The HIV-1 envelope glycoproteins: folding, function and vaccine design

Sanders, R.W.

Publication date
2004
Document Version
Final published version

The HIV-1 envelope glycoproteins:
folding, function and vaccine design

Omslagontwerp en ontwerp binnenwerk: René Staelenberg, Amsterdam

ISBN 90 5356 667 8
NUR 870

The research described in this thesis was performed in the department of Human Retrovirology at the Academic Medical Center of the University of Amsterdam. Part of the work was performed at Cornell University (New York), the Aaron Diamond AIDS Research Center (New York) and the Scripps Research Institute (San Diego).
Printing of this thesis was supported financially by Progenics Pharmaceuticals, the University of Amsterdam, Bristol-Myers Squibb and Boehringer-Ingelheim.
Parts of this thesis were reprinted with permission from the *Journal of Virology* (Copyright © 2003, the American Society for Microbiology) and the Los Alamos *HIV Sequence Compendium 2002* (Copyright © 1998-2003 The Regents of the University of California).

The HIV-1 envelope glycoproteins: folding, function and vaccine design

De HIV-1 envelop glycoproteïnen: vouwing, functie en vaccinontwerp

Academisch proefschrift,
ter verkrijging van de graad van doctor
aan de Universiteit van Amsterdam
op gezag van de Rector Magnificus
prof.mr. P.F. van der Heijden
ten overstaan van een door het college voor promoties ingestelde
commissie, in het openbaar te verdedigen in de Aula der Universiteit
op vrijdag 23 januari 2004, te 14.00 uur

door

Rogier Willem Sanders

geboren te IJsselstein

Promotiecommissie

promotores:	prof.dr. B. Berkhout
	prof.dr. J.P. Moore
overige leden:	prof.dr. I. Braakman
	prof.dr. J. Goudsmit
	prof.dr. M.L. Kapsenberg
	prof.dr. F. Miedema
	prof.dr. A.D.M.E. Osterhaus
	prof.dr. P.J. Rottier

Faculteit der Geneeskunde

Contents

Chapter 1

Introduction

General Introduction

With a total of 62 million infections and 20 million deaths worldwide, acquired immunodeficiency syndrome (AIDS) is one of the world's major death causes (http://www.unaids.org). The most–affected countries are in subsaharan Africa and are least able to cope with the devastating consequences. In some countries more than one in three persons is infected with HIV (Zimbabwe, 33,7% and Botswana, 38,8% prevalence). Efforts to develop an effective vaccine are therefore of the utmost importance.

Although an earlier case (1959) has retrospectively been identified (48,96, 236,251), the first cases of what later became known as AIDS were described in 1981 (85,102,139,205). In 1983 a novel retrovirus was identified as the causative agent: HIV-1 (9,76). Its cousin HIV-2 was identified three years later (43,44). While HIV-1 originated from a related immunodeficiency virus (SIV_{cpz}) in African chimpanzees, HIV-2 evolved from a SIV variant in sooty mangabeys (79,203). SIV_{cpz} crossed the species barrier between its natural host and humans probably before 1940 and subsequently evolved to adapt to the new human host and become manifest as HIV-1 (86,116). HIV-1 counts many subtypes of which subtype C is the most common throughout the world and subtype B is the most common in western countries (168).

HIV-1 is a retrovirus belonging to the subfamily of lentiviruses (82,83). In general, lentiviruses cause a slow degenerative disease, characterized by an acute phase, a latent phase and finally disease progression (82,217). Many lentiviruses have been described that cause immune deficiency in a variety of hosts (64,82), with examples being feline immunodeficiency virus (FIV) in cats, bovine immunodeficiency virus (BIV) in cattle and SIV in monkeys (64,82). Lentiviruses have evolved mechanisms to persist for many years in the hostile environment of an immune-competent host. Infecting and killing cells of the immune system, HIV-1 causes gradual depletion and dysfunction of the immune system, which finally leads to opportunistic infections and death.

The HIV-1 genome consists of two identical positively stranded RNA molecules of approximately 10.000 nucleotides (Fig. 1). The three major and typical retroviral genes are *gag*, *pol* and *env* (176,189,231). The *gag* gene encodes the structural proteins which are posttranslationally cleaved from the Gag precursor: the capsid protein (CA-p24), the matrix protein (MA-p17), the nucleocapsid protein (NC-p7), p6 and p2 (45,132,215,230). The *pol* gene encodes the protease (PR), responsible for the posttranslational cleavage of various gene products; the reverse transcriptase (RT), responsible for reverse transcription of the RNA

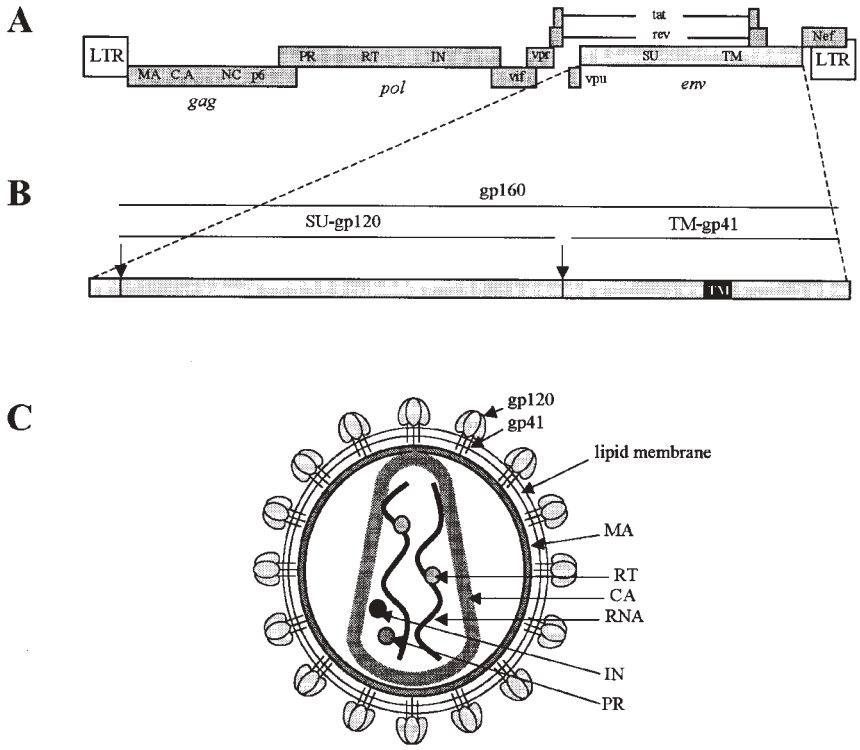

Fig. 1. **A**. Genetic organization of HIV-1. **B**. The *env* gene. Env is produced as a gp160 precursor protein. The cleavage sites between the leader peptide and gp160 and between gp120 and gp41 are marked by arrows. The transmembrane domain (TM) is also indicated. **C**. Schematic of an HIV-1 virus particle.

genome into DNA; and integrase (IN), responsible for the integration of the viral DNA genome into the host genome (26,45,132,215,219,230). The *env* gene encodes the viral envelope glycoproteins (Env) gp120 and gp41, the subject of this thesis (Fig. 1B). In addition to these typical retroviral genes, the HIV-1 genome encodes several accessory and regulatory proteins: Vpr, Vif, Vpu, Tat, Rev, and Nef, with various functions in the viral life cycle (50,132,217,224). Besides the 9 genes, the HIV-1 genome contains many sequence and/or structure motifs with important functions at the RNA or DNA level (11,128).

The structure of the virus and the functions of the various proteins are outlined in Fig. 1 and 2. In short, the structural proteins make up the inner cone shaped core (CA) and shell (MA) (45,132,215,230). Env resides in the lipid membrane that forms the external surface of the virus particle and mediates entry into cells expressing the appropriate receptors (101,132). Env is also the major component of the virus exposed to the immune system. The reverse transcriptase (RT) enzymes reside in the virion core together with the RNA genome, which is coated with the NC protein. (26,65,73,219). Once the viral genome is reverse transcribed and integrated in the host genome, RNA synthesis from the integrated DNA and protein expression result in the production of new virus particles that bud from the cell membrane to initiate a new round of infection.

HIV-1 cell tropism and transmission

HIV-1 resides in cells of the immune system expressing the appropriate receptors: CD4 and one of the chemokine receptors CCR5 or CXCR4 as a second receptor, also termed coreceptor (2,12,40,53,55,56,58,111,133). These receptors are required for Env-mediated viral entry into the host cell. Cells that are susceptible to HIV-1 infection are $CD4^+$ T cells (helper T cells), thymocytes, monocytes, macrophages, microglia and dendritic cells (DC) (23,75,91,155,186,187,250). The cell tropism of a particular virus isolate is mainly dependent on whether is uses CCR5 or CXCR4 as coreceptor (20,110,206). Although the reasons are not completely clear, transmitted viruses predominantly use CCR5 (227,250) and individuals with a mutant CCR5 gene are strongly resistant to HIV-1 infection (99,130,167). CCR5-using virus isolates are able to infect memory T cells and macrophages (1,91,169,198,252). In approximately 50% of the individuals

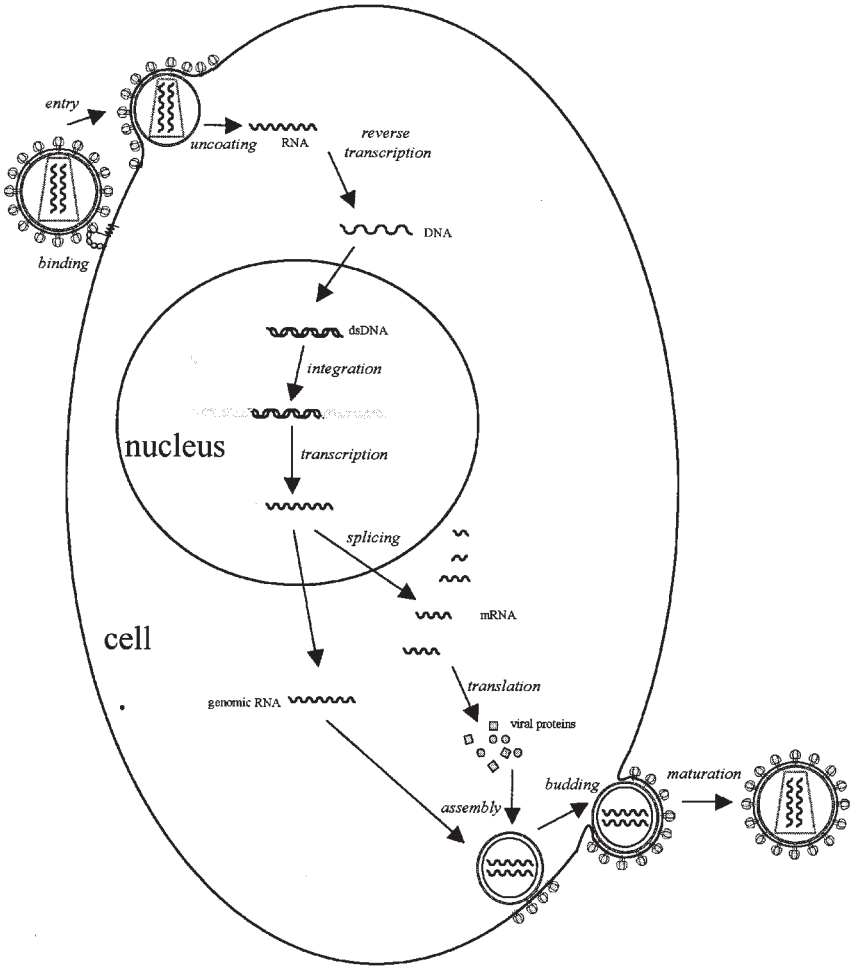

Fig. 2. The HIV-1 life cycle. See text for further details.

infected with HIV-1 subtype B, coreceptor use eventually changes from CCR5 to CXCR4 and this usually correlates with a more rapid disease progression due to broadening of the host cell range (21,47,115). CXCR4-using virus variants are able to infect naïve T cells in addition to memory T cells (21,47,115,226). Of note is that HIV-1 has a preference to infect HIV-1 specific T cells (57).

Sexual transmission of HIV-1 is thought to require the help of dendritic cells (DC) to cross the mucosal barrier before infection of T cells can occur (97,109,174,177,185,208,212). DC residing in peripheral tissues are able to capture HIV-1 and to facilitate transport to a draining lymph node, which subsequently becomes the center of viral replication. Although HIV-1 can infect certain DC such as Langerhans cells (30,31,166,234), other DC specifically bind HIV-1 and present the virus particle to T cells, without becoming infected themselves (22,29,81,89). Various lectins on DC, the best characterized being DC-SIGN (CD209), can facilitate specific binding of HIV (and also other viruses), through an interaction with gp120. Virions are internalised and remain in an infectious form in an intracellular compartment (72,81,118,118,170,225).

Crucial in HIV transmission mediated by DC is the interaction between Env on the virus and DC-SIGN on the DC. DC-SIGN is a C-type lectin that binds mannose residues on the outer surface of gp120. Although other lectins can substitute for DC-SIGN on certain types of DC (225), the interaction between DC-SIGN and gp120 has been studied most intensively. Subsequent interactions between the T cell and the DC facilitate virus transfer by local recruitment of adhesion molecules and the HIV-1 receptors, and the formation of an "infectious synapse" (chapter 2)(140,190).

Env biosynthesis, structure and function

The entry process of HIV-1 is mediated by the envelope glycoproteins (Env). Env is arranged on the virus particle in trimeric spikes, comprising three gp120 (SU) and three gp41 (TM) molecules, anchored within the viral membrane via the gp41 transmembrane domain (172,241). The surface subunit gp120 is ~480 amino-acids long and contains 9 disulfide bonds and 20-24 *N*-linked carbohydrates, contributing almost half of gp120s molecular weight (126) (see also Fig. 1A in chapter 3.1, Fig. 1 in chapter 4.1 and Fig. 3 in chapter 5.1). gp120 is divided into five conserved regions (C1-C5) interspaced by five variable regions (V1-V5) (144). The V1-V4 loops are separated from the gp120 core by disulfide bonds at the base of each loop structure (126). The atomic structure of the core of gp120 in complex with CD4 and an antibody, solved by X-ray crystallography, revealed that it consists of three domains: an inner and outer domain bridged by a four-stranded β-sheet (122). Viral attachment to susceptible target cells involves the binding of CD4 to gp120. The CD4 binding site is located at the edge of the three domains and binding of CD4 causes drastic conformational changes involving refolding of ~100 amino-acids (151). This refolding results in a movement of the V1/V2 and V3 loops away from each other, allowing the exposure and/or creation of the coreceptor binding site in the bridging sheet that was previously obscured (Fig. 3)(122,183,222,237,239,240). The conformational changes in gp120 that result from receptor and coreceptor binding trigger the

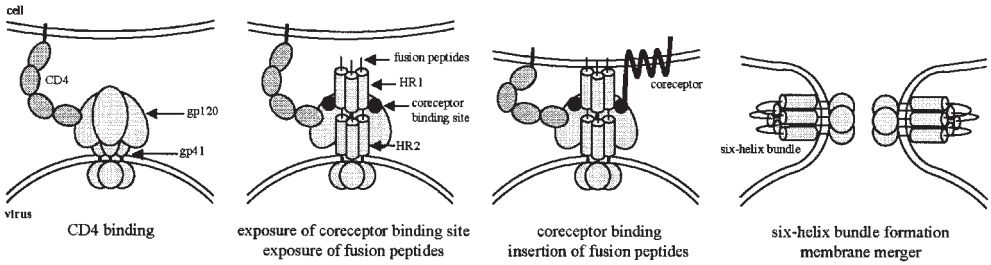

Fig. 3. Model for Env-mediated entry of HIV-1. CD4 binding induces conformational changes that result in the exposure and/or creation of the coreceptor binding site (black circle) and the exposure of the fusion peptides in gp41 towards the target cell membrane by the formation of an extended triple stranded coiled coil, also termed the pre-hairpin intermediate. Coreceptor binding results in insertion of the fusion peptides into the cell membrane. Subsequent conformational changes involve the formation of a six-helix bundle structure, or triple hairpin, and finally result in membrane fusion.

fusion of viral and cellular membranes, which is mediated by gp41.

The transmembrane subunit gp41 consists of ~340 amino-acids with ~180 residues in the ectodomain (gp41e), which contains four *N*-linked carbohydrates and one small disulfide bond-bonded loop (see also Fig. 3 in chapter 5.1, Fig. 1 in chapter 5.6 and Fig. 1 in chapter 5.7). gp41 has an unusual long intracytoplasmic tail with various motifs that contribute to viral replication (73,100). The binding of the receptors to gp120 leads to the insertion of the hydrophobic N-terminal fusion peptide of gp41 into the target cell membrane (Fig. 3). Subsequent changes within gp41e involve two leucine zipper-like motifs, heptad repeat 1 (HR1) and heptad repeat 2 (HR2). Ultimately, the HR1 and HR2 regions from three gp41 molecules assemble into a six-helix bundle structure, which juxtaposes the viral and cellular membranes for fusion (Fig. 3)(10,36,46,63,77,142,216,233). Formation of the six-helix bundle structure stabilizes the initial membrane pore and causes lipid mixing and finally complete membrane merger, resulting in the release of the viral core into the cytoplasm (54,77,78,136,142).

Although a considerable amount of structural and functional data has been accumulated on the separate subunits, relatively little is known about their concerted functioning, in particular the mechanism by which receptor-triggered conformational changes in gp120 activate the fusion machinery of gp41. Mutagenesis analyses indicate that the Env subunits contact each other in the N- and C-terminal regions (C1 and C5) of gp120 and the loop and HR1 regions of gp41 (17,32,37,38,74,92,134,175,191,201,235,238,248). However, the available atomic structures of gp120 and gp41 do not reveal the contact regions, because they were deleted in order to obtain crystals with high resolution diffraction (36,120-122,216,233). There is ample evidence suggesting intimate interactions between the two subunits. For example, substitutions in gp41 can influence inhibition by compounds directed to gp120 and *vice versa* (5,152,159,178,180,213,220,221).

The entry process in general and the fusion process in particular are promising targets for novel therapeutic agents. Although we and others have reviewed the recent progress made in this field (6,54,63,145), it is worth noting that the first

entry inhibitor (enfuvirtide, fuzeon, ENF, T-20, DP178) has been approved by the US Food and Drug Administration (FDA) in march 2003 (http://www.fda.gov)..

The Env complex is synthesized as a gp160 precursor protein (Fig. 1B), which is translocated cotranslationally into the Endoplasmic Reticulum (ER). Here, Env acquires carbohydrates and disulfide bonds, it folds, trimerizes and looses its leader peptide (124). As for any other glycoprotein, gp160 folding is assisted by molecular chaperones. gp160 transiently associates with the ER resident chaperones BiP, calnexin and calreticulin (61,113,156). The formation of Env's intricate disulfide bonded architecture is the topic of chapter 4 (for details on glycoprotein folding and oxidation in the ER, see the introduction of chapter 4.1).

Once oxidative folding in the ER is completed, gp160 is transported to the Golgi complex where it is cleaved by cellular proteases of the furin family into the gp120 and gp41 subunits, which remain associated non-covalently (Fig. 1B)(148,211). However, not all gp160 molecules are cleaved into gp120 and gp41, which is relevant to later sections in this general introduction and chapter 5. In addition, the carbohydrate moieties are modified in the Golgi network (126). Many glycans on Env are not at all or not completely processed to complex carbohydrates (see also the introduction and Fig. 1 of chapter 3.1), which results in the presence of mannose residues on the outer surface of gp120. The exposed mannose residues are important for the binding of various Env ligands: DC-SIGN and other lectins that facilitate DC-mediated virus transmission, the broadly neutralizing antibody 2G12, and cyanovirin-N, a cyanobacterial protein that inhibits virus replication (chapters 2 and 3)(13-15,28,67,95,143,193,197). The glycans are also important for Env folding in the ER (chapter 4) and for immune evasion (see below). The native envelope glycoprotein complex is finally transported to the cell surface where virus particles are assembled that bud from the cell membrane.

Env antigenicity and immunogenicity

Env is embedded in the viral membrane and the membrane of infected cells, thereby rendering it as the major target for virus-neutralizing antibodies (165,172). Hence, Env is the focus for the development of subunit vaccines based on the induction of humoral immunity, but Env based vaccines have not been able to elicit protective neutralizing antibody responses (165,200). The antibody response to Env has been studied extensively, mostly through isolation of antibodies from infected individuals and immunized animals. Over 100 monoclonal antibodies have been identified that are directed to distinct Env domains. Combining antigenic data revealed that the gp120 surface can be roughly divided into a neutralizing face with the epitopes for several neutralizing antibodies, a non-neutralizing face with solely non-neutralizing epitopes, and an immunologically silent face that is largely covered with carbohydrate (147,239).

The neutralizing face harbors the receptor binding sites, which are obvious targets for neutralizing antibodies. The CD4 binding site epitopes overlap with the binding site for CD4 and antibodies directed to these epitopes block binding of CD4 to soluble gp120. CD4 binding induces the exposure of another set of epitopes, termed CD4-induced (CD4i) epitopes, the majority of which overlap with

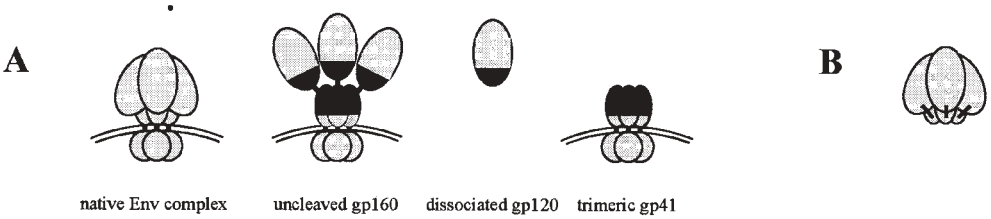

Fig. 4. **A**. Different forms of Env. The regions indicated in black are the non-neutralizing decoy epitopes in the gp120 C1 and C5 regions and gp41 cluster I and II. **B**. A soluble and stable mimic of the functional native Env complex as described in this thesis (chapter 5.6). Intermolecular disulfide bonds between gp120 and gp41 (chapter 5.1) are indicated.

the coreceptor binding site (183). The N- and C-termini of gp120 (C1 and C5 regions) contribute to most of the non-neutralizing face, which is thought to be occluded by other gp120 subunits in the trimer, and by gp41 (Fig. 4A) (92,238, 239,248). Antibodies directed to these regions are non-neutralizing, because they are unable to recognize the functional Env complex and unable to block the viral entry process. An unique antibody, 2G12, binds to the silent face of gp120, and seems to indirectly block coreceptor binding (223).

The antigenic domains described above encompass the conserved regions of gp120. The variable loops, which camouflage the neutralizing face from the humoral response, can efficiently elicit neutralizing antibodies, but these antibodies are usually specific for the strain to which they were elicited and viral escape through mutation of the variable loops renders these antibodies ineffective. The V3 region is of special interest for several reasons. First, it is an immunodominant neutralization epitope. Second, it is part of the coreceptor binding domain and important for the switch from CCR5 to CXCR4 usage (25,49,51,52,87, 88,98,173,229,253). The V3 domain can fold in two conformations, which are suggested to mimic the natural ligands for CCR5 (MIP-1α, MIP-1β and RANTES) and CXCR4 (SDF-1) (202,210).

Gp41 has three important epitope clusters: cluster I in the immunodominant loop region, cluster II in the N-terminal part of HR2, and the 2F5/4E10/z13 cluster proximal to the membrane (Fig. 4A, see also Fig. 1B in chapter 5.6) (7,16,59, 149,150,160,214,244,254). Although the majority of the antibodies raised against gp41 during natural infection are directed against the cluster I and II regions, they are ineffective in virus neutralization because these regions are not exposed on the native functional Env complex (Fig. 1B) (84,146,165,184,218,244). Other domains in gp41 may also occasionally elicit antibodies (16,59). The only neutralizing antibodies to gp41, however, bind to the membrane proximal region (2F5/4E10/z13).

Several properties of Env are known to contribute to the failure of the immune system to raise sufficient neutralizing antibodies in natural infection or in a vaccine setting. The first mechanism of antibody evasion concerns the inaccessibility of the receptor binding sites to antibodies. The CD4 binding site is located in a recessed cavity that is not very accessible to antibodies and neutralizing antibodies are not easily elicited against it, the exception being b12 (122,239). CD4

binding is in part mediated by Cα atoms in gp120 and mutation of the side chains is thus possible without affecting CD4 contacts. Furthermore, the CD4-gp120 interface contains several cavities and residues around these cavities can also be changed to escape from antibodies without affecting CD4 binding (122,239). In addition, the binding of antibodies to the CD4 binding site is energetically unfavourable due to its location on the edge of the three domains, the specific domain organization and the intrinsic flexibility of gp120 (119). The coreceptor binding site is only exposed after CD4 binding, thereby limiting space and time available for antibody interference (122,239). Indeed, CD4i antibodies are usually unable to neutralize primary isolates because of steric constraints (123). The complete IgG molecules do not fit between the CD4-bound Env and the cell membrane, in contrast to Fab or single chain Fv versions of the same antibodies that neutralize primary isolates efficiently (123). The variable loops are instrumental in shielding these sites (122,183,222,237,239,240). The heavy glycosylation, mostly located on the silent face, also functions as a shield against the humoral immune response because the immune system does not recognize sugars as foreign. Thus, specific antibodies are rarely raised against these sugars, the only exception for HIV-1 gp120 being 2G12 (24,114,122,153,179,239).

In contrast to the shielding of neutralization epitopes on functional Env, non-functional Env exposes decoy epitopes that exclusively raise non-neutralizing antibodies. gp120 is easily shed from the viral and/or cellular surface and gp160 is incompletely cleaved, both leading to the exposure of decoy epitopes in the C1 and C5 regions of gp120, and in cluster I and II in gp41, the regions that normally comprise the intersubunit interface (Fig. 4A) (17,32,37,38,74,84,92,134,146, 165,175,184,191,201,218,235,238,244,248). Similarly, lysis of virus-infected cells leads to the exposure of these decoy epitopes on immature Env forms (17,93,161,163,165,188). Since these non-functional species of Env are abundant in natural infection, the initial immune response is likely to be directed to these Env forms, and this may in fact suppress the antibody response to the functional form of Env by the mechanism of “original antigenic sin” (161,163).

Env’s formidable defenses against antibodies forces the humoral immune response to find rare solutions. Many of the known neutralizing antibodies (b12, 2G12, 2F5/4E10/z13, CD4i antibodies) have unusual properties. b12 has an unusually long complementarity determining region (CDR) H3 domain with an aromatic tryptophan at its apex that mimics the phenylalanine of CD4, which protrudes into the recessed CD4 binding cavity (27,195). b12 exhibits a small binding entropy to gp120 in contrast to non-neutralizing antibodies to the CD4 binding site (119). 2F5 also has an unusually long CDR H3 domain that was probably generated through an extremely rare recombination event on the immunoglobulin heavy chain locus (117). The glycan shield that serves to protect conserved protein domains is the target of the 2G12 monoclonal antibody, which specifically binds mannose residues on a cluster of carbohydrates on the silent face of gp120, but close to the coreceptor binding site (chapter 3.1)(28,193,197,223). To facilitate this unusual multivalent carbohydrate recognition, the V_H domains are swapped, resulting in a Fab-dimerized antibody with an extended antigen binding surface (28). Another set of unusual neutralizing antibodies bind the coreceptor binding site on gp120 and are characterized by sulfation of tyrosines in their

antigen binding sites, thus mimicking the sulfated N-terminus of CCR5 (41).

Thus, only a few known human monoclonal antibodies can efficiently neutralize diverse HIV strains. The sulfated antibodies mentioned above belong to a group of weakly neutralizing antibodies that bind the coreceptor binding site. 2G12 indirectly blocks coreceptor binding (223) and b12 blocks CD4 binding. Another group of neutralizing antibodies (2F5, 4E10 and z13) bind to the membrane proximal region in gp41. Their mechanism of neutralization is not completely understood, but it has been suggested that the presence of a bulky antibody so close to the viral membrane interferes with the merger of the viral and cellular membranes (172).

Although some properties of neutralizing antibodies are understood, the correlates of neutralization are for a major part unclear. For example, why are most of the CD4 binding site antibodies unable to neutralize primary isolates, while they are capable of blocking the interaction of CD4 with monomeric gp120? It is assumed that neutralizing antibodies bind to the functional Env complex, presumably the cleaved trimer, while non-neutralizing antibodies do not (69,196). Non-neutralizing antibodies can bind to non-functional forms of Env that are present on the surface of infectious virions and although non-neutralizing antibodies can compete with neutralizing antibodies for binding to virions, they can not compete for neutralization (93,171).

Notably, Env may also elicit antibodies that increase HIV infectivity. Enhancing antibodies to HIV and other viruses have been described (34,90,112,125, 184). The enhancing effect of vaccination with Env subunit vaccines on challenge infection has been extensively studied for FIV in cats, and accelerated infection has been observed in vaccinated cats (106,107,154,204). Although no enhancing effects have been observed in the current clinical trials using recombinant gp120 (71), Env subunit vaccines are not by definition safe: they may elicit antibodies that increase virus infectivity.

Env-based vaccine strategies

In our HIV-1 vaccine research, we focused on the humoral immune response and a review on the cytotoxic T lymphocyte (CTL) response to HIV-1 is therefore beyond the scope of this thesis. There is compelling evidence that antibodies may play an important role in vaccine-induced immunity against HIV. First, hu-SCID-PBL mice can be protected against HIV-1 after passive immunization with neutralizing antibodies (162). Second, passive infusion of neutralizing antibodies can protect monkeys against infection (94,137,138,164). Third, intravaginal administration of neutralizing antibodies can protect monkeys against intravaginal challenge (228). Fourth, vaccine-induced antibodies can sometimes protect monkeys (39,62,127). Fifth, during natural infection in humans, rapid escape from neutralizing antibodies can occur (3,4,182,232). The key problem, however, is how to raise such broadly neutralizing antibodies by a vaccine in humans.

As anticipated for some time, the first generation of Env-based subunit vaccines (recombinant gp120) failed completely (165,200). Thus, it became apparent that the natural gp120 is not suitable as a vaccine antigen (165,200). The current available knowledge on how Env fools the immune system has led to the development

of several sophisticated candidate immunogens. Over the last few years, much progress has been made in antigen presentation in the context of recombinant viruses, DNA, protein vaccines or combinations thereof. A review of this research is beyond the scope of this thesis, but all progress in antigen presentation will be irrelevant if the antigen itself is very poor at eliciting neutralizing antibodies, which is certainly the case for HIV-1 gp120. Therefore, increasing attention is drawn to antigen modification. This research is in part independent of questions about which particular Env (i.e. the Env of which particular strain or subtype of HIV-1) has the best intrinsic immunogenic properties, and which Env will raise antibodies that optimally neutralize diverse HIV-1 strains (80).

One of the first modifications tested was the addition of gp41 sequences to yield soluble, oligomeric gp140 immunogens (60). This strategy slightly improves the induction of neutralizing antibodies (60,62,181). Another modification is the deletion of variable loops, which results in a better exposure of the receptor binding sites (19,33,104,192,207,209). The immunogenicity data are moderately encouraging (8,103,131,141). Similarly, elimination of carbohydrates has been shown to lead to the exposure of conserved regions and increased elicitation of neutralizing antibodies (24,114,153,179). The converse of eliminating carbohydrate to uncover neutralizing epitopes, that is hyperglycosylation of non-neutralizing decoy epitopes, is also under investigation (158). To overcome the intrinsic flexibility of gp120 and the entropic masking of the CD4 binding site, substitutions are designed that either stabilize or disupt the CD4-bound state of gp120 (242). Env immunogens with increased affinity for neutralizing antibody b12 and decreased affinity for non-neutralizing antibodies to the CD4 binding site have also been generated by targeted mutagenesis using the recent structural data on the b12 antibody and its footprint on gp120 (157). Since the trimer is most likely the functional form of Env, stabilization of the trimer interactions has been proposed as a modification strategy. The first stabilized trimers were based on the use of trimer stabilizing coiled coil motifs at the C-terminus of the gp41 ectodomain (66,245-247). These trimer-stabilizing motifs were tested either alone, or in combination with disulfide bond linkage of the gp41 subunits. The cleavage site was inactivated in these immunogens, and the initial immunogenicity results have been moderately encouraging (249). Recently, we described the generation of cleaved stabilized trimers (chapter 5.6)(194). Another option is the complexing of Env with receptors or receptor mimetics, and such Env-receptor complexes can be used for immunization. This approach may facilitate elicitation of neutralizing antibodies to epitopes that are obscured in uncomplexed Env (68,70). Other modification strategies, some of which are aimed at the exposure of fusion intermediate structures, are currently under investigation (35,42,135). We have discussed immunogens that comprise whole modified Env, but immunization with individual peptides of neutralizing epitopes (V3, 2F5, b12) is also under evaluation (105,108,129,243).

Outline of this thesis

The current knowledge on Env biosynthesis, structure and function and the implications for immunogenicity is insufficient to tackle the HIV vaccine problem.

Therefore, fundamental research in combination with rational vaccine design may contribute to a better understanding of Env and the immune responses raised against it. The results from such an approach will hopefully eventually lead to the design of Env immunogens that are able to induce neutralizing antibodies that can prevent transmission or clear infection, perhaps in combination with effective CTL vaccines. Chapter 2, 3 and 4 describe our fundamental research on various properties of Env. Chapter 2 deals with the Env-mediated transmission of HIV-1 by dendritic cells and sheds light on which molecules participate in this process alongside Env (190). Chapter 3 reveals the nature of the carbohydrate epitope of the unique 2G12 antibody that efficiently neutralizes HIV-1 (193). The role of the native disulfide bonds in Env biosynthesis, folding and virus replication is the topic of chapter 4.1. An escape virus variant is presented in chapter 4.2. This virus lacks the essential disulfide bond at the base of the V4 domain, but restores Env folding and virus replication through stabilization of a local β-sheet fold. Other escape viruses lack the N-terminal disulfide bond in gp120 and have local and distal compensatory substitutions that reveal interesting interactions between gp120 and gp41 (chapter 4.3). These studies increase our knowledge on Env biosynthesis and protein folding in general.

Chapter 5 describes studies on Env modifications that should improve its properties as vaccine antigen. Stabilization of the normally weak non-covalent interactions between gp120 and gp41 is the subject of chapter 5.1 (17). The intersubunit instability can be overcome by the introduction of an appropriately positioned intermolecular cysteine bridge (SOS). The SOS disulfide bond allows proper precursor cleavage, but prevents gp120 – gp41 dissociation, which leads to the undesirable exposure of immunogenic decoy epitopes. We combined the SOS technology with the deletion of variable loops in order to increase the exposure of the receptor binding sites (chapter 5.2)(192). In chapter 5.3 we describe the purification and oligomeric properties of SOS gp140 (199), which appears to be mostly monomeric. We also assessed the effect of the SOS mutations on virus replication and attempted to generate improved SOS variants through virus evolution (chapter 5.4). In chapter 5.5 new Env variants are presented with modified cleavage sites that are more efficiently used by cellular proteases of the furin family (18). These variants may help to improve vaccine systems that do not allow complete Env cleavage. Finally, chapters 5.6 and 5.7 describe mutations that increase the trimeric stability of SOS gp140 and their effects on virus replication and evolution (194). The literature survey on gp41 mutagenesis in the appendix may be seen as a preparative study for chapter 5.6 (191). Since it becomes more and more clear that the Env trimer is the functionally and immunologically relevant form of Env, trimer stabilization as described in this thesis may be valuable for vaccine research and structural studies (Fig. 4B).

References

1. **Alkhatib, G., C. C. Broder, and E. A. Berger**. 1996. Cell type-specific fusion cofactors determine human immunodeficiency virus type 1 tropism for T-cell lines versus primary macrophages. J. Virol. **70**:5487-5494.
2. **Alkhatib, G., C. Combadiere, C. C. Broder, Y. Feng, P. M. Murphy, and E. A. Berger**. 1996. CC CKR5: a RANTES, MIP-1a, MIP-1b receptor as a fusion co-factor for macrophage-tropic HIV-1. Science **272**:1955-1958.
3. **Arendrup, M., C. Nielsen, J. E. Hansen, C. Pedersen, L. Mathiesen, and J. O. Nielsen**. 1992. Autologous HIV-1 neutralizing antibodies: emergence of neutralization-resistant escape virus and subsequent development of escape virus neutralizing antibodies. J. Acquir. Immune Defic. Syndr. **5**:303-307.
4. **Arendrup, M., A. Sonnerborg, B. Svennerholm, L. Akerblom, C. Nielsen, H. Clausen, S. Olofsson, J. O. Nielsen, and J. E. Hansen**. 1993. Neutralizing antibody response during human immunodeficiency virus type 1 infection: type and group specificity and viral escape. J. Gen. Virol. **74 (Pt 5)**:855-863.
5. **Back, N. K., L. Smit, M. Schutten, P. L. Nara, M. Tersmette, and J. Goudsmit**. 1993. Mutations in human immunodeficiency virus type 1 gp41 affect sensitivity to neutralization by gp120 antibodies. J. Virol. **67**:6897-6902.
6. **Baldwin, C. E., R. W. Sanders, and B. Berkhout**. 2003. Inhibiting HIV-1 Entry with Fusion Inhibitors. Curr. Med. Chem. **10**:1633-1642.
7. **Barbato, G., E. Bianchi, P. Ingallinella, W. H. Hurni, M. D. Miller, G. Ciliberto, R. Cortese, R. Bazzo, J. W. Shiver, and A. Pessi**. 2003. Structural analysis of the epitope of the anti-HIV antibody 2F5 sheds light into its mechanism of neutralization and HIV fusion. J. Mol. Biol. **330**:1101-1115.
8. **Barnett, S. W., S. Lu, I. Srivastava, S. Cherpelis, A. Gettie, J. Blanchard, S. Wang, I. Mboudjeka, L. Leung, Y. Lian, A. Fong, C. Buckner, A. Ly, S. Hilt, J. Ulmer, C. T. Wild, J. R. Mascola, and L. Stamatatos**. 2001. The ability of an oligomeric human immunodeficiency virus type 1 (HIV- 1) envelope antigen to elicit neutralizing antibodies against primary HIV-1 isolates is improved following partial deletion of the second hypervariable region. J. Virol. **75**:5526-5540.
9. **Barré-Sinoussi, F., J. C. Chermann, P. Rey, M. T. Nugeyre, S. Chamaret, J. Gruest, C. Dauguet, C. Axler-Blin, F. Vezinet-Brun, C. Rouzioux, W. Rozenbaum, and L. Montagnier**. 1983. Isolation of a T-lymphotropic retrovirus from a patient at risk for acquired immune deficiency syndrome (AIDS). Science **220**:868-871.
10. **Bentz, J.** 2000. Membrane fusion mediated by coiled coils: a hypothesis. Biophys. J. **78**:886-900.
11. **Berkhout, B.** 1996. Structure and function of the human immunodeficiency virus leader RNA. Progr. Nucl. Acid. Res. Mol. Biol. **54**:1-34.
12. **Berson, J. F., D. Long, B. J. Doranz, J. Rucker, F. R. Jirik, and R. W. Doms**. 1996. A seven-transmembrane domain receptor involved in fusion and entry of T-cell-tropic human immunodeficiency virus type 1 strains. J. Virol. **70**:6288-6295.
13. **Bewley, C. A.** 2001. Solution structure of a cyanovirin-N:Man alpha 1-2Man alpha complex: structural basis for high-affinity carbohydrate-mediated binding to gp120. Structure (Camb.) **9**:931-940.
14. **Bewley, C. A., K. R. Gustafson, M. R. Boyd, D. G. Covell, A. Bax, G. M. Clore, and A. M. Gronenborn**. 1998. Solution structure of cyanovirin-N, a potent HIV-inactivating protein. Nat. Struct. Biol **5**:571-578.
15. **Bewley, C. A., S. Kiyonaka, and I. Hamachi**. 2002. Site-specific discrimination by cyanovirin-N for alpha-linked trisaccharides comprising the three arms of Man(8) and Man(9). J. Mol. Biol. **322**:881-889.
16. **Binley, J. M., H. J. Ditzel, C. F. Barbas, III, N. Sullivan, J. Sodroski, P. W. Parren, and D. R. Burton**. 1996. Human antibody responses to HIV type 1 glycoprotein 41 cloned in phage display libraries suggest three major epitopes are recognized and give evidence for conserved antibody motifs in antigen binding. AIDS Res. Hum. Retroviruses **12**:911-924.
17. **Binley, J. M., R. W. Sanders, B. Clas, N. Schuelke, A. Master, Y. Guo, F. Kajumo, D. J. Ansel-**

ma, P. J. Maddon, W. C. Olson, and J. P. Moore. 2000. A recombinant HIV-1 envelope glycoprotein complex stabilized by an intermolecular disulfide bond between the gp120 and gp41 subunits is an antigenic mimic of the trimeric virion-associated structure. J. Virol. **74**:627-643.

18. **Binley, J. M., R. W. Sanders, A. Master, C. S. Cayanan, C. L. Wiley, L. Schiffner, B. Travis, S. Kuhmann, D. R. Burton, S.-L. Hu, W. C. Olson, and J. P. Moore**. 2002. Enhancing the proteolytic maturation of human immunodeficiency virus type 1 envelope glycoproteins. J. Virol. **76**:2606-2616.
19. **Binley, J. M., R. Wyatt, E. Desjardins, P. D. Kwong, W. Hendrickson, J. P. Moore, and J. Sodroski**. 1998. Analysis of the interaction of antibodies with a conserved enzymatically deglycosylated core of the HIV type 1 envelope glycoprotein 120. AIDS Res. Hum. Retroviruses **14**:191-198.
20. **Bjorndal, A., H. Deng, M. Jansson, J. R. Fiore, C. Colognesi, A. Karlsson, J. Albert, G. Scarlatti, D. R. Littman, and E. M. Fenyo**. 1997. Coreceptor usage of primary human immunodeficiency virus type 1 isolates varies according to biological phenotype. J. Virol. **71**:7478-7487.
21. **Blaak, H., A. B. van't Wout, M. Brouwer, B. Hooibrink, E. Hovenkamp, and H. Schuitemaker**. 2000. *In vivo* HIV-1 infection of CD45RA(+)CD4(+) T cells is established primarily by syncytium-inducing variants and correlates with the rate of CD4(+) T cell decline. Proc. Natl. Acad. Sci. USA **97**:1269-1274.
22. **Blauvelt, A., H. Asada, M. W. Saville, V. Klaus-Kovtun, D. J. Altman, R. Yarchoan, and S. I. Katz**. 1997. Productive infection of dendritic cells by HIV-1 and their ability to capture virus are mediated through separate pathways. J. Clin. Invest. **100**:2043-2053.
23. **Bleul, C. C., L. Wu, J. A. Hoxie, T. A. Springer, and C. R. Mackay**. 1997. The HIV coreceptors CXCR4 and CCR5 are differentially expressed and regulated on human T lymphocytes. Proc. Natl. Acad. Sci. USA **94**:1925-1930.
24. **Bolmstedt, A., J. Hinkula, E. Rowcliffe, M. Biller, B. Wahren, and S. Olofsson**. 2001. Enhanced immunogenicity of a human immunodeficiency virus type 1 env DNA vaccine by manipulating N-glycosylation signals. Effects of elimination of the V3 N306 glycan. Vaccine **20**:397-405.
25. **Briggs, D. R., D. L. Tuttle, J. W. Sleasman, and M. M. Goodenow**. 2000. Envelope V3 amino-acid sequence predicts HIV-1 phenotype (co-receptor usage and tropism for macrophages). AIDS **14**:2937-2939.
26. **Brown, P. O.** 1997. Integration, p. 161-204. *In* J. M. Coffin, S. H. Hughes, and H. E. Varmus (eds.), Retroviruses. Cold Spring Harbor Laboratory Press, New York.
27. **Burton, D. R., J. Pyati, R. Koduri, S. J. Sharp, G. B. Thornton, P. W. Parren, L. S. Sawyer, R. M. Hendry, N. Dunlop, P. L. Nara, and .** 1994. Efficient neutralization of primary isolates of HIV-1 by a recombinant human monoclonal antibody. Science **266**:1024-1027.
28. **Calarese, D. A., C. N. Scanlan, M. B. Zwick, S. Deechongkit, Y. Mimura, R. Kunert, P. Zhu, M. R. Wormald, R. L. Stanfield, K. H. Roux, J. W. Kelly, P. M. Rudd, R. A. Dwek, H. Katinger, D. R. Burton, and I. A. Wilson**. 2003. Antibody domain exchange is an immunological solution to carbohydrate cluster recognition. Science **300**:2065-2071.
29. **Cameron, P. U., P. S. Freudenthal, J. M. Barker, S. Gezelter, K. Inaba, and R. M. Steinman**. 1992. Dendritic cells exposed to human immunodeficiency virus type-1 transmit a vigorous cytopathic infection to CD4+ T cells. Science **257**:383-387.
30. **Cameron, P. U., M. G. Lowe, S. M. Crowe, U. O'Doherty, M. Pope, S. Gezelter, and R. M. Steinman**. 1994. Susceptibility of dendritic cells to HIV-1 infection *in vitro*. J. Leukoc. Biol. **56**:257-265.
31. **Canque, B., Y. Bakri, S. Camus, M. Yagello, A. Benjouad, and J. C. Gluckman**. 1999. The susceptibility to X4 and R5 human immunodeficiency virus-1 strains of dendritic cells derived *in vitro* from CD34(+) hematopoietic progenitor cells is primarily determined by their maturation stage. Blood **93**:3866-3875.
32. **Cao, J., L. Bergeron, E. Helseth, M. Thali, H. Repke, and J. Sodroski**. 1993. Effects of amino-acid changes in the extracellular domain of the human immunodeficiency virus type 1 gp41 envelope glycoprotein. J. Virol. **67**:2747-2755.
33. **Cao, J., N. Sullivan, E. Desjardin, C. Parolin, J. Robinson, R. Wyatt, and J. Sodroski**. 1997. Replication and neutralization of human immunodeficiency virus type 1 lacking the V1 and V2 variable loops of the gp120 envelope glycoprotein. J. Virol. **71**:9808-9812.

34. **Cardosa, M. J., J. S. Porterfield, and S. Gordon**. 1983. Complement receptor mediates enhanced flavivirus replication in macrophages. J. Exp. Med. **158**:258-263.
35. **Chakrabarti, B. K., W. P. Kong, B. Y. Wu, Z. Y. Yang, J. Friborg, X. Ling, S. R. King, D. C. Montefiori, and G. J. Nabel**. 2002. Modifications of the human immunodeficiency virus envelope glycoprotein enhance immunogenicity for genetic immunization. J. Virol. **76**:5357-5368.
36. **Chan, D. C., D. Fass, J. M. Berger, and P. S. Kim**. 1997. Core structure of gp41 from the HIV envelope glycoprotein. Cell **89**:263-273.
37. **Chen, S. S.** 1994. Functional role of the zipper motif region of human immunodeficiency virus type 1 transmembrane protein gp41. J. Virol. **68**:2002-2010.
38. **Chen, S. S., C. N. Lee, W. R. Lee, K. McIntosh, and T. H. Lee**. 1993. Mutational analysis of the leucine zipper-like motif of the human immunodeficiency virus type 1 envelope transmembrane glycoprotein. J. Virol. **67**:3615-3619.
39. **Cho, M. W., Y. B. Kim, M. K. Lee, K. C. Gupta, W. Ross, R. Plishka, A. Buckler-White, T. Igarashi, T. Theodore, R. Byrum, C. Kemp, D. C. Montefiori, and M. A. Martin**. 2001. Polyvalent envelope glycoprotein vaccine elicits a broader neutralizing antibody response but is unable to provide sterilizing protection against heterologous simian/human immunodeficiency virus infection in pigtailed macaques. J. Virol. **75**:2224-2234.
40. **Choe, H., M. Farzan, Y. Sun, N. Sullivan, B. Rollins, P. D. Ponath, L. Wu, C. R. Mackay, G. LaRosa, W. Newman, N. Gerard, C. Gerard, and J. Sodroski**. 1996. The β-chemokine receptors CCR3 and CCR5 facilitate infection by primary HIV-1 isolates. Cell **85**:1135-1148.
41. **Choe, H., W. Li, P. L. Wright, N. Vasilieva, M. Venturi, C. C. Huang, C. Grundner, T. Dorfman, M. B. Zwick, L. Wang, E. S. Rosenberg, P. D. Kwong, D. R. Burton, J. E. Robinson, J. G. Sodroski, and M. Farzan**. 2003. Tyrosine sulfation of human antibodies contributes to recognition of the CCR5 binding region of HIV-1 gp120. Cell **114**:161-170.
42. **Chow, Y. H., O. L. Wei, S. Phogat, I. A. Sidorov, T. R. Fouts, C. C. Broder, and D. S. Dimitrov**. 2002. Conserved structures exposed in HIV-1 envelope glycoproteins stabilized by flexible linkers as potent entry inhibitors and potential immunogens. Biochemistry **41**:7176-7182.
43. **Clavel, F.** 1987. HIV-2, the West African AIDS virus (editorial review). AIDS **1**:135-140.
44. **Clavel, F., D. Guétard, F. Brun-Vézinet, S. Chamaret, M.-A. Rey, M. O. Santos-Ferreira, A. G. Laurent, C. Dauguet, C. Katlama, C. Rouzioux, D. Klatzmann, J. L. Champalimaud, and L. Montagnier**. 1986. Isolation of a new human retrovirus from West African patients with AIDS. Science **233**:343-346.
45. **Coffin, J. M.** 1990. Retroviridae and their replication, p. 1437-1500. *In* B. N. Fields and D. M. Knipe (eds.), Virology. Raven Press, New York, N.Y.
46. **Colman, P. M. and M. C. Lawrence**. 2003. The structural biology of type I viral membrane fusion. Nat. Rev. Mol. Cell Biol. **4**:309-319.
47. **Connor, R. I., K. E. Sheridan, D. Ceradini, S. Choe, and N. R. Landau**. 1997. Change in coreceptor use correlates with disease progression in HIV-1-infected individuals. J. Exp. Med. **185**:621-628.
48. **Corbitt, G., A. S. Bailey, and G. Williams**. 1990. HIV infection in Manchester, 1959. Lancet **336**:51.
49. **Cormier, E. G. and T. Dragic**. 2002. The crown and stem of the V3 loop play distinct roles in human immunodeficiency virus type 1 envelope glycoprotein interactions with the CCR5 coreceptor. J. Virol. **76**:8953-8957.
50. **Cullen, B. R.** 1998. HIV-1 auxiliary proteins: making connections in a dying cell. Cell **93**:685-692.
51. **De Jong, J.-J., J. Goudsmit, W. Keulen, B. Klaver, W. Krone, M. Tersmette, and A. de Ronde**. 1992. Human immunodeficiency virus type 1 clones chimeric for the envelope V3 domain differ in syncytium formation and replication capacity. J. Virol. **66**:757-765.
52. **De Jong, J.-J., A. Ronde de, W. Keulen, M. Tersmette, and J. Goudsmit**. 1992. Minimal requirements for the human immunodeficiency virus type 1 V3 domain to support the syncytium-inducing (SI) phenotype: analysis by single amino-acid substitution. J. Virol. **66**:6777-6780.
53. **Deng, H., R. Liu, W. Ellmeier, S. Choe, D. Unutmaz, M. Burkhart, P. Di Marzio, S. Marmon, R. E. Sutton, C. M. Hill, C. B. Davis, S. Peiper, T. J. Schall, D. R. Littman, and N. R. Landau**. 1996. Identification of a major co-receptor for primary isolates of HIV-1. Nature **381**:661-666.

54. **Doms, R. W. and J. P. Moore**. 2000. HIV-1 membrane fusion: targets of opportunity. J. Cell Biol. **151**:F9-14.
55. **Doranz, B. J., J. F. Berson, J. Rucker, and R. W. Doms**. 1997. Chemokine receptors as fusion cofactors for human immunodeficiency virus type 1 (HIV-1). Immunol. Res. **16**:15-28.
56. **Doranz, B. J., J. Rucker, Y. Yi, R. J. Smyth, M. Samson, S. Peiper, M. Parmentier, R. G. Collman, and R. W. Doms**. 1996. A dual-tropic primary HIV-1 isolate that uses fusin and the beta-chemokinereceptors CKR-5, CKR-3, and CKR-2beta as fusion cofactors. Cell **85**:1149-1158.
57. **Douek, D. C., J. M. Brenchley, M. R. Betts, D. R. Ambrozak, B. J. Hill, Y. Okamoto, J. P. Casazza, J. Kuruppu, K. Kunstman, S. Wolinsky, Z. Grossman, M. Dybul, A. Oxenius, D. A. Price, M. Connors, and R. A. Koup**. 2002. HIV preferentially infects HIV-specific CD4+ T cells. Nature **417**:95-98.
58. **Dragic, T., V. Litwin, G. P. Allaway, S. R. Martin, Y. Huang, K. A. Nagashima, C. Cayanan, P. J. Maddon, R. A. Koup, J. P. Moore, and W. A. Paxton**. 1996. HIV-1 entry into CD4+ cells is mediated by the chemokine receptor CC-CKR5. Nature **381**:667-673.
59. **Earl, P. L., C. C. Broder, R. W. Doms, and B. Moss**. 1997. Epitope map of human immunodeficiency virus type 1 gp41 derived from 47 monoclonal antibodies produced by immunization with oligomeric envelope protein. J. Virol. **71**:2674-2684.
60. **Earl, P. L., C. C. Broder, D. Long, S. A. Lee, J. Peterson, S. Chakrabarti, R. W. Doms, and B. Moss**. 1994. Native oligomeric human immunodeficiency virus type 1 envelope glycoprotein elicits diverse monoclonal antibody reactivities. J. Virol. **68**:3015-3026.
61. **Earl, P. L., B. Moss, and R. W. Doms**. 1991. Folding, interaction with GRP78-BiP, assembly, and transport of the human immunodeficiency virus type 1 envelope protein. J. Virol. **65**:2047-2055.
62. **Earl, P. L., W. Sugiura, D. C. Montefiori, C. C. Broder, S. A. Lee, C. Wild, J. Lifson, and B. Moss**. 2001. Immunogenicity and protective efficacy of oligomeric human immunodeficiency virus type 1 gp140. J. Virol. **75**:645-653.
63. **Eckert, D. M. and P. S. Kim**. 2001. Mechanisms of viral membrane fusion and its inhibition. Annu. Rev. Biochem. **70**:777-810.
64. **Egberink, H. and M. C. Horzinek**. 1992. Animal immunodeficiency viruses. Vet. Microbiol. **33**:311-331.
65. **Esposito, D. and R. Craigie**. 1999. HIV integrase structure and function. Adv. Virus Res. **52**:319-333.
66. **Farzan, M., H. Choe, E. Desjardins, Y. Sun, J. Kuhn, J. Cao, D. Archambault, P. Kolchinsky, M. Koch, R. Wyatt, and J. Sodroski**. 1998. Stabilization of human immunodeficiency virus type 1 envelope glycoprotein trimers by disulfide bonds introduced into the gp41 glycoprotein ectodomain. J. Virol. **72**:7620-7625.
67. **Feinberg, H., D. A. Mitchell, K. Drickamer, and W. I. Weis**. 2001. Structural basis for selective recognition of oligosaccharides by DC-SIGN and DC-SIGNR. Science **294**:2163-2166.
68. **Fouts, T., K. Godfrey, K. Bobb, D. Montefiori, C. V. Hanson, V. S. Kalyanaraman, A. DeVico, and R. Pal**. 2002. Crosslinked HIV-1 envelope-CD4 receptor complexes elicit broadly cross-reactive neutralizing antibodies in rhesus macaques. Proc. Natl. Acad. Sci. USA **99**:11842-11847.
69. **Fouts, T. R., J. M. Binley, A. Trkola, J. E. Robinson, and J. P. Moore**. 1997. Neutralization of the human immunodeficiency virus type 1 primary isolate JR-FL by human monoclonal antibodies correlates with antibody binding to the oligomeric form of the envelope glycoprotein complex. J. Virol **71**:2779-2785.
70. **Fouts, T. R., R. Tuskan, K. Godfrey, M. Reitz, D. Hone, G. K. Lewis, and A. L. DeVico**. 2000. Expression and characterization of a single-chain polypeptide analogue of the human immunodeficiency virus type 1 gp120-CD4 receptor complex. J. Virol. **74**:11427-11436.
71. **Francis, D. P., W. L. Heyward, V. Popovic, P. Orozco-Cronin, K. Orelind, C. Gee, A. Hirsch, T. Ippolito, A. Luck, M. Longhi, V. Gulati, N. Winslow, M. Gurwith, F. Sinangil, and P. W. Berman**. 2003. Candidate HIV/AIDS vaccines: lessons learned from the World's first phase III efficacy trials. AIDS **17**:147-156.
72. **Frank, I., M. Piatak, Jr., H. Stoessel, N. Romani, D. Bonnyay, J. D. Lifson, and M. Pope**. 2002. Infectious and whole inactivated simian immunodeficiency viruses interact similarly with primate dendritic cells (DCs): differential intracellular fate of virions in mature and immature DCs. J. Virol. **76**:2936-2951.

73. **Freed, E. O.** 2001. HIV-1 replication. Somat.Cell Mol. Genet. **26**:13-33.
74. **Freed, E. O., D. J. Myers, and R. Risser**. 1990. Characterization of the fusion domain of the human immunodeficiency virus type 1 envelope glycoprotein gp41. Proc. Natl. Acad. Sci. USA **87**:4650-4654.
75. **Funke, I., A. Hahn, E. P. Rieber, E. Weiss, and G. Riethmuller**. 1987. The cellular receptor (CD4) of the human immunodeficiency virus is expressed on neurons and glial cells in human brain. J. Exp. Med. **165**:1230-1235.
76. **Gallo, R. C., S. Z. Salahuddin, M. Popovic, G. M. Shearer, M. Kaplan, B. F. Haynes, T. J. Palker, R. Redfield, J. Oleske, B. Safai, G. White, P. Foster, and P. D. Markham**. 1984. Frequent detection and isolation of cytopathic retroviruses (HTLV-III) from patients with AIDS and at risk for AIDS. Science **224**:500-503.
77. **Gallo, S. A., C. M. Finnegan, M. Viard, Y. Raviv, A. Dimitrov, S. S. Rawat, A. Puri, S. Durell, and R. Blumenthal**. 2003. The HIV Env-mediated fusion reaction. Biochim. Biophys. Acta **1614**:36-50.
78. **Gallo, S. A., A. Puri, and R. Blumenthal**. 2001. HIV-1 gp41 six-helix bundle formation occurs rapidly after the engagement of gp120 by CXCR4 in the HIV-1 Env-mediated fusion process. Biochemistry **40**:12231-12236.
79. **Gao, F., E. Bailes, D. L. Robertson, Y. Chen, C. M. Rodenburg, S. F. Michael, L. B. Cummins, L. O. Arthur, M. Peeters, G. M. Shaw, P. M. Sharp, and B. H. Hahn**. 1999. Origin of HIV-1 in the chimpanzee Pan troglodytes troglodytes. Nature **397**:436-441.
80. **Gaschen, B., J. Taylor, K. Yusim, B. Foley, F. Gao, D. Lang, V. Novitsky, B. Haynes, B. H. Hahn, T. Bhattacharya, and B. Korber**. 2002. Diversity considerations in HIV-1 vaccine selection. Science **296**:2354-2360.
81. **Geijtenbeek, T. B., D. S. Kwon, R. Torensma, S. J. van Vliet, G. C. van Duijnhoven, J. Middel, I. L. Cornelissen, H. S. Nottet, V. N. KewalRamani, D. R. Littman, C. G. Figdor, and Y. van Kooyk**. 2000. DC-SIGN, a dendritic cell-specific HIV-1-binding protein that enhances trans-infection of T cells. Cell **100**:587-597.
82. **Gonda, M. A., M. J. Braun, J. E. Clements, J. M. Pyper, F. Wong-Staal, R. C. Gallo, and R. V. Gilden**. 1986. Human T-cell lymphotropic virus type III shares sequence homology with a family of pathogenic lentiviruses. Proc. Natl. Acad. Sci. USA **83**:4007-4011.
83. **Gonda, M. A., F. Wong-Staal, R. C. Gallo, J. E. Clements, O. Narayan, and R. V. Gilden**. 1985. Sequence homology and morphologic similarity of HTLV-III and visna virus, a pathogenic lentivirus. Science **227**:173-177.
84. **Gorny, M. K. and S. Zolla-Pazner**. 2000. Recognition by human monoclonal antibodies of free and complexed peptides representing the prefusogenic and fusogenic forms of human immunodeficiency virus type 1 gp41. J. Virol. **74**:6186-6192.
85. **Gottlieb, M. S., R. Schroff, H. M. Schanker, J. D. Weisman, P. T. Fan, R. A. Wolf, and A. Saxon**. 1981. Pneumocystis carinii pneumonia and mucosal candidiasis in previously healthy homosexual men: evidence of a new acquired cellular immunodeficiency. N. Engl. J. Med. **305**:1425-1431.
86. **Goudsmit, J.** 1997. Viral sex. Oxford University Press, New York.
87. **Goudsmit, J., C. A. Boucher, R. H. Meloen, L. G. Epstein, L. Smit, H. L. van Der, and M. Bakker**. 1988. Human antibody response to a strain-specific HIV-1 gp120 epitope associated with cell fusion inhibition. AIDS **2**:157-164.
88. **Goudsmit, J., C. Debouck, R. H. Meloen, L. Smit, M. Bakker, D. M. Asher, A. V. Wolff, C. J. Gibbs, Jr., and D. C. Gajdusek**. 1988. Human immunodeficiency virus type 1 neutralization epitope with conserved architecture elicits early type-specific antibodies in experimentally infected chimpanzees. Proc. Natl. Acad. Sci. USA **85**:4478-4482.
89. **Granelli-Piperno, A., E. Delgado, V. Finkel, W. Paxton, and R. M. Steinman**. 1998. Immature dendritic cells selectively replicate macrophagetropic (M-tropic) human immunodeficiency virus type 1, while mature cells efficiently transmit both M- and T-tropic virus to T cells. J. Virol. **72**:2733-2737.
90. **Guillon, C., M. Schutten, P. H. Boers, R. A. Gruters, and A. D. Osterhaus**. 2002. Antibody-mediated enhancement of human immunodeficiency virus type 1 infectivity is determined by the structure of gp120 and depends on modulation of the gp120-CCR5 interaction. J. Virol. **76**:2827-2834.

91. **He, J., Y. Chen, M. Farzan, H. Choe, A. Ohagen, S. Gartner, J. Busciglio, X. Yang, W. Hofmann, W. Newman, C. R. Mackay, J. Sodroski, and D. Gabuzda**. 1997. CCR3 and CCR5 are co-receptors for HIV-1 infection of microglia. Nature **385**:645-649.
92. **Helseth, E., U. Olshevsky, C. Furman, and J. Sodroski**. 1991. Human immunodeficiency virus type 1 gp120 envelope glycoprotein regions important for association with the gp41 transmembrane glycoprotein. J. Virol. **65**:2119-2123.
93. **Herrera, C., C. Spenlehauer, M. S. Fung, D. R. Burton, S. Beddows, and J. P. Moore**. 2003. Nonneutralizing antibodies to the CD4-binding site on the gp120 subunit of human immunodeficiency virus type 1 do not interfere with the activity of a neutralizing antibody against the same site. J. Virol. **77**:1084-1091.
94. **Hofmann-Lehmann, R., J. Vlasak, R. A. Rasmussen, B. A. Smith, T. W. Baba, V. Liska, F. Ferrantelli, D. C. Montefiori, H. M. McClure, D. C. Anderson, B. J. Bernacky, T. A. Rizvi, R. Schmidt, L. R. Hill, M. E. Keeling, H. Katinger, G. Stiegler, L. A. Cavacini, M. R. Posner, T. C. Chou, J. Andersen, and R. M. Ruprecht**. 2001. Postnatal passive immunization of neonatal macaques with a triple combination of human monoclonal antibodies against oral simian-human immunodeficiency virus challenge. J. Virol. **75**:7470-7480.
95. **Hong, P. W., K. B. Flummerfelt, A. de Parseval, K. Gurney, J. H. Elder, and B. Lee**. 2002. Human immunodeficiency virus envelope (gp120) binding to DC-SIGN and primary dendritic cells is carbohydrate dependent but does not involve 2G12 or cyanovirin binding sites: implications for structural analyses of gp120-DC-SIGN binding. J. Virol. **76**:12855-12865.
96. **Hooper, E. and W. D. Hamilton**. 1996. 1959 Manchester case of syndrome resembling AIDS. Lancet **348**:1363-1365.
97. **Hu, J., M. B. Gardner, and C. J. Miller**. 2000. Simian immunodeficiency virus rapidly penetrates the cervicovaginal mucosa after intravaginal inoculation and infects intraepithelial dendritic cells. J. Virol. **74**:6087-6095.
98. **Hu, Q., J. O. Trent, G. D. Tomaras, Z. Wang, J. L. Murray, S. M. Conolly, J. M. Navenot, A. P. Barry, M. L. Greenberg, and S. C. Peiper**. 2000. Identification of ENV determinants in V3 that influence the molecular anatomy of CCR5 utilization. J. Mol. Biol. **302**:359-375.
99. **Huang, Y., W. A. Paxton, S. M. Wolinsky, A. U. Neumann, L. Zhang, T. He, S. Kang, D. Ceradini, Z. Jin, K. Yazdanbakhsh, K. Kunstman, D. Erickson, E. Dragon, N. R. Landau, J. Phair, D. D. Ho, and R. A. Koup**. 1996. The role of a mutant CCR5 allele in HIV-1 transmission and disease progression. Nat. Med. **2**:1240-1243.
100. **Hunter, E.** 1997. gp41, a multifunctional protein involved in HIV entry and pathogenesis, p. III-55-III-73. *In* B. Korber, B. Hahn, B. Foley, J. W. Mellors, T. Leitner, G. Myers, F. McCutchan, and C. L. Kuiken (eds.), Human Retroviruses and AIDS 1997. Theoretical Biology and Biophysics Group, Los Alamos National Laboratory, Los Alamos, NM.
101. **Hunter, E.** 1997. Viral entry and receptors, p. 71-119. *In* J. M. Coffin, S. H. Hughes, and H. E. Varmus (eds.), Cold Spring Harbor Laboratory Press, New York.
102. **Hymes, K. B., T. Cheung, J. B. Greene, N. S. Prose, A. Marcus, H. Ballard, D. C. William, and L. J. Laubenstein**. 1981. Kaposi's sarcoma in homosexual men-a report of eight cases. Lancet **2**:598-600.
103. **Jeffs, S. A., C. Shotton, P. Balfe, and J. A. McKeating**. 2002. Truncated gp120 envelope glycoprotein of human immunodeficiency virus 1 elicits a broadly reactive neutralizing immune response. J. Gen. Virol. **83**:2723-2732.
104. **Johnson, W. E., J. Morgan, J. Reitter, B. A. Puffer, S. Czajak, R. W. Doms, and R. C. Desrosiers**. 2002. A replication-competent, neutralization-sensitive variant of simian immunodeficiency virus lacking 100 amino-acids of envelope. J. Virol. **76**:2075-2086.
105. **Joyce, J. G., W. M. Hurni, M. J. Bogusky, V. M. Garsky, X. Liang, M. P. Citron, R. C. Danzeisen, M. D. Miller, J. W. Shiver, and P. M. Keller**. 2002. Enhancement of alpha -helicity in the HIV-1 inhibitory peptide DP178 leads to an increased affinity for human monoclonal antibody 2F5 but does not elicit neutralizing responses *in vitro*. Implications for vaccine design. J. Biol. Chem. **277**:45811-45820.
106. **Karlas, J. A., K. H. Siebelink, M. A. Peer, W. Huisman, A. M. Cuisinier, G. F. Rimmelzwaan, and A. D. Osterhaus**. 1999. Vaccination with experimental feline immunodeficiency virus vaccines, based on autologous infected cells, elicits enhancement of homologous challenge infection. J. Gen. Virol. **80 (Pt 3)**:761-765.

107. **Karlas, J. A., K. H. Siebelink, M. A. Peer, W. Huisman, G. F. Rimmelzwaan, and A. D. Osterhaus**. 1998. Accelerated viraemia in cats vaccinated with fixed autologous FIV-infected cells. Vet. Immunol. Immunopathol. **65**:353-365.
108. **Kawahara, M., K. Matsuo, T. Nakasone, T. Hiroi, H. Kiyono, S. Matsumoto, T. Yamada, N. Yamamoto, and M. Honda**. 2002. Combined intrarectal/intradermal inoculation of recombinant Mycobacterium bovis bacillus Calmette-Guerin (BCG) induces enhanced immune responses against the inserted HIV-1 V3 antigen. Vaccine **21**:158-166.
109. **Kawamura, T., S. S. Cohen, D. L. Borris, E. A. Aquilino, S. Glushakova, L. B. Margolis, J. M. Orenstein, R. E. Offord, A. R. Neurath, and A. Blauvelt**. 2000. Candidate microbicides block HIV-1 infection of human immature Langerhans cells within epithelial tissue explants. J. Exp. Med. **192**:1491-1500.
110. **Klatzmann, D., F. Barre-Sinoussi, M. T. Nugeyre, C. Danquet, E. Vilmer, C. Griscelli, F. Brun-Veziret, C. Rouzioux, J. C. Gluckman, J. C. Chermann, and et al.** 1984. Selective tropism of lymphadenopathy associated virus for helper-inducer T lymphocytes. Science **225**:59-63.
111. **Klatzmann, D., E. Champagne, and S. Chamaret**. 1984. T-lymphocyte T4 molecule behaves as the receptor for human retrovirus LAV. Nature **312**:767-768.
112. **Kliks, S. C., A. Nisalak, W. E. Brandt, L. Wahl, and D. S. Burke**. 1989. Antibody-dependent enhancement of dengue virus growth in human monocytes as a risk factor for dengue hemorrhagic fever. Am. J. Trop. Med. Hyg. **40**:444-451.
113. **Knarr, G., S. Modrow, A. Todd, M. J. Gething, and J. Buchner**. 1999. BiP-binding sequences in HIV gp160. Implications for the binding specificity of bip. J. Biol. Chem. **274**:29850-29857.
114. **Koch, M., M. Pancera, P. D. Kwong, P. Kolchinsky, C. Grundner, L. Wang, W. A. Hendrickson, J. Sodroski, and R. Wyatt**. 2003. Structure-based, targeted deglycosylation of HIV-1 gp120 and effects on neutralization sensitivity and antibody recognition. Virology **313**:387-400.
115. **Koot, M., I. P. M. Keet, A. H. V. Vos, R. E. Y. de Goede, M. Th. L. Roos, R. A. Coutinho, F. Miedema, P. Th. A. Schellekens, and M. Tersmette**. 1993. Prognostic value of human immunodeficiency virus type 1 biological phenotype for rate of CD4+ cell depletion and progression to AIDS. Ann. Int. Med. **118**:681-688.
116. **Korber, B., M. Muldoon, J. Theiler, F. Gao, R. Gupta, A. Lapedes, B. H. Hahn, S. Wolinsky, and T. Bhattacharya**. 2000. Timing the ancestor of the HIV-1 pandemic strains. Science **288**:1789-1796.
117. **Kunert, R., F. Ruker, and H. Katinger**. 1998. Molecular characterization of five neutralizing anti-HIV type 1 antibodies: identification of nonconventional D segments in the human monoclonal antibodies 2G12 and 2F5. AIDS Res. Hum. Retroviruses **14**:1115-1128.
118. **Kwon, D. S., G. Gregorio, N. Bitton, W. A. Hendrickson, and D. R. Littman**. 2002. DC-SIGN-mediated internalization of HIV is required for trans-enhancement of T cell infection. Immunity **16**:135-144.
119. **Kwong, P. D., M. L. Doyle, D. J. Casper, C. Cicala, S. A. Leavitt, S. Majeed, T. D. Steenbeke, M. Venturi, I. Chaiken, M. Fung, H. Katinger, P. W. Parren, J. Robinson, D. Van Ryk, L. Wang, D. R. Burton, E. Freire, R. Wyatt, J. Sodroski, W. A. Hendrickson, and J. Arthos**. 2002. HIV-1 evades antibody-mediated neutralization through conformational masking of receptor-binding sites. Nature **420**:678-682.
120. **Kwong, P. D., R. Wyatt, E. Desjardins, J. Robinson, J. S. Culp, B. D. Hellmig, R. W. Sweet, J. Sodroski, and W. A. Hendrickson**. 1999. Probability analysis of variational crystallization and its application to gp120, the exterior envelope glycoprotein of type 1 human immunodeficiency virus (HIV-1). J. Biol. Chem. **274**:4115-4123.
121. **Kwong, P. D., R. Wyatt, S. Majeed, J. Robinson, R. W. Sweet, J. Sodroski, and W. A. Hendrickson**. 2000. Structures of HIV-1 gp120 envelope glycoproteins from laboratory- adapted and primary isolates. Struct. Fold. Des. **8**:1329-1339.
122. **Kwong, P. D., R. Wyatt, J. Robinson, R. W. Sweet, J. Sodroski, and W. A. Hendrickson**. 1998. Structure of an HIV gp120 envelope glycoprotein in a complex with the CD4 receptor and a neutralizing human antibody. Nature **393**:648-659.
123. **Labrijn, A. F., P. Poignard, A. Raja, M. B. Zwick, K. Delgado, M. Franti, J. Binley, V. Vivona, C. Grundner, C. C. Huang, M. Venturi, C. J. Petropoulos, T. Wrin, D. S. Dimitrov, J. Robinson, P. D. Kwong, R. T. Wyatt, J. Sodroski, and D. R. Burton**. 2003. Access of anti-

body molecules to the conserved coreceptor binding site on glycoprotein gp120 is sterically restricted on primary human immunodeficiency virus type 1. J. Virol. **77**:10557-10565.

124. **Land, A., D. Zonneveld, and I. Braakman**. 2003. Folding of HIV-1 envelope glycoprotein involves extensive isomerization of disulfide bonds and conformation-dependent leader peptide cleavage. FASEB J. **17**:1058-1067.
125. **Lee, S., K. Peden, D. S. Dimitrov, C. C. Broder, J. Manischewitz, G. Denisova, J. M. Gershoni, and H. Golding**. 1997. Enhancement of human immunodeficiency virus type 1 envelope-mediated fusion by a CD4-gp120 complex-specific monoclonal antibody. J. Virol. **71**:6037-6043.
126. **Leonard, C. K., M. W. Spellman, L. Riddle, R. J. Harris, J. N. Thomas, and T. J. Gregory**. 1990. Assignment of intrachain disulfide bonds and characterization of potential glycosylation sites of the type 1 recombinant human immunodeficiency virus envelope glycoprotein (gp120) expressed in chinese hamster ovary cells. J. Biol. Chem. **265(18)**:10373-10382.
127. **Letvin, N. L., D. C. Montefiori, Y. Yasutomi, H. C. Perry, M. E. Davies, C. Lekutis, M. Alroy, D. C. Freed, C. I. Lord, L. K. Handt, M. A. Liu, and J. W. Shiver**. 1997. Potent, protective anti-HIV immune responses generated by bimodal HIV envelope DNA plus protein vaccination. Proc. Natl. Acad. Sci. USA **94**:9378-9383.
128. **Leulliot, N. and G. Varani**. 2001. Current topics in RNA-protein recognition: control of specificity and biological function through induced fit and conformational capture. Biochemistry **40**:7947-7956.
129. **Li, H., Z. Q. Liu, J. Ding, and Y. H. Chen**. 2002. Recombinant multi-epitope vaccine induce predefined epitope-specific antibodies against HIV-1. Immunol. Lett. **84**:153-157.
130. **Liu, R., W. A. Paxton, S. Choe, D. Ceradini, S. R. Martin, R. Horuk, M. E. MacDonald, H. Stuhlmann, R. A. Koup, and N. R. Landau**. 1996. Homozygous defect in HIV-1 coreceptor accounts for resistance of some multiply-exposed individuals to HIV-1 infection. Cell **86**:367-377.
131. **Lu, S., R. Wyatt, J. F. Richmond, F. Mustafa, S. Wang, J. Weng, D. C. Montefiori, J. Sodroski, and H. L. Robinson**. 1998. Immunogenicity of DNA vaccines expressing human immunodeficiency virus type 1 envelope glycoprotein with and without deletions in the V1/2 and V3 regions. AIDS Res. Hum. Retroviruses **14**:151-155.
132. **Luciw, P.** 1996. Human Immunodeficiency Viruses and their replication, *In* B. N. Fields, D. M. Knipe, and P. M. Howley (eds.), Virology. Lippincott-Raven Publishers, Philadelphia, New York.
133. **Maddon, P. J., A. G. Dalgleish, J. S. McDougal, P. R. Clapham, R. A. Weiss, and R. Axel**. 1986. The T4 gene encodes the AIDS virus receptor and is expressed in the immune system and the brain. Cell **47**:333-348.
134. **Maerz, A. L., H. E. Drummer, K. A. Wilson, and P. Poumbourios**. 2001. Functional analysis of the disulfide bond-bonded loop/chain reversal region of human immunodeficiency virus type 1 gp41 reveals a critical role in gp120-gp41 association. J. Virol. **75**:6635-6644.
135. **Mantis, N. J., P. A. Kozlowski, D. W. Mielcarz, W. Weissenhorn, and M. R. Neutra**. 2001. Immunization of mice with recombinant gp41 in a systemic prime/mucosal boost protocol induces HIV-1-specific serum IgG and secretory IgA antibodies. Vaccine **19**:3990-4001.
136. **Markosyan, R. M., F. S. Cohen, and G. B. Melikyan**. 2003. HIV-1 envelope proteins complete their folding into six-helix bundles immediately after fusion pore formation. Mol. Biol. Cell **14**:926-938.
137. **Mascola, J. R., M. G. Lewis, G. Stiegler, D. Harris, T. C. VanCott, D. Hayes, M. K. Louder, C. R. Brown, C. V. Sapan, S. S. Frankel, Y. Lu, M. L. Robb, H. Katinger, and D. L. Birx**. 1999. Protection of Macaques against pathogenic simian/human immunodeficiency virus 89.6PD by passive transfer of neutralizing antibodies. J. Virol. **73**:4009-4018.
138. **Mascola, J. R., G. Stiegler, T. C. VanCott, H. Katinger, C. B. Carpenter, C. E. Hanson, H. Beary, D. Hayes, S. S. Frankel, D. L. Birx, and M. G. Lewis**. 2000. Protection of macaques against vaginal transmission of a pathogenic HIV-1/SIV chimeric virus by passive infusion of neutralizing antibodies. Nat. Med. **6**:207-210.
139. **Masur, H., M. A. Michelis, J. B. Greene, I. Onorato, R. A. Stouwe, R. S. Holzman, G. Wormser, L. Brettman, M. Lange, H. W. Murray, and S. Cunningham-Rundles**. 1981. An outbreak of community-acquired Pneumocystis carinii pneumonia: initial manifestation of cel-

lular immune dysfunction. N. Engl. J. Med. **305**:1431-1438.
140. **McDonald, D., L. Wu, S. M. Bohks, V. N. KewalRamani, D. Unutmaz, and T. J. Hope**. 2003. Recruitment of HIV and its receptors to dendritic cell-T cell junctions. Science **300**:1295-1297.
141. **McKeating, J. A., C. Shotton, S. Jeffs, C. Palmer, A. Hammond, J. Lewis, K. Oliver, J. May, and P. Balfe**. 1996. Immunogenicity of full length and truncated forms of the human immunodeficiency virus type I envelope glycoprotein. Immunol. Lett. **51**:101-105.
142. **Melikyan, G. B., R. M. Markosyan, H. Hemmati, M. K. Delmedico, D. M. Lambert, and F. S. Cohen**. 2000. Evidence that the transition of HIV-1 gp41 into a six-helix bundle, not the bundle configuration, induces membrane fusion. J. Cell Biol. **151**:413-423.
143. **Mitchell, D. A., A. J. Fadden, and K. Drickamer**. 2001. A novel mechanism of carbohydrate recognition by the C-type lectins DC-SIGN and DC-SIGNR. Subunit organization and binding to multivalent ligands. J. Biol. Chem. **276**:28939-28945.
144. **Modrow, S., B. H. Hahn, G. M. Shaw, R. C. Gallo, F. Wong-Staal, and H. Wolf**. 1987. Computer-assisted analysis of envelope protein sequences of seven human immunodeficiency virus isolates: prediction of antigenic epitopes in conserved and variable regions. J. Virol. **61,2**:570-578.
145. **Moore, J. P. and R. W. Doms**. 2003. The entry of entry inhibitors: A fusion of science and medicine. Proc. Natl. Acad. Sci. USA **100**:10598-10602.
146. **Moore, J. P., P. W. H. I. Parren, and D. R. Burton**. 2001. Genetic subtypes, humoral immunity, and human immunodeficiency virus type 1 vaccine development. J. Virol. **75**:5721-5729.
147. **Moore, J. P. and J. Sodroski**. 1996. Antibody cross-competition analysis of the human immunodeficiency virus type 1 gp120 exterior envelope glycoprotein. J. Virol. **70**:1863-1872.
148. **Moulard, M. and E. Decroly**. 2000. Maturation of HIV envelope glycoprotein precursors by cellular endoproteases. Biochim. Biophys. Acta **1469**:121-132.
149. **Muster, T., R. Guinea, A. Trkola, M. Purtscher, A. Klima, F. Steindl, P. Palese, and H. Katinger**. 1994. Cross-neutralizing activity against divergent human immunodeficiency virus type 1 isolates induced by the gp41 sequence ELDKWAS. J. Virol. **68**:4031-4034.
150. **Muster, T., F. Steindl, M. Purtscher, A. Trkola, A. Klima, G. Himmler, F. Ruker, and H. Katinger**. 1993. A conserved neutralizing epitope on gp41 of human immunodeficiency virus type 1. J. Virol. **67**:6642-6647.
151. **Myszka, D. G., R. W. Sweet, P. Hensley, M. Brigham-Burke, P. D. Kwong, W. A. Hendrickson, R. Wyatt, J. Sodroski, and M. L. Doyle**. 2000. Energetics of the HIV gp120-CD4 binding reaction. Proc. Natl. Acad. Sci. USA **97**:9026-9031.
152. **Nagashima, K. A., D. A. Thompson, S. I. Rosenfield, P. J. Maddon, T. Dragic, and W. C. Olson**. 2001. Human immunodeficiency virus type 1 entry inhibitors PRO 542 and T-20 are potently synergistic in blocking virus-cell and cell-cell fusion. J. Infect. Dis. **183**:1121-1125.
153. **Olofsson, S. and J. E. Hansen**. 1998. Host cell glycosylation of viral glycoproteins—a battlefield for host defence and viral resistance. Scand. J. Infect. Dis. **30**:435-440.
154. **Osterhaus, A. D., E. Tijhaar, R. C. Huisman, W. Huisman, I. H. Darby, M. J. Francis, G. F. Rimmelzwaan, and K. H. Siebelink**. 1996. Accelerated viremia in cats vaccinated with recombinant vaccinia virus expressing envelope glycoprotein of feline immunodeficiency virus. AIDS Res. Hum. Retroviruses **12**:437-441.
155. **Ostrowski, M. A., S. J. Justement, A. Catanzaro, C. A. Hallahan, L. A. Ehler, S. B. Mizell, P. N. Kumar, J. A. Mican, T. W. Chun, and A. S. Fauci**. 1998. Expression of chemokine receptors CXCR4 and CCR5 in HIV-1-infected and uninfected individuals. J. Immunol. **161**:3195-3201.
156. **Otteken, A., P. L. Earl, and B. Moss**. 1996. Folding, assembly, and intracellular trafficking of the human immunodeficiency virus type 1 envelope glycoprotein analyzed with monoclonal antibodies recognizing maturational intermediates. J. Virol. **70**:3407-3415.
157. **Pantophlet, R., S. E. Ollmann, P. Poignard, P. W. Parren, I. A. Wilson, and D. R. Burton**. 2003. Fine mapping of the interaction of neutralizing and nonneutralizing monoclonal antibodies with the CD4 binding site of human immunodeficiency virus type 1 gp120. J. Virol. **77**:642-658.
158. **Pantophlet, R., I. A. Wilson, and D. R. Burton**. 2003. Hyperglycosylated mutants of human immunodeficiency virus (HIV) type 1 monomeric gp120 as novel antigens for HIV vaccine design. J. Virol. **77**:5889-5901.

159. **Park, E. J., M. K. Gorny, S. Zolla-Pazner, and G. V. Quinnan, Jr.** 2000. A global neutralization resistance phenotype of human immunodeficiency virus type 1 is determined by distinct mechanisms mediating enhanced infectivity and conformational change of the envelope complex. J. Virol. **74**:4183-4191.
160. **Parker, C. E., L. J. Deterding, C. Hager-Braun, J. M. Binley, N. Schulke, H. Katinger, J. P. Moore, and K. B. Tomer**. 2001. Fine definition of the epitope on the gp41 glycoprotein of human immunodeficiency virus type 1 for the neutralizing monoclonal antibody 2F5. J. Virol. **75**:10906-10911.
161. **Parren, P. W., D. R. Burton, and Q. J. Sattentau**. 1997. HIV-1 antibody—debris or virion? Nat. Med. **3**:366-367.
162. **Parren, P. W., H. J. Ditzel, R. J. Gulizia, J. M. Binley, C. F. Barbas, III, D. R. Burton, and D. E. Mosier**. 1995. Protection against HIV-1 infection in hu-PBL-SCID mice by passive immunization with a neutralizing human monoclonal antibody against the gp120 CD4-binding site. AIDS **9**:F1-F6.
163. **Parren, P. W., M. C. Gauduin, R. A. Koup, P. Poignard, P. Fisicaro, D. R. Burton, and Q. J. Sattentau**. 1997. Relevance of the antibody response against human immunodeficiency virus type 1 envelope to vaccine design. Immunol. Lett. **57**:105-112.
164. **Parren, P. W., P. A. Marx, A. J. Hessell, A. Luckay, J. Harouse, C. Cheng-Mayer, J. P. Moore, and D. R. Burton**. 2001. Antibody protects macaques against vaginal challenge with a pathogenic R5 simian/human immunodeficiency virus at serum levels giving complete neutralization *in vitro*. J. Virol. **75**:8340-8347.
165. **Parren, P. W. H. I., J. P. Moore, D. R. Burton, and Q. J. Sattentau**. 1999. The neutralizing antibody response to HIV-1: viral evasion and escape from humoral immunity. AIDS **13 (Suppl. A)**:S137-S162.
166. **Patterson, S., A. Rae, N. Hockey, J. Gilmour, and F. Gotch**. 2001. Plasmacytoid dendritic cells are highly susceptible to human immunodeficiency virus type 1 infection and release infectious virus. J. Virol. **75**:6710-6713.
167. **Paxton, W. A., S. R. Martin, D. Tse, T. R. O'Brien, J. Skurnick, N. L. VanDevanter, N. Padian, J. F. Braun, D. P. Kotler, S. M. Wolinsky, and R. A. Koup**. 1996. Relative resistance to HIV-1 infection of CD4 lymphocytes from persons who remain uninfected despite multiple high-risk sexual exposure. Nat. Med **2**:412-417.
168. **Perrin, L., L. Kaiser, and S. Yerly**. 2003. Travel and the spread of HIV-1 genetic variants. Lancet Infect. Dis. **3**:22-27.
169. **Platt, E. J., K. Wehrly, S. E. Kuhmann, B. Chesebro, and D. Kabat**. 1998. Effects of CCR5 and CD4 cell surface concentrations on infections by macrophagetropic isolates of human immunodeficiency virus type 1. J. Virol. **72**:2855-2864.
170. **Pohlmann, S., F. Baribaud, B. Lee, G. J. Leslie, M. D. Sanchez, K. Hiebenthal-Millow, J. Munch, F. Kirchhoff, and R. W. Doms**. 2001. DC-SIGN interactions with human immunodeficiency virus type 1 and 2 and simian immunodeficiency virus. J. Virol. **75**:4664-4672.
171. **Poignard, P., M. Moulard, E. Golez, V. Vivona, M. Franti, S. Venturini, M. Wang, P. W. Parren, and D. R. Burton**. 2003. Heterogeneity of envelope molecules expressed on primary human immunodeficiency virus type 1 particles as probed by the binding of neutralizing and nonneutralizing antibodies. J. Virol. **77**:353-365.
172. **Poignard, P., E. O. Saphire, P. W. Parren, and D. R. Burton**. 2001. gp120: Biologic aspects of structural features. Annu. Rev. Immunol. **19**:253-274.
173. **Pollakis, G., S. Kang, A. Kliphuis, M. I. Chalaby, J. Goudsmit, and W. A. Paxton**. 2001. N-linked glycosylation of the HIV type-1 gp120 envelope glycoprotein as a major determinant of CCR5 and CXCR4 coreceptor utilization. J. Biol. Chem. **276**:13433-13441.
174. **Pope, M., S. Gezelter, N. Gallo, L. Hoffman, and R. M. Steinman**. 1995. Low levels of HIV-1 infection in cutaneous dendritic cells promote extensive viral replication upon binding to memory CD4+ T cells. J. Exp. Med. **182**:2045-2056.
175. **Poumbourios, P., A. L. Maerz, and H. E. Drummer**. 2003. Functional evolution of the HIV-1 envelope glycoprotein gp120-association site of gp41. J. Biol. Chem. **278**: 42149-42160.
176. **Ratner, L., W. Haseltine, R. Patarca, K. J. Livak, B. Starcich, S. F. Josephs, E. R. Doran, J. A. Rafalski, E. A. Whitehorn, K. Baumeister, L. Ivanoff, S. R. Petteway, Jr., M. L. Pearson, J. A. Lautenberger, T. S. Papas, J. Ghrayeb, N. T. Chang, R. C. Gallo, and F. Wong-Staal**.

1985. Complete nucleotide sequence of the AIDS virus, HTLV-III. Nature **313**:277-284.

177. **Reece, J. C., A. J. Handley, E. J. Anstee, W. A. Morrison, S. M. Crowe, and P. U. Cameron**. 1998. HIV-1 selection by epidermal dendritic cells during transmission across human skin. J. Exp. Med. **187**:1623-1631.
178. **Reeves, J. D., S. A. Gallo, N. Ahmad, J. L. Miamidian, P. E. Harvey, M. Sharron, S. Pohlmann, J. N. Sfakianos, C. A. Derdeyn, R. Blumenthal, E. Hunter, and R. W. Doms**. 2002. Sensitivity of HIV-1 to entry inhibitors correlates with envelope/coreceptor affinity, receptor density, and fusion kinetics. Proc. Natl. Acad. Sci. USA **99**:16249-16254.
179. **Reitter, J. N., R. E. Means, and R. C. Desrosiers**. 1998. A role for carbohydrates in immune evasion in AIDS. Nat. Med. **4**:679-684.
180. **Reitz, M. S., Jr., C. Wilson, C. Naugle, R. C. Gallo, and M. Robert-Guroff**. 1988. Generation of a neutralization-resistant variant of HIV-1 is due to selection for a point mutation in the envelope gene. Cell **54**:57-63.
181. **Richardson, T. M., B. L. Stryjewski, C. C. Broder, J. A. Hoxie, J. R. Mascola, P. L. Earl, and R. W. Doms**. 1996. Humoral response to oligomeric HIV-1 envelope protein. J. Virol. **70**:753-762.
182. **Richman, D. D., T. Wrin, S. J. Little, and C. J. Petropoulos**. 2003. Rapid evolution of the neutralizing antibody response to HIV type 1 infection. Proc. Natl. Acad. Sci. USA **100**:4144-4149.
183. **Rizzuto, C. D., R. Wyatt, N. Hernandez-Ramos, Y. Sun, P. D. Kwong, W. A. Hendrickson, and J. Sodroski**. 1998. A conserved HIV gp120 glycoprotein structure involved in chemokine receptor binding. Science **280**:1949-1953.
184. **Robinson, W. E., Jr., T. Kawamura, M. K. Gorny, D. lake, J. Y. Xu, Y. Matsumoto, T. Sugano, Y. Masuho, W. M. Mitchell, E. Hersh, and S. Zolla-Pazner**. 1990. Human monoclonal antibodies to the human immunodeficiency virus type 1 (HIV-1) transmembrane glycoprotein gp41 enhance HIV-1 infection *in vitro*. Proc. Natl. Acad. Sci. USA **87**:3185-3189.
185. **Rowland-Jones, S. L.** 1999. HIV: The deadly passenger in dendritic cells. Curr. Biol. **9**:R248-R250.
186. **Rubbert, A., C. Combadiere, M. Ostrowski, J. Arthos, M. Dybul, E. Machado, M. A. Cohn, J. A. Hoxie, P. M. Murphy, A. S. Fauci, and D. Weissman**. 1998. Dendritic cells express multiple chemokine receptors used as coreceptors for HIV entry. J. Immunol. **160**:3933-3941.
187. **Ruiz, M. E., C. Cicala, J. Arthos, A. Kinter, A. T. Catanzaro, J. Adelsberger, K. L. Holmes, O. J. Cohen, and A. S. Fauci**. 1998. Peripheral blood-derived CD34+ progenitor cells: CXC chemokine receptor 4 and CC chemokine receptor 5 expression and infection by HIV. J. Immunol. **161**:4169-4176.
188. **Sakurai, H., R. A. Williamson, J. E. Crowe, J. A. Beeler, P. Poignard, R. B. Bastidas, R. M. Chanock, and D. R. Burton**. 1999. Human antibody responses to mature and immature forms of viral envelope in respiratory syncytial virus infection: significance for subunit vaccines. J. Virol. **73**:2956-2962.
189. **Sanchez-Pescador, R., M. D. Power, P. J. Barr, K. S. Steimer, M. M. Stempien, S. L. Brown-Shimer, W. W. Gee, A. Renard, A. Randolph, J. A. Levy, D. Dina, and P. A. Luciw**. 1985. Nucleotide sequence and expression of an AIDS-associated retrovirus (ARV-2). Science **227**:484-492.
190. **Sanders, R. W., E. C. de Jong, C. E. Baldwin, J. H. Schuitemaker, M. L. Kapsenberg, and B. Berkhout**. 2002. Differential transmission of human immunodeficiency virus type 1 by distinct subsets of effector dendritic cells. J. Virol. **76**:7812-7821.
191. **Sanders, R. W., B. Korber, M. Lu, B. Berkhout, and J. P. Moore**. 2002. Mutational analyses and natural variablility of the gp41 ectodomain, p. 43-68. *In* C. Kuiken, B. Foley, E. Freed, B. Hahn, P. Marx, F. McCutchan, J. Mellors, S. Wolinsky, and B. Korber (eds.), HIV Sequence compendium 2002. Los Alamos National Laboratory, Theoretical Biology and Biophysics Group, Los Alamos, New Mexico.
192. **Sanders, R. W., L. Schiffner, A. Master, F. Kajumo, Y. Guo, T. Dragic, J. P. Moore, and J. M. Binley**. 2000. Variable-loop-deleted variants of the human immunodeficiency virus type 1 envelope glycoprotein can be stabilized by an intermolecular disulfide bond between the gp120 and gp41 subunits. J. Virol. **74**:5091-5100.
193. **Sanders, R. W., M. Venturi, L. Schiffner, R. Kalyanaraman, H. Katinger, K. O. Lloyd, P. D. Kwong, and J. P. Moore**. 2002. The mannose-dependent epitope for neutralizing antibody 2G12

on human immunodeficiency virus type 1 glycoprotein gp120. J. Virol. **76**:7293-7305.

194. **Sanders, R. W., M. Vesanen, N. Schuelke, A. Master, L. Schiffner, R. Kalyanaraman, M. Paluch, B. Berkhout, P. J. Maddon, W. C. Olson, M. Lu, and J. P. Moore**. 2002. Stabilization of the soluble, cleaved, trimeric form of the envelope glycoprotein complex of human immunodeficiency virus type 1. J. Virol. **76**:8875-8889.
195. **Saphire, E. O., P. W. Parren, R. Pantophlet, M. B. Zwick, G. M. Morris, P. M. Rudd, R. A. Dwek, R. L. Stanfield, D. R. Burton, and I. A. Wilson**. 2001. Crystal structure of a neutralizing human IgG against HIV-1: a template for vaccine design. Science **293**:1155-1159.
196. **Sattentau, Q. J. and J. P. Moore**. 1995. Human immunodeficiency virus type 1 neutralization is determined by epitope exposure on the gp120 oligomer. J. Exp. Med. **182**:185-196.
197. **Scanlan, C. N., R. Pantophlet, M. R. Wormald, S. E. Ollmann, R. Stanfield, I. A. Wilson, H. Katinger, R. A. Dwek, P. M. Rudd, and D. R. Burton**. 2002. The broadly neutralizing antihuman immunodeficiency virus type 1 antibody 2G12 recognizes a cluster of alpha1—>2 mannose residues on the outer face of gp120. J. Virol **76**:7306-7321.
198. **Schuitemaker, H., N. A. Kootstra, R. E. de Goede, F. de Wolf, F. Miedema, and M. Tersmette**. 1991. Monocytotropic human immunodeficiency virus type 1 (HIV-1) variants detectable in all stages of HIV-1 infection lack T-cell line tropism and syncytium-inducing ability in primary T-cell culture. J. Virol **65**:356-363.
199. **Schulke, N., M. S. Vesanen, R. W. Sanders, P. Zhu, M. Lu, D. J. Anselma, A. R. Villa, P. W. Parren, J. M. Binley, K. H. Roux, P. J. Maddon, J. P. Moore, and W. C. Olson**. 2002. Oligomeric and conformational properties of a proteolytically mature, disulfide bond-stabilized human immunodeficiency virus type 1 gp140 envelope glycoprotein. J. Virol. **76**:7760-7776.
200. **Schultz, A. M. and J. A. Bradac**. 2001. The HIV vaccine pipeline, from preclinical to phase III. AIDS **15 Suppl 5**:S147-S158.
201. **Schulz, T. F., B. A. Jameson, L. Lopalco, A. G. Siccardi, R. A. Weiss, and J. P. Moore**. 1992. Conserved structural features in the interaction between retroviral surface and transmembrane glycoproteins? AIDS Res. Hum. Retroviruses **8**:1571-1580.
202. **Sharon, M., N. Kessler, R. Levy, S. Zolla-Pazner, M. Gorlach, and J. Anglister**. 2003. Alternative conformations of HIV-1 V3 loops mimic beta hairpins in chemokines, suggesting a mechanism for coreceptor selectivity. Structure (Camb.) **11**:225-236.
203. **Sharp, P. M., E. Bailes, R. R. Chaudhuri, C. M. Rodenburg, M. O. Santiago, and B. H. Hahn**. 2001. The origins of acquired immune deficiency syndrome viruses: where and when? Philos. Trans. R. Soc. Lond. B. Biol. Sci. **356**:867-876.
204. **Siebelink, K. H., E. Tijhaar, R. C. Huisman, W. Huisman, A. de Ronde, I. H. Darby, M. J. Francis, G. F. Rimmelzwaan, and A. D. Osterhaus**. 1995. Enhancement of feline immunodeficiency virus infection after immunization with envelope glycoprotein subunit vaccines. J. Virol. **69**:3704-3711.
205. **Siegal, F. P., C. Lopez, G. S. Hammer, A. E. Brown, S. J. Kornfeld, J. Gold, J. Hassett, S. Z. Hirschman, C. Cunningham-Rundles, and B. R. Adelsberg.** 1981. Severe acquired immunodeficiency in male homosexuals, manifested by chronic perianal ulcerative herpes simplex lesions. N. Engl. J. Med. **305**:1439-1444.
206. **Simmonds, G., D. Wilkinson, J. D. Reeves, M. T. Dittmar, S. Beddows, J. Weber, G. Carnegie, U. Desselberger, P. W. Gray, R. A. Weiss, and P. R. Clapham**. 1996. Primary, syncytium-inducing human immunodeficiency virus type 1 isolates are dual-tropic and most can use either Lestr or CCR5 as coreceptors for virus entry. J. Virol. **70**:8355-8360.
207. **Srivastava, I. K., L. Stamatatos, E. Kan, M. Vajdy, Y. Lian, S. Hilt, L. Martin, C. Vita, P. Zhu, K. H. Roux, L. Vojtech, C. Montefiori, J. Donnelly, J. B. Ulmer, and S. W. Barnett**. 2003. Purification, characterization, and immunogenicity of a soluble trimeric envelope protein containing a partial deletion of the V2 loop derived from SF162, an R5-tropic human immunodeficiency virus type 1 isolate. J. Virol. **77**:11244-11259.
208. **Stahl-Hennig, C., R. M. Steinman, K. Tenner-Racz, M. Pope, N. Stolte, K. Matz-Rensing, G. Grobschupff, B. Raschdorff, G. Hunsmann, and P. Racz**. 1999. Rapid infection of oral mucosal-associated lymphoid tissue with simian immunodeficiency virus. Science **285**:1261-1265.
209. **Stamatatos, L., M. Wiskerchen, and C. Cheng-Mayer**. 1998. Effect of major deletions in the V1 and V2 loops of a macrophage-tropic HIV type 1 isolate on viral envelope structure, cell

entry, and replication. AIDS Res. Hum. Retroviruses **14**:1129-1139.
210. **Stanfield, R., E. Cabezas, A. Satterthwait, E. Stura, A. Profy, and I. Wilson**. 1999. Dual conformations for the HIV-1 gp120 V3 loop in complexes with different neutralizing fabs. Structure. Fold. Des. **7**:131-142.
211. **Stein, B. S. and E. G. Engleman**. 1990. Intracellular processing of the gp160 HIV-1 envelope precursor. J. Biol. Chem. **265**:2640-2649.
212. **Steinman, R. M. and K. Inaba**. 1999. Myeloid dendritic cells. J. Leukoc. Biol. **66**:205-208.
213. **Stern, T. L., M. S. Reitz, Jr., and M. Robert-Guroff**. 1995. Spontaneous reversion of human immunodeficiency virus type 1 neutralization-resistant variant HXB2thr582: *in vitro* selection against cytopathicity highlights gp120-gp41 interactive regions. J. Virol. **69**:1860-1867.
214. **Stiegler, G., R. Kunert, M. Purtscher, S. Wolbank, R. Voglauer, F. Steindl, and H. Katinger**. 2001. A potent cross-clade neutralizing human monoclonal antibody against a novel epitope on gp41 of human immunodeficiency virus type 1. AIDS Res. Hum. Retroviruses **17**:1757-1765.
215. **Swanstrom, R. and J. W. Wills**. 1997. Synthesis, assembly, and processing of viral proteins, p. 263-334. *In* J. M. Coffin, S. H. Hughes, and H. E. Varmus (eds.), Retroviruses. Cold Spring Harbor Laboratory press, Plainview, New York.
216. **Tan, K., J. Liu, J. Wang, S. Shen, and M. Lu**. 1997. Atomic structure of a thermostable subdomain of HIV-1 gp41. Proc. Natl. Acad. Sci. USA **94**:12303-12308.
217. **Tang, H., K. L. Kuhen, and F. Wong-Staal**. 1999. Lentivirus replication and regulation. Annu. Rev. Genet. **33**:133-170.
218. **Taniguchi, Y., S. Zolla-Pazner, Y. Xu, X. Zhang, S. Takeda, and T. Hattori**. 2000. Human monoclonal antibody 98-6 reacts with the fusogenic form of gp41. Virology **273**:333-340.
219. **Telesnitsky, A. and S. P. Goff**. 1997. Reverse Transcriptase and the generation of retroviral DNA, p. 121-160. *In* J. M. Coffin, S. H. Hughes, and H. E. Varmus (eds.), Retroviruses. New York: Cold Spring Harbor Laboratory Press.
220. **Tremblay, C. L., F. Giguel, C. Kollmann, Y. Guan, T. C. Chou, B. M. Baroudy, and M. S. Hirsch**. 2002. Anti-human immunodeficiency virus interactions of SCH-C (SCH 351125), a CCR5 antagonist, with other antiretroviral agents *in vitro*. Antimicrob. Agents Chemother. **46**:1336-1339.
221. **Tremblay, C. L., C. Kollmann, F. Giguel, T. C. Chou, and M. S. Hirsch**. 2000. Strong *in vitro* synergy between the fusion inhibitor T-20 and the CXCR4 blocker AMD-3100. J. Acquir. Immune. Defic. Syndr. **25**:99-102.
222. **Trkola, A., T. Dragic, J. Arthos, J. M. Binley, W. C. Olson, G. P. Allaway, C. Cheng-Mayer, J. Robinson, P. J. Maddon, and J. P. Moore**. 1996. CD4-dependent, antibody-sensitive interactions between HIV-1 and its co-receptor CCR-5. Nature **384**:184-187.
223. **Trkola, A., M. Purtscher, T. Muster, C. Ballaun, A. Buchacher, N. Sullivan, K. Srinivasan, J. Sodroski, J. P. Moore, and H. Katinger**. 1996. Human monoclonal antibody 2G12 defines a distinctive neutralization epitope on the gp120 glycoprotein of human immunodeficiency virus type 1. J. Virol. **70**:1100-1108.
224. **Trono, D.** 1995. HIV accessory proteins: leading roles for the supporting cast. Cell **82**:189-192.
225. **Turville, S. G., P. U. Cameron, A. Handley, G. Lin, S. Pohlmann, R. W. Doms, and A. L. Cunningham**. 2002. Diversity of receptors binding HIV on dendritic cell subsets. Nat. Immunol. **3**:975-983.
226. **van Rij, R. P., H. Blaak, J. A. Visser, M. Brouwer, R. Rientsma, S. Broersen, A. M. Roda Husman, and H. Schuitemaker**. 2000. Differential coreceptor expression allows for independent evolution of non-syncytium-inducing and syncytium-inducing HIV-1. J. Clin. Invest. **106**:1039-1052.
227. **van't Wout, A. B., N. A. Kootstra, G. A. Mulder-Kampinga, N. Albrecht-van Lent, H. J. Scherpbier, J. Veenstra, K. Boer, R. A. Coutinho, F. Miedema, and H. Schuitemaker**. 1994. Macrophage-tropic variants initiate human immunodeficiency virus type 1 infection after sexual, parenteral, and vertical transmission. J. Clin. Invest. **94**:2060-2067.
228. **Veazey, R. S., R. J. Shattock, M. Pope, J. C. Kirijan, J. Jones, Q. Hu, T. Ketas, P. A. Marx, P. J. Klasse, D. R. Burton, and J. P. Moore**. 2003. Prevention of virus transmission to macaque monkeys by a vaginally applied monoclonal antibody to HIV-1 gp120. Nat. Med. **9**:343-346.
229. **Verrier, F., A. M. Borman, D. Brand, and M. Girard**. 1999. Role of the HIV type 1 glycoprotein 120 V3 loop in determining coreceptor usage. AIDS Res. Hum. Retroviruses **15**:731-743.

230. **Vogt, V. M.** 1997. Retroviral virions and genomes, p. 27-69. *In* J. M. Coffin, S. H. Hughes, and H. E. Varmus (eds.), Retroviruses. Cold Spring Harbor Laboratory Press, New York.
231. **Wain-Hobson, S., P. Sonigo, O. Danos, S. Cole, and M. Alizon**. 1985. Nucleotide sequence of the AIDS virus, LAV. Cell **40**:9-17.
232. **Wei, X., J. M. Decker, S. Wang, H. Hui, J. C. Kappes, X. Wu, J. F. Salazar-Gonzalez, M. G. Salazar, J. M. Kilby, M. S. Saag, N. L. Komarova, M. A. Nowak, B. H. Hahn, P. D. Kwong, and G. M. Shaw**. 2003. Antibody neutralization and escape by HIV-1. Nature **422**:307-312.
233. **Weissenhorn, W., A. Dessen, S. C. Harrison, J. J. Skehel, and D. C. Wiley**. 1997. Atomic structure of the ectodomain from HIV-1 gp41. Nature **387**:426-430.
234. **Weissman, D., Y. Li, J. Ananworanich, L. J. Zhou, J. Adelsberger, T. F. Tedder, M. Baseler, and A. S. Fauci**. 1995. Three populations of cells with dendritic morphology exist in peripheral blood, only one of which is infectable with human immunodeficiency virus type 1. Proc. Natl. Acad. Sci.USA **92**:826-830.
235. **Wild, C., J. W. Dubay, T. Greenwell, T. Baird, Jr., T. G. Oas, C. McDanal, E. Hunter, and T. Matthews**. 1994. Propensity for a leucine zipper-like domain of human immunodeficiency virus type 1 gp41 to form oligomers correlates with a role in virus- induced fusion rather than assembly of the glycoprotein complex. Proc. Natl. Acad. Sci. USA **91**:12676-12680.
236. **Williams, G., T. B. Stretton, and J. C. Leonard**. 1983. AIDS in 1959? Lancet **2**:1136.
237. **Wu, L., N. P. Gerard, R. Wyatt, H. Choe, C. Parolin, N. Ruffing, A. Borsetti, A. A. Cardoso, E. Desjardin, W. Newman, C. Gerard, and J. Sodroski**. 1996. CD4-induced interaction of primary HIV-1 gp120 glycoproteins with the chemokine receptor CCR-5. Nature **384**:179-183.
238. **Wyatt, R., E. Desjardin, U. Olshevsky, C. Nixon, J. Binley, V. Olshevsky, and J. Sodroski**. 1997. Analysis of the interaction of the human immunodeficiency virus type 1 gp120 envelope glycoprotein with the gp41 transmembrane glycoprotein. J. Virol. **71**:9722-9731.
239. **Wyatt, R., P. D. Kwong, E. Desjardins, R. W. Sweet, J. Robinson, W. A. Hendrickson, and J. G. Sodroski**. 1998. The antigenic structure of the HIV gp120 envelope glycoprotein. Nature **393**:705-711.
240. **Wyatt, R., J. Moore, M. Accola, E. Desjardin, J. Robinson, and J. Sodroski**. 1995. Involvement of the V1/V2 variable loop structure in the exposure of human immunodeficiency virus type 1 gp120 epitopes induced by receptor binding. J. Virol. **69**:5723-5733.
241. **Wyatt, R. and J. Sodroski**. 1998. The HIV-1 envelope glycoproteins: fusogens, antigens, and immunogens. Science **280**:1884-1888.
242. **Xiang, S. H., P. D. Kwong, R. Gupta, C. D. Rizzuto, D. J. Casper, R. Wyatt, L. Wang, W. A. Hendrickson, M. L. Doyle, and J. Sodroski**. 2002. Mutagenic stabilization and/or disruption of a CD4-bound state reveals distinct conformations of the human immunodeficiency virus type 1 gp120 envelope glycoprotein. J. Virol. **76**:9888-9899.
243. **Xiao, Y., Y. Zhao, Y. Lu, and Y. H. Chen**. 2000. Epitope-vaccine induces high levels of ELDKWA-epitope-specific neutralizing antibody. Immunol. Invest. **29**:41-50.
244. **Xu, J. Y., M. K. Gorny, T. Palker, S. Karwowska, and S. Zolla-Pazner**. 1991. Epitope mapping of two immunodominant domains of gp41, the transmembrane protein of human immunodeficiency virus type 1, using ten human monoclonal antibodies. J. Virol. **65**:4832-4838.
245. **Yang, X., M. Farzan, R. Wyatt, and J. Sodroski**. 2000. Characterization of stable, soluble trimers containing complete ectodomains of human immunodeficiency virus type 1 envelope glycoproteins. J. Virol. **74**:5716-5725.
246. **Yang, X., L. Florin, M. Farzan, P. Kolchinsky, P. D. Kwong, J. Sodroski, and R. Wyatt**. 2000. Modifications that stabilize human immunodeficiency virus envelope glycoprotein trimers in solution. J. Virol. **74**:4746-4754.
247. **Yang, X., J. Lee, E. M. Mahony, P. D. Kwong, R. Wyatt, and J. Sodroski**. 2002. Highly stable trimers formed by human immunodeficiency virus type 1 envelope glycoproteins fused with the trimeric motif of T4 bacteriophage fibritin. J. Virol. **76**:4634-4642.
248. **Yang, X., E. Mahony, G. H. Holm, A. Kassa, and J. Sodroski**. 2003. Role of the gp120 inner domain beta-sandwich in the interaction between the human immunodeficiency virus envelope glycoprotein subunits. Virology **313**:117-125.
249. **Yang, X., R. Wyatt, and J. Sodroski**. 2001. Improved elicitation of neutralizing antibodies against primary human immunodeficiency viruses by soluble stabilized envelope glycoprotein trimers. J. Virol. **75**:1165-1171.

250. **Zaitseva, A. and et al**. 1997. Expression and function of CCR5 and CXCR4 on human Langerhans cells and macrophages: implications for HIV primary infection. Nat. Med. **3**:1369-1375.
251. **Zhu, T., B. T. Korber, A. J. Nahmias, E. Hooper, P. M. Sharp, and D. D. Ho**. 1998. An african HIV-1 sequence from 1959 and implications for the origin of the epidemic. Nature **391**:594-597.
252. **Zhu, T., H. Mo, N. Wang, D. S. Nam, Y. Cao, R. A. Koup, and D. D. Ho**. 1993. Genotypic and phenotypic characterization of HIV-1 patients with primary infection. Science **261**:1179-1181.
253. **Zwart, G., L. Van der Hoek, N. K. T. Back, C. Ramautarsing, T. Wolfs, J.-J. De Jong, A. Ronde de, J. Goudsmit, H. Langedijk, and P. Nara**. 1991. Antigenicity and antigenic variation of the V3 neutralization domain on the envelope glycoprotein gp120 of HIV-1, p. 45-50. *In* R. M. Chanock, H. S. Ginsberg, F. Brown, and R. A. Lerner (eds.), Vaccines 91. Cold Spring Harbor Laboratory Press, New York.
254. **Zwick, M. B., A. F. Labrijn, M. Wang, C. Spenlehauer, E. O. Saphire, J. M. Binley, J. P. Moore, G. Stiegler, H. Katinger, D. R. Burton, and P. W. Parren**. 2001. Broadly neutralizing antibodies targeted to the membrane-proximal external region of human immunodeficiency virus type 1 glycoprotein gp41. J. Virol. **75**:10892-10905.

Chapter 2.1

Differential transmission of HIV-1 by distinct subsets of effector dendritic cells

(*Journal of Virology,* August 2002, p. 7812-7821)

Rogier W. Sanders[1], Esther C. de Jong[2,3], Christopher E. Baldwin[1], Joost H. N. Schuitemaker[2], Martien L. Kapsenberg[2,3], Ben Berkhout[1]

Dept. of Human Retrovirology
[2]Dept. of Cell Biology and Histology
[3]Dept. of Dermatology, Academic Medical Center, University of Amsterdam, the Netherlands

Dendritic cells (DC) support HIV-1 transmission by capture of the virus particle in the mucosa and subsequent transport to the draining lymph node, where HIV-1 is presented to $CD4^+$ Th-cells. Virus transmission involves a high affinity interaction of the DC-specific surface molecule DC-SIGN and the viral envelope glycoprotein gp120 and subsequent internalization of the virus, which remains infectious. The mechanism of viral transmission from DC to T cells is currently unknown. Sentinel immature DC (iDC) develop into Th1-promoting effector DC1 or Th2-promoting DC2, depending on the activation signals. We studied the ability of these effector DC subsets to support HIV-1 transmission *in vitro*. Compared with iDC, virus transmission is greatly upregulated for the DC1 subset, whereas DC2 cells are inactive. Increased transmission by DC1 correlates with increased expression of ICAM-1, and blocking studies confirm that ICAM-1 expression on DC is important for HIV transmission. The ICAM-1 – LFA-1 interaction is known to be important for immunological cross-talk between DC and T cells, and our results indicate that this cell – cell contact is exploited by HIV-1 for efficient transmission.

Introduction

Human immunodeficiency virus type 1 (HIV-1) infects human $CD4^+$ T cells via interactions between the viral envelope glycoprotein gp120 and the CD4 receptor and a chemokine coreceptor on the T cell (9). Sexual transmission of HIV-1 requires the help of dendritic cells (DC) to cross the mucosal barrier before infection of T cells can occur (19,23,33-35,41,43). DC residing in peripheral tissues are able to capture HIV-1 and to facilitate transport to a draining lymph node, which becomes the center of viral replication. Although HIV-1 can infect certain DC such as Langerhans cells (4,5,16,30,47), other DC specifically bind HIV-1 and present the virus particle to T cells without becoming infected themselves (2,3,14,16). The recently identified DC-specific receptor DC-SIGN (CD209) facilitates specific binding of HIV-1, HIV-2 and SIV through interaction with the

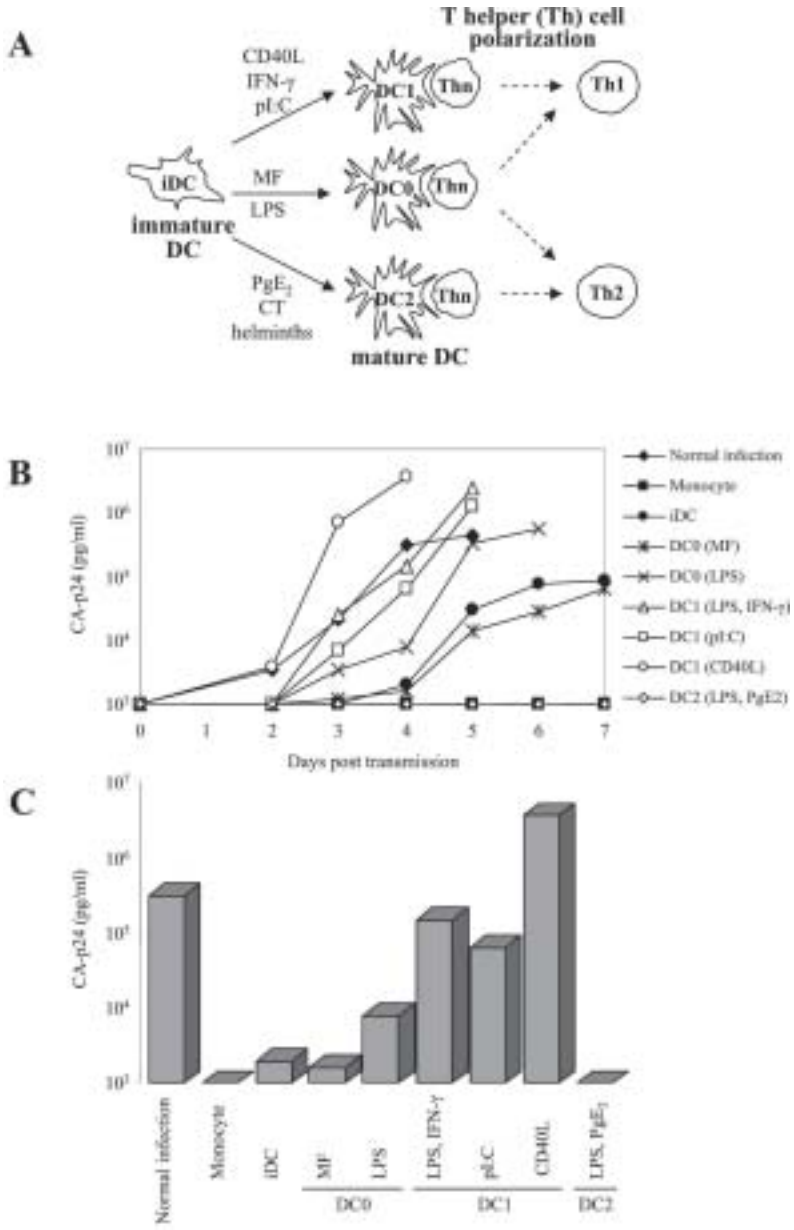

Fig. 1. Differential HIV-1 transmission by DC subsets. **A**. Maturation of iDC to obtain distinct subsets of mDC. Purified monocytes were cultured for 6 days in the presence of GM-CSF and IL-4 to obtain $CD1a^{+}CD14^{-}CD83^{-}$ iDC. These iDC were then cultured with diverse stimuli for two additional days to obtain $CD1a^{+}CD83^{+}$ mDC of the DC1, DC2 and DC0 type. The T helper (Th) cell polarizing capacities of the DC subsets are indicated. **B**. Replication of HIV-1 in T cells after transmission by different subsets of DC. In brief, 50 x 10^3 DC were pulsed with HIV-1 LAI (150 pg/well CA-p24) for two hours and unbound virus was washed out, except in the control experiment without DC (normal infection). DC were subsequently cocultured with 50 x 10^3 SupT1 T cells and virus spread in SupT1 cells after transmission was monitored for 7 days by CA-p24 production. **C**. The same data from day 4 in panel B are represented as bars. Similar results were obtained in more than 10 independent experiments.

viral envelope glycoprotein gp120 and mediates internalization of virions, which remain in an infectious form in an intracellular compartment (11,14,24,31)**.** The mechanism of subsequent virus transmission to T cells remains unknown.

DC are professional antigen presenting cells that take up antigen at sites of pathogen entry (1). Upon encounter with antigen, immature sentinel DC (iDC) develop into mature effector DC (mDC) that are specialized to stimulate naïve T cells. *In vitro* studies with monocyte-derived DC indicate that these effector DC express distinct molecules (20,21)**.** Depending on the type of pathogen and the micro-environment of the iDC, different subsets of effector DC develop that promote the development of Th1 cells or Th2 cells from naïve precursors. In this way, the type of T cell response is adapted to the type of invading pathogen and the source of infected tissue (21). These distinct subsets of effector DC bias the polarization of Th cells into Th1 cells (DC1), Th2 cells (DC2), or both (DC0) (8). The differential DC maturation is illustrated in Fig. 1A. Unbiased DC0 are obtained with maturation factors such as IL-1, TNF-α or lipopolysaccharides (LPS), and induce both IL-4-producing Th1 cells and IFN-producing Th2 cells (37), of which the balance varies with the cell donor and the antigen dose (36). The presence of IFN-γ, dsRNA (polyI:C) or viral RNA induces the development of DC into effector DC1, characterized by their capacity to promote Th1 responses in naïve T cells (6,40,44,46). DC2 can be induced by cholera toxin, helminths and prostraglandins, and these cells express high levels of OX40L that bias Th2 responses (10,13,22,48).

To study the ability of differentially matured DC to support HIV-1 transmission, we used an *in vitro* assay for DC-mediated HIV-1 infection of T cells. We found that the efficiency of virus transmission to T cells is largely influenced by the type of DC subset. The DC1 subset shows a markedly increased ability to mediate HIV-1 transmission compared to iDC, which correlates with increased surface expression of ICAM-1. Antibody blocking studies indicate that ICAM-1 plays an important role in transmission. The DC2 subset is very inefficient in HIV-1 transmission and the DC0 cells display an intermediate phenotype, similar to iDC. Our observations suggest that the DC1 subset with high ICAM-1 expression is a key player in HIV-1 transmission and that cell-cell contact between the DC and the T cell, mediated by ICAM-1 and LFA-1, is instrumental for efficient virus transmission.

Materials and Methods

Cytokines, antigens and reagents

Human rGM-CSF (500 U/ml) was a gift from Schering-Plough, Uden, The Netherlands. Human rIFN- (1000 U/ml) was a gift from Dr P.H. van der Meide (Biomedical Primate Research Center, Rijswijk, The Netherlands). Human rIL-2 was obtained from Chiron, Amsterdam, The Netherlands. Human rIL-4 (250 U/ml) and human rTNFα (50 ng/ml) were obtained from PBH (Hannover, Germany). Human rIL-1β (10 ng/ml) was obtained from Boehringer Mannheim (Mannheim, Germany). Prostraglandin E2 (PgE2), poly I:C (Sigma, St. Louis, MN) cholera toxin (CT; Sigma) were used at 10^{-6} M, 20 μg/ml and 1 μg/ml, respectively. Lipopolysaccharide (LPS) (Difco, Detroit, MI) was used at a final

concentration of 100 ng/ml. Superantigen *Staphylococcus aureus* enterotoxin B (SEB; Sigma Chemical Co., St. Louis, Mo) was used at a final concentration of 1 ng/ml. Stromal cell derived factor (SDF)-1 (R&D, Minneapolis, MN) was used at a final concentration of 2.0 μg/ml and azidothymidine (AZT) at 10 μM. Antibodies to ICAM-1,2,3 and LFA-1,2,3 were acquired from Immunotech, Marseille, France and used at a final concentration of 10 μg/ml for blocking experiments and 1 μg/ml for FACS staining. The anti-DC-SIGN antibody was a gift from Dr. Yvette van Kooyk, Nijmegen, The Netherlands.

In vitro generation of iDC from peripheral blood monocytes (PBMC) and subsequent maturation

Venous blood from healthy donors was collected by venipuncture in sodium-heparin containing tubes (VT100H; Venoject, Terumo Europe, Leuven, Belgium). PBMC were isolated by density centrifugation on Lymphoprep (Nycomed, Torshov, Norway). Subsequently, PBMC were layered on a Percoll (Pharmacia, Uppsala, Sweden) gradient with three density layers (1.076, 1.059 and 1.045 g/ml). The light fraction with predominantly monocytes was collected, washed and seeded in 24-well culture plates (Costar, Cambridge, MA) at a density of $5x10^5$ cells/well. After 60 min. at 37ºC, non-adherent cells were removed and adherent cells were cultured in Iscove's modified Dulbecco's medium (IMDM; Life Technologies Ltd., Paisley, UK) with gentamycin (86 μg/ml; Duchefa, Haarlem, The Netherlands) and 1% FCS (Hyclone, Logan, UT), and supplemented with GM-CSF and IL-4 to obtain iDC as described elsewhere (13). At day 3, the culture medium with supplements was refreshed. At day 6, $CD1a^+CD14^-$ iDC were treated with different reagents to initiate distinct maturation pathways.

Immature DC were treated either with maturation factors (rIL-1/rTNF-), CT, LPS or poly I:C, or a combination of LPS and PgE2 or IFN-γ. Maturation in response to CD40-ligand (CD40L) was obtained by stimulation of iDC with irradiated mouse fibroblast cells (J558 cells) stably expressing CD40L. After 48 hours, fully mature $CD1a^+$ (>95%) $CD83^+$ (>90%) mDC were obtained. The cytokine secretion profiles and Th-polarizing properties of different mDC will be described elsewhere. All subsequent tests were performed after harvesting and extensive washing of the cells to remove all induction factors.

Flow cytometry

Mouse anti-human mAbs against the following molecules were used: CD1a (OKT6; Ortho Diagnostic system, Beerse, Belgium), CD83 (Hb15a, IgG2b, Immunotech, Marseille, France), CD86 (IgG2a; Innogenetics, Ghent, Belgium), ICAM-1, ICAM-2, ICAM-3 (all three obtained from R&D systems, Abingdon, U.K.), CD4 (Becton Dickinson, San Jose, CA), CCR5, CXCR4 (both obtained from PharMingen, San Diego, CA), and DC-SIGN. Bound mAbs were detected by FITC-conjugated goat F(ab')2 anti-mouse IgG and IgM (Jackson Immunoresearch Laboratories Inc., West Grove, PA). Samples were analyzed on a FACScan (Becton Dickinson).

T cells

$CD4^+CD45RA^+CD45RO^-$ naïve Th cells (>98% pure as assessed by flow cytometry) were purified from peripheral blood lymphocytes (PBL; heterologous to DC) using a human $CD4^+/CD45RO^-$ column kit (R&D, Minneapolis, MN). Naïve T-cells, PBL and the SupT1 T-cell line were cultured in RPMI medium (Life Technologies Ltd., Paisley, UK) supplemented with 10% FCS, penicillin (100 U/ml), streptomycin (100 µg/ml) and for naïve T-cells and PBL we also added IL-2 (100 U/ml) and SEB.

Virus stocks

SupT1 T cells and C33A cervix carcinoma cells were transfected by electroporation and $CaPO_4$ precipitation, respectively, with 10 µg of the molecular clone of the T-tropic HIV-1 LAI strain as described previously (7). The virus containing supernatant was harvested 3 days post transfection, filtered and stored at -80ºC. The concentration of virus was measured by CA-p24 ELISA.

Mixed lymphocyte reaction

Mature DC where tested for their ability to stimulate allogeneic naïve T cells in a mixed lymphocyte reaction (MLR). $CD4^+$ $CD45RA^+$ $CD45RO^-$ Th cells (2.5 x 10^5/200 ml) were cocultured in 96-well flat-bottom culture plates with increasing numbers of different mDC. T cell proliferation was measured after 5 days by the thymidine incorporation assay. [^{3}H]-thymidine (0.3 mQ/well, Radiochemical Centre, Amersham, Little Chalfont, U.K.) was added to the culture for 16 hours and the sample was analyzed by liquid scintillation counting.

HIV capture by DC

Dendritic cells (150 x 10^3/100 µl/well) were incubated with a high virus dose (20 ng CA-p24) for 2 hours at 37ºC. Cells were washed extensively with PBS to remove unbound virus, and subsequently lysed to release the captured CA-p24, which was measured by ELISA.

HIV-1 transmission assay

A previously described transmission assay (14,32) was used with some modifications. In short, iDC or fully mature $CD83^+$ mDC were incubated on a 96 well plate (40 x 10^3 cells/100 µl/well) with virus (0.15 ng CA-p24 per well, unless indicated otherwise) for 2 hours in RPMI medium. We used the CXCR4-using primary virus isolate LAI. The DC were washed twice with PBS to remove unbound virus and cocultured with T cells (40 x 10^3/100µl/well) for 7 days in RPMI medium. Virus spread in T cells was measured by CA-p24 ELISA and the cultures were inspected for the appearance of HIV-syncytia. The CA-p24 values at day 4 post infection are shown for most experiments. In some experiments, DC were incubated with AZT, SDF-1, or anti-ICAM-1 antibodies during the virus pulse. These inhibitors were washed out together with unbound virus prior to coculture with T cells. Maturation of DC by CD40L was performed with irradiated mouse cells stably expressing CD40L (J558 cells). Because these cells are present in the transmission assay, we tested their ability to promote HIV-1 transmission. The irradiated mouse cells do not support HIV-1 transmission. To con-

trol for the presence of contaminating T cells and the presence of residual free virus after washing, we performed transmission experiments with the precursor Monocytes, which were consistently negative in transmission. In some experiments, T cells were added to virus-preincubated DC in a Transwell culture dish, such that both cell types were separated by a membrane. To test the effect of soluble DC-derived factors on HIV-1 transmission, we collected the supernatants of immature and differentially matured DC, which were activated with J558-CD40L for 24 hours. Supernatants were harvested, filtered and frozen at –20°C before use in the infection experiments.

Results

DC subsets differ significantly in their ability to transmit HIV-1

Monocyte-derived iDC were treated with different stimuli to generate distincts subsets of $CD83^+$ mDC. The different maturation pathways are illustrated in Fig. 1A, and the expression of the maturation marker CD83 is included in the FACS analysis of Fig. 3. The final state of maturation was confirmed by upregulation of CD80, CD86 and HLA-DR, downregulation of the mannose receptor, and the loss of phagocytotic capacity (results not shown). Based on their ability to induce the development of IFN-γ-producing Th1 or IL-4-producing Th2 cells from naïve precursors, the mDC were designated DC1 or DC2, and unbiased mDC were termed DC0. These effector phenotypes are stable over time. A detailed description of the DC subsets, their cytokine production profile and their T cell effector function is presented elsewhere (8). DC1 were generated either by IFN-γ treatment or by poly I:C stimulation. We also obtained cells with DC1-like properties by treatment of iDC with CD40-ligand (CD40L). Stimulation of iDC with CT or with LPS plus PgE2 resulted in two types of DC2 cells. The DC0 cells were induced with maturation factors IL-1β plus TNF-α or LPS. In this study, we analyzed the DC subsets for their ability to transmit HIV-1 to $CD4^+$ T cells.

We used a previously described transmission assay with some modifications (14,32). DC were incubated for 2 hours with the CXCR4-using primary HIV-1 isolate LAI, washed extensively to remove unbound virus and cocultured with SupT1 T cells for 7 days. Virus spread was measured in the culture supernatant by CA-p24 ELISA. The result of a representative transmission experiment with the different DC subsets is shown in Fig. 1, which represents the replication kinetics after transmission (Fig. 1B) and the CA-p24 values at day 4 (Fig. 1C). Consistent with previous results, iDC were able to transfer HIV-1 to T cells. Interestingly, we observed profound differences for the three classes of mDC. All DC1 samples displayed a dramatically increased HIV-1 transmission capacity compared to iDC. The DC1 transmission efficiency is comparable with direct infection of T cells without the wash to remove unbound virus. The DC2 cells were largely inactive, and the DC0 cells showed an intermediate transmission activity similar to that of iDC. Similar results were obtained with DC derived from different donors (table 1). To control for the presence of contaminating T cells and the presence of residual free virus after washing, we performed transmission experiments with the precursor monocytes, that were consistently negative in transmission, presumably because these cells lack DC-SIGN (15). DC in

Table 1. Virus transmission[a] by DC derived from different donors

	donor 1	donor 2	donor 3	donor 4	donor 5
iDC	240,000	7,800	2,000	22,000	14,600
DC0[b]	44,000	<1,000	1,600	6,500	nd[e]
DC1[c]	250,000	720,000	65,000	36,000	145,000
DC2[d]	6,400	<1,000	<1,000	3,500	1,800

[a] Virus spread in SupT1 (pg/ml CA-p24) after DC-mediated transmission
[b] MF treated
[c] pI:C treated, except for donor 4 (CD40L treated)
[d] MF, PgE2 treated
[e] Not determined

the absence of T cells did not support virus replication (results not shown).

We titrated the amount of HIV-1 in the transmission assay with the relatively inefficient transmitter iDC and the efficient transmitter DC1 (Fig. 2A). A virus dose of only 45 pg CA-p24 is sufficient for DC1 cells to initiate a spreading infection in T cells, but at least 30-fold more virus is needed with iDC as transmitter. In another experiment, we omitted the wash step that removes unbound virus (Fig. 2B). This experiment was performed with an extremely low virus dose (15 pg CA-p24) that is not sufficient to initiate a spreading infection of T cells in the absence of DC. T cell infection can be rescued with iDC, but the DC1 subset is again the most efficient virus transmitter. We further analyzed DC mediated transmission to primary T cells. The different effector DC display the same relative transmission efficiencies in a coculture with heterologous peripheral blood lymphocytes (PBL) (Fig. 2C). Experiments with purified naïve T cells produced similar results (Fig. 2D), indicating that DC1 cells are particularly suited for HIV-1 transmission.

To investigate whether differences in the induction of T cell proliferation by the DC subsets could account for the observed differences in virus spread in T cells, we performed mixed lymphocyte reactions (MLR). DC0, DC1 and DC2 subsets were incubated with naïve T cells and T cell proliferation was measured by [^{3}H]thymidine incorporation (Fig. 3A). Among the mDC subsets, we measured no significant difference in their capacity to induce T cell proliferation, supporting the idea that the DC subsets differ in their ability to transmit HIV-1. We also performed transmission experiments with a mixture of the efficiently transmitting iDC cells and the inactive DC2 cells (Fig. 3B). The presence of DC2 cells did not inhibit the efficient transmission obtained with iDC cells. This result confirms that the inability of DC2 cells to transmit virus is not due to inhibition of T cell proliferation. Instead, we reason that DC2 cells lack a factor that is critical for HIV-1 transmission.

Phenotypic analysis of DC subsets

We analyzed several DC surface markers to elucidate the mechanism underlying the profound differences in transmission efficiency. We thereby focused on molecules that are important in DC-HIV and DC-T cell interactions. The DC marker CD1a and DC-maturation markers CD83 and CD86 were included as controls.

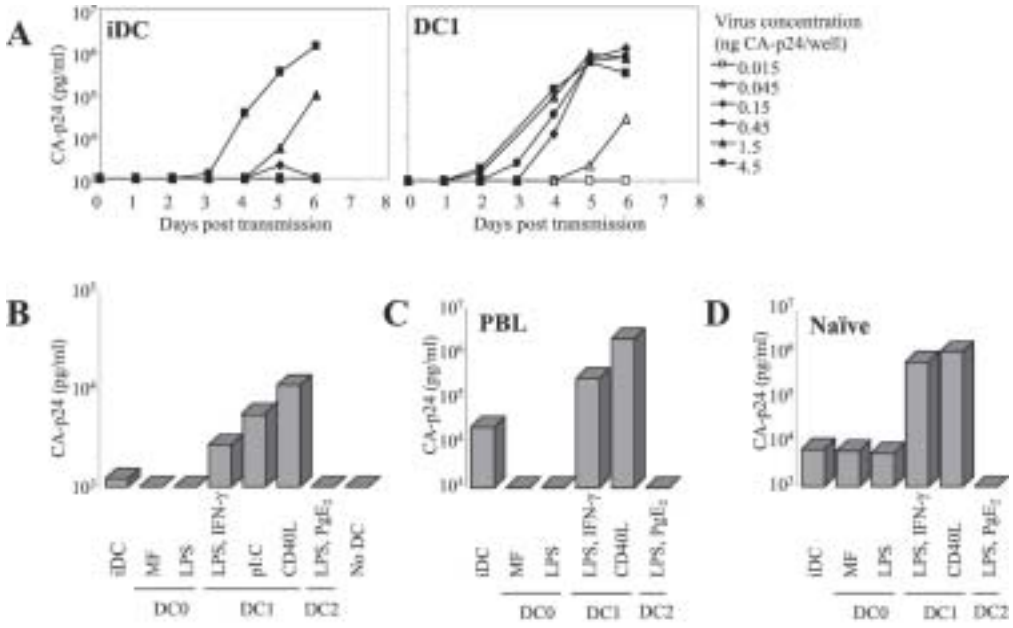

Fig. 2. DC1 are superior in HIV-1 transmission. **A**. Transmission assay as described in the legend of Fig. 1B. The amount of virus incubated with iDC or DC1 was titrated, and virus spread in SupT1 cells was measured. The DC1 cells were obtained by CD40L stimulation. **B**. DC-mediated enhancement of HIV-1 infection. A minimal dose of 15 pg CA-p24 per well of C33A-produced virus was used to infect T cells in the absence or presence of distinct DC subsets. No wash step was performed to remove unbound virus. **C** and **D**. Transmission to primary T cells. DC were preincubated with virus (150 pg CA-p24 per well), subsequently washed, and cocultured with PBL (C) or naïve T cells (Thn; D). The CA-p24 values of day 4 post-transmission are shown.

Binding of the virus particle is mediated by DC-SIGN, which is expressed upon generation of iDC from monocytes (results not shown (15)). FACS analyses showed that DC-SIGN expression is slightly decreased upon DC maturation, but to a similar extent for the different mDC subsets (Fig. 4). Next, we investigated the expression of the HIV (co-)receptors as factors for potential entry of HIV-1 in DC (results not shown). CD4 was not differentially expressed and CCR5 was in fact downregulated on all mDC subsets. Elevated CXCR4 expression was only apparent for the DC2 subset, but this subset has a poor capacity to transmit HIV-1. Downregulation of CCR5 and upregulation of CXCR4 during maturation of DC has been described previously (38). We then focused on adhesions molecules on DC that are involved in DC – T cell contacts. Most of these molecules such as LFA-1, ICAM-3, CD40 and CD86 are equally expressed on the DC subsets, and ICAM-2 is not expressed on mDC (Fig. 4, data not shown and ref. (40)). Interestingly, ICAM-1 varies significantly among the DC subsets and its expression correlates with the transmission capacity (Fig. 4). In particular, DC1 cells have higher ICAM-1 expression levels than iDC, DC2 and DC0 cells. Similar results with DC derived from different donors (table 2). This raises the interesting possibility that DC1 transmit HIV-1 efficiently because these cells interact more effi-

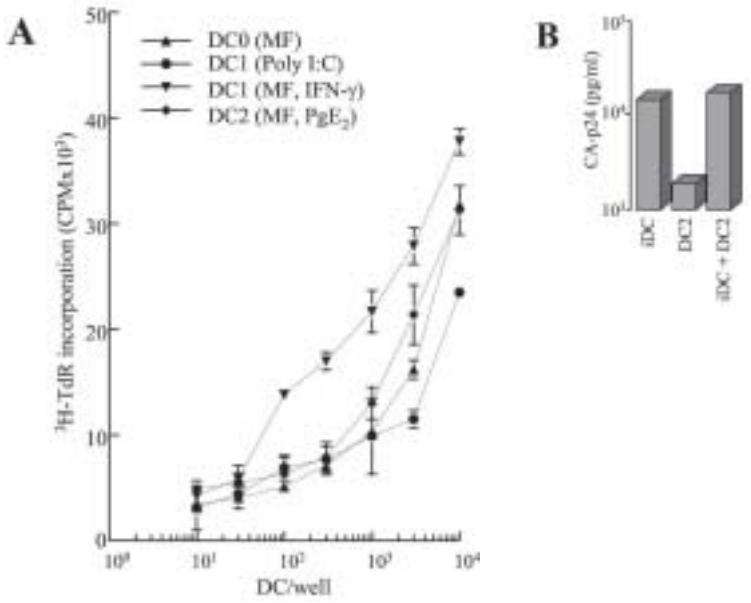

Fig. 3. **A**. The mDC subsets and stimulation of T cells. iDC were matured as described in the legend to Fig. 1. mDC (10 x 10^4 cells/well) were cultured at different numbers with 2.5 x 10^5 allogeneic naïve ($CD45RA^+$) $CD4^+$ T cells. After 5 days, T cell proliferation was measured by [^{3}H]thymidine incorporation (shown in counts per minute, cpm). Similar results were obtained with DC from two other donors. **B**. HIV-1 transmission in mixed DC cultures. Transmission was performed with iDC, DC2 and a mixture of iDC and DC2. The CA-p24 values measured at day 4 post-transmission are shown.

ciently with the recipient T cell through the well-established ICAM-1 – LFA-1 interaction.

Cell-cell contact by means of the ICAM-1 – LFA-1 interaction facilitates HIV-1 transmission

Antibody blocking studies were performed to establish the importance of ICAM-1 expression for DC-mediated virus transmission (Fig. 5A). Virus transmission was performed in the presence or absence of an antibody to ICAM-1 that blocks LFA-1 binding. DC1-mediated transmission was compared with that of iDC, and a normal infection (without wash step) served as control experiment. Blocking of ICAM-1 greatly reduced the transmission efficiency of both iDC and DC1, but the spreading infection in T cells was not affected. Preincubation of DC with antibodies to LFA-1 or ICAM-3 did not block virus transmission to T cells (results not shown). To test whether direct cell-cell contact is required for the efficient virus transmission observed for DC1, we performed an experiment with the DC (preincubated with virus) and T cells in two compartments separated by a membrane that is permeable only for virus particles (transwell culture dish; Fig. 5B). Virus transmission from DC1 to T cells was completely abolished in the transwell experiment, indicating the requirement for cell-cell contact. The same result was obtained in transmission studies with iDC. Thus, iDC are also likely to use the ICAM-1 – LFA-1 interaction, which is confirmed by the blocking experiment

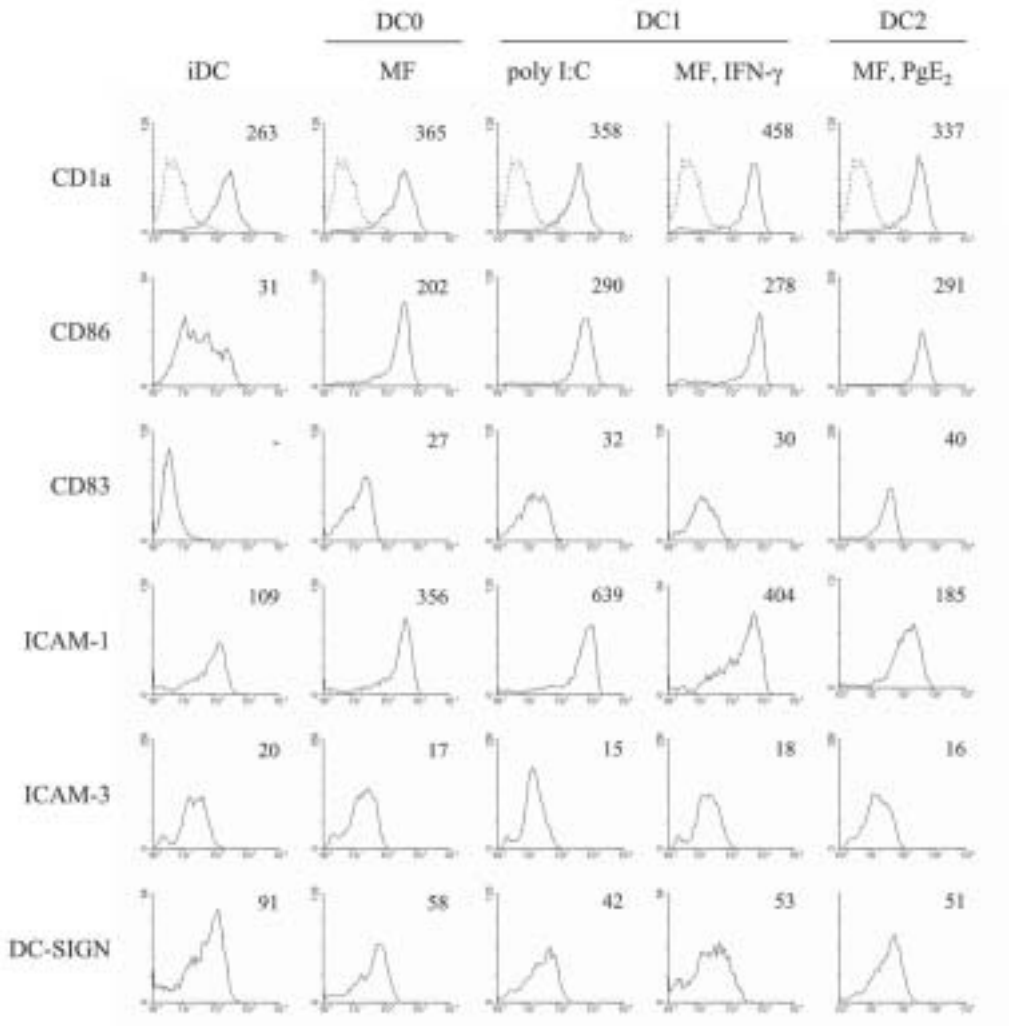

Fig. 4. DC1 express enhanced levels of ICAM-1 but not DC-SIGN. iDC were matured as described in the legend to Fig. 1. The expression of CD1a, CD86, CD83, ICAM-1, ICAM-3 and DC-SIGN was determined by FACS (broken line represents the isotype matched control and the solid line the specific staining). The mean fluorescence intensity is indicated. Similar results were obtained with DC of four different donors (see also Table 2).

with anti-ICAM-1 antibodies (Fig. 5A). Alternatively, it is possible that DC-secreted factors play a role in the transmission of HIV-1 to T cells. To test this, we performed a regular T cell infection in the presence of conditioned DC medium (Fig. 5C). The supernatants of the mDC subsets did not affect the T cell infection rate significantly, but the supernatant from iDC displayed an enhancing effect. Similar results were obtained when the supernatant was added 1 day post infection (results not shown), suggesting that the stimulatory effect of the iDC supernatant is not at the level of virus entry. Combined with the slightly elevated

Table 2. CD83 and ICAM-1 expression[a] by DC derived from different donors

	donor 1	donor 2	donor 3	donor 4	donor 5
CD83					
iDC	-	-	-	-	-
DC0[b]	27	86	79	65	15
DC1[c]	32	109	140	58	14
DC2[d]	40	123	nd[e]	67	21
ICAM-1					
iDC	109	329	347	268	78
DC0[b]	356	827	1068	640	107
DC1[c]	639	1899	2279	992	306
DC2[d]	185	311	nd[e]	207	122

[a] CD83 and ICAM-1 expression measured on effector DC by FACS. Given are mean fluorescence intensities (MFI)
[b] MF treated
[c] pI:C treated
[d] MF, PgE2 treated
[e] Not determined

DC-SIGN expression on iDC, these results provide an explanation for the fair transmission capacity of iDC, despite a moderate ICAM-1 level. Most importantly, these results exclude the possibility that the high transmission capacity of DC1 is due to a soluble factor. These observations suggest that the interaction between ICAM-1 on DC1 and LFA-1 on T cells is critical for efficient HIV-1 transmission. DC1 appear superior in the second phase of virus transmission, that is the presentation of HIV-1 to T cells. Based on the similar level of DC-SIGN expression on iDC and all mDC subsets, one would predict that DC1 is not special in the first phase of transmission, that is virus binding. To test this, iDC and the mDC subsets were incubated with HIV-1 for two hours, washed extensively, and subsequently lysed to quantitate the amount of bound virus by CA-p24 ELISA. We measured a similar virus-binding activity with DC1, iDC and DC0 (Fig. 5D). This result is consistent with a previous study indicating that the efficiency of virus uptake is similar for iDC and mDC, although a different uptake mechanism was proposed (11).

Discussion

We studied the transmission of HIV by different subsets of effector dendritic cells (mDC) that were obtained from monocyte-derived iDC through distinct maturation pathways. These mDC display profound differences in their ability to support HIV-1 transmission to T cells. Compared with iDC, the DC1 subset shows greatly improved virus transmission efficiency, both to a T cell line and PBL target cells. In contrast, DC2 are poor transmitters, which is not caused by a negative impact of DC2 on the T cells. Unbiased mDC show an intermediate ability to mediate HIV transmission. We set out to analyze the mechanism of increased transmission by DC1. It could be excluded that secreted factors determine the enhanced transmission capacity of DC1. A major factor in the DC – HIV-1 interactions is the recently identified DC-SIGN molecule that binds the viral envelope glycoprotein gp120 (14,14,15). We show all mDC subsets express approximate-

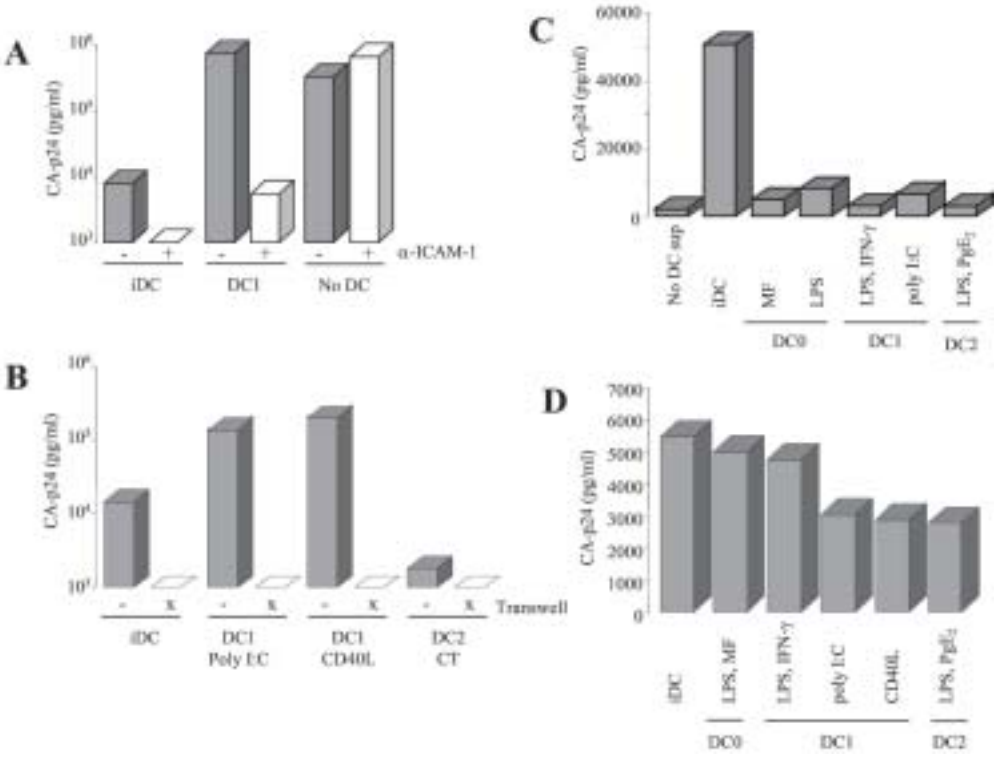

Fig. 5. Cell-cell contact via ICAM-1 – LFA-1 is essential for DC1-mediated transmission. **A**. Blocking of ICAM-1. Transmission of HIV-1 by DC was performed in the absence or presence of a neutralizing anti-ICAM-1 antibody. The antibody was present in the 2 hr DC – HIV-1 incubation and washed out together with unbound virus prior to coculture with T cells. The DC1 cells used in this experiment were obtained by poly I:C stimulation. The right two bars represent a normal infection control. No wash was performed with these samples. **B**. DC mediated transmission was performed with or without a permeable membrane (transwell) between the virus-preincubated DC and T cells. **C**. The effect of DC-conditioned medium on a regular T cell infection. SupT1 cells were infected with HIV-1 (150 pg CA-p24) in the presence or absence of the respective DC supernatants. The CA-p24 values measured at day 3 post infection are shown. **D**. Virus capture by DC. 150 x 10^3 DC were incubated with virus (20 ng CA-p24) for 2 hours. After extensive washing, DC were lysed and bound virus was quantitated by ELISA.

ly equal levels of DC-SIGN (Fig. 4), and virus capture was similar for the DC subsets tested (Fig. 5D). Thus, there must be another reason for the increased transmission capacity of the DC1 subset. Our results indicate that increased ICAM-1 expression, which is observed exclusively for the DC1 subset, plays a major role in virus transmission to T cells by facilitating cell-cell contact. First, we demonstrated that DC – T cell contact is critical for transmission in the transwell experiment (Fig. 5B). Second, HIV-1 transmission by DC1 could be blocked, albeit not completely, by anti-ICAM-1 antibodies (Fig. 5A). The partial inhibition may indicate that other cell surface molecules participate in the DC – T cell contact. These combined results are translated in the transmission model shown in Fig. 6, which depicts three essential interactions: 1) the DC – HIV interaction through DC-SIGN – gp120; 2) the DC – T cell interaction through ICAM-

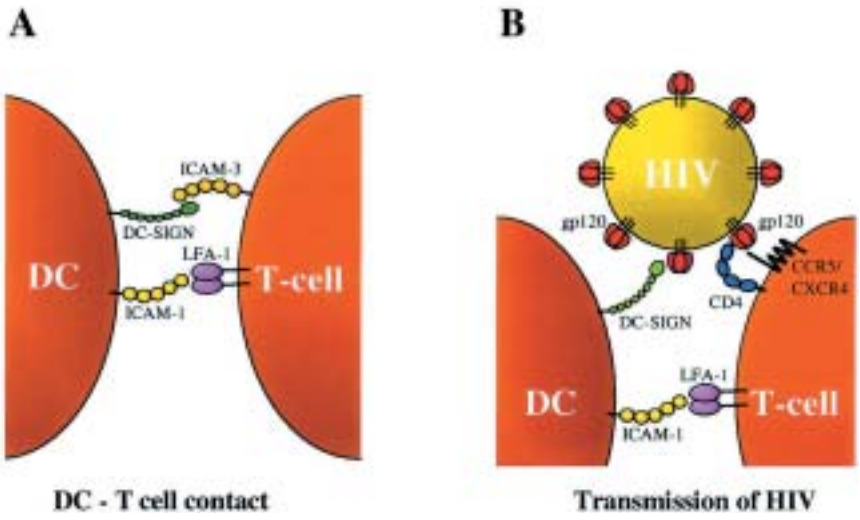

Fig. 6. Transmission model. **A**. In regular DC – T cell contacts, the initial interaction involves ICAM-1 and LFA-1, as well as DC-SIGN and ICAM-3 (15). **B**. In HIV-1 transmission, DC-SIGN captures the virus particle through interaction with gp120. When the DC subsequently contact T cells through the ICAM-1 – LFA-1 interaction, HIV-1 is juxtaposed to the T cell surface with the CD4 and CXCR4 receptors.

1 – LFA-1, and 3) the HIV – T cell interactions through gp120 – CD4 and CCR5/CXCR4. In this model, the "DC-SIGN arm" of the DC binds HIV-1 and the "ICAM-1 arm" binds the T cell, thus juxtaposing the virus particle and the T cell surface. The ICAM-1 – LFA-1 interaction also plays important roles in immune reactions, e.g. in DC1-induced Th1 polarization (27,39). Thus, HIV exploits the human immune system in its mode of transmission.

An extensive microarray/proteomics analysis of the gene expression profile of maturing DC was recently reported (25). Interestingly, this survey showed decreased expression of integrins and other cell adhesion molecules and increased expression of cell motility genes, which is consistent with the enhanced migration properties of mature DC. Increased ICAM-1 expression may therefore be a relatively unique property of the DC1 subset that allows the functional interaction with T cells in the lymph node.

ICAM-1 has been implicated in DC – T cell contacts through interaction with LFA-1 (45), and we now propose that this interaction facilitates HIV transmission. As an alternative explanation of our results, increased ICAM-1 expression on DC1 could establish a stronger DC – HIV interaction through binding of virion-associated LFA-1 (12). In fact, HIV and SIV specifically incorporate cellular adhesion molecules such as LFA-1 and these molecules facilitate adhesion of virions to T cells and thereby enhance viral infectivity (18,29). The incorporation of LFA-1 on HIV-1 particles varies with the cell type that is used for virus production. To critically test this hypothesis, we produced virus in cell types that do not express LFA-1 (and ICAM-1). Similar transmission results were obtained with these virus stocks, including efficient transmission with DC1 cells (Fig. 2B

and results not shown). Furthermore, we measured no difference in virus binding capacity for iDC and different mDC subsets. Thus, the ICAM-1 interaction partner LFA-1 is required on the T cell to facilitate the DC – T cell contact. This cell-cell contact may trigger intracellular events in the T cell that favor productive infection. For instance, ICAM-1 binding to LFA-1 has been demonstrated to upregulate the activities of PI 3-kinase, sphingomyelinase and c-Jun N-terminal kinase (28).

There is evidence that M-tropic HIV-1 isolates can infect iDC through the CCR5 coreceptor (16,17,35). To exclude DC infection in our transmission assay, we used the CXCR4-using LAI primary isolate. CXCR4 is not expressed on iDC, but could be upregulated during maturation, coinciding with increased entry of CXCR4-using HIV-1 (5,26,39,49). We therefore analyzed the cell surface expression of the HIV receptor CD4 and coreceptors CCR5 and CXCR4, but did not measure significant differences among the mDC. Furthermore, we did not observe any virus replication in prolonged DC cell cultures without T cells, and the presence of antiviral compounds like AZT and SDF-1α in the DC1 – virus preincubation step did not affect transmission in the regular assay (results not shown). We therefore exclude the possibility that DC-infection plays a major role in this transmission assay.

This study provides new insight into the mechanism of virus transmission from DC to T cells. The *in vivo* biological significance of the increased transmission that we observed with DC1 remains to be elucidated. We speculate that HIV can enhance its own transmission by a selective trigger of maturation of this specific DC1 subset. In this scenario, sub-epithelial DC-SIGN$^+$ iDC would capture HIV originating from infected epithelial DC-SIGN$^-$ DC (Langerhans cells) that are permissive for HIV infection (42). The iDC-virus complex would subsequently start to migrate, coinciding with maturation into DC1. At the time of encounter with T cells in the lymph node, increased ICAM-1 expression on the DC1 surface will facilitate the DC – T cell contact and thus stimulate the transfer of the virus particle to the T cell. Alternatively, prior or simultaneous infection by bacterial or viral pathogens may enhance the chance of HIV-1 transmission by local enrichment of mature cells of the DC1 type. The highly efficient *in vitro* transmission assay with DC1 cells that we report in this study provides a framework for further mechanistic studies and for the screening of potential transmission inhibitors.

Acknowledgements

We thank Melissa Pope and John Moore for critical reading of the manuscript, and Bill Paxton and Moustapha Chalaby for helpful discussions. This work was sponsored in part by the Dutch AIDS Fund (Amsterdam).

References

1. **Banchereau, J. and R. M. Steinman**. 1998. Dendritic cells and the control of immunity. Nature **392**:245-252.
2. **Blauvelt, A., H. Asada, M. W. Saville, V. Klaus-Kovtun, D. J. Altman, R. Yarchoan, and S. I. Katz**. 1997. Productive infection of dendritic cells by HIV-1 and their ability to capture virus are mediated through separate pathways. J.Clin.Invest **100**:2043-2053.
3. **Cameron, P. U., P. S. Freudenthal, J. M. Barker, S. Gezelter, K. Inaba, and R. M. Steinman**. 1992. Dendritic cells exposed to human immunodeficiency virus type-1 transmit a vigorous cytopathic infection to CD4+ T cells. Science **257**:383-387.
4. **Cameron, P. U., M. G. Lowe, S. M. Crowe, U. O'Doherty, M. Pope, S. Gezelter, and R. M. Steinman**. 1994. Susceptibility of dendritic cells to HIV-1 infection *in vitro*. J.Leukoc.Biol. **56**:257-265.
5. **Canque, B., Y. Bakri, S. Camus, M. Yagello, A. Benjouad, and J. C. Gluckman**. 1999. The susceptibility to X4 and R5 human immunodeficiency virus-1 strains of dendritic cells derived *in vitro* from CD34(+) hematopoietic progenitor cells is primarily determined by their maturation stage. Blood **93**:3866-3875.
6. **Cella, M., M. Salio, Y. Sakakibara, H. Langen, I. Julkunen, and A. Lanzavecchia**. 1999. Maturation, activation, and protection of dendritic cells induced by double-stranded RNA. J.Exp.Med. **189**:821-829.
7. **Das, A. T., B. Klaver, and B. Berkhout**. 1999. A hairpin structure in the R region of the Human Immunodeficiency Virus type 1 RNA genome is instrumental in polyadenylation site selection. J.Virol. **73**:81-91.
8. **de Jong, E. C., P. L. Vieira, P. Kalinski, J. H. Schuitemaker, Y. Tanaka, E. A. Wierenga, M. Yazdanbakhsh, and M. L. Kapsenberg**. 2002. Microbial compounds selectively induce Th1 cell-promoting or Th2-cell promoting dendritic cells *in vitro* with diverse Th cell-polarizing signals. J.Immunol. **168**:1704-1709.
9. **Doms, R. W. and J. P. Moore**. 2000. HIV-1 membrane fusion: targets of opportunity. J.Cell Biol. **151**:F9-14.
10. **Flynn, S., K. M. Toellner, C. Raykundalia, M. Goodall, and P. Lane**. 1998. CD4 T cell cytokine differentiation: the B cell activation molecule, OX40 ligand, instructs CD4 T cells to express interleukin 4 and upregulates expression of the chemokine receptor, Blr-1. J.Exp.Med. **188**:297-304.
11. **Frank, I., M. Piatak, Jr., H. Stoessel, N. Romani, D. Bonnyay, J. D. Lifson, and M. Pope**. 2002. Infectious and whole inactivated simian immunodeficiency viruses interact similarly with primate dendritic cells (DCs): differential intracellular fate of virions in mature and immature DCs. J.Virol. **76**:2936-2951.
12. **Fujiwara, M., R. Tsunoda, S. Shigeta, T. Yokota, and M. Baba**. 1999. Human follicular dendritic cells remain uninfected and capture human immunodeficiency virus type 1 through CD54-CD11a interaction. J.Virol. **73**:3603-3607.
13. **Gagliardi, M. C., F. Sallusto, M. Marinaro, A. Langenkamp, A. Lanzavecchia, and M. T. De Magistris**. 2000. Cholera toxin induces maturation of human dendritic cells and licences them for Th2 priming. Eur.J.Immunol. **30**:2394-2403.
14. **Geijtenbeek, T. B., D. S. Kwon, R. Torensma, S. J. van Vliet, G. C. van Duijnhoven, J. Middel, I. L. Cornelissen, H. S. Nottet, V. N. KewalRamani, D. R. Littman, C. G. Figdor, and Y. van Kooyk**. 2000. DC-SIGN, a dendritic cell-specific HIV-1-binding protein that enhances trans-infection of T cells. Cell **100**:587-597.
15. **Geijtenbeek, T. B., R. Torensma, S. J. van Vliet, G. C. van Duijnhoven, G. J. Adema, Y. van Kooyk, and C. G. Figdor**. 2000. Identification of DC-SIGN, a novel dendritic cell-specific ICAM-3 receptor that supports primary immune responses. Cell **100**:575-585.
16. **Granelli-Piperno, A., E. Delgado, V. Finkel, W. Paxton, and R. M. Steinman**. 1998. Immature dendritic cells selectively replicate macrophagetropic (M-tropic) human immunodeficiency virus type 1, while mature cells efficiently transmit bo. J.Virol. **72**:2733-2737.

17. **Granelli-Piperno, A., V. Finkel, E. Delgado, and R. M. Steinman**. 1999. Virus replication begins in dendritic cells during the transmission of HIV-1 from mature dendritic cells to T cells. Curr.Biol. **9**:21-29.
18. **Hioe, C. E., L. Bastiani, J. E. Hildreth, and S. Zolla-Pazner**. 1998. Role of cellular adhesion molecules in HIV type 1 infection and their impact on virus neutralization. AIDS Res.Hum.Retroviruses **14 Suppl 3**:S247-S254.
19. **Hu, J., M. B. Gardner, and C. J. Miller**. 2000. Simian immunodeficiency virus rapidly penetrates the cervicovaginal mucosa after intravaginal inoculation and infects intraepithelial dendritic cells. J.Virol. **74**:6087-6095.
20. **Huang, Q., d. Liu, P. Majewski, l. Schulte, J. M. Korn, R. A. Young, E. S. Lander, and N. Hacohen**. 2001. The plasticity of dendritic cell responses to pathogens and their components. Science **294**:870-875.
21. **Kalinski, P., C. M. Hilkens, E. A. Wierenga, and M. L. Kapsenberg**. 1999. T-cell priming by type-1 and type-2 polarized dendritic cells: the concept of a third signal. Immunol.Today **20**:561-567.
22. **Kalinski, P., J. H. Schuitemaker, C. M. Hilkens, and M. L. Kapsenberg**. 1998. Prostaglandin E2 induces the final maturation of IL-12-deficient CD1a+CD83+ dendritic cells: the levels of IL-12 are determined during the final dendritic cell maturation and are resistant to further modulation. J.Immunol. **161**:2804-2809.
23. **Kawamura, T., S. S. Cohen, D. L. Borris, E. A. Aquilino, S. Glushakova, L. B. Margolis, J. M. Orenstein, R. E. Offord, A. R. Neurath, and A. Blauvelt**. 2000. Candidate microbicides block HIV-1 infection of human immature Langerhans cells within epithelial tissue explants. J.Exp.Med. **192**:1491-1500.
24. **Kwon, D. S., G. Gregorio, N. Bitton, W. A. Hendrickson, and D. R. Littman**. 2002. DC-SIGN-mediated internalization of HIV is required for trans- enhancement of T cell infection. Immunity. **16**:135-144.
25. **Le Naour, F., L. Hohenkirk, A. Grolleau, D. E. Misek, P. Lescure, J. D. Geiger, S. Hanash, and L. Beretta**. 2001. Profiling changes in gene expression during differentiation and maturation of monocyte-derived dendritic cells using both oligonucleotide microarrays and proteomics. J.Biol.Chem. **276**:17920-17931.
26. **Lee, B., M. Sharron, L. J. Montaner, D. Weissman, and R. W. Doms**. 1999. Quantification of CD4, CCR5, and CXCR4 levels on lymphocyte subsets, dendritic cells, and differentially conditioned monocyte-derived macrophages. Proc Natl Acad Sci USA **96** :5215-5220.
27. **Luksch, C. R., O. Winqvist, M. E. Ozaki, L. Karlsson, M. R. Jackson, P. A. Peterson, and S. R. Webb**. 1999. Intercellular adhesion molecule-1 inhibits interleukin 4 production by naive T cells. Proc.Natl.Acad.Sci.U.S.A **96**:3023-3028.
28. **Ni, H. T., M. J. Deeths, W. Li, D. L. Mueller, and M. F. Mescher**. 1999. Signaling pathways activated by leukocyte function-associated Ag-1- dependent costimulation. J.Immunol. **162**:5183-5189.
29. **Orentas, R. J. and J. E. Hildreth**. 1993. Association of host cell surface adhesion receptors and other membrane proteins with HIV and SIV. AIDS Res.Hum.Retroviruses **9**:1157-1165.
30. **Patterson, S., A. Rae, N. Hockey, J. Gilmour, and F. Gotch**. 2001. Plasmacytoid dendritic cells are highly susceptible to human immunodeficiency virus type 1 infection and release infectious virus. J.Virol. **75**:6710-6713.
31. **Pohlmann, S., F. Baribaud, B. Lee, G. J. Leslie, M. D. Sanchez, K. Hiebenthal-Millow, J. Munch, F. Kirchhoff, and R. W. Doms**. 2001. DC-SIGN interactions with human immunodeficiency virus type 1 and 2 and simian immunodeficiency virus. J.Virol. **75**:4664-4672.
32. **Pope, M., M. G. Betjes, N. Romani, H. Hirmand, P. U. Cameron, L. Hoffman, S. Gezelter, G. Schuler, and R. M. Steinman**. 1994. Conjugates of dendritic cells and memory T lymphocytes from skin facilitate productive infection with HIV-1. Cell **78**:389-398.
33. **Pope, M., S. Gezelter, N. Gallo, L. Hoffman, and R. M. Steinman**. 1995. Low levels of HIV-1 infection in cutaneous dendritic cells promote extensive viral replication upon binding to memory CD4+ T cells. J.Exp.Med. **182**:2045-2056.
34. **Reece, J. C., A. J. Handley, E. J. Anstee, W. A. Morrison, S. M. Crowe, and P. U. Cameron**. 1998. HIV-1 selection by epidermal dendritic cells during transmission across human skin. J.Exp.Med. **187**:1623-1631.

35. **Rowland-Jones, S. L.** 1999. HIV: The deadly passenger in dendritic cells. Curr.Biol. **9**:R248-R250.
36. **Sallusto, F., M. Cella, C. Danieli, and A. Lanzavecchia**. 1995. Dendritic cells use macropinocytosis and the mannose receptor to concentrate macromolecules in the major histocompatibility complex class II compartment: downregulation by cytokines and bacterial products. J.Exp.Med. **182**:389-400.
37. **Sallusto, F. and A. Lanzavecchia**. 1994. Efficient presentation of soluble antigen by cultured human dendritic cells is maintained by granulocyte/macrophage colony-stimulating factor plus interleukin 4 and downregulated by tumor necrosis factor alpha. J.Exp.Med. **179**:1109-1118.
38. **Sallusto, F., A. Lanzavecchia, and C. R. Mackay**. 1998. Chemokines and chemokine receptors in T-cell priming and Th1/Th2- mediated responses. Immunol.Today **19**:568-574.
39. **Salomon, B. and J. A. Bluestone**. 1998. LFA-1 interaction with ICAM-1 and ICAM-2 regulates Th2 cytokine production. J.Immunol. **161**:5138-5142.
40. **Smits, H. H., E. C. de Jong, J. H. Schuitemaker, T. B. Geijtenbeek, Y. van Kooyk, M. L. Kapsenberg, and E. A. Wierenga**. 2002. Intercellular adhesion molecule-1/LFA-1 ligation favors human Th1 development. J.Immunol. **168**:1710-1716.
41. **Stahl-Hennig, C., R. M. Steinman, K. Tenner-Racz, M. Pope, N. Stolte, K. Matz-Rensing, G. Grobschupff, B. Raschdorff, G. Hunsmann, and P. Racz**. 1999. Rapid infection of oral mucosal-associated lymphoid tissue with simian immunodeficiency virus. Science **285**:1261-1265.
42. **Steinman, R. M.** 2000. DC-SIGN: a guide to some mysteries of dendritic cells. Cell **100**:491-494.
43. **Steinman, R. M. and K. Inaba**. 1999. Myeloid dendritic cells. J.Leukoc.Biol. **66**:205-208.
44. **Trinchieri, G.** 1995. Interleukin-12: a proinflammatory cytokine with immunoregulatory functions that bridge innate resistance and antigen-specific adaptive immunity. Annu.Rev.Immunol. **13**:251-276.
45. **Tsunetsugu-Yokota, Y., S. Yasuda, A. Sugimoto, T. Yagi, M. Azuma, H. Yagita, K. Akagawa, and T. Takemori**. 1997. Efficient virus transmission from dendritic cells to CD4+ T cells in response to antigen depends on close contact through adhesion molecules. Virol. **239**:259-268.
46. **Vieira, P. L., E. C. de Jong, E. A. Wierenga, M. L. Kapsenberg, and P. Kalinski**. 2000. Development of Th1-inducing capacity in myeloid dendritic cells requires environmental instruction. J.Immunol. **164**:4507-4512.
47. **Weissman, D., Y. Li, J. Ananworanich, L. J. Zhou, J. Adelsberger, T. F. Tedder, M. Baseler, and A. S. Fauci**. 1995. Three populations of cells with dendritic morphology exist in peripheral blood, only one of which is infectable with human immunodeficiency virus type 1. Proc.Natl.Acad.Sci.U.S.A **92**:826-830.
48. **Whelan, M., M. M. Harnett, K. M. Houston, V. Patel, W. Harnett, and K. P. Rigley**. 2000. A filarial nematode-secreted product signals dendritic cells to acquire a phenotype that drives development of Th2 cells. J.Immunol. **164**:6453-6460.
49. **Zoeteweij, J. P., H. Golding, H. Mostowski, and A. Blauvelt**. 1998. Cytokines regulate expression and function of the HIV coreceptor CXCR4 on human mature dendritic cells. J.Immunol. **161**:3219-3223.

Chapter 3.1

The mannose-dependent epitope for neutralizing antibody 2G12 on HIV-1 glycoprotein gp120

(*Journal of Virology,* July 2002, p. 7293-7305)

Rogier W. Sanders[1,2], Miro Venturi[3], Linnea Schiffner[1], Roopa Kalyanaraman[1], Hermann Katinger[4], Kenneth O. Lloyd[5], Peter D. Kwong[3], John P. Moore[1]

[1]Dept. of Microbiology and Immunology, Weill Medical College of Cornell University, 1300 York Ave., New York, NY 10021.

[2]Dept. of Human Retrovirology, Academic Medical Center, University of Amsterdam, Meibergdreef 15, 1105 AZ Amsterdam, The Netherlands.

[3]Vaccine Research Center, NIAID, National Institutes of Health, Bethesda, MD 20892

[4]Institute for Applied Microbiology, University of Agriculture and Forestry, Muthgasse 18, 1190 Vienna, Austria.

[5]Immunology Program, Memorial Sloan-Kettering Cancer Center, 1275 York Avenue, New York, NY 10021.

We have analyzed the unique epitope for the broadly neutralizing human monoclonal antibody (MAb) 2G12 on the gp120 surface glycoprotein of human immunodeficiency virus type 1 (HIV-1). Sequence analysis, focusing on the conservation of relevant residues across multiple HIV-1 isolates, refined the epitope that was defined previously by substitutional mutagenesis (Trkola, A., M. Purtscher, T. Muster, C. Ballaun, A. Buchacher, N. Sullivan, K. Srinivasan, J. Sodroski, J. P. Moore, and H. Katinger. 1996. J. Virol. 70, 1100-1108). In a biochemical study, we digested recombinant gp120 with various glycosidase enzymes of known specificity, and showed that the 2G12 epitope is lost when gp120 is treated with mannosidases. Computational analyses were used to position the epitope in the context of the virion-associated envelope glycoprotein complex, to determine the variability of the surrounding surface, and to calculate the surface accessibility of possible glycan- and polypeptide-epitope components. Together, these analyses suggest that the 2G12 epitope is centered on the high mannose/hybrid glycans of residues 295, 332 and 392, with peripheral glycans from 386 and 448 on either flank. The epitope is mannose-dependent and composed primarily of carbohydrate, with probably no direct involvement of the gp120 polypeptide surface. It resides on a face orthogonal to the CD4 binding face, on a surface proximal to, but distinct from, that implicated in co-receptor binding. Its conservation amidst an otherwise highly variable gp120 surface suggests a functional role for the 2G12 binding site, perhaps related to the mannose-dependent attachment of HIV-1 to DC-SIGN or related lectins that facilitate virus entry into susceptible target cells.

Introduction

Only a very few monoclonal antibodies (MAbs) are capable of neutralizing primary isolates of human immunodeficiency virus type 1 (HIV-1) and the polyclonal response is also weak (10,19,42,44,57,65). Effective antibodies are scarce because HIV-1 has evolved various protective mechanisms to enable it to resist the binding of antibodies to its envelope glycoprotein (Env) complex (30-32,41,50,56,57,59,71,72). Among the antibodies that can overcome these defenses is the human MAb 2G12 (65,66). The 2G12 antibody recognizes a unique epitope on the surface glycoprotein gp120 that is not directly associated with the receptor-binding sites on this protein (43,67). However, 2G12 is capable of inhibiting the interactions of HIV-1 with its cell surface binding sites and thereby neutralizing infectivity (23,40,64,66,67). The success of 2G12 at neutralizing HIV-1 *in vitro* is reinforced by its ability in passive immunization experiments, usually in combination with other antibodies, to protect macaques from simian-human immunodeficiency virus challenge (2,35,36).

The precise nature of the 2G12 epitope is uncertain. Antibody mapping studies using monomeric gp120 showed that 2G12 forms a unique competition group, in that no other MAb is able to prevent its binding to gp120, and *vice versa* (47). Moreover, a mutagenesis analysis revealed that the only amino-acid substitutions in gp120 which disrupt the 2G12 epitope are at residues specifying sites for *N*-linked glycosylation in the C2, C3, C4 and V4 domains (Fig.1A) (66). The crystal structure of a gp120 fragment comprising the conserved core with truncations of the V1, V2 and V3 variable loops and of the gp41 interactive region, has been obtained (30,31). It showed that most of the predicted glycosylation sites thought be relevant to 2G12 binding are likely to be sufficiently proximal to one another to be within the footprint of an antibody epitope (71,72). Furthermore, several of the relevant glycans are close to the receptor-binding sites on gp120, and probably play an important role in shielding these sites from antibody recognition (41,71,72). Thus 2G12 may actually exploit the very glycan defenses that normally help protect HIV-1 from neutralizing antibodies (52). Because knowledge of neutralization epitopes might be exploitable for vaccine design, we have further analyzed the 2G12 epitope. Our results implicate a conserved patch of high mannose/hybrid glycans as being involved in the formation of this epitope, with mannose residues an essential component. There may be similarities between the 2G12 epitope and the mannose-dependent binding sites on gp120 for DC-SIGN, a lectin that facilitates HIV-1 entry by enhancing the presentation of virions to susceptible cells (3,22,24,38,58), and cyanovirin-N (CV-N), a cyanobacterial protein that inhibits HIV-1 infectivity (8,18,21).

Materials and methods

Sequence analysis

The sequences of isolates sensitive to neutralization by 2G12 (6,42,44) were obtained from the Los Alamos HIV Databank (http://hiv-web.lanl.gov/) and from D. Montefiori (D. Montefiori, personal communication), and their degree of conservation analyzed. The sequences of 15 different isolates, BK132, HXBc2,

JR-FL, QH0515, QH0692, PVO, TVO, 301593, 301657, 301660, 301727, 92BR030, 92RW009, 92RW021 and 92TH014, were analyzed for conservation. Each of these viruses is successfully neutralized by 2G12 (7,65,66). The sequence and structure of the gp120 core fragment for HXBc2 has been described (30,31); the sequences for HIV-1 isolates PVO and TVO were obtained from D. Montefiori; database protein accession numbers for the other sequences were L03697, U63632, AF277061, AF277065, U08444, U04908, U04909, U04925, U08714, U88823, U08645 and U08801 respectively.

A variability criterion was devised, based upon whether a change would disrupt the binding of a hypothetical antibody. For example, a change of Lys to Glu conserves amino-acid type, both being charged; however, such a substitution would disrupt the binding of an antibody that recognized the Glu residue, resulting in a variable classification. Residues were classified as "variable" only if such changes were present in at least 2 of the 15 sequences analyzed.

Deglycosylation of gp120

HIV-1_{JR-FL} gp120, expressed and purified from Chinese Hamster Ovary (CHO) cells was obtained from Progenics Pharmaceuticals, Tarrytown, NY (64). The gp120 protein (1 μg) was incubated with various glycosidases for 16h at 37ºC in 100 μl of the appropriate buffer for each enzyme. Controls included untreated and mock-treated gp120 (digestion buffer, no enzyme). Every enzyme has its own optimal digestion buffer, as indicated by the manufacturer. We selected the buffer for Endo F2 and Endo F3 for the mock-treated control as it had the lowest pH; its composition was 50 mM sodium acetate, pH 4.5. All glycosidases were obtained from Calbiochem, La Jolla, CA. The amounts of each enzyme used were: NgF, 50 U; Endo D, 25 mU; Endo-β-galactosidase, 25 mU; Endo F1, 175 mU; Endo F2, 50 mU; Endo F3, 50 mU; Endo H, 50 mU; α2-3,6, 8,9-neuraminidase, 62.5 mU; α1-2,3,6-mannosidase, 2500 mU. Denaturation and reduction of gp120 was performed by boiling in 1% SDS and 50 mM DTT.

SDS-PAGE and western blot

Glycosidase-treated gp120 (20 ng) was analyzed by sodium dodecyl sulfate polyacrylamide gel electrophoresis (SDS-PAGE) (6). Western blotting was performed following established protocols using the anti-gp120 V3-loop MAb PA-1 (1:5000; 0.2 μg/ml final; Progenics) (64) and HRP-labeled anti-mouse IgG (1:5000; 0.2 μg/ml final; Kierkegaard & Perry Laboratories, Gaithersburg, MD). Luminometric detection of envelope glycoproteins was performed using the Renaissance Western Blot Chemiluminescence Reagent Plus system (NEN Life Science Products, Boston, MA).

Enzyme-linked immunosorbent assays (ELISA)

ELISAs were performed as described previously (46,47). Glycosylated or deglycosylated gp120 (100 ng/ml) was captured onto the solid phase using antibody D7324 to the C5 region (46,47), then bound gp120 was detected with either 2G12 or serum from HIV-1-infected individual LSS. Denaturation of gp120 by boiling in the presence of SDS and dithiothreitol (DTT), followed by ELISA, was per-

formed as described elsewhere (46). The IgG1b12 MAb was a gift from Dennis Burton (Scripps Research Institute, La Jolla, CA) (11).

Structure-based analyses

The following structures were used: the crystal structure of core gp120 in complex with the N-terminal two domains of CD4 (D1D2) and the antigen-binding portion (Fab) of the human antibody 17b, as determined for the T-cell line-adapted isolate HXBc2 (28,29); a model (71) of the HXBc2 core extended by molecular dynamics to include the protein proximal pentasaccharide structure consisting of the two N-acetylglycosamine and three mannose residues (GlcNAc-GlcNAc-Man-$(Man)_2$) common to all *N*-linked sites (Fig.1B); a model (32) further extended by using steric constraints to graft the NMR structure (13) of a V3 loop onto the gp120 core; and a trimeric model (32) obtained by optimization of quantifiable surface parameters. This trimeric model represents the orientation that gp120 most likely assumes in the functional viral spike (32).

Calculations of the accessibility of glycan and polypeptide components of the 2G12 epitope were made with the model containing the GlcNAc-GlcNAc-Man-$(Man)_2$ moieties. This model probably underestimates the glycan contribution, since it only contains the central glycan core. All surface areas and distance measurements were made using the program GRASP (51).

Results

Sequence analysis

A substitutional mutagenesis study has implicated several *N*-linked glycans as being important components of the 2G12 epitope on gp120 (66). Amino-acid substitutions that directly or indirectly affected the *N*-linked glycan sites at positions 295, 332, 386, 392, 397 and 448 were found to com-pletely or partially reduce 2G12 binding (66) (Fig.1). To gain insight into the conservation of the 2G12 epitope, the sequence variability of the above *N*-linked glycan sites was analyzed (Table 1). The Los Alamos Database (http://hiv-web-lanl.gov) was used, as it has been designed to represent the total sequence diversity of HIV-1. This database has 20 representative HIV-1 sequences from subtype A, 107 from subtype B and 30 from subtype C (12). To make estimates of "total" variability for each residue, the total number of differences in subtypes A through C was divided by the total number of sequences (Table 1). Of the above six *N*-linked glycan sites, four were relatively well conserved, while two (Asn-295 and Asn-397) were moderately variable. The variability was subtype-dependent; Asn-295 for example was relatively conserved in subtype B, but highly variable in subtypes A and C (12).

The variability of the complete amino-acid sequence was also analyzed among the different HIV-1 isolates that are efficiently neutralized by 2G12, and so must express the 2G12 epitope (7,65,66). We chose 15 isolates for which there was sequence information available (7,65,66). How the extent of sequence variability mapped onto the surface of gp120 is shown in Fig. 2. Despite our use of only 15 sequences, the variation appeared similar to that described previously using sequences from the entire spectrum of primate immunodeficiency viruses (31),

with much of the gp120 surface being variable. The only conserved surfaces were associated with either the CD4 or the co-receptor binding surfaces, or involved oligomer contact sites that were occluded within the functional viral spike (31,42).

Among the *N*-linked sites implicated as probably being contributory to the 2G12 epitope (66), the sites at residues 332, 386 and 392 were conserved in all test isolates, the site at residue 295 in all but isolate 92RW021, and the site at residue 448 in all but isolate QH0515 (Fig.2). In contrast, the *N*-linked glycan site at residue 397 was variable in most strains; this site is located within the highly variable V4 loop region. The conservation analysis therefore indicates that the glycan at residue 397 is probably not part of the 2G12 epitope. Note that, in the published substitutional mutagenesis study, residue 397 was only analyzed in the context of a double substitution that simultaneously disrupted the glycan sites at both residues 392 and 397 (66). The observed loss of 2G12 binding to this 392 + 397 double mutant is therefore likely to be due to the change at position 392, and not to the change at position 397.

Treatment of gp120 with endo- and exoglycosidases

We next used a biochemical technique to analyze the 2G12 epitope on gp120 from the HIV-$1_{JR\text{-}FL}$ strain, expressed in CHO cells. The gp120 protein from the IIIB isolate, also expressed in CHO cells, has been shown experimentally to contain 13 complex glycans and 11 high mannose and/or hybrid chains (33). JR-FL gp120 is predicted to have all of the complex glycan sites that are present in IIIB gp120, 8 of the high mannose and/or hybrid sites, and 2 additional *N*-linked sites that are absent from IIIB gp120 (Fig.1A).

N-linked carbohydrates can be divided into three categories termed high mannose, hybrid and complex (Fig.1B) (27). These share a common pentasaccharide core structure. High mannose oligosaccharides usually have two to six mannose residues attached to this core. Complex carbohydrates can have different outer branches; bi-, tri-, and tetraantennary chains with a typical sialyllactosamine sequence are shown in Fig. 1B. Hybrid oligosaccharides contain elements of both high mannose and complex carbohydrate structures. Sugars are transferred to asparagines in the rough endoplasmic reticulum, then trimmed to yield $Man_8GlcNAc_2$ oligosaccharide species. These high mannose carbohydrates can be further modified during passage through the Golgi network to become complex type carbohydrates (27). The theoretical molecular weights of the examples shown in Fig. 1B are 1.7 kDa for hybrid oligosaccharides, 2.0 kDa for high mannose oligosaccharides and 2.4 kDa for biantennary complex chains. The molecular weights of the equivalent tri- and tetraantennary complex chains are 3.1 kDa and 3.8 kDa, respectively.

We treated monomeric JR-FL gp120 with a selection of endo- and exoglycosidases. These enzymes have different specificities for the three classes of carbohydrates, as indicated in Fig. 1B (27,53,62). *N*-glycosidase F (NgF) cleaves all three carbohydrate classes between the asparagine and the innermost *N*-acetylglucosamine residue. Endoglycosidases D, F1, F2, F3 and H cleave between the two core *N*-acetylglucosamine residues but they differ in their specificities: Endo F1 and Endo H cleave high mannose and hybrid carbohydrates; Endo F2 cuts

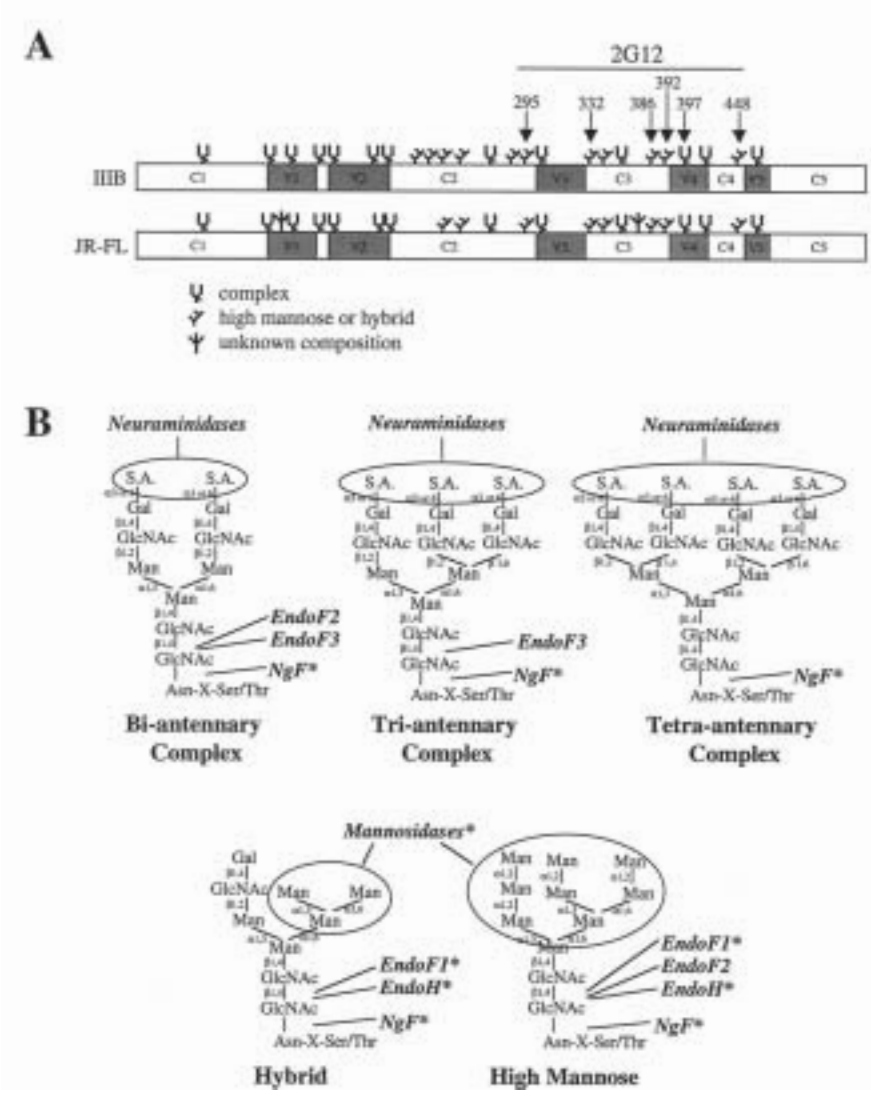

Fig.1. **A**. Carbohydrates on gp120 and their contribution to the 2G12 epitope as identified by substitutional mutagenesis. The schematic of CHO-expressed IIIB and JR-FL gp120 has the *N*-linked glycosylation sites indicated. The composition of the carbohydrates in IIIB gp120 was experimentally determined (33); the carbohydrate designations in the schematic of JR-FL gp120 are based on that study, assuming that glycans are processed similarly on the two Env glycoproteins. Three sites in JR-FL gp120 that are not present in IIIB gp120 are designated as being of unknown carbohydrate composition. Arrows indicate sites that were shown to be important for 2G12 binding, in a substitutional mutagenesis study. Note that the sites at 392 and 397 were only deleted in combination (66). **B**. Specificities of glycosidases. The schematic is derived from ref.27. The cleavage sites of some of the endo- and exoglycosidases used in this study are indicated on the structures of the three classes of carbohydrates: complex, hybrid and high mannose. Note that the number and characteristics of the sugar residues in the outer branches can vary. Complex glycans generally have two to four outer branches and may have a fucose residue attached to the inner N-acetylglucosamine. Asterisks indicate enzymatic cleavages that affect 2G12 binding (see Fig. 4). Abbreviations: GlcNAc, N-acetylglucosamine; Man, mannose; Gal, galactose; S.A., sialic acid.

high mannose and biantennary complex chains, but not hybrid chains; and Endo F3 cleaves bi- and triantennary complex chains. Endo D generally acts on Man_3 and Man_4 sugars. Endo-β-galactosidase cuts β1-4 galactosidase linkages in unbranched poly-*N*-acetyllactosamine chains. Neuraminidase removes terminal sialic acid residues from complex chains, and α-mannosidase cleaves terminal α-linked mannose residues.

The removal of carbohydrate chains from gp120 by glycosidase treatment was monitored by determining whether gp120 migrated with a lower molecular weight when analyzed by SDS-PAGE and western blotting with the anti-V3 loop MAb, PA-1 (Fig. 3). A substantial reduction in the molecular weight of gp120, to ~60 kDa, was caused by NgF treatment, indicating that most carbohydrates had been removed. No proteolytic degradation of HIV-1 gp120 was observed after NgF treatment, in contrast to what occurs with virion-derived gp120 from simian immunodeficiency virus (SIV) (37). Endo F2- or Endo F3-treated gp120s migrated diffusely with glycoprotein species running from around 80 to 110 kDa. The diffuseness is probably caused by heterogeneity in the complex carbohydrates, only some of which are cleaved by these enzymes. Thus, Endo F2 digests only biantennary complex chains and high mannose chains, whereas Endo F3 cleaves bi- and triantennnary, but not tetraantennary chains. A shift of 40 kDa corresponds to a predicted loss of 15 biantennary complex oligosaccharides plus 4 high mannose carbohydrates in the case of Endo F2, and of 14 triantennary oligosaccharides in the case of Endo F3. Smaller changes in the mobility of HIV-1 gp120 were observed in response to treatment with Endo F1 or Endo H (both

Table 1. Variability of *N*-linked sites identified by substitutional mutagenesis as being part of the 2G12 epitope.

		Variability (%):			
N-linked site	Glycan type*	Clade A	Clade B	Clade C	Total
295	mannose	40	15	80	31
332	mannose	25	14	13	15
386	mannose	15	15	15	15
392	mannose	5	11	16	11
397	complex	45	26	37	31
448	mannose	5	4	10	6

*mannose refers to either high mannose or hybrid glycans

of ~10 kDa, corresponding to 5 to 7 hybrid or high mannose chains), with α-mannosidase (~10 kDa, corresponding to ~55 mannose residues, each of 0.18 kDa), or with neuraminidase (~10 kDa, corresponding to ~30 sialic acid residues, each 0.32 kDa in size, on complex oligosaccharide chains).

The loss of ~30 sialic acid residues is consistent with the removal of all the residues from 15 biantennary or 10 triantennary complex chains, assuming they are of the type depicted in Fig. 1B. Hence, many of the complex carbohydrate chains must be susceptible to neuraminidase modification. Similarly, mannosidase must affect most of the hybrid and high mannose oligosaccharides, since the molecular weight loss is so substantial (Fig. 1B).

No changes in gp120 migration were observed after exposure of the glycoprotein to Endo D or Endo-β-galactosidase (Fig. 3). Hence these particular glycosidases were probably unable to remove any glycan components from the gp120 surface, either because their function is blocked by the presence of terminal sugars (Endo D) or their sites of action were either absent (Endo-β-galactosidase) or inaccessible.

2G12 binding to deglycosylated gp120

We next used an ELISA to assess whether 2G12 was able to bind to gp120 that had been exposed to the various glycosidases (Fig. 4). Treatment of gp120 with NgF, Endo F1, Endo H or α-mannosidase completely destroyed its ability to bind 2G12. Conversely, Endo F2, Endo F3, neuraminidase, Endo D or Endo-β-galactosidase treatment had no significant effect on 2G12 binding (Fig. 4A, left panel). Endo-β-galactosidase had a very modest apparent effect on 2G12 binding but this was not reproducible in repeat experiments (data not shown). In contrast to what was observed with 2G12 binding, most of the above enzyme treatments had little effect on the gp120 binding of polyclonal antibodies from the serum of an HIV-1-infected person, LSS, although NgF digestion of gp120 did significantly reduce the binding of the serum antibodies (Fig. 4A, right panel).

To further assess whether glycosidases that affected the binding of 2G12 did so through a specific effect on the 2G12 epitope, or through a non-specific perturbation of gp120 structure, we compared the ability of enzyme-treated gp120 to bind 2G12 and another neutralizing MAb to a discontinuous gp120 epitope, IgG1b12 (Fig. 4B). We observed that IgG1b12 binding was not significantly affected by gp120 deglycosylation by Endo F1, Endo F2, Endo F3, Endo H or α-mannosidase although NgF treatment did significantly reduce IgG1b12 binding (Fig. 4B and data not shown). Thus, the overall antigenic structure of gp120 was not substantially perturbed by the various glycosidases or by the moderately low pH buffers that were used in the digests. An exception was NgF treatment, which did significantly reduce the extent of serum antibody binding and substantially reduced IgG1b12 and serum binding (Fig. 4A and data not shown). This is perhaps not surprising given that NgF converts each relatively hydrophobic *N*-linked site into a hydrophilic aspartic acid. This modification of so many carbohydrates could affect the structure of multiple antibody epitopes, including but not limited to that for IgG1b12, either directly or by affecting the overall conformation of gp120. However, Endo F1, Endo H and α-mannosidase clearly destroy the 2G12 epitope without affecting the IgG1b12 epitope (Fig. 4B).

When gp120 was denatured by boiling in SDS and DTT, 2G12 was still able to bind, but with an approximately 500-fold reduction in affinity (Fig. 4C, left panel). In contrast, serum antibody binding was only reduced 10-fold by denaturation and reduction of gp120 (Fig. 4C, middle panel) (43). The binding of IgG1b12 was completely eliminated by gp120 denaturation and reduction (Fig. 4C, right panel).

Together, these findings imply that the 2G12 epitope is discontinuous in nature, or otherwise sensitive to gp120 conformation (46), and that it contains mannose residues. Moreover, consistent with our conservation analysis, the complex glycan at residue 397 is probably not involved in 2G12 binding.

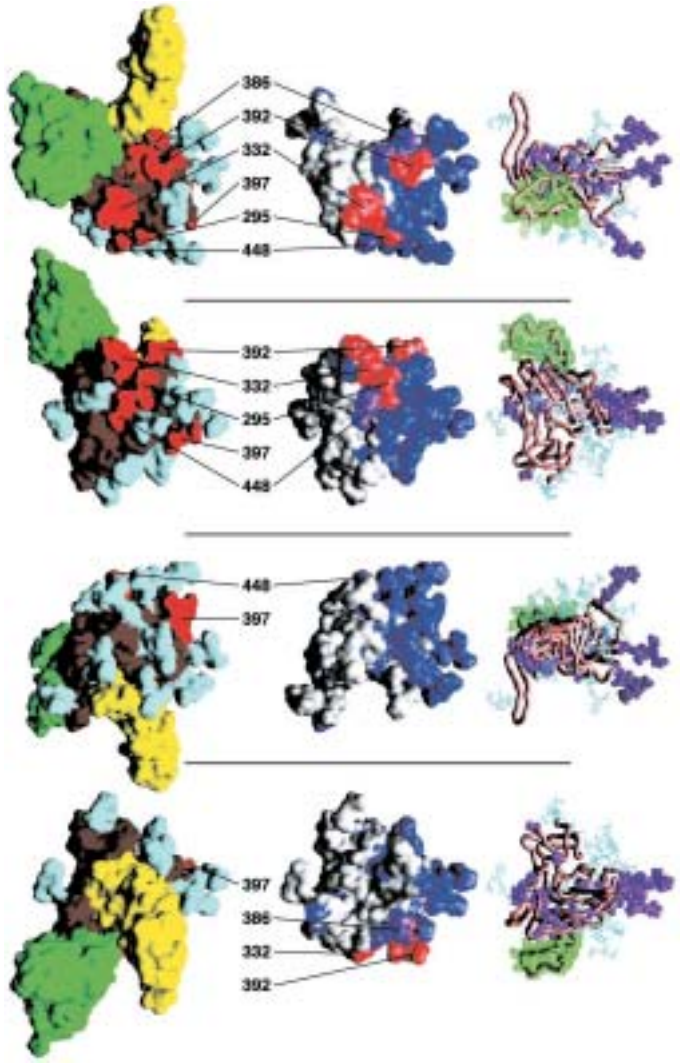

Fig. 2. The 2G12 epitope. Four different orientations of an HIV-1 gp120 monomer are shown in three different representations. The top panel shows gp120 as viewed from the target cell membrane, looking towards the virus. Each subsequent panel shows a view rotated by 90°, with the bottom panel showing core gp120 oriented such that the viral membrane would be positioned above, the target cell below. The left-most column of figures depicts the solvent-accessible surface of gp120, colored according to the functionality of the underlying atoms. Red, residues and associated glycans identified by mutagenesis as being part of the 2G12 epitope; cyan, carbohydrate; brown, remaining gp120 surface. Shown for reference are the solvent accessible surfaces of CD4 (yellow, N-terminal two-domains) and the human neutralizing antibody 17b (green, variable (Fv) portion), as they are oriented in the core gp120: CD4:17b ternary crystal structure (30,31). The right-most column of figures depicts a carbon-alpha worm of gp120 (brown), the molecular surface of the V3 loop as modeled into the gp120 core context (32) (green), the atoms of neutral mutants for 2G12 binding identified previously (66) (purple), and the bonds of modeled carbohydrate (71) (cyan). The middle column of figures depicts the variability of strains that 2G12 neutralizes efficiently, mapped onto the solvent-accessible gp120 core surface. Conserved residues are shown in white, variable residues in blue, and the mutationally identified 2G12 epitope in red, for substitutions that decrease 2G12 binding by at least 90%, or in purple, for substitutions that decrease binding by 60-90%. Selected residues are labeled to aid in orientation.

Structue-based analysis of the 2G12 epitope

Antibodies against almost all the carbohydrate-free surface of the gp120 core have been characterized (46,47,71). Since 2G12 forms a unique competition group, these other ligands do not sterically compete with 2G12 binding (47). This restriction on the definition of the 2G12 epitope is graphically demonstrated in Fig. 2, which illustrates the binding to gp120 of the CD4 ligand and the 17b MAb.

The substitution mutagenesis data and the sequence-variation information were placed into the context of the gp120 structure (Fig.2). This sequence/structure-based analysis implicated a high mannose/hybrid carbohydrate-rich region, centered upon the glycans of residues 295, 332 and 392, with the glycans at residues 386 and 448 flanking opposite ends (Fig.2). The earlier mutagenesis study showed that residues 295, 332, and 392 were critical to 2G12 binding, in that substitutions at these positions caused a complete or substantial loss of 2G12 binding, whereas removal of the glycans from residues 386 or 448 had a significant, although incomplete, inhibitory effect (66). The central 295/332/392 glycan site (Asn + pentasaccharide core) displays a solvent-accessible surface of 2161 $Å^2$, with glycan sites at 386 and 448 contributing 770 $Å^2$ and 730 $Å^2$ respectively.

The glycans at residues 386 and 392 are slightly separated from the rest of the 2G12 epitope by the V3 loop. Deletion of the V3 loop from gp120, either completely or partially (removal of residues 303-323), modestly reduces 2G12 binding (7,66). Thus, the V3 loop is unlikely to be part of the 2G12 epitope, but its close proximity suggests that its removal could indirectly perturb the structure of the epitope.

Directly proximal to residues 295, 332 and 448 is the high mannose/hydrid glycan of Asn-262 (in Fig. 2, this is the conserved carbohydrate directly left of

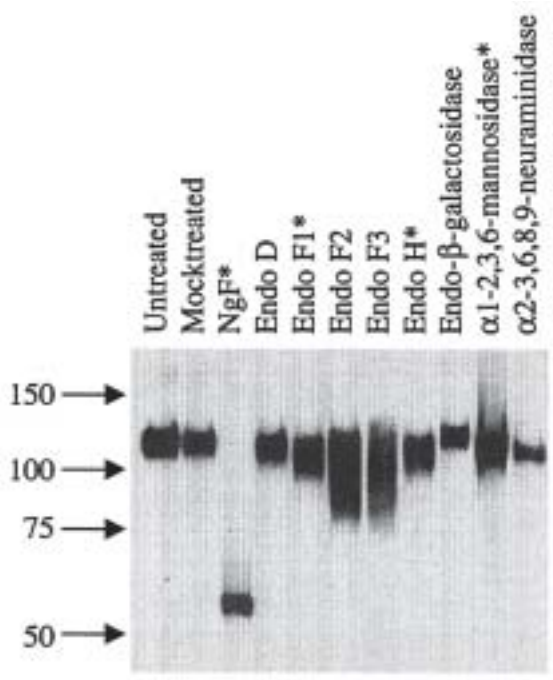

Fig.3. Mobilities of glycosidase-treated gp120 on SDS-PAGE. CHO-expressed JR-FL gp120 was incubated with various endo- and exoglycosidases, then analyzed by SDS-PAGE and western blotting. Control lanes included untreated and mock-treated gp120 (digestion buffer, no enzyme). Asterisks indicate enzymes that affect 2G12 binding (see Fig. 4).

residues 295/448 in the second panel from the top). Asn-262 is conserved in all primate immunodeficiency viruses. A substitution at residue 262 that eliminates this glycosylation site (262N/T) causes a substantial enhancement in 2G12 binding (66). Thus while the glycan on residue 262 cannot form part of the 2G12 epitope, its absence probably affects the orientation and accessibility of the nearby glycans on residues 295 and 332. Substitutions at residue 262 are known to have a substantial impact on the overall folding of gp120 that affect multiple antibody epitopes (48). The other substitutions associated with an increase in 2G12 binding involve residues 88, 103 and 256 (66). The change at position 88 (88N/P) is likely to significantly distort the β-strand at the gp41-interactive region of gp120, whereas residues 103 and 256 are both buried within the gp120 structure; their substitution with larger residues (103Q/F and 256S/Y) probably adversely affects gp120 folding. Indeed, the 256S/Y substitution has a very similar phenotype to that of the 262N/T change, in that it significantly perturbs the structure of many antibody epitopes (J.P.M. and J. Sodroski, unpublished data).

Because our biochemical analysis demonstrated the importance of the mannose residues on the glycans, we analyzed the mannoses of residues 295, 332, 386, 392 and 448 within the context of the functional envelope trimer (Fig.5). These glycans form a surface that is proximal to the chemokine receptor binding surface, on a face orthogonal to the CD4 binding face. In terms of amino-acid substitution among different natural isolates, much of this surface is relatively variable, with the most conserved portions being the base of the V3 loop, and the glycans at positions 262, 332, 386, 392 and 448 that make up or surround the 2G12 epitope. A small portion of this surface is also made up of polypeptide main-chain (Fig.5, right-most column).

The mutational, sequence-variation, biochemical and structure-based analyses all suggested that the 2G12 epitope was composed of high mannose/hybrid glycans. We therefore investigated the extent to which the polypeptide surface of gp120 in this region was accessible to antibody binding (Table 2). We investigated a range of different radial distances from the mannoses of residues 295, 332, 386, 392 and 448. The average diameter of an antibody epitope is 15-20 Å with a surface area of approximately 600-800 $Å^2$ (17,55). With a 5 Å radial cutoff, the total solvent accessible surface surrounding the mannoses of residues 295, 332, 386, 392 and 448 is 3403 $Å^2$; at 10 Å, 6014 $Å^2$; and at 15 Å, 9513 $Å^2$. Thus the actual 2G12 epitope must represent only a small portion of this total surface. We removed from consideration the gp120 surface associated with the binding of CD4 and MAb 17b, because 2G12 does not compete with these ligands for binding to gp120 (47).

We next investigated a variety of probe radii. A 1.4 Å probe, the radius of a water molecule, provides a rough approximation of the penetration of a side-chain to the protein surface. A radius of between 2.5 and 5 Å approximates the penetration of a β-hairpin turn, for example from a CDR-loop of an antibody. A radius of 10 Å approximates the reach of an entire antibody-combining region (17,55). We found that even in the extreme of a 15 Å radial distance with a 1.4 Å probe, the glycan-to-protein surface area ratio was 2.3. This corresponds to a surface that is 70% carbohydrate. At the other extreme, a 5 Å radial distance with a 10 Å probe, the glycan-to-protein surface area ratio was 13.9, which corresponds

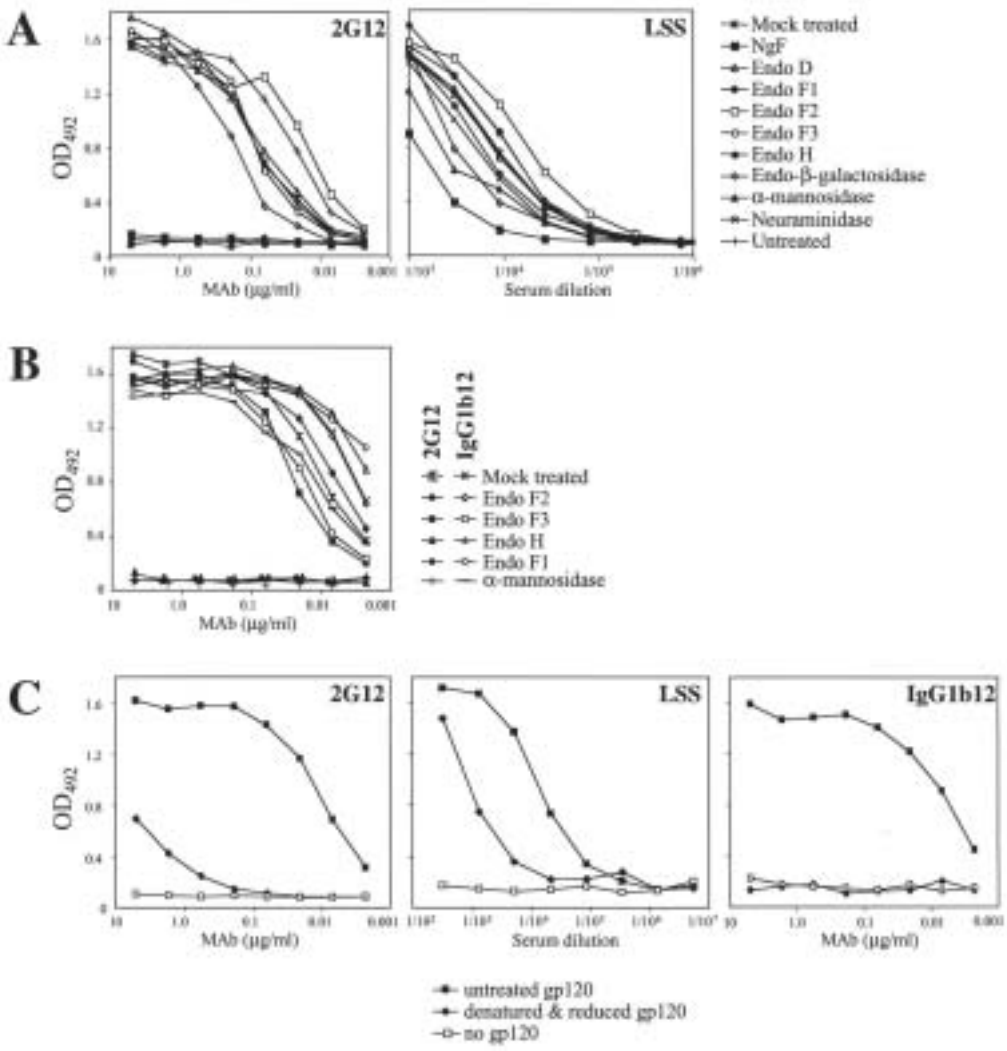

Fig.4. Mannosidase treatment of gp120 abrogates 2G12 binding. **A**. 2G12 binding of glycosidase-treated gp120. Aliquots of the same glycosidase-treated gp120 preparations analyzed by SDS-PAGE (Fig.3) were tested for 2G12 reactivity in ELISA. Bound gp120 was detected with either 2G12 (left panel) or serum from HIV-1-infected individual LSS (right panel). Modest variations in the ELISA signals derived from different enzymatic digests probably reflect small variations in the amounts of gp120 captured from the individual reaction buffers, and are not considered experimentally significant. The results shown are representative of three independent experiments with similar outcomes. **B**. Deglycosylation of gp120 does not significantly affect IgG1b12 binding. A similar experiment as shown in (A) was performed with IgG1b12 (right panel) using a representative subset of glycosidases. The symbols to indicate the various treatments of gp120 are the same as used (A). **C**. Denaturation and reduction of gp120 decreases 2G12 binding dramatically. Gp120 was denatured and reduced as described in the materials and methods section and MAb or serum binding was measured. The symbols used are indicated below the figure.

to a surface of 93% carbohydrate. These results probably underestimate the true amount of the glycan component of the 2G12 epitope, since they were derived from a model that only contains the protein proximal pentasaccharide, and most glycans would be twice this size. On the other hand, glycans are also flexible, and may permit better penetration in an induced fit scenario than would be predicted

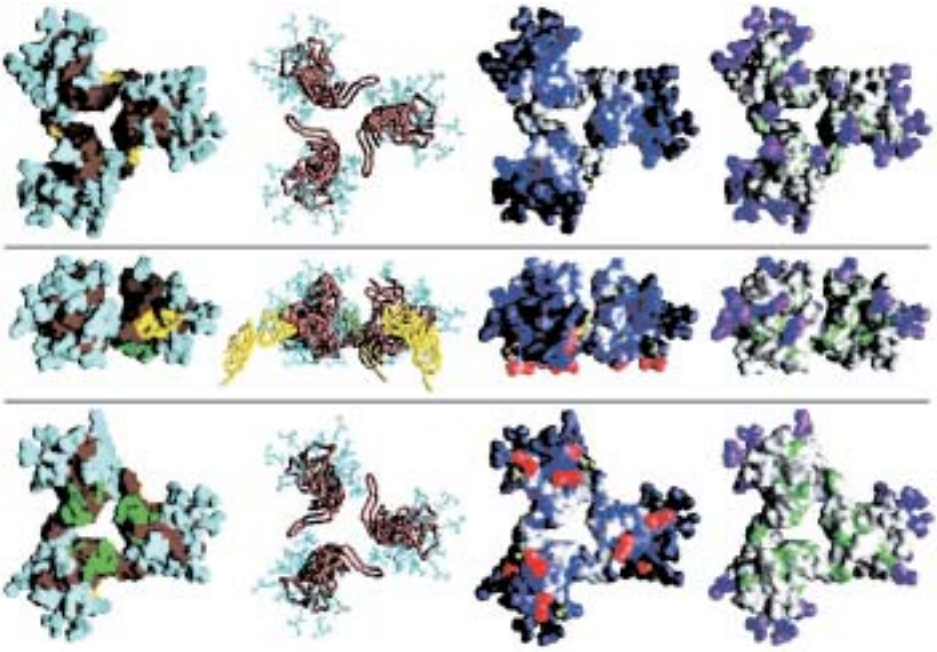

Fig. 5. The 2G12 epitope in the context of the functional envelope trimer. Various representations of gp120 are displayed in the trimeric orientation that it mostly assumes in the functional, virion-associated Env complex. This orientation was determined by optimization of quantifiable surface parameters, as described previously (32). Three different views of the trimer are shown, each rotated by 90° about a horizontal axis. The top panel shows gp120 as viewed from the virus, the middle panel, a side view with the virus membrane positioned above, the target cell below, and the bottom panel, a view from the perspective of the target cell. (Note: the right most protomer in the bottom panel corresponds in orientation to the top panel of gp120 monomers in Fig. 2). The left column of figures depicts the solvent-accessible surface of gp120 colored according to functionality: cyan, surface associated with carbohydrate; yellow, surface within 3 Å of CD4; green, surface associated with residues that are part of the CCR5 binding surface (61), and brown, the remaining gp120 surface. The next column of figures depicts a carbon-alpha worm trace of gp120 (brown), carbohydrate (cyan) and a carbon-alpha worm of CD4 (yellow). The third column of figures depicts gp120 colored according to the sequence variability of the underlying residues, ranging from white (conserved) to dark blue (highly variable). The conservation scheme depicted here was described earlier in the structure analysis of core gp120 (30). Shown in red are the mannose residues of glycans 295, 332, 386, 392 and 448 which we have identified here as being critical for 2G12 binding. The right-most column of figures depicts in purple, the solvent accessible surface associated with complex carbohydrates, and in green, the surface associated with main-chain atoms. Since main-chain atoms do not change upon amino-acid variation, this portion is less subject to change upon side chain variation. Comparison of the left-most and right-most panels shows that much of the gp120 surface facing the cell is dominated by high-mannose or hybrid glycans. The figure was made using the program GRASP (51). (The left two columns were previously shown in ref.22, and are reproduced here as a visual aid for orienting the other panels).

Table 2. Antibody accessibility of the gp120 polypeptide surface containing the 2G12 epitope

Radius of probe (Å)	Glycan-protein surface area ratio when radial distance from mannose epitope (Å) is:		
	5.0	10.0	15.0
1.4	6.8	3.1	2.3
2.5	9.9	4.1	3.2
5.0	9.1	5.0	4.7
10.0	13.9	10.2	9.0

Surface accessibility is dependent on the size of the probe, with water for example being able to penetrate into small crevices that are not accessible to bulky aromatic side chains. To analyze the degree to which the gp120 polypeptide surface was accessible beneath overlying glycan residues, the 2G12 epitope was analyzed with spherical probes of different radii, ranging from 1.4 Å, the radius of a water molecule, to 10 Å, the radius of an antibody epitope. Because the precise extent of the 2G12 epitope is not known, a range of boundaries extending from the known 2G12 mannose binding site was considered. At each radial boundary distance (horizontal axis) and probe radius (vertical axis), the ratio of glycan surface area to polypeptide surface area was calculated for different potential epitopes. The actual 2G12 paratope is likely to be a mixture of different probe radii, with the 2G12 epitope boundary within the range of radial distances presented here.

by the rigid model used in our probe analysis. Nonetheless, these results demonstrate that the 2G12 epitope is primarily composed of high mannose/hybrid glycans.

Discussion

Our experiments indicate that mannose residues in *N*-linked high mannose/hybrid glycan chains are essential for 2G12 binding to recombinant gp120. Thus, exomannosidase treatment is sufficient to destroy the 2G12 epitope, without affecting the discontinuous epitope for the neutralizing MAb IgG1b12 (Fig.4). Endo F1 and Endo H treatment also abolished 2G12 binding to CHO cell-expressed gp120 whereas Endo F2 had no effect, indicating that the mannose residues of hybrid, rather than high mannose, carbohydrates may be involved in the 2G12 epitope (Fig.1). This conclusion can be drawn because Endo F2 is able to remove mannose residues from high mannose chains, but not from hybrid chains (27,53,62); moreover, Endo F2 does successfully digest gp120 (Fig.3) while leaving the 2G12 epitope intact (Fig.4). However, the efficiency of Endo F2 at cleaving high mannose carbohydrates is at least 20-fold lower than its cleavage of complex chains (62). It is therefore possible that, in addition to hybrid chain carbohydrates, high mannose chains resistant to Endo F2 treatment could also be involved in 2G12 binding. Endo H and Endo D treatment of JR-FL gp120 produced from Drosophila cells has been shown to remove at most only 90% of the high mannose carbohydrate (29), although SIV gp160 has been reported to be completely sensitive to Endo H (14). Thus while we expect most high mannose glycans on HIV-1 gp120 to be sensitive to Endo H, Endo F1 or Endo F2, the observed mobility change of only 10 kDa after Endo F1 and Endo H treatment suggests that part of the high mannose and hybrid carbohydrates on HIV-$1_{JR\text{-}FL}$ gp120 are not, in fact, accessible to endoglycosidases.

N-linked glycans are added onto proteins during synthesis as high mannose, preformed oligosaccharides; only through later modification in the Golgi apparatus do these oligosaccharides lose their terminal mannose sugars. The precise characterization of *N*-linked glycans has been carried out only on recombinant, monomeric gp120, so it is possible that the glycans on the native, trimeric Env complex might be modified differently. However, since 2G12 neutralizes HIV-1 virions derived from human cells (66), the MAb must be able to recognize the native Env complex. The recognition of terminally-linked mannose residues by 2G12 is not, therefore, an artefact of our use of recombinant gp120 expressed in CHO cells; the critical mannose residues must be exposed for 2G12 binding on the surfaces of both the monomeric gp120 molecule and the native, trimeric Env complex.

Mannosidase treatment reduces the infectivity of SIV virions (37). This observation further confirms that terminal mannoses are present on the functionally relevant, trimeric Env complex. Indeed, the oligomerization of Env late in its biosynthesis may decrease the accessibility of gp120 to the glycan-modifying enzymes in the Golgi apparatus, and thereby increase the retention of high mannose glycans on the native Env complex. Consistent with this view, an analysis of *N*-linked oligosaccharides on gp120 derived from chronically virus-infected, human H9 cells showed that more than 80% of the gp120 glycans are of the high mannose or hybrid variety (39).

In contrast to the inhibitory effect of mannosidases, neuraminidase treatment increased the infectivity of SIV (37). One explanation for this might be that the complex, sialic acid-containing carbohydrates of the variable loops are involved in shielding conserved functional regions of gp120 on the native Env complex (41,72); another is that alterations in the electrostatic properties of virions caused by neuraminidase treatment might increase their binding to the cell surface. Regardless of the precise explanation, the results obtained using neuraminidase show that it is not glycosidase treatment in general that decreases virion infectivity, but rather the specific activity of the particular glycosidases that are used.

A mutagenesis study on LAI gp120 revealed that the 2G12 epitope is destroyed by amino-acid substitutions that affected several different *N*-linked glycan residues in the C2, C3, C4 and V4 regions of gp120 (Fig.1A) (66). Most of these glycans consist of high mannose and/or hybrid chains, not complex chains (33,66). An exception is the complex glycan at residues 397, but our data indicate that this residues is probably not involved in 2G12 binding. In general, complex carbohydrates are present on the variable loops of gp120 and their positions often differ among HIV-1 isolates (12,33,34). In contrast, gp120 glycans of high mannose/hybrid character that are located in the less variable regions of the protein, are usually conserved among divergent HIV-1 isolates, and may play an important structural role by facilitating the correct folding of gp120 (12,33).

The sequence analysis of isolates sensitive to 2G12 neutralization proved to be unexpectedly powerful in defining the 2G12 epitope. Such variational analysis works well in the context of the dense information provided by the highly variable HIV-1 genome. A similar, but less detailed analysis helped to define some features of the epitope for the broadly neutralizing anti-gp41 MAb 2F5 (65). The variational analysis of amino-acids that are conserved in the 2G12-sensitive isolates,

but highly variable in HIV-1 otherwise (30), defines eight amino-acids including that at position 295. These residues are scattered across the surface, but only position 295 is a site of *N*-linked glycosylation. Thus, even in the absence of any substitutional mutagenesis data, the sensitivity of the 2G12 epitope to deglycosylation would have been sufficient for the variational analysis to locate this epitope on gp120. However, a limitation of the variational analysis method of epitope definition is that there needs to be significant natural sequence variation within the epitope; it is thus most useful for defining the less conserved gp120 epitopes.

Although 2G12 is broadly reactive with many HIV-1 isolates, it is not panreactive (65). For example, analysis of 2G12 neutralization resistance has identified subtype C viruses that were 2G12 resistant (9). We analyzed the subset of those resistant viruses for which sequence information was available (isolates DU151, DU179 and DU422 (9). All of them lacked glycan 295. While the diversity represented by database sequences probably does not reflect the frequency of viral populations, it nonetheless shows that many HIV-1 isolates will naturally lack some of the *N*-linked glycans required for the formation of the 2G12 epitope (12). Indeed, glycan 295 is poorly conserved among subtype C strains (Table 1), suggesting that most subtype C isolates will be resistant to 2G12 neutralization. The 2G12 epitope that we have identified on gp120 contains, or is directly proximal, to seven of the eight high mannose/hybrid sites that are conserved between the JR-FL and HXBc2 isolates. Indeed, the site is the only conserved, exposed surface on the gp120 trimer that does not interact with the known cellular receptors, CD4 and a chemokine receptor (32). Nonetheless, 2G12 is able to interfere with the binding of gp120 to CCR5 (64) and with the attachment of HIV-1 virions to cells (67). The positioning of its epitope on the gp120 moieties of the native Env trimer suggests that this inhibition is an indirect, steric effect manifested by the sheer bulk of an antibody molecule located physically close to the receptor-binding sites. Such interference is particularly relevant in the context of the physically crowded virion-receptor complex on the cell surface.

Terminal mannose residues are rarely found on mammalian cell-surface or serum glycoproteins (reviewed in 63,68,70). Indeed, the presence of a terminal mannose results in binding of proteins to hepatic lectin receptors and their rapid clearance from the plasma. Virions expressing HIV-1 envelope glycoproteins are very rapidly removed from plasma after their infusion into macaques, with a half-life measured in minutes (26). Thus the presence of terminal high mannose residues on gp120 glycans represents a paradox: these residues appear to be highly conserved and so presumably have a relevant function, yet their presence should be detrimental to the viral life cycle by accelerating the rate of virion clearance.

What could be an evolutionarily conserved function for the terminal mannose residues of gp120? One explanation is that HIV-1 is known to use the mannose components of its gp120 *N*-linked glycans to bind to the cell-surface receptors DC-SIGN and DC-SIGNR (3,24,58). These dendritic cell and macrophage receptors augment the efficiency of both vertical and horizontal HIV-1 transmission, by enhancing the presentation of virions to both macrophages and T cells (reviewed in 3,58). Structural and biochemical analyses of DC-SIGN and DC-SIGNR show that these proteins bind to the central, protein-proximal mannose residues of high mannose glycans (22,38). The rate-limiting step for retroviral infection is known

to be the initial stage of virus-cell attachment (15,49,54,60,69), so the use of DC-SIGN as a high-affinity attachment site provides a significant advantage to HIV-1 (3,24,58). The high mannose/hybrid sugars that form and surround the 2G12 epitope are a possible component of the binding site for DC-SIGN and related proteins. Of note is that the location of these high mannose sugars on a surface distal from the viral membrane (Fig.5), facing outwards from the virus, is optimal for cell surface binding.

There is precedence for the glycan residues of gp120 being the target of an antiviral compound. The cyanobacterial protein, CV-N, is an inhibitor of HIV-1 entry that acts by binding to gp120 (8,18,21). The binding site for CV-N on gp120 comprises exclusively mannose residues on *N*-linked glycans, specifically Manα1-2Manα moieties presented on Man_8 or Man_9 high mannose structures (4,5). CV-N has high affinity and low affinity binding sites, each of which recognizes the mannose moieties of a single *N*-linked glycan (4). CV-N can block 2G12 binding to gp120, but does not inhibit the gp120 binding of other neutralizing or non-neutralizing MAbs (21). The converse competition does not occur, however, in that 2G12 does not inhibit CV-N binding to gp120, most probably because there are multiple binding sites for CV-N, only some of which are occluded by 2G12 (Table 3) (4,21). Overall, however, there are clear similarities in the gp120 binding sites of 2G12 and cyanovirin-N, and probably also in the mechanisms of action of these infection-inhibitors. However, 2G12 does not inhibit DC-SIGN binding to gp120 (Table 3). This is, again, probably a result of the relatively promiscuous binding of DC-SIGN to gp120, in that DC-SIGN can probably recognize any of the exposed high-mannose glycans, whereas 2G12 is a more selective in its interactions. The converse competition between DC-SIGN and 2G12 has not been reported (Table 3). Any partial overlap that does occur between the DC-SIGN and 2G12 binding sites could help explain why unusually low concentrations of 2G12 are able to protect some macaques from vaginal challenge with SHIV-89.6P, albeit inconsistently (36). Much greater concentrations of other anti-Env MAbs are required to achieve the same degree of protection (56).

Our principal conclusion is that the 2G12 MAb recognizes an epitope that is dependent on the presence of mannose residues on *N*-linked glycans. In all probability, the epitope is completely composed of sugars, with no involvement of the gp120 peptide backbone. This will need to be confirmed by crystallographic

Table 3. Competition between reagents that bind mannose residues on gp120

	Competition with inhibitor[c]		
Ligand	2G12	DC-SIGN	CV-N
2G12	X	?	YES[b]
DC-SIGN	NO[a]	X	?
CV-N	NO[b]	?	X

[a] T. B. Geijtenbeek, and Y. van Kooyk, personal communication.
[b] Derived from reference 19.
[c] X, autologous cross-competition; YES, heterologous competition occurs; NO, no competition; ?, no information available.

analysis of the 2G12-gp120 complex. However, for several reasons, we believe that 2G12 is not a conventional "anti-carbohydrate" antibody (25). Firstly, 2G12 is specific for HIV-1 gp120 and does not, for example, recognize SIV gp120 expressed in the same cells (our unpublished data). Secondly, denaturation of gp120 with SDS and DTT causes at least a 500-fold reduction in 2G12 binding, yet the mannose residues are still present on denatured gp120. Thirdly, the *N*-linked moieties that 2G12 recognizes are present on many extracellular, host proteins. For 2G12 to avoid being self-reactive, it cannot bind with high affinity to just a single *N*-linked moiety. Furthermore, given the flexibility of *N*-linked attachments, a binding site involving even two or three moieties would probably not provide enough specificity. Hence, we think that 2G12 recognizes a discontinuous structure that comprises the mannose elements of several individual glycan chains, folded into proximity. Based on our analyses, up to five individual *N*-linked glycans could be involved in forming the 2G12 epitope.

If we are correct that the 2G12 epitope is a discontinuous structure comprising only carbohydrate residues, it may be very difficult to exploit this information for HIV-1 vaccine development. Common *N*-linked glycans are rarely immunogenic, and sera from HIV-1 infected individuals do not compete with 2G12 binding to gp120 (62). In addition, raising anti-carbohydrate antibodies of broad specificity could cause problems from the perspective of auto-immunity. On the other hand, if the 2G12 epitope is indeed a discontinuous structure unique to gp120, perhaps that structure could be appropriately immunogenic in the context of a vaccine antigen if it can be further defined and then appropriately presented. After all, the structure was immunogenic in the individual whose immune system made 2G12, and the resulting antibody does recognize and neutralize a broad range of HIV-1 isolates (65,66).

There are very few conserved neutralization epitopes on gp120, yet there is a great need to exploit these limited weaknesses in the otherwise efficient defenses present on gp120 (45). HIV-1 sequence analysis demonstrates that gp120 glycans are often conserved. Moreover, a loss of five glycosylation sites when SIV was cultured *in vitro* was reversed when the virus replicated in macaques (20). This confirms the functional requirement to preserve gp120 glycans, probably to help resist the humoral immune response (52,71). Unusual approaches to raising "2G12-like" antibodies that focus on carbohydrate chemistry should, therefore, now be explored. For example, a synthetic structure containing clustered mannosyl structures on a peptide scaffold, resembling the recently synthesized trimeric Le-y conjugate (28), could be considered. Alternatively, peptide mimeotopes of carbohydrate antigens might be a useful technique (1,16). Our results also suggest that vaccine-design strategies intended to deglycosylate gp120, and thereby uncover hidden neutralization epitopes, should focus on the complex carbohydrates and perhaps leave the high mannose-containing structures intact, in the hope that 2G12-like antibodies might somehow still be induced.

Acknowledgements

We thank Paul Maddon and Bill Olson for gifts of JR-FL gp120 and the PA-1 MAb, and Dennis Burton for the IgG1b12 MAb. We are grateful to Larry Shapiro

for helpful comments, to Bette Korber and Brian Foley for suggestions on protein sequence analysis, and to David Montefiori for sequences of 2G12 sensitive and resistance subtype C isolates. This work was supported by NIH grants AI36082, AI39420 and AI45463. JPM is a Stavros S. Niarchos Scholar. PDK was a recipient of a Burroughs Wellcome Career Development award. The Department of Microbiology and Immunology at the Weill Medical College gratefully acknowledges the support of the William Randolph Hearst Foundation.

References

1. **Agadjanyan, M., P. Luo, M. A. Westerink, L. A. Carey, W. Hutchins, Z. Steplewski, D. B. Weiner, and T. Kieber-Emmons.** 1997. Peptide mimicry of carbohydrate epitopes on human immunodeficiency virus. Nat. Biotechnol. **15:**547-551.
2. **Baba, T. W., V. Liska, R. Hofmann-Lehmann, J. Vlasak, W. Xu, S. Ayehunie, L. A. Cavacini, M. R. Posner, H. Katinger, G. Stiegler, B. J. Bernacky, T. A. Rizvi, R. Schmidt, L. R. Hill, M. E. Keeling, Y. Lu, J. E. Wright, T. C. Chou, and R. M. Ruprecht.** 2000. Human neutralizing monoclonal antibodies of the IgG1 subtype protect against mucosal simian-human immunodeficiency virus infection. Nat. Med. **6:**200-206.
3. **Baribaud, F., S. Pohlmann, and R. W. Doms.** 2001. The role of DC-SIGN and DC-SIGNR in HIV and SIV attachment, infection, and transmission. Virology **286:**1-6.
4. **Bewley, C. A.** 2001. Solution structure of a cyanovirin-N:Man1-2Man complex: structural basis for high-affinity carbohydrate-mediated binding to gp120. Structure **9:**931-940.
5. **Bewley, C. A., and S. Otero-Quinten.** 2001. The potent anti-HIV protein cyanovirin-N contains two novel carbohydrate binding sites that selectively bind to Man_8D1D3 and Man_9 with nanomolar affinity: implications for binding to HIV envelope glycoprotein gp120. J. Am. Chem. Soc. **123:**3892-3902.
6. **Binley, J. M., R. W. Sanders, B. Clas, N. Schuelke, A. Master, Y. Guo, F. Kajumo, D. J. Anselma, P. J. Maddon, W. C. Olson, and J. P. Moore.** 2000. A recombinant HIV-1 envelope glycoprotein complex stabilized by an intermolecular disulfide bond between the gp120 and gp41 subunits is an antigenic mimic of the trimeric virion-associated structure. J. Virol. **74:**627-643.
7. **Binley, J. M., R. Wyatt, E. Desjardins, P. D. Kwong, W. Hendrickson, J. P. Moore, and J. Sodroski.** 1998. Analysis of the interaction of antibodies with a conserved, enzymatically deglycosylated core of the HIV type 1 envelope glycoprotein. AIDS Res. Hum. Retrovir. **14:**191-198.
8. **Boyd, M. R., K. R. Gustafson, J. B. McMahon, R. H. Shoemaker, B. R. O'Keefe, T. Mori, R. J. Gulakowski, L. Wu, M. I. Rivera, C. M. Laurencot, M. J. Currens, J. H. Cardellina II, R. W. Buckheit, Jr., P. L. Nara, L. K. Pannell, R. C. Sowder II, and L. E. Henderson.** 1997. Discovery of cyanovirin-N, a novel human immunodeficiency virus-inactivating protein that binds viral surface envelope glycoprotein gp120: potential applications to microbicide development. Antimicrob. Agents Chemother. **7:**1521-1530.
9. **Bures, R., L. Morris, C. Williamson, G. Ramjee, M. Deers, S. A. Fiscus, A. Abdool-Karim, and D. C. Montefiori.** 2002. Regional clustering of shared neutralization determinants on primary isolates of clade C human immunodeficiency virus type 1 from South Africa. J. Virol. **76:**2233-2244.
10. **Burton, D. R., and D. C. Montefiori.** 1997. The antibody response in HIV-1 infection. AIDS **11**(Suppl. A)**:**587-598.
11. **Burton, D. R., J. Pyati, R. Koduri, G. B. Thornton, L. S. W. Sawyer, R. M. Hendry, N. Dunlop, P. L. Nara, M. Lamacchia, E. Garratty, E. R. Stiehm, Y. J. Bryson, J. P. Moore, D. D. Ho, and C. F. Barbas III.** 1994. Efficient neutralization of primary isolates of HIV-1 by a recombinant human monoclonal antibody. Science **266:**1024-1027.
12. **Carr, J. K., B. T. Foley, T. Leitner, M. Salminen, B. Korber, and F. McCutchan.** 1998. Reference sequences representing the principal genetic diversity of HIV-1 in the pandemic. *In* B. Korber, C. L. Kuiken, B. Foley, B. Hahn, F. McCutchan, J. W. Mellors, and J. Sodroski (ed.), Human

retroviruses and AIDS 1998: a compilation and analysis of nucleic acid and amino acid sequences. Theoretical Biology and Biophysics Group, Los Alamos National Laboratory, Los Alamos, N.Mex.

13. **Catasti, P., J. D. Fontenot, E. M. Bradbury, and G. Gupta.** 1995. Local and global structural properties of the HIV-MN V3 loop. J. Biol. Chem. **270:**2224-2232.
14. **Chen, B., G. Zhou, M. Kim, R. E. Hussey, B. Elly, J. J. Skehel, E. L. Reinherz, S. C. Harrison, and D. C. Wiley.** 2000. Expression, purification, and characterization of gp160e, the soluble, trimeric ectodomain of the simian immunodeficiency virus envelope glycoprotein, gp160. J. Biol. Chem. **275:**34946-34953.
15. **Chuck, A. S., and B. O. Palsson.** 1996. Consistent and high rates of gene transfer can be obtained using flow-through transduction over a wide range of retroviral titers. Hum. Gene Ther. **7:**743-750.
16. **Clackson, T., and J. A. Wells.** 1991. A hot spot of binding energy in a hormone-receptor interface. Science **267:**383-386.
17. **Cunto-Amnesty, G., T. K. Dam, P. Luo, B. Monzavi-Karbassi, C. F. Brewer, T. C. Van Cott, and T. Kieber-Emmon.** 2001. Directing the immune response to carbohydrate antigens. J. Biol. Chem. **276:**30490-30498.
18. **Davies, D. R., and G. H. Cohen.** 1996. Interactions of protein antigens with antibodies. Proc. Natl. Acad. Sci. USA **93:**7-12.
19. **Dey, B., D. L. Lemer, P. Lusso, M. R. Boyd, J. H. Elder, and E. A. Berger.** 2000. Multiple antiviral activities of cyanovirin-N: blocking of human immunodeficiency virus type 1 gp120 interaction with CD4 and coreceptor and inhibition of diverse enveloped viruses. J. Virol. **74:**4562-4569.
20. **D'Souza, M. P., D. Livnat, J. A. Bradac, S. Bridges, et al.** 1997. Evaluation of monoclonal antibodies to HIV-1 primary isolates by neutralization assays: performance criteria for selecting candidate antibodies for clinical trials. J. Infect. Dis. **175:**1056-1062.
21. **Edmonson, P., M. Murphey-Corb, L. N. Martin, C. Delahunty, J. Heeney, H. Kornfeld, P. R. Donahue, G. H. Learn, L. Hood, and J. I. Mullins.** 1998. Evolution of a simian immunodeficiency virus pathogen. J. Virol. **72:**405-414.
22. **Esser, M. T., T. Mori, I. Mondor, Q. J. Sattentau, B. Dey, E. A. Berger, M. R. Boyd, and J. D. Lifson.** 1999. Cyanovirin-N binds to gp120 to interfere with CD-dependent human immunodeficiency virus type 1 virion binding, fusion, and infectivity but does not affect the CD4 binding site on gp120 or soluble CD4-induced conformational changes in gp120. J. Virol. **73:**4360-4371.
23. **Feinberg, H., D. A. Mitchell, K. Drickamer, and W. I. Weis.** 2001. Structural basis for selective recognition of oligosaccharides by DC-SIGN and DC-SIGNR. Science **294:**2163-2166.
24. **Fouts, T. R., J. M. Binley, A. Trkola, J. E. Robinson, and J. P. Moore.** 1997. Neutralization of the human immunodeficiency virus type 1 primary isolate JR-FL by human monoclonal antibodies correlates with antibody binding to the oligomeric form of the envelope glycoprotein complex. J. Virol. **71:**2779-2785.
25. **Geijtenbeek, T. B., D. S. Kwon, R. Torensma, S. J. van Vliet, G. C. van Duijnhoven, J. Middel, I. L. Cornelissen, H. S. Nottet, V. N. KewalRamani, D. R. Littman, C. G. Figdor, and Y. van Kooyk.** 2000. DC-SIGN, a dendritic cell-specific HIV-1-binding protein that enhances trans-infection of T cells. Cell **100:**587-597.
26. **Hansen, J. E., H. Clausen, C. Nielsen, L. S. Teglbjaerg, L. L. Hansen, C. M. Nielsen, E. Dabelsteen, L. Mathiesen, S. I. Hakomori, and J. O. Nielsen.** 1990. Inhibition of human immunodeficiency virus (HIV) infection in vitro by anticarbohydrate monoclonal antibodies: peripheral glycosylation of HIV envelope glycoprotein gp120 may be a target for virus neutralization. J. Virol. **64:**2833-2840.
27. **Igarashi, T., C. Brown, A. Azadegan, N. Haigwood, D. Dimitrov, M. A. Martin, and R. Shibata.** 1999. Human immunodeficiency virus type 1 neutralizing antibodies accelerate clearance of cell-free virions from blood plasma. Nat. Med. **5:**211-216.
28. **Kornfeld, R., and S. Kornfeld.** 1985. Assembly of asparagine-linked oligosaccharides. Annu. Rev. Biochem. **54:**631-664.
29. **Kudryashov, V., P. W. Glunz, L. J. Williams, S. Hinterman, S. J. Danishevsky, and K. O. Lloyd.** 2001. Towards optimized carbohydrate-based anticancer vaccines: epitope clustering, carrier structure, and adjuvant all influence antibody responses to Lewis(y) conjugates in mice. Proc. Natl. Acad. Sci. USA **98:**3264-3269.

30. **Kwong, P. D., R. Wyatt, E. Desjardins, J. Robinson, J. S. Culp, B. D. Hellmig, R. W. Sweet, J. Sodroski, and W. A. Hendrickson.** 1999. Probability analysis of variational crystallization and its application to gp120, the exterior envelope glycoprotein of type 1 human immunodeficiency virus (HIV-1). J. Biol. Chem. **274:**4115-4123.
31. **Kwong, P. D., R. Wyatt, S. Majeed, J. Robinson, R. W. Sweet, J. Sodroski, and W. A. Hendrickson.** 2000. Structures of HIV-1 gp120 envelope glycoproteins from laboratory-adapted and primary isolates. Structure **8:**1329-1339.
32. **Kwong, P. D., R. Wyatt, J. Robinson, R. W. Sweet, J. Sodroski, and W. A. Hendrickson.** 1998. Structure of an HIV gp120 envelope glycoprotein in complex with the CD4 receptor and a neutralizing human antibody. Nature **393:**648-659.
33. **Kwong, P., R. Wyatt, Q. J. Sattentau, J. Sodroski, and W. A. Hendrickson.** 2000. Oligomeric modeling and electrostatic analysis of the gp120 envelope glycoprotein of human immunodeficiency virus. J. Virol. **74:**1961-1972.
34. **Lee, S. J., S. Evers, D. Roeder, A. F. Parlow, J. Risteli, L. Risteli, Y. C. Lee, T. Feizi, H. Langen, and M. C. Nussenzweig.** 2002. Mannose receptor-mediated regulation of serum glycoprotein homeostasis. Science **295:**1898-1901.
35. **Leonard, C. K., M. W. Spellman, L. Riddle, R. J. Harris, J. N. Thomas, and T. J. Gregory.** 1990. Assignment of intrachain disulfide bonds and characterization of potential glycosylation sites of the type 1 recombinant human immunodeficiency virus envelope glycoprotein (gp120) expressed in Chinese hamster ovary cells. J. Biol. Chem. **265:**10373-10382.
36. **Li, Y., L. Luo, N. Rasool, and C. Y. Kang.** 1993. Glycosylation is necessary for the correct folding of human immunodeficiency virus gp120 in CD4 binding. J. Virol. **67:**584-588.
37. **Mascola, J. R., M. G. Lewis, G. Stiegler, D. Harris, T. C. VanCott, D. Hayes, M. K. Louder, C. R. Brown, C. V. Sapan, S. S. Frankel, Y. Lu, M. L. Robb, H. Katinger, and D. L. Birx.** 1999. Protection of macaques against pathogenic simian/human immunodeficiency virus 89.6PD by passive transfer of neutralizing antibodies. J. Virol. **73:**4009-4018.
38. **Mascola, J. R., G. Stiegler, T. C. VanCott, H. Katinger, C. B. Carpenter, C. E. Hanson, H. Beary, D. Hayes, S. S. Frankel, D. L. Birx, and M. G. Lewis.** 2000. Protection of macaques against vaginal transmission of a pathogenic HIV-1/SIV chimeric virus by passive infusion of neutralizing antibodies. Nat. Med. **6:**207-210.
39. **Means, R. E., and R. C. Desrosiers.** 2000. Resistance of native, oligomeric envelope on simian immunodeficiency virus to digestion by glycosidases. J. Virol. **74:**11181-11190.
40. **Mitchell, D. A., A. J. Fadden, and K. Drickamer.** 2001. A novel mechanism of carbohydrate recognition by the C-type lectins DC-SIGN and DC-SIGNR. J. Biol. Chem. **276:**28939-28945.
41. **Mizuochi, T., T. J. Matthews, M. Kato, J. Hamako, K. Titani, J. Solomon, and T. Feizi.** 1990. Diversity of oligosaccharide structures on the envelope glycoprotein gp120 of human immunodeficiency virus 1 from the lymphoblastoid cell line H9. J. Biol. Chem. **265:**8519-8524.
42. **Mondor, I., M. Moulard, S. Ugolini, P.-J. Klasse, J. Hoxie, A. Amara, T. Delaunay, R. Wyatt, J. Sodroski, and Q. Sattentau.** 1998. Interactions among HIV gp120, CD4, and CXCR4: dependence on CD4 expression level, gp120 viral origin, conservation of the gp120 COOH- and NH_2-termini and V1/V2 and V3 variable loops, and sensitivity to neutralizing antibodies. Virology **248:**394-405.
43. **Moore, J. P., and J. M. Binley.** 1998. Envelope's letters boxed into shape. Nature **393:**630-631.
44. **Moore, J. P., Y. Cao, L. Qing, Q. J. Sattentau, J. Pyati, R. Koduri, J. Robinson, C. F. Barbas III, D. R. Burton, and D. D. Ho.** 1995. Primary isolates of human immunodeficiency virus type 1 are relatively resistant to neutralization by monoclonal antibodies to gp120 and their neutralization is not predicted by studies with monomeric gp120. J. Virol. **69:**101-109.
45. **Moore, J. P., and D. D. Ho.** 1993. Antibodies to discontinuous or conformationally sensitive epitopes on the gp120 glycoprotein of human immunodeficiency virus type 1 are highly prevalent in sera of infected humans. J. Virol. **67:**863-875.
46. **Moore, J. P., and D. D. Ho.** 1995. HIV-1 neutralization: the consequences of viral adaptation to growth on transformed T cells. AIDS **9**(Suppl. A)**:**S117-S136.
47. **Moore, J. P., P. W. H. I. Parren, and D. R. Burton.** 2001. Genetic subtypes, humoral immunity and human immunodeficiency virus type 1 vaccine development. J. Virol. **75:**5721-5729.
48. **Moore, J. P., Q. J. Sattentau, R. Wyatt, and J. Sodroski.** 1994. Probing the structure of the human immunodeficiency virus surface glycoprotein gp120 with a panel of monoclonal antibod-

ies. J. Virol. **68:**469-484.
49. **Moore, J. P., and J. Sodroski.** 1996. Antibody cross-competition analysis of the human immunodeficiency virus type 1 gp120 exterior envelope glycoprotein. J. Virol. **70:**1863-1872.
50. **Moore, J. P., R. L. Willey, G. K. Lewis, J. Robinson, and J. Sodroski.** 1994. Immunological evidence for interactions between the first, second and fifth conserved domains of the gp120 surface glycoprotein of human immunodeficiency virus type 1. J. Virol. **68:**6836-6847.
51. **Morgan, J. R., J. M. LeDoux, R. G. Snow, R. G. Tompkins, and M. L. Yarmush.** 1995. Retrovirus infection: effect of time and target cell number. J. Virol. **69:**6994-7000.
52. **Myzska, D. G., R. W. Sweet, P. Hensley, M. Brigham-Burke, P. D. Kwong, W. A. Hendrickson, R. Wyatt, J. Sodroski, and M. L. Doyle.** 2000. Energetics of the HIV gp120-CD4 binding reaction. Proc. Natl. Acad. Sci. USA **97:**9026-9031.
53. **Nicholls, A., K. A. Sharp, and B. Honig.** 1991. Protein folding and association: insight from the interfacial and thermodynamic properties of hydrocarbons. Proteins Struct. Funct. Genet. **11:**281-296.
54. **Olofsson, S., and J. E. Hansen.** 1998. Host cell glycosylation of viral glycoproteins—a battlefield for host defence and viral resistance. Scand. J. Infect. Dis. **30:**435-440.
55. **O'Neill, R. A.** 1996. Enzymatic release of oligosaccharides from glycoproteins for chromatographic and electrophoretic analysis. J. Chromatogr. A **720:**201-215.
56. **Orloff, G. M., S. L. Orloff, M. S. Kennedy, P. J. Maddon, and J. S. McDougal.** 1991. Penetration of CD4 T cells by HIV-1. The CD4 receptor does not internalize with HIV, and CD4-related signal transduction events are not required for entry. J. Immunol. **146:**2578-2587.
57. **Padlan, E. A.** 1996. X-ray crystallography of antibodies. Adv. Protein Chem. **49:**57-133.
58. **Parren, P. W. H. I., and D. R. Burton.** 2001. The antiviral activity of antibodies in vitro and in vivo. Adv. Immunol. **77:**195-262.
59. **Parren, P. W. H. I., J. P. Moore, D. R. Burton, and Q. J. Sattentau.** 1999. The neutralizing antibody response to HIV-1: viral evasion and escape from humoral immunity. AIDS **13**(Suppl. A)**:**S137-S162.
60. **Pearce, K. H., Jr., M. H. Ultsch, R. F. Kelley, A. M. de Vos, and J. A. Wells.** 1996. Structural and mutational analysis of affinity-inert contact residues at the growth hormone-receptor interface. Biochemistry **35:**10300-10307.
61. **Pohlmann, S., F. Baribaud, and R. W. Doms.** 2001. DC-SIGN and DC-SIGNR: helping hands for HIV. Trends Immunol. **22:**643-646.
62. **Poignard, P., E. Ollman Saphire, P. W. H. I. Parren, and D. R. Burton.** 2001. gp120: biologic aspects of structural features. Annu. Rev. Immunol. **19:**253-274.
63. **Poret, C. D., K. V. Lukacs, G. Box, Y. Takeuchi, and M. K. L. Collins.** 1998. Cationic liposomes enhance the rate of transduction by a recombinant retroviral vector in vitro and in vivo. J. Virol. **72:**4832-4840.
64. **Rizzuto, C. D., R. Wyatt, N. Hernandez-Ramos, Y. Sun, P. D. Kwong, W. A. Hendrickson, and J. Sodroski.** 1998. A conserved HIV gp120 glycoprotein structure involved in chemokine receptor binding. Science **280:**1949-1953.
65. **Tarentino, A. L., and T. H. Plummer, Jr.** 1994. Enzymatic deglycosylation of asparagine-linked glycans: purification, properties, and specificity of oligosaccharide-cleaving enzymes from *Flavobacterium meningosepticum*. Methods Enzymol. **230:**44-57.
66. **Taylor, M. E.** 1993. Recognition of complex carbohydrates by the macrophage mannose receptor. Biochem. Soc. Trans. **21:**468-473.
67. **Trkola, A., T. Dragic, J. Arthos, J. M. Binley, W. C. Olson, G. P. Allaway, C. Cheng Mayer, J. Robinson, P. J. Maddon, and J. P. Moore.** 1996. CD4-dependent, antibody-sensitive interactions between HIV-1 and its co-receptor CCR-5. Nature **384:**184-187.
68. **Trkola, A., A. B. Pomales, H. Yuan, B. Korber, P. J. Maddon, G. P. Allaway, H. Katinger, C. F. Barbas, I. I. I., D. R. Burton, D. D. Ho, and J. P. Moore.** 1995. Cross-clade neutralization of primary isolates of human immunodeficiency virus type 1 by human monoclonal antibodies and tetrameric CD4 IgG. J. Virol. **69:**6609-6617.
69. **Trkola, A., M. Purtscher, T. Muster, C. Ballaun, A. Buchacher, N. Sullivan, K. Srinivasan, J. Sodroski, J. P. Moore, and H. Katinger.** 1996. Human monoclonal antibody 2G12 defines a distinctive neutralization epitope on the gp120 glycoprotein of human immunodeficiency virus type 1. J. Virol. **70:**1100-1108.

70. **Ugolini, S., I. Mondor, P. W. H. I. Parren, D. R. Burton, S. A. Tilley, P. J. Klasse, and Q. J. Sattentau.** 1997. Inhibition of attachment to $CD4^+$ target cells is a major mechanism of T cell line-adapted HIV-1 neutralization. J. Exp. Med. **186:**1287-1298.
71. **Vasta, G. R., M. Quesenberry, H. Ahmed, and N. O'Leary.** 1999. C-type lectins and galectins mediate innate and adaptive immune functions: their roles in the complement activation pathway. Dev. Comp. Immunol. **23:**401-420.
72. **Wang, H., R. Paul, R. E. Burgeson, D. R. Keene, and D. Kabat.** 1991. Plasma membrane receptors for ecotropic murine retroviruses require a limiting accessory factor. J. Virol. **65:**6468-6477.
73. **Weis, W. I., M. E. Taylor, and K. Drickamer.** 1998. The C-type lectin superfamily in the immune system. Immunol. Rev. **163:**19-34.
74. **Wyatt, R., P. D. Kwong, E. Desjardins, R. W. Sweet, J. Robinson, W. A. Hendrickson, and J. G. Sodroski.** 1998. The antigenic structure of the HIV gp120 envelope glycoprotein. Nature **393:**705-711.
75. **Wyatt, R., and J. Sodroski.** 1998. The HIV-1 envelope glycoproteins: fusogens, antigens, and immunogens. Science **280:**1884-1888.

Chapter 4.1

Folding and functionality of HIV-1 envelope glycoprotein disulfide bond mutants: discrepancies between ER quality control verdicts and viral fitness requirements

Eelco van Anken[1], Rogier W. Sanders[2], Marije Liscaljet[1], Maarten de Kok[1], Sonja Tilleman[1], Kati Holopainen[1], Martijn Dankers[2], Mirjam Dierdorp[1], Els Busser[2], Ben Berkhout[2], Ineke Braakman[1]

[1]Dept. of Bio-organic chemistry, Bijvoet Center, Utrecht University, Padualaan 8, 3584 CH Utrecht, The Netherlands

[2]Dept. of Human Retrovirology, Academic Medical Center, University of Amsterdam, 1105 AZ Amsterdam, The Netherlands

The strict conservation of the ten disulfide bonds in the HIV-1 envelope glycoproteins (Env) suggests that they are important for folding in the endoplasmic reticulum (ER) or for viral entry. To investigate the role of individual disulfide bonds, we systematically replaced cysteines by alanines. We found that five disulfide bonds are essential for both folding and viral entry. Surprisingly, two disulfide bonds could be mutagenized without abrogating folding or function. The remaining three disulfide bonds are elementary for viral fitness despite their dispensability for folding. Thus, approval from the quality control to leave the ER is based on 'foldedness', which in turn does not necessarily warrant protein functionality.

Introduction

The HIV-1 envelope glycoproteins (Env) are the sole viral proteins present on the surface of virions (2). Env is synthesized as a 160 kDa precursor protein (gp160), which folds and trimerizes in the endoplasmic reticulum (ER) of the host cell, where it obtains ten disulfides and up to 30 *N*-linked glycans depending on the viral isolate (24). In the Golgi complex, gp160 is cleaved by a cellular protease into a soluble subunit, gp120, and a transmembrane subunit, gp41 (30, 44), and the two subunits remain non-covalently associated on the surface of infected cells and virions. Together, the two Env subunits mediate viral entry: gp120 is responsible for binding to the receptor (CD4) and the coreceptor (CCR5 or CXCR4) on the host cell, and gp41 is needed for subsequent fusion of the viral and cellular membranes (11, 13, 51). Although viral entry is accomplished only by the joint effort of the two subunits, some gp120 dissociates from gp41. Whether gp120 dissociation is necessary for gp41 mediated membrane fusion is still a matter of debate, but shedding of gp120 may enhance viral immune evasion, because freely floating gp120 molecules could act as decoy to fool the immune system of the host (29, 36, 39).

Maturing Env is a substrate for the same folding machinery as any cellular protein that travels along the secretory pathway. Both signal sequence (or leader peptide) removal and *N*-glycosylation occur cotranslationally as soon as maturing ER substrates enter into the lumen of the ER. Folding and disulfide bond formation also commence cotranslationally, but these processes continue for minutes or hours after translation is completed. Folding is assisted by ER resident proteins or so-called chaperones. They transiently associate with folding intermediates to catalyze slow folding events and to prevent aggregation or other unwanted interactions with their environment (45). To ensure fidelity in the maturation process, a variety of quality control mechanisms monitor the folded state of ER substrates. As a rule, only correctly folded proteins can exit the ER, while incompletely folded and misfolded proteins are retained in the ER through association with the ensemble of ER resident proteins (14). To prevent overpopulation of the ER lumen with misfolded proteins, they can be disposed of via retrotranslocation from the ER lumen back into the cytosol, followed by proteasomal degradation, a process referred to as ER-associated degradation (ERAD) (15, 38).

Folding of Env is slow to extremely slow depending on the viral isolate: IIIB Env leaves the ER with a $t_{1/2}$ of 30 min (12, 33), while for LAI Env exit from the ER takes hours (22). Folding intermediates with few or non-native disulfides can persist for hours after translation. Evidence for the employment of ER chaperones during the folding process of Env is its association with BiP, calnexin and calreticulin (12, 34, 35). Special to the folding process of Env is the late removal of its leader peptide with a $t_{1/2}$ of ~15 min for IIIB Env (25) and ~30 min for LAI Env (22). This occurs in a conformation-dependent fashion, since some initial folding of Env is required for leader peptide cleavage (22). Rate-limiting for folding of the gp160 precursor is the folding of gp120 (22), probably because it harbours the majority of glycans and disulfide bonds. Therefore, folding of the gp120 soluble subunit alone largely reflects the folding of Env as a whole. Although slow, the folding process is productive: few if any Env molecules are degraded or end up in aggregates. Instead, the majority of Env reaches the native state (22).

Sequence variability of Env among different HIV strains is notorious and in part explains why the humoral response of many HIV-infected individuals is inadequate. The cysteine residues however are strictly conserved among different HIV strains. This suggests that the antigenic shield of Env may vary, but that the disulfide-bonded structure of Env and, hence, the basic architecture of the molecule is constant. The question is why the ten disulfide bonds of Env are conserved. One reason could be that they contribute to the overall stability (of domains) of the molecule. It is also possible that disulfide bonds play a part in the conformational changes of Env during receptor binding or fusion of the viral and the host cell. Alternatively, disulfide bonds are likely to play a critical part during the folding process itself.

Disulfide-bond deletion mutants of ER client proteins have often shown to be excellent tools to provide detailed insight into oxidative folding pathways and into the contribution of disulfide bonds to the structural stability and function of these proteins. ER client proteins that lack a particular disulfide bond are often maturation incompetent. They either fail to fold at all and aggregate or they oxi-

dize to species that correpond to folding intermediates of the wild-type (wt). Some data were generated from employment of Env cysteine mutants (5, 10, 16, 18, 23, 46, 49), but together they do not give a consistent idea of the relative importance of the ten disulfide bonds of Env for folding and function.

To systematically assess the role of all individual disulfide bonds in Env folding and function, we analyzed a complete series of mutants, where all cysteines were replaced by alanines both individually and pair-wise. Here we report that none of the Env disulfide bond mutants were prone to aggregation. Instead, most mutants underwent oxidative folding at least to a certain extent. Strikingly, five of the ten disulfide bonds could be mutagenized without preventing the formation of a native-like conformation. These Env mutants passed the quality control and could exit the ER. Even more surprisingly, two disulfide bonds were dispensable for Env function.

Materials and methods

Cells

HeLa cells were cultured in MEM (Life technologies) supplemented with 10% FCS (Hybond), penicillin (100 U/ml), streptomycin (100 µg/ml). C33A cervix carcinoma cells were maintained in DMEM (Life Technologies), supplemented with 10% FCS, penicillin and streptomycin. SupT1 T cells were cultured in RPMI medium supplemented with 10% FCS, penicillin and streptomycin. LuSIV cells were cultured in RPMI medium supplemented with 10% FCS, penicillin, streptomycin and hygromycin B (41). Peripheral blood mononuclear cells (PBMCs) were isolated from buffy coats from healthy individuals by Ficoll-Isopaque density centrifugation. PBMCs were cultured for three days in RPMI medium (Life Technologies Ltd., Paisley, UK) supplemented with 10% FCS, penicillin (100 U/ml), streptomycin (100 µg/ml) and phytohemagglutinin (PHA; 5 µg/ml) and subsequently cultured in the absence of PHA but in the presence of IL-2 (100 U/ml).

Site-directed mutagenesis and subcloning

Both single mutants and double mutants of cysteine pairs were generated to eliminate corresponding disulfide bonds in Env. Mutants were generated by site directed mutagenesis, either by the pALTER system (Promega), or by the Quickchange system (Invitrogen) according to the manufacturer's instructions. Mutagenic oligos were designed as follows: TGT or TGC cysteine encoding codons were changed into GCT or, respectively, GCC alanine encoding codons with flanking sequences of 12-14 ncts on either side. Double mutants were generated by an extra round of site-directed mutagenesis of one of the corresponding single mutants. Mutations were confirmed by dideoxynucleotide sequencing of the mutant Env ORFs in entirety.

From a full length molecular clone pLAI (37) of the HIV-1_{LAI} isolate we cloned the *Sal*I-*Xho*I fragment into pBlueScript-KS(+) (Stratagene), yielding pBS-HIV-SX. The *vpu* and *tat* sequences were eliminated by digestion with *Sal*I and *Bbs*I, Klenow treatment and subsequent religation. To render the *Kpn*I site unique to the Env encoding sequence, the *Kpn*I site in the polylinker was

destroyed by Klenow treatment and subsequent religation. To render the *Hin*dIII site unique to the *env* sequence, the *Xbal*I and *Hin*dIII site in the polylinker were filled in with Klenow and religated, destroying the *Hin*dIII site but restoring the *Xba*I site, yielding pBS-gp160. A stop codon was introduced just behind the cleavage site between the gp120 and gp41 sequences by PCR, yielding pBS-gp120. For some site directed mutagenesis rounds pALTER-Env was used, which was constructed by cloning the *Kpn*I-*Hin*dIII fragment from pBS-Env-gp160 into the polylinker of pALTER. For folding assays, mutant Env ORFs were excized from pBS-gp160 or pBS-gp120 as *Not*I-*Xho*I fragments before they were subcloned into pcDNA3 (Invitrogen), yielding pcDNA3-gp160 or pcDNA3-gp120. For functional assays, mutant Env ORFs were first excized from pBS-gp160 as *Nde*I-*Hin*dIII fragments and subcloned into pRS1. pRS1 was generated as follows. First, the *Sal*I-*Bam*HI fragment from pLAI was cloned into pUC18 (Roche). Second, the *Pst*I-*Stu*I fragment from the resulting plasmid was cloned into pBS-gp160, rendering the *Hind*III site in the Env ORF unique. pRS1 does contain the *vpu* and *tat* sequences. Subsequently, mutant Env ORFs were cloned back from pRS1 into pLAI as *Sal*I-*Bam*HI fragments.

Heterologous expression and folding assays

Recombinant vaccinia virus expressing the T7 polymerase (17) was used to drive expression of Env mutants under control of the T7 promoter. Subconfluent HeLa cells were grown at 37°C in 35 mm dishes and infected with a multiplicity of infection (m.o.i.) of 4. Thirty minutes post-infection, cells were transfected with a mixture of 4 mg of mutant or wild-type (wt) pcDNA-gp120 or pcDNA3-gp160, and 10 µl Lipofectase (Invitrogen), according to the manufacturer's instructions.

Pulse-chase experiments were performed essentially as described (6, 22). Five hours after infection, cells were depleted of cysteine and methionine for 15 min before they were pulse-labeled for 2 min with 50 µCi of Redivue pro-mix L-[^{35}S] *in vitro* labeling mix (AP Biotech). Cells were chased for various intervals in medium containing excess unlabeled cysteine and methionine. At the end of the chase, cells were transferred on ice and free sulfhydryl groups were alkylated by addition of NEM. Cells were lysed with detergent and the nuclei were removed by centrifugation. Post-nuclear lysates were immunoprecipitated with polyclonal antibodies directed against Env. In addition, secreted gp120 molecules were immunoprecipitated from the culture media at later chase times. Immune precipitates of Env proteins were treated with Endoglycosidase H and samples were analyzed by reducing or non-reducing SDS-PAGE. Gels were dried and signals were detected on Biomax MR films (Kodak).

Viruses and infections

SupT1 cells were transfected with 10 µg wt or mutant pLAI constructs by electroporation as described previously (9). Virus spread was measured for 14 days using CA-p24 ELISA as described previously (19). Virus stocks were produced as follows: C33A cells were transfected with 10 µg WT or mutant pLAI constructs by $CaPO_4$ precipitation. Three days post-transfection of C33A cells, virus containing culture supernatants were harvested, filtered and stored at -80ºC. Virus concentrations were quantitated by capsid CA-p24 ELISA. These values were

used to normalize the amount of virus for infection experiments. $50x10^3$ PBMCs were infected with 50 ng CA-p24 of C33A-produced HIV-1_{LAI} per well in a 96-well plate and subsequent virus spread was measured as described above.

Virus entry and infectivity assays

$300x10^3$ cells LuSIV cells, stably transfected with an LTR-luciferase construct (41), were incubated with 100 ng CA-p24 of C33A-produced HIV-1_{LAI} per well in a 48-well plate. Cells were maintained in the presence of 200 nM saquinavir to prevent additional rounds of virus replication. Luciferase activity was determined after 48 hrs as a measure for viral entry. The 50% tissue culture infectious dose ($TCID_{50}$) in SupT1 cells was determined after 14 days by endpoint dilution.

Ultracentrifugation of virions

C33A cells were tranfected with 40 µg pLAI per T75 flask. Medium was refreshed at day one post-transfection. At 3 days post-transfection, cells and culture media were harvested. Cells were resuspended in 1.0 ml of lysis buffer. Culture media were centrifuged and passed through a 0.45 µm filter to remove residual cells and debris. Virus particles were pelleted from filtered culture media by ultracentrifugation (100.000 *g* for 45 min at 4°C) and resuspended in 0.5 ml lysis buffer (50mM Tris (pH 7.4) 10mM EDTA, 100mM NaCl, 1% SDS). The virus-free supernatant, containing shed gp120, was concentrated using Amicon centrifugal filter units (Millipore, Bedford, MA) and SDS was added to a final solution of 1%.

Quantitation of gp120 by ELISA

Concentrations of gp120 in cell, virion and supernatant fractions were measured as described previously (28, 42), with some modifications. ELISA plates were coated overnight with sheep antibody D7324 (10 µg/ml; Aalto Bioreagents, Ratharnham, Dublin, Ireland), directed to the gp120 C5 region, in 0.1 M $NaHCO_3$. After blocking by 2% milk in Tris-buffered saline (TBS) for 30 min., gp120 was captured by incubation for 2 hr at room temperature. Recombinant HIV-1_{LAI} gp120 (Progenics Pharmaceuticals, Inc. Tarrytown, NY) was used as a reference. Unbound gp120 was washed away with TBS and purified HIV-1^+ serum Ig (HIVIg) was added for 1.5 hr in 2% milk, 20% sheep serum (SS), 0.5% Tween. HIVIg binding was detected with alkaline phosphatase conjugated goat anti-human Fc (1:10000, Jackson Immunoresearch, West Grove, PA) in 2% milk, 20% SS, 0.5% Tween. Detection of alkaline phosphatase activity was performed using AMPAK reagents (DAKO, Carpinteria, CA). The measured gp120 contents in cells, virus and supernatant were normalized for CA-p24.

Nomenclature of cysteine mutants and distribution of disulfide bond

Although we used HIV-1_{LAI} Env, numbering is based on the HIV-1_{HXB2} isolate to facilitate the identification of amino-acid positions in Env (http://www.hiv.lanl.gov/content/hiv-db). C54A and C74A refer to the single mutants and, respectively, C54A/C74A to the double mutant of disulfide bond 54-74; C119A/C205A to the double mutant of disulfide bond 119-205, etc. The gp41 part of Env contains a single disulfide bond: 598-604, while the gp120 part harbours the remaining nine disulfide bonds (Fig. 1A). The gp120 soluble subunit (SU) consists of a core that is

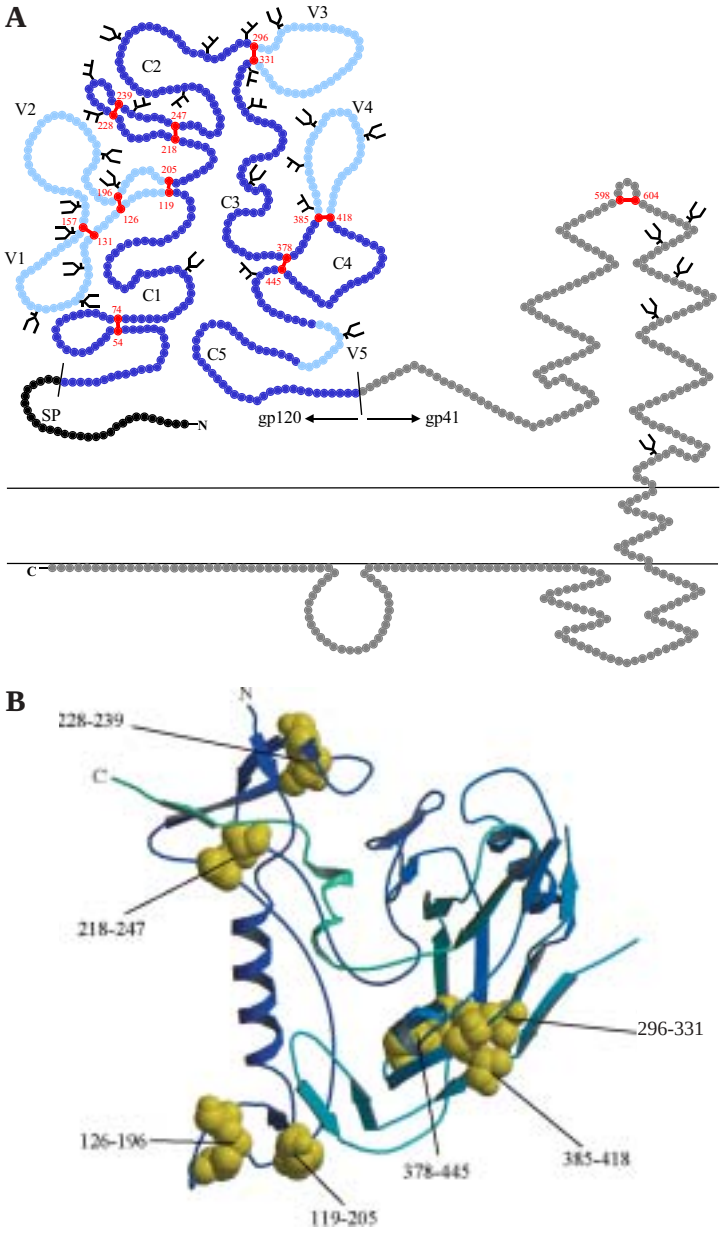

Fig. 1. Schematic of the gp160 precursor. **A**. The gp41 membrane spanning subunit (TM) is depicted in grey and the signal peptide is indicated in black. Disulfide bonds and cysteines are depicted in red. Cysteine residue numbers are indicated. The gp120 soluble subunit (SU) consists of a core that is composed of conserved regions C1 to C5 (indicated in dark blue). The protein loops that protrude from the gp120 core (indicated in light blue) contain the variable regions V1 to V5. *N*-glycans of both the modified (Y) and high mannose type (F) are indicated (24). **B**. Ribbon structure is shown for the crystal structure of gp120 (21). The cysteines and hence disulfide bonds are shown as space filling yellow spheres. Note that the C1 region including the 54-74 disulfide bond is absent. Only the stem of the V1/V2 loops is present. Consequently, the 131-157 disulfide bond at the stem of the V1 loop alone is absent. The V3 and V4 loops are also absent from the core crystal structure of gp120.

composed of conserved regions C1 to C5. This gp120 core forms the CD4 binding part of Env and largely overlaps with the available with available crystal structures of gp120 (21)(Fig. 1B). The protein loops that protrude from the gp120 core contain the variable regions V1 to V5. The most prominent loops, which harbour the V1 and V2 regions, have three disulfide bonds at their stem: 119-205, 126-196, and 131-157. The gp120 core counts six disulfide bonds. Two of these are found at the base of the V3 and V4 loops: 296-331 and, respectively, 385-418. The C1 region contains a single disulfide bond: 54-74, while the C2 region harbors two disulfide bonds: 218-247 and 228-239. The C3 and C4 regions are covalently linked by the 378-445 disulfide bond.

Results

Maturation of Env in a vaccinia T7 expression system

To investigate Env maturation we chose to express gp160 or the soluble subunit gp120 in HeLa cells from plasmids under control of the T7 promoter, by using a recombinant Vaccinia virus vector system (17). We employed three previously developed assays (22), to monitor maturation of both gp160 and gp120 proteins by pulse-chase analysis. 1) We analyzed SDS PAGE mobility changes in alkylated, nonreduced samples after various chase periods as a measure for disulfide bond formation. 2) By analyzing the same samples by SDS PAGE under reducing conditions, we followed signal peptide cleavage as a second measure for Env folding. 3) gp120 was harvested from the culture media at later chase times and analyzed by SDS PAGE as a measure for exit from the ER and subsequent secretion.

In nonreduced samples wt gp120 appeared as a faint fuzzy band in the 0 min chase sample (Fig. 2, left panels). The corresponding reduced sample appeared as a discrete band, which implied that already directly after the pulse the protein was subject to initial disulfide bond formation. Both the reduced and nonreduced

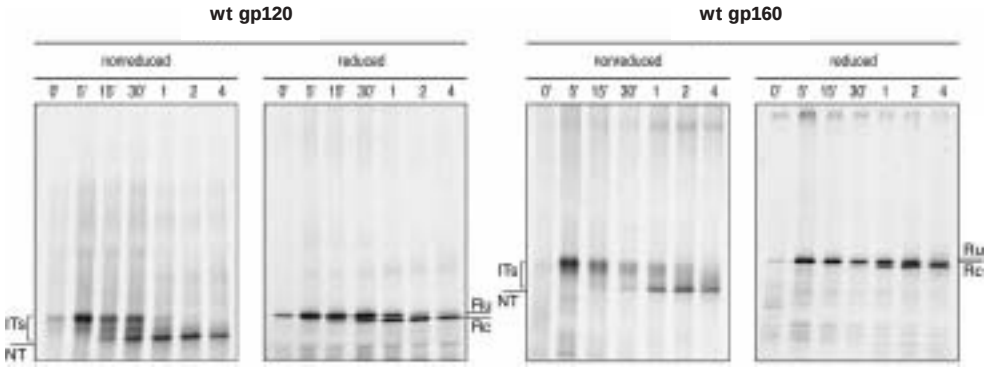

Fig. 2. Folding of wt Env as monitored for VVT7 expressed gp120 and gp160. HeLa cell were infected with VVT7 and transfected with plasmids encoding gp120 (left panels) or gp160 (right panels). Cells were pulse labeled for 2 min and chased for the indicated times. Cells were lysed and Env proteins were immunoprecipitated from lysates. Immunoprecipitates were deglycosylated and analyzed by nonreducing or reducing 7.5% (gp120) or 6% (gp160) SDS PAGE. Folding intermediates (ITs), the native form (NT), the reduced state from which the signal peptide was cleaved off (Rc) or not (Ru) are indicated.

bands rapidly increased in intensity at 5 min after the pulse, indicating that very early folding intermediates were poorly recognized by the antibodies. At intermediary chase times most nonreduced gp120 molecules were present in a smear of various partially oxidized folding intermediates (ITs). Through progressive oxidizing steps they reached a band of highest mobility that corresponded to the native fully, oxidized form of the protein (NT). Concomitantly, a second band of higher mobility appeared in the reduced samples, which increased with time. This band represented gp120 molecules from which the signal peptide was removed. The majority of gp120 molecules had correctly folded at later chase times as evident from appearance of the native band and signal peptide removal (Rc = reduced cleaved *versus* Ru = reduced uncleaved).

For gp160 we observed similar folding kinetics as for gp120 when expressed alone, except that differences in mobility were somewhat less evident because of the larger size of gp160 (Fig. 2, right panels). Neither gp120 nor gp160 did form aggregates. Moreover, the total signal of intracellular and secreted gp120 did not markedly decrease with time, indicating that no gp120 was degraded. Thus, maturation of Env was slow but productive. That Env folded correctly and eventually could exit the ER and travel further along the secretory pathway was evident from the appearance of gp120 in the culture media at later chase times (results not shown).

Taken together, our findings were in agreement with earlier studies that studied Env maturation in HIV infected SupT1 cells (9) or in the context of gp120 or gp160 expressing recombinant vaccinia viruses (22). This validated the T7 promoter driven expression system as an excellent tool to monitor differences in the maturation of our collection of Env cysteine mutants.

Variable effects of cysteine deletions on Env maturation

To investigate the role of particular disulfide bonds in maturation of Env, we expressed cysteine mutants in the VVT7 system and analyzed them by pulse-chase analysis. The elimination of single cysteines or cysteine pairs had variable effects on maturation kinetics and efficiency of Env, as shown for gp120 (Fig. 3A). Some mutants clearly displayed oxidative folding, as evident from the appearance of discrete folding intermediates or even native bands in nonreduced gels. Other mutants were folding deficient as evident from the absence of folding intermediates or native bands. Results were similar for corresponding gp160 variants (data not shown). Ofcourse, for gp41 mutants gp160 variants are shown (Fig. 3A). Data on maturation of the complete set of mutants are summarized in table 1.

Env mutants defective in folding

Mutants of five out of ten disulfide bonds were folding deficient: mutants of the single disulfide bond in the C1 region (54-74), of the two disulfide bonds in the C2 region (218-247 and 228-239), of the single disulfide bond at the stem of the V3 loop (296-331), and of the single disulfide bond at the stem of the V4 loop (385-418) (Fig. 1A). Maturation was most severely affected in mutants of 218-247: signal sequence cleavage was undetectable (Fig. 3, reduced) and appearance of more oxidized Env species was minimal although faint ‘smears’ of Env species at later chase periods with faster mobility than the Env species at 0 min chase

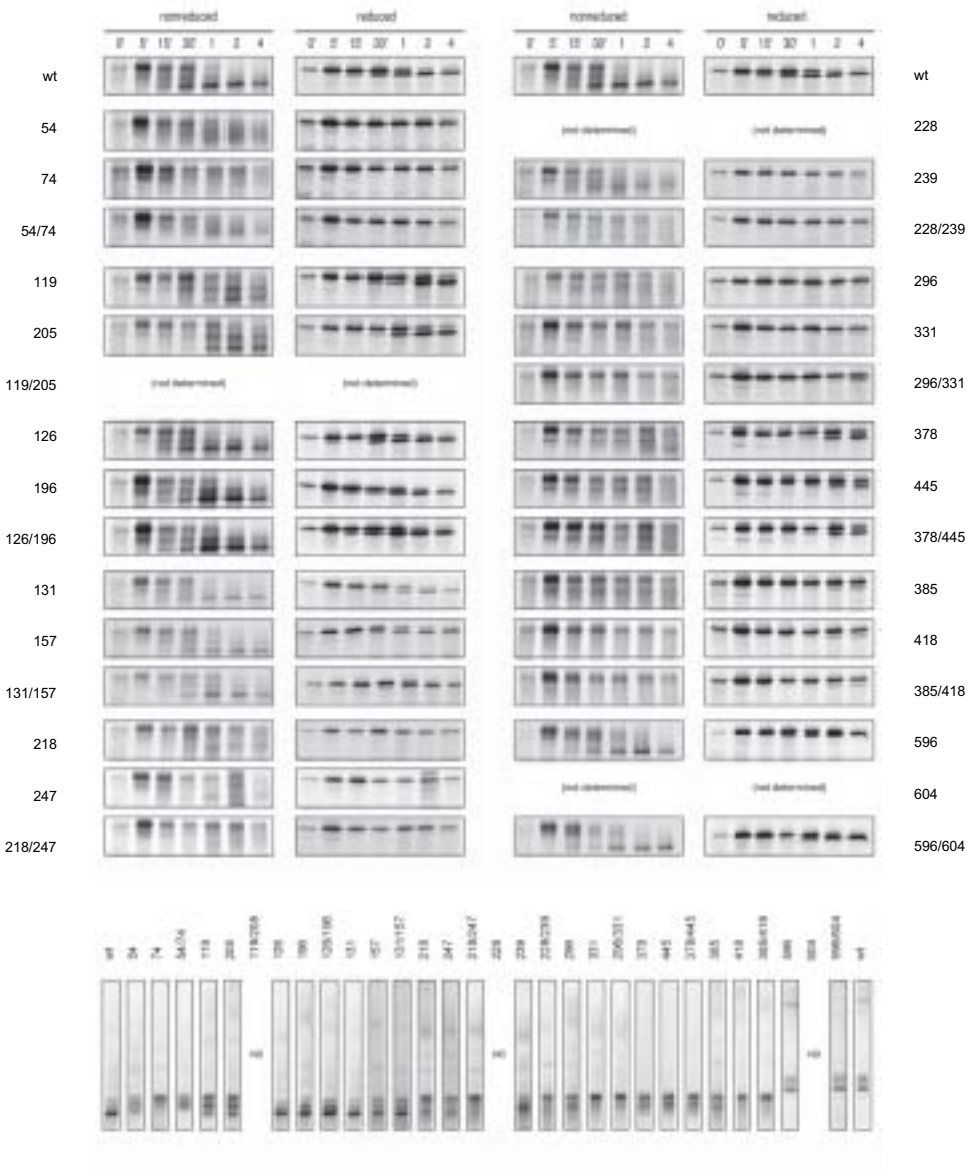

Fig. 3. Folding of cysteine mutants of Env. **A**. Mutants were analyzed as in Fig. 2. Excerpts of gels displaying folding intermediates etc. are shown for all mutants. For 598-604 mutants gp160 variants are shown, but for all other mutants gp120 variants are shown. **B**. From the corresponding nonreduced gels as shown in A, full lanes are shown of the 1 hr chase sample.

were indicative for some residual disulfide bond formation (Fig. 3, nonreduced). The double mutant of 228-239 was similarly folding defective as the 218-247 mutants. Conversely, the corresponding C239A single mutant underwent oxidative folding, although it did not reach the NT form. In accordance with its partial folding competence, C239A displayed some residual signal sequence cleavage (Fig. 3A). We found similar kinetics of signal peptide cleavage from the two single mutants of 296-331. Signal peptide removal from the corresponding C296A/C331A double mutant was even slightly faster. Still, all 296-331 mutants only modestly formed intermediate oxidized species as compared to C239A; C296A more convincingly so than C331A and the double mutant.

The 385-418 mutants showed a similar variation in oxidative folding competence as 296-331 mutants: C385A clearly formed folding intermediates, but C418 and C385A/C418A much less so. Signal peptide cleavage of all 385-418 mutants mutants was however similar: low but detectable. In contrast, all mutants of 54-74 partially folded to heterogeneously oxidized endpoints, although C74A reached less oxidized species than C54A or C54A/C74A. Still, signal peptide removal of all 54-74 mutants was minimal; only C54A/C74A displayed some residual cleavage. In contrast to other folding deficient mutants, minute amounts of C54A and C54A/C74A were secreted into the culture medium when expressed as gp120 variants (table 1).

Taken together, all these mutants displayed severe folding defects. None reached detectable amounts of NT. Some reached partially oxidized species, indicating that they still folded to a certain extent. Other mutants underwent only residual disulfide bond formation as evident from the ‘smears’. The majority of these mutant Env species nevertheless remained non-oxidized, as evident from the persistence of the reduced-like band that was already present at 0 min chase. Accordingly, signal sequence cleavage and secretion of these folding incompetent mutants was minimal to non-existent.

Folding deficiency leads to aggregation and/or degradation for most mutant proteins studied so far. Strikingly, folding incompetence of Env mutants did not lead to their aggregation, as is clear from the absence of higher molecular weight species at 1 hr chase (Fig. 3B). That signals of any Env mutant did not decrease at later chase time periods any more rapidly than wt, implied that none of the mutants were prone to degradation either, despite their prolonged ER residency as unfolded (or misfolded) species.

Maturation competent Env mutants

Surprisingly, mutants of five disulfide bonds were maturation competent: mutants of the two disulfide bonds at the stem of the V1/V2 loops (119-205 and 126-196), of the single disulfide bond at the stem of the V1 loop alone (131-157), of the disulfide bond that bridges the C3 and C4 region (378-445), and of the single disulfide bond in gp41 (598-604) (Fig. 1A). Folding kinetics of 126-196 and 131-157 mutants were identical to those of wt: they reached the native state and their signal peptide was cleaved off at a similar pace as wt (Fig. 3A). Accordingly, they could exit from the ER as evident from secretion of gp120 variants of these mutants, although their secretion was slightly less efficient than of wt (table 1). The 598-604 mutants were also equally folding competent as wt (Fig. 3A).

		appearance of folding intermediates	signal peptide cleavage	appearance of NT	gp120 secretion	gp120 sheddin g	virion incorpo- ration	infectivity	replication
	wt								
C1	54	++	-	-	-/+				-
	74	+	-	-	-				-
	54/74	++	-/+	-	-/+	-	-/+	-/+	-/+
V1/V2	119							+	++
	205								+
	119/205								
	126							-	-
	196							-	-
	126/196					-	-/+	-	-
	131							-	-
	157							-	-
	131/157					++++	++	-	-
C2	218		-	-	-				
	247		-	-	-				-
	218/247		-	-	-				-
	228								-
	239	++	-/+	-	-				-
	228/239	-/+	-	-	-				-
V3	296	++		-	-				-
	331			-	-				-
	296/331		+	-	-				-
C3/C4	378	++	++	-/+	+			++	++
	445	++	++	-/+	+			++	++
	378/445	++	++	-/+	+	+	+	+++	+++
V4	385			-	-				
	418			-	-				
	385/418			-	-				
gp41	598								
	604								
	598/604								

Table 1. Summary of maturation and functional abilities of all Env cysteine mutants. All data on the maturation and functionality of Env mutants were compared with wt. Behaviour of mutants as compared to wt in various assays is arbitrarily indicated: (—) incompetence of mutants to follow wt phenotype; (-/+) residual competence; (+), (++) and (+++) increasing competence similar to wt.

Folding kinetics of 119-205 mutants were slightly slower than of wt: they reached NT and their signal peptide was cleaved off with a $t_{1/2}$ of ~1 hr as opposed to ~30 min for wt (Fig. 3A). Maturation of 378-445 mutants was even slower: $t_{1/2}$ of signal peptide removal was 2-4 hrs. Some molecules of these mutants also fully oxidized at later chase periods, although the NT band was faint. These mutants reached NT with kinetics more similar to wt at 30°C (results not shown), confirming their folding competence. Except for the 598-604 mutants, all folding competent mutants displayed a discrete folding intermediate band that persisted longer than in the folding process of wt. This suggests that, albeit perhaps equally productive, their folding pathways were not identical to that of wt.

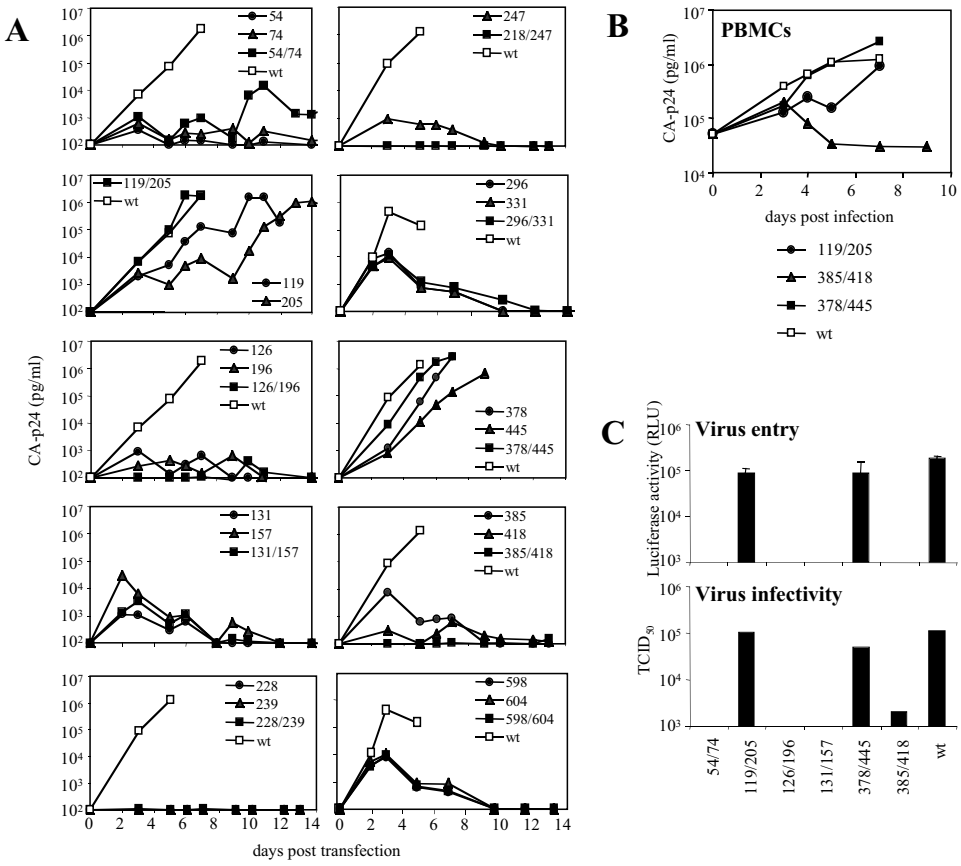

Fig. 4. Replication and infectivity of HIV-1_{LAI} containing cysteine substitutions in Env. **A**. SupT1 cells were transfected with 10 µg pLAI and virus spread was monitored for 14 days using CA-p24 ELISA. **B**. Virus spread in PBMCs was measured after infection with C33A-produced virus (50 ng CA-p24). **C**. Viral entry into LuSIV cells was quantified by measuring luciferase activity 48 hours after infection (upper panel). The infectivities ($TCID_{50}$) in SupT1 cells were measured by endpoint dilution (lower panel). The exact $TCID_{50}$ values of the respective mutants per µg CA-p24 are as follows: 43 (C54A/C74A); 105167 (C119A/C205A); 0 (C126A/C 196A); 0 (C131A/C157A); 50814 (C378A/C445A); 1980 (C385A/C418A) and 111169 (wt).

Variable effects of cysteine mutations on Env function

To investigate the role of particular disulfide bonds in Env function, we analyzed the entry and replication of viruses with wt and mutant Env proteins. SupT1 cells were transfected with infectious molecular clones (pLAI), containing the wt or mutant Env sequences and virus spread was monitored for 14 days by CA-p24 ELISA (Fig. 4A). Note, that the peak at day 3, which is present in many mutants represents transient CA-p24 production and not virus replication. Most mutant viruses did not replicate as was reported earlier for 296-331 mutants (16, 47, 49) and 385-418 mutants (5, 18, 23, 49). For folding incompetent mutants replication deficiency was anticipated, but also some folding competent mutants did not replicate. The lack of 126-196, 131-157 or 598-604 disulfide bonds were incompatible with viral function. In agreement with our results, defective cell entry of C131G and C196V single mutants was reported earlier (49). Likewise, replication deficiency of the 598-604 mutants was in agreement with other studies (10, 46).

Strikingly, viruses lacking the 119-205 or the 378-445 disulfide bond did replicate efficiently. The double mutants C119A/C205A and C378A/C445A replicated with higher efficiency than the corresponding single mutants (Fig. 4A), indicating that an odd number of cysteines in gp120 is disadvantageous for virus replication. The C119A/C205A and C378A/C445A double mutants also replicated with kinetics similar to wt in PBMCs, indicating that these viruses could propagate in natural host cells (Fig. 4B). When an extremely high virus dose was used for infection, a very low level of virus spread could be measured for some of the other cysteine mutants (results not shown). Interestingly, this was most evident for C54A/C74A and C385A/C418A in spite of their folding deficiencies (Fig. 3A).

To establish whether these mutants could mediate viral entry and infectivity, LuSIV cells, which contain a LTR-luciferase reporter construct (41), were infected with the respective viruses. After 48 hrs, luciferase activity was determined as a measure for entry. The $TCID_{50}$ in SupT1 cells was calculated by endpoint dilution as a measure for infectivity. As anticipated, C119A/C205A and C378A/C445A double mutants sustained viral entry and infectivity, almost equally efficiently as wt (Fig. 4C). However, we could not detect any Env activity of the C54A/C74A mutant in the entry assay (Fig. 4C, upper panel). $TCID_{50}$ experiments confirmed that this mutant was virtually non-infectious: more than 3 logs lower than wt (Fig. 4C, lower panel). The C378A/C445A double mutant was also defective in viral entry (Fig. 4C, upper panel), although it displayed some low infectivity (Fig. 4C, lower panel).

Variable incorporation of mutant Env spikes into virions

The lack of replication of the 126-196, 131-157 mutants could be caused by inefficient incorporation of Env proteins, despite proper folding. We therefore measured the incorporation of gp120 in virus particles by using a gp120 ELISA on purified virus fractions. For comparison, we measured the fraction of Env that was retained intracellularly and the fraction of gp120 that was shed into the culture medium. For the wt construct we recovered 14% of the total amount of gp120 from the cell fraction, 21% from the virus fraction, and 65% from the supernatant (results not shown). In comparison we found 17% of CA-p24 protein

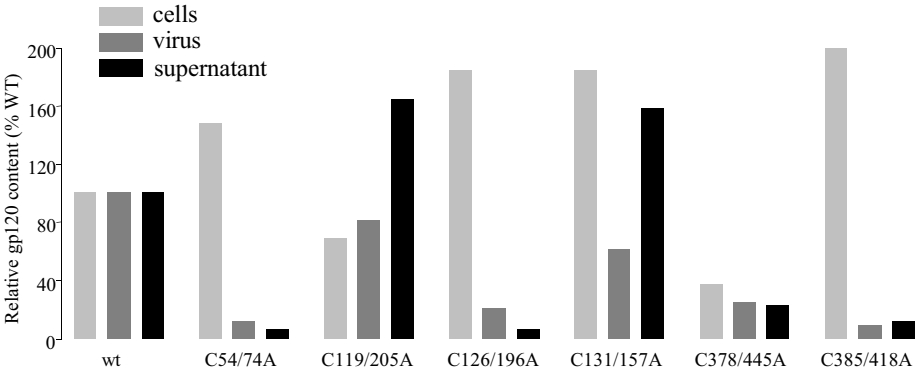

Fig. 5. Gp120 content in cell, virus and supernatant fractions of virus producing cells. gp120 and CA-p24 contents were measured by ELISA. The gp120 amounts were standardized for CA-p24 input and the gp120 contents of mutants in the respective fractions are given as percentages of the wt gp120 contents. Similar results were obtained in independent experiments.

in cells, 58% in the virus, and 25% in the supernatant (results not shown). The differential distribution of gp120 and CA-p24 in the virus fraction *versus* supernatant was indicative for considerable shedding of the LAI gp120 molecules from cells and/or from viruses. We found that the molar Gag-to-Env ratio in the wt virus sample was approximately 100:1. This corresponds to an average of 4-8 trimeric Env spikes per virus particle, which is in accordance with previously published results (8, 31).

As expected, considerable amounts of C119A/C205A Env spikes were incorporated onto virions (Fig. 5). Still, the percentage of incorporated C119A/C205A molecules was slightly lower than wt (~80%), while a higher percentage of gp120 was shed from this mutant into the culture supernatant as compared wt. Incorporation of C378A/C445A spikes into virions and gp120 shedding however was lower than wt, but this correlated with slower folding kinetics of this mutant (Fig. 3A). Low spike density correlated with slightly lower viral entry and infectivity compared to wt (Fig. 4B). Nevertheless, replication in both SupT1 (Fig. 4A) and PBMCs (Fig. 4C) was similar to wt. In accordance with the maturation defects of C54A/C74A and C385A/C418A alike, these mutants accumulated intracellularly, while minimal amounts of gp120 were shed into the medium, and incorporation was ~10-fold lower than wt (Fig. 5). This would amount to less than one spike per virion, explaining the poor infection and replication capacity of these mutants.

The C131A/C157A mutant was incorporated into virions with only slightly lower efficiency than wt (~60%) and more gp120 was shed from this mutant than from wt (Fig. 5). The Env spikes were however dysfunctional, because they could not mediate viral entry or sustain viral infectivity (Fig. 4C). Only very low levels of C126A/C196A Env molecules were incorporated in virus particles or shed into the supernatant (Fig. 5), although the C126A/C196A gp120 variant was secreted with near wt efficiency (table 1).

Discussion

Interference with the disulfide bonded structure of proteins that travel through the ER generally leads to misfolding, aggregation and loss of function. In contrast, Env was remarkably tolerant towards manipulation of its ten disulfide bonds. Two disulfide bonds were completely dispensable for virus replication. Three disulfide bonds were essential for the virus, but dispensable for folding, indicating that ER quality control standards do not necessarily overlap with those of the virus.

The gp120 core folds independently from the gp41 subunit and the V1/V2 region
All Env mutants underwent oxidative folding i.e. at least some molecules of all Env mutants obtained disulfide bond(s). Mutants of disulfide bonds in the gp120 core displayed mild to severe folding problems. Dependent on the mutation, they reached different partially oxidized endpoints, as judged by differences in mobility of these species in non-reduced gels. Altogether, this implies that the gp120 core likely folds in a co-operative manner and that folding of Env as a whole is dependent on the folding of this core. In agreement with such a scenario, conformational antibodies raised against the gp120 core simultaneously recognize the Env structure as it arises in the ER (A. Land, D. Zonneveld and I.B., manuscript in preparation).

In contrast to the gp120 core mutants, mutants of gp41 and the V1/V2 region folded to a native state with similar kinetics as wt. The appearance of a distinct intermediate in the folding process of the V1/V2 mutants could indicate that they have (a minor) folding problem. Apparently, kinetics of completing the disulfide bonded structure of the V1/V2 region were different from wt. Oxidative folding of the V1/V2 could form a kinetic bottleneck for oxidative folding of Env at large when one of the V1/V2 disulfide bonds was absent. That the subtle difference in folding kinetics did not influence productivity of Env folding, implies that folding of the mutagenized domains did not interfere with folding of other domains. Thus, folding of the gp41 and V1/V2 domains must be independent of the folding of the gp120 core.

Misfolding and narrow escapes
Dependent on the consequences for folding and function of their elimination, we clustered the ten disulfide bonds of Env into three classes (Fig. 6): Folding and function incompetent (class I), folding competent, but function incompetent (class II), and folding and function competent (class III). We divided class I into two subclasses. Class Ia contains the disulfide bonds of Env that were absolutely essential for both folding and viral entry: 218-247, 218-239 and 296-331. Similarly as the class Ia mutants the class Ib mutants (of the 54-74 and 385-418 disulfide bonds) only gave rise to partially oxidized Env species, that in majority still contained their signal peptides. Unlike the class Ia mutants, the class Ib double mutants however showed residual functionality.

How can we reconcile misfolding with viral function of Env? On average only a single Env spike or less was incorporated per virus particle in these mutants, which explains why infectivity was low. The fact that these mutants could repli-

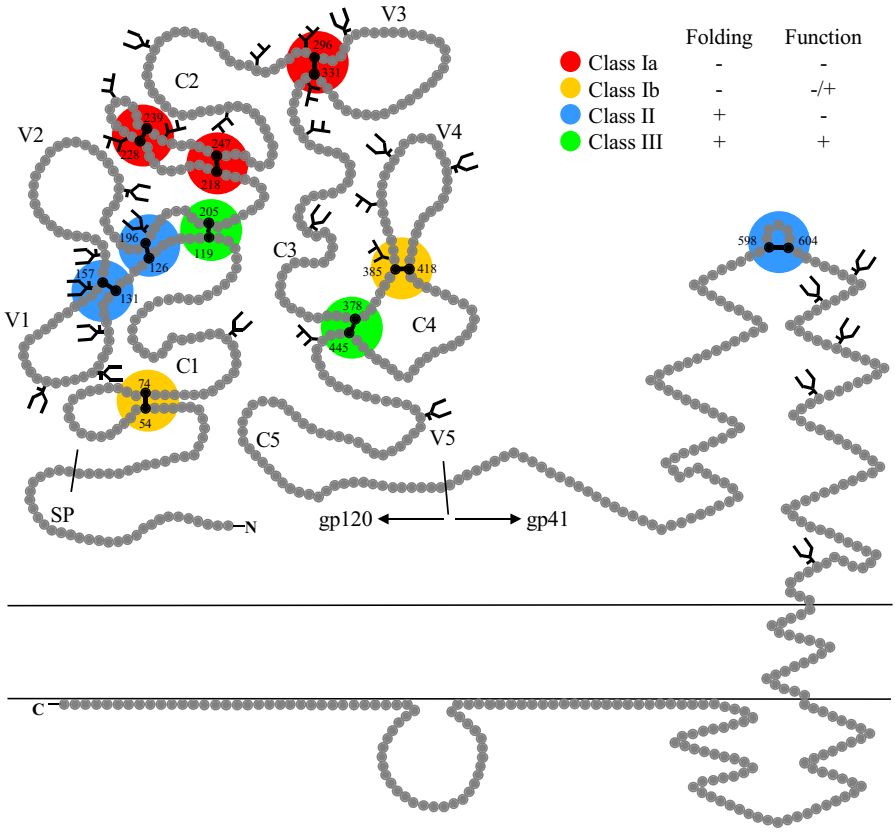

Fig. 6. Classification of disulfide bonds of Env. Based on the effect of their elimination disulfide bonds were clustered in four classes. Class Ia represents disulfide bonds that were both essential for maturation and function Env (depicted in red). Class Ib represents disulfide bonds that are important for folding and function, but whose elimination was still compatible with residual viral functionality of Env (depicted in orange). Class II represents disulfide bonds that were dispensable for folding, yet elementary for the function of Env (depicted in blue). Class III represents disulfide bonds that were both dispensable for maturation and function of Env (depicted in green).

cate at all indicates that the scarce Env spikes that were incorporated into the virus particle were fully functional. Hence, a small minority of mutant Env molecules managed to overcome the folding problems to acquire a native-like conformation and exit from the ER. Thus, the 54-74 and 385-418 disulfide bonds 'only' seem to be relevant for increasing the probability of correct folding.

That mutants of 385-418 are maturation incompetent has been reported earlier (5, 18, 23, 49). That folding capacity of these mutants can easily be restored is supported by the earlier observation that mutagenesis of the 385 cysteine into a valine instead of an alanine allowed residual infectivity (49). Accordingly, we found that *in vitro* evolution of the class Ib mutants readily gave rise to Env revertants with increased replication capacity, while we never observed evolution of Ia mutants (chapters 4.2 and 4.3).

Plasticity of the disulfide bonded structure of Env

Since all mutants differed from wt at least by the lack of one disulfide bond, one could argue that none of the mutants could ever fold correctly, depending on the definition of 'correct folding'. For the class III mutants, i.e. mutants of disulfide bonds 119-205 and 378-445, this argument is perhaps too academic, since they must have folded to a structure comparable enough to wt to maintain their function. Similarly, a replicating SIV could be generated lacking 100 amino-acids within gp120, including two absolutely conserved cysteines (20).

The dispensability of these disulfide bonds raises the question why they have been conserved during viral evolution. The loss of disulfide bonds during evolution would necessarily involve Env variants with odd cysteines, because simultaneous pair-wise elimination of cysteines is very unlikely to occur. We found that the single mutants of these disulfide bonds replicated with lower efficiency than the corresponding double mutants. This may imply that a single cysteine intermediate could be too much of an obstacle on the evolutionary path towards Env variants lacking a disulfide bond altogether, and hence would rule out their occurrance. Alternatively, these two disulfide bonds contribute to the strict integrity of the outer antigenic shield that disguises the susceptible core of Env. In such a scenario, these two disulfide bonds would be important for immune evasion and their relevance would become manifest only during natural infection.

Apart from its tolerance to disulfide bond deletions, the plasticity of the Env structure is further illustrated by its leniency towards insertion of additional disulfide bonds. Nature itself provides us with a few good examples. In some HIV-1 isolates extra cysteine pairs were found in the V1 and V4 regions and, in HIV-2 and SIV isolates, also in the V2 region and the gp41 ectodomain (26, 43, 50). In addition, it is possible to introduce a non-native disulfide bond between the gp120 C5 region and gp41. This intersubunit disulfide bond renders the protein non-functional, but upon reduction of the disulfide bond it is fully active, indicating that folding is unaffected by this extra cysteine pair (1, 3, 4). Still, engineering additional disulfide bonds into Env is not easy. Cysteine pairs were introduced in the gp120 core at distances sufficiently close to covalently link the inner and outer domains by disulfide bonds. Although these mutants correctly folded as indicated by X-ray crystallography studies, the intended additional disulfide bonds did not form (P. Kwong, personal communication).

Envelope mutants expose fallibility of the ER quality control mechanisms

Disulfide bonds of class II, 126-196, 131-157 in the V1/V2 region and 598-604 in gp41, were essential for the virus, although mutants of these disulfide bonds folded as efficiently as wt. Although we still need to confirm that the gp41 mutants could leave the ER, exit was evident for the V1/V2 mutants. Cleavage of the gp160 precursor into gp120 and gp41, which occurs in the Golgi complex, is impaired for 598-604 mutants (10, 46), explaining their loss of function. Efficient cleavage of the gp160 precursor was however reported for a C131G and a C196V mutant (49) and we witnessed shedding from C131A/C157A, and residually from C126A/C196A. The V1/V2 class II mutants therefore had structural defects other than the gp41 mutants. The quality control mechanisms in the ER however must have failed to detect their defects. Apparently, Quality Control standards for

'foldedness' are no guarantee for functionality of the 'folded' proteins.

Central to ER quality control of glycoproteins stands the folding sensor UDP-glucose:glycoprotein glucosyltransferase (UGGT). It probes the folded state of the maturing ER substrates by interacting with both their *N*-glycans and peptide backbones. Even minor local deviations from the native state trigger UGGT to reglucosylate *N*-glycans, which in turn sentences the incompletely folded molecules to (re-)associate with calnexin or calreticulin for an additional folding cycle (14). UGGT however fails to recognize unstructured peptides (40, 48). The V1/V2 region is highly flexible (Shang-Te Hsu and Alexandre Bonvin, manuscript in preparation) and very hydrophilic, which may explain why UGGT failed to recognize structural shortcomings of this region.

Apart from the retention of incompletely folded proteins, quality control must ensure that terminally misfolded proteins are cleared from the ER lumen. Remarkably, none of the mutants were prone to aggregation or seemed to be degraded via ERAD, even though for the mutants of class I and II the majority of Env molecules never reached a native-like state and were likely beyond rescue. Apparently, quality control failed to discriminate these mutants as misfolded species. The ER folding machinery seemed to treat them as rather *bona fide* folding intermediates, irrespective of whether some domains had not folded yet or whether they never would. The most oxidized species of these mutants did not appear as discrete bands, but were fuzzy instead. In line with the idea of ongoing folding attempts, the 'fuzziness' of these bands could reflect incessant disulfide bond isomerization, which is characteristic for the folding pathway of wt Env as well (22).

Glycans of ER substrates are exploited by the quality control to distinguish genuine folding intermediates from misfolded proteins. High mannose glycans on partially folded ER substrates allow association of the ER chaperones calnexin and calreticulin. In that way, immature molecules remain substrate to the 'on-road' folding pathway. By an as yet poorly understood mechanism, a mannose monosaccharide unit is trimmed from the middle branch of *N*-glycans on terminally misfolded ER clients by ER resident mannosidases (7). By virtue of their trimmed mannoses, misfolded proteins are transferred from calnexin to the mannose lectin EDEM. This transfer targets misfolded proteins to the 'off-road' pathway that ultimately results in ERAD (14). Because of the abundance of glycans that decorate Env, complete mannose trimming of misfolded Env species may be difficult to achieve for the mannosidase. Since release from calnexin seems necessary for sequestering of ERAD candidates by EDEM (27, 32), dislocation from the ER lumen could be impeded. That viral envelope proteins on average are extensively glycosylated, could explain in such a scenario why they are poor ERAD substrates. Because ERAD furnishes peptides for antigenic presentation by MHC molecules, it indeed may be fortuitous for viruses to safeguard their envelope glycoproteins from ERAD.

Acknowledgements

We thank members of the Braakman and Berkhout group for helpful discussions and Aafke Land in particular for sharing her expertise in folding assays for Env. We thank Stephan Heynen for technical assistance. In addition, we thank Peter

Kwong, Shang-Te Hsu and Alexandre Bonvin for sharing unpublished data. We are grateful to James Binley for the gift of HIVIg, Norbert Schülke and Bill Olson for the gift of recombinant gp120 and Janice Clements for the donation of LuSIV cells. This work was supported by grants from NWO-MW (EvA, IB) and the Dutch AIDS fund (IB, BB)

References

1. **Abrahamyan, L. G., R. M. Markosyan, J. P. Moore, F. S. Cohen, and G. B. Melikyan** 2003. Human immunodeficiency virus type 1 Env with an intersubunit disulfide bond engages coreceptors but requires bond reduction after engagement to induce fusion. J. Virol. **77:**5829-36.
2. **Allen, J., T. H. Lee, M. F. McLane, J. Sodroski, W. Haseltine, and M. Essex** 1983. Identification of the major envelope glycoprotein product of HTLV-III. Science. **228:**1091-1094.
3. **Binley, J. M., C. S. Cayanan, C. Wiley, N. Schulke, W. C. Olson, and D. R. Burton** 2003. Redox-triggered infection by disulfide-shackled human immunodeficiency virus type 1 pseudovirions. J. Virol. **77:**5678-84.
4. **Binley, J. M., R. W. Sanders, B. Clas, N. Schuelke, A. Master, Y. Guo, F. Kajumo, D. J. Anselma, P. J. Maddon, W. C. Olson, and J. P. Moore** 2000. A recombinant human immunodeficiency virus type 1 envelope glycoprotein complex stabilized by an intermolecular disulfide bond between the gp120 and gp41 subunits is an antigenic mimic of the trimeric virion-associated structure. J. Virol. **74:**627-43.
5. **Bolmstedt, A., A. Hemming, P. Flodby, P. Berntsson, B. Travis, J. P. Lin, J. Ledbetter, T. Tsu, H. Wigzell, S. L. Hu, and et al.** 1991. Effects of mutations in glycosylation sites and disulphide bonds on processing, CD4-binding and fusion activity of human immunodeficiency virus envelope glycoproteins. J. Gen. Virol. **72:**1269-77.
6. **Braakman, I., H. Hoover-Litty, K. R. Wagner, and A. Helenius** 1991. Folding of influenza hemagglutinin in the endoplasmic reticulum. J. Cell Biol. **114:**401-11.
7. **Cabral, C. M., Y. Liu, and R. N. Sifers** 2001. Dissecting glycoprotein quality control in the secretory pathway. Trends Biochem. Sci. **26:**619-24.
8. **Chertova, E., J. W. Bess Jr, Jr., B. J. Crise, I. R. Sowder, T. M. Schaden, J. M. Hilburn, J. A. Hoxie, R. E. Benveniste, J. D. Lifson, L. E. Henderson, and L. O. Arthur** 2002. Envelope glycoprotein incorporation, not shedding of surface envelope glycoprotein (gp120/SU), Is the primary determinant of SU content of purified human immunodeficiency virus type 1 and simian immunodeficiency virus. J. Virol. **76:**5315-25.
9. **Das, A. T., A. Land, I. Braakman, B. Klaver, and B. Berkhout** 1999. HIV-1 evolves into a nonsyncytium-inducing virus upon prolonged culture *in vitro*. Virology **263:**55-69.
10. **Dedera, D., R. L. Gu, and L. Ratner** 1992. Conserved cysteine residues in the human immunodeficiency virus type 1 transmembrane envelope protein are essential for precursor envelope cleavage. J. Virol. **66:**1207-9.
11. **Doms, R. W., and J. P. Moore** 2000. HIV-1 membrane fusion: targets of opportunity. J. Cell Biol. **151**:F9-14.
12. **Earl, P. L., B. Moss, and R. W. Doms** 1991. Folding, interaction with GRP78-BiP, assembly, and transport of the human immunodeficiency virus type 1 envelope protein. J. Virol. **65:**2047-55.
13. **Eckert, D. M., and P. S. Kim** 2001. Mechanisms of viral membrane fusion and its inhibition. Annu. Rev. Biochem. **70:**777-810.
14. **Ellgaard, L., and A. Helenius** 2003. Quality control in the endoplasmic reticulum. Nat. Rev. Mol. Cell Biol. **4:**181-91.
15. **Fewell, S. W., K. J. Travers, J. S. Weissman, and J. L. Brodsky** 2001. The action of molecular chaperones in the early secretory pathway. Annu. Rev. Genet. **35:**149-91.
16. **Freed, E. O., and R. Risser** 1991. Identification of conserved residues in the human immunodeficiency virus type 1 principal neutralizing determinant that are involved in fusion. AIDS Res. Hum. Retroviruses. **7:**807-11.

17. **Fuerst, T. R., E. G. Niles, F. W. Studier, and B. Moss** 1986. Eukaryotic transient-expression system based on recombinant vaccinia virus that synthesizes bacteriophage T7 RNA polymerase Proc. Natl. Acad. Sci. USA **83:**8122-6.
18. **Hemming, A., A. Bolmstedt, P. Flodby, L. Lundberg, M. Gidlund, H. Wigzell, and S. Olofsson** 1989. Cystein 402 of HIV gp 120 is essential for CD4-binding and resistance of gp 120 to intracellular degradation. Arch. Virol. **109:**269-76.
19. **Jeeninga, R. E., M. Hoogenkamp, M. Armand-Ugon, M. de Baar, K. Verhoef, and B. Berkhout** 2000. Functional differences between the long terminal repeat transcriptional promoters of human immunodeficiency virus type 1 subtypes A through G. J. Virol. **74:**3740-51.
20. **Johnson, W. E., J. Morgan, J. Reitter, B. A. Puffer, S. Czajak, R. W. Doms, and R. C. Desrosiers** 2002. A replication-competent, neutralization-sensitive variant of simian immunodeficiency virus lacking 100 amino-acids of envelope. J. Virol. **76:**2075-86.
21. **Kwong, P. D., R. Wyatt, J. Robinson, R. W. Sweet, J. Sodroski, and W. A. Hendrickson** 1998. Structure of an HIV gp120 envelope glycoprotein in complex with the CD4 receptor and a neutralizing human antibody. Nature. **393:**648-59.
22. **Land, A., D. Zonneveld, and I. Braakman** 2003. Folding of HIV-1 envelope glycoprotein involves extensive isomerization of disulfide bonds and conformation-dependent leader peptide cleavage. FASEB J. **17:**1058-67.
23. **Lekutis, C., U. Olshevsky, C. Furman, M. Thali, and J. Sodroski** 1992. Contribution of disulfide bonds in the carboxyl terminus of the human immunodeficiency virus type I gp120 glycoprotein to CD4 binding. J. Acquir. Immune Defic. Syndr. **5:**78-81.
24. **Leonard, C. K., M. W. Spellman, L. Riddle, R. J. Harris, J. N. Thomas, and T. J. Gregory** 1990. Assignment of intrachain disulfide bonds and characterization of potential glycosylation sites of the type 1 recombinant human immunodeficiency virus envelope glycoprotein (gp120) expressed in Chinese hamster ovary cells. J. Biol. Chem. **265:**10373-82.
25. **Li, Y., L. Luo, D. Y. Thomas, and C. Y. Kang** 1994. Control of expression, glycosylation, and secretion of HIV-1 gp120 by homologous and heterologous signal sequences. Virology. **204:**266-78.
26. **Mokili, J. L., M. Rogers, J. K. Carr, P. Simmonds, J. M. Bopopi, B. T. Foley, B. T. Korber, D. L. Birx, and F. E. McCutchan** 2002. Identification of a novel clade of human immunodeficiency virus type 1 in Democratic Republic of Congo. AIDS Res. Hum. Retroviruses. **18:**817-23.
27. **Molinari, M., V. Calanca, C. Galli, P. Lucca, and P. Paganetti** 2003. Role of EDEM in the release of misfolded glycoproteins from the calnexin cycle. Science. **299:**1397-400.
28. **Moore, J. P., and D. D. Ho** 1993. Antibodies to discontinuous or conformationally sensitive epitopes on the gp120 glycoprotein of human immunodeficiency virus type 1 are highly prevalent in sera of infected humans. J. Virol. **67:**863-75.
29. **Moore, J. P., P. W. Parren, and D. R. Burton** 2001. Genetic subtypes, humoral immunity, and human immunodeficiency virus type 1 vaccine development. J. Virol. **75:**5721-9.
30. **Moulard, M., and E. Decroly** 2000. Maturation of HIV envelope glycoprotein precursors by cellular endoproteases. Biochim. Biophys. Acta. **1469:**121-32.
31. **O'Brien, W. A., S. H. Mao, Y. Cao, and J. P. Moore** 1994. Macrophage-tropic and T-cell line-adapted chimeric strains of human immunodeficiency virus type 1 differ in their susceptibilities to neutralization by soluble CD4 at different temperatures. J. Virol. **68:**5264-9.
32. **Oda, Y., N. Hosokawa, I. Wada, and K. Nagata** 2003. EDEM as an acceptor of terminally misfolded glycoproteins released from calnexin. Science. **299:**1394-7.
33. **Otteken, A., P. L. Earl, and B. Moss** 1996. Folding, assembly, and intracellular trafficking of the human immunodeficiency virus type 1 envelope glycoprotein analyzed with monoclonal antibodies recognizing maturational intermediates. J. Virol. **70:**3407-15.
34. **Otteken, A., and B. Moss** 1996. Calreticulin interacts with newly synthesized human immunodeficiency virus type 1 envelope glycoprotein, suggesting a chaperone function similar to that of calnexin. J. Biol. Chem. **271:**97-103.
35. **Ou, W. J., J. J. Bergeron, Y. Li, C. Y. Kang, and D. Y. Thomas** 1995. Conformational changes induced in the endoplasmic reticulum luminal domain of calnexin by Mg-ATP and Ca2+. J. Biol. Chem. **270:**18051-9.
36. **Parren, P. W., D. R. Burton, and Q. J. Sattentau** 1997. HIV-1 antibody—debris or virion? Nat. Med. **3:**366-7.

37. **Peden, K., M. Emerman, and L. Montagnier** 1991. Changes in growth properties on passage in tissue culture of viruses derived from infectious molecular clones of HIV-1LAI, HIV-1MAL, and HIV-1ELI. Virology **185:**661-72.
38. **Plemper, R. K., and D. H. Wolf** 1999. Retrograde protein translocation: ERADication of secretory proteins in health and disease. Trends Biochem. Sci. **24:**266-70.
39. **Poignard, P., E. O. Saphire, P. W. Parren, and D. R. Burton** 2001. gp120: Biologic aspects of structural features. Annu. Rev. Immunol. **19:**253-74.
40. **Ritter, C., and A. Helenius** 2000. Recognition of local glycoprotein misfolding by the ER folding sensor UDP-glucose:glycoprotein glucosyltransferase. Nat. Struct. Biol. **7:**278-80.
41. **Roos, J. W., M. F. Maughan, Z. Liao, J. E. Hildreth, and J. E. Clements** 2000. LuSIV cells: a reporter cell line for the detection and quantitation of a single cycle of HIV and SIV replication Virology **273:**307-15.
42. **Sanders, R. W., M. Venturi, L. Schiffner, R. Kalyanaraman, H. Katinger, K. O. Lloyd, P. D. Kwong, and J. P. Moore** 2002. The mannose-dependent epitope for neutralizing antibody 2G12 on human immunodeficiency virus type 1 glycoprotein gp120. J. Virol. **76:**7293-305.
43. **Santiago, M. L., F. Bibollet-Ruche, E. Bailes, S. Kamenya, M. N. Muller, M. Lukasik, A. E. Pusey, D. A. Collins, R. W. Wrangham, J. Goodall, G. M. Shaw, P. M. Sharp, and B. H. Hahn** 2003. Amplification of a complete simian immunodeficiency virus genome from fecal RNA of a wild chimpanzee. J. Virol. **77:**2183-42.
44. **Stein, B. S., and E. G. Engleman** 1990. Intracellular processing of the gp160 HIV-1 envelope precursor. Endoproteolytic cleavage occurs in a cis or medial compartment of the Golgi complex. J. Biol. Chem. **265:**2640-9.
45. **Stevens, F. J., and Y. Argon** 1999. Protein folding in the ER. Semin. Cell. Dev. Biol. **10:**443-54.
46. **Syu, W. J., W. R. Lee, B. Du, Q. C. Yu, M. Essex, and T. H. Lee** 1991. Role of conserved gp41 cysteine residues in the processing of human immunodeficiency virus envelope precursor and viral infectivity. J. Virol. **65:**6349-52.
47. **Travis, B. M., T. I. Dykers, D. Hewgill, J. Ledbetter, T. T. Tsu, S. L. Hu, and J. B. Lewis** 1992. Functional roles of the V3 hypervariable region of HIV-1 gp160 in the processing of gp160 and in the formation of syncytia in CD4+ cells. Virology **186:**313-7.
48. **Trombetta, E. S., and A. Helenius** 2000. Conformational requirements for glycoprotein reglucosylation in the endoplasmic reticulum. J. Cell Biol. **148:**1123-29.
49. **Tschachler, E., H. Buchow, R. C. Gallo, and M. S. Reitz, Jr.** 1990. Functional contribution of cysteine residues to the human immunodeficiency virus type 1 envelope. J. Virol. **64:**2250-9.
50. **Wang, W. K., M. Essex, and T. H. Lee** 1996. Single amino-acid substitution in constant region 1 or 4 of gp120 causes the phenotype of a human immunodeficiency virus type 1 variant with mutations in hypervariable regions 1 and 2 to revert. J. Virol. **70:**607-11.
51. **Wyatt, R., and J. Sodroski** 1998. The HIV-1 envelope glycoproteins: fusogens, antigens, and immunogens. Science. **280:**1884-8.

Chapter 4.2

A stable β-sheet fold can substitute for a disulfide bond in HIV-1 gp120

Rogier W. Sanders[1], Shang-Te D. Hsu[2], Eelco van Anken[3], Marije Liscaljet[3], Sonja Tillemans[3], Els Busser[1], Martijn Dankers[1], Ineke Braakman[3], Alexandre M. J. J. Bonvin[2], Ben Berkhout[1]

[1]Dept. of Human Retrovirology, Academic Medical Center, University of Amsterdam, Meibergdreef 15, 1105 AZ Amsterdam, The Netherlands

[2]Dept. NMR Spectroscopy, Bijvoet Center for Biomolecular Research, Utrecht University, Padualaan 8, 3584 CH Utrecht, The Netherlands

[3]Dept. Bio-organic chemistry, Bijvoet Center for Biomolecular Research, Utrecht University, Padualaan 8, 3584 CH Utrecht, The Netherlands

Protein folding is studied at several levels. First, the formation of secondary structure elements such as α-helices and β-sheets can be investigated. Second, the acquisition of tertiary structure and disulfide bonds during oxidative folding in the endoplasmic reticulum (ER) *in vivo* can be studied. Third, one can analyze the results of a completed folding process as a protein is secreted or expressed at the cell surface, the ultimate test being the analysis of function. The correlates of these different levels of protein folding are mostly unclear. We generated an HIV-1 gp120 variant through virus evolution that is functional despite the lack of the disulfide bond at the base of the V4 domain that is otherwise required for virus replication and gp120 activity. Biochemical and computational analyses indicate that virus replication is restored through the improvement of local hydrogen bonding and stabilization of a local β-sheet fold. This study provides proof that a critically important disulfide bond can be functionally replaced by an alternative protein structure motif. It also provides evidence for the proposal that local protein stability is an important factor in escape from ER quality control during protein biosynthesis. Furthermore, our data indicate that β-sheet preference is a determinant in directing protein stability and protein folding *in vivo* and that β-sheet rules deduced from experiments with small model proteins also hold for the intricate chaperone-assisted folding of a complicated glycoprotein such as gp120.

Introduction

The HIV-1 envelope glycoprotein complex (Env) mediates viral attachment and entry in susceptible cells. The surface subunit (SU; gp120) sequentially binds the CD4 receptor and either CCR5 or CXCR4 as a coreceptor (41, 60). Subsequent conformational changes result in fusion of viral and cellular membranes, mediated by the transmembrane glycoprotein (TM; gp41) (13, 18). Env is synthesized as a gp160 precursor protein, which is cotranslationally translocated into the

endoplasmic reticulum (ER). Here, Env acquires carbohydrate chains and disulfide bonds, it folds, trimerizes and looses its leader peptide (30). Like folding of any other glycoprotein, gp160 folding is assisted by molecular chaperones. gp160 transiently associates with the ER resident chaperones BiP, calnexin and calreticulin (12, 26, 39). Subsequently, gp160 is transported to the Golgi complex where it is cleaved into gp120 and gp41, which stay associated non-covalently (38, 54). In addition, part of the ~30 carbohydrates are modified here (31).

Most proteins have the intrinsic capacity to acquire their unique three-dimensional structure in a spontaneous and autonomous manner, depending only on the amino-acid sequence and a native environment (22). It was assumed that folding rules based on *in vitro* folding experiments with small model proteins could be applied to the description of protein folding in living cells. However, complicated proteins need assistance from chaperones to fold properly and there is no direct evidence that these simple folding rules also apply to chaperone–assisted protein folding in the ER.

We have previously studied the role of individual disulfide bonds in oxidative Env folding. Five out of ten disulfide bonds were dispensable for folding. Surprisingly, two were also largely dispensable for Env function and viral replication. The remaining five disulfide bonds were required for proper oxidative folding of Env in the ER. The advantage of using Env over other models for glycoprotein folding is that HIV-1 provides the possibility for protein evolution when a mutant protein is tested in replication competent HIV-1. We used virus-driven protein evolution to further characterize the significance and role of specific disulfide bonds. In the current study, we describe an escape variant of an Env mutant lacking the conserved disulfide bond at the base of the V4 domain. This disulfide bond excludes the V4 loop from the gp120 core and is required for proper oxidative folding of wt gp120 and virus replication. In the evolved variant, the role of the disulfide bond during folding is replaced by increased local hydrogen bonding within a β-sheet fold, which results in an escape from ER quality control and restored virus replication.

Materials and Methods

Cloning

The pRS1, pcDNA3-Env-gp120 and pLAI plasmids containing the appropriate mutations in the *env* gene were generated as described previously (chapter 4.1). PCR-generated gp120 sequences from evolved viruses (see below) were cloned into the pRS1 shuttle vector using the *Bsa*B1 and *Nhe*1 sites and subsequently cloned into the pLAI infectious molecular clone (40) as *Sal*I-*Bam*HI fragments. *Not*I-*Xho*I fragments were subcloned into the pcDNA3 expression vector for use in folding experiments. Numbering of individual amino-acids is based on the sequence of HXB2 gp160.

Cells and transfections

HeLa cells (ATCC) and HT1080 cells were cultured in MEM (Life technologies) supplemented with 10% FCS (Hybond), penicillin (100 U/ml), streptomycin (100 µg/ml). Peripheral blood mononuclear cells (PBMCs) were isolated from buffy

coats from healthy individuals by Ficoll-Isopaque density centrifugation. PBMCs were cultured for three days in RPMI medium (Life Technologies Ltd., Paisley, UK) supplemented with 10% FCS, penicillin (100 U/ml), streptomycin (100 µg/ml) and phytohemagglutinin (PHA; 5 µg/ml) and subsequently cultured without PHA, but with IL-2 (100 U/ml). SupT1 cells were cultured in RPMI medium supplemented with 10% FCS, penicillin and streptomycin. LuSIV cells were cultured in RPMI medium supplemented with 10% FCS, penicillin, streptomycin and hygromycin B (44). C33A cervix carcinoma cells were maintained in DMEM (Life Technologies), supplemented with 10% FCS, penicillin and streptomycin, as previously described (45). SupT1 and C33A cells were transfected with pLAI by electroporation and $Ca_3(PO_4)_2$ precipitation, respectively, as described previously (9).

Viruses and infections

Virus stocks were produced by transfecting C33A cells with the appropriate pLAI constructs. The virus containing supernatant was harvested 3 days post-transfection, filtered and stored at -80ºC and the virus concentration was quantitated by capsid CA-p24 ELISA as described previously (23). These values were used to normalize the amount of virus in subsequent infection experiments. Infection experiments were performed as follows. $50x10^3$ SupT1 T cells or PBMCs were infected with 20 or 500 ng CA-p24, respectively, of C33A-produced HIV-1_{LAI} per well in a 24-well plate, and virus spread was measured for 14 days using CA-p24 ELISA.

Virus evolution

For evolution experiments, SupT1 cells were transfected with 10 µg pLAI constructs by electroporation, and virus cultures were inspected regularly for the emergence of revertant viruses by CA-p24 ELISA and/or the appearance of syncytia. At regular intervals, cells and filtered supernatant were stored at -80ºC and virus was quantitated by CA-p24 ELISA. When a revertant virus was identified, DNA was extracted from infected cells (10) and proviral gp120 sequences were PCR-amplified with primers A (5'-GCTCCATGGCTTAGGGCAACATATATCTATG-3') and B (5'-GTCTCGAGATGCTGCTCC -3') and sequenced.

Virus entry, infectivity and neutralization

LuSIV cells, stably transfected with an LTR-luciferase construct (44), were infected with 200 ng CA-p24/$300x10^3$ cells/ml in a 48 well plate. Cells were maintained in the presence of 200 nM saquinavir to prevent additional rounds of virus replication. Luciferase activity was measured after 48 hrs. Neutralization experiments were performed similarly, but virus was preincubated for 30 min at room temperature, with the appropriate concentration of either monoclonal antibody 2G12 (4, 46, 50, 56) or IgG1b12 (3, 48). The 50% tissue culture infectious dose ($TCID_{50}$) was determined by endpoint dilution.

Quantitation of gp120 in cell, virion and supernatant fractions

C33A cells were transfected with 40 µg pLAI per T75 flask. Medium was refreshed at day one post-transfection. The culture supernatant was harvested at

3 days post-transfection, centrifuged and passed through a 0.45 µm filter to remove residual cells and debris. Cells were resuspended in 1.0 ml lysis buffer (50mM Tris (pH 7.4) 10mM EDTA, 100mM NaCl, 1% SDS). Virus particles were pelleted by ultracentrifugation (100.000 *g* for 45 min at 4°C) and resuspended in 0.5 ml lysis buffer. The virus free supernatant, containing gp120 shedded from the cell and virion surface, was concentrated using Amicon centrifugal filter units (Millipore, Bedford, MA) and SDS was added to a 1% end concentration.

Gp120 in cell, virion and supernatant fractions was measured as described previously (37, 46), with minor modifications. ELISA plates were coated overnight with sheep antibody D7324 (10 µg/ml; Aalto Bioreagents, Ratharnham, Dublin, Ireland), directed to the gp120 C5 region, in 0.1 M $NaHCO_3$. After blocking with 2% milk in Tris-buffered saline (TBS) for 30 min, gp120 was captured by incubation for 2 hr at room temperature. Recombinant HIV-1_{LAI} gp120 (Progenics Pharmaceuticals, Inc. Tarrytown, NY) was used as a reference. Unbound gp120 was washed away with TBS and purified serum Ig from an HIV-1 positive individual (HIVIg) was added for 1.5 hr in 2% milk, 20% sheep serum (SS), 0.5% Tween-20. HIVIg binding was detected with alkaline phosphatase conjugated goat anti-human Fc (1:10000, Jackson Immunoresearch, West Grove, PA) in 2% milk, 20% SS, 0.5% Tween-20. Detection of alkaline phosphatase activity was performed using AMPAK reagents (DAKO, Carpinteria, CA). The measured gp120 contents in cells, virus and supernatant were normalized for CA-p24.

Env folding

For folding assays, mutant gp120 was expressed using a recombinant Vaccinia virus vector system (chapter 4.1). Folding of gp120 mutants was analyzed by pulse-chase labeling and immunoprecipition with anti-Env sera as described (chapter 4.1)(30). Formation of disulfide bonds was assayed by SDS-PAGE mobility changes of deglycosylated, alkylated, non-reduced samples. Reduced samples were used to follow signal sequence cleavage.

Molecular dynamics simulations

The starting structures were generated with SWISS-MODEL (19) using modeling templates as structural analogs (PDB entries 1G9M, 1GC1 for the HXB2 isolate (28, 29) and 1G9N for the YU2 isolate (28). The flexible N- and C-termini and the hypervariable V1, V2 and V3 loops, which are missing in the crystal structures, were not included to limit the size of the simulations. The missing V4 loop was modeled by SWISS-MODEL. In addition to the wild-type sequence of HXB2 (wt), point mutations were introduced *in silico* by modifying the input primary sequences for model generations. Four variants were used in this study: the inactive mutant: C385A/C418A; the active revertant: C385A C418V T415I; the corresponding core sequence of LAI isolate; and the HXB2 core sequence with all cysteine residues replaced by alanines.

The GROMACS 3.0 molecular dynamics package (33) was used with the GROMOS 43A1 force field (11). Starting structures were solvated using the single point charge (SPC) water model (2) in a periodic cubic box with a 1.4 nm solute-wall minimum distance. After a first steepest descent energy minimization with positional restraints on the solute, chloride ions were introduced in all three

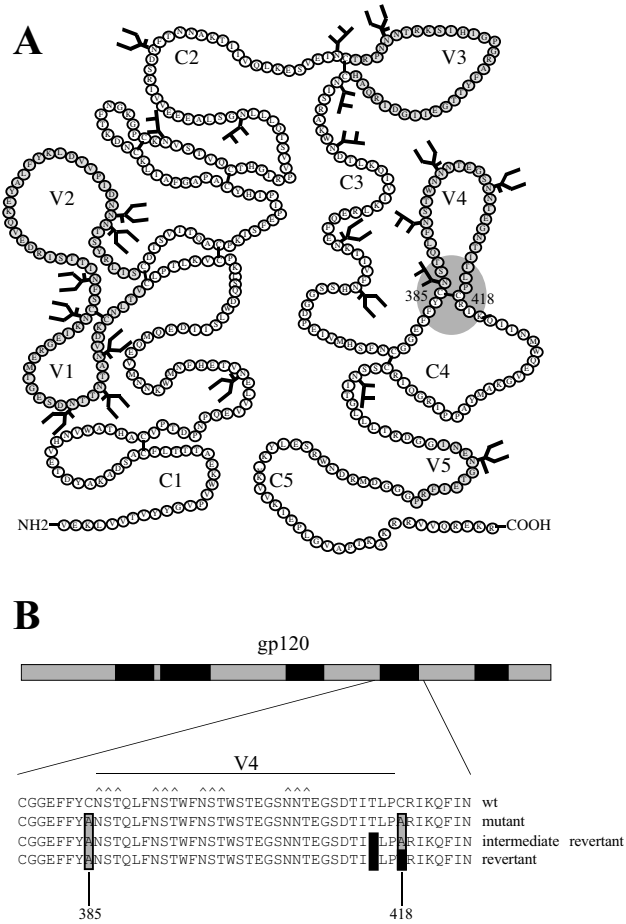

Fig. 1. Local reversion in HIV-1 gp120. **A.** Schematic of gp120 with the 5 conserved domains (C1-C5 and five variable domains (V1-V5). The location of the V4 base disulfide bond is indicated (grey sphere). *Fig.* is adapted from (31). Sites for *N*-linked glycosylation are given. **B.** Sequences of the V4 loop and flanking regions of wt, mutant and revertant viruses. No mutations were found outside this region. The original mutations are indicated with grey boxes, the reversion with black boxes. *N*-linked glycosylation sites are indicated by (^^^).

systems to obtain an electro-neutralized system. The resulting systems are comprised of 317 amino-acids and about 30,500 water molecules that give a total number of about 93,900 atoms. A second energy minimization was then performed, followed by five successive 20 ps MD runs with decreasing positional restraint force constants on the solutes (K_{posres} = 1000, 1000, 100, 10 and 0 kJ mol^{-1} nm^{-2}) prior to the production runs.

The simulations were run for a period of 10 ns at 300K and 1 atm for all variants except for the core LAI gp120 (5ns). Short 1 ns simulations at 400K and 1atm were performed starting from different time points of the 300K simulations (1, 1.5 and 2 ns) for all variants to assess their thermostability. Furthermore, 10 ns simulation at 400K and 1 atm were carried out for the wt, mutant and rever-

tant core gp120s starting from configurations taken at 2 ns of the 300K simulations. For all simulations, solute, solvent and counterions were weakly coupled independently to reference temperature and pressure baths (1). Non-bonded interactions were calculated using twin range cutoffs of 0.8 and 1.4 nm. Long range electrostatic interactions beyond the cutoff were treated with the generalized reaction field model using a dielectric constant of 54 (55). A 4 fs integration time step was used in conjunction with dummy atoms (16). Bond lengths were constrained with the LINCS algorithm (20). The simulations required about 50 hours per nanosecond in parallel on four 1.3 GHz AMD CPUs.

Results

Evolution of gp120 lacking the conserved disulfide bond at the base of the V4
In our previous work we found that five out of ten absolutely conserved disulfide bonds are essential for the oxidative folding of the HIV-1 Env protein. However, for some mutants that were folding incompetent we could still observe a minimal but reproducible infectivity when placed in a replicating virus, although not sufficient to cause a spreading infection (class Ib, chapter 4.1). One of these mutants was the C385A/C418A double mutant, lacking the disulfide bond at the base of the V4 variable loop (Fig. 1A). This virus appeared to be a good candidate for protein evolution studies, with the aim of identifying and investigating escape routes that result in restoration of gp120 folding and virus replication. After prolonged culturing (80 days) on SupT1 T cells, we identified a replicating virus in a culture of the C385A/C418A mutant virus. Proviral *env* sequences were PCR-amplified and sequenced. Population sequencing revealed two reversions: a first-site pseudoreversion A418V and a second-site reversion at a nearby residue: T415I (Fig. 1B). Thus, the wt cysteine at position 418 is not restored, which may be caused by the design of the mutant alanine codon, which requires at least two point mutation to become a cysteine codon. This combined with the fact that the original C385A substitution was still present implies that the disulfide bond at the base of the V4 is not restored. Sequencing of individual *env* clones revealed several with only the T415I reversion, implying that this mutation appeared first during the course of evolution (Fig. 1). For simplicity we will hereafter refer to the respective variants as mutant (C385A/C418A), intermediate revertant (C385A/C418A T415I) and revertant (C385A C418V T415I).

To establish whether the identified substitutions accounted for the revertant phenotype, the relevant *env* fragments were subcloned into a molecular clone of HIV-1_{LAI}. Virus stocks were produced by DNA transfection of non-susceptible C33A cells. SupT1 T cells were infected with wt, mutant and revertant viruses and virus spread was monitored by CA-p24 ELISA (Fig. 2A). The C385A/C418A mutant virus did not cause a spreading infection (chapter 4.1). The intermediate revertant (C385A/C418A T415I) replicated poorly, and revertant (C385A C418V T415I) showed greatly improved replication, although it was still somewhat impaired compared to the wt virus. Similar results were obtained in primary cells, indicating that the revertant phenotype is not specific for the SupT1 T cell line that was used for the evolution experiment (Fig. 2B). The differences in viral replication could not be attributed to differences in virus production, since the virus pro-

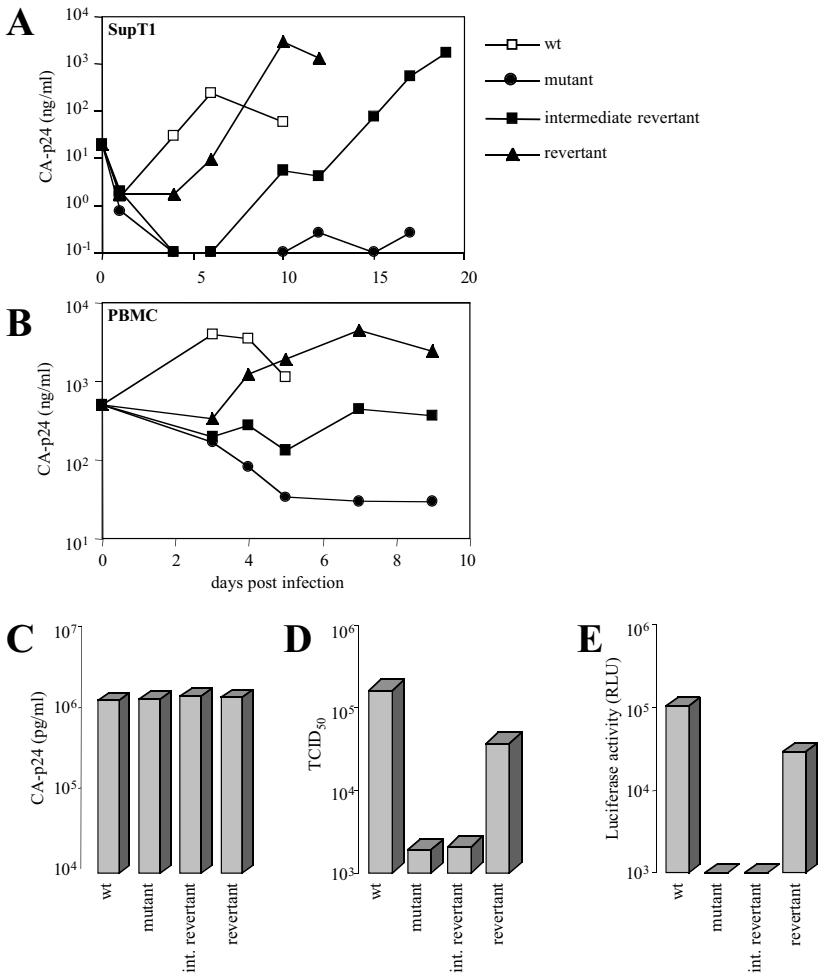

Fig. 2. Restoration of viral infectivity and replication. **A.** 300x10³ SupT1 T cells were infected with 20 ng CA-p24 and virus spread was measured for 20 days. **B.** 100x10³ PBMCs were infected with 50 ng of the respective molecular clones and virus spread was monitored for 10 days. **C.** Virus stocks were produced by transfection of C33A cells and the amount of virus was quantitated using ELISA. **D.** The infectivities ($TCID_{50}$) were measured by endpoint dilution. The exact $TCID_{50}$ values of the respective mutants per g CA-p24 are as follows: 162658 (wt); 1900 (mutant); 2083 (intermediate revertant) and 36745 (revertant). **E.** 300x10³ LuSIV cells were infected with 200 ng CA-p24 in the presence of 200 nM Saquinavir. Viral entry into cells was quantified by measuring luciferase activity 48 hours after infection.

duction, which is essentially Env-independent, was similar for wt, mutant and revertant viruses (Fig. 2C). Infectivity measurements ($TCID_{50}$; Fig. 2D) and single cycle viral entry experiments (Fig. 2E) further corroborated the replication results and firmly established that Env-mediated entry of the revertant virus was restored. We did measure a minor increase in infectivity and no increased entry for the intermediate revertant (Fig. 2D and E), but the replication advantage is obvious (Fig. 2A and B). The combined results indicate that a two-step evolution process took

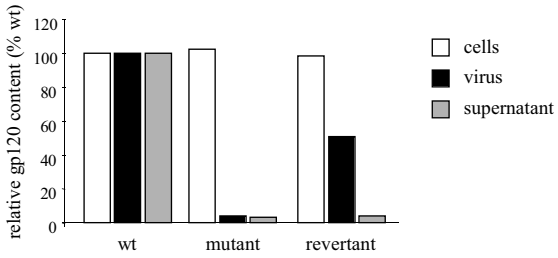

Fig. 3. Restoration of Env incorporation into virions. gp120 content in cell, virus and supernatant fractions of virus producing cells. gp120 and CA-p24 contents were measured by ELISA. The gp120 amounts were standardized for CA-p24 input and the gp120 contents of mutants in the respective fractions are given as percentages of the wt gp120 contents (arbitrarily set at 1).

place upon removal of the V4 base disulfide bond, and both reversions at and near residue 418 contribute to the final revertant phenotype.

The T415I and A418V reversions restore gp120 incorporation into virus particles
To study the effect of the various substitutions on the expression of Env in cells and on the surface of virus particles, we analyzed the gp120 content of cells and viruses using a gp120 ELISA. C33A cells were transiently transfected with the respective molecular clones. Cells were harvested after 48 hr and the virus fraction was purified from the culture supernatant by ultracentrifugation, which allowed us not only to determine the gp120 content of viruses, but also how much gp120 is shed into the supernatant from the cellular and viral surfaces. For the wild-type construct, ~14% of the total amount of gp120 was present in the cell fraction, ~21% in the virus fraction, and ~65% in the supernatant, indicating considerable shedding of the LAI gp120 molecules from cells and/or viruses (chapter 4.1). The corresponding numbers for the viral CA-p24 protein are ~17% in cells, ~58% in the virus, and ~25% in the supernatant. We determined the gp120/CA-p24 ratio's in the respective fractions for mutant and revertant viruses and compared these to the wt gp120/CA-p24 ratio's that were arbitrarily set at 1 (Fig. 3). The C385A/C418A mutant accumulated gp120 in the cell fraction, but virtually no gp120 was incorporated into virus particles or shed into the medium (~4% gp120 incorporation into virions compared to wt). This result is consistent with the severe folding defect measured for this mutant (see below and chapter 4.1). The revertant significantly increased gp120 incorporation into virions (~51% of wt). Strikingly, the revertant did hardly shed gp120 in the culture medium, suggesting that it has stabilized the gp120-gp41 interaction (~4% of wt shedding).

The T415I and A418V reversions slightly improve gp120 folding
The poor replication capacity of the mutant Env could be explained by its low folding efficiency in the ER (chapter 4.1). Apparently too few correctly folded Env molecules could leave the ER and be incorporated onto virus particles. The increased incorporation into virus particles of the revertant Env suggests that the evolutionary repair of virus replication did occur through increased folding competence of the revertant. We therefore analyzed oxidative folding of the revertant

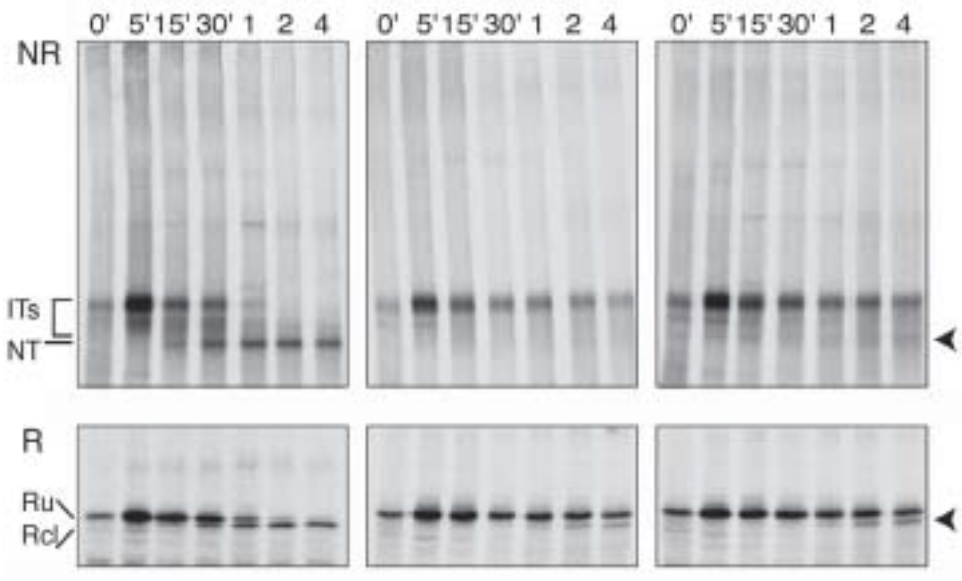

Fig. 4. Partial restoration of gp120 folding. Hela cells were infected with VVT7 and transfected with plasmids encoding wt (left panels), mutant (middle panels) or revertant (right panels) gp120. Cells were pulse labeled for 2 min and chased for the indicated times. Cells were lysed and gp120 proteins were immunoprecipitated from lysates. Immunoprecipitates were deglycosylated and analyzed by nonreducing (upper panels) or reducing (lower panels) 7.5% SDS PAGE. Folding intermediates (ITs), the native form (NT), the reduced uncleaved (Ru) and cleaved (Rc) forms of gp120 are indicated.

gp120 in comparison with wt and mutant gp120 by pulse-chase analysis (Fig. 4). wt gp120 progressed with time via a 'smear' of partially oxidized folding intermediates (ITs) to a fully oxidized native form (NT) in nonreduced gels (Fig. 4, upper left panel). Concomitantly, the signal peptide was removed from gp120 (Reduced uncleaved (Ru) vs Reduced cleaved (Rc) with time (Fig. 4, lower left panel), as reported previously (chapter 4.1). In contrast, mutant gp120 failed to display detectable amounts of NT even after 4 hrs of chase (Fig. 4, upper middle panel) and the signal peptide was cleaved only from a minority of mutant gp120 molecules (Fig. 4, lower middle panel), as we had observed previously (chapter 4.1). In case of the revertant a faint NT-like band appeared at later chase periods (Fig. 4, upper right panel, indicated by an arrowhead). Also, the revertant displayed slightly more signal peptide cleavage in comparison to the mutant periods (Fig. 3, lower right panel, indicated by an arrowhead). Altogether, this indicates that the revertant phenotype correlates with slightly increased folding competence of gp120, although folding kinetics are far from restored to wt levels.

The revertant gp120 on virions is antigenically similar to wt Env

It is clear that the two local amino-acid substitutions in the revertant improved gp120 folding, expression and virus incorporation compared to the original mutant. However, the question remained how these mutations could compensate for the lack of a disulfide bond that is absolutely conserved among natural HIV-1 isolates. To investigate whether the global fold of revertant gp120 was distinct

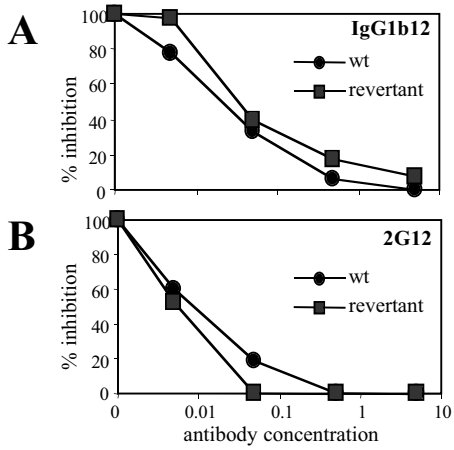

Fig. 5. Neutralization of wt and revertant viruses by monoclonal antibodies IgG1b12 and 2G12. Viral entry (as assayed in Fig. 2D) was measured in the presence of varying concentrations of IgG1b12 and 2G12.

from that of wt gp120, we performed neutralization experiments using the 2G12 monoclonal antibody (Fig. 5). 2G12 recognizes a conformational carbohydrate epitope on the outer domain of gp120, and its epitope includes the carbohydrates that are attached to the asparagines at positions 332 and 392 in close proximity to the V4 base (chapter 3.1)(4, 46, 50, 56). In addition, the glycans attached to N295, N386 and N448 contribute directly or indirectly to the proper presentation of the 2G12 epitope. The glycan at position 386 is immediately adjacent to the 385-418 disulfide bond, and N392 is located only a few residues further downstream. Local structural alterations caused by the absence of the disulfide bond, with the additional amino-acid changes causing the phenotypic reversion, could perturb the composition and/or orientation of these carbohydrates and thereby affect 2G12 binding and neutralization. The monoclonal antibody IgG1b12, which binds to an conformational epitope that overlaps with the CD4 binding site was also included in the experiment (3, 49). Neutralization experiments show that both the wt and revertant virus are inhibited by 2G12 and IgG1b12 with comparable IC_{50} values (Fig. 5). The mutant virus could not be analyzed in this assay because it does not replicate. These results indicate that wt and revertant gp120 molecules that reach the virus particle are not dramatically different in their conformation. Therefore, the restoration of replication capacity can be attributed to an increased yield of correctly folded Env species.

Molecular dynamics simulations show no apparent effect on the global structure of gp120

To analyze in further detail the effects of the substitutions on gp120 structure and stability, we performed molecular dynamics simulations. Simulations performed at 300K revealed a remarkable stability of both wt and all variants of gp120 (results not shown). Increasing the temperature to 400K only enhanced local fluctuations, mainly in loop regions, e.g., the V1/V2, V4 and V5 loops, without significant changes in energy or secondary structure. Even the removal of all disulfide bonds by alanine substitution did not lead to global unfolding or loss of secondary or tertiary structure, suggesting that the disulfide bonds do not play an important role in maintaining gp120 structure once it is folded (simulations per-

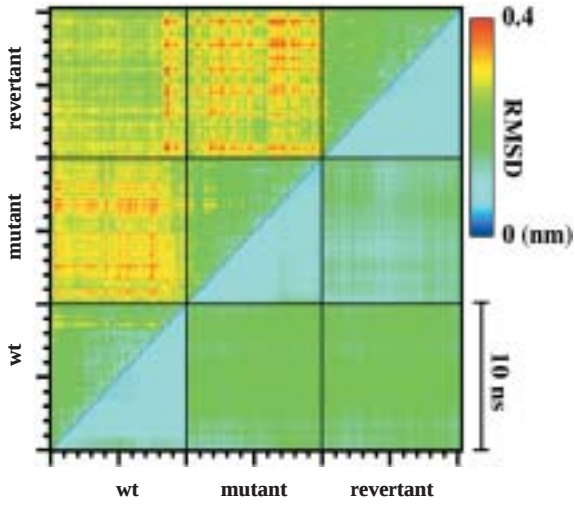

Fig. 6. Pair-wise backbone RMSD matrix of wt, mutant (C385A/C418A) and revertant (C385A C418V T415I) gp120. Each section represents a 10 ns simulation at 300K. Each colored dot represents a positional root-mean-square deviation (RMSD) between two conformations taken from the respective trajectories indicated on the axes, and is color-coded according to the scale shown on the right. The conformations are taken every 10 ps. The upper left panel shows the backbone RMSD fitted on the backbone atoms (N, C and Cα) of the secondary structure elements of the starting structure as identified by DSSP (24). The lower right panel shows the backbone RMSD of theβ-sheet that includes β-strands β-13 (299-305), β-16 and β-17 (373-386), and β-19 (412-422), fitted on the backbone atoms of these residues. An equilibrated conformational sampling period is found when an off-diagonal region shows a continuous low RMSD (blue to green).

formed at elevated temperature (400K) for 10 ns; results not shown). A complete sampling of the unfolding pathway for such a large system is beyond the reach of the current computational power. Instead, we will focus on the further description of the equilibrium state of each variant. Note that the core sequences of HXB2, present in the crystal structures, and LAI, used in our virus and folding experiments, differ by six amino-acids, which are all remote from the mutation sites of interest. Comparison of the first 5 ns simulations of the HXB2 and LAI model structures revealed no significant difference (results not shown). We therefore used the HXB2 structure as wt reference and introduced point mutations *in silico* in order to minimize changes of structural variables so that the calculation of pre-equilibrating period can be reduced.

Positional root-mean-square deviation (RMSD) analysis of wt, mutant and revertant gp120s indicates that a 2 to 4 ns equilibration period is required for all backbone atoms to reach equilibrium. The four β-strands (β-13:299-305, β-16/β-17:373-386 and β-19:412-422) around the mutation sites stabilized much faster with very little RMSD fluctuation (<0.1 nm). Therefore, to ensure the proper sampling of the equilibrium states only the last 5 ns of all simulations were used for the analysis. A comparison of the three variants by RMSD matrix analysis also indicates that the overall backbone of the mutant core deviates slightly from wt and revertants with a maximum RMSD of 0.4 nm. The conformation of the four-stranded β-sheet that constitutes the region of interest in mutant and revertant gp120s is nevertheless very similar with only minor deviations from the wt (RMSD < 0.2 nm) (Fig. 6). The presence of the blue-to-green off-diagonal regions indicates sampling of similar regions of conformational space among these variants. Thus, no significant differences in the global structures were seen.

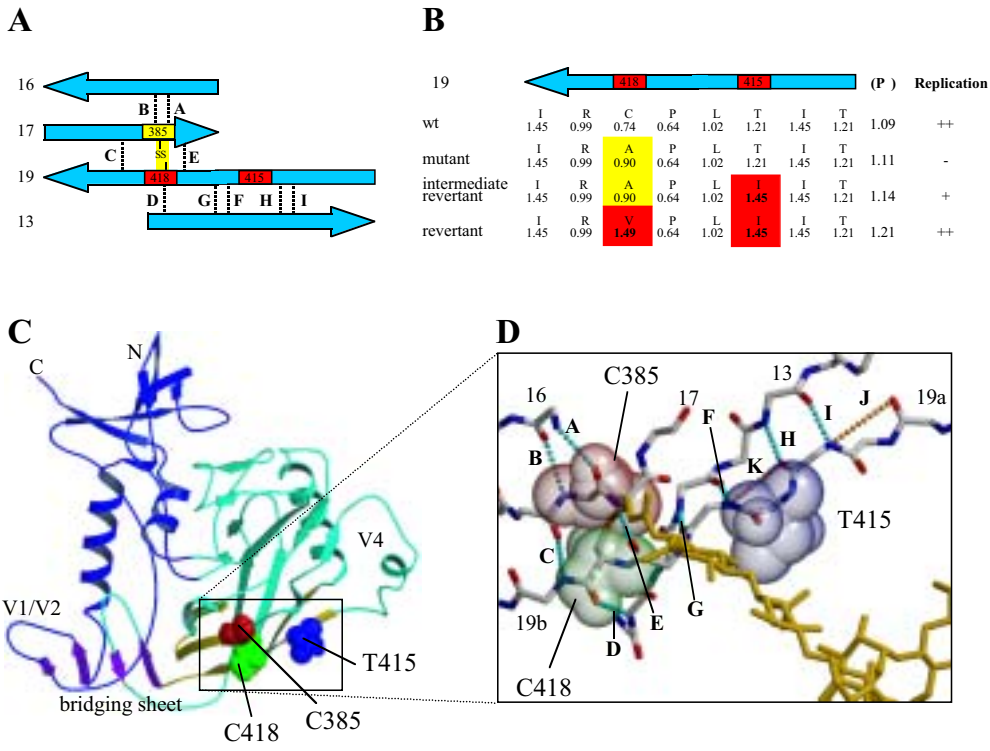

Fig. 7. **A.** Schematic representation of the β-sheet fold of β-strands β-13, β-16, β-17 and β-19. The interstrand hydrogen bonds residues 385, 415 and 418 are indicated (see also Fig. 7D and Table 1). **B.** β-sheet propensities of residues in β-19 including these of mutant and revertant residues, according to Levitt (32). The composite β-sheet propensity (Pβ) of β-19 is also given (7). **C.** Ribbon representation of the starting structure of core gp120 for simulation studies. The inner and outer domains are colored blue and cyan, respectively. The bridging sheet is colored magenta. Mutation sites of C385, C418 and T415 are indicated in red, green and blue spheres and the b-sheet formed by β-13, β-16, β-17 and β-19 is colored gold. The missing V4 loop is modeled by SWISS-MODEL. Detailed structure of the boxed region is shown on the right with the observed backbone-backbone hydrogen bonds around the mutation sites. Inter- and intrastrand backbone-backbone hydrogen bonds are displayed in cyan and orange dashed-lines, respectively. Alphabetic labels correspond to the identities listed in Table 1. Glycan structure of the *N*-glycosylation at N386 is taken and modified from PDB entry 1H3U (27).

The T415I and A418V reversions increase local backbone-backbone hydrogen bonding

Since no differences in the overall structures were seen, analysis at residual or atomic level may provide more insights into the effect of these mutations. The amino-acids at positions 385, 415 and 418 are located in a four-stranded antiparallel β-sheet (Fig. 7). Central in this β-sheet is strand β-19 with an unusual proline (P417) that causes the strand to bend. The N-terminal part of β-19 (β-19a) forms a double-stranded antiparallel β-sheet with β-13, but downstream of the unusual residue P417, β-19b interacts with β-17 to form a triple-stranded β-sheet also

involving β-16. In the wt protein, C385 in β-17 and C418 in β-19 are covalently linked by the disulfide bond, conferring stability to the β-sheet that comprises the V4 base region. Inspection of the β-sheet propensities of the side chains of the revertant amino-acids, revealed that both T415I and A418V increase the β-sheet propensity (Fig. 7B)(7, 32). The overall β-sheet propensity of β-19 increases from 1.11 for the mutant to 1.14 and 1.21 for the intermediate and final revertants, compared to 1.09 for the wt β-19, although it should be noted that the contribution of a disulfide bond is not taken into account for the wt β-19. Interestingly, the two reversions are on either side of the β-sheet destabilizing residue P417.

The formation of interresidue backbone hydrogen bonds is the determinant for secondary structure (24) and is therefore important for protein folding. A loss or a reduction in the presence of specific hydrogen bonds can lead to a deficiency in protein folding. A detailed molecular dynamics investigation into the hydrogen bond network in the vicinity of the mutation sites revealed an intriguing compensation effect. Four interstrand hydrogen bonds that are stable in wt gp120, are lost in the mutant, but are partially or fully restored in revertant (hydrogen bonds B, C, D and H in table 1 and Fig. 7C). In contrast, hydrogen bonds E and I, which are virtually absent in the wt, but present in the mutant are destabilized in the revertant. These particular hydrogen bonds may have a disadvantageous effect on the topology of the β-sheet. Some hydrogen donors and acceptors switch from

Table 1. Statistics of hydrogen bond occurrence in the vicinity of the mutation and reversion sites.

	Backbone-backbone hydrogen bond	Hydrogen bond occurrence (%) during 5-10 ns		
		wt	mutant	revertant
A	C385[e](O)-H374(N)	86.8	90.2	99.6
B	C385[e](N)-H374(O)	97.4	0.0	34.1
C	Y384(O)-R419(N)	90.6	10.2	85.6
D[a]	C418[e](N)-G329(O)	94.0	0.2	34.3
E[b]	P417(O)-N386(N)	6.6	94.4	35.5
F[d]	C331(O)-L416(N)	14.4	0.2	0.2
G	C331(N)-L416(N)	92.6	98.0	86.2
H[c]	I414(O)-I333(N)	61.9	0.2	97.6
I	I414(N)-I333(O)	0.2	96.2	4.4
J[d]	I414(N)-N412(O)	96.4	17.0	0.2
K[c,d]	I414(O)-L416(N)	86.8	97.2	99.4
	Overall average	*66.2*	*45.8*	*52.5*

[a] G329 is the first linker residue for the truncated V3 loop
[b] *N*-glycosylation at N386 was not taken into account during simulation
[c] hydrogen bonds that are located directly proximal to residue 415 (see Fig. 7)
[d] intrastrand backbone hydrogen bonds. A hydrogen bond is considered to exist when the donor-hydrogen-acceptor angle is larger than 135° and the donor-acceptor distance is smaller than 0.25 nm
[e] Cysteines in the wt protein, but not in the mutant or revertant proteins

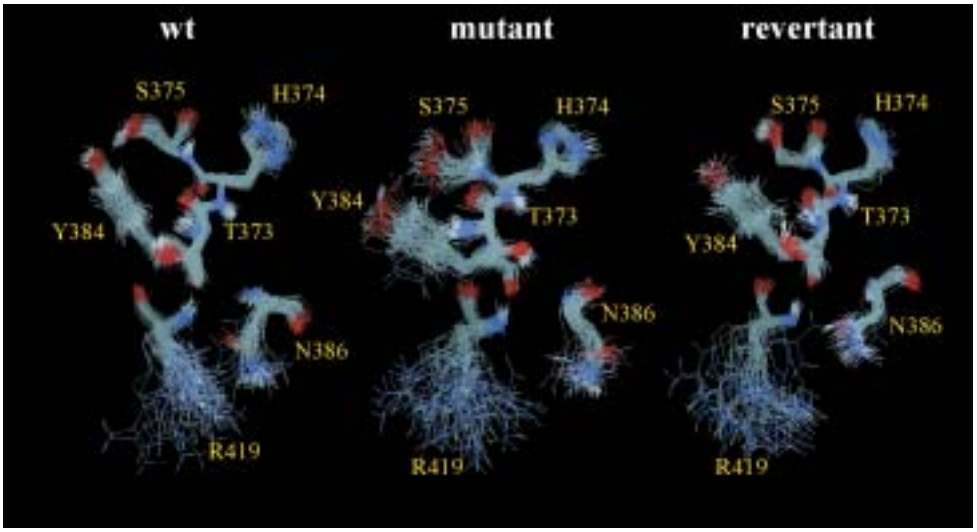

Fig. 8. Snapshots of selected hydrophilic residues around the mutation sites, that can potentially form interstrand hydrogen bonds. The structures are sampled every 100 ps during the 5-10 ns trajectories. All structures are fitted on the backbone atoms of these residues. The atoms are colored in white, red, blue and gray for hydrogen, oxygen, nitrogen and carbon, respectively.

interstrand bonding to intrastrand bonding (for example see hydrogen bond I and J in table 1 and Fig. 7C). Finally, in line with the experimental data, comparison of the overall average occurrence of the eleven hydrogen bonds that are in close proximity to the mutation sites indicates that wt gives the highest stability to this particular hydrogen bond network (66.2%), with partial restoration in revertant (52.5%) compared to the mutant (45.8%). The restoration of hydrogen bonding in the revertant is even more significant when one considers the absence of the disulfide bond that fixes these interactions in the wt protein.

The T415I and A418V reversions improve local interstrand side chain packing

In addition to the backbone hydrogen bonding that defines the secondary structure of protein folds, the side chain packing is also an important stabilizing factor. The electrostatic interactions among side chains provide a long range attracting gradient and therefore might be crucial for protein folding during the search of the native fold. An overlay of snapshots of selected hydrophilic residues around the mutation site during molecular dynamics simulations shows a remarkable well-defined side chain packing in the wt protein, except for R419, which exhibits a main cluster close to N386 with the remaining being poorly defined (Fig. 8). Using the same criteria as for the backbone hydrogen bond network, interstrand side chain hydrogen bond are found for S375(Oγ)-Y384(Oη) (29.7% in 5-10 ns trajectory) and N386(Nδ2)-R419(Nη) (25.0%) despite the intrinsic flexibility of R419. Note that the side chain hydrogen bonding geometry of S375(Oγ)-S375(Hγ)-Y384(Oη) is surprisingly well-defined despite the intrinsic mobility of serine and tyrosine side chains. The geometry of S375 and Y384

becomes clearly disordered in the mutant and no cluster can be found in R419 that is in contact with N386. The overall geometry of the side chain organization is slightly different and, as a consequence, both side chain hydrogen bonds are absent in the mutant. The side chain packing is substantially restored in the revertant, particularly for S375 and Y384. However, the gain in structural integrity is not sufficient to restore the hydrogen bonds that are present in the wt protein. Nevertheless, these results illustrate that the reversions contribute to an improvement of local side chain packing.

The analysis of backbone-backbone and side chain interactions illustrate that the effects of the mutations and reversions at positions 385, 415 and 418 are regional. Besides local effects on the interactions between strands β-17 and β-19 that are normally linked by the disulfide bond, there are also effects on interactions between β-17 and β-16 (e.g. S375-Y384; H374-C385A) and between β-19 and β-13 (e.g. I333-I414; L416-C331; G329-C418A). Thus, the mutations and reversions affect all four strands of the antiparallel β-sheet.

Discussion

We describe an HIV-1 gp120 variant that emerged through virus evolution and that is functional despite the lack of the disulfide bond at the base of the V4 domain, which is otherwise required for virus replication and gp120 activity. Virological, biochemical and computational analyses suggest that virus replication is restored through improvement of a local β-sheet fold. This study provides evidence that a critically important disulfide bond can be functionally replaced by an alternative protein structure motif. It also provides evidence for the proposal that local protein stability is an important factor in escape from ER quality control during protein biosynthesis.

Our data are surprisingly well in accordance with both theoretical β-sheet propensities (Fig. 7B)(7, 32) and β-sheet preferences as established in small model proteins (25, 35, 51). The first reversion (T415I) slightly increases the β-sheet preference and viral replication is slightly improved. The second A418V reversion has a considerable effect on both β-sheet preference and viral replication. The generalized rules on β-sheet preference apply to β-19 since it is a central strand and not an edge strand (34)(Fig. 7). The counterbalancing effect of the reversions on the presence of the β-sheet disfavouring P417 is presumably only possible because β-19 is not an edge strand (47). Thus, β-sheet preference is a major determinant in directing protein folding and protein stability and our data point out that the simple rules deduced from experiments with small model proteins also hold for the intricate folding of a complicated glycoprotein such as gp120 in living cells.

The increase of hydrogen bonding might in part be a result of the increase of van der Waals interactions where T415I is flanked by I414 and L416 with several hydrophobic residues in the opposite strand, β-13. A recent study suggested that a hydrophobic core is the stabilizing factor for a β-stranded Betanova peptide (8). Kumagai and co-workers also showed that a Thr-to-Ile mutation at position 29 does not change the structure of α-lactalbumin but has a significant positive effect on its thermostability due to the increase of hydrophobic side chain

packing and hydrogen bonding (21). We also did not find significant overall structural perturbation when mutations were introduced *in silico* in the native state of gp120.

The local restoration of a folding defect of a disulfide bond mutant provides new insights on the relevance of disulfide bonds for folding in the ER and on the discrimination between immature and correctly folded client proteins by ER quality control. The well-characterized calnexin/calreticulin cycle plays a role in oxidative folding in the ER and ER quality control of virtually all glycoproteins (14, 15, 57). Calnexin and calreticulin are lectins that recognize monoglucosylated carbohydrate moieties on glycoproteins. They associate with Erp57, an ER resident thiol-oxidoreductase that forms transient disulfide bonds with glycoproteins bound to calnexin or calreticulin and mediates isomerization of disulfide bonds (36). Glucosidase II hydrolyses glucose from monoglucosylated carbohydrates on folding glycoproteins, which results in glycoprotein release from calnexin and calreticulin. An other important player in the calnexin/calreticulin cycle and in ER quality control is UDP-glucose:glycoprotein glucosyltransferase (UGGT), which recognizes improperly folded domains on folding glycoproteins and reglucosylates carbohydrates in the misfolded region so that it can reassociate with calnexin or calreticulin for another attempt to properly fold the domain. The determinants for recognition of improperly folded glycoprotein domains by UGGT are not completely clear (5, 17, 43, 52, 53, 58). UGGT recognizes only the improperly folded parts of the protein, and it does not recognize random coil. Although the carbohydrate is important for tagging the protein to be recognized by calnexin or calreticulin, it is not involved in the recognition of misfolding. It has been suggested that UGGT recognizes exposed hydrophobic patches, instable domains or mobile groups.

Our results indicate that local instability and/or mobility may be important in the recognition of UGGT. In gp120 lacking the 385/418 disulfide bond, local strengthening of non-covalent interactions stabilizes a local β-sheet fold. The reversions do not alter the local β-sheet structure, but increase the stability of the β-sheet and thereby the correct fold or a quasi-correct fold. UGGT does not recognize the protein anymore as being improperly folded and the protein is allowed to leave the ER. Although other molecular chaperones, such as BiP, play a role in the recognition of misfolding, no BiP binding sites were detected in the V4 region (26).

When UGGT senses misfolding, it tags the protein for reentering the calnexin/calreticulin pathway by reglucosylation of a local carbohydrate. The obvious candidate for marking the misfolded V4 base region is the glycan attached to N386, immediately neighboring the 385/418 disulfide bond in the wt protein. We have observed an alternative escape route in a similar evolution experiment with a C418A single mutant virus. In that particular case, the increase in viral replication and escape from ER quality control involved the elimination of the 386 glycan (results not shown). Thus, these studies may represent two different pathways for ER quality control escape: increase of local stability of protein structure or elimination of a nearby carbohydrate.

The number of revertant gp120 molecules that reached a native state was still modest compared to wt. Since only native gp120 can exit the ER, also limited

amounts of revertant Env could reach the cell surface to be incorporated into virions. Nevertheless, incorporation reached levels that were close to wt. Apparently, the few Env molecules that did reach the cell surface were sufficient to produce virions with a normal Env content. This suggests that other factors are limiting in the intricate virion assembly process. This also suggests that in wt only a fraction of Env is incorporated. We note that the increase in replication capacity could be correlated directly with an increase of gp120 incorporation into virions, suggesting that the reversions cause the escape from ER quality control, but that they do not contribute to improvement of subsequent Env functions *per se* (e.g. (co)receptor binding, membrane fusion).

This study indicates that the 385-418 disulfide bond is not specifically required for gp120 folding, i.e. it can be compensated for by alternative means of protein stabilization. There is a precedent for this phenomenon. Single chain antibody fragments (scFv) could be generated by molecular evolution, in which disulfide bonds were replaced by, for example, a salt bridge (42). We have observed another escape route in a C418A single mutant, also lacking the V4 base. In addition, we have generated various escape variants from HIV-1 lacking the 54-74 disulfide bond in the C1 region of gp120 (chapter 4.3). Restoration of the original disulfide bonds was never seen in these escape variants. Taken together with our earlier studies in which we showed that 5 out of 10 disulfide bonds were not essential for ER folding, we can now conclude that 7 out of 10 disulfide bonds are not absolutely and specifically required for oxidative folding of gp120. 5 disulfide bonds can be replaced without penalty on folding, 2 can be replaced by other stabilizing mechanisms. Whether the formation of specific native or nonnative disulfide bonds plays a role in directing protein folding is unclear (6, 59), but if such a mechanism is required for oxidative folding of Env, our work clearly indicates that most of the cysteines in Env are not involved. An exception might be formed by the cysteines in the C2-V3 region, which are absolutely required for folding. This region might act as an initiator or director for Env folding.

Of note is that the exemplary short term evolution experiments that we performed never resulted in an Env that folded as efficiently as wt and a virus that replicated at wt levels. It would be of interest to prolong the evolution of the revertant virus presented here, to see whether it can in fact reach wt levels of folding without the 385-418 disulfide bond. It is possible that, although not essential for Env folding *per se*, it increases the chances of efficient folding.

The question remains why the V4 base disulfide bond is absolutely conserved *in vivo*. One reason could be that the best alternative for this disulfide bond, such as a stabilized β-sheet, may never completely compensate for the lack of the disulfide bond and restore wt levels of replication. Prolonged evolution experiments with the revertant virus described here, might also answer this question. The loss of the disulfide bond may also be prevented because the virus would have to go through an intermediate with a free cysteine, which is usually disadvantageous because it may interfere with the formation of the correct disulfide bonds (chapter 4.1). Alternatively, it is possible that this disulfide bond has a more distinct function *in vivo*, for example in immune evasion. It may play a role in positioning of the V4 domain so that it can optimally exert its function as antigenic shield, or it could be involved in maintaining an optimally loose gp120-

gp41, resulting in shedding and the presence of immunological decoy gp120. This study underlines the evolutionary potential of HIV-1 not only because of its high mutation rate but also because of the structural plasticity of its proteins.

Acknowledgements

We thank James Binley and Dennis Burton for the gift of antibodies, Norbert Schülke and Bill Olson for the gift of recombinant gp120, Janice Clements for the donation of LuSIV cells, and Stephan Heynen for technical assistance. This work was sponsored in part by the Dutch AIDS fund (Amsterdam).

References

1. **Berendsen, H. J. C., J. P. M. Postma, W. F. Van Gunsteren, A. Di-Nola, and J. R. Haak.** 1984. Molecular dynamics with coupling to an external bath. J. Chem. Phys. **81**:3684-3690.
2. **Berendsen, H. J. C., J. P. M. Postma, W. F. Van Gunsteren, and J. Hermans.** 1981. Interaction models for water in relation to protein hydration. Reidel Publishing Company, Dordrecht.
3. **Burton, D. R., J. Pyati, R. Koduri, S. J. Sharp, G. B. Thornton, P. W. Parren, L. S. Sawyer, R. M. Hendry, N. Dunlop, P. L. Nara, and .** 1994. Efficient neutralization of primary isolates of HIV-1 by a recombinant human monoclonal antibody. Science **266**:1024-1027.
4. **Calarese, D. A., C. N. Scanlan, M. B. Zwick, S. Deechongkit, Y. Mimura, R. Kunert, P. Zhu, M. R. Wormald, R. L. Stanfield, K. H. Roux, J. W. Kelly, P. M. Rudd, R. A. Dwek, H. Katinger, D. R. Burton, and I. A. Wilson.** 2003. Antibody domain exchange is an immunological solution to carbohydrate cluster recognition. Science **300**:2065-2071.
5. **Caramelo, J. J., O. A. Castro, L. G. Alonso, G. Prat-Gay, and A. J. Parodi.** 2003. UDP-Glc:glycoprotein glucosyltransferase recognizes structured and solvent accessible hydrophobic patches in molten globule-like folding intermediates. Proc. Natl. Acad. Sci. USA **100**:86-91.
6. **Cemazar, M., S. Zahariev, J. J. Lopez, O. Carugo, J. A. Jones, P. J. Hore, and S. Pongor.** 2003. Oxidative folding intermediates with nonnative disulfide bridges between adjacent cysteine residues. Proc. Natl. Acad. Sci. USA **100**:5754-5759.
7. **Chou, P. Y. and G. D. Fasman.** 1974. Conformational parameters for amino-acids in helical, beta-sheet, and random coil regions calculated from proteins. Biochemistry 13:211-222.
8. **Colombo, G., D. Roccatano, and A. E. Mark.** 2002. Folding and stability of the three-stranded beta-sheet peptide Betanova: insights from molecular dynamics simulations. Proteins **46**:380-392.
9. **Das, A. T., B. Klaver, and B. Berkhout.** 1999. A hairpin structure in the R region of the Human Immunodeficiency Virus type 1 RNA genome is instrumental in polyadenylation site selection. J. Virol. **73**:81-91.
10. **Das, A. T., B. Klaver, B. I. F. Klasens, J. L. B. van Wamel, and B. Berkhout.** 1997. A conserved hairpin motif in the R-U5 region of the human immunodeficiency virus type 1 RNA genome is essential for replication. J. Virol. **71**:2346-2356.
11. **Daura, X., A. E. Mark, and W. F. Van Gunsteren.** 1998. Parametrization of aliphatic CHn united atoms of GROMOS96 force field. J. Comput. Chem. **19**:535-547.
12. **Earl, P. L., B. Moss, and R. W. Doms.** 1991. Folding, interaction with GRP78-BiP, assembly, and transport of the human immunodeficiency virus type 1 envelope protein. J. Virol. **65**:2047-2055.
13. **Eckert, D. M. and P. S. Kim.** 2001. Mechanisms of viral membrane fusion and its inhibition. Annu. Rev. Biochem. **70**:777-810.
14. **Ellgaard, L. and A. Helenius.** 2003. Quality control in the endoplasmic reticulum. Nat. Rev. Mol. Cell Biol. **4**:181-191.
15. **Ellgaard, L., M. Molinari, and A. Helenius.** 1999. Setting the standards: quality control in the secretory pathway. Science **286**:1882-1888.
16. **Feenstra, K. A., B. Hess, and H. J. C. Berendsen.** 1999. Improving efficiency of large time-

scale molecular dynamics of hydrogen-rich systems. J. Comput. Chem. **20**:786-798.
17. **Fernandez, F., C. D'Alessio, S. Fanchiotti, and A. J. Parodi.** 1998. A misfolded protein conformation is not a sufficient condition for *in vivo* glucosylation by the UDP-Glc:glycoprotein glucosyltransferase. EMBO J. **17**:5877-5886.
18. **Gallo, S. A., C. M. Finnegan, M. Viard, Y. Raviv, A. Dimitrov, S. S. Rawat, A. Puri, S. Durell, and R. Blumenthal.** 2003. The HIV Env-mediated fusion reaction. Biochim. Biophys. Acta **1614**:36-50.
19. **Guex, N. and M. C. Peitsch.** 1997. SWISS-MODEL and the Swiss-PdbViewer: an environment for comparative protein modeling. Electrophoresis **18**:2714-2723.
20. **Hess, B., H. Bekker, H. J. C. Berendsen, and J. Fraaije.** 1997. LINCS: a linear constraint solver for comparative protein modeling. J. Comput. Chem. **18**:1463-1472.
21. **Horii, K., M. Saito, T. Yoda, K. Tsumoto, M. Matsushima, K. Kuwajima, and I. Kumagai.** 2001. Contribution of Thr29 to the thermodynamic stability of goat alpha-lactalbumin as determined by experimental and theoretical approaches. Proteins **45**:16-29.
22. **Jaenicke, R.** 1999. Stability and folding of domain proteins. Prog. Biophys. Mol Biol **71**:155-241.
23. **Jeeninga, R. E., M. Hoogenkamp, M. Armand-Ugon, M. de Baar, K. Verhoef, and B. Berkhout.** 2000. Functional differences between the LTR transcriptional promoters of HIV-1 subtypes A through G. J. Virol. **74**:3740-3751.
24. **Kabsch, W. and C. Sander.** 1983. Dictionary of protein secondary structure: pattern recognition of hydrogen-bonded and geometrical features. Biopolymers **22**:2577-2637.
25. **Kim, C. A. and J. M. Berg.** 1993. Thermodynamic beta-sheet propensities measured using a zinc-finger host peptide. Nature **362**:267-270.
26. **Knarr, G., S. Modrow, A. Todd, M. J. Gething, and J. Buchner.** 1999. BiP-binding sequences in HIV gp160. Implications for the binding specificity of bip. J. Biol. Chem. **274**:29850-29857.
27. **Krapp, S., Y. Mimura, R. Jefferis, R. Huber, and P. Sondermann.** 2003. Structural analysis of human IgG-Fc glycoforms reveals a correlation between glycosylation and structural integrity. J. Mol. Biol. **325**:979-989.
28. **Kwong, P. D., R. Wyatt, S. Majeed, J. Robinson, R. W. Sweet, J. Sodroski, and W. A. Hendrickson.** 2000. Structures of HIV-1 gp120 envelope glycoproteins from laboratory- adapted and primary isolates. Structure Fold. Des. **8**:1329-1339.
29. **Kwong, P. D., R. Wyatt, J. Robinson, R. W. Sweet, J. Sodroski, and W. A. Hendrickson.** 1998. Structure of an HIV gp120 envelope glycoprotein in a complex with the CD4 receptor and a neutralizing human antibody. Nature **393**:648-659.
30. **Land, A., D. Zonneveld, and I. Braakman.** 2003. Folding of HIV-1 envelope glycoprotein involves extensive isomerization of disulfide bonds and conformation-dependent leader peptide cleavage. FASEB J. **17**:1058-1067.
31. **Leonard, C. K., M. W. Spellman, L. Riddle, R. J. Harris, J. N. Thomas, and T. J. Gregory.** 1990. Assignment of intrachain disulfide bonds and characterization of potential glycosylation sites of the type 1 recombinant human immunodeficiency virus envelope glycoprotein (gp120) expressed in chinese hamster ovary cells. J. Biol. Chem. **265**(18):10373-10382.
32. **Levitt, M.** 1978. Conformational preferences of amino-acids in globular proteins. Biochem. **17**:4277-4285.
33. **Lindahl, E., B. Hess, and D. Van der Spoel.** 2001. GROMACS 3.0: a package for molecular simulation and trajectory analysis. J. Mol. Model. **7**:306-317.
34. **Minor, D. L., Jr. and P. S. Kim.** 1994. Context is a major determinant of beta-sheet propensity. Nature **371**:264-267.
35. **Minor, D. L., Jr. and P. S. Kim.** 1994. Measurement of the beta-sheet-forming propensities of amino-acids. Nature **367**:660-663.
36. **Molinari, M. and A. Helenius.** 1999. Glycoproteins form mixed disulphides with oxidoreductases during folding in living cells. Nature **402**:90-93.
37. **Moore, J. P. and D. D. Ho.** 1993. Antibodies to discontinuous or conformationally sensitive epitopes on the gp120 glycoprotein of human immunodeficiency virus type 1 are highly prevalent in sera of infected humans. J. Virol. **67**:863-875.
48. **Moulard, M. and E. Decroly.** 2000. Maturation of HIV envelope glycoprotein precursors by cellular endoproteases. Biochim. Biophys. Acta 1**469**:121-132.

39. **Otteken, A., P. L. Earl, and B. Moss.** 1996. Folding, assembly, and intracellular trafficking of the human immunodeficiency virus type 1 envelope glycoprotein analyzed with monoclonal antibodies recognizing maturational intermediates. J. Virol. **70**:3407-3415.
40. **Peden, K., M. Emerman, and L. Montagnier.** 1991. Changes in growth properties on passage in tissue culture of viruses derived from infectious molecular clones of HIV-1_{LAI}, HIV-1_{MAL}, and HIV-1_{ELI}. Virology **185**:661-672.
41. **Poignard, P., E. O. Saphire, P. W. Parren, and D. R. Burton.** 2001. gp120: Biologic aspects of structural features. Annu. Rev. Immunol. **19**:253-274.
42. **Proba, K., A. Worn, A. Honegger, and A. Pluckthun.** 1998. Antibody scFv fragments without disulfide bonds made by molecular evolution. J. Mol. Biol. **275**:245-253.
43. **Ritter, C. and A. Helenius.** 2000. Recognition of local glycoprotein misfolding by the ER folding sensor UDP-glucose:glycoprotein glucosyltransferase. Nat. Struct. Biol **7**:278-280.
44. **Roos, J. W., M. F. Maughan, Z. Liao, J. E. Hildreth, and J. E. Clements.** 2000. LuSIV cells: a reporter cell line for the detection and quantitation of a single cycle of HIV and SIV replication. Virology **273**:307-315.
45. **Sanders, R. W., E. C. de Jong, C. E. Baldwin, J. H. Schuitemaker, M. L. Kapsenberg, and B. Berkhout.** 2002. Differential transmission of human immunodeficiency virus type 1 by distinct subsets of effector dendritic cells. J. Virol. **76**:7812-7821.
46. **Sanders, R. W., M. Venturi, L. Schiffner, R. Kalyanaraman, H. Katinger, K. O. Lloyd, P. D. Kwong, and J. P. Moore.** 2002. The mannose-dependent epitope for neutralizing antibody 2G12 on human immunodeficiency virus type 1 glycoprotein gp120. J. Virol. **76**:7293-7305.
47. **Santiveri, C. M., M. Rico, M. A. Jimenez, M. T. Pastor, and E. Perez-Paya.** 2002. Insights into the determinants of beta-sheet stability: 1H and 13C NMR conformational investigation of three-stranded antiparallel beta-sheet-forming peptides. J. Pept. Res. **61**:177-188.
48. **Saphire, E. O., P. W. Parren, R. Pantophlet, M. B. Zwick, G. M. Morris, P. M. Rudd, R. A. Dwek, R. L. Stanfield, D. R. Burton, and I. A. Wilson.** 2001. Crystal structure of a neutralizing human IGG against HIV-1: a template for vaccine design. Science **293**:1155-1159.
49. **Saphire, E. O., P. W. Parren, R. Pantophlet, M. B. Zwick, G. M. Morris, P. M. Rudd, R. A. Dwek, R. L. Stanfield, D. R. Burton, and I. A. Wilson.** 2001. Crystal structure of a neutralizing human IGG against HIV-1: a template for vaccine design. Science **293**:1155-1159.
50. **Scanlan, C. N., R. Pantophlet, M. R. Wormald, S. E. Ollmann, R. Stanfield, I. A. Wilson, H. Katinger, R. A. Dwek, P. M. Rudd, and D. R. Burton.** 2002. The broadly neutralizing anti-human immunodeficiency virus type 1 antibody 2G12 recognizes a cluster of alpha1—>2 mannose residues on the outer face of gp120. J. Virol. **76**:7306-7321.
51. **Smith, C. K., J. M. Withka, and L. Regan.** 1994. A thermodynamic scale for the beta-sheet forming tendencies of the amino-acids. Biochemistry **33**:5510-5517.
52. **Sousa, M. and A. J. Parodi.** 1995. The molecular basis for the recognition of misfolded glycoproteins by the UDP-Glc:glycoprotein glucosyltransferase. EMBO J. **14**:4196-4203.
53. **Sousa, M. C. and A. J. Parodi.** 1996. The interaction of the UDP-GLC:glycoprotein glucosyltransferase with the acceptor glycoprotein. Cell Mol. Biol. (Noisy. -le-grand) **42**:609-616.
54. **Stein, B. S. and E. G. Engleman.** 1990. Intracellular processing of the gp160 HIV-1 envelope precursor. J. Biol. Chem. **265**:2640-2649.
55. **Tironi, I. G., R. Sperb, P. E. Smith, and W. F. Van Gunsteren.** 1995. A generalized reaction field method for molecular dynamics simulations. J. Chem. Phys. **102**:5451-5459.
56. **Trkola, A., M. Purtscher, T. Muster, C. Ballaun, A. Buchacher, N. Sullivan, K. Srinivasan, J. Sodroski, J. P. Moore, and H. Katinger.** 1996. Human monoclonal antibody 2G12 defines a distinctive neutralization epitope on the gp120 glycoprotein of human immunodeficiency virus type 1. J. Virol. **70**:1100-1108.
57. **Trombetta, E. S. and A. Helenius.** 1998. Lectins as chaperones in glycoprotein folding. Curr. Opin. Struct. Biol **8**:587-592.
58. **Trombetta, E. S. and A. Helenius.** 2000. Conformational requirements for glycoprotein reglucosylation in the endoplasmic reticulum. J. Cell Biol. **148**:1123-1129.
59. **Weissman, J. S. and P. S. Kim.** 1992. Kinetic role of nonnative species in the folding of bovine pancreatic trypsin inhibitor. Proc. Natl. Acad. Sci. USA **89**:9900-9904.
60. **Wyatt, R. and J. Sodroski.** 1998. The HIV-1 envelope glycoproteins: fusogens, antigens, and immunogens. Science **280**:1884-1888.

Chapter 4.3

Local and distal compensatory changes upon evolution of the HIV-1 envelope glycoproteins lacking the N-terminal disulfide bond in gp120

Rogier W. Sanders[1], Els Busser[1], Martijn M. Dankers[1], Min Lu[2], Ben Berkhout[1]

[1]Dept. of Human Retrovirology, Academic Medical Center, University of Amsterdam, 1105 AZ Amsterdam, The Netherlands

[2]Dept. of Biochemistry, Weill Medical College of Cornell University, 1300 York Ave., New York, NY 10021, USA

We have previously studied the role of individual disulfide bonds in the oxidative folding of the HIV-1 envelope glycoproteins (Env) in the endoplasmic reticulum (ER)(chapter 4.1). Five out of the ten disulfide bonds in Env are dispensable for folding. Surprisingly, two of these disulfide bonds are even dispensable for Env function and viral replication. The remaining five disulfide bonds are required for proper folding of Env. We used protein evolution through *in vitro* virus replication to further characterize the significance and role of specific disulfide bonds. In the current study, we describe evolved Env variants lacking the disulfide bond in the N-terminal C1 domain of the gp120 subunit. Compensatory changes were found both locally near the leader cleavage site and distally in the gp41 ectodomain. The results suggest that these two Env domains interact during folding.

The HIV-1 Envelope glycoproteins (Env) mediate viral entry into target cells. Much is known about the separate subunits, the surface subunit gp120 and the transmembrane subunit gp41, but relatively little is known about their concerted functioning. Even less is known about the concerted folding of the two subunits as part of the gp160 precursor protein, although we reported that folding of the two subunits is relatively independent (chapter 4.1). In our previous work we found that five out of ten absolutely conserved disulfide bonds are essential for oxidative folding of the Env protein (chapter 4.1). For example, mutation of the disulfide bond in the N-terminal C1 domain (C54A/C74A) results in incomplete oxidative folding, abrogation of leader peptide cleavage, and abrogation of gp120 secretion and Env incorporation onto virions. When placed in the context of a replicating virus, we could still observe a minimal but reproducible infectivity for some of these Env disulfide bond mutants, most notably the C54A/C74A and the C385A/C418A double mutants (class Ib mutants, chapter 4.1). These viruses appeared to be promising candidates for evolution studies that are aimed at identifying and investigating evolution routes that result in restoration of gp120 folding in the absence of a particular disulfide bond. We already reported interesting virus variants that emerged from evolution of the C385A/C418A mutant virus lacking

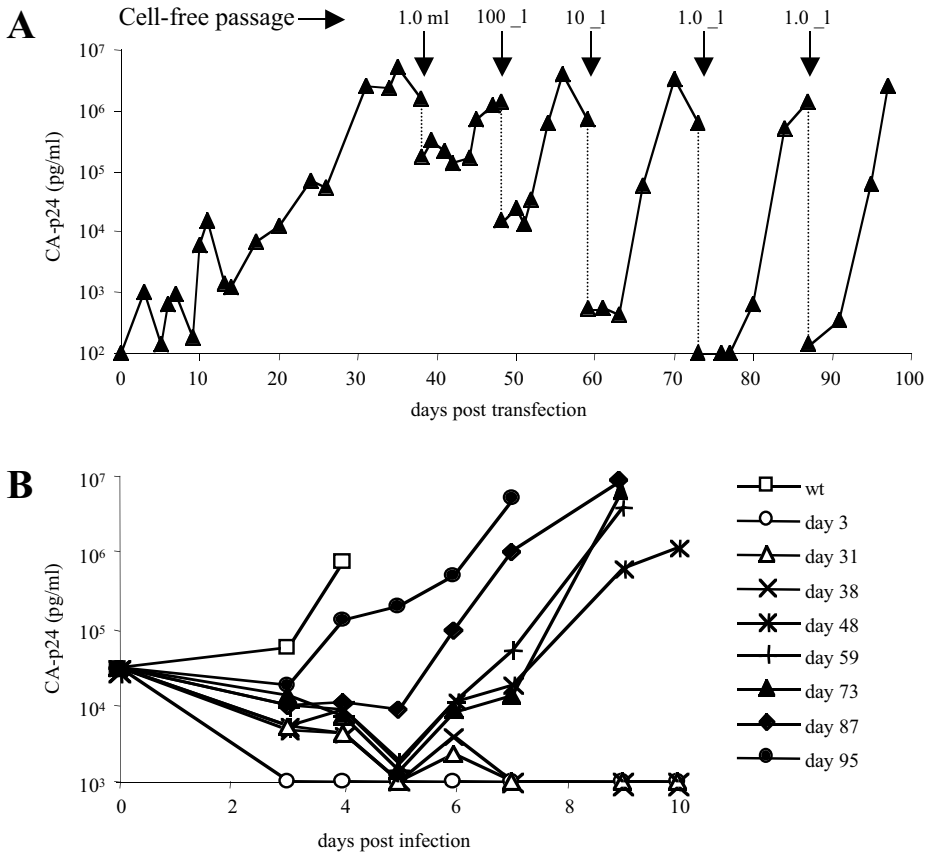

Fig. 1. Evolution of the HIV-1_{LAI} C54A/C74A virus. **A**. Virus spread in culture B was measured over a period of 95 days after the initial transfection of SupT1 T cells with 10 μg of the molecular clone pLAI. The virus-containing supernatant was passaged cell-free onto fresh cells at peak infection. The volume of passaged supernatant was gradually decreased, which is indicated on top of the graph. **B**. Viruses collected at various time points over the course of infection were stored at –80°C and compared in an infection experiment on SupT1 cells (input 20 ng/ml CA-p24 of each virus).

the disulfide bond at the base of the V4 loop (chapter 4.2). Here we describe evolved Env variants that lack the disulfide bond in the N-terminal C1 domain.

Evolution of HIV-1 lacking the N-terminal disulfide bond in gp120

We initiated three evolution cultures (cultures A-C) by transfecting SupT1 T cells with the molecular clone of the C54A/C74A virus. The methodology used for these experiments is similar to that described in chapter 4.2. Cell-free virus was passaged onto fresh cells at peak infection as monitored by CA-p24 production. As the viruses regained replication capacity, less and less virus could be passaged. For example, a detailed scheme of the prolonged infection in culture B is illustrated in Fig. 1A. Similar results were obtained in cultures A and C (results not shown). The wild-type (wt) HIV-1_{LAI} virus uses the CXCR4 coreceptor and induces the formation of syncytia in SupT1 T cells. During the course of evolu-

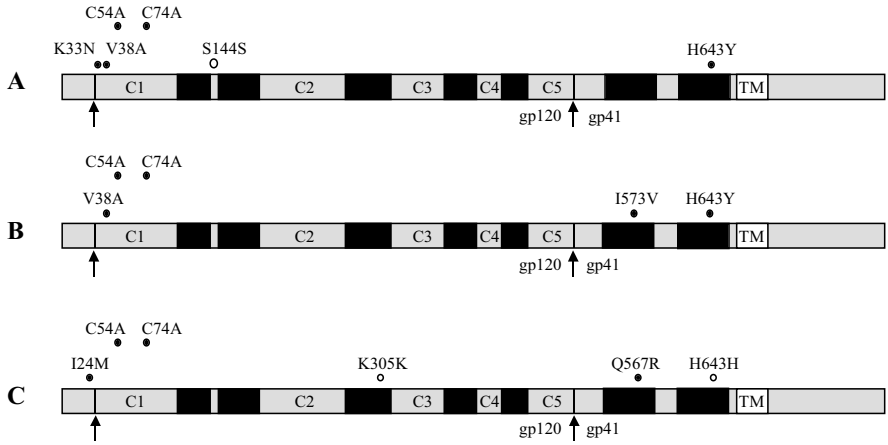

	substitution	codon change	remarks	region	occurrence in natural isolates (98 isolates, clade A-O)
	C54A	TGT to GCT		C1	98xC
	C74A	TGT to GCT		C1	98xC
A	K33N	AAA to AAT	not fixed	C1	48xN, 20xK, 18xQ, 7xD, 2xH, 1xP
	V38A	GTC to GCC		C1	97xV, 1xI
	S144S	AGC to AGN	silent	V1	
	H643Y	CAC to TAC		HR2	95xY, 2xF, 1xH
B	V38A	GTC to GCC		C1	97xV, 1xI
	I573V	ATC to GTC		HR1	96xI, 2xV
	H643Y	CAC to TAC		HR2	95xY, 2xF, 1xH
C	I24M	ATA to ATG	change in VpU I78V	leader	56xM, 18xI, 15xL, 4xC, 3xT, 1xS, 1xW
	K305K	AAA to AAG	silent	V3	
	Q567R	CAA to CGA		HR1	72xQ, 14xK, 10xR, 1xH, 1xE
	H643H	CAC to CAT	silent	HR2	95xY, 2xF, 1xH

Fig. 2. Schematic of the substitutions found in evolution cultures A, B and C. The complete ectodomain of Env was PCR-amplified from proviral DNA and sequenced. Direct sequencing of the quasispecies revealed the presence of the mutations indicated by circles. Amino-acid changes are indicated by closed circles and open circles indicate silent changes. The sites of leader peptide cleavage and gp160 precursor cleavage are indicated by arrows. The locations of the conserved regions (C1-C5), the variable loops (V1-V5), the heptad repeat regions (HR1 and HR2), and the transmembrane domain (TM) are indicated. Note that cultures A and B were passaged in parallel and the fact that two substitutions (V38A and H643Y) are present in both cultures suggests that a contamination took place at some stage. However, the subsequent changes (K33N in A and I573V in B) occurred independently. The table lists the codon changes. In addition, the occurence of alternative amino-acids at the specific residues in natural HIV-1 isolates is shown.

tion, we never observed the formation of syncytia in cultures A and B and only rarely in culture C. To characterize the evolution process we collected virus samples at several time points and an equal amount of virus was used in an infection experiment to compare their replication capacity (Fig. 1B). Virus variants that emerged around day 48 had gained some replication capacity compared to the original mutant virus. Viruses sampled later in evolution at day 87 and 95 displayed a further increase in replication capacity. These results suggest that the evolutionary repair of the C54A/C74A mutant is a multi-step process. Virus variants that were present when the experiment was stopped (day 95) were still some-

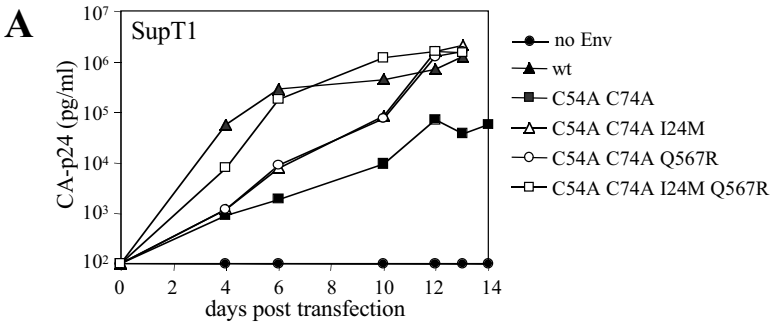

C

SupT1

4	6	7	10	day
-	-	-	-	no Env
+	++++	++++	†	wt
-	-	-	-	C54A C74A
-	-	-	-	C54A C74A I24M
-	-	-	-	C54A C74A Q567R
-	-	++	†	C54A C74A I24M Q567R

Fig. 3. Virus spread after transfection of SupT1 cells (**A**) or MT-2 cells (**B**) with 10 μg of the respective molecular clones. **C**. The appearance of syncytia in the SupT1 experiment is indicated on an arbitrary scale: – (no syncytia), + (very few syncytia) to ++++ (nearly all cells involved in syncytia). † indicates massive cell death.

what delayed in replication compared to the wt virus.

To identify the changes that caused the revertant phenotype, chromosomal DNA was isolated from the cells at day 95, and the entire *env* gene was PCR-amplified. Sequencing of the viral quasispecies in culture A revealed three amino-acid changes (closed circles: K33N, V38A, and H643Y), and one silent mutation (open circle: S144S) (Fig. 2). The K33N substitution was not fixed in the culture at day 95 since the sequence was mixed with the wt sequence. Three changes were observed in culture B (V38A, I573V and H643Y) and two changes (I24M, Q567R) in addition to two silent mutations were present in culture C. Details on the codon changes are provided in the bottom panel of Fig. 2, which also lists the natural amino-acid variation at these positions. Some reversion are actually changes to the consensus residues (K33N in culture A, H643Y in culture B, and I24M in culture C). The original C54A/C74A mutations were still present in all cultures, indicating that the disulfide bond was not restored. In fact, the design of the disulfide bond mutants was meant to prevent such an escape route because it requires a total of four nucleotide changes in the two codons to restore both cysteines and thus the disulfide bond. Sequencing of individual *env* clones revealed that some clones from culture B did not contain the I573V mutation, implying that this substitution appeared later during the course of evolution than the other two reversions. Likewise, the K33N substitution appeared late in culture A (Fig. 2). Thus, 6 different substitutions were found in total, one in the leader peptide, two in the mutated C1 region and three in the distal gp41 domain.

Both proximal and distal reversions contribute to the regain of replication capacity

We decided to focus on the Env variant present in culture C for the subsequent virological analyses. To investigate the significance of the observed substitutions for the revertant phenotype, the relevant *env* fragments were inserted into a molecular clone (C54A/C74A I24M Q567R). We also generated the two possible single revertants (C54A/C74A I24M and C54A/C74A Q567R). SupT1 cells were transfected with the mutant, revertant and wt molecular clones and virus spread was measured by CA-p24 ELISA (Fig. 3A). The single revertants exhibited improved replication compared to the original mutant virus and the double revertant replicated even better. The improvement of virus replication was less pronounced in MT-2 cells but the same ranking order was observed (Fig. 3B). These cell type differences may indicate a degree of host cell specificity of the revertant phenotype. The ability of the revertant viruses to induce the formation of syncytia in SupT1 cells was also scored (Fig. 3C). Syncytia were not observed in the cultures with the single revertant viruses, even at peak infection and high CA-p24 levels. We did observe some syncytia in the double revertant culture. However, whereas virus spread of the double revertant virus in SupT1 cells was similar to that of the wt virus as monitored by CA-p24 production, the syncytia appeared later and never reached the maximum score. Since SupT1 cells only express the CXCR4 coreceptor and since the revertant viruses have no changes in the coreceptor binding domains, the single revertant viruses are examples of non-syncytium-inducing CXCR4-using viruses (2, 4, 6). These results clearly indicate that a multi-step evolution process took place and that both the proximal (I24M) and distal substitutions (Q567R) contribute to the revertant phenotype.

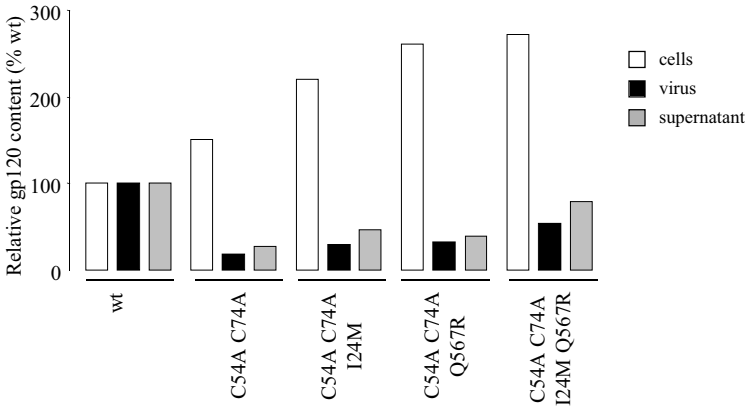

Fig. 4. Env production and incorporation onto virions. Non-permissive C33A cells were transfected with the molecular clones of the respective variant viruses and virions were pelleted by ultracentrifugation and separated from the supernatant. Cells and viruses were lysed and the gp120 and CA-p24 content of cell, virus and supernatant fractions was measured by ELISA. The gp120 amounts were standardized for CA-p24 input and the values obtained for wt were set at one for each fraction.

Improvement of gp120 expression and virion incorporation

To study the effect of the disulfide bond removal and the compensatory changes on the expression of Env in cells and on the surface of virus particles, we analyzed the gp120 content of cells and viruses using a gp120 ELISA. C33A cells were transiently transfected with the respective molecular clones. Cells were collected and the virus fraction was purified from the culture supernatant by ultracentrifugation. This allowed us not only to determine the gp120 content of viruses, but also to determine how much gp120 is shed into the supernatant from the cellular and viral surfaces. We determined the gp120/CA-p24 ratio in the respective fractions for the wt, mutant and revertant viruses. All values were related to that of the wt virus, which were set at 1 for each fraction (Fig. 4). The C54A/C74A mutant accumulated more gp120 intracellularly than the wt virus and virtually no gp120 was incorporated onto virus particles or shed into the medium. We measured approximately 18% gp120 incorporation onto virions compared to wt. This result is consistent with the folding defect described for this mutant (chapter 4.1). All revertants significantly increased the amount of cell-associated gp120 compared with the mutant, and this correlated with increased Env incorporation onto virions. We measured 29% and 33% Env incorporation for the I24M and Q567R single revertants, respectively, and 54% for the double revertant. The amount of gp120 shedding into the supernatant correlated with the level of Env incorporation onto virions, suggesting that the gp120 - gp41 association was not affected. In conclusion, both reversions contributed to higher Env expression and virion incorporation, thus explaining the increased replication capacity.

The substitutions in gp41 do not affect the six-helix bundle conformation

It is likely that the reversions in gp41 restore an early protein biosynthesis defect in the context of the C54A/C74A mutant. However, an alternative explanation

Table 1: Physicochemical data of the gp41 core mutants

N34(L6)C28 peptide	$-[\theta]_{222}$[a] (deg cm^2 dmol^{-1})	T_m[a] (°C)	molecular mass (kDa)
wt	-31,300	70	3.1
Q567R	-31,900	72	3.0
I573V	-31,100	65	3.1

[a] All CD scans and melts were performed with 10 μM peptide solutions in PBS (pH 7.0). The midpoint of thermal denaturation (T_m) was estimated from the thermal dependence of the CD signal at 222 nm.

[b] Sedimentation equilibrium results are reported as a ratio of the experimental molecular weight to the calculated molecular weight for a monomer (M_{obs}/M_{calc}).

seems possible. The Q567R and I573V substitutions are located centrally in the coiled coil domain in the post-fusion structure of gp41 and could affect this conformation and thus a late Env function: membrane fusion. To investigate this, we introduced the Q567R and I573V substitutions in the recombinant polypeptide HIV-1_{LAI} N34(L6)C28, which represents the core of the gp41 ectodomain and the biophysical properties were compared to those of wt as described previously (5, 8). We did not analyze the H643Y reversion because it is located on the outside of the six-helix bundle and less likely to affect its structure and/or stability. Circular dichroism was used to measure the α-helical content. The wt peptide is >95% α-helical at 4ºC as indicated by the typical wavelength dependency pattern shown in figure 5A. The Q567R and I573V peptides are >95% α-helical and their wavelength dependency is similar to that of the wt peptide. Under these conditions, the mid-point of thermal denaturation (T_m) of the wt peptide is 70ºC, and the T_m for the Q567R and I573V peptides is 72ºC and 65ºC, respectively (table 1, Fig. 5B). Thus, the I573V substitution slightly destabilizes the six-helix bundle. Sedimentation equilibrium experiments indicate that the Q567R and I573V peptides form discrete trimers over a ten-fold range of peptide concentration (10 to 100 μM) (table 1, Fig. 5C and D). In conclusion, these data indicate that the Q567R and I573V reversions have minimal effects on the gp41 six-helix bundle structure, which is in accordance with the assumption that they primarily restore virus replication by compensating for an early biosynthesis defect.

In other evolution experiments with Env mutants we exclusively found that reversions occur locally (chapters 4.2, 5.4 and 5.7). Here we describe variants that have changes at two spots within Env: around the leader peptide cleavage site and in the gp41 ectodomain. It may not be surprising that reversions near the leader peptide cleavage site occur in the C54A/C74A virus, because leader peptide cleavage is almost completely abrogated in this variant (chapter 4.1). The substitutions at position 24, 33 and 38 may thus have a positive effect on leader peptide cleavage, and this possibility is currently under investigation. It may also not be a complete surprise that mutations in gp41 compensate for a defect caused by mutations in the C1 region, because it is known that this gp120 domain is involved in the intersubunit interaction with gp41 (3, 9). The structural changes in C1 due to the loss of the disulfide bond can have a major impact on this interaction. Although the region around residues Q567 and I573 is involved in the

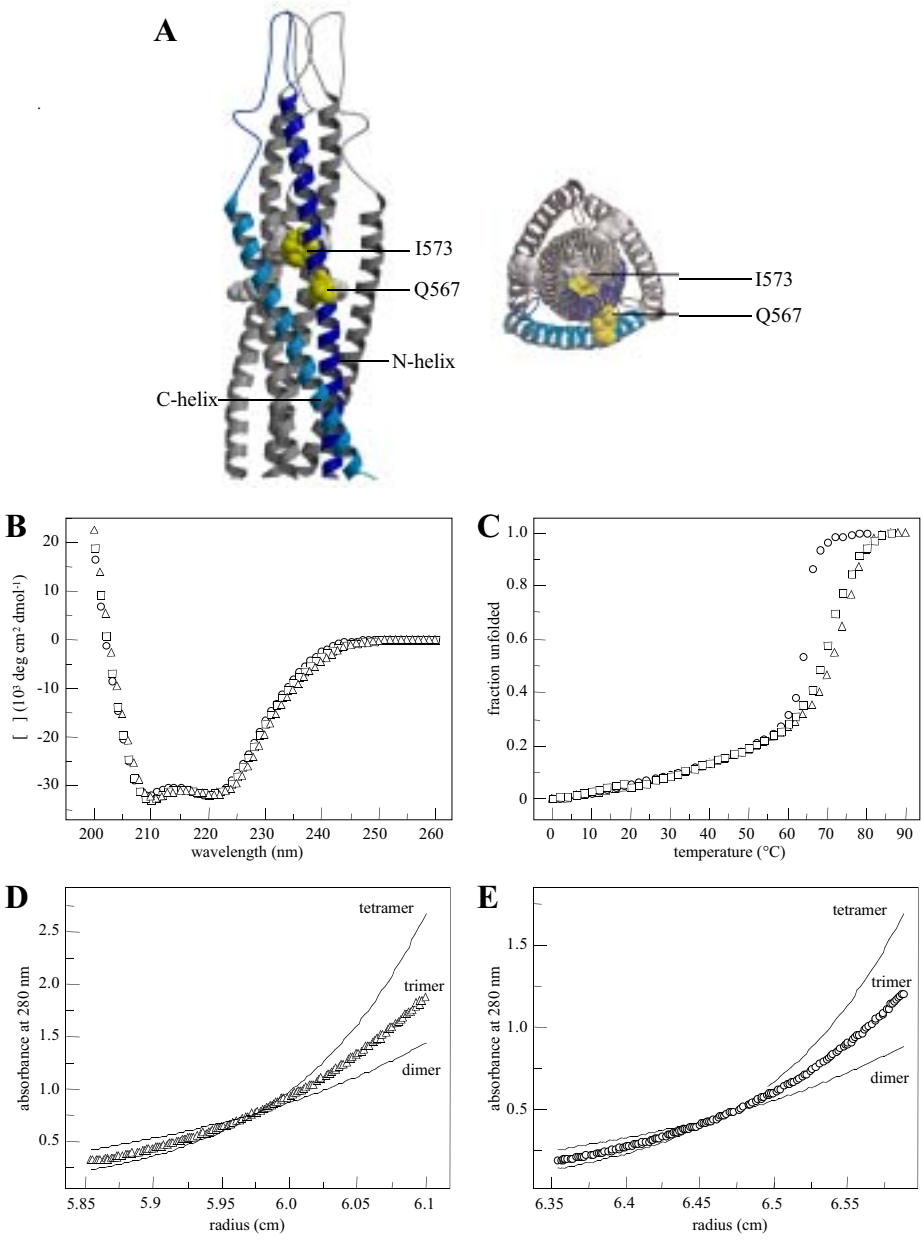

Fig. 5. Properties of the wt and mutant gp41 peptidess. **A**. Location of the Q567R and I573V substitutions in the structure model of the gp41 ectodomain (1). **B**. Circular dichroism spectra of the wt N34(L6)C28 peptide (open squares), Q567R (open triangles), and I573V (open circles) at 4°C in PBS (pH 7.0) and 10 μM peptide concentration. **C**. Thermal melting experiments monitored by circular dichroism at 222 nm. The decrease in the fraction of a folded molecule is shown as a function of temperature. **D**. Representative sedimentation equilibrium data of a 100 μM solution of Q567R collected at 4°C and 20,000 rpm in PBS (pH 7.0). The data fit best to a trimer model. Curves for dimer and tetramer states are indicated for comparison. **E**. Representative equilibrium sedimentation data of a 30 μM solution of I573V at 4°C in PBS (pH 7.0). The data fit to a trimer model.

gp120 - gp41 interaction (7), we did not measure a significant effect of the Q567R substitution on gp120 shedding (Fig. 4). However, the effect of this substitution may be very subtle. Alternatively, the effect of this substitution on the interaction between the C1 region and gp41 may be more important in a transient intermediate during Env folding.

Acknowledgements

We thank Norbert Schülke and Bill Olson for the gift of recombinant gp120, James Binley for the gift of HIVIg, Janice Clements for the donation of LuSIV cells, Stephan Heynen for technical assistance, and Ineke Braakman and Eelco van Anken for helpful discussions. This work was sponsored by the Dutch AIDS Fund (Amsterdam).

References

1. **Caffrey, M.** 2001. Model for the structure of the HIV gp41 ectodomain: insight into the intermolecular interactions of the gp41 loop. Biochim. Biophys. Acta **1536**:116-122.
2. **Das, A. T., A. Land, I. Braakman, B. Klaver, and B. Berkhout.** 1999. HIV-1 evolves into a nonsyncytium-inducing virus upon prolonged culture *in vitro*. Virology **263**:55-69.
3. **Helseth, E., U. Olshevsky, C. Furman, and J. Sodroski.** 1991. Human immunodeficiency virus type 1 gp120 envelope glycoprotein regions important for association with the gp41 transmembrane glycoprotein. J. Virol. **65**:2119-2123.
4. **Kozak, S. L., E. J. Platt, N. Madani, F. E. Ferro, K. Peden, and D. Kabat.** 1997. CD4, CXCR-4, and CCR-5 dependencies for infections by primary patient and laboratory-adapted isolates of human immunodeficiency virus type 1. J. Virol. **71**:873-882.
5. **Lu, M., H. Ji, and S. Shen.** 1999. Subdomain folding and biological activity of the core structure from human immunodeficiency virus type 1 gp41: implications for viral membrane fusion. J. Virol. **73**:4433-4438.
6. **Peden, K., M. Emerman, and L. Montagnier.** 1991. Changes in growth properties on passage in tissue culture of viruses derived from infectious molecular clones of HIV-1_{LAI}, HIV-1_{MAL}, and HIV-1_{ELI}. Virology **185**:661-672.
7. **Sanders, R. W., B. Korber, M. Lu, B. Berkhout, and J. P. Moore. 2002. Mutational analyses and natural variablility of the gp41 ectodomain,** p. 43-68. *In* C. Kuiken, B. Foley, E. Freed, B. Hahn, P. Marx, F. McCutchan, J. Mellors, S. Wolinsky, and B. Korber (eds.), HIV Sequence compendium 2002. Los Alamos National Laboratory, Theoretical Biology and Biophysics Group, Los Alamos, New Mexico.
8. **Sanders, R. W., M. Vesanen, N. Schuelke, A. Master, L. Schiffner, R. Kalyanaraman, M. Paluch, B. Berkhout, P. J. Maddon, W. C. Olson, M. Lu, and J. P. Moore.** 2002. Stabilization of the soluble, cleaved, trimeric form of the envelope glycoprotein complex of human immunodeficiency virus type 1. J. Virol. **76**:8875-8889.
9. **Wyatt, R., E. Desjardin, U. Olshevsky, C. Nixon, J. Binley, V. Olshevsky, and J. Sodroski.** 1997. Analysis of the interaction of the human immunodeficiency virus type 1 gp120 envelope glycoprotein with the gp41 transmembrane glycoprotein. J. Virol. **71**:9722-9731.

Chapter 5.1

A recombinant HIV-1 envelope glycoprotein complex stabilized by an intermolecular disulfide bond between the gp120 and gp41 subunits is an antigenic mimic of the trimeric virion-associated structure

(*Journal of Virology,* January 2000, p. 627-643, Vol. 74, No. 2)

James M. Binley[1], Rogier W. Sanders[2], Brian Clas[1], Norbert Schuelke[3], Aditi Master[1], Yong Guo[1], Francis Kajumo[1], Deborah J. Anselma[3], Paul J. Maddon[3], William C. Olson[3], John P. Moore[1]

[1]Aaron Diamond AIDS Research Center, The Rockefeller University, New York, New York 10016

[2]Dept. of Human Retrovirology, Academic Medical Center, University of Amsterdam, 1105 AZ Amsterdam, The Netherlands

[3]Progenics Pharmaceuticals, Inc., Tarrytown, New York 10591

The few antibodies that can potently neutralize human immunodeficiency virus type 1 (HIV-1) recognize the limited number of envelope glycoprotein epitopes exposed on infectious virions. These native envelope glycoprotein complexes comprise three gp120 subunits noncovalently and weakly associated with three gp41 moieties. The individual subunits induce neutralizing antibodies inefficiently but raise many nonneutralizing antibodies. Consequently, recombinant envelope glycoproteins do not elicit strong antiviral antibody responses, particularly against primary HIV-1 isolates. To try to develop recombinant proteins that are better antigenic mimics of the native envelope glycoprotein complex, we have introduced a disulfide bond between the C-terminal region of gp120 and the immunodominant segment of the gp41 ectodomain. The resulting gp140 protein is processed efficiently, producing a properly folded envelope glycoprotein complex. The association of gp120 with gp41 is now stabilized by the supplementary intermolecular disulfide bond, which forms with approximately 50% efficiency. The gp140 protein has antigenic properties which resemble those of the virion-associated complex. This type of gp140 protein may be worth evaluating for immunogenicity as a component of a multivalent HIV-1 vaccine.

Introduction

The urgent need for an effective vaccine against human immunodeficiency virus type 1 (HIV-1) is undoubted, for only by vaccination will the worldwide spread of AIDS be stemmed (44, 46, 62). Although there is not yet universal consensus on

what components will be needed in a vaccine that is able to induce protective immunity against HIV-1 infection or disease, a popular view is that both the humoral and the cellular arms of the human immune system should be efficiently stimulated (12-14, 43, 44, 46, 57, 64, 94). To do this will probably require the creation of a multivalent vaccine that incorporates several categories of immunogen, each intended to optimally evoke different, necessary immune responses. Examples would be a live recombinant virus or a DNA vector to stimulate cellular immunity, combined with a subunit protein to generate antibody responses (4, 5, 32, 93).

There has, arguably, been more progress with evoking HIV-1-specific cellular immunity than humoral immunity in recent years, although some new concepts relating to neutralizing-antibody induction that merit continued evaluation have recently been described (18, 52, 81, 90, 103). The most widely tried method of neutralizing-antibody induction, i.e., that involving recombinant monomeric gp120 proteins, has not been successful at inducing antibodies able to neutralize heterologous primary isolates at significant titers (4, 5, 22, 40, 58, 59, 81, 111, 120). This raises serious questions about the protective efficacy of vaccines that include such proteins, either alone or in combination with other immunogens (14). One of the major obstacles to neutralizing-antibody induction is the inherent resistance of primary HIV-1 isolates to such antibodies (10, 12, 13, 58, 59, 64, 66-68, 80, 81, 102, 107, 112, 120), a feature that HIV-1 shares with other lentiviruses and one which is probably necessary for viral persistence *in vivo* (3, 23, 65). The native HIV-1 envelope glycoprotein complex on virions, a heterotrimer containing three gp120 proteins noncovalently associated with three gp41 moieties, is recognized poorly by antibodies that efficiently bind to the individual gp120 and gp41 subunits (51, 66, 81, 98, 102, 122).

Notwithstanding the natural defenses used by HIV-1 to resist or evade humoral immunity, proteins which faithfully represent the antigenic structure of the virion-associated envelope glycoprotein complex may be worth evaluating as vaccine immunogens. For instance, the three most potent HIV-1 neutralizing antibodies yet identified, immunoglobulin b12 (IgG1b12), 2G12, and 2F5, have a high affinity for the native trimer which is comparable to or sometimes greater than their affinity for the individual gp120 or gp41 subunits (15, 34, 77, 92, 96, 98, 102, 109). These antibodies may therefore have been raised by an immune response to virions rather than to viral debris or dissociated subunits (13, 68, 80, 81).

The lability of the noncovalent interaction between gp120 and gp41, which causes extensive gp120 dissociation from virions or virus-infected cells (38, 61, 70, 87), is a major obstacle to making stable recombinant, oligomeric envelope glycoproteins. Initial attempts at making stable oligomers therefore involved the introduction of mutations to remove or replace the gp120-gp41 cleavage recognition sequence (6, 27-29). Usually, such proteins are also truncated N-terminal to the transmembrane-spanning region of gp41, so that they are efficiently secreted as soluble proteins (the internal segment of gp41 is of limited relevance for induction of humoral immune responses). A broadly similar nonrecombinant protein was isolated from a virus-infected cell line (110). The resulting proteins (gp140s) contain the gp120 moiety linked to the 20-kDa gp41 ectodomain by a peptide bond between the C terminus of gp120 and the N terminus of gp41, which is not present in the virion-associated complex. Although these uncleaved gp140 pro-

teins (designated $gp140_{UNC}$) are oligomerized by strong, noncovalent intermolecular interactions between gp41 subunits (19, 101, 116), it is questionable whether they truly mimic the native envelope glycoprotein complex. Thus, epitopes are exposed on $gp140_{UNC}$ proteins that are not accessible on virions (27, 28), and there are indications that coreceptor interactions of $gp140_{UNC}$ proteins are inefficient (31). Together, these observations imply that a structural perturbation is caused to the gp120 component by the covalently attached, improperly associated gp41 ectodomain (31). For whatever reason, immunogenicity studies carried out to date with $gp140_{UNC}$ proteins have not been particularly encouraging, in that primary virus-neutralizing antibodies have not been induced (27, 90, 110).

We have therefore pursued a different approach: the expression of gp140 proteins with the natural gp120-gp41 cleavage site preserved but with a disulfide bond introduced between gp120 and the gp41 ectodomain to stabilize the association of these two subunits. We report here on the antigenic properties of such a gp140 protein.

Materials and methods

Cloning of gp140 and furin

Plasmid pPPI4 is a eukaryotic shuttle vector generated at Progenics Pharmaceuticals Inc. The expression of HIV-1 envelope proteins is under the control of the cytomegalovirus major immediate-early promoter-enhancer with a tissue plasminogen activator leader and bovine growth hormone poly(A) signal (106). The vector contains the dihydroxyfolate reductase gene and a simian virus 40 SV40 origin of replication, which promotes high-level replication and transient expression of open reading frames in cells expressing the SV40 large T antigen. PCR was used to clone DNA encoding the gp140 segment of the *env* genes of isolates JR-FL (50), DH123 (100), HxB2 (88), GUN-1wt (104), and 89.6 (21) from the corresponding HIV-1 genomic plasmids. The primers used were 5'Kpnlenv (5'-GTCTATTATGGGGTACCTGTGTGGAAAGAAGC-3') and 3'BstB1env (5'-CGCAGACGCAGATTCGAATTAATACCACAGCCAGTT-3'). The restriction sites are underlined. The PCR products were cloned into pPPI4 by using *Kpn*I and *Bst*B1. These plasmids are designated $gp140_{WT}$ (wild type) to distinguish them from the mutated forms described below. A furin-expressing plasmid, pGEMfurin, was obtained from Gary Thomas, Vollum Institute, Portland, Oreg. (63). The *Eco*RI-*Hin*dIII fragment of furin was subcloned into pcDNA3.1 (Invitrogen Inc.) to make pcDNA3.1furin.

Mutagenesis of gp140

A variety of double cysteine substitutions were introduced into the gp120 and gp41 moieties of $gp140_{WT}$ (HIV-1_{JR-FL}) in pPPI4 by using Quickchange mutagenesis kits (Stratagene, La Jolla, Calif.) and verified by sequencing. Details of the positions of these substitutions are provided in Results (see Fig. 3). A similar strategy was used to make the corresponding cysteine substitutions in other HIV-1 gp140 proteins. A gp120-gp41 cleavage site mutant of JR-FL $gp140_{UNC}$ was generated by substitution of the sequence Lys-Arg-Arg-Val-Val-Gln-Arg-Glu-Lys-Arg-Ala-Val (the C terminus of gp120 and the first two residues of gp41) by

a hexameric Leu-Arg motif. This eliminates the furin cleavage motif (underlined), as described previously (30) (see Fig. 3). The PCR primers were 3'140M (TCGAAGGCGGAGACGAAGTCGTAGCCGCAGTGCCTTGGTGGGTGC TACTCCTAATGGTTC) with 5'KpnIenv and 5'140M (5'-CTACGACTTGTCT CCGCCTTCGACTACGGGGAATAGGAGCTGTGTTCCTTGGGTTCTTG-3') with 3'BstB1env. The PCR products of these two reactions were purified, and an overlap PCR reaction was performed to generate a full-length *env* gene that was cloned into pPPI4 by *Kpn*I-*Bst*BI digestion.

Note that the numbering system used to denote the positions of gp120 and gp41 residues in HIV-1_{JR-FL} is based on the numbering of residues in HIV-1_{HxBc2}, to facilitate comparison with structural information published on this envelope glycoprotein (51, 122).

Transfection, labeling, and immunoprecipitation

Adherent 293T cells were grown in Dulbecco's modified Eagle's medium (Gibco) supplemented with 10% fetal calf serum, penicillin, streptomycin, and L-glutamine. Transient transfection of 293T cells was performed by calcium phosphate precipitation. The gp140 expression plasmids pPPI4-gp140 were transfected with or without cotransfection of the furin expression vector pcDNA3.1-furin, each at 10 μg per 10-cm^2 plate. At 1 day posttransfection, the medium was changed to Dulbecco's modified Eagle's medium supplemented with 0.2% bovine serum albumin, penicillin, streptomycin and L-glutamine. For radioimmunoprecipitation analysis (RIPA), [^{35}S]cysteine and [^{35}S]methionine (200 μCi per plate; Amersham International PLC) were added for 24 h. The culture supernatants were then cleared of debris by centrifugation before addition of concentrated RIPA buffer to adjust the composition to 50 mM Tris-HCl-150 mM NaCl-1 mM EDTA (pH 7.2). Envelope glycoproteins were immunoprecipitated with monoclonal antibodies (MAbs) to a variety of epitopes. In some instances, the MAbs had been labeled with biotin (42). The MAbs were added in a 1-ml volume for 10 min at room temperature and then precipitated by incubation overnight at 4°C with either streptavidin-coated agarose beads (Vector Laboratories) or protein G-coated agarose beads (Pierce Inc.), as appropriate. The beads were washed three times with RIPA buffer containing 1% Nonidet P-40 detergent, and then the proteins were eluted by heating at 100°C for 5 min in 60 μl of polyacrylamide gel electrophoresis (PAGE) buffer supplemented with 2% sodium dodecyl sulfate (SDS) and, when indicated, 100 mM dithiothreitol (DTT). The immunoprecipitates were fractionated by SDS-PAGE (8% polyacrylamide) at 200 V for 1 h. Unless otherwise specified (e.g., see Fig. 2 and 10), the amounts of immunoprecipitated envelope glycoproteins loaded onto each lane were comparable, in that fixed numbers of cells were transfected with the same amount of plasmid and then a constant volume of supernatant was precipitated with a standard amount of MAb. The gels were dried and exposed to a phosphor screen. The positions of the radiolabeled proteins were determined by using a PhosphorImager with ImageQuant software (Molecular Dynamics Inc.).

MAbs to HIV-1 envelope glycoprotein epitopes, and sCD4

The epitopes for, and some immunochemical properties of, anti-gp120 MAbs from various donors have been described previously (9, 71, 72). These include 19b and 83.1 to the V3 loop (74, 118), IgG1b12 and F91 to the CD4 binding site (CD4bs) (15, 72), 2G12 to a unique C3-V4 glycan-dependent epitope (108, 109), M90 to the C1 region (113), 23A and sheep antibody D7324 to the C5 region (69, 72), C11 to a discontinuous C1-C5 epitope (75), 17b to a CD4-inducible epitope (9, 47, 72, 91, 103, 105, 122, 123), A32 to a CD4-inducible C1-C4 epitope (72, 103), and G3-519 and G3-42 to C4 and C4/V3 epitopes, respectively (72, 73). MAbs to gp41 epitopes included 7B2 to epitope cluster I (a gift from James Robinson); 4D4 to cluster I (11); T4, an oligomer-specific MAb overlapping the cluster I region (28); 2.2B to cluster II (a gift from James Robinson); T15G1 to cluster II (a gift from Ab Notkins); and 2F5 to a neutralizing epitope encompassing residues 653 to 659 (11, 77, 108). The tetrameric CD4-IgG2 and monomeric soluble CD4 (sCD4) molecules, from Progenics Pharmaceuticals Inc., have also been described previously (2).

Quantitation of gp120 and gp140 proteins by ELISA

To measure the secretion of gp120 and gp140 proteins from transfected 293T cells, we used a gp120 antigen capture enzyme-linked immunosorbent assay (ELISA) based on one that has been described previously (7, 69, 71). Briefly, envelope glycoproteins in the culture supernatants were denatured and reduced by boiling with 1% SDS and 50 mM DTT. Purified monomeric JR-FL gp120 treated in the same way was used as a reference standard for gp120 expression (106). The denatured proteins were captured on plastic by sheep antibody D7324, which was raised to the continuous sequence APTKAKRRVVQREKR at the C terminus of gp120. Bound envelope glycoproteins were detected by using a mixture of MAbs B12 and B13 against epitopes exposed on denatured gp120 (1, 71). This assay allows the efficient detection of both gp120 and any gp140 molecules in which the peptide bond between gp120 and the gp140 ectodomain is still intact (71, 106).

Sucrose velocity gradient centrifugation

Culture supernatants from *env*-transfected 293T cells were concentrated by 100-fold on Millipore concentrators, and then a 100-µl aliquot was layered onto a 5 to 20% sucrose step gradient of 8.8 ml comprising 11 steps of 800 µl each. The gradient was overlaid to bring the volume up to 12 ml and then centrifuged for 20 h at 40,000 *g* in an SW41Ti rotor at 4°C. Gradient fractions of 500 µl taken sequentially from the top were immunoprecipitated with MAb 2G12, boiled with SDS, and analyzed by SDS-PAGE.

Gel filtration analysis

Culture supernatants from ^{35}S-labeled *env*-transfected 293T cells were concentrated 100-fold on Millipore concentrators. A 100-µl aliquot of the concentrate was loaded onto fast protein liquid chromatography Superdex 200 HR 10/30 column (Pharmacia, Piscataway, N.J.), equilibrated with Ca^{2+}- and Mg^{2+}-free phosphate-buffered saline. The column was eluted at a flow rate of 0.4 ml/min, and

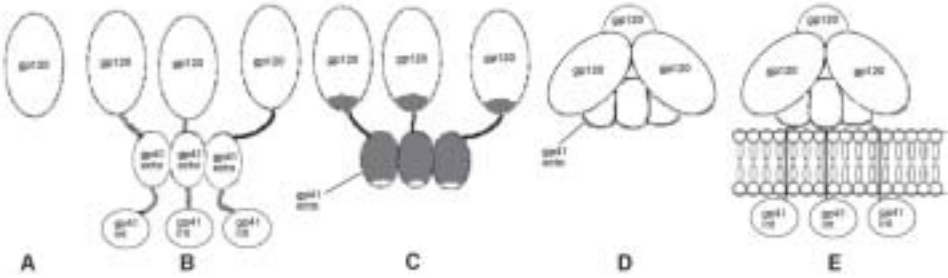

Fig. 1. Different forms of the HIV-1 envelope glycoproteins. **A.** Monomeric gp120. **B.** Full-length recombinant gp160 (in practice, this protein may form higher-order aggregates in solution because of associations between various hydrophobic domains). **C.** Proteolytically unprocessed gp140 trimer with the peptide bond maintained between gp120 and gp41 ($gp140_{UNC}$ or $gp140_{NON}$). **D.** The SOS gp140 protein, a proteolytically processed gp140 stabilized by an intermolecular disulfide bond. **E.** Native, virion-associated gp120-gp41 trimer. The topologies of these proteins are inferred from previous reports cited in the text and from studies described in this paper. The shading of the $gp140_{UNC}$ protein (**C**) indicates the major antibody-accessible regions that are poorly or not exposed on the SOS gp140 protein or on the native gp120-gp41 trimer. The trimeric state of the SOS gp140 protein (**D**) has not yet been confirmed experimentally.

0.25-ml fractions were collected. Identical fractions from four runs were pooled and immunoprecipitated with MAb 2G12 as described above. Comparison of the envelope glycoprotein elution profiles with those of known protein standards allowed an approximate assessment of molecular weights.

Results

Wild-type gp140 is incompletely processed by cellular proteases

We chose to use the $HIV\text{-}1_{JR\text{-}FL}$ strain (subtype B) as our template for studies of the antigenic structure of oligomerized envelope glycoproteins. Several reasons underlay this choice: (i) $HIV\text{-}1_{JR\text{-}FL}$ is a primary R5 isolate with a typical neutralization resistance profile and so is representative of the most commonly transmitted HIV-1 strains (34, 107); (ii) it is a molecularly cloned virus with a well-characterized *env* gene (50); (iii) we have previously expressed the gp120 monomer protein from $HIV\text{-}1_{JR\text{-}FL}$ (106); and (iv) we have already studied the MAb reactivity profiles of the $HIV\text{-}1_{JR\text{-}FL}$ gp120 monomer and cell surface-expressed gp120/gp140 complex and so are familiar with their antigenic properties (34, 35, 106).

To gain experience with the gp140 form of the $HIV\text{-}1_{JR\text{-}FL}$ envelope glycoprotein, we expressed a protein which had the natural cleavage site between gp120 and gp41 maintained intact ($gp140_{WT}$). In common with all the mutants that we subsequently describe, the $gp140_{WT}$ protein has the gp41 moiety truncated close to the transmembrane-spanning region, so that it contains both gp120 and the gp41 ectodomain ($gp41_{ECTO}$) (Fig. 1). When we expressed the $gp140_{WT}$ construct in 293T cells by transient transfection, we could detect envelope glycoproteins in the supernatants at between 100 and 500 ng per ml by using an antigen-capture ELISA that recognizes both gp120 and gp140 proteins after they have been deliberately denatured. When the culture supernatants were immunoprecipitated with various anti-gp120 antibodies and then subjected to denaturing SDS-PAGE

analysis, two bands appeared consistently on the gels. The results of one such immunoprecipitation experiment, with the 2G12 MAb as the precipitating antibody, are shown in Fig. 2. Although higher-molecular-mass aggregates were also present, two discrete bands can be seen; one of these, which we assumed to be free gp120, migrated at 120 kDa, and the other ran at 140 kDa (Fig. 2, lane 1). This latter protein migrated identically to a gp140 protein that we had mutated in the gp120-gp41 cleavage site ($gp140_{UNC}$) (lane 3).

We reasoned that the 140-kDa band produced during expression of the $gp140_{WT}$ construct in transient transfections most probably arises because the host cell proteases of the furin family only incompletely cleave the scissile peptide bond between gp120 and the gp41 ectodomain. This could occur because the proteases are saturated by the large amount of gp140 expressed during a transient-transfection procedure. We therefore cotransfected a furin-encoding plasmid with the $gp140_{WT}$-expressing plasmid, since such a procedure has been shown to increase the proteolytic processing of Ebola virus envelope glycoproteins (114).

In the presence of exogenous furin, the $gp140_{WT}$ protein was completely processed into its gp120 and $gp41_{ECTO}$ components (Fig. 2, lane 2). Of these, only the gp120 band is clearly visible on SDS-PAGE gels after immunoprecipitation;

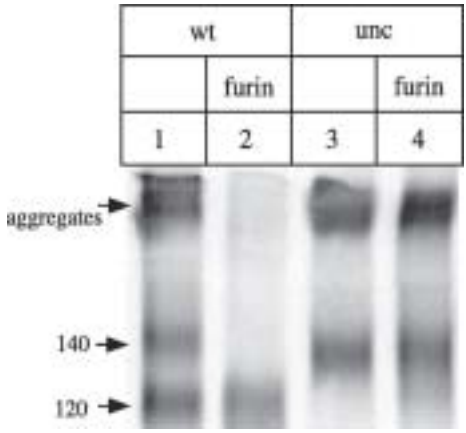

Fig. 2. Cotransfection of furin increases the efficiency of cleavage of the peptide bond between gp120 and gp41. 293T cells were transfected with DNA expressing the $HIV\text{-}1_{JR\text{-}FL}$ $gp140_{WT}$ or $gp140_{UNC}$ (gp120-gp41 cleavage site mutant) proteins, in the presence or absence of a cotransfected furin-expressing plasmid. The ^{35}S-labeled envelope glycoproteins secreted from the cells were immunoprecipitated with the anti-gp120 MAb 2G12, boiled with SDS, and analyzed by SDS-PAGE. Lanes: 1, $gp140_{WT}$ (gp140/gp120 doublet); 2, $gp140_{WT}$ plus furin (gp120 only); 3, $gp140_{UNC}$ (gp140 only); 4, $gp140_{UNC}$ plus furin (gp140 only). The approximate molecular masses, in kilodaltons, of the major species are recorded on the left, as are higher-molecular-mass aggregates. Only one-fifth of the immunoprecipitated proteins from the transfections shown in lanes 1 and 3 were loaded onto the gel, to ensure that the amounts of envelope glycoproteins analyzed in each lane were approximately comparable.

this is probably because the hydrophobic fusion peptide causes the 20-kDa gp41 ectodomain to self-aggregate when it is not bound to gp120. In contrast to $gp140_{WT}$, the $gp140_{UNC}$ mutant was unaffected by the cotransfection of endogenous furin, still giving rise to only a single 140-kDa band in immunoprecipitates, because the cleavage site for furin proteases has been eliminated by mutation (lane 4). Furin cotransfection did, however, reduce by approximately fivefold the overall secretion of HIV-1_{JR-FL} envelope glycoproteins, as judged by the results of immunoprecipitations with polyclonal sera pooled from HIV-1-infected individuals (data not shown). This may be due to competition between the gp140- and furin-expressing plasmids for transcription or translation. We therefore adjusted the volume of supernatant used in each immunoprecipitation procedure with MAbs, to ensure that the total amounts of envelope glycoproteins present were comparable.

The above results confirm our assumption that the 140-kDa band obtained when the $gp140_{WT}$ protein is expressed in the absence of exogenous furin arises because of incomplete proteolytic cleavage of the peptide bond between gp120 and the gp140 ectodomain. We therefore designate this noncleaved gp140 protein $gp140_{NON}$ (Fig. 1). Another feature of furin cotransfection was that it eliminated the production of the high molecular weight aggregates that were visible in immunoprecipitates of both the $gp140_{WT}$ and $gp140_{UNC}$ proteins (Fig. 2, compare lane 2 with lanes 1, 3, and 4). When furin is cotransfected, the gp41 ectodomains cleaved off the gp120 subunits presumably still aggregate but are not precipitated by anti-gp120 antibodies.

Stabilization of the gp120-gp41 interaction by introduction of double cysteine substitutions

With furin cotransfection, we could now express a soluble gp140 protein in which the gp120 and $gp41_{ECTO}$ components were associated only through a noncovalent linkage, mimicking what occurs in the native trimeric envelope glycoprotein complex on virions. However, the natural, noncovalent association between gp120 and gp41 is weak, leading to the gradual shedding of gp120 from virions and the surface of infected cells (38, 61, 70, 87). In practice, an unstable gp120-$gp41_{ECTO}$ complex is unlikely to be useful for vaccination purposes; it would, for example, be difficult to purify. We therefore sought ways to stabilize the gp120-gp41 interaction by the introduction of an intermolecular disulfide bond between the gp120 and gp41 subunits. Of note is that such bonds occur in at least a fraction of the envelope glycoprotein complexes of type C retroviruses, such as murine leukemia virus (MuLV) and human T-lymphotropic virus type 1 (HTLV-1) (25, 37, 48, 54, 55, 78, 82-86, 99).

Our mutagenesis strategy was guided by our earlier theoretical consideration of which regions of gp120 and gp41 were involved in their association (99). This analysis had, itself, been influenced by the mutational studies of Helseth et al. (45). Thus, there is strong mutagenic evidence that the first and last conserved regions of gp120 (C1 and C5 domains) are the contact sites for gp41 (45, 121). The corresponding sites on gp41 are known with less certainty. However, the positions of cysteine residues available for intermolecular disulfide bond formation in, e.g., the MuLV and HTLV-1 envelope glycoproteins strongly suggested

that we should focus our attention on the central region of the gp41 ectodomain, in proximity to the intramolecular disulfide-linked loop (99). This loop is a conserved feature of retroviral envelope glycoproteins (37, 82). More recent information on the structure on the gp41 ectodomain supports this choice (8, 16, 19, 116). Precedent for the introduction of paired cysteine residues leading to the formation of intermolecular disulfide bonds has arisen from studies of HIV-1 gp41 (33) and of other viral envelope glycoproteins (39).

We therefore substituted single cysteine residues at several different positions in the C1 and C5 regions of gp120, focusing on amino-acids previously shown to be important for the gp120-gp41 interaction (Fig. 3A). Simultaneously, we introduced a second cysteine substitution at several residues near the intramolecular disulfide loop of gp41 (Fig. 3B). The intent was to identify pairs of cysteine residues whose physical juxtaposition during gp140 processing was such that an intermolecular disulfide bond would form spontaneously. In all, 53 different double-cysteine substitution mutants were generated in the context of the JR-FL $gp140_{WT}$ protein and then coexpressed with furin by transient transfection of 293T cells (Fig. 4 and 5).

An initial analysis of the transfection supernatants by antigen capture ELISA indicated that all the gp140 mutants were efficiently expressed as secreted proteins, except those which contained a cysteine at residue 495 of gp120 (data not shown). We next characterized the secreted proteins by immunoprecipitation with the anti-gp120 MAbs 2G12 and F91 followed by SDS-PAGE. In this procedure, the envelope glycoproteins were eluted from the beads by boiling for 5 min in SDS-PAGE loading buffer, in the absence of any reducing agent such as DTT. In addition to the 120-kDa band (gp120), a second band of approximately 140 kDa (gp140) was precipitated by 2G12 and F91 from most of the double-cysteine mutant transfection supernatants (Fig. 4). This was not always the case, however, as exemplified by the A497C/W610C mutant, for which no 140-kDa band was visible (Fig. 4, lanes 9 and 10). There was some variation in how far the 140 kDa proteins from the different mutants migrated on the SDS-PAGE gels. For example, the V36C/W596C and T499C/T605C mutants were particularly slow moving (lanes 7 and 8 and lanes 11 and 12, respectively). The presence of diffuse bands with reduced mobility on SDS-PAGE gels is probably indicative of incomplete or improper envelope glycoprotein maturation (25, 27-30, 79). High-molecular-weight aggregates similar to those in Fig. 2 were present in the immunoprecipitates of most of the double-cysteine mutants (data not shown, but see Fig. 10).

To determine which among the double-cysteine mutants was the most suitable for further analysis, we determined the relative intensities of the 140 and 120-kDa bands derived after immunoprecipitation of each mutant by MAb 2G12 followed by SDS-PAGE and densitometry (Fig. 5). We sought the mutant that produced the highest fraction of gp140 in relation to the total amount of secreted gp120 plus gp140 (i.e., the highest ratio of gp140 to gp140 + gp120). Our interpretation was that such a mutant would have the most efficient formation of the intermolecular disulfide bond, while producing a 140-kDa protein that was reactive with a potently neutralizing anti-gp120 MAb.

Among the double-cysteine mutants, the one that most efficiently produced a 2G12-precipitable gp140 protein was a protein containing cysteine substitutions

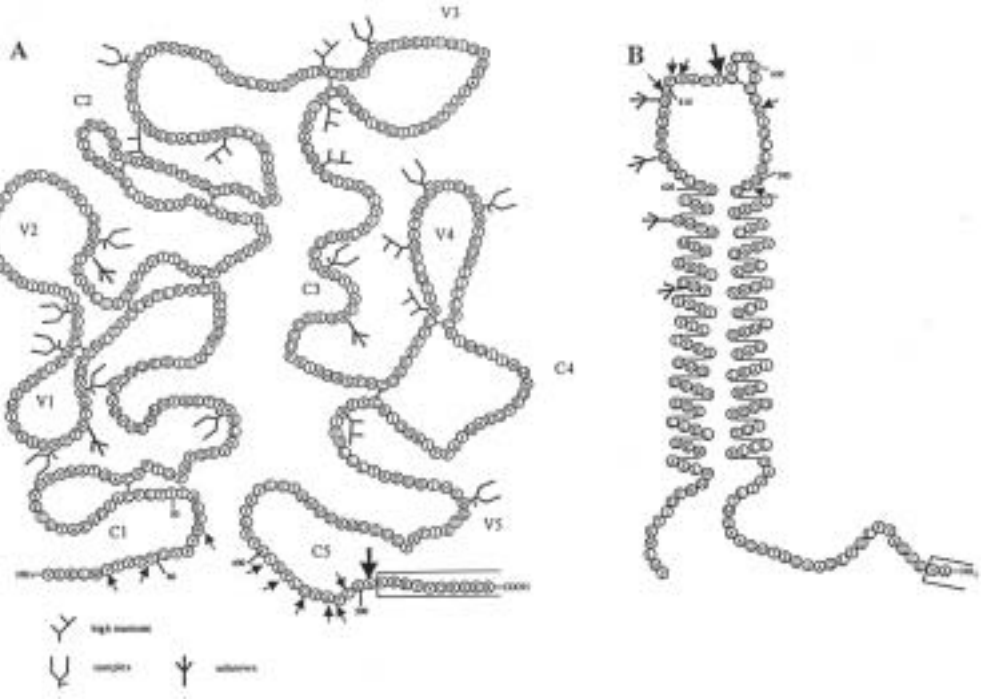

Fig. 3. Positions of cysteine substitutions in JR-FL gp140. The various residues of the JR-FL $gp140_{WT}$ protein that have been mutated to cysteines in one or more mutants are indicated by arrows on the schematics of the gp120 and $gp41_{ECTO}$ subunits. The positions of the alanine-501 and threonine-605 residues that are both mutated to cysteine in the SOS gp140 protein are indicated by the larger arrows. **A.** The depiction of JR-FL gp120, including the positioning of canonical sites for complex and high-mannose *N*-linked carbohydrates, is based on that of Leonard et al. (56), adjusted to reflect the sequence numbering of $HIV\text{-}1_{HXB2}$. **B.** The cartoon of the JR-FL gp41-ectodomain is derived from reference 37, also adjusted to reflect the HXB2 sequence numbering. The open boxes at the C terminus of gp120 and the N terminus of gp41 indicate the regions that are mutated in the $gp140_{UNC}$ protein to eliminate the cleavage site between gp120 and gp41.

at alanine-501 of gp120 and threonine-605 of gp41 (A501C/T605C) (Fig. 5). Of note is that this protein migrated on SDS-PAGE gels as a discrete gp140 band with a mobility identical to that of the uncleaved gp140 protein from JR-FL (Fig. 4, compare lanes 13 and 14 with lane 15). The A501C/T605C mutant was the only one to have this property among the double cysteine mutants that we tested, a finding which suggests that a properly folded and processed gp140 protein is produced. Below, we refer to the A501C/T605C double cysteine mutant as the SOS gp140 protein.

Characterization of the SOS gp140 protein

We verified that the SOS gp140 protein was indeed stabilized by an intermolecular disulfide bond by boiling the 2G12-immunoprecipitated proteins with SDS and DTT prior to gel electrophoresis; under these conditions, only a 120-kDa band was detected (Fig. 6A, lane 4, and Fig. 6B, lane 3). However, boiling with SDS alone did not eliminate the 140-kDa band (Fig. 6A and B, lanes 1). Taken

together, the data imply the presence of a covalent bond between the gp120 moiety and the gp41 ectodomain of the SOS gp140 protein that is sensitive to the presence of a reducing agent, i.e., a disulfide bond. In contrast, the 140-kDa bands produced from the $gp140_{NON}$ ($gp140_{WT}$ without furin) and $gp140_{UNC}$ proteins were unaffected by boiling in the presence of DTT (Fig. 6A, lanes 5 and 6). In these two proteins, the gp120 and $gp41_{ECTO}$ subunits are attached via the uncleaved peptide bond, which is unaffected by reducing agents.

As noted above, SDS-PAGE gels revealed that the mobility and sharpness of the 140-kDa band derived from the SOS gp140 protein was indistinguishable from those of the bands derived from the $gp140_{NON}$ and $gp140_{UNC}$ proteins (Fig. 6A, lanes 1 to 3). We also confirmed that cotransfection of furin was important for the correct formation of the SOS gp140 protein. Thus, in the absence of furin, the 140-kDa band was unaffected by boiling the immunoprecipitated proteins in the presence of DTT, suggesting that an uncleaved peptide bond still links the gp120 and $gp41_{ECTO}$ subunits (Fig. 6B, compare lanes 3 and 4).

Mutants containing only one of the two cysteines present in the SOS gp140 protein (gp140 mutants A501C and T605C) were also evaluated by RIPA with the 2G12 MAb (Fig. 6C). The A501C mutant produced no 140-kDa protein, and the T605C mutant produced a little, but the resulting ratio of gp140 to gp140 + gp120 was much lower with this mutant than with the SOS gp140 protein (Fig. 6C, compare lanes 1 and 3). Furthermore, the 140-kDa band derived from the T605C mutant had a lower mobility than the corresponding band from the SOS gp140 protein and probably represents a misfolded species (Fig. 6C, lane 3). Overall, this study with single cysteine substitutions provides further evidence that the 140-kDa band from the double-cysteine mutants is due to the formation of an intermolecular disulfide bond between gp120 and the gp41 ectodomain.

Attempts to improve the efficiency of disulfide bond formation in the SOS gp140 protein

Although disulfide-stabilized gp140 proteins are secreted from cells expressing the SOS gp140 mutant, there is also significant production of gp120 monomers (Fig. 4 and 6). This implies that the disulfide bond between gp120 and the gp41 ectodomain forms with imperfect efficiency. We attempted to improve this by introducing additional amino-acid substitutions near the inserted cysteines or by varying where the cysteines were positioned in gp120. We retained the gp41 cysteine at residue 605, where it is in the SOS gp140 protein, because this position seemed to be the one at which intermolecular disulfide bond formation was most favored (Fig. 5).

We first varied the position of the cysteine substitution in gp120, by placing it either N-terminal or C-terminal to alanine-501. The ratio of gp140 to gp140 + gp120 was not increased in any of these new mutants; it remained comparable to, or lower than, the ratio derived from the SOS gp140 protein (Fig. 7, lanes 1 to 8). Furthermore, there was a decrease in the mobility and sharpness of the gp140 band compared to that derived from the SOS gp140 protein (lanes 1 to 8). Next, we considered whether the bulky, charged side chains of the lysine residues adjacent to alanine-501 might interfere with disulfide bond formation. We therefore mutated either or both of the lysines at positions 500 and 502 to alanines in the

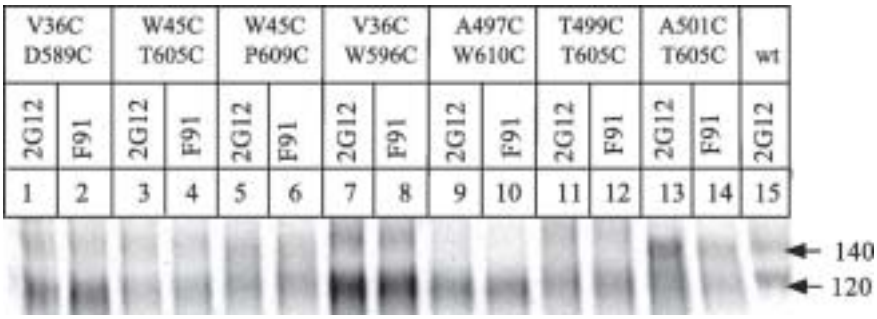

Fig. 4. Immunoprecipitation analysis of selected double cysteine mutants of JR-FL gp140. The ^{35}S-labeled envelope glycoproteins secreted from transfected 293T cells were immunoprecipitated with an anti-gp120 MAb, boiled with SDS, and analyzed by SDS-PAGE. The MAbs used were either 2G12 (odd-numbered lanes) or F91, which recognizes a CD4-binding site-related epitope (even-numbered lanes). The positions of the two cysteine substitutions in each protein (one in gp120, the other in $gp41_{ECTO}$) are noted above the lanes. The $gp140_{WT}$ protein is shown in lane 15. All proteins were expressed in the presence of cotransfected furin, except for the $gp140_{WT}$ protein in lane 15, which serves as a reference standard for the position of 120-kDa (gp120) and 140-kDa ($gp140_{NON}$) bands. Note that in this and all subsequent figures (except Fig. 10) that depict the outcome of RIPA experiments, the photographs have been cropped to show only the 120- and 140-kDa bands, since other regions of the gels were not informative.

context of the SOS gp140 protein, but these changes neither increased the ratio of gp140 to gp140 + gp120 nor affected the migration of gp140 (lanes 9 to 11). Finally, we introduced a second pair of cysteines into the SOS gp140 protein at residues 45 of gp120 and 609 of gp41, since a disulfide bond formed fairly efficiently when this cysteine pair was introduced into the wild-type protein (Fig. 5). The quadruple-cysteine mutant (W45C/A501C/T605C/P609C) was, however, poorly expressed, and the gp120 and gp140 bands that were produced both migrated unusually slowly. The same was observed with two other similar mutants (W45C/K500C/T605C/P609C) and (W45C/K502C/T605C/P609C) (Fig. 7, lanes 12 to 14). This implies that there may be protein-folding or other expression problems with quadruple-cysteine mutants of gp140.

Antigenic properties of the SOS gp140 protein

Among the JR-FL *env* mutants we have yet made, the efficiency of intermolecular disulfide bond formation is apparently the highest in the SOS gp140 protein (A501C/T605C). We therefore characterized the antigenic structure of this protein, by probing its topology with a panel of MAbs to a variety of gp120 and gp41 epitopes (Fig. 8). For comparison, we studied the reactivity of the same MAbs with the $gp140_{NON}$ protein produced when the $gp140_{WT}$ gene is expressed in the absence of cotransfected furin. The $gp140_{NON}$ protein still contains a peptide bond between the gp120 and $gp140_{ECTO}$ subunits (Fig. 6). Structurally, the $gp140_{NON}$ protein is essentially identical to the $gp140_{UNC}$ protein, in which the gp120-gp140 cleavage site has been deliberately replaced by mutagenesis (see Fig. 9). As an additional comparator, we used a double-cysteine mutant in which the gp120 cysteine substitution was in the C1 domain, the W45C/T605C gp140 protein (Fig. 8).

	gp41					
	D589C	W596C	T605C	V608C	P609C	W610C
V36C	0.45	0.40	0.35	0.30	0.40	0.30
Y40C	0.35	0.30	0.60	0.45	0.45	N.D.
W45C	0.45	0.45	0.65	0.50	0.65	0.45

gp120 C1

P493C	0.35	0.30	0.45	0	0	0
G495C	0	0	0.25	0.20	0.30	0
A497C	0	0	0.05	0	0	0
P498C	0	0.10	0.30	0.15	0.05	0
T499C	0	0.15	0.55	0.25	0.25	0.10
A501C	0.05	0	0.75	0.50	0.10	0.25

gp120 C5

Fig. 5. The efficiency of intermolecular disulfide bond formation is dependent upon the positions of the cysteine substitutions. The ^{35}S-labeled envelope glycoproteins secreted from 293T cells cotransfected with furin and the various gp140 mutants were immunoprecipitated with the anti-gp120 MAb 2G12, boiled with SDS, and analyzed by SDS-PAGE. For each mutant, the intensities of the 140- and 120-kDa bands were determined by densitometry and the ratio of gp140 to gp140 + gp120 was calculated and recorded. The extent of shading is proportional to the magnitude of the ratio. The positions of the amino-acid substitutions in gp41 and the C1 and C5 domains of gp120 are recorded along the top and down the sides, respectively. N.D., not done.

Compared to $gp140_{NON}$, the SOS gp140 protein has several antigenic differences that we believe are desirable for a protein intended to mimic the structure of the virion-associated gp120-gp41 complex. These are summarized below.

(i) The SOS gp140 protein is efficiently recognized by the potently neutralizing antibodies IgG1b12 and 2G12 and also by the CD4-IgG2 molecule (Fig. 8A). Although the RIPA method is not sufficiently quantitative to allow a precise determination of relative affinities, the reactivities of these MAbs and of the CD4-IgG2 molecule with the SOS gp140 protein appear to be substantially greater than with the $gp140_{NON}$ and gp120 proteins. Clearly, the SOS gp140 protein has an intact CD4 binding site. Epitopes in the V3 loop are also accessible on the SOS gp140 protein, as shown by its reactivity with MAbs 19b and 83.1 (Fig. 8A). There is very little exposure on the SOS gp140 protein of epitopes for MAbs G3-42 and G3-519 (Fig. 8B). These MAbs bind to the C4 region of gp120, in proximity to the V3 loop and the CD4 binding site, and have neutralizing activity

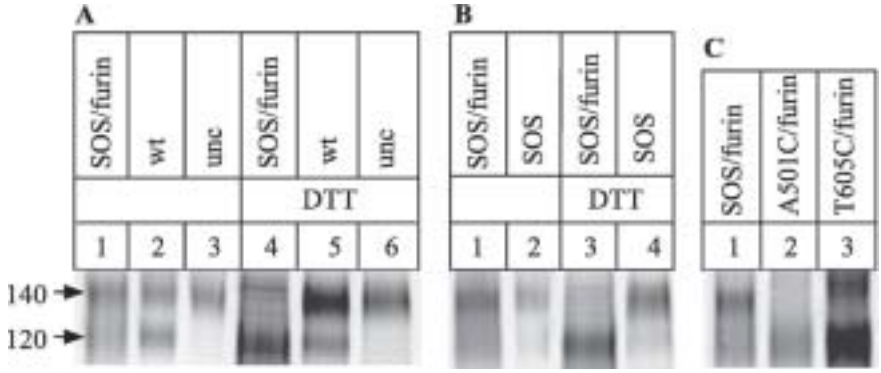

Fig. 6 Confirmation that an intermolecular gp120-gp41 bond forms in the SOS gp140 protein. 293T cells were transfected with plasmids expressing gp140 proteins and, when indicated, a furin-expressing plasmid. The secreted, ^{35}S-labeled glycoproteins were immunoprecipitated with the anti-gp120 MAb 2G12, boiled in the presence of SDS or, when indicated, SDS plus DTT, and analyzed by SDS-PAGE. **A.** Lanes: 1 and 4, SOS gp140 protein (double cysteine mutant A501C/T605C) plus furin; 2 and 5, $gp140_{WT}$ protein, no furin; 3 and 6, $gp140_{UNC}$ protein, no furin. In lanes 1 to 3 the immunoprecipitated proteins were boiled with SDS; in lanes 4 to 6 they were boiled with SDS plus DTT. **B.** Lanes: 1 and 3, SOS gp140 protein plus furin; 2 and 4, SOS gp140 protein without furin. In lanes 1 and 2 the immunoprecipitated proteins were boiled with SDS; in lanes 3 and 4 they were boiled with SDS plus DTT. **C.** Lanes: 1, SOS gp140 protein (double cysteine mutant A501C/T605C) plus furin; 2, single cysteine gp140 mutant A501C plus furin; 3, single cysteine gp140 mutant T605C plus furin. The immunoprecipitated proteins in each case were boiled with SDS. High-molecular-weight aggregates were also present in immunoprecipitates of the SOS gp140 protein (data not shown but see Fig. 10).

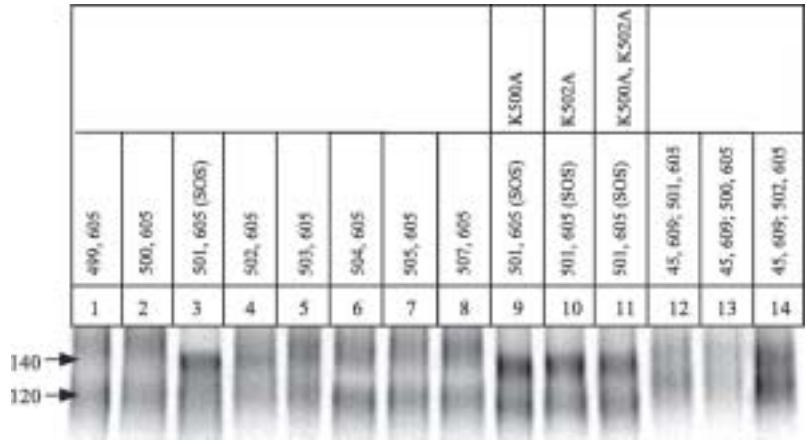

Fig. 7. Analysis of cysteine mutants of JR-FL gp140. The ^{35}S-labeled envelope glycoproteins secreted from gp140-transfected 293T cells in the presence of cotransfected furin were immunoprecipitated with the anti-gp120 MAb 2G12, boiled with SDS, and analyzed by SDS-PAGE. Lanes: 1 to 8, each of the different gp140 double cysteine mutants contained the T605C substitution in gp41, in combination with a second cysteine substitution at the indicated residue in the C5 region of gp120 (the SOS gp140 protein is in lane 3); 9 to 11, gp140 proteins containing the A501C/T605C double cysteine substitutions together with the indicated lysine to alanine substitutions at residue 500 (lane 9), residue 502 (lane 10) or both residues 500 and 502 (lane 11); 12 to 14, gp140 proteins containing quadruple cysteine substitutions; each protein contained the W45C, T605C, and P609C substitutions, plus K500C (lane 12), A501C (lane 13), or K502C (lane 14).

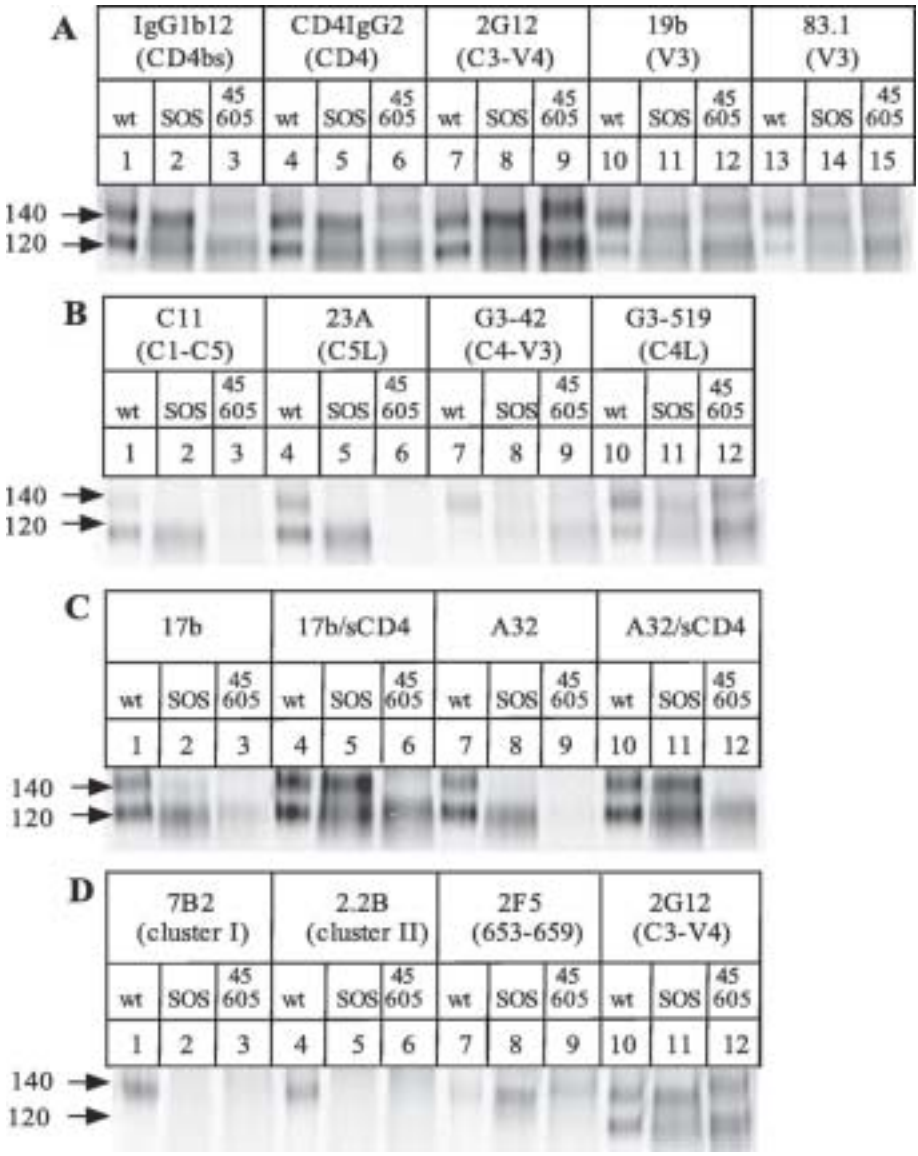

Fig. 8. Comparison of the antigenic structures of the SOS gp140 protein, the $gp140_{NON}$ protein and gp120. The ^{35}S-labeled envelope glycoproteins secreted from transfected 293T cells were immunoprecipitated with different anti-gp120 **A** to **C** or anti-gp41 (**D.**) MAbs, boiled with SDS, and analyzed by SDS-PAGE. Lanes: 1, 4, 7, 10, and 13, $gp140_{WT}$ with no cotransfected furin, producing gp120 and the $gp140_{NON}$ protein; 2, 5, 8, 11, and 14, SOS gp140 protein plus cotransfected furin; 3, 6, 9, 12, and 15, gp140 protein containing the W45C/T605C double cysteine substitutions, plus co-transfected furin. Brief descriptions of the epitopes recognized by each MAb are noted above each lane; for more details, see the primary references listed in Materials and Methods. D, discontinuous epitope; L, linear epitope.

against T-cell-line-adapted but not primary HIV-1 isolates (67, 72, 73, 122). Each of the above MAbs also recognized the $gp140_{NON}$ and gp120 proteins derived from expression of $gp140_{WT}$ in the absence of furin (Fig. 8A). The V3 loop MAbs 19b and 83.1 and the C4-V3 MAb G3-42 bound to the $gp140_{NON}$ protein more strongly than to the corresponding gp120 (note the relative intensities of the 140- and 120-kDa bands in lanes 10 and 13 of Fig. 8A and lane 7 of Fig. 8B, compared to lanes 1, 4, and 7 of Fig. 8A). The V3 loop may be unusually well exposed in the uncleaved gp140 protein.

(ii) Conversely, the nonneutralizing anti-gp120 MAbs C11 and 23A did not bind detectably to the SOS gp140 protein (Fig. 8B). These MAbs recognize epitopes in the C1 and C5 domains, regions of gp120 that are involved in gp41 association and are occluded in the context of a properly formed gp120-gp41 complex (71, 121). Although the cysteine residue at position 501 of the SOS gp140 protein is located near the epitopes for MAbs C11 and 23A, it did not destroy these epitopes; thus, MAbs C11 and 23A bound efficiently to the gp120 derived from the SOS gp140 protein, which also contains the A501C substitution (Fig. 8B). In addition, MAb M90, to a discontinuous C1 epitope, bound weakly to gp120 derived from the SOS gp140 protein but not to the SOS gp140 protein itself. M90 did, however, bind to both the gp120 and gp140 components of $gp140_{WT}$ (data not shown). In contrast to the poor reactivity of the C1- and C5-directed MAbs with the SOS gp140 protein, these MAbs all bound to the $gp140_{NON}$ and gp120 proteins (Fig. 8B) and also to $gp140_{UNC}$ (see Fig. 9) (data not shown). This implies that the C1 and C5 regions of gp120 are abnormally accessible when a peptide bond links gp120 with the gp41 ectodomain.

(iii) The induction of the epitope for MAb 17b by the prior binding of sCD4 occurred far more efficiently on the SOS gp140 protein than on the $gp140_{NON}$ or gp120 protein (Fig. 8C, compare lanes 5 and 2 with lanes 4 and 1). Indeed, in the absence of sCD4, there was very little reactivity of 17b with the SOS gp140 protein (lane 2). The CD4-induced epitope for MAb 17b overlaps the coreceptor binding site on gp120 (91); it is considered that this site becomes exposed on the virion-associated gp120-gp41 complex during the conformational changes which initiate virus-cell fusion after CD4 binding (47, 91, 95, 97, 103). The induction of the 17b epitope on the SOS gp140 protein suggests that the conformation of the gp120 moieties resembles what is present on virions and is not significantly affected by the intermolecular disulfide bond with the gp41 ectodomain. The $gp140_{NON}$ protein bound 17b constitutively, and although there was some induction of the 17b epitope upon soluble CD4 binding, this was much less pronounced than what occurred with the SOS gp140 protein (Fig. 8C).

(iv) Another CD4-inducible epitope on gp120 is that recognized by MAb A32 (72, 103). There was negligible binding of A32 to the SOS gp140 protein in the absence of sCD4, but the epitope was strongly induced by sCD4 binding (Fig. 8C, compare lanes 11 and 8). As observed with 17b, the A32 epitope was much less efficiently induced on the $gp140_{NON}$ protein than on the SOS gp140 protein (compare lanes 10 and 7).

(v) Neither of the nonneutralizing anti-gp41 MAbs 7B2 and 2.2B recognized the SOS gp140 protein, whereas each bound strongly to the $gp140_{NON}$ protein (Fig. 8D). These anti-gp41 MAbs recognize the two major epitope clusters of the

gp41 ectodomain, both of which are considered to be occluded by gp120 in the virion-associated gp120-gp41 complex (71, 98). Similar results were obtained with several other MAbs to these regions, T4, T15G1, and 4D4 (data not shown). The failure of these anti-gp41 MAbs to bind to the SOS gp140 protein is another indication that this protein adopts a configuration similar to that of the native trimer. However, we cannot exclude the possibility that the formation of an intermolecular disulfide bond involving the central region of gp41 perturbs the epitopes for several gp41 MAbs by a different mechanism. The efficient recognition of the $gp140_{NON}$ protein by several gp41 MAbs is consistent with the view that proteins of this type have an aberrant conformation because of the peptide bond linking gp120 with gp41 (31).

(vi) In marked contrast to what was observed with the nonneutralizing anti-gp41 MAbs, the neutralizing anti-gp41 MAb 2F5 bound efficiently to the SOS gp140 protein but not detectably to the $gp140_{NON}$ protein (Fig. 8D, compare lanes 11 and 10). When the experiment was repeated with a higher concentration of the $gp140_{WT}$ protein, some 2F5 reactivity could be observed (data not shown). However, when equivalent amounts of the $gp140_{WT}$ and SOS gp140 proteins were compared, it was found that 2F5 reacted more strongly with the latter (Fig. 8D). Of note is that the 2F5 epitope is the only region of gp41 thought to be well exposed in the context of native gp120-gp41 complexes (98). The ability of the SOS gp140 protein to bind 2F5 is again consistent with the view that this protein adopts a configuration similar to that of the native trimer.

We also examined whether sCD4 binding could cause the exposure of other previously occult epitopes in the C1 and C5 regions of gp120 or in several areas of the gp41 ectodomain, as happens when sCD4 induces the shedding of gp120 from gp41 on the native envelope glycoprotein complex (87, 98). However, we could not detect any increase in the exposure of any other gp41 epitopes on the SOS gp140 protein in the presence of sCD4 (data not shown). This indicates that the presence of the intermolecular disulfide bond prevents gp120 from dissociating from the gp41 ectodomain, despite the conformational changes that are induced in the gp120 moiety upon sCD4 binding.

The antigenic properties of the SOS gp140 protein were compared with those of the W45C/T605C gp140 protein. Among the set of mutants that contained a cysteine substitution within the C1 domain, this was the most efficient at gp140 formation (Fig. 5). Although the W45C/T605C gp140 protein reacted well with the 2G12 MAb (Fig. 8A, lane 9), it bound CD4-IgG2 and IgG1b12 very poorly (lanes 3 and 6). Furthermore, there was little induction of the 17b and A32 epitopes on the W45C/T605C gp140 protein by sCD4, although these epitopes were induced on the gp120 moiety from this mutant (Fig. 8C, compare lanes 6 and 12 with lanes 3 and 9). There was some reactivity of anti-gp41 MAbs with the W45C/T605C gp140 protein (Fig. 8D). The anti-gp120 MAbs C11 and 23A recognized neither the gp140 nor the gp120 form of the W45C/T605C mutant (Fig. 8B). For the C1-C5-directed MAb C11, this may be due to a direct effect of the W45C substitution on the epitope (75). Inappropriate protein folding due to the aberrant formation of disulfide bonds in the C1 and C5 regions of gp120 may be an explanation for the lack of 23A reactivity with the W45C/T605C mutant. Taken together with the fact that the gp140 bands from the W45C/T605C protein

are diffuse and of relatively low mobility, these results suggest that this mutant has suboptimal antigenic properties. Indeed, the contrast between the properties of the W45C/T605C gp140 protein and the SOS gp140 protein implies that the positioning of the intermolecular disulfide bonds has a significant influence on the antigenic structure of the resulting gp140 molecule.

Comparing the antigenic structures of $gp140_{NON}$ and $gp140_{UNC}$

We next studied the antigenic structure of the gp140 protein produced when the cleavage site between gp120 and gp41 is replaced by mutation ($gp140_{UNC}$), since this type of protein is being used in vaccine-related studies on the grounds that it is oligomeric (27, 90, 110). We compared $gp140_{UNC}$ with the $gp140_{NON}$ and gp120 proteins produced when $gp140_{WT}$ is expressed in the absence of cotransfected furin (Fig. 9). The $gp140_{NON}$ and $gp140_{UNC}$ proteins could not be distinguished from one another by the reactivity of any of the test MAbs; they are essentially isomorphic. The major differences in antigenic structure between the SOS gp140 protein and the $gp140_{NON}$ protein that were demonstrated in Fig. 8 therefore also apply to the $gp140_{UNC}$ protein. Of particular note is the negligible induction of the 17b epitope on the $gp140_{UNC}$ protein by sCD4 (Fig. 9, compare lanes 6 and 8), which may help explain why proteins of the $gp140_{UNC}$ type interact poorly with the CCR5 coreceptor (31). The aberrant exposure of gp41 in the $gp140_{UNC}$ and $gp140_{NON}$ proteins is also clearly revealed (compare Fig. 9, lanes 11 and 12, with Fig. 8D, lane 2).

Intersubunit disulfide bonds form in SOS gp140 proteins from other HIV-1 isolates

To assess the generality of our observations with gp140 proteins derived from the R5 HIV-1 isolate JR-FL, we generated double-cysteine mutants of gp140s from four other HIV-1 strains. These were the R5X4 viruses GUN-1wt, 89.6, and DH123 and the T-cell-line-adapted X4 virus HxB2. In each case, the cysteines were introduced at the residues equivalent to alanine-501 and threonine-605 of HxB2. The resulting SOS gp140 proteins were precipitated with the 2G12 MAb, in comparison with the $gp140_{WT}$ proteins from each isolate (Fig. 10). In general,

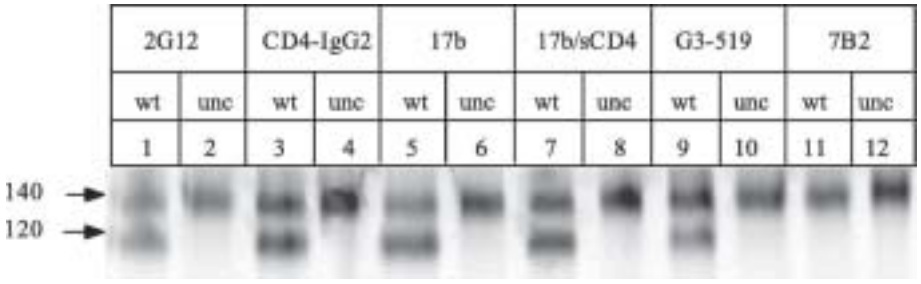

Fig. 9. Comparison of the antigenic structures of the $gp140_{NON}$ and $gp140_{UNC}$ proteins. The ^{35}S-labeled envelope glycoproteins secreted from transfected 293T cells were immunoprecipitated with different anti-gp120 MAbs, boiled with SDS, and analyzed by SDS-PAGE. Odd-numbered lanes contained $gp140_{WT}$ with no cotransfected furin, producing gp120 and the $gp140_{NON}$ protein. Even-numbered lanes contained $gp140_{UNC}$ protein with no cotransfected furin.

the results obtained with the GUN-1wt, 89.6, DH123, and HxB2 proteins were very similar to what was observed with JR-FL gp140s. Disulfide-stabilized gp140 proteins could be efficiently expressed from each isolate, as confirmed by the disappearance of the 140-kDa band when the immunoprecipitates were boiled with DTT before being subjected to SDS-PAGE analysis. In each case, the ratio of gp140 to gp140 + gp120 was comparable to or greater than that observed for the JR-FL SOS gp140 protein. One unexpected but advantageous observation was that furin cotransfection significantly increased the secretion of envelope glycoproteins from 89.6 gp140-transfected cells (Fig. 10B, compare lanes 6 and 7 with lane 5). This may be due to a decrease in the degradation of misfolded proteins when the scissile bond between gp120 and gp41 is correctly cleaved. We do not yet know why this should be an isolate-dependent phenomenon. To some extent, it occurs also with DH123 proteins.

Sucrose gradient analysis of the SOS gp140 and gp140UNC proteins

The oligomeric state of the secreted gp140 complex cannot be determined by immunoprecipitations of unfractionated supernatants, since the proteins are subsequently denatured by boiling with SDS prior to gel electrophoresis. To obtain information on the size of the gp140 protein complex under nondenaturing conditions, we performed a sucrose velocity gradient analysis on 100-fold concentrates of the proteins secreted from 293T cells transfected with SOS gp140 (JR-FL) and furin or, for comparison, with the $gp140_{UNC}$ mutant (Fig. 11A). To detect where various molecular species had migrated on the sucrose velocity gradient, the gradient fractions were immunoprecipitated with MAb 2G12, boiled with SDS, and analyzed by SDS-PAGE.

Three forms of envelope glycoproteins were detected after sucrose gradient fractionation of the SOS gp140 protein (Fig. 11A). Fractions 23 and 24 contained material of a very high molecular mass, which probably correspond to the aggregates that were noted in RIPA experiments (Fig. 2). A broad peak containing envelope glycoproteins with a subunit molecular mass of 140 kDa was centered on fraction 20. A second peak containing 120-kDa subunits was present in fractions 17 to 19, separated from the 140-kDa proteins by two fractions, or 1 ml (Fig. 11A).

When the $gp140_{UNC}$ protein was analyzed, the very-high-molecular-mass aggregates were again present (fractions 22 to 24), and they were more abundant than with the SOS gp140 protein (Fig. 11B). This is consistent with what was observed in the immunoprecipitation analysis shown in Fig. 2. Envelope glycoproteins with a subunit weight of 140-kDa were spread throughout fractions 18 to 24 (Fig. 11B). The 140-kDa proteins in fractions 22 to 24 were most probably derived from high-molecular-mass aggregates formed when the immunoprecipitates were boiled with SDS before being subjected to SDS-PAGE. The 140-kDa proteins in fractions 19 to 21 migrate in the same position as the 140-kDa components of the SOS gp140 preparation.

We interpret the sucrose velocity gradients to indicate that the SOS gp140 preparation contains monomeric gp120 proteins which peak in fractions 17 and 18, together with oligomeric proteins containing 140-kDa subunits which peak in fractions 19 and 20. Excluding the products of protein aggregation, only the

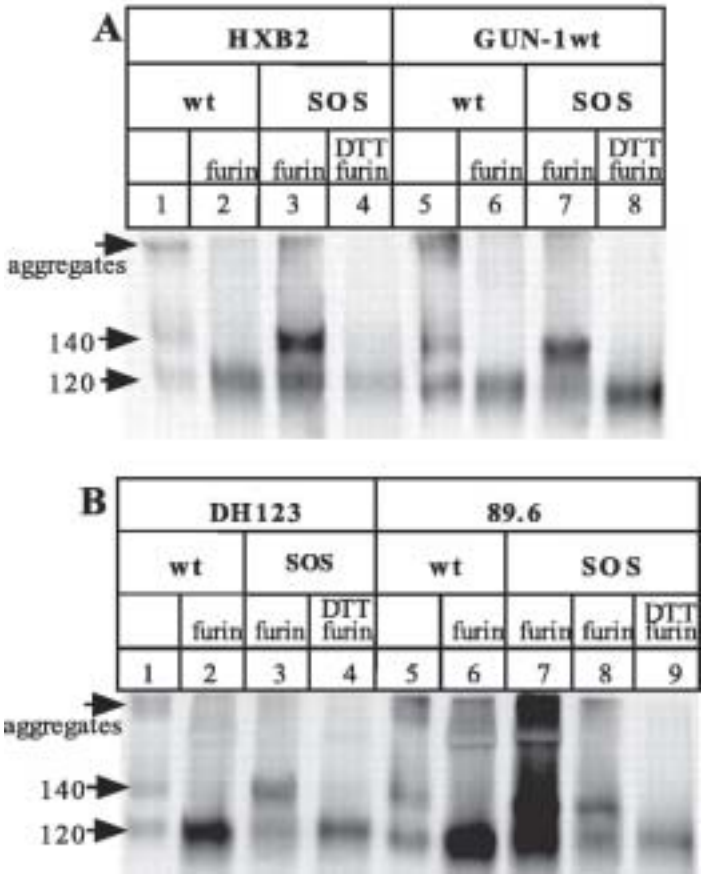

Fig. 10. Preparation of disulfide bond-stabilized gp140 proteins from various HIV-1 isolates. 293T cells were transfected with plasmids expressing gp140 proteins from different isolates and, when indicated, a furin-expressing plasmid. The secreted, ^{35}S-labeled glycoproteins were immunoprecipitated with the anti-gp120 MAb 2G12, boiled with SDS (and, when indicated, DTT), and analyzed by SDS-PAGE. The SOS gp140 protein from each isolate contained double cysteine substitutions at positions equivalent to alanine-501 and threonine-605 of the JR-FL gp140 protein. **A**. HxB2 (lanes 1 to 4) and GUN-1wt (lanes 5 to 8). Lanes: 1 and 5, $gp140_{WT}$ with no cotransfected furin, producing gp120 and the $gp140_{NON}$ protein; 2 and 6, $gp140_{WT}$ plus furin, producing gp120; 3 and 7, SOS gp140 protein plus furin; 4 and 8, as lanes 3 and 7 except that the immunoprecipitates were boiled with both SDS and DTT prior to SDS-PAGE. **B.** DH123 (lanes 1 to 4) and 89.6 (lanes 5 to 9). The layout of the lanes is as in panel A, except that for 89.6, lane 8 is the same as lane 7 but with only one-fifth of the immunoprecipitate loaded onto the gel and lane 9 is the same as lane 8 but with the immunoprecipitates boiled with both SDS and DTT prior to SDS-PAGE. The positions of the 120- and 140-kDa bands, and of higher-molecular-mass aggregates, are indicated on the left of each panel. Only one-fifth of the immunoprecipitated proteins from the $gp140_{WT}$ plus furin transfections (lanes 2 and 6) was loaded onto each gel, to approximately compensate for the increased envelope glycoprotein expression that was observed with the JR-FL $gp140_{WT}$ protein under these conditions.

latter proteins are present in the $gp140_{UNC}$ preparation. From this analysis, we cannot determine the exact molecular mass, and hence the subunit composition, of the oligomeric proteins. However, the fact that they were clearly separated from the 120-kDa gp120 monomers by an approximately 1-ml volume on a standard 5 to 20% sucrose velocity gradient of 8.8 ml (i.e., by a density difference of approximately 1.5% sucrose) indicates that they are probably of several hundred kilodaltons (a 140-kDa monomer would not be separable from a 120-kDa protein under these conditions). This would be consistent with their composition being oligomeric gp120-$gp41_{ECTO}$ complexes, although this cannot be proven by this type of analysis.

Gel filtration analysis of the SOS gp140 and $gp140_{UNC}$ proteins

To obtain additional information on the molecular size of the gp140 protein complexes under nondenaturing conditions, we used size exclusion gel filtration chromatography (Fig. 12). This was performed on concentrates of the proteins secreted from 293T cells transfected with SOS gp140 (JR-FL) plus furin (Fig. 12A) and, for comparison, $gp140_{UNC}$ (Fig. 12B). To detect where various molecular species had migrated, the gradient fractions were immunoprecipitated with MAb 2G12, boiled with SDS, and analyzed by SDS-PAGE.

Three forms of envelope glycoproteins were detected after fractionation of the SOS gp140 protein (Fig. 12A). Fractions 12 to 19 contained material of a high molecular weight, which may again correspond to the aggregates noted in RIPA experiments (Fig. 2). A broad peak containing envelope glycoproteins with a subunit molecular mass of 140 kDa was centered on fractions 20 and 21. This, we believe, is the oligomeric component of the SOS gp140 protein (see below and also Discussion). A more rapidly migrating peak containing 120-kDa subunits was found in and around fractions 24 and 25; this most probably represents the position of gp120 monomers (Fig. 12A).

When the $gp140_{UNC}$ protein was analyzed, the very-high-molecular-weight aggregates were again present (fractions 12 to 19), and they were more abundant than was observed with the SOS gp140 protein (Fig. 12B). This is consistent with the immunoprecipitation analysis in Fig.Fig. 2. Envelope glycoproteins with a subunit weight of 140 kDa were spread throughout fractions 15 to 23, with an apparent peak around fractions 15 and 16 (Fig. 12B). The aggregates in fractions 12 to 18 are probably derived from the unfolding of gp140 and the intermolecular association of hydrophobic gp41 moieties when the immunoprecipitates are boiled with SDS before being subjected SDS-PAGE. Of note is that the gp140 proteins in fractions 20 and 21 migrate in the same position as the 140-kDa components of the SOS gp140 preparation. The radiographs shown in Fig. 12A and B were scanned to determine the density of each band (Fig. 12C). We estimate that approximately 40 to 50% of the nonaggregated protein in the SOS gp140 protein is in the higher-molecular-weight form, with the rest being gp120. The positions of the protein standards thyroglobulin (669 kDa), ferritin (440 kDa), and aldolase (158 kDa) are also indicated (Fig. 12C). Note that the monomeric gp120 protein migrates more rapidly, and hence appears to be of higher molecular mass, than a standard, globular protein of 158 kDa, aldolase. However, the higher-molecular-mass, oligomeric component of the SOS gp140

protein migrates more slowly, and so appears to be of lower molecular mass, than the 440-kDa ferritin standard (Fig. 12C). The unusually abundant glycosylation of the HIV-1 envelope glycoproteins is likely to affect their biophysical properties and limit the value of comparisons with traditional protein molecular weight standards.

Discussion

Our goals are to make a recombinant HIV-1 envelope glycoprotein with antigenic properties mimicking those of the native, trimeric gp120/gp41 complex found on virions or virus-infected cells and then evaluate whether such a protein might be a useful component of a multivalent HIV-1 vaccine. We believe we have accomplished the initial phase in creating the SOS gp140 protein. Whether this protein will be a superior immunogen to gp120 monomers, gp140 proteins with a peptide linkage retained between the gp120 and $gp41_{ECTO}$ moieties, or full-length gp160, remains to be determined. We believe that the disulfide bridge in the SOS gp140 protein should provide sufficient stability for this to be a practical immunogen, considering that the 140-kDa band survives boiling and SDS treatment during PAGE analysis.

There were two technical steps necessary for the generation of the SOS gp140 protein. The first was the use of cotransfected furin to increase the efficiency with which a secreted gp140 protein is proteolytically processed into gp120 and $gp41_{ECTO}$ moieties. The second was the introduction of a disulfide bond, at an appropriate position, to cross-link the gp120 subunit to the gp41 ectodomain and thereby increase its stability. During the synthesis of envelope glycoproteins in HIV-1-infected cells, trimerization of the gp41 moieties in the context of the gp160 precursor precedes the cleavage of the peptide bond linking gp120 to gp41 (25, 79). The cleavage step is mediated by proteases of the furin family (25, 41, 76). This step is inefficient, but unprocessed gp160 is generally sorted intracellularly into the lysosomal pathway, and little or no uncleaved gp160 is incorporated into virions (25, 26, 60, 119). However, when the HIV-1 *env* gene is expressed at high levels in mammalian cells, uncleaved gp160 cleavage can be found at the cell surface, perhaps because the natural cellular complement of furin proteases is saturated or because of differences in how gp160s are routed in infected and transfected cells (60, 119; Q. J. Sattentau, personal communication). These differences may be exacerbated when soluble rather than membrane-associated proteins are expressed, as is the case with gp140s. For whatever reason, when we expressed the JR-FL $gp140_{WT}$ gene in 293T cells, only a fraction of the secreted gp140 proteins were properly cleaved to gp120 and $gp41_{ECTO}$ subunits. This problem was overcome by the exogenous supplementation of furin via transfection, a device previously used to increase the efficiency of Ebola virus envelope glycoprotein proteolytic processing (114) and one that may have general relevance for vaccine development. Furin transfection did, however, reduce the extent of envelope glycoprotein expression (except with 89.6 and perhaps DH123), perhaps because of competition between plasmids for protein translation. Careful optimization of the furin content of permanent cell lines will be required when scaling up the production of the SOS gp140 protein.

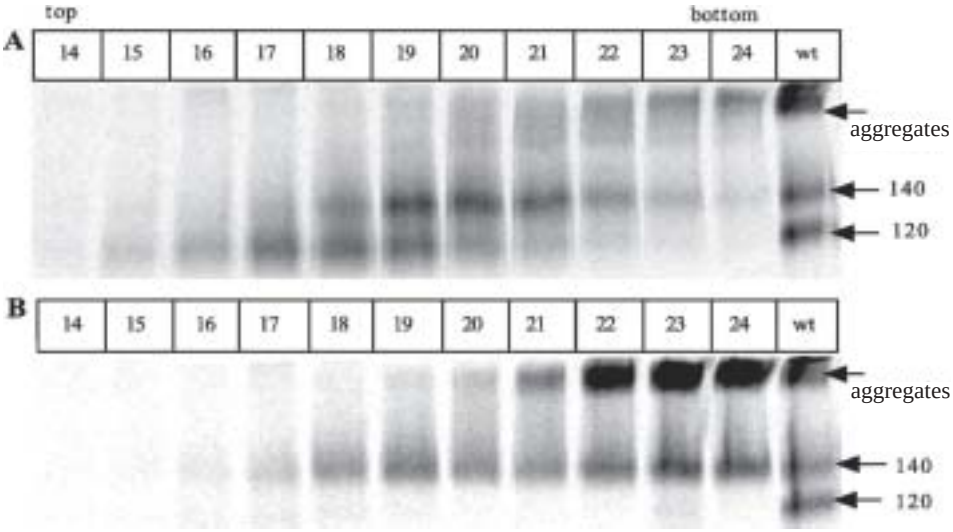

Fig. 11. Sucrose gradient analysis of the JR-FL SOS gp140 and $gp140_{UNC}$ proteins. Envelope glycoproteins secreted from transfected 293T cells were concentrated 100-fold and then fractionated by sucrose velocity gradient centrifugation. The gradient fractions (500 µl) were immunoprecipitated with MAb 2G12, boiled with SDS, and analyzed by SDS-PAGE to detect envelope glycoproteins and determine the sizes of their denatured components. **A.** JR-FL SOS gp140 protein. **B.** JR-FL $gp140_{UNC}$ protein. The last lane in each panel shows an unconcentrated supernatant containing the JR-FL $gp140_{WT}$ protein expressed in the absence of furin and then immunoprecipitated with 2G12 to provide a reference standard for the positions of gp120 and gp140 proteins on the gel. These bands are marked on the right of each panel, together with the position of high-molecular-weight aggregates.

The solution to the first problem created the second: the properly processed gp120 and $gp41_{ECTO}$ subunits are only weakly associated by noncovalent interactions. Consequently, the gp120 moieties are rapidly shed as the complex disassembles (38, 61, 70). To overcome this, we considered whether we could modify the gp120 or gp41 primary sequences to increase the strength of the noncovalent interaction between the subunits. However, in the absence of detailed information on the structure of the gp120-gp41 interactive sites, there was no good way to predict what amino-acid substitutions might work. Indeed, most of the substitutions in relevant regions of gp120 and gp41 that have been described in the literature actually weaken rather than strengthen the intersubunit association (17, 20, 45). We therefore focused on a second strategy: the stabilization of the gp120-gp41 interaction by the formation of an intersubunit disulfide bond between cysteine residues introduced into appropriate positions within gp120 and gp41.

We found that the precise positioning of the two cysteine residues introduced into gp120 and gp41 was important. Of the many double-cysteine mutants that we evaluated, the SOS gp140 protein (A501C/T605C) had the highest efficiency of disulfide bond formation, the fewest indications of poor folding, and the most favorable antigenic properties. In this protein, the cysteine substitution in gp120 is at a residue previously shown to be critical for any association of gp120 with

gp41 (45). The N- and C-terminal ends of gp120 probably assume disordered, flexible conformations, a factor which provoked their deletion from the crystallized gp120 core fragment (51, 122). The flexibility of these regions may explain why so many different cysteine substitutions of residues near the gp120 N and C termini permitted at least some disulfide linking to gp140. However, several such mutants were associated with smearing of gp140 bands on SDS-PAGE gels, suggesting that an imperfectly positioned disulfide bond does have some negative effects on envelope glycoprotein folding.

The corresponding substitution in gp41 is at a location exactly equivalent to where a cysteine residue is naturally positioned in the transmembrane glycoproteins of many retroviruses, including MuLV and HTLV-1 (37, 82, 99). This cysteine is immediately C-terminal to a small loop bounded by an intramolecular disulfide bond that is a common feature of retrovirus and lentivirus transmembrane glycoproteins (37, 82). On intuitive grounds, we postulated that this region of HIV-1 gp41 was involved in gp120 binding (99); the additional cysteine present in other retroviruses probably accounts for the disulfide bond that can sometimes form between the surface and transmembrane glycoproteins (25, 54, 55, 78, 83-86). There may be a conserved mechanism of subunit association among many viral families, sometimes with the involvement of a disulfide bond and sometimes not (36, 37, 99, 124). The crystal structure of the major fragment of the gp41 ectodomain in its postfusion conformation reveals that the C-terminal helix of the gp41 trimeric coiled coil is positioned antiparallel to, and stacked on the outside of, an N-terminal trimer (19, 101, 116). This implies that the cysteine residue substituted for alanine-605 protrudes outward in the postfusion conformation of gp41. The crystal structures of the TM glycoproteins of other viruses, such as MuLV and Ebola virus, also show that the region near the intramolecular disulfide-bonded loop is solvent accessible (16, 117). At present, the conformation of the prefusion form of the gp41 ectodomain is unknown, but presumably alanine-605 must also protrude in this form of the protein since the cysteine residue substituted at this position is available for disulfide bond formation with cysteine-501 of gp120. In the correctly folded, prefusion form of the gp120-gp41 complex, these two residues must be sufficiently proximal for disulfide bond formation to be possible. If and when the prefusion form of the gp41 ectodomain is crystallized, the exact positioning of alanine-605 will be revealed.

Although we can clearly make a gp140 protein in which the gp120 and $gp41_{ECTO}$ moieties are stabilized by an intermolecular disulfide bond, the formation of the disulfide bond occurs with imperfect efficiency. Thus, only a fraction (perhaps 40 to 50%) of the envelope glycoprotein complexes secreted from 293T cells expressing the A501C/T605C double cysteine mutant in the presence of furin are in the form of the SOS gp140 protein (Fig.Fig. 12C). The remaining proteins are present as gp120 monomers. This reflects inefficient formation of the intermolecular disulfide bond in the transfected 293T cells, rather than a lability of this bond once it has formed; the gp120 subunit still remains attached to the gp41 ectodomain even when the SOS gp140 protein is boiled in SDS and partially denatured, indicating that the intermolecular disulfide bond is quite stable. Preliminary studies of a permanent CHO cell line show that these cells secrete essentially only disulfide-stabilized SOS gp140 proteins, with virtually no gp120

moieties being present (data not shown). The efficiency of intermolecular disulfide bond formation is probably cell type dependent.

Biophysical analyses showed that the SOS gp140 protein has a higher molecular weight than monomeric gp120. It also differs in its biophysical properties

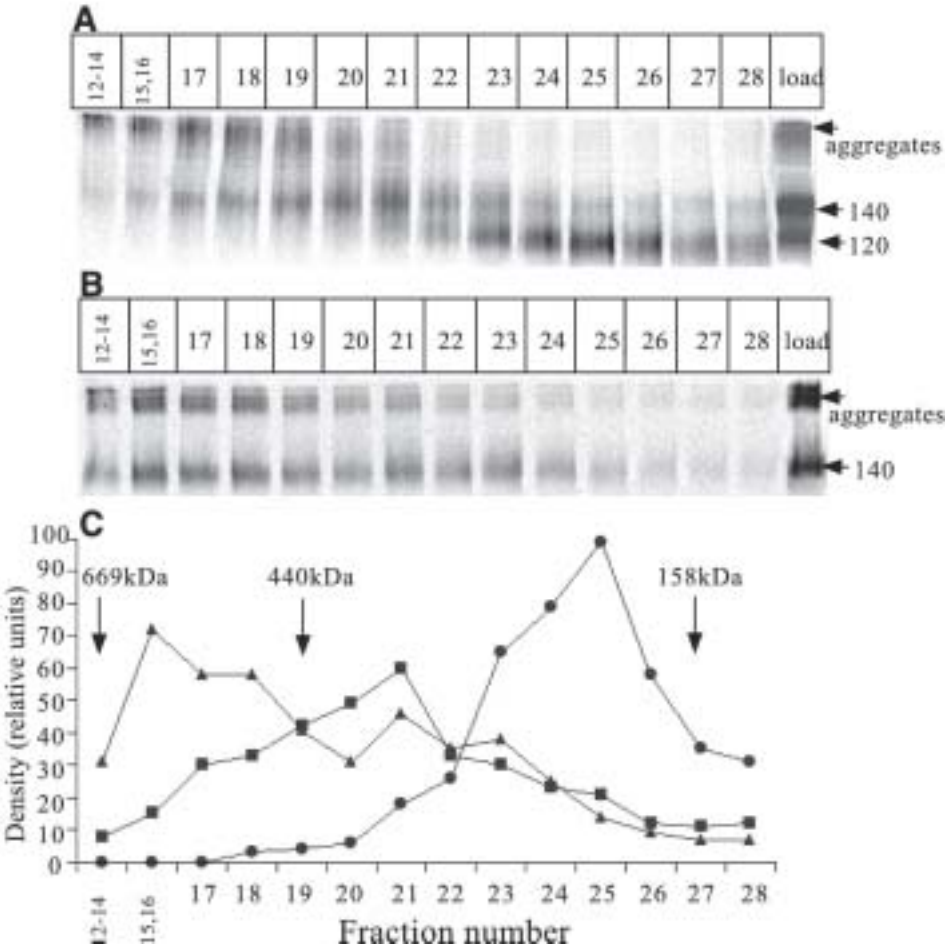

Fig. 12. Gel filtration analysis of the JR-FL SOS gp140 and gp140$_{UNC}$ proteins. Envelope glycoproteins from transfected 293T cells were concentrated 100-fold and then fractionated by gel filtration chromatography. The fractions (250 µl) were immunoprecipitated with MAb 2G12, boiled with SDS, and analyzed by SDS-PAGE to detect envelope glycoproteins and determine the size of their constituent subunits. **A.** JR-FL SOS gp140 protein. **B.** JR-FL gp140$_{UNC}$ protein. The last lane in each panel shows an unconcentrated supernatant containing the protein under analysis and immunoprecipitated with 2G12 to provide a reference standard. These bands are marked on the right of each panel, together with the position of high-molecular-weight aggregates. **C.** Densitometric analysis of the elution profile derived from the SOS gp140 protein (**A** and **B**). , gp140$_{UNC}$; , the 140-kDa component of SOS gp140; , the 120-kDa component of SOS gp140. The positions of molecular mass standards are indicated by arrows. These were thyroglobulin (669 kDa), ferritin (440 kDa), and aldolase (158 kDa).

from uncleaved gp140. However, we have not yet determined whether the SOS gp140 protein contains three gp41 ectodomains, each linked to a gp120 moiety via a disulfide bond, or whether only one or two gp120s are successfully attached to trimerized gp41 subunits. A mixture of molecular species may be present. Additional studies of SOS gp140 proteins purified from a permanent cell line are necessary to address these issues.

We are, however, encouraged by the antigenic properties of the SOS gp140 protein; it has a MAb reactivity pattern that is consistent with what has been learnt from prior studies of the native trimer and of the relationship between MAb binding and HIV-1 neutralization (34, 71, 72, 98, 102, 106, 115). Thus the most commonly exposed regions on the gp120 moiety of the SOS gp140 protein correspond to neutralizing-antibody epitopes. These include areas near the CD4 binding site (e.g., the binding sites for MAb IgG1b12 and the CD4-IgG2 molecule), the C3-V4 glycan-dependent epitope for MAb 2G12, the V3 loop, and, in the presence of sCD4, the CD4-induced epitope for MAb 17b that overlaps the coreceptor binding site. For some MAbs, notably 2G12, the reactivity with the SOS gp140 protein is better than with the gp120 monomer. MAbs to nonneutralizing epitopes in the C1 and C5 domains do not bind to the SOS gp140 protein, although they recognize the uncleaved gp140 proteins quite efficiently because of the abnormal conformation conferred upon the gp120 moiety when the gp41 ectodomain is attached via a peptide bond.

Some MAbs to CD4-binding site and V3 loop epitopes (e.g., F91 and 19b) do, however, bind efficiently to the SOS gp140 protein while lacking strong neutralization activity against HIV-1_{JR-FL}. The binding of the nonneutralizing A32 MAb to the SOS gp140 protein in the presence of sCD4 is another example. The ability of weakly neutralizing MAbs to bind to native envelope glycoprotein complexes on the cell surface has been described previously (35). Factors such as the on-rate may be important in determining precisely which MAbs to closely related epitopes do (e.g., IgG1b12) and do not (e.g., F91) neutralize HIV-1. Kinetic parameters might not be identical in RIPA and neutralization assays, in that the slow binding of some MAbs to the native trimer might be rapid enough to be detectable in a binding assay yet too slow to be able to interfere with virus attachment and entry in a neutralization assay. There may also be differences in the rates at which neutralizing antibodies bind to soluble and membrane-associated forms of the same protein complex.

On the gp41 moiety of the SOS gp140 protein, only the epitope for the neutralizing MAb 2F5 is accessible. Nonneutralizing gp120 and gp41 antibody epitopes components are not exposed on the SOS gp140 protein, just as they are inaccessible on native trimers (71, 98). However, we cannot rule out the possibility that the occlusion of the nonneutralizing gp41 epitopes is a direct consequence of the formation of the intermolecular disulfide bond. The almost complete occlusion of the CD4-induced epitope on the SOS gp140 protein in the absence of CD4, combined with its substantial induction upon CD4 binding, is consistent with how the gp120 moieties in a native trimer are thought to be arranged (122). In this conformation, the CD4-induced epitopes are partially covered by the V1/V2 and V3 loop structures and partially occluded by interactions between the individual gp120 components of a trimer. In the gp120 monomer, the occlusion

of the CD4-induced epitopes is only partial (105, 122, 123), and we observed this to be the case also in the uncleaved gp140 proteins. Thus the MAb reactivity patterns of the SOS gp140 protein are, in general, consistent with its existing as a native, oligomeric structure. We believe that the SOS gp140 protein is in a prefusion conformation, judged by the dramatic induction of the 17b epitope upon sCD4 binding.

The above properties of the SOS gp140 protein contrast markedly with the antigenic structure of gp140 proteins that retain the peptide bond between gp120 and the gp41 ectodomain. Proteins of this category have not, to date, been significantly superior to gp120 monomers as immunogens (27, 90, 110). This may be because they do not properly mimic the structure of the native trimer, as indicated by their limited ability to interact with coreceptors (31); it is probably not the ability of a protein to oligomerize that most strongly influences its immunogenicity, but its overall structure. The acid test of the value of our work to vaccine development will come from immunogenicity studies, the outcomes of which are inherently unpredictable. The preservation of the best neutralizing-antibody epitopes on the SOS gp140 protein (those for MAbs IgG1b12, 2G12, and 2F5), combined with the elimination of irrelevant epitopes, might be valuable for focusing the humoral immune response.

It may, however, be found necessary to further modify the antigenic structure of the SOS gp140 protein to improve its immunogenicity, for example by removing some of its glycan residues or variable loops (18, 89). In preliminary studies, we have found that such modifications can be made to the SOS gp140 protein without having significant effects on the efficiency of intermolecular disulfide bond formation (R. Sanders, F. Kajumo, A. Master, L. Schiffner, T. Dragic, J. P. Moore, and J. M. Binley, unpublished results). The ability of the SOS gp140 protein to bind soluble CD4 and undergo relevant conformational changes allows a further way to explore its immunogenicity, i.e., as an sCD4 complex (49). It may also be possible to make full-length, membrane-bound versions of the SOS gp140 protein by restoring the transmembrane domain. Such a protein, expressed in the context of a DNA plasmid or a live recombinant virus vector, might be useful for priming the immune system prior to boosting with a soluble version.

That the A501C/T605C double cysteine substitution works in the context not only of HIV-$1_{JR\text{-}FL}$ but also with several other primary and T-cell-line-adapted subtype B isolates (Gun-1wt, DH123, 89.6, and HxB2) suggests that the method will be generally useful for generating stable trimers. We are presently making similar mutants derived from HIV-1 subtype C isolates. Thus, if the SOS gp140 mutant, or antigenic variants thereof, does induce superior neutralizing-antibody responses in small-animal models, its overall utility as a vaccine antigen could be evaluated in monkey models by using homologous and heterologous SHIVs as challenge viruses (24, 53). It may also be possible to make SOS gp140 proteins derived from SIV_{mac} or other lentiviruses, given the likely similarity of the gp120-gp41 association among retroviruses (99). This could have useful implications for the development of vaccines against retroviruses in general and perhaps other viral families as well.

Acknowledgements

We thank Gary Thomas for provision of the pGEMfurin plasmid and James Robinson and Herman Katinger for the gifts of several monoclonal antibodies. We are grateful for the sage advice of Dennis Burton and Bob Doms on the biophysical properties of HIV-1 envelope glycoproteins. We appreciate the technical assistance of Daryl Schiller. This work was supported by RO1 grants AI 39420 and AI 45463.

References

1. **Abacioglu, Y. H., T. R. Fouts, J. D. Laman, E. Claassen, S. H. Pincus, J. P. Moore, C. A. Roby, R. Kamin-Lewis, and G. K. Lewis.** 1994. Epitope mapping and topology of baculovirus expressed HIV-1 gp160 determined with a panel of murine monoclonal antibodies. AIDS Res. Hum. Retroviruses **10:**371-381
2. **Allaway, G. P., K. L. Davis-Bruno, G. A. Beaudry, E. B. Garcia, E. L. Wong, A. M. Ryder, K. W. Hasel, M.-C. Gauduin, R. A. Koup, J. S. McDougal, and P. J. Maddon.** 1995. Expression and characterization of CD4lgG2, a novel heterotetramer which neutralizes primary HIV-1 isolates. AIDS Res. Hum. Retroviruses **11:**533-540
3. **Baldinotti, F., D. Matteucci, P. Mazzetti, C. Giannelli, P. Bandecchi, F. Tozzini, and M. Bendinelli.** 1994. Serum neutralization of feline immunodeficiency virus is markedly dependent on passage history of the virus and host system. J. Virol. **68:**4572-4579.
4. **Barnett, S. W., S. Rajasekar, H. Legg, B. Doe, D. H. Fuller, J. R. Haynes, C. M. Walker, and K. S. Steimer.** 1997. Vaccination with HIV-1 gp120 DNA induces immune responses that are boosted by a recombinant gp120 protein subunit. Vaccine **15:**869-873
5. **Belshe, R. B., G. J. Gorse, M. J. Mulligan, T. G. Evans, M. C. Keefer, J.-L. Excler, A. M. Duliege, J. Tartaglia, W. I. Cox, J. McNamara, K.-L. Hwang, A. Bradney, D. C. Montefiori, and K. J. Weinhold.** 1998. Induction of immune responses to HIV-1 by canarypox virus (ALVAC) HIV-1 and gp120 SF-2 recombinant vaccines in uninfected volunteers. AIDS **12:**2407-2415
6. **Berman, P. W., W. M. Nunes, and O. K. Haffar.** 1988. Expression of membrane associated and secreted variants of gp160 of human immunodeficiency virus type 1 *in vitro* and in continuous cell lines. J. Virol. **62:**3135-3142
7. **Binley, J. M., P. J. Klasse, Y. Cao, I. M. Jones, M. Markowitz, D. D. Ho, and J. P. Moore.** 1997. Differential regulation of the antibody responses to gag and env proteins of human immunodeficiency virus type 1. J. Virol. **71:**2799-2809.
8. **Binley, J. M., and J. P. Moore.** 1997. The viral mousetrap. Nature **387:**346-348
9. **Binley, J. M., R. Wyatt, E. Desjardins, P. D. Kwong, W. Hendrickson, J. P. Moore, and J. Sodroski.** 1998. Analysis of the interaction of antibodies with a conserved, enzymatically deglycosylated core of the HIV type 1 envelope glycoprotein 120. AIDS Res. Hum. Retroviruses **14:**191-198
10. **Bou-Habib, D. C., G. Roderiquez, T. Oravecz, P. W. Berman, P. Lusso, and M. A. Norcross.** 1994. Cryptic nature of envelope V3 region epitopes protects primary human immunodeficiency virus type 1 from antibody neutralization. J. Virol. **68:**6006-6013.
11. **Buchacher, A., R. Predl, K. Strutzenberger, W. Steinfellner, A. Trkola, M. Purtscher, G. Gruber, C. Tauer, F. Steindl, A. Jungbauer, and H. Katinger.** 1994. Generation of human monoclonal antibodies against HIV-1 proteins: electrofusion and Epstein-Barr virus transformation for peripheral blood lymphocyte immortalization. AIDS Res. Hum. Retroviruses **10:**359-369
12. **Burton, D. R.** 1997. A vaccine for HIV type 1: the antibody perspective. Proc. Natl. Acad. Sci. USA **94:**10018-10023.
13. **Burton, D. R., and D. C. Montefiori.** 1997. The antibody response in HIV-1 infection. AIDS **11**(Suppl. A)**:**587-598

14. **Burton, D. R., and J. P. Moore.** 1998. Why do we not have an HIV vaccine and how can we make one? Nat. Med. **4:**495-498
15. **Burton, D. R., J. Pyati, R. Koduri, G. B. Thornton, L. S. W. Sawyer, R. M. Hendry, N. Dunlop, P. L. Nara, M. Lamacchia, E. Garratty, E. R. Stiehm, Y. J. Bryson, J. P. Moore, D. D. Ho, and C. F. Barbas, III.** 1994. Efficient neutralization of primary isolates of HIV-1 by a recombinant human monoclonal antibody. Science **266:**1024-1027
16. **Caffrey, M., M. Cai, J. Kaufman, S. J. Stahl, P. T. Wingfield, D. G. Covell, A. M. Gronenborn, and G. M. Clore.** 1998. Three dimensional solution structure of the 44 kDa ectodomain of SIV gp41. EMBO J. **17:**4572-4584.
17. **Cao, J., L. Bergeron, E. Helseth, M. Thali, H. Repke, and J. Sodroski.** 1993. Effects of amino-acid changes in the extracellular domain of the HIV-1 gp41 envelope glycoprotein. J. Virol. **67:**2747-2755.
18. **Cao, J., N. Sullivan, E. Desjardin, C. Parolin, J. Robinson, R. Wyatt, and J. Sodroski.** 1997. Replication and neutralization of human immunodeficiency virus type 1 lacking the V1 and V2 variable loops of the gp120 envelope glycoprotein. J. Virol. **71:**9808-9812.
19. **Chan, D. C., D. Fass, J. M. Berger, and P. S. Kim.** 1997. Core structure of gp41 from the HIV envelope glycoprotein. Cell **89:**263-273
20. **Chen, S. L.** 1994. Functional role of the leucine zipper motif region of HIV-1 transmembrane protein gp41. J. Virol. **68:**2002-2010.
21. **Collman, R., J. W. Balliet, S. A. Gregory, H. Friedman, D. L. Kolson, N. Nathanson, and A. Srinivasan.** 1992. An infectious molecular clone of an unusual macrophage-tropic and highly cytopathic strain of human immunodeficiency virus type 1. J. Virol. **66:**7517-7521.
22. **Connor, R. I., B. T. M. Korber, B. S. Graham, B. H. Hahn, D. D. Ho, B. D. Walker, A. U. Neumann, S. H. Vermund, J. Mestecky, S. Jackson, E. Fenamore, Y. Cao, F. Gao, S. Kalams, K. Kuntsman, D. McDonald, N. McWilliams, A. Trkola, J. P. Moore, and S. M. Wolinsky.** 1998. Immunological and virological analyses of persons infected by human immunodeficiency virus type 1 while participating in trials of recombinant gp120 subunit vaccines. J. Virol. **72:**1552-1576.
23. **Cook, R. F., S. L. Berger, K. E. Rushlow, J. E. McManus, S. J. Cook, S. Harrold, M. L. Raabe, R. C. Montelaro, and C. J. Issel.** 1995. Enhanced sensitivity to neutralizing antibodies in a variant of equine infectious anemia virus is linked to amino-acid substitutions in the surface unit envelope glycoprotein. J. Virol. **69:**1493-1499.
24. **Desrosiers, R. C.** 1995. Non-human primate models for AIDS vaccines. AIDS **9**(Suppl. A)**:**S137-S141
25. **Doms, R. W., R. A. Lamb, J. K. Rose, and A. Helenius.** 1993. Folding and assembly of viral membrane proteins. Virology **193:**545-562
26. **Dubay, J. W., S. R. Dubay, H.-J. Shin, and E. Hunter.** 1995. Analysis of the cleavage site of the human immunodeficiency virus type glycoprotein: requirement of precursor cleavage for glycoprotein incorporation. J. Virol. **69:**4675-4682.
27. **Earl, P. L., C. C. Broder, R. W. Doms, and B. Moss.** 1997. Epitope map of human immunodeficiency virus type 1 gp41 derived from 47 monoclonal antibodies produced by immunization with oligomeric envelope protein. J. Virol. **71:**2674-2684.
28. **Earl, P. L., C. C. Broder, D. Long, S. A. Lee, J. Peterson, S. Chakrabarti, R. W. Doms, and B. Moss.** 1994. Native oligomeric human immunodeficiency virus type 1 envelope glycoprotein elicits diverse monoclonal antibody reactivities. J. Virol. **68:**3015-3026.
29. **Earl, P. L., R. W. Doms, and B. Moss.** 1990. Oligomeric structure of the human immunodeficiency virus type 1 envelope glycoprotein. Proc. Natl. Acad. Sci. USA **87:**648-652.
30. **Earl, P. L., S. Koenig, and B. Moss.** 1991. Biological and immunological properties of human immunodeficiency virus type 1 envelope glycoprotein: analysis of proteins with truncations and deletions expressed by recombinant vaccinia viruses. J. Virol. **65:**31-41
31. **Edinger, A. L., C. Blanpain, K. J. Kuntsman, S. M. Wolinsky, M. Parmentier, and R. W. Doms.** 1999. Functional dissection of CCR5 coreceptor function through the use of CD4-independent simian immunodeficiency virus strains. J. Virol. **73:**4062-4073.
32. **Excler, D., and S. Plotkin.** 1997. The prime-boost concept applied to HIV preventive vaccines. AIDS **11**(Suppl. A)**:**S127-S137
33. **Farzan, M., H. Choe, E. Desjardins, Y. Sun, J. Kuhn, J. Cao, D. Archambault, P. Kolchin-**

sky, M. Koch, R. Wyatt, and J. Sodroski. 1998. Stabilization of human immunodeficiency virus type 1 envelope glycoprotein trimers by disulfide bonds introduced into the gp41 ectodomain. J. Virol. **72:**7620-7625.

34. **Fouts, T. R., J. M. Binley, A. Trkola, J. E. Robinson, and J. P. Moore.** 1997. Neutralization of the HIV-1 primary isolate JR-FL by human monoclonal antibodies correlates with antibody binding to the oligomeric form of the envelope glycoprotein complex. J. Virol. **71:**2779-2785.
35. **Fouts, T. R., A. Trkola, M. S. Fung, and J. P. Moore.** 1998. Interactions of polyclonal and monoclonal anti-glycoprotein 120 antibodies with oligomeric glycoprotein 120-glycoprotein 41 complexes of a primary HIV type 1 isolate: relationship to neutralization. AIDS Res. Hum. Retroviruses **14:**591-598
36. **Gallaher, W. R.** 1996. Similar structural models of the transmembrane proteins of Ebola and avian sarcoma viruses. Cell **85:**477-478
37. **Gallaher, W. R., J. M. Ball, R. F. Garry, A. M. Martin-Amedec, and R. C. Montelaro.** 1995. A general model for the surface glycoproteins of HIV and other retroviruses. AIDS Res. Hum. Retroviruses **11:**191-202
38. **Gelderblom, H. R., H. Reupke, and G. Pauli.** 1985. Loss envelope antigens of HTLV-III/LAV, a factor in AIDS pathogenesis? Lancet **ii:**1016-1017.
39. **Godley, L., J. Pfeifer, D. Steinhauer, B. Ely, G. Shaw, R. Kaufmann, E. Suchanek, C. Pabo, J. J. Skehel, D. C. Wiley, and S. Wharton.** 1992. Introduction of intersubunit disulfide bonds in the membrane-distal region of the influenza hemagglutinin abolishes membrane fusion activity. Cell **68:**635-645
40. **Graham, B. S., M. J. McElrath, R. I. Connor, D. H. Schwartz, G. J. Gorse, M. C. Keefer, M. J. Mulligan, T. J. Matthews, S. M. Wolinsky, D. C. Montefiori, S. H. Vermund, J. S. Lambert, L. Corey, R. B. Belshe, R. Dolin, P. F. Wright, B. T. Korber, M. C. Wolff, and P. E. Fast.** 1998. Analysis of intercurrent human immunodeficiency virus type 1 infections in phase I and II trials of current AIDS vaccines. J. Infect. Dis. **177:**310-319
41. **Hallenberger, S., V. Bosch, H. Angliker, E. Shaw, H. D. Klenk, and W. Garten.** 1992. Inhibition of furin-mediated cleavage activation of HIV-1 glycoprotein gp160. Nature **360:**358-361
42. **Harlow, E., and D. Lane.** 1988. Antibodies: a laboratory manual. Cold Spring Harbor Laboratory Press, Cold Spring Harbor, N.Y.
43. **Haynes, B. F., G. Pantaleo, and A. S. Fauci.** 1996. Towards an understanding of the correlates of protective immunity to HIV infection. Science **271:**324-328.
44. **Heilman, C. A., and D. Baltimore.** 1998. HIV vaccineswhere are we going? Nat. Med. **4:**532-534
45. **Helseth, E., U. Olshevsky, C. Furman, and J. Sodroski.** 1991. Human immunodeficiency virus type 1 gp120 envelope glycoprotein regions important for association with the gp41 transmembrane glycoprotein. J. Virol. **65:**2119-2123
46. **Hilleman, M. R.** 1998. A simplified vaccinologist's vaccinology and the pursuit of a vaccine against AIDS. Vaccine **16:**778-793
47. **Hoffman, T. L., C. C. LaBranche, W. Zhang, G. Canziani, J. Robinson, I. Chaiken, J. A. Hoxie, and R. W. Doms.** 1999. Stable exposure of the coreceptor-binding site in a CD4-independent HIV-1 envelope protein. Proc. Natl. Acad. Sci. USA **96:**6359-6364.
48. **Hunter, E., and R. Swanstrom.** 1990. Retrovirus envelope glycoproteins. Curr. Top. Microbiol. Immunol. **157:**187-253
49. **Kang, C.-Y., K. Hariharan, P. L. Nara, J. Sodroski, and J. P. Moore.** 1994. Immunization with a soluble CD4-gp120 complex preferentially induces neutralizing anti-human immunodeficiency virus type 1 antibodies directed to conformation-dependent epitopes of gp120. J. Virol. **68:**5854-5862.
50. **Koyanagi, Y., S. Miles, R. T. Mitsuyasu, J. E. Merrill, H. V. Vinters, and I. S. Chen.** 1987. Dual infection of the central nervous system by AIDS viruses with distinct cellular tropisms. Science **236:**819-822
51. **Kwong, P. D., R. Wyatt, J. Robinson, R. W. Sweet, J. Sodroski, and W. A. Hendrickson.** 1998. Structure of an HIV gp120 envelope glycoprotein complex with the CD4 receptor and a neutralizing human antibody. Nature **393:**648-659
52. **LaCasse, R. A., K. E. Follis, M. Trahey, J. D. Scarborough, D. R. Littman, and J. H. Nunberg.** 1999. Fusion-competent vaccines: broad neutralization of primary isolates of HIV. Science **283:**357-362.

53. **Lamb-Wharton, R. J., S. V. Joag, E. B. Stephens, and O. Narayan.** 1997. Primate models of AIDS vaccine development. AIDS **11**(Suppl. A)**:**S121-S126.
54. **Leamnson, R. N., and M. S. Halpern.** 1976. Subunit structure of the glycoprotein complex of avian tumor virus. J. Virol. **18:**956-968
55. **Leamnson, R. N., M. H. M. Shander, and M. S. Halpern.** 1977. A structural protein complex in Moloney leukemia virus. Virology **76:**437-439
56. **Leonard, C. K., M. W. Spellman, L. Riddle, R. J. Harris, J. N. Thomas, and T. J. Gregory.** 1990. Assignment of intrachain disulfide bonds and characterization of potential glycosylation sites of the type 1 recombinant human immunodeficiency virus envelope glycoprotein (gp120) expressed in Chinese hamster ovary cells. J. Biol. Chem. **265:**10373-10382.
57. **Letvin, N. L.** 1998. Progress in the development of an HIV-1 vaccine. Science **280:**1875-1880.
58. **Mascola, J. R., S. W. Snyder, O. S. Weislow, S. M. Belay, R. B. Belshe, D. H. Schwartz, M. L. Clements, R. Dolin, B. S. Graham, G. J. Gorse, M. C. Keefer, M. J. McElrath, M. C. Walker, K. F. Wagner, J. G. McNeil, F. E. McCutchan, D. S. Burke, and the National Institute of Allergy and Infectious Diseases AIDS Vaccine Evaluation Group.** 1996. Immunization with envelope subunit vaccine products elicits neutralizing antibodies against laboratory adapted but not primary isolates of human immunodeficiency virus type 1. J. Infect. Dis. **173:**340-348
59. **Matthews, T. J.** 1994. Dilemma of neutralization resistance of HIV-1 field isolates and vaccine development. AIDS Res. Hum. Retroviruses **10:**631-632
60. **McCune, J. M., L. B. Rabin, M. B. Feinberg, M. Lieberman, J. C. Kosek, G. Reyes, and I. L. Weissman.** 1988. Endoproteolytic cleavage of gp160 is required for the activation of human immunodeficiency virus. Cell **53:**55-67
61. **McKeating, J. A., A. McKnight, and J. P. Moore.** 1991. Differential loss of envelope glycoprotein gp120 from virions of human immunodeficiency virus type 1 isolates: effect on infectivity and neutralization. J. Virol. **65:**852-860
62. **Mertens, T. E., and A. Burton.** 1996. Global estimates and epidemiology of HIV-1 infection and AIDS. AIDS **10**(Suppl. A)**:**S221-S228
63. **Molloy, S. S., L. Thomas, J. K. VanSlyke, P. E. Stenberg, and G. Thomas.** 1994. Intracellular trafficking and activation of the furin proprotein convertase: localization to the TGN and recycling from the cell surface. EMBO J. **13:**18-33.
64. **Montefiori, D. C., and T. G. Evans.** 1999. Toward an HIV type 1 vaccine that generates potent, broadly cross-reactive neutralizing antibodies. AIDS Res. Hum. Retroviruses **15:**689-698
65. **Montefiori, D. C., K. A. Reimann, M. S. Wyand, K. Manson, M. G. Lewis, R. G. Collman, J. G. Sodroski, D. P. Bolognesi, and N. L. Letvin.** 1998. Neutralizing antibodies in sera from macaques infected with chimeric simian-human immunodeficiency virus containing the envelope glycoproteins of either a laboratory-adapted variant or a primary isolate of human immunodeficiency virus type 1. J. Virol. **72:**3427-3431.
66. **Moore, J. P., and J. M. Binley.** 1998. Envelope's letters boxed into shape. Nature **393:**630-631
67. **Moore, J. P., Y. Cao, L. Qing, Q. J. Sattentau, J. Pyati, R. Koduri, J. Robinson, C. F. Barbas III, D. R. Burton, and D. D. Ho.** 1995. Primary isolates of human immunodeficiency virus type 1 are relatively resistant to neutralization by monoclonal antibodies to gp120 and their neutralization is not predicted by studies with monomeric gp120. J. Virol. **69:**101-109.
68. **Moore, J. P., and D. D. Ho.** 1995. HIV-1 neutralization: the consequences of viral adaptation to growth on transformed T cells. AIDS **9**(Suppl. A)**:**S117-S136
69. **Moore, J. P., J. A. McKeating, I. M. Jones, P. E. Stephens, G. Clements, S. Thomson, and R. A. Weiss.** 1990. Characterisation of recombinant gp120 and gp160 from HIV-1: binding to monoclonal antibodies and sCD4. AIDS **4:**307-315
70. **Moore, J. P., J. A. McKeating, R. A. Weiss, and Q. J. Sattentau.** 1990. Dissociation of gp120 from HIV-1 virions induced by soluble CD4. Science **250:**1139-1142
71. **Moore, J. P., Q. J. Sattentau, R. Wyatt, and J. Sodroski.** 1994. Probing the structure of the human immunodeficiency virus surface glycoprotein gp120 with a panel of monoclonal antibodies. J. Virol. **68:**469-484.
72. **Moore, J. P., and J. Sodroski.** 1996. Antibody cross-competition analysis of the human immunodeficiency virus type 1 exterior envelope glycoprotein. J. Virol. **70:**1863-1872.
73. **Moore, J. P., M. Thali, B. A. Jameson, F. Vignaux, G. K. Lewis, S.-W. Poon, M. S. Fung, N. C. Sun, M. Charles, P. J. Durda, L. Åkerblom, B. Wahren, D. D. Ho, Q. J. Sattentau, and J.**

Sodroski. 1993. Immunochemical analysis of human immunodeficiency virus type 1: probing the structure of the C4 and V4 domains and the interaction of the C4 domain with the V3 loop. J. Virol. **67:**4785-4796.

74. **Moore, J. P., A. Trkola, B. Korber, L. J. Boots, J. A. Kessler II, F. E. McCutchan, J. Mascola, D. D. Ho, J. Robinson, and A. J. Conley.** 1995. A human monoclonal antibody to a complex epitope in the V3 region of gp120 of human immunodeficiency virus type 1 has broad reactivity within and outside clade B. J. Virol. **69:**122-130.
75. **Moore, J. P., R. L. Willey, G. K. Lewis, J. Robinson, and J. Sodroski.** 1994. Immunological evidence for interactions between the first, second and fifth conserved domains of the gp120 surface glycoprotein of human immunodeficiency virus type 1. J. Virol. **68:**6836-6847.
76. **Morikawa, Y., E. Barsov, and I. Jones.** 1993. Legitimate and illegitimate cleavage of human immunodeficiency virus glycoproteins by furin. J. Virol. **167:**3601-3604.
77. **Muster, T., R. Guinea, A. Trkola, M. Purtscher, A. Klima, F. Steindl, P. Palese, and H. Katinger.** 1994. Cross-neutralizing antibodies against divergent human immunodeficiency virus type 1 isolates induced by the gp41 sequence ELDKWAS. J. Virol. **68:**4031-4034.
78. **Opstelten, D. E., M. Wallin, and H. Garoff.** 1998. Moloney murine leukemia virus envelope subunits, gp70 and Pr15E, form a stable disulfide-linked complex. J. Virol. **72:**6537-6545.
79. **Otteken, A., P. L. Earl, and B. Moss.** 1996. Folding, assembly, and intracellular trafficking of the HIV-1 envelope glycoprotein analyzed with monoclonal antibodies recognizing maturational intermediates. J. Virol. **70:**3407-3415.
80. **Parren, P. W. H. I., D. R. Burton, and Q. J. Sattentau.** 1997. HIV-1 antibodydebris or virion? Nat. Med. **3:**366-367
81. **Parren, P. W. H. I., J. P. Moore, D. R. Burton, and Q. J. Sattentau.** 1999. The neutralizing antibody response to HIV-1: viral evasion and escape from humoral immunity. AIDS **13**(Suppl. A)**:**S137-S162
82. **Patarca, R., and W. A. Haseltine.** 1984. Similarities among retrovirus proteins. Nature **312:**496
83. **Pinter, A., and E. Fleissner.** 1977. The presence of disulfide-linked gp70 p15(E) complexes in AKR MuLV. Virology **83:**417-422
84. **Pinter, A., and E. Fleissner.** 1979. Characterization of oligomeric complexes of murine and feline leukemia virus envelope and core components formed upon cross-linking. J. Virol. **30:**157-165
85. **Pinter, A., R. Kopelman, Z. Li, S. C. Kayman, and D. A. Sanders.** 1997. Localization of the labile disulfide bond between SU and TM of the murine leukemia virus protein complex to a highly conserved CWLC motif in SU that resembles the active-site sequence of thiol-disulfide exchange enzymes. J. Virol. **71:**8073-8077.
86. **Pique, C., D. Pham, T. Tursz, and M. C. Dokhelar.** 1992. Human T-cell leukemia virus type 1 envelope protein maturation process: requirements for syncytium formation. J. Virol. **66:**906-913.
87. **Poignard, P., T. Fouts, D. Naniche, J. P. Moore, and Q. J. Sattentau.** 1996. Neutralizing antibodies to human immunodeficiency virus type-1 gp120 induce envelope glycoprotein subunit dissociation. J. Exp. Med. **183:**473-484.
88. **Ratner, L., A. Fisher, L. L. Jagodzinski, H. Mitsuya, R.-S. Liou, R. C. Gallo, and F. Wong-Staal.** 1987. Complete nucleotide sequences of functional clones of the AIDS virus. AIDS Res. Hum. Retroviruses **3:**57-69
89. **Reiter, J. N., R. E. Means, and R. C. Desrosiers.** 1998. A role for carbohydrates in immune evasion in AIDS. Nat. Med. **4:**679-684
90. **Richardson, T. M., Jr., B. L. Stryjewski, C. C. Broder, J. A. Hoxie, J. R. Mascola, P. L. Earl, and R. W. Doms.** 1996. Humoral response to oligomeric human immunodeficiency virus type 1 envelope protein. J. Virol. **70:**753-762.
91. **Rizzuto, C. D., R. Wyatt, N. Hernandez-Ramos, Y. Sun, P. D. Kwong, W. A. Hendrickson, and J. G. Sodroski.** 1998. A conserved HIV gp120 glycoprotein structure involved in chemokine receptor binding. Science **280:**1949-1953.
92. **Roben, P., J. P. Moore, M. Thali, J. Sodroski, C. F. Barbas III, and D. R. Burton.** 1994. Recognition properties of a panel of human recombinant Fab fragments to the CD4 binding site of gp120 showing differing ability to neutralize human immunodeficiency virus type 1. J. Virol. **68:**4821-4828.
93. **Robinson, H. L.** 1997. DNA vaccines for immunodeficiency viruses. AIDS **11**(Suppl. A)**:**S109-S119

94. **Rowland-Jones, S., R. Tan, and A. McMichael.** 1997. The role of cellular immunity in protection against HIV infection. Adv. Immunol. **65:**448-455.
95. **Sattentau, Q. J., and J. P. Moore.** 1991. Conformational changes induced in the human immunodeficiency virus envelope glycoproteins by soluble CD4 binding. J. Exp. Med. **174:**407-415.
96. **Sattentau, Q. J., and J. P. Moore.** 1995. Human immunodeficiency virus type 1 neutralization is determined by epitope exposure on the glycoprotein gp120 oligomer. J. Exp. Med. **182:**185-196.
97. **Sattentau, Q. J., J. P. Moore, F. Vignaux, F. Traincard, and P. Poignard.** 1993. Conformational changes induced in the envelope glycoproteins of the human and simian immunodeficiency viruses by soluble receptor binding. J. Virol. **67:**7383-7393.
98. **Sattentau, Q. J., S. Zolla-Pazner, and P. Poignard.** 1995. Epitope exposure on functional, oligomeric HIV-1 gp41 molecules. Virology **206:**713-717
99. **Schultz, T. F., B. A. Jameson, L. Lopalco, A. G. Siccardi, R. A. Weiss, and J. P. Moore.** 1992. Conserved structural features in the interaction between retroviral surface and transmembrane glycoproteins. AIDS Res. Hum. Retroviruses **8:**1585-1594.
100. **Shibata, R., M. D. Hoggan, C. Broscius, G. Englund, T. S. Theodore, A. Buckler White, L. O. Arthur, Z. Israel, A. Schultz, H. C. Lane, and M. A. Martin.** 1995. Isolation and characterization of a syncytium inducing macrophage/T-cell line tropic human immunodeficiency virus type 1 isolate that readily infects chimpanzee cells *in vitro* and *in vivo*. J. Virol. **69:**4453-4462.
101. **Shu, W., H. Ji, and M. Lu.** 1999. Trimerization specificity in HIV-1 gp41: analysis with a GCN4 leucine zipper model. Biochemistry **38:**5378-5385
102. **Sullivan, N., Y. Sun, J. Li, W. Hofmann, and J. Sodroski.** 1995. Replicative function and neutralization sensitivity of envelope glycoprotein from primary and T-cell-line-passaged human immunodeficiency virus type isolates. J. Virol. **69:**4413-4422.
103. **Sullivan, N., Y. Sun, Q. Sattentau, M. Thali, D. Wu, G. Denisova, J. Gershoni, J. Robinson, J. P. Moore, and J. Sodroski.** 1998. CD4-induced conformational changes in the human immunodeficiency virus type 1 gp120 glycoprotein: consequences for virus entry and neutralization. J. Virol. **72:**4694-4703.
104. **Takeuchi, Y., M. Akutsu, K. Murayama, N. Shimizu, and H. Hoshino.** 1991. Host range mutant of human immunodeficiency virus type 1: modification of cell tropism by a single point mutation at the neutralization epitope in the *env* gene. J. Virol. **65:**1710-1718
105. **Thali, M., J. P. Moore, C. Furman, M. Charles, D. D. Ho, J. Robinson, and J. Sodroski.** 1993. Characterization of human immunodeficiency virus type 1 (HIV-1) gp120 neutralization epitopes exposed upon gp120-CD4 binding. J. Virol. **67:**3978-3988.
106. **Trkola, A., T. Dragic, J. Arthos, J. M. Binley, W. C. Olson, G. P. Allaway, C. Cheng Mayer, J. Robinson, P. J. Maddon, and J. P. Moore.** 1996. CD4-dependent, antibody-sensitive interactions between HIV-1 and its co-receptor CCR-5. Nature **384:**184-187
107. **Trkola, A., T. Ketas, V. N. KewalRamani, F. Endorf, J. M. Binley, H. Katinger, J. Robinson, D. R. Littman, and J. P. Moore.** 1998. Neutralization sensitivity of human immunodeficiency virus type 1 primary isolates to antibodies and CD4-based reagents is independent of coreceptor usage. J. Virol. **72:**1876-1885.
108. **Trkola, A., A. B. Pomales, H. Yuan, B. Korber, P. J. Maddon, G. P. Allaway, H. Katinger, C. F. Barbas III, D. R. Burton, D. D. Ho, and J. P. Moore.** 1995. Cross-clade neutralization of primary isolates of human immunodeficiency virus type 1 by human monoclonal antibodies and tetrameric CD4 IgG. J. Virol. **69:**6609-6617.
109. **Trkola, A., M. Purtscher, T. Muster, C. Ballaun, A. Buchacher, N. Sullivan, K. Srinivasan, J. Sodroski, J. P. Moore, and H. Katinger.** 1996. Human monoclonal antibody 2G12 defines a distinctive neutralization epitope on the gp120 glycoprotein of human immunodeficiency virus type 1. J. Virol. **70:**1100-1108.
110. **VanCott, T. C., J. R. Mascola, R. W. Kaminski, V. Kalyanraman, P. L. Hallberg, P. R. Burnett, J. T. Ulrich, D. J. Rechtman, and D. L. Birx.** 1997. Antibodies with specificity to native gp120 and neutralization activity against primary human immunodeficiency virus type 1 isolates elicited by immunization with oligomeric gp160. J. Virol. **71:**4319-4330.
111. **VanCott, T. C., J. R. Mascola, L. D. Loomis-Price, F. Sinangil, N. Zitomersky, J. McNeil,**

M. L. Robb, D. L. Birx, and S. Barnett. 1999. Cross-subtype neutralizing antibodies induced in baboons by a subtype E gp120 immunogen based on an R5 primary human immunodeficiency virus type 1 envelope. J. Virol. **73:**4640-4650.

112. **Van Cott, T. C., V. R. Polonis, L. D. Loomis, N. L. Michael, P. L. Nara, and D. L. Birx.** 1995. Differential role of V3-specific antibodies in neutralization assays involving primary and laboratory adapted isolates of HIV-1. AIDS Res. Hum. Retroviruses **11:**1379-1392
113. **Veronese, F. D., R. Rahman, R. Pal, C. Boyer, J. Romano, V. S. Kalyanaraman, B. C. Nair, R. C. Gallo, and M. G. Sarngadharan.** 1992. Delineation of immunoreactive, conserved regions in the external envelope glycoprotein of the human immunodeficiency virus type 1. AIDS Res. Hum. Retroviruses **8:**1125-1132
114. **Volchkov, V. E., H. Feldmann, V. A. Volchkova, and H. D. Klenk.** 1998. Processing of the ebola virus glycoprotein by the proprotein convertase furin. Proc. Natl. Acad. Sci. USA **95:**5762-5767.
115. **Watkins, B. A., S. Buge, K. Aldrich, A. E. Davis, J. Robinson, M. S. Reitz, and M. Robert-Guroff.** 1996. Resistance of human immunodeficiency virus type 1 to neutralization by natural antisera occurs through single amino-acid substitutions that cause changes in antibody binding at multiple sites. J. Virol. **70:**8431-8437.
116. **Weissenhorn, W., A. Dessen, S. C. Harrison, J. J. Shekel, and D. C. Wiley.** 1997. Atomic structure of the ectodomain from HIV-1 gp41. Nature **387:**426-430
117. **Weissenhorn, W., A. Carfi, K. H. Lee, J. J. Skehel, and D. C. Wiley.** 1998. Crystal structure of Ebola virus membrane fusion subunit, GP2, from the envelope glycoprotein ectodomain. Mol. Cell **2:**605-616
118. **White-Scharf, M. E., B. J. Potts, L. M. Smith, K. A. Sokolowski, J. R. Rusche, and S. Silver.** 1993. Broadly neutralizing monoclonal antibodies to the V3 region of HIV-1 can be elicited by peptide immunization. Virology **192:**197-206
119. **Willey, R. L., J. S. Bonifacino, B. J. Potts, M. A. Martin, and R. D. Klausner.** 1988. Biosynthesis, cleavage, and degradation of the human immunodeficiency virus type 1 envelope protein. Proc. Natl. Acad. Sci. USA **85:**9580-9584
120. **Wrin, T., and J. H. Nunberg.** 1994. HIV-1 MN recombinant gp120 vaccine serum, which fails to neutralize primary isolates of HIV-1, does not antagonize neutralization by antibodies from infected individuals. AIDS **8:**1622-1623
121. **Wyatt, R., E. Desjardin, U. Olshevsky, C. Nixon, J. Binley, V. Olshevsky, and J. Sodroski.** 1997. Analysis of the interaction of the human immunodeficiency virus type 1 gp120 envelope glycoprotein with the gp41 transmembrane glycoprotein. J. Virol. **71:**9722-9731.
122. **Wyatt, R., P. D. Kwong, E. Desjardin, R. W. Sweet, J. Robinson, W. A. Hendrickson, and J. G. Sodroski.** 1998. The antigenic structure of the HIV gp120 envelope glycoprotein. Nature **393:**705-711
123. **Wyatt, R., J. P. Moore, M. Accola, E. Desjardin, J. Robinson, and J. Sodroski.** 1995. Involvement of the V1/V2 variable loop structure in the exposure of human immunodeficiency virus type 1 gp120 epitopes induced by receptor binding. J. Virol. **69:**5723-5733.
124. **Zhou, N., C. M. Kay, and R. S. Hodges.** 1993. Disulphide bond contribution to protein stability: positional effects of substitution in the hydrophobic core of the two-stranded alpha-helical coiled-coil. Biochemistry **32:**3178-3187

Chapter 5.2

Variable-loop-deleted variants of the HIV-1 envelope glycoprotein can be stabilized by an intermolecular disulfide bond between the gp120 and gp41 subunits

(*Journal of Virology,* 2000, p. 5091-5100, Vol. 74)

Rogier W. Sanders[1], Linnea Schiffner[2], Aditi Master[2], Francis Kajumo[2], Yong Guo[2], Tatjana Dragic[2], John P. Moore[2], and James M. Binley[2]

[1]*Dept. of Human Retrovirology, Academic Medical Center, University of Amsterdam, 1105 AZ Amsterdam, The Netherlands*

[2]*Aaron Diamond AIDS Research Center, The Rockefeller University, New York, New York 10016*

We have described an oligomeric gp140 envelope glycoprotein from human immunodeficiency virus type 1 that is stabilized by an intermolecular disulfide bond between gp120 and the gp41 ectodomain, termed SOS gp140 (J. M. Binley, R. W. Sanders, B. Clas, N. Schuelke, A. Master, Y. Guo, F. Kajumo, D. J. Anselma, P. J. Maddon, W. C. Olson, and J. P. Moore, J. Virol. 74:627-643, 2000). In this protein, the protease cleavage site between gp120 and gp41 is fully utilized. Here we report the characterization of gp140 variants that have deletions in the first, second, and/or third variable loop (V1, V2, and V3 loops). The SOS disulfide bond formed efficiently in gp140s containing a single loop deletion or a combination deletion of the V1 and V2 loops. However, deletion of all three variable loops prevented formation of the SOS disulfide bond. Some variable-loop-deleted gp140s were not fully processed to their gp120 and gp41 constituents even when the furin protease was cotransfected. The exposure of the gp120-gp41 cleavage site is probably affected in these proteins, even though the disabling change is in a region of gp120 distal from the cleavage site. Antigenic characterization of the variable-loop-deleted SOS gp140 proteins revealed that deletion of the variable loops uncovers cryptic, conserved neutralization epitopes near the coreceptor-binding site on gp120. These modified, disulfide-stabilized glycoproteins might be useful as immunogens.

Introduction

An immunogen able to induce effective humoral immune responses would be a valuable component of combination vaccines against human immunodeficiency virus type 1 (HIV-1). Such vaccines include ones in which cellular immunity is stimulated by live, recombinant viruses or DNA-based vectors (3, 19, 23, 30, 52).

The monomeric HIV-1 gp120 glycoprotein does not elicit broadly neutralizing antibody responses against representative primary isolates (3, 14, 49). However, such proteins are still being included in combination vaccines, for want of anything better.

The HIV-1 envelope glycoprotein complex contains two subunits, the transmembrane glycoprotein gp41 and the surface glycoprotein gp120. The latter contributes most of the exposed surface area to the complex and contains the binding sites for the CD4 receptor and a coreceptor, either CCR5 or CXCR4 or both (35, 53, 64, 71, 72). The crystal structures of the core fragments of both gp41 and gp120 have been described (11, 26, 28, 68, 72). During envelope glycoprotein synthesis, a peptide bond that links the gp120 and gp41 components of the precursor polyprotein, gp160, is cleaved by proteases in the Golgi complex (17, 24, 31, 58, 69, 70). The gp120 and gp41 subunits are then noncovalently but weakly associated (22, 32, 38, 57). On the cell and virion surface, the envelope glycoproteins are organized in trimers via noncovalent gp41-gp41 interactions (11, 28, 29, 68).

The trimeric envelope glycoprotein complex mediates HIV-1 attachment and fusion. First, gp120 binds to the CD4 receptor, inducing conformational changes that expose the normally occult coreceptor binding site (64, 71). This involves the movement of the first, second, and third variable loops (V1, V2, and V3 loops) away from the coreceptor-binding site (59, 61, 73). Once gp120 interacts with the coreceptor, additional conformational changes expose fusion peptides at the N termini of the gp41 moieties, which then mediate fusion of the viral and cell membranes (11, 13, 25, 45, 68).

The envelope glycoproteins are important targets for the humoral immune response in that neutralizing antibodies are known that interfere with virus-cell attachment and fusion (41, 49, 50). To persist as a chronic infection in the face of a vigorous humoral response, HIV-1 has evolved ways to limit the generation of neutralizing antibodies and/or to minimize their effect on its life cycle. There is unusually extensive shielding of the conserved regions of gp120 by nonimmunogenic carbohydrates (48, 51); the CD4-binding site is recessed (26, 72); escape mutants can be generated in a relatively facile way, even to antibodies against the CD4-binding site (26, 72); variable loops hide the coreceptor-binding site until after the CD4 interaction has occurred, thereby minimizing the time and space available for antibodies to intervene against this stage of the fusion process (26, 36, 53, 59, 72).

Another defense mechanism is that the trimeric envelope glycoprotein spikes are poorly immunogenic compared to their dissociated subunits (9, 40, 50). Most infection-induced antienvelope antibodies are raised to uncleaved gp160 precursors, dissociated gp120, or gp41 ectodomains from which gp120 has been shed (39, 40, 50, 56), as is also the case in respiratory syncytial virus infection (55). Such “viral debris” does not antigenically mimic the native trimeric complex, so although the immune response to viral antigens is strong, that against infectious virus is weak. Viral debris might not just create an irrelevant immune responseit may even actively decoy antibody production away from the functionally important forms of the envelope glycoproteins (40, 50, 55).

All these factors impact upon the design of vaccines for inducing humoral immunity: The natural mechanisms used by HIV-1 to limit the immunogenicity of its envelope glycoproteins need to be understood and overcome. One approach

that we and others are pursuing is the development of antigenic mimics of the native complex (5, 20, 74). We previously described such a protein (SOS gp140) in which the weak association between gp120 and the gp41 ectodomain is stabilized by the introduction of an intersubunit disulfide bond (5). However, it may be necessary to modify this protein to improve its immunogenicity. Several mutants of HIV-1 and simian immunodeficiency virus (SIV) gp120s have been made with the intent of immunogenicity enhancement; these include proteins that lack glycosylation sites or one or more of the variable loops (6, 10, 30, 51). Variable-loop-deleted gp120s are properly folded (4); indeed, one such protein from the HxBc2 strain was successfully crystallized as a ternary complex with soluble CD4 (sCD4) and the Fab fragment of the human monoclonal antibody (MAb) 17b (26, 72).

Here, we describe versions of the SOS gp140 protein with deletions of the V1, V2, and V3 loops. These modifications uncover conserved neutralization epitopes around the coreceptor-binding site in the context of a properly folded, fully processed, oligomeric envelope glycoprotein complex.

Materials and methods

Plasmids

The envelope glycoproteins used in this study were derived from HIV-1_{JR-FL}, a subtype B, CCR5-using primary isolate. The pPPI4 plasmid expressing soluble gp140 lacking the transmembrane and intracytoplasmic domains of gp41 has been described elsewhere (5). Furin was expressed from the plasmid pcDNA3.1-furin (5, 62).

Construction of mutant envelope glycoproteins

Plasmids encoding single-loop-deletion mutants were generated as follows; restriction sites are underlined. To delete the V1 sequences, two primers were designed that contain a unique *Nae*I site: 5JV1-N (5'-GTCTGAGTCGCCG-GCTCCCTTGCAATTTAAAGTAACACAGAG-3') and 3JV1-N (5'-GTCT-GAGTCGGAGCCGGCAACTGCTCTTTCAATATCACC-3'). PCR amplification with primer pair 5'Kpn1env (5'-GTCTATTATGGGGTACCTGTGTGG AAAGAAGC-3', which contains a unique *Kpn*I site) and 5JV1-N and with primer pair 3JV1-N and 3'BstB1env (5'-GTCTGAGTCTTCGAATTAATAAC-CACAGCCATTTTG-3', which contains a unique *Bst*BI site) produced two fragments without the V1 sequences that contained the *Nae*I site. Cloning of these fragments into pPPI4 using the *Kpn*I, *Nae*I, and *Bst*BI sites produced the plasmid lacking the V1 sequences. Plasmids lacking the V2 or V3 sequence were constructed in an analogous manner. The primer pairs used to create ΔV2-env were 5'Kpn1env and 5JV2-B (5'-GTCTGAGTCGGATCCGGCACCAGAGCAGTT TTTTATTTCTCC-3'') and 3'BstB1env and 3JV2-B (5'-GTCTGAGTCGGATC CTGTGACACCTCAGTCATTACACAG-3'). Primers 5JV2-B and 3JV2-B both contain a unique *Bam*HI site. The fragments were cloned into pPPI4 using the *Kpn*I, *Bam*HI, and *Bst*BI sites. The primers used to create the ΔV3 *env* gene were 5'Kpn1env and 5JV3-N (5' - GTCTGAGTCGGAGCCGGCGATATAAGACA AGCACATTGTAAC - 3') and 3'BstB1env and 3JV3-N (5'-GTCTGAGTCGC-CGGCTCCATTGTTGTTGGGTCTTGTACAATTAATTTC-3'). Primers 5JV3-

N and 3JV3-N both contain a unique *Nae*I site. The fragments were cloned into pPPI4 using the *Kpn*I, *Nae*I, and *Bst*BI sites. In the encoded glycoproteins, amino-acids 133 to 155 (ΔV1), 159 to 194 (ΔV2), or 303 to 324 (ΔV3) were replaced by a glycine-alanine-glycine linker (GAG) (Fig. 1). The numbering of amino-acids was based on the HxBc2 sequence, with the initiator methionine designated residue 1.

PCR amplification by primers 5'KpnIenv and 5JV1V2-B (5'-GTCT-GAGTCGGATCCGGCACCAGAGCAGT TGCCGGCTCCCT TGCAAT TTAA AGTAACAA-3'), using a DNA template (pPPI4) coding for a V1-deleted Env, followed by digestion by *Kpn*I and *Bam*HI generated a fragment lacking the sequences encoding the V1 loop. This fragment was cloned into a pPPI4 plasmid lacking the sequences for the V2 loop using the *Kpn*I and *Bam*HI restriction sites. The resulting plasmid encoded gp140 lacking both the V1 and V2 loops and was named ΔV1V2' (Fig. 1). A gp140 protein without the V1, V2, and V3 loops was created in a similar way but using a DNA fragment generated by PCR on a ΔV3 template with primers 3JV2-B and J140-BB. This was cloned into the ΔV1V2' plasmid by using *Bam*HI and *Bst*BI. The resulting *env* sequences were named ΔV1V2'V3. Another, more extensively deleted form of ΔV1V2, termed ΔV1V2*, was also constructed (Fig. 1). Here, PCR amplification was performed with primers 3'ΔV1V2STU1 (5'-GGCTCAAAGGATATCT TTGGACAGGCCTG T GTAATGACTGAGG TGTCACATCCTGCACCACAGAG TGGGG TTAATTT TACACATGGC-3', containing an *Stu*I site) and 5'Kpn1env. The resulting fragment was digested with *Stu*I and *Kpn*I and cloned into a pPPI4 gp140 vector using the internal *Stu*I site. The resulting ΔV1V2* gp140 protein had amino-acids 127 to 195 replaced by the GAG linker (Fig. 1). The ΔV1V2*V3 protein was constructed in an analogous manner to ΔV1V2'V3. Amino-acid substitutions were made with the Quickchange site-directed mutagenesis kit (Stratagene Inc.) using appropriate primers. The fidelity of all mutations was confirmed by sequencing. The absence of variable-loop epitopes from the loop-deleted proteins was confirmed by enzyme-linked immunosorbent assay (ELISA) with appropriate antibodies (4, 37, 39, 41, 42).

Transfection, labeling, and immunoprecipitation

Adherent 293T cells were grown in Dulbecco's modified Eagle's medium (DMEM; Gibco) supplemented with 10% fetal calf serum, penicillin, streptomycin, and L-glutamine. Transient transfection of 293T cells was performed by calcium phosphate precipitation. The plasmids based on pPPI4 gp140 were transfected with and without the furin expression vector pcDNA3.1-furin, each at 10 µg per 10-cm^2 plate. One day post-transfection, the medium was changed to DMEM supplemented with 0.2% bovine serum albumin, penicillin, streptomycin, and L-glutamine. For radioimmunoprecipitation analysis (RIPA), [^{35}S]cysteine and [^{35}S]methionine (200 µCi per plate; Amersham International PLC) were added for 24 h in DMEM lacking cysteine and methionine as described previously (5). The culture supernatants were cleared of debris by low-speed centrifugation before addition of concentrated RIPA buffer to adjust the composition to 50 mM Tris-HCl, 150 mM NaCl, and 1 mM EDTA (pH 7.2). Envelope glycoproteins were immunoprecipitated with biotin-labeled or unlabeled MAbs in a

1-ml volume for 10 min at room temperature, followed by incubation overnight at 4°C with either streptavidin-coated agarose beads (Vector Labs) or protein G-coated agarose beads (Pierce Inc.), as appropriate. The beads were washed three times with RIPA buffer containing 1% NP-40 detergent. Proteins were eluted by heating the beads at 100°C for 5 min in 60 µl of polyacrylamide gel electrophoresis (PAGE) buffer supplemented with 2% sodium dodecyl sulfate (SDS) and, when indicated, 100 mM dithiothreitol (DTT). The immunoprecipitates were fractionated by electrophoresis on SDS-8% PAGE gels at 200 V for 1 h. The gels were dried and exposed to a phosphor screen, and the positions of the radiolabeled proteins were determined using a PhosphorImager with ImageQuant software (Molecular Dynamics Inc.).

MAbs to HIV-1 envelope glycoprotein epitopes and sCD4

The epitopes and immunochemical properties of all the anti-gp120 and anti-gp41 MAbs used in this study have been described previously, as have their donors (5). Additional information on these MAbs has also been published (4, 7, 8, 18, 37, 39, 41-43, 46, 47, 53, 61, 65, 66, 72, 73). The tetrameric CD4-immunoglobulin G2 (CD4-IgG2) and monomeric sCD4 molecules, from Progenics Pharmaceuticals Inc., have also been described elsewhere (2).

Quantitation and characterization of gp120 and gp140 proteins by ELISA

To measure the secretion of gp120 and gp140 proteins from transfected 293T cells, we used a gp120 antigen capture ELISA based on a previously described assay (4, 37, 39). Briefly, envelope glycoproteins in the culture supernatants were denatured and reduced by boiling with 1% SDS and 50 mM DTT. Purified, monomeric JR-FL gp120 treated in the same way was used as a reference standard for gp120 expression (5, 64). The denatured proteins were captured onto plastic via sheep antibody D7324, which was raised against the continuous sequence APTKAKRRVVQREKR at the C terminus of gp120. Bound envelope glycoproteins were detected using a mixture of MAbs B12 and B13 against continuous epitopes exposed on denatured gp120 (1, 39). This assay allows the efficient detection of both gp120 and any gp140 molecules in which the peptide bond between gp120 and the gp140 ectodomain is still intact (5, 64). Nondenatured envelope glycoproteins were detected using the QC256 pool of sera from HIV-1-infected individuals (37, 38).

Results

Generation of variable-loop-deleted versions of the wild-type and SOS gp140 proteins

Throughout the text, we refer to proteins that contain gp120 and the gp41 ectodomain ($gp41_{ECTO}$) as wild-type (wt) gp140 proteins. The variants with cysteine substitutions that form an intermolecular disulfide bond between residues 501 of gp120 and 605 of gp41 are designated SOS gp140 proteins. Versions of these proteins without additional mutations are sometimes referred to as full-length to distinguish them from proteins from which one or more variable loops have been deleted; the latter are described as ΔV1, ΔV1 SOS, etc. For convenience, we refer to

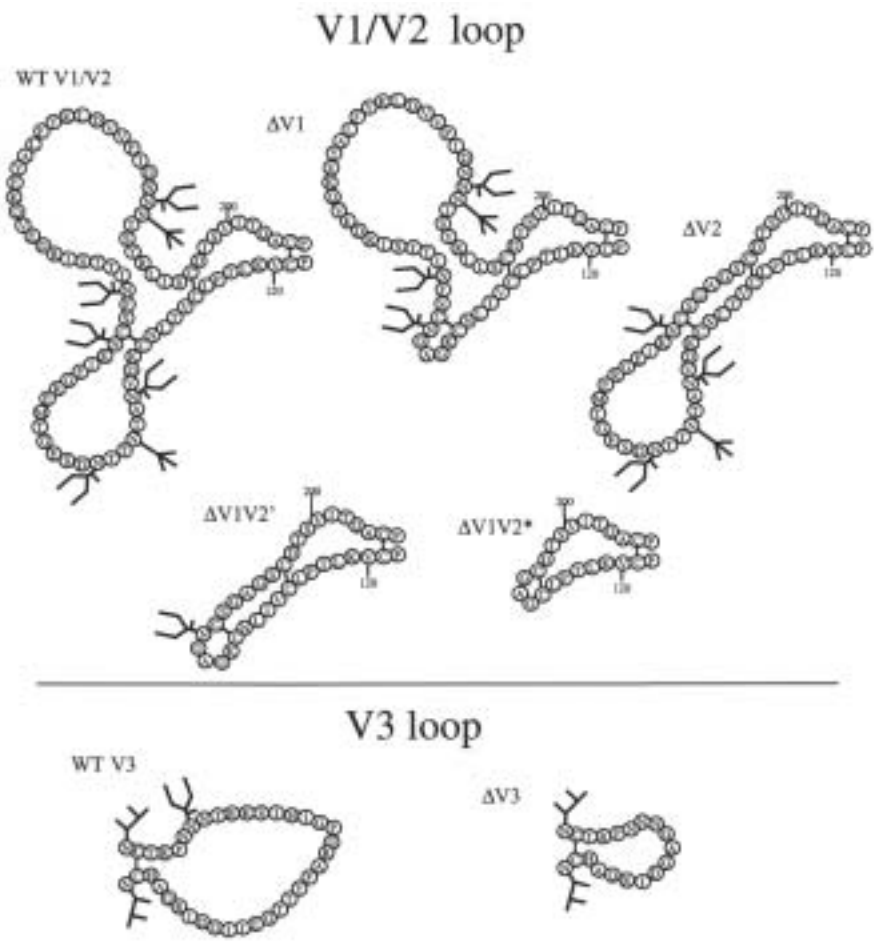

Fig. 1. Schematic representation of the V1, V2, and V3 regions of JR-FL gp120 and the deletions made in the various mutants. The structures and residue numbering scheme are based on the representation of JR-FL gp120 in reference 5, which is in turn based on the gp120 secondary structure described by Leonard et al. (27).

the variable-loop-deleted mutants as gp120s or gp140s irrespective of their actual size, the gp140s possessing the gp41 ectodomain in each case.

We generated a set of wt and SOS gp140 proteins with a deletion in one or more of the variable loops (Fig. 1). These were ΔV1 (amino-acids 133 to 155 replaced by the GAG tripeptide), ΔV2 (amino-acids 159 to 194 replaced by GAG), ΔV3 (amino-acids 303 to 324 replaced by GAG), ΔV1V2' (amino-acids 133 to 155 and 159 to 194 replaced by GAG), and ΔV1V2* (amino-acids 127 to 195 replaced by GAG). Two proteins with multiple loop deletions were also made, ΔV1V2'V3 and ΔV1V2*V3. Unlike the ΔV1V2* and ΔV1V2*V3 proteins, the ΔV1V2' and ΔV1V2'V3 proteins still contained natural sequences between the V1 and V2 loops, including the glycosylation site at position 156 and the cysteines at

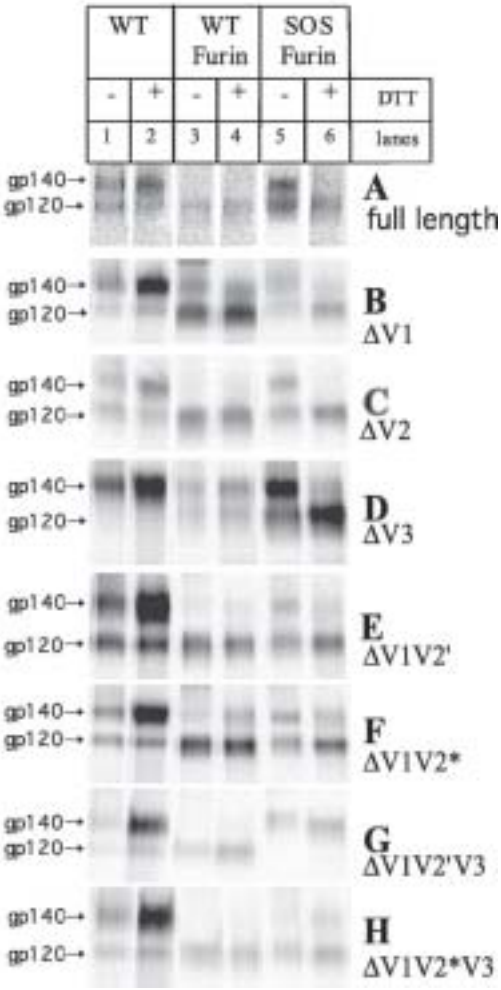

Fig. 2. Analysis of cleavage and intermolecular disulfide bond formation in full-length and variable-loop-deleted gp140 proteins. Envelope glycoproteins secreted from transfected 293T cells were immunoprecipitated with MAb 2G12. Furin was cotransfected only with the SOS gp140 proteins. The wt gp140 proteins were produced in the absence (lanes 1 and 2) or presence (lanes 3 and 4) of cotransfected furin. The SOS gp140 proteins were produced in the presence of cotransfected furin (lanes 5 and 6). In each lane, the upper band represents a gp140 protein containing gp120 plus the gp41 ectodomain. These bands from wt proteins comprise uncleaved gp140 species in which the gp120-$gp41_{ECTO}$ cleavage site is unprocessed. In the case of SOS gp140 proteins, the upper bands represent disulfide-stabilized, proteolytically cleaved gp140s. In all cases, the lower bands are gp120 proteins, with or without deletions in their variable loops. The precipitated proteins were treated with DTT or not treated, as indicated. The full-length proteins are analyzed in panel A, and different variable-loop-deleted proteins are analyzed in panels B through H.

positions 131 and 157 that form an intramolecular disulfide bond (Fig. 1). The designs of these various mutants were based on the results from previous studies with loop-deleted versions of gp120 monomers (4, 72, 73). To create disulfide-stabilized versions of the variable-loop-deleted gp140 proteins (loop-deleted SOS gp140 proteins), we substituted residues alanine-501 of gp120 and threonine-605 of gp41 with cysteines, as previously described for the full-length gp140 protein (5).

To investigate whether variable-loop-deleted gp140 proteins were properly folded and cleaved and whether they formed the SOS disulfide bond, they were expressed in the presence and absence of cotransfected furin and then immunoprecipitated with MAb 2G12. This recognizes a neutralizing, glycan-dependent epitope in the C3 and V4 regions of gp120 (similar results were obtained using anti-gp41 MAb 2F5; data not shown). The precipitated proteins were incubated with or without DTT prior to SDS-PAGE analysis to determine whether there was

an uncleaved peptide bond or a reducible disulfide bond between gp120 and $gp41_{ECTO}$ (Fig. 2). The full-length gp140 proteins were also analyzed for comparison (Fig. 2A). Because of variations in the expression of the different gp140 variants and in their immunoprecipitation efficiencies, the intensities of different bands in Fig. 2 cannot be precisely compared. However, the various envelope proteins appeared to be secreted with different efficiencies. For example, ΔV1 SOS gp140 (Fig. 2B, lane 5) and ΔV2 gp140 (Fig. 2C, lane 1) were expressed relatively poorly, whereas ΔV3 SOS gp140 was expressed with significantly greater efficiency than the others (Fig. 2D, lane 5). Measurements of protein expression by ELISA were consistent with the RIPA analyses (data not shown).

In most cases, both a gp120 band (or the variable-loop-deleted equivalent) and a gp140 band (or the variable-loop-deleted equivalent) were detected. Note that a gp140 (upper) band can represent either an uncleaved gp140 protein, in which gp120 is still linked to $gp41_{ECTO}$ by a peptide bond (Fig. 2, lanes 1 to 4), or an SOS gp140 protein, in which the gp120 and $gp41_{ECTO}$ moieties are associated by an intermolecular disulfide bond (Fig. 2, lane 5) that is susceptible to reduction by DTT (Fig. 2, lane 6). The two forms of gp140 proteins migrate identically on SDS-PAGE gels (5).

Like full-length wt gp140, none of the variable-loop-deleted gp140 proteins was completely cleaved in the absence of cotransfected furin, as indicated by the presence of uncleaved gp140 bands that survived DTT treatment (Fig. 2, compare lanes 1 and 2). In the presence of furin, the different variable-loop-deleted proteins were cleaved to various extents (Fig. 2, lane 3). For example, the ΔV2 and ΔV1V2' gp140 proteins were efficiently cleaved, in that no gp140 band was now visible (Fig. 2C and E, lanes 3 and 4), whereas some residual uncleaved gp140 was produced from the ΔV1 and ΔV1V2* gp140 constructs, even in the presence of furin (Fig. 2B and F, lanes 3 and 4).

An intermolecular disulfide bond forms successfully in the SOS versions of the ΔV1, ΔV2, ΔV3, ΔV1V2', and ΔV1V2* proteins (Fig. 2B to F, lanes 5 and 6). These are generally processed efficiently in the presence of furin, although some uncleaved gp140 protein is still present with ΔV1V2* SOS gp140 (Fig. 2F, lane 6). This apparently DTT-resistant gp140 is probably derived from high-molecular-weight aggregates that are disrupted by boiling with DTT (5). Such aggregates are produced from transient transfections with gp140- or SOS gp140-expressing plasmids but not from CHO cells stably expressing the SOS gp140 protein and furin (5) (data not shown).

Although the majority of the variable-loop deletants behaved like their full-length counterparts, some did not. The most notable differences were the absence of a gp140 band derived from the ΔV1V2*V3 SOS gp140 construct (Fig. 2H, lane 5) and the absence of gp120 bands derived from the ΔV3 gp140 and ΔV1V2'V3 SOS gp140 constructs even in the presence of furin and/or DTT (Fig. 2D, lanes 1 to 4, and Fig. 2G, lanes 5 and 6).

*SOS bond does not form in ΔV1V2*V3 gp140*

No gp140 band was expressed from the ΔV1V2*V3 SOS gp140 construct (Fig. 2H, lane 5). However, when ΔV1V2*V3 SOS gp140 was treated with DTT, a faint DTT-insensitive gp140 band was visible (Fig. 2H, lane 6), derived from the

DTT disruption of uncleaved gp140 aggregates. That the ΔV1V2*V3 SOS gp140 construct does not yield a gp140 protein while producing a gp120 could have one of two explanations. Either the 2G12 MAb does not bind the gp140 form of this protein because of structural perturbations introduced by the triple loop deletion that limit 2G12 epitope exposure, or the disulfide bond between cysteine residues 501 of gp120 and 605 of gp41 does not form in the context of this triple-loop-deleted protein.

To investigate the first possibility, we used a panel of MAbs to the CD4-binding site (CD4BS), CD4-induced (CD4i), and C4 epitopes on gp120 and the neutralizing anti-gp41 MAb 2F5. None of these MAbs precipitated a gp140 protein from the ΔV1V2*V3 SOS gp140 transfection. In contrast, every MAb, including 2G12, was able to precipitate an uncleaved ΔV1V2*V3 wt gp140 protein (data not shown). Hence, the deletion of all three variable loops does not cause a major structural perturbation to the gp120 core and its conserved epitopes.

The most likely explanation of the failure of multiple MAbs to detect the ΔV1V2*V3 SOS gp140 protein is that the protein is simply not secreted. Hence, when the V1, V2, and V3 loops are all deleted, the intermolecular disulfide bond cannot form between gp120 and gp41, so that no stable gp140 is produced. This is not the case when only the V1 and V2 loops are deleted or when only the V3 loop is removed (Fig. 2D to F, lane 5). Presumably, the triple-loop-deleted gp140 protein folds in such a way that the cysteine residues at positions 501 and 605 are not close enough to form a disulfide bond. On this assumption, we tried moving the gp120 cysteine from residue 501 to residue 500 or 502, but this did not restore the formation of the intermolecular disulfide bond (data not shown).

Some gp140 mutants are incompletely processed to gp120 and gp41$_{ECTO}$

The most likely explanation for the absence of gp120 bands from the ΔV3 gp140 (Fig. 2D, lanes 1 to 4) and ΔV1V2'V3 SOS gp140 preparations (Fig. 2G, lanes 5 and 6), even in the presence of furin, is due to inefficient cleavage of gp140 into gp120 and gp41$_{ECTO}$ subunits. In contrast to the extremely limited cleavage of the wt ΔV3 gp140 protein (Fig. 2D, lanes 1 to 4), the ΔV3 SOS gp140 protein was fully cleaved (Fig. 2D, lanes 5 and 6). It appears, then, that the deletion of the V3 loop modifies the conformation of the wt gp140 protein in such a way that its cleavage into gp120 and gp41$_{ECTO}$ subunits becomes inefficient. However, the introduction of the intermolecular disulfide bond into the SOS version of the ΔV3 gp140 protein restores the protein's conformation and permits cleavage to occur.

In contrast to wt ΔV3 gp140, the wt ΔV1V2'V3 gp140 protein was cleaved efficiently to gp120 in the presence of furin (Fig. 2G, lanes 3 and 4). Moreover, while the cleavage deficiency of the wt ΔV3 gp140 was rescued by introduction of an SOS bond, the ΔV1V2'V3 SOS gp140 expressed uncleaved gp140 (Fig. 2G, lanes 5 and 6). The diffuseness of the band and its low mobility compared with its wt gp140 counterpart (this is more easily discernable on gels that were run further; data not shown) suggests that the ΔV1V2'V3 SOS gp140 is a misfolded protein (5, 16) (Fig. 2G, compare lanes 5 and 1). Hence, the cysteine residues at positions 501 and 605 must inhibit the processing of the triple-loop-deleted SOS gp140 protein.

The processing efficiencies of the various loop-deleted wt and SOS gp140 proteins are summarized in Table 1.

Table 1. Proteolytic cleavage and intermolecular disulfide bond formation in full-length and loop-deleted wt and SOS gp140 proteins[a]

gp140 mutant	gp140 cleavage		Disulfide bond formation
	wt protein	SOS protein	
wt, full length	+++	+++	+
ΔV1	++	+++	+
ΔV2	+++	+++	+
ΔV3	–	+++	+
ΔV1V2'	+++	+++	+
ΔV1V2*	++	++	+
ΔV1V2'V3	+++	–	–
ΔV1V2*V3	+++	+++	–

a The original data are presented in Fig. 3 and 4. The extent of gp140 cleavage in the presence of cotransfected furin was determined. +++, 90 to 100% cleavage; ++, 60 to 90% cleavage; +, 30 to 60% cleavage; –, 0 to 30% cleavage. The formation of intermolecular disulfide bonds was determined in SOS gp140.

Exposure of gp120 C5 and gp41 epitopes on loop-deleted SOS gp140 proteins

We have shown that full-length uncleaved gp140 proteins differ in their antigenic structure from the SOS gp140 protein (5). Nonneutralizing epitopes in the C1 and C5 domains of gp120 and all gp41 epitopes except the neutralizing 2F5 epitope are obscured in the SOS gp140 protein, whereas they are exposed on the uncleaved gp140 proteins. In this respect, the SOS gp140 protein has antigenic properties similar to those of the native, virion-associated envelope glycoprotein complex, in which the C1 and C5 domains and much of the gp41 surface are involved in intersubunit interactions (5, 39, 56).

To study the antigenic structures of loop-deleted SOS gp140 proteins, we first performed immunoprecipitations with MAb 23A, directed to the gp120 C5 domain, and to several regions of gp41 (MAb 7B2 to cluster I, MAb 25C2 to the cluster II/fusion domain, and MAb 2F5 to neutralization epitope ELDKWAS). The SOS gp140 forms of the full-length, ΔV3, and ΔV1V2* proteins (Fig. 3, even-numbered lanes) were compared with the wt versions of the same proteins, which produce gp120 and uncleaved gp140 (Fig. 3, odd-numbered lanes).

The gp120 C5 MAb 23A failed to recognize the properly processed full-length SOS, ΔV1V2* SOS, and ΔV3 SOS gp140 proteins, but it bound to the uncleaved gp140 version of each of these proteins. The recognition by MAb 23A of the gp120 bands derived from the SOS gp140 transfections indicates that its epitope was not destroyed by the nearby cysteine substitution in the C5 domain (Fig. 3, compare lane 2 with lane 1). The nonneutralizing anti-gp41 MAbs 25C2 and 7B2 also did not bind to the full-length SOS, ΔV1V2* SOS, and ΔV3 SOS gp140 proteins, but they reacted efficiently with the corresponding uncleaved wt gp140 proteins (Fig. 3, compare lanes 4 and 6 with lanes 3 and 5). Similar results were

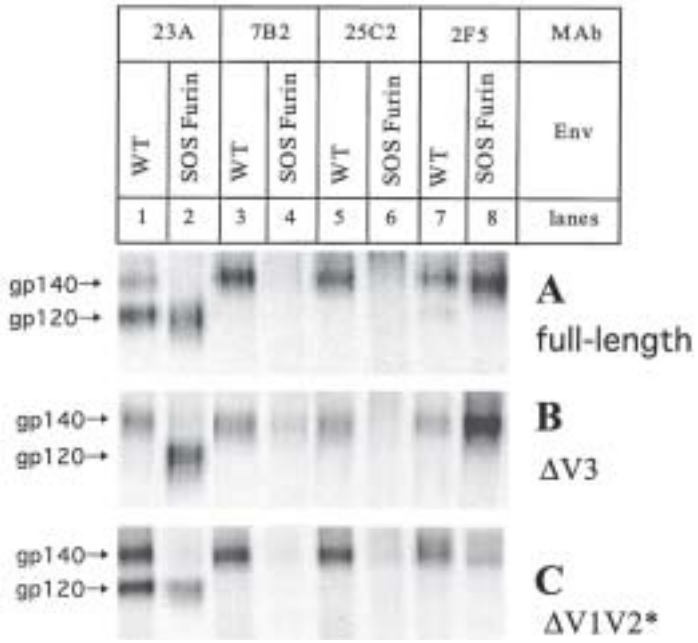

Fig. 3. Antigenic structure analysis of variable-loop-deleted gp140 proteins. Envelope glycoproteins from **A.** full-length, **B.** V3, and **C.** V1V2* WT and SOS gp140 proteins were precipitated with MAb 23A to the gp120 C5 region or with MAb 2F5, 25C2, or 7B2 to the gp41 ectodomain, as indicated. The WT gp140 proteins were expressed in the absence of cotransfected furin, yielding gp120 and uncleaved gp140 (odd-numbered lanes). Furin was cotransfected with the SOS gp140 proteins (even-numbered lanes).

obtained with several other nonneutralizing MAbs to various gp41 epitopes, such as 4D4, T15G1, and 2.2B (data not shown).

In contrast to what was found with the nonneutralizing MAbs, the neutralizing MAb 2F5 bound much more efficiently to the full-length and ΔV3 SOS gp140 proteins than to the uncleaved WT gp140 proteins (Fig. 3, compare lane 8 with lane 7). Taking into account the slightly reduced expression of the ΔV1V2* SOS gp140 protein compared with the wt ΔV1V2* gp140 protein (Fig. 3C, lanes 1 and 2), 2F5 reactivity was also greater with the SOS gp140 version (Fig. 3C, lanes 7 and 8). A similar pattern of data on 2F5 reactivity was obtained with other variable-loop-deleted gp140 and SOS gp140 proteins (data not shown).

aken together, these experiments confirm that the ΔV1V2* SOS and ΔV3 SOS gp140 proteins are processed properly and that they retain the fundamental antigenic properties of the full-length SOS gp140 protein.

Exposure of CD4-binding site and CD4-induced epitopes on loop-deleted SOS gp140 proteins

To assess whether the receptor-binding sites were preserved on the ΔV2 SOS, ΔV3 SOS, and ΔV1V2* SOS gp140 proteins, we first performed immunoprecip-

itations with the tetrameric CD4-IgG2 molecule (Fig. 4A). Like the full-length SOS gp140 protein, the variable-loop-deleted SOS gp140 proteins could be efficiently precipitated with CD4-IgG2, confirming that the CD4-binding site was retained on these proteins (Fig. 4A). Similar results were obtained using MAbs IgG1b12 and F91 to epitopes which overlapped the CD4BS (data not shown). There was, however, reduced reactivity of IgG1b12 with SOS gp140 proteins lacking the V2 loop, consistent with the known influence of the V2 loop structure on the epitope for this MAb (8, 34, 54, 73).

Important elements of the coreceptor-binding site on gp120 overlap the epitopes for the human MAbs 17b and 48d, so these MAbs can be used as surrogates for the coreceptor interactions of gp120 proteins (26, 53, 72). The variable loops of gp120 partially occlude the 17b/48d epitope cluster until the binding of CD4 induces conformational changes that fully expose these epitopes; hence their designation as CD4i epitopes (59, 64, 71-73). The removal of the variable loops, especially the V1 and V2 loop structure, from monomeric gp120 constitutively increases the exposure of the CD4i epitopes (4, 73). We have shown that the CD4i epitopes are almost completely occluded on the SOS gp140 protein but that their exposure is greatly increased by sCD4 binding (5). We now sought to determine the effect on these epitopes of removing the variable loops from the SOS gp140 protein.

The full-length, ΔV2, ΔV3, and ΔV1V2* SOS gp140 proteins were immunoprecipitated with MAb 17b in the presence and absence of sCD4 (Fig. 4B). Similar results were obtained with MAb 48d and also with MAb A32 to a separate CD4i epitope (data not shown). Without sCD4, the 17b epitope was almost completely obscured on the full-length SOS gp140 protein, but it was strongly induced by sCD4 binding (Fig. 4B, compare lanes 1 and 5). In the absence of sCD4, the 17b epitope was partially exposed on the ΔV2 SOS and ΔV3 SOS gp140 proteins and well exposed on the ΔV1V2* SOS gp140 protein (Fig. 4B, compare lanes 2 to 4 with lanes 6 to 8). The binding of sCD4 strongly induced the 17b epitope on the ΔV3 SOS gp140 (Fig. 4B, lanes 3 and 7) but had little or no effect on the binding of 17b to the ΔV2 SOS and the ΔV1V2* SOS gp140 proteins (Fig. 4B, compare lanes 2 and 4 with lanes 6 and 8).

These results confirm that the CD4i epitopes are present on the variable-loop-deleted SOS gp140 proteins. They are also consistent with the known involvement of the V1-V2 loop structure in shielding the CD4i epitopes (4, 73); the CD4i epitopes can be exposed either by removal of the variable loops or by sCD4 binding. Although both mechanisms can operate, once the CD4i epitopes are well exposed (as on the ΔV1V2* SOS gp140 protein), they can be further uncovered to only a limited extent by sCD4 binding.

The effect of sCD4 on 17b binding was much greater on the full-length and ΔV3 SOS gp140 proteins than on the corresponding gp120 monomers (compare the effect of sCD4 on the upper and lower bands in Fig. 4B, lanes 1, 3, 5, and 7). This presumably reflects the additional involvement of intersubunit interactions as part of the mechanisms that shield the CD4i epitopes on oligomeric envelope glycoproteins (5).

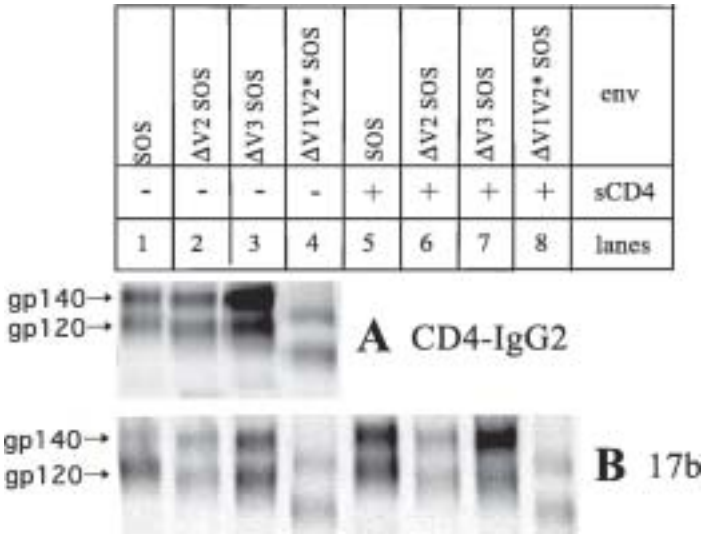

Fig. 4. Exposure of CD4BS and CD4i epitopes on variable-loop-deleted SOS gp140 proteins. Envelope glycoproteins expressed from the full-length SOS gp140 protein and the V2 SOS, V3 SOS, and V1V2* SOS gp140 proteins in the presence of cotransfected furin were immunoprecipitated with (A) the CD4-IgG2 molecule or (B) MAb 17b to a CD4i epitope in the presence and absence of sCD4.

Discussion

We aim to create envelope glycoproteins that are more immunogenic than presently available gp120 monomers or oligomers in which a peptide bond links gp120 with the gp41 ectodomain either by design or because of inefficient processing of the cleavage site. We have described oligomeric gp140 proteins stabilized by an intermolecular disulfide bond between gp120 and $gp41_{ECTO}$ (SOS gp140 proteins). These proteins mimic the antigenic structure of the native, fusion-competent glycoprotein complex found on the surfaces of virions or infected cells (5). The immunogenicity of the SOS gp140 proteins has yet to be evaluated, but we have anticipated the possibility that it might be necessary to alter their structure to improve the presentation of conserved neutralization epitopes.

Here, we describe SOS gp140 proteins from which one or more of the gp120 variable loops have been deleted to better expose underlying, conserved regions around the CD4- and coreceptor-binding sites. Two parameters that required characterization were whether an intermolecular disulfide bond could form between gp120 and $gp41_{ECTO}$ after deletion of variable loops and whether loop-deleted proteins could be properly processed at the gp120-$gp41_{ECTO}$ proteolytic cleavage site.

It was not possible to remove all three of the V1, V2, and V3 loop structures without adversely affecting the formation of the intermolecular disulfide bond

and/or the proper proteolytic processing and folding of SOS gp140 proteins. However, each of the individual loops could be safely deleted, as could the V1 and V2 loops in combination. When the disulfide bond did form, the cleavage site was always efficiently utilized in the presence of cotransfected furin. Thus, we could successfully make the ΔV1, ΔV2, ΔV3, ΔV1V2', and ΔV1V2* SOS gp140 proteins.

In the context of the wt gp140 protein, deletion of the V3 loop prevented cleavage of gp120 from $gp41_{ECTO}$ so that only uncleaved gp140 proteins were secreted, even when furin was cotransfected. An unexpected observation was that the formation of the intermolecular disulfide bond in the ΔV3 SOS gp140 protein completely reversed the cleavage deficiency. The removal of the V3 loop from gp120 appears to prevent the ΔV3 gp140 protein from folding correctly, so that the proteolytic cleavage site becomes inaccessible. The formation of the intermolecular disulfide bond presumably rescues the folding defect at an early stage of the synthesis of the ΔV3 SOS gp140 protein, so that the cleavage site becomes properly exposed (Table 1).

Introduction of the same intermolecular disulfide bond into the ΔV1V2'V3 gp140 protein had the opposite effect, however, in that this protein was efficiently cleaved but the ΔV1V2'V3 SOS gp140 protein was not. Conversely, the ΔV1V2*V3 SOS protein, which lacks the intramolecular disulfide bond at the base of the V1-V2 loop structure, was fully cleaved. However, in this protein, the intermolecular disulfide bond between gp120 and $gp41_{ECTO}$ did not form (Table 1). Neither triple-loop-deleted SOS gp140 construct gave rise to a disulfide-stabilized SOS gp140 protein.

Other than the presence or absence of the REKR cleavage site for furin proteases at the gp120 C terminus (24, 31, 44, 58, 69), several factors influence gp160 proteolysis. The cysteine residues at the base of the V3 loop are important for proper gp160 processing, at least in the context of envelope glycoproteins from the LAI isolate (12, 21, 63, 67). Substitutions within and around the small intramolecular disulfide-bonded loop in the gp41 ectodomain also impair the efficiency of gp160 cleavage (15, 60), especially in primary-isolate envelope glycoproteins (33). This loop is proximal to the gp41 cysteine substitution in the SOS gp140 proteins and is implicated in gp120 binding (5).

Many other cysteine residues in gp120 are also indispensable for proper processing and folding of the envelope glycoproteins (67). We therefore made two different ΔV1V2 proteins, one of which (ΔV1V2*) lacked the cysteines at positions 131 and 157 near the base of the V1-V2 loop structure. This protein was processed efficiently, indicating that these two cysteines are dispensable for the folding and cleavage of gp140. Deleting these cysteines is a known not to affect the folding of monomeric gp120 (72, 73). A Leu-to-Asp substitution at residue 266 in the third constant region of gp120 also dramatically impaired gp160 cleavage (70).

Overall, the efficiency of gp160 or gp140 cleavage can be sensitive to changes in multiple regions of the envelope glycoproteins in an unpredictable fashion. It may be that amino-acid substitutions, even at distal locations, influence the folding of the envelope glycoprotein complex in a way that affects the exposure of the cleavage site and hence the extent to which it is processed by proteases. The

wt gp140 proteins from a variety of HIV-1 and SIV isolates differ significantly in their cleavage efficiency (5) (data not shown). This again indicates the sensitivity of the conserved cleavage site to differences in protein conformation during envelope glycoprotein synthesis. A similar hypothesis could explain the lack of SOS bond formation in the triple-loop deletants.

Notwithstanding what remains to be learned about envelope glycoprotein processing pathways, we were able to make the ΔV1, ΔV2, ΔV3, ΔV1V2', and ΔV1V2* SOS gp140 proteins. Among these, we have characterized the antigenic structure of the ΔV3 SOS gp140 and the ΔV1V2* SOS gp140 proteins in the most detail. These variable-loop-deleted SOS gp140 proteins retain the desirable features of their full-length counterpart. Thus, the C5 region of gp120 and all the gp41 epitopes (except the 2F5 neutralization epitope) are not exposed on any of the SOS gp140 proteins. In contrast, gp120 epitopes relevant to virus neutralization are well exposed on the variable-loop-deleted SOS gp140 proteins; indeed, on the ΔV1V2* SOS gp140 protein, the CD4i epitope for MAb 17b is constitutively exposed without sCD4 addition. The CD4i epitopes are moderately accessible on the ΔV3 SOS gp140 protein but are still inducible by sCD4. On the full-length SOS gp140 protein, MAb reactivity with the CD4i epitopes is almost entirely dependent upon the presence of sCD4. Of note is that the occlusion of the CD4i epitopes is greater on the full-length, oligomeric SOS gp140 protein than in the corresponding gp120 monomer. This suggests that oligomerization increases the extent to which the CD4i epitopes, and presumably the proximal coreceptor-binding site, are shielded prior to CD4 binding.

Further modifications can be made to the SOS gp140 proteins, including reductions in their carbohydrate content. Deletion of the V1-V2 loop region removes almost one-third of the gp120 *N*-linked glycans, but we have found that other glycosylation sites in the C3 and V4 regions can be eliminated from the ΔV1V2* SOS gp140 protein without affecting its overall conformation. Removing variable loops and glycans from SOS gp140 proteins might also be useful for structural studies, based on how the gp120 core was crystallized (26, 72).

In summary, we have now made disulfide-stabilized SOS gp140 proteins with deletions of the V3 or the V1 and V2 loops. These proteins are properly processed and have favorable antigenic properties. The deletion of the variable loops increases the accessibility of the underlying, conserved neutralization epitopes on the gp120 moieties. However, the entire approach of deleting the variable loops depends upon the assumption that any antibodies that are induced to previously cryptic epitopes will be capable of binding back to the same structures on native virions and thereby neutralizing HIV-1 infectivity. The virions that must be countered by a vaccine contain the unmodified envelope glycoproteins on which the conserved epitopes remain shielded. Of note is that the 17b and 48d MAbs to the conserved, CD4i epitopes have little or no ability to neutralize primary isolates (59, 64, 71, 73). The deletion of the V1, V2, and V3 loops from gp120, uncleaved gp140, and gp160 forms of the envelope glycoproteins from the T-cell-line-adapted strain HXB2 either decreased the ability of the proteins to induce autologous neutralizing antibodies or had little effect (30). Whether modifications to the antigenic structure of SOS gp140 glycoproteins by variable-loop deletion translate into improvements in their immunogenicity remains to be determined.

Acknowledgments

We thank Gary Thomas for provision of the pGEMfurin plasmid and James Robinson and Herman Katinger for the gifts of several monoclonal antibodies. We appreciate the use of expression vectors and other reagents from Paul Maddon, Norbert Schuelke, and William Olson at Progenics Pharmaceuticals, as well as their advice and support. This work was supported by RO1 grants AI 39420 and AI 45463.

References

1. **Abacioglu, Y. H., T. R. Fouts, J. D. Laman, E. Claassen, S. H. Pincus, J. P. Moore, C. A. Roby, R. Kamin-Lewis, and G. K. Lewis.** 1994. Epitope mapping and topology of baculovirus-expressed HIV-1 gp160 determined with a panel of murine monoclonal antibodies. AIDS Res. Hum. Retroviruses **10:**371-381
2. **Allaway, G. P., K. L. Davis-Bruno, G. A. Beaudry, E. B. Garcia, E. L. Wong, A. M. Ryder, K. W. Hasel, M. C. Gauduin, R. A. Koup, J. S. McDougal, and P. J. Maddon.** 1995. Expression and characterization of CD4-IgG2, a novel heterotetramer that neutralizes primary HIV type 1 isolates. AIDS Res. Hum. Retroviruses **11:**533-539
3. **Barnett, S. W., S. Rajasekar, H. Legg, B. Doe, D. H. Fuller, J. R. Haynes, C. M. Walker, and K. S. Steimer.** 1997. Vaccination with HIV-1 gp120 DNA induces immune responses that are boosted by a recombinant gp120 protein subunit. Vaccine **15:**869-873
4. **Binley, J. M., R. Wyatt, E. Desjardins, P. D. Kwong, W. Hendrickson, J. P. Moore, and J. Sodroski.** 1998. Analysis of the interaction of antibodies with a conserved enzymatically deglycosylated core of the HIV type 1 envelope glycoprotein 120. AIDS Res. Hum. Retroviruses **14:**191-198
5. **Binley, J. M., R. W. Sanders, B. Clas, N. Schuelke, A. Master, Y. Guo, F. Kajumo, D. J. Anselma, P. J. Maddon, W. C. Olson, and J. P. Moore.** 2000. A recombinant human immunodeficiency virus type 1 envelope glycoprotein complex stabilized by an intermolecular disulfide bond between the gp120 and gp41 subunits is an antigenic mimic of the trimeric virion-associated structure. J. Virol. **74**:627-643.
6. **Bolmstedt, A., S. Sjolander, J. E. Hansen, L. Akerblom, A. Hemming, S. L. Hu, B. Morein, and S. Olofsson.** 1996. Influence of *N*-linked glycans in V4-V5 region of human immunodeficiency virus type 1 glycoprotein gp160 on induction of a virus-neutralizing humoral response. J. Acquir. Immune Defic. Syndr. Hum. Retrovirol. **12:**213-220
7. **Buchacher, A., R. Predl, K. Strutzenberger, W. Steinfellner, A. Trkola, M. Purtscher, G. Gruber, C. Tauer, F. Steindl, A. Jungbauer, and H. Katinger.** 1994. Generation of human monoclonal antibodies against HIV-1 proteins: electrofusion and Epstein-Barr virus transformation for peripheral blood lymphocyte immortalization. AIDS Res. Hum. Retroviruses **10:**359-369
8. **Burton, D. R., J. Pyati, R. Koduri, S. J. Sharp, G. B. Thornton, P. W. Parren, L. S. Sawyer, R. M. Hendry, N. Dunlop, P. L. Nara, M. Lamacchia, E. Garratty, E. R. Stiehm, Y. J. Bryson, J. P. Moore, D. D. Ho, and C. F. Barbas, III.** 1994. Efficient neutralization of primary isolates of HIV-1 by a recombinant human monoclonal antibody. Science **266:**1024-1027
9. **Burton, D. R.** 1997. A vaccine for HIV type 1: the antibody perspective. Proc. Natl. Acad. Sci. USA **94:**10018-10023.
10. **Cao, J., N. Sullivan, E. Desjardin, C. Parolin, J. Robinson, R. Wyatt, and J. Sodroski.** 1997. Replication and neutralization of human immunodeficiency virus type 1 lacking the V1 and V2 variable loops of the gp120 envelope glycoprotein. J. Virol. **71:**9808-9812.
11. **Chan, D. C., D. Fass, J. M. Berger, and P. S. Kim.** 1997. Core structure of gp41 from the HIV envelope glycoprotein. Cell **89:**263-273
12. **Chiou, S. H., E. O. Freed, A. T. Panganiban, and W. R. Kenealy.** 1992. Studies on the role of the V3 loop in human immunodeficiency virus type 1 envelope glycoprotein function. AIDS Res.

Hum. Retroviruses **8:**1611-1618
13. **Cladera, J., I. Martin, J. M. Ruysschaert, and P. O'Shea.** 1999. Characterization of the sequence of interactions of the fusion domain of the simian immunodeficiency virus with membranes. Role of the membrane dipole potential. J. Biol. Chem. **274:**29951-29959.
14. **Connor, R. I., B. T. M. Korber, B. S. Graham, B. H. Hahn, D. D. Ho, B. D. Walker, A. U. Neumann, S. H. Vermund, J. Mestecky, S. Jackson, E. Fenamore, Y. Cao, F. Gao, S. Kalams, K. Kuntsman, D. McDonald, N. McWilliams, A. Trkola, J. P. Moore, and S. M. Wolinsky.** 1998. Immunological and virological analyses of persons infected by human immunodeficiency virus type 1, while participating in trials of recombinant gp120 subunit vaccines. J. Virol. **72:**1552-1576.
15. **Dedera, D., R. L. Gu, and L. Ratner.** 1992. Conserved cysteine residues in the human immunodeficiency virus type 1 transmembrane envelope protein are essential for precursor envelope cleavage. J. Virol. **66:**1207-1209.
16. **Doms, R. W., R. A. Lamb, J. K. Rose, and A. Helenius.** 1993. Folding and assembly of viral membrane proteins. Virology **193:**545-562
17. **Dubay, J. W., S. R. Dubay, H. J. Shin, and E. Hunter.** 1995. Analysis of the cleavage site of the human immunodeficiency virus type 1 glycoprotein: requirement of precursor cleavage for glycoprotein incorporation. J. Virol. **69:**4675-4682.
18. **Earl, P. L., C. C. Broder, D. Long, S. A. Lee, J. Peterson, S. Chakrabarti, R. W. Doms, and B. Moss.** 1994. Native oligomeric human immunodeficiency virus type 1 envelope glycoprotein elicits diverse monoclonal antibody reactivities. J. Virol. **68:**3015-3026.
19. **Excler, J. L., and S. Plotkin.** 1997. The prime-boost concept applied to HIV preventive vaccines. AIDS **11**(Suppl. A)**:**S127-S137
20. **Farzan, M., H. Choe, E. Desjardins, Y. Sun, J. Kuhn, J. Cao, D. Archambault, P. Kolchinsky, M. Koch, R. Wyatt, and J. Sodroski.** 1998. Stabilization of human immunodeficiency virus type 1 envelope glycoprotein trimers by disulfide bonds introduced into the gp41 glycoprotein ectodomain. J. Virol. **72:**7620-7625.
21. **Freed, E. O., and R. Risser.** 1991. Identification of conserved residues in the human immunodeficiency virus type 1 principal neutralizing determinant that are involved in fusion. AIDS Res. Hum. Retroviruses **7:**807-811
22. **Gelderblom, H. R., H. Reupke, and G. Pauli.** 1985. Loss of envelope antigens of HTLV-III/LAV, a factor in AIDS pathogenesis? Lancet **ii:**1016-1017.
23. **Hu, S. L., J. Klaniecki, T. Dykers, P. Sridhar, and B. M. Travis.** 1991. Neutralizing antibodies against HIV-1 BRU and SF2 isolates generated in mice immunized with recombinant vaccinia virus expressing HIV-1 (BRU) envelope glycoproteins and boosted with homologous gp160. AIDS Res. Hum. Retroviruses **7:**615-620
24. **Inocencio, N. M., J. F. Sucic, J. M. Moehring, M. J. Spence, and T. J. Moehring.** 1997. Endoprotease activities other than furin and PACE4 with a role in processing of HIV-1 gp160 glycoproteins in CHO-K1 cells. J. Biol. Chem. **272:**1344-1348.
25. **Jones, P. L., T. Korte, and R. Blumenthal.** 1998. Conformational changes in cell surface HIV-1 envelope glycoproteins are triggered by cooperation between cell surface CD4 and co-receptors. J. Biol. Chem. **273:**404-409.
26. **Kwong, P. D., R. Wyatt, J. Robinson, R. W. Sweet, J. Sodroski, and W. A. Hendrickson.** 1998. Structure of an HIV gp120 envelope glycoprotein in complex with the CD4 receptor and a neutralizing human antibody. Nature **393:**648-659
27. **Leonard, C. K., M. W. Spellman, L. Riddle, R. J. Harris, J. N. Thomas, and T. J. Gregory.** 1990. Assignment of intrachain disulfide bonds and characterization of potential glycosylation sites of the type 1 recombinant human immunodeficiency virus envelope glycoprotein (gp120) expressed in Chinese hamster ovary cells. J. Biol. Chem. **265:**10373-10382.
28. **Lu, M., S. Blackow, and P. Kim.** 1995. A trimeric structural domain of the HIV-1 transmembrane glycoprotein. Nat. Struct. Biol. **2:**1075-1085
29. **Lu, M., H. Ji, and S. Shen.** 1999. Subdomain folding and biological activity of the core structure from human immunodeficiency virus type 1 gp41: implications for viral membrane fusion. J. Virol. **73:**4433-4438.
30. **Lu, S., R. Wyatt, J. F. Richmond, F. Mustafa, S. Wang, J. Weng, D. C. Montefiori, J. Sodroski, and H. L. Robinson.** 1998. Immunogenicity of DNA vaccines expressing human immunode-

ficiency virus type 1 envelope glycoprotein with and without deletions in the V1/2 and V3 regions. AIDS Res. Hum. Retroviruses **14:**151-155

31. **McCune, J. M., L. B. Rabin, M. B. Feinberg, M. Lieberman, J. C. Kosek, G. R. Reyes, and I. L. Weissman.** 1988. Endoproteolytic cleavage of gp160 is required for the activation of human immunodeficiency virus. Cell **53:**55-67
32. **McKeating, J. A., A. McKnight, and J. P. Moore.** 1991. Differential loss of envelope glycoprotein gp120 from virion of human immunodeficiency virus type 1 isolates: effects on infectivity and neutralization. J. Virol. **65:**852-860
33. **Merat, R., H. Raoul, T. Leste-Lasserre, P. Sonigo, and G. Pancino.** 1999. Variable constraints on the principal immunodominant domain of the transmembrane glycoprotein of human immunodeficiency virus type 1. J. Virol. **73:**5698-5706.
34. **Mo, H., L. Stamatatos, J. E. Ip, C. F. Barbas, P. W. H. I. Parren, D. R. Burton, J. P. Moore, and D. D. Ho.** 1997. Human immunodeficiency virus type 1 mutants that escape neutralization by human monoclonal antibody IgG1b12. J. Virol. **71:**6869-6874.
35. **Moore, J. P.** 1997. Co-receptors: implications for HIV pathogenesis and therapy. Science **276:**51-52.
36. **Moore, J. P., and J. Binley.** 1998. HIV: envelope's letters boxed into shape. Nature **393:**630-631
37. **Moore, J. P., J. A. McKeating, I. M. Jones, P. E. Stephens, G. Clements, S. Thomson, and R. A. Weiss.** 1990. Characterization of recombinant gp120 and gp160 from HIV-1: binding to monoclonal antibodies and soluble CD4. AIDS **4:**307-315
38. **Moore, J. P., J. A. McKeating, R. A. Weiss, and Q. J. Sattentau.** 1990. Dissociation of gp120 from HIV-1 virions induced by soluble CD4. Science **250:**1139-1142
39. **Moore, J. P., Q. J. Sattentau, R. Wyatt, and J. Sodroski.** 1994. Probing the structure of the human immunodeficiency virus surface glycoprotein gp120 with a panel of monoclonal antibodies. J. Virol. **68:**469-484.
40. **Moore, J. P., and D. D. Ho.** 1995. HIV-1 neutralization: the consequences of viral adaptation to growth on transformed T cells. AIDS **9**(Suppl. A)**:**S117-S136
41. **Moore, J. P., and J. Sodroski.** 1996. Antibody cross-competition analysis of the human immunodeficiency virus type 1 gp120 exterior envelope glycoprotein. J. Virol. **70:**1863-1872.
42. **Moore, J. P., M. Thali, B. A. Jameson, F. Vignaux, G. K. Lewis, S. W. Poon, M. Charles, M. S. Fung, B. Sun, P. J. Durda, L. Akerblom, B. Wahren, D. D. Ho, Q. J. Sattentau, and J. Sodroski.** 1993. Immunochemical analysis of the gp120 surface glycoprotein of human immunodeficiency virus type 1: probing the structure of the C4 and V4 domains and the interaction of the C4 domain with the V3 loop. J. Virol. **67:**4785-4796.
43. **Moore, J. P., A. Trkola, B. Korber, L. J. Boots, J. A. Kessler, 2nd, F. E. McCutchan, J. Mascola, D. D. Ho, J. Robinson, and A. J. Conley.** 1995. A human monoclonal antibody to a complex epitope in the V3 region of gp120 of human immunodeficiency virus type 1 has broad reactivity within and outside clade B. J. Virol. **69:**122-130.
44. **Morikawa, Y., E. Barsov, and I. Jones.** 1993. Legitimate and illegitimate cleavage of human immunodeficiency virus glycoproteins by furin. J. Virol. **67:**3601-3604.
45. **Munoz-Barroso, I., K. Salzwedel, E. Hunter, and R. Blumenthal.** 1999. Role of the membrane-proximal domain in the initial stages of human immunodeficiency virus type 1 envelope glycoprotein-mediated membrane fusion. J. Virol. **73:**6089-6092.
46. **Muster, T., R. Guinea, A. Trkola, M. Purtscher, A. Klima, F. Steindl, P. Palese, and H. Katinger.** 1994. Cross-neutralizing activity against divergent human immunodeficiency virus type 1 isolates induced by the gp41 sequence ELDKWAS. J. Virol. **68:**4031-4034.
47. **Muster, T., F. Steindl, M. Purtscher, A. Trkola, A. Klima, G. Himmler, F. Ruker, and H. Katinger.** 1993. A conserved neutralizing epitope on gp41 of human immunodeficiency virus type 1. J. Virol. **67:**6642-6647.
48. **Olofsson, S., and J. E. Hansen.** 1998. Host cell glycosylation of viral glycoproteinsΔa battlefield for host defence and viral resistance. Scand. J. Infect. Dis. **30:**435-440
49. **Parren, P. W. H. I., J. P. Moore, D. R. Burton, and Q. J. Sattentau.** 1999. The neutralizing antibody response to HIV-1: viral evasion and escape from humoral immunity. AIDS **13**(Suppl. A)**:**S137-S162
50. **Parren, P. W. H. I., D. R. Burton, and Q. J. Sattentau.** 1997. HIV-1 antibodyΔdebris or virion? Nat. Med. **3:**366-367

51. **Reitter, J. N., R. E. Means, and R. C. Desrosiers.** 1998. A role for carbohydrates in immune evasion in AIDS. Nat. Med. **4:**679-684
52. **Richmond, J. F., S. Lu, J. C. Santoro, J. Weng, S. L. Hu, D. C. Montefiori, and H. L. Robinson.** 1998. Studies of the neutralizing activity and avidity of anti-human immunodeficiency virus type 1 Env antibody elicited by DNA priming and protein boosting. J. Virol. **72:**9092-10000.
53. **Rizzuto, C. D., R. Wyatt, N. Hernandez-Ramos, Y. Sun, P. D. Kwong, W. A. Hendrickson, and J. Sodroski.** 1998. A conserved HIV gp120 glycoprotein structure involved in chemokine receptor binding. Science **280:**1949-1953.
54. **Roben, P., J. P. Moore, M. Thali, J. Sodroski, C. F. Barbas, 3rd, and D. R. Burton.** 1994. Recognition properties of a panel of human recombinant Fab fragments to the CD4 binding site of gp120 that show differing abilities to neutralize human immunodeficiency virus type 1. J. Virol. **68:**4821-4828.
55. **Sakurai, H., R. A. Williamson, J. E. Crowe, J. A. Beeler, P. Poignard, R. B. Bastidas, R. M. Chanock, and D. R. Burton.** 1999. Human antibody responses to mature and immature forms of viral envelope in respiratory syncytial virus infection: significance for subunit vaccines. J. Virol. **73:**2956-2962.
56. **Sattentau, Q. J., S. Zolla-Pazner, and P. Poignard.** 1995. Epitope exposure on functional, oligomeric HIV-1 gp41 molecules. Virology **206:**713-717
57. **Schneider, J., O. Kaaden, T. D. Copeland, S. Oroszlan, and G. Hunsmann.** 1986. Shedding and interspecies type sero-reactivity of the envelope glycopolypeptide gp120 of the human immunodeficiency virus. J. Gen. Virol. **67:**2533-2538.
58. **Stein, B. S., and E. G. Engleman.** 1990. Intracellular processing of the gp160 HIV-1 envelope precursor. Endoproteolytic cleavage occurs in a cis or medial compartment of the Golgi complex. J. Biol. Chem. **265:**2640-2649.
59. **Sullivan, N., Y. Sun, Q. Sattentau, M. Thali, D. Wu, G. Denisova, J. Gershoni, J. Robinson, J. P. Moore, and J. Sodroski.** 1998. CD4-induced conformational changes in the human immunodeficiency virus type 1 gp120 glycoprotein: consequences for virus entry and neutralization. J. Virol. **72:**4694-4703.
60. **Syu, W. J., W. R. Lee, B. Du, Q. C. Yu, M. Essex, and T. H. Lee.** 1991. Role of conserved gp41 cysteine residues in the processing of human immunodeficiency virus envelope precursor and viral infectivity. J. Virol. **65:**6349-6352
61. **Thali, M., J. P. Moore, C. Furman, M. Charles, D. D. Ho, J. Robinson, and J. Sodroski.** 1993. Characterization of conserved human immunodeficiency virus type 1 gp120 neutralization epitopes exposed upon gp120-CD4 binding. J. Virol. **67:**3978-3988.
62. **Thomas, G., B. A. Thorne, L. Thomas, R. G. Allen, D. E. Hruby, R. Fuller, and J. Thorner.** 1988. Yeast KEX2 endoprotease correctly cleaves a neuroendocrine prohormone in mammalian cells. Science **241:**226-230
63. **Travis, B. M., T. I. Dykers, D. Hewgill, J. Ledbetter, T. T. Tsu, S. L. Hu, and J. B. Lewis.** 1992. Functional roles of the V3 hypervariable region of HIV-1 gp160 in the processing of gp160 and in the formation of syncytia in CD4+ cells. Virology **186:**313-317
64. **Trkola, A., T. Dragic, J. Arthos, J. M. Binley, W. C. Olson, G. P. Allaway, C. Cheng-Mayer, J. Robinson, P. J. Maddon, and J. P. Moore.** 1996. CD4-dependent, antibody-sensitive interactions between HIV-1 and its co-receptor CCR-5. Nature **384:**184-187
65. **Trkola, A., A. B. Pomales, H. Yuan, B. Korber, P. J. Maddon, G. P. Allaway, H. Katinger, C. F. Barbas, 3rd, D. R. Burton, D. D. Ho, and J. P. Moore.** 1995. Cross-clade neutralization of primary isolates of human immunodeficiency virus type 1 by human monoclonal antibodies and tetrameric CD4-IgG. J. Virol. **69:**6609-6617.
66. **Trkola, A., M. Purtscher, T. Muster, C. Ballaun, A. Buchacher, N. Sullivan, K. Srinivasan, J. Sodroski, J. P. Moore, and H. Katinger.** 1996. Human monoclonal antibody 2G12 defines a distinctive neutralization epitope on the gp120 glycoprotein of human immunodeficiency virus type 1. J. Virol. **70:**1100-1108.
67. **Tschachler, E., H. Buchow, R. C. Gallo, and M. S. Reitz, Jr.** 1990. Functional contribution of cysteine residues to the human immunodeficiency virus type 1 envelope. J. Virol. **64:**2250-2259
68. **Weissenhorn, W., A. Dessen, S. C. Harrison, J. J. Skehel, and D. C. Wiley.** 1997. Atomic structure of the ectodomain from HIV-1 gp41. Nature **387:**426-430
69. **Willey, R. L., J. S. Bonifacino, B. J. Potts, M. A. Martin, and R. D. Klausner.** 1988. Biosyn-

thesis, cleavage, and degradation of the human immunodeficiency virus 1 envelope glycoprotein gp160. Proc. Natl. Acad. Sci. USA **85:**9580-9584

70. **Willey, R. L., T. Klimkait, D. M. Frucht, J. S. Bonifacino, and M. A. Martin.** 1991. Mutations within the human immunodeficiency virus type 1 gp160 envelope glycoprotein alter its intracellular transport and processing. Virology **184:**313-321.
71. **Wu, L., N. P. Gerard, R. Wyatt, H. Choe, C. Parolin, N. Ruffing, A. Borsetti, A. A. Cardoso, E. Desjardin, W. Newman, C. Gerard, and J. Sodroski.** 1996. CD4-induced interaction of primary HIV-1 gp120 glycoproteins with the chemokine receptor CCR-5. Nature **384:**179-183
72. **Wyatt, R., P. D. Kwong, E. Desjardins, R. W. Sweet, J. Robinson, W. A. Hendrickson, and J. G. Sodroski.** 1998. The antigenic structure of the HIV gp120 envelope glycoprotein. Nature **393:**705-711
73. **Wyatt, R., J. P. Moore, M. Accola, E. Desjardin, J. Robinson, and J. Sodroski.** 1995. Involvement of the V1/V2 variable loop structure in the exposure of human immunodeficiency virus type 1 gp120 epitopes induced by receptor binding. J. Virol. **69:**5723-5733.
74. **Yang, X., L. Florin, M. Farzan, P. Kolchinsky, P. D. Kwong, J. Sodroski, and R. Wyatt.** 2000. Modifications that stabilize human immunodeficiency virus envelope glycoprotein trimers in solution. J. Virol. **74:**4746-4754.

Chapter 5.3

Oligomeric and conformational properties of a proteolytically mature, disulfide-stabilized HIV-1 gp140 envelope glycoprotein

(*Journal of Virology*, August 2002, p. 7760-7776)

Norbert Schülke[1], Mika S. Vesanen[2], Rogier W. Sanders[2], Ping Zhu[3], Min Lu[4], Deborah J. Anselma[1], Anthony R. Villa[1], Paul W. H. I. Parren[5], James M. Binley[2], Kenneth H. Roux[1], Paul J. Maddon[1], John P. Moore[2], William C. Olson[1]

[1]*Progenics Pharmaceuticals Inc., Tarrytown, New York 10591*
[2]*Dept. of Microbiology and Immunology*
[3]*Dept. of Biochemistry, Weill Medical College of Cornell University, New York, New York 10021*
[4]*Dept. of Biological Science and Structural Biology Program, Florida State University, Tallahassee, Florida 32306*
[5]*Dept. of Immunology, The Scripps Research Institute, La Jolla, California 92037*

We describe the further properties of a protein, designated SOS gp140, wherein the association of the gp120 and gp41 subunits of the human immunodeficiency virus type 1 (HIV-1) envelope glycoprotein is stabilized by an intersubunit disulfide bond. HIV-1_{JR-FL} SOS gp140, proteolytically uncleaved gp140 ($gp140_{UNC}$), and gp120 were expressed in stably transfected Chinese hamster ovary cells and analyzed for antigenic and structural properties before and after purification. Compared with $gp140_{UNC}$, SOS gp140 reacted more strongly in surface plasmon resonance and radioimmunoprecipitation assays with the neutralizing monoclonal antibodies (MAbs) 2G12 (anti-gp120), 2F5 (anti-gp41), and 17b (to a CD4-induced epitope that overlaps the CCR5-binding site). In contrast, $gp140_{UNC}$ displayed the greater reactivity with nonneutralizing anti-gp120 and anti-gp41 MAbs. Immunoelectron microscopy studies suggested a model for SOS gp140 wherein the gp41 ectodomain ($gp41_{ECTO}$) occludes the "nonneutralizing" face of gp120, consistent with the antigenic properties of this protein. We also report the application of Blue Native polyacrylamide gel electrophoresis (BN-PAGE), a high-resolution molecular sizing method, to the study of viral envelope proteins. BN-PAGE and other biophysical studies demonstrated that SOS gp140 was monomeric, whereas $gp140_{UNC}$ comprised a mixture of noncovalently associated and disulfide-linked dimers, trimers, and tetramers. The oligomeric and conformational properties of SOS gp140 and $gp140_{UNC}$ were largely unaffected by purification. An uncleaved gp140 protein containing the SOS cysteine mutations (SOS $gp140_{UNC}$) was also oligomeric. Surprisingly, variable-loop-deleted SOS gp140 proteins were expressed (although not yet purified) as cleaved, noncovalently associated oligomers that were significantly more stable than the

full-length protein. Overall, our findings have relevance for rational vaccine design.

Introduction

The native, fusion-competent form of the human immunodeficiency virus type 1 (HIV-1) envelope glycoprotein complex is a trimeric structure composed of three gp120 subunits and three gp41 subunits; the receptor-binding (CD4 and coreceptor) sites are located in the gp120 moieties, and the fusion peptides are located in the gp41 components (10, 33, 34, 52, 69, 78, 83). In the generally accepted model of HIV-1 fusion, the sequential binding of gp120 to CD4 and a coreceptor induces a series of conformational changes in the gp41 subunits, leading to the insertion of the fusion peptides into the host cell membrane in a highly dynamic process (14, 31, 39, 59, 68, 72, 81, 84, 91). The associations between the six components of the fusion-competent complex are maintained via noncovalent interactions between gp120 and gp41 and between the gp41 subunits (52, 84). These interactions are relatively weak, making the fusion-competent complex unstable. This instability perhaps facilitates the conformational changes in the various components that are necessary for the fusion reaction to proceed efficiently, but it greatly complicates the task of isolating the native complex in purified form. Put simply, the native complex falls apart before it can be purified, leaving only the dissociated subunits.

One reason it would be desirable to produce the native HIV-1 envelope complex is to explore its potential as an immunogen, perhaps after modification to improve its exposure of critical neutralization epitopes. The limited neutralizing-antibody response to HIV-1 in infected people is directed at the native complex and is probably raised against it (6, 40, 49, 51). In contrast, the isolated subunits have not proven efficient at inducing relevant neutralizing antibodies (reviewed in references 6, 49, and 51). We and others are therefore attempting to make more-stable forms of the envelope glycoprotein complex that better mimic the native structure. Usually, these efforts have focused on making various forms of soluble gp140 glycoproteins which contain gp120 but only the ectodomain of gp41 (4, 11, 13, 17, 19-21, 57, 66, 76, 85-87, 90).

An approach to resolving the instability of the native complex is to remove the cleavage site that naturally exists between the gp120 and gp41 subunits. Doing so means that proteolysis of this site does not occur, leading to the expression of gp140 glycoproteins in which the gp120 subunit is covalently linked to the gp41 ectodomain ($gp41_{ECTO}$) by means of a peptide bond (2, 3, 16-18). Such proteins can be oligomeric, sometimes trimeric (11, 16-21, 54, 66, 85-87, 90). However, it is not clear that they truly represent the structure of the native, fusion-competent complex in which the gp120-gp41 cleavage site is fully utilized. Hence the receptor-binding properties of uncleaved gp140 ($gp140_{UNC}$) proteins tend to be impaired, and nonneutralizing antibody epitopes are exposed on them that probably are not accessible on the native structure (4, 6, 28, 60, 90).

We have taken an alternative approach to the problem of gp120-gp41 instability, which is to retain the cleavage site but to introduce a disulfide bond between the gp120 and $gp41_{ECTO}$ subunits (4, 57). Properly positioned, this intermolecular disulfide bond forms efficiently during envelope glycoprotein (Env) synthesis,

allowing the secretion of gp140 proteins that are proteolytically processed but in which the association between the gp120 and $gp41_{ECTO}$ subunits is maintained by the disulfide bond.

Here we show that the gp41-gp41 interactions are unstable in the SOS gp140 protein, which is expressed and purified primarily as a monomer. In contrast, $gp140_{UNC}$ proteins—with or without the SOS cysteine substitutions—are multimeric, implying that cleavage of the peptide bond between gp120 and gp41 destabilizes the native complex. Despite being monomeric, the purified and unpurified forms of SOS gp140 are better antigenic structural mimics of the native, fusion-competent Env structure than are the corresponding gp120 or $gp140_{UNC}$ proteins. This may be because the presence and orientation of $gp41_{ECTO}$ occludes certain nonneutralization epitopes on SOS gp140 while preserving the presentation of important neutralization sites. This explanation is consistent with immunoelectron microscopy studies of the protein. Unexpectedly, proteolytically mature, but variable-loop-deleted, SOS gp140 glycoproteins have enhanced oligomeric stability, so these molecules warrant further study for their structural and immunogenic properties.

Materials and methods

Plasmids

The pPPI4 eukaryotic expression vectors encoding SOS and uncleaved forms of $HIV\text{-}1_{JR\text{-}FL}$ gp140 have been described previously (4, 72). The SOS gp140 protein contains cysteine substitutions at residues A501 in the C5 region of gp120 and T605 in gp41 (4, 57). In $gp140_{UNC}$, the sequence KRRVVQREKRAV at the junction between gp120 and $gp41_{ECTO}$ has been replaced with a hexameric Leu-Arg motif to prevent scission of gp140 into gp120 and $gp41_{ECTO}$ (4). Plasmids encoding variable-loop-deleted forms of $HIV\text{-}1_{JR\text{-}FL}$ SOS gp140 have been described (57). In these constructs, the tripeptide GAG is used to replace V1 loop sequences (D133-K155) and V2 loop sequences (F159-I194), alone or in combination. The SOS $gp140_{UNC}$ protein contains the same cysteine substitutions that are present in SOS gp140, but the residues REKR at the gp120-$gp41_{ECTO}$ cleavage site have been replaced by the sequence IEGR, to prevent gp140 cleavage. Relative to the GenBank $HIV\text{-}1_{JR\text{-}FL}$ env sequence (accession no. AAB05604), the gp140 proteins contained a K668N substitution near the carboxy terminus of the molecules, consistent with the consensus subtype B sequence. The furin gene (71) was expressed from plasmid pcDNA3.1furin (4).

MAbs and CD4-based proteins

The following anti-gp120 monoclonal antibodies (MAbs) were used: IgG1b12 (against the CD4 binding site [7]), 2G12 (against a unique C3-V4 glycan-dependent epitope [75]), 17b (against a CD4-inducible epitope [70]), 19b (against the V3 loop [42]), and 23A (against the C5 region [41]). The anti-gp41 MAbs were 2F5 (against an epitope centered on the sequence ELDKWA [44, 48, 93]) and 2.2B (against epitope cluster II). MAbs IgG1b12, 2G12, and 2F5 are broadly neutralizing (74). MAb 17b weakly neutralizes diverse strains of HIV-1, more so in the presence of soluble CD4 (70), whereas the neutralizing activity of MAb 19b

against primary isolates is limited (73). MAbs 23A and 2.2B are nonneutralizing. Soluble CD4 (sCD4) and the CD4-based molecule CD4-IgG2 have been described elsewhere (1).

HIV-1 gp140 and gp120 glycoproteins

To create stable cell lines that secrete full-length HIV-1_{JR-FL} SOS gp140 or V1V2 SOS gp140, we cotransfected DXB-11 dihydrofolate reductase-negative Chinese hamster ovary (CHO) cells with pcDNA3.1furin and either pPPI4-SOS gp140 (4) or pPPI4-V1V2$_*$ SOS gp140 (57), respectively, using the calcium phosphate precipitation method. Doubly transformed cells were selected by passaging the cells in nucleoside-free -minimum essential medium containing 10% fetal bovine serum, Geneticin (Life Technologies, Rockville, Md.), and methotrexate (Sigma, St. Louis, Mo.). The cells were amplified for gp140 expression by stepwise increases in methotrexate concentration, as described elsewhere (1). Clones were selected for SOS gp140 expression, assembly, and endoproteolytic processing based on sodium dodecyl sulfate-polyacrylamide gel electrophoresis (SDS-PAGE) and Western blot analyses of culture supernatants. CHO cells expressing SOS $gp140_{UNC}$ were created using similar methods, except that pcDNA3.1furin and Geneticin were not used. Full-length SOS gp140 was purified from CHO cell culture supernatants by *Galanthus nivalis* lectin affinity chromatography (Sigma) and Superdex 200 gel filtration chromatography (Amersham-Pharmacia, Piscataway, N.J.), as described elsewhere (72). The $gp140_{UNC}$ glycoprotein was purified by lectin chromatography only. The concentration of purified Envs was measured by UV spectroscopy as described previously (61) and was corroborated by enzyme-linked immunosorbent assay and densitometric analysis of SDS-PAGE gels. Recombinant HIV-1_{JR-FL}, HIV-1_{LAI}, and HIV-1_{YU2} gp120 glycoproteins were produced using methods that have been previously described (72, 81). Where indicated, HIV-1 envelope glycoproteins were transiently expressed in adherent 293T cells by transfection with Env- and furin-expressing plasmids, as described previously (4). For radioimmunoprecipitation assays, the proteins were metabolically labeled with [^{35}S]cysteine and [^{35}S]methionine for 24 h prior to analysis.

SDS-PAGE, radioimmunoprecipitation, Blue Native PAGE, and Western blot analyses

SDS-PAGE analyses were performed as described elsewhere (4). Reduced and nonreduced samples were prepared by boiling for 2 min in Laemmli sample buffer (62.5 mM Tris-HCl [pH 6.8], 2% SDS, 25% glycerol, 0.01% bromophenol blue) in the presence or absence, respectively, of 50 mM dithiothreitol (DTT). Protein purity was determined by densitometric analysis of the stained gels followed by the use of ImageQuant software (Molecular Devices, Sunnyvale, Calif.). Radioimmunoprecipitation assays (RIPAs) were performed on Env-containing cell culture supernatants, as previously described (4, 57).

Blue Native (BN)-PAGE was carried out with minor modifications to the published method (62, 63). Thus, purified protein samples or cell culture supernatants were diluted with an equal volume of a buffer containing 100 mM 4-(*N*-morpholino)propane sulfonic acid (MOPS), 100 mM Tris-HCl, pH 7.7, 40% glycerol, 0.1% Coomassie blue, just prior to loading onto a 4 to 12% Bis-Tris NuPAGE gel

(Invitrogen). Typically, gel electrophoresis was performed for 2 h at 150V (0.07A) using 50 mM MOPS, 50 mM Tris, pH 7.7, 0.002% Coomassie blue as cathode buffer, and 50 mM MOPS, 50 mM Tris, pH 7.7 as anode buffer. When purified proteins were analyzed, the gel was destained with several changes of 50 mM MOPS, 50 mM Tris, pH 7.7 subsequent to the electrophoresis step. Typically, 5 µg of purified protein were loaded per lane.

For Western blot analyses, gels and polyvinylidene difluoride (PVDF) membranes were soaked for 10 min in transfer buffer (192 mM glycine, 25 mM Tris, 0.05% SDS [pH 8.8] containing 20% methanol). Following transfer, PVDF membranes were destained of Coomassie blue dye using 25% methanol and 10% acetic acid and air dried. Destained membranes were probed using the anti-V3 loop MAb PA1 (Progenics) followed by horseradish peroxidase-labeled anti-mouse immunoglobulin G (IgG) (Kirkegaard & Perry), each used at a final concentration of 0.2 µg/ml. Luminometric detection of the envelope glycoproteins was obtained with the Renaissance Western blot Chemiluminescence Reagent *Plus* system (Perkin-Elmer Life Sciences, Boston, Mass.). Bovine serum albumin (BSA), apoferritin, and thyroglobulin were obtained from Amersham Biosciences (Piscataway, N.J.) and used as molecular mass standards.

Matrix-assisted laser desorption ionization-time-of-flight (MALDI-TOF) mass spectrometry

Proteins were dialyzed overnight against water prior to analysis. Where indicated, SOS gp140 (1 mg/ml) was reduced with 10 mM DTT (Sigma), after which iodoacetamide (Sigma) was added to a final concentration of 100 mM, before dialysis. The samples were mixed with an equal volume of sinapinic acid matrix solution, dried at room temperature, and analyzed by MALDI-TOF mass spectrometry (37). MALDI-TOF mass spectra were acquired on a PerSeptive Biosystems Voyager-STR mass spectrometer with delayed extraction. Samples were irradiated with a nitrogen laser (Laser Science Inc.) operated at 337 nm. Ions produced in the sample target were accelerated with a deflection voltage of 30,000 V.

Sedimentation equilibrium analysis

Sedimentation equilibrium measurements were performed on a Beckman XL-A Optima analytical ultracentrifuge with an An-60 Ti rotor at 20°C. Protein samples were dialyzed overnight into run buffer (50 mM sodium phosphate, 150 mM NaCl [pH 7.0]) diluted to 0.15, 0.30, and 0.60 mg/ml and centrifuged in a six-sector cell at rotor speeds of 6,000 and 9,000 rpm. Data were acquired at two wavelengths per rotor speed and were fit using the program NONLIN to a single species model of the natural logarithm of the absorbance versus radial distance squared (29). Solvent density and protein partial specific volume were calculated according to solvent and protein composition, respectively (36).

Size exclusion chromatography

Purified, CHO cell-expressed SOS gp140, $gp140_{UNC}$, and gp120 proteins were analyzed by size exclusion chromatography on a TSK $G3000SW_{XL}$ high-performance liquid chromatography column (TosoHaas, Montgomeryville, Pa.) using phosphate-buffered saline as the running buffer. The protein retention time

was determined by monitoring the UV absorbance of the column effluent at a wavelength of 280 nm. The column was calibrated using ferritin as a model protein that exists in oligomeric states of 220, 440, and 880 kDa (24).

Surface plasmon resonance measurements

A Biacore X optical biosensor was used. Each MAb was immobilized at 8,000 to 10,000 resonance units by the amine coupling method to a CM5 sensor chip, according to the manufacturer's instructions (Biacore, Inc., Piscataway, N.J.). A reference surface (lacking antibody) was used as a background control. Binding experiments were performed at 25°C in HSB-EP buffer (10 mM HEPES [pH 7.4], 150 mM NaCl, 3 mM EDTA, 0.005% [vol/vol] Surfactant P20). Purified Envs (25 nM) were run over the test and control chips at a flow rate of 30 μl/min, whereas CHO cell culture supernatants (5 nM Env) were analyzed at 10 μl/min. To study the exposure of CD4-induced epitopes, sCD4 was added to the envelope glycoproteins at an 8-molar excess concentration for at least 1 h prior to analysis. The sensor surface was regenerated with a short pulse of 3.5 M $MgCl_2$.

Immunoelectron microscopy

Immunoelectron-microscopic analyses of SOS gp140 and gp120 alone and in complex with MAb, MAb fragments, and sCD4 were performed by negative staining with uranyl formate as previously described (55, 56). The samples were examined on a JEOL JEM CX-100 electron microscope and photographed at a magnification of 100,000 diameters.

Immune complex image digitalizing and averaging

The electron micrographs of immune complex images were digitalized on an AGFA (Ridgefield Park, N.J.) DUOSCAN T2500 negative scanner at a scanning resolution of 2,500 pixels per inch. Potentially informative complexes were selected and windowed as 256- by 256-pixel images. Approximately 500 randomly oriented examples of each complex combination were windowed, brought into alignment, and then averaged using the SPIDER software package (23). Windowed images were first normalized by scaling to adjust the image pixel values to a mean of 1. Complexes were then centered and masked for an alignment through classification (multiple references [multireference] alignment [23]). For this alignment procedure, the particles were first assigned to six classes using k-means clustering (23). The images in each class were then averaged, and the six class averages were taken as the multireference for the realignment of all of the original windowed complexes. Complexes with mirrored (inverted) orientation were automatically righted for averaging. The newly aligned complexes were then reclassified, and class averages were calculated as the new references. All of the complexes were then realigned based on the new multiple references. The classification and multireference alignment processes were repeated until no further improvement was evident.

For image subtraction comparisons, a threshold value was first applied to the averaged images. They were then manually aligned for best fit, and one image was subtracted from the other.

Molecular modeling

The SwissPDBviewer program (25) and Viewerlite software (Accelrys, Inc., San Diego, Calif.) were used to enhance the electron microscopy-based interpretations and to investigate the likely location of the gp41 domain in SOS gp140.

Results

Assembly and cleavage of purified SOS gp140

We have previously described the antigenic properties of unpurified HIV-1_{JR-FL} SOS gp140 proteins produced via transient transfection of 293T cells (4). To facilitate preparation of larger amounts of this protein for evaluation in purified form, we constructed a stable CHO cell line that expresses both SOS gp140 and human furin. Heterologous furin was expressed to facilitate efficient proteolytic processing of SOS gp140 (4).

The SOS gp140 protein was purified from CHO cell supernatants to >91% homogeneity as determined by SDS-PAGE and densitometric analysis of the nonreduced protein (Fig. 1, lane 8). Only minor amounts of free gp120 were present in the SOS gp140 preparation, indicating that the intersubunit disulfide bond remained substantially intact during purification. No high-molecular-mass SOS gp140 oligomers or aggregates were observed (Fig. 1, lane 8). Under nonreducing conditions, SOS gp140 migrated as a predominant 140-kDa band. The major contaminant was bovine alpha 2-macroglobulin, which migrates as a 170-kDa band on a reducing SDS-PAGE gel (Fig. 1, lane 3) and can be eliminated by adaptation of the CHO cell line to serum-free culture (unpublished results). Upon reduction with DTT, the purified SOS gp140 protein migrated as a predominant 120-kDa band, with a minor (14%) fraction of the 140-kDa band present (Fig. 1,

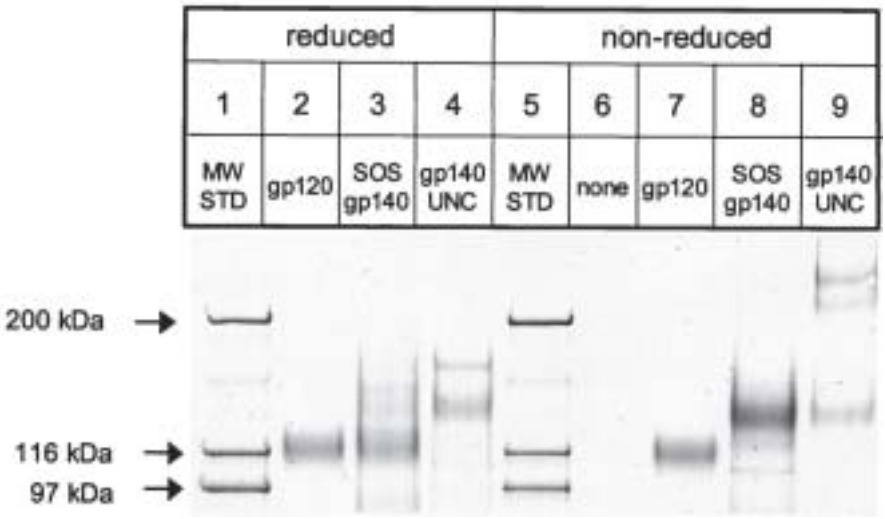

Fig. 1. SDS-PAGE analysis of purified HIV-1_{JR-FL} SOS gp140, $gp140_{UNC}$, and gp120 proteins. CHO cell-expressed proteins (0.5 µg) in Laemmli sample buffer with (reduced) or without (non-reduced) 50 mM DTT were resolved on a 3 to 8% polyacrylamide gradient gel.

lane 3). These data indicated that approximately 86% of the SOS gp140 protein was proteolytically processed.

The HIV-1_{JR-FL} $gp140_{UNC}$ protein was expressed in CHO cells using similar methods, although without cotransfected furin, and was also obtained at 90% purity. It too contained alpha 2-macroglobulin as the major contaminant, but no free gp120 was detectable (Fig. 1, lanes 4 and 9). In the absence of DTT, alpha 2-macroglobulin migrates as a 350-kDa dimer and is not clearly resolved from $gp140_{UNC}$ oligomers (Fig. 1, lane 9). Under nonreducing conditions, bands consistent with $gp140_{UNC}$ monomers (140 kDa), dimers (280 kDa), and trimers (420 kDa) were observed in roughly equal amounts (Fig. 1, lane 9). These proteins were reactive with anti-gp120 MAbs in Western blot analysis (data not shown). When treated with DTT, $gp140_{UNC}$ gave rise to an intensified monomer band at 140 kDa and an alpha 2-macroglobulin monomer band at 170 kDa; but gp140 oligomers were absent (Fig. 1, compare lanes 4 and 9). Thus, disulfide-linked, reducible oligomers comprise half or more of the $gp140_{UNC}$ preparation. Comparable amounts of reducible oligomers have been observed in $gp140_{UNC}$ protein preparations derived from subtype A, B, and E viruses, with minor strain-to-strain differences (46, 67). Reducible gp160 oligomers of this type have been proposed to contain aberrant intermolecular disulfide bonds (46). If so, at least some of the oligomers present in $gp140_{UNC}$ preparations represent misfolded protein aggregates.

Biophysical properties of purified SOS gp140

(i) Matrix-assisted laser desorption ionization mass spectrometry

This technique was used to determine the absolute molecular masses of HIV-1_{JR-FL} gp120 and SOS gp140. The measured molecular masses were 121.9 kDa for SOS gp140 and 91.3 kDa for gp120. Reduced SOS gp140 gave rise to a small peak of uncleaved gp140 at 118.5 kDa, a gp120 peak at 91.8 kDa, and a $gp41_{ECTO}$ peak at 27 kDa. Differences in glycosylation between cleaved and uncleaved SOS gp140 proteins could account for the 3.4-kDa difference in their measured masses. A difference of 0.5 kDa was observed in the mass of gp120 when expressed alone and in the context of SOS gp140. This difference is not significant but rather is within the range of assay variation for a heavily glycosylated protein. The measured mass of HIV-1_{JR-FL} gp120 is comparable to previously reported molecular masses of CHO cell-expressed HIV-1_{GB8} gp120 (91.8 kDa) and *Drosophila* cell-expressed HIV-1_{WD61} gp120 (99.6 kDa) (30, 45). The anomalously high molecular masses (120 and 140 kDa, respectively [Fig. 1]) observed for gp120 and SOS gp140 by SDS-PAGE reflect the high carbohydrate content of these proteins. The extended structure of the glycans and their poor reactivity with the dodecyl sulfate anion retard the electrophoretic migration of the glycoproteins through SDS-PAGE gel matrices (30).

(ii) Ultracentrifugation

Sedimentation equilibrium measurements were used to examine the oligomeric state of purified SOS gp140. Over protein concentrations ranging from 0.15 to 0.60 mg/ml, the apparent molecular mass of SOS gp140 was consistently found to be 155 kDa (Fig. 2A). Hence, the purified SOS gp140 protein is monomeric in solution. There was no systematic dependence of molecular mass on protein con-

centration over the range studied, since the molecular masses were all within 15% of those calculated for an ideal monomer. However, the residuals (the difference between the data and the theoretical curve for a monomer) deviated from zero in a systematic fashion (Fig. 2A), suggesting the presence of small amounts of oligomeric material. The difference in molecular masses observed using mass spectrometry (122 kDa) and sedimentation equilibrium (155 kDa) may reflect imprecisions in the latter technique. In particular, the uncertain composition of the SOS gp140 glycans introduces an error of this magnitude into calculations of the molecule's partial specific volume. However, this issue does not obscure our chief conclusion that the SOS gp140 protein is a monomer.

(iii) Analytical gel filtration chromatography

Purified HIV-$1_{JR\text{-}FL}$ SOS gp140, $gp140_{UNC}$, and gp120 proteins were also examined using size exclusion chromatography. Monomeric gp120 eluted with a retention time of 6.24 min and an apparent molecular mass of 200 kDa (Fig. 2B). The apparently large size of this protein reflects the extended structures of its carbohydrate moieties. The retention time (5.95 min) and apparent molecular mass (220 kDa) of the SOS gp140 protein are consistent with it being a monomer that is slightly larger than gp120. In contrast, the $gp140_{UNC}$ protein eluted at 4.91 min as a broad peak with an average molecular mass of >500 kDa, which is consistent with it comprising a mixture of oligomeric species. Although the chromatogram suggests the existence of multiple species in the $gp140_{UNC}$ preparation, this gel filtration technique cannot resolve mixtures of gp140 dimers, trimers, and tetramers.

(iv) Blue Native polyacrylamide gel electrophoresis

BN-PAGE was used to examine the oligomeric state of the purified SOS gp140 and $gp140_{UNC}$ proteins. In BN-PAGE, most proteins are fractionated according to their Stokes radius (62, 63). We first applied this technique to a model set of soluble proteins, including gp120 alone and in complex with sCD4 (Fig. 2C). The model proteins included thyroglobulin and ferritin, which naturally comprise a distribution of noncovalent oligomers of various sizes. The oligomeric states of these multisubunit proteins, as determined by BN-PAGE, are similar to those observed using other nondenaturing techniques (24, 77). BSA exists as monomers, dimers, and higher-order species in solution (35); the same ladder of oligomers was observed in BN-PAGE. Not surprisingly, the gp120/sCD4 complex, which has an association constant in the nanomolar range (1), remained intact during BN-PAGE analysis.

The purified SOS gp140 protein was largely monomeric by BN-PAGE (Fig. 2D), although a minor amount (<10%) of dimeric species was also observed. The purified $gp140_{UNC}$ protein migrated as well-resolved dimers, trimers, and tetramers, with trace amounts of monomer present (Fig. 2D). The $gp140_{UNC}$ dimer represented the major oligomeric form of the protein present under nondenaturing conditions. Although tetrameric $gp140_{UNC}$ is a distinct minor species on BN-PAGE gels (Fig. 2D), it is absent from nonreduced SDS-PAGE gels (Fig. 1). Upon treatment with SDS and heat, the $gp140_{UNC}$ tetramers probably revert to lower-molecular-weight species, such as monomers and/or disulfide-linked dimers. As expected, HIV-$1_{JR\text{-}FL}$ gp120 migrated as a predominant 120-kDa monomeric protein. BN-

PAGE analyses of unpurified gp140 proteins are described below (see Fig. 7).

Overall, ultracentrifugation, gel filtration, and BN-PAGE analyses were in excellent agreement as to the oligomeric states of these purified Env proteins. BN-PAGE, however, was the only method capable of clearly resolving the mixture of oligomeric species contained in the $gp140_{UNC}$ preparation.

Immunoelectron microscopy of SOS gp140.

(i) SOS gp140 and SOS gp140-MAb complexes

In the absence of antibodies, the electron micrographs revealed SOS gp140 to be mostly monomeric, randomly oriented, and multilobed (Fig 3A). Qualitatively similar images were obtained with HIV-1_{JR-FL} gp120 (data not shown), and the two proteins could not be clearly distinguished in the absence of MAbs or other means of orienting the images.

Electron micrographs were also obtained of SOS gp140 in complex with MAbs 2F5 (Fig. 3B), IgG1b12 (Fig. 3C), and 2G12 (Fig. 3D). To aid in interpretation, the complexes were masked and rotated such that the presumptive Fc of the MAb points downward. Schematic diagrams are also provided for each complex in order to illustrate the basic geometry and stoichiometry observed. In each case, the complexes shown represent the majority or plurality species present. However, other species, such as free MAb and monovalent MAb-SOS gp140 complexes, were also present in each sample (data not shown).

When combined with IgG1b12 or 2F5, SOS gp140 formed rather typical immune complexes composed of a single MAb and up to two SOS gp140s (Fig. 3B and C). The complexes adopted the characteristic Y-shaped antibody structure, with a variable angle between the Fab arms of the MAb. In contrast, the 2G12-SOS gp140 complexes produced strikingly different images (Fig. 3D). Y-shaped complexes comprising two distinct Fab arms with bound SOS gp140s were rare. Instead, the 2G12-SOS gp140 images were highly linear and appeared to represent one MAb bound to two SOS gp140 proteins aligned in parallel. Similar structures were observed less frequently for 2G12 in a complex with HIV-1_{JR-FL} gp120, but not with HIV-1_{YU2} gp120 (data not shown). We suspect that the parallel alignment of the SOS gp140s forces the two Fab arms into similar alignment, resulting in an overall linear structure. These complexes are unprecedented in our immunoelectron microscopy studies of Env-MAb complexes (55, 56, 92; K. H. Roux, unpublished observations). One hypothesis is that 2G12 binds to HIV-1_{JR-FL} gp120 and SOS gp140 in an orientation that promotes residual weak gp120-gp120 and/or gp41-gp41 interactions, which then stabilize the complex in the parallel configuration observed. Additional studies are ongoing to further explore this finding.

Combinations of these well-characterized MAbs were used to examine the relative placement of their epitopes on SOS gp140. In the first combination, SOS gp140-2F5-IgG1b12, multiple ring structures were observed which appeared to be composed of two SOS gp140 proteins bridged by two antibody molecules (data not shown). To distinguish between the 2F5 and IgG1b12 MAbs, we examined complexes formed between IgG1b12 $F(ab')_2$, SOS gp140, and the intact 2F5 MAb. Characteristic ring structures were again observed (Fig. 3E). The ring complexes were then subjected to computational analysis using the SPIDER program

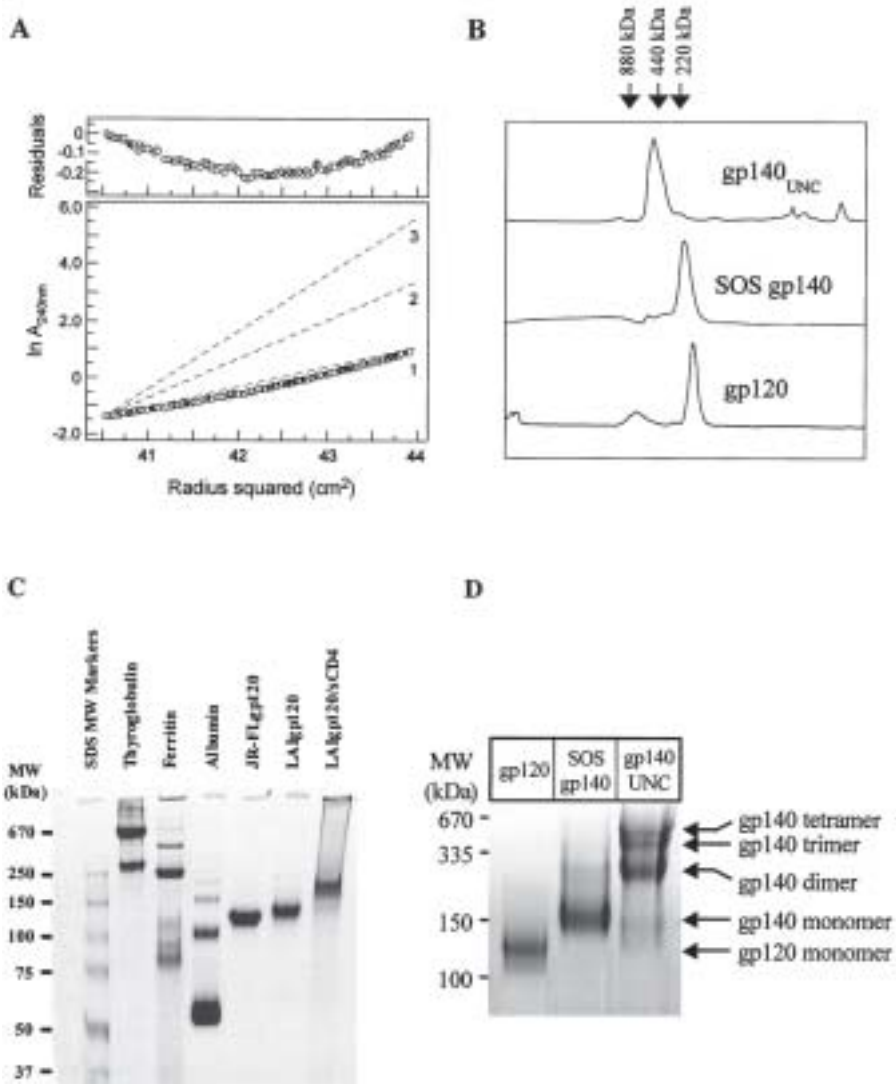

Fig. 2. Biophysical analyses of purified, CHO cell-expressed HIV-1_{JR-FL} envelope glycoproteins. **A.** Sedimentation equilibrium studies of SOS gp140 indicate that it is monomeric in solution. Representative data (open circles) obtained at a rotor speed of 9,000 rpm and a protein concentration of 0.6 mg/ml are plotted as ln(absorbance) versus the square of the axis of rotation. The slope is proportional to the molecular weight of the protein oligomer. Dashed lines with increasing slopes indicate, respectively, the predicted data for monomeric (1), dimeric (2), and trimeric (3) states of the protein. Deviations from the calculated values are plotted as residuals in the upper portion of the figure. **B.** Analytical size exclusion chromatography. Purified SOS gp140, $gp140_{UNC}$, and gp120 proteins were resolved on a TSK $G3000SW_{XL}$ column in phosphate-buffered saline, and their retention times were compared with those of known molecular mass (MW) standard proteins of 220, 440, and 880 kDa (arrowed). The main peak retention time of SOS gp140 (5.95 min) is consistent with it being a monomer that is slightly larger than monomeric gp120 (retention time, 6.24 min), whereas $gp140_{UNC}$ (retention time, 4.91 min) migrates as an oligomeric species. **C.** The oligomeric status of pure standard proteins, thyroglobulin, ferritin, and albumin, were compared with gp120 and gp120 in complex with soluble CD4 using BN-PAGE. The proteins were visualized on the gel using Coomassie blue. **D.** BN-PAGE analysis of CHO cell-derived, purified HIV-1_{JR-FL} gp120, SOS gp140, and $gp140_{UNC}$ glycoproteins.

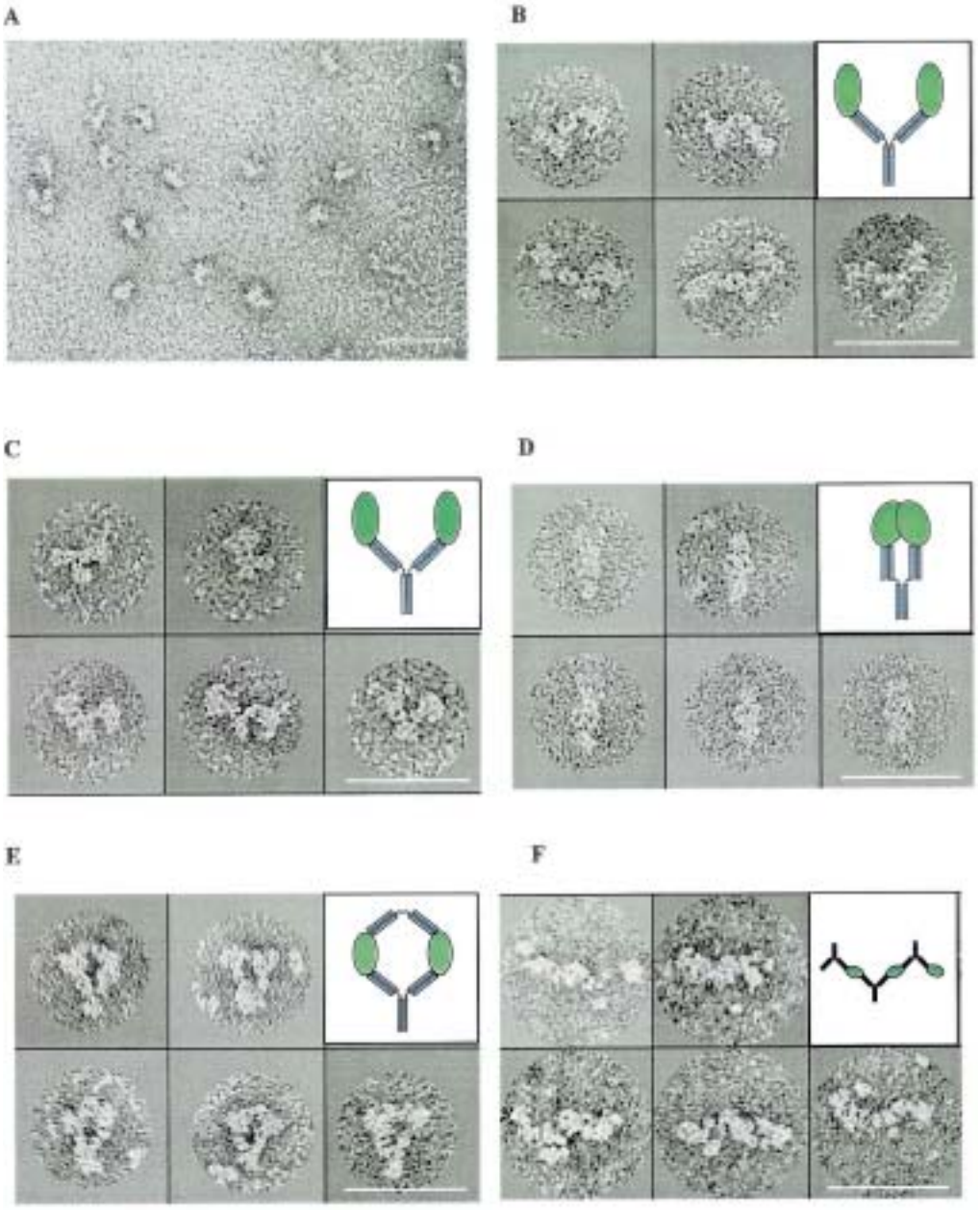

Fig. 3. Negative-stain electron micrographs of SOS gp140 alone (**A**) and in complex with MAbs (**B to F**). Bar, 40 nm. In panels B to F, the panels were masked and rotated so that the presumptive Fc of the MAb is oriented downward. When multiple MAbs were used, the presumptive Fc of MAb 2F5 is oriented downward. In panels B to F, interpretative diagrams are also provided to illustrate the basic geometry and stoichiometry of the immune complexes. SOS gp140, intact MAb, and F(ab)'$_2$ are illustrated by ovals, Y-shaped structures, and V-shaped structures, respectively, in the schematic diagrams, which are not drawn to scale. The MAbs used are as follows: 2F5 (B), IgG1b12 (C), 2G12 (D), MAb 2F5 plus F(ab')$_2$ IgG1b12 (E), and MAb 2F5 plus MAb 2G12 (F).

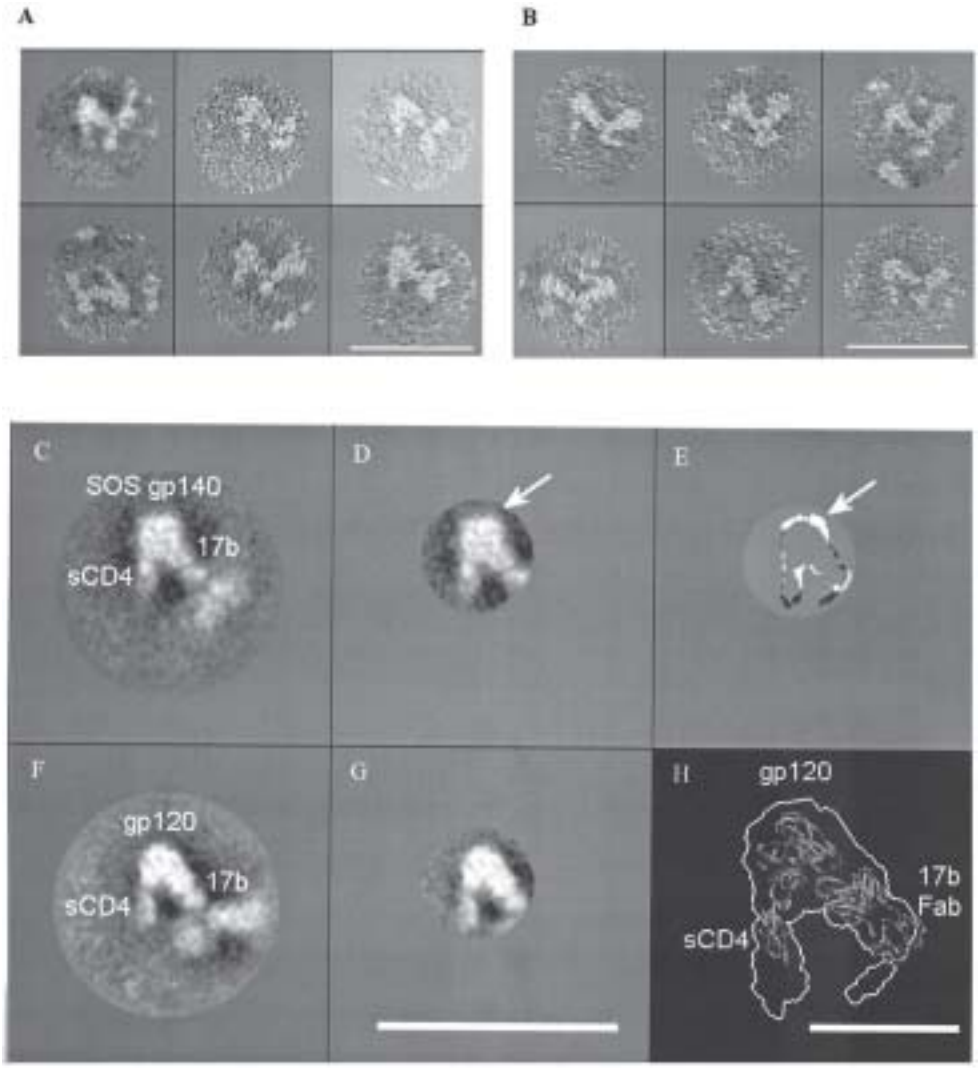

Fig. 4. Individual, averaged and subtracted electron micrographs of SOS gp140 and gp120 in complex with sCD4 and MAb 17b. Panels A and B are individual electron micrographs of ternary complexes of SOS gp140 (A) and YU2 gp120 (B). The Fc region of MAb 17b is aligned downward. Panels C and F are averaged electron micrographs of ternary complexes of SOS gp140 (C) and gp120 (F). Panels D and G are masked and averaged electron micrographs of the SOS gp140 complex (D) and the gp120 complex (G). Panel E represents the density remaining upon subtraction of the gp120 complex (G) from the gp140 complex (D). In panels D and E, the arrow indicates the area of greatest residual density, which represents the presumptive $gp41_{ECTO}$ moiety that is present in SOS gp140 but not in gp120. Panel H indicates the outline of the gp120 complex (G) overlaid upon a ribbon diagram of the X-ray crystal structure of the gp120 core in complex with sCD4 and the 17b Fab fragment (PDB code 1GC1) (33). The gp120 complex was enlarged to facilitate viewing. Bar, 40 nm (A to G) or 10 nm (H).

package to yield several categories of averaged images (data not shown). The MAb 2F5 and IgG1b12 $F(ab')_2$ components can be clearly delineated in the images, as can the SOS gp140 molecule. When bound to a given SOS gp140 mol-

ecule, the Fab arms of 2F5 and IgG1b12 lie at approximately right angles, as indicated in the schematic diagram (Fig. 3E).

In marked contrast to the IgG1b12-containing ternary complexes, those composed of SOS, 2F5, and 2G12 formed extended chains rather than closed rings (Fig. 3F). These observations place the 2F5 and 2G12 epitopes at opposite ends of the SOS gp140 molecule. There was significant heterogeneity in the stoichiometry of the 2F5/2G12/SOS gp140 complexes, just one example of which is indicated in the schematic diagram.

(ii) Immunoelectron microscopy of SOS gp140 and gp120 in complex with sCD4 and MAb 17b

In an effort to further characterize the topology of SOS gp140, we reacted it with MAb 17b and/or sCD4. We generated the corresponding YU2 gp120 complexes for comparison. As expected, the combination of MAb 17b plus SOS gp140 or gp120 alone did not form complexes, consistent with the need for sCD4 to induce the 17b epitope. Similarly, unremarkable complexes were obtained when sCD4 was mixed with SOS gp140 or gp120 in the absence of MAb 17b (data not shown). However, complexes with clearly defined geometry were obtained for sCD4/Env/17b (Fig. 4A and B).

These complexes were composed of 17b with one or two attached SOS gp140s or gp120s, together with tangentially protruding sCD4 molecules. These complexes were then subjected to computer-assisted averaging (Fig. 4C and F). The free arm and the Fc region of MAb 17b were disordered in these images due to the flexibility of the MAb, so the averaged images, based on multireference alignment (23), were masked to highlight the better-resolved sCD4, Env, and 17b Fab structures (Fig. 4D and G). The gp120 and SOS gp140 images were qualitatively similar, but an image subtraction of one from the other revealed the presence of additional mass on the SOS gp140 protein (arrowed in Fig. 4D and E). For this process, a threshold cutoff value was first applied to the averaged SOS gp140/sCD4/17b (Fig. 4D) and gp120/sCD4/17b (Fig. 4G) images. The two profiles were then manually aligned for best fit, and the image of the gp120 complex was subtracted from that of the SOS gp140 complex. This additional mass may represent $gp41_{ECTO}$, although we cannot strictly exclude other explanations, such as differences in the primary sequence and/or glycosylation of the gp120 and SOS gp140 proteins used. The resolution of the technique does not enable us to estimate the molecular weight of the additional mass. Moreover, a significant portion of the $gp41_{ECTO}$ moiety of SOS gp140 could reside "under" gp120 and thus be hidden in the image.

In order to orient the putative $gp41_{ECTO}$ moiety in relation to the remaining structures seen in the electron micrographs, the X-ray structure of the gp120 core in complex with the D1D2 domain of sCD4 and Fab 17b (33) was docked, using Program O, into the profile map obtained for the sCD4/gp120/MAb 17b complex (Fig. 4H). Given that there are differences in the gp120 (whole versus core) and CD4 (four-domain versus two-domain) molecules used for the electron microscopy and crystallization studies, there is reasonable agreement in the overall topology of the structures generated.

This agreement in structures (Fig. 4H) enabled us to position the putative $gp41_{ECTO}$ moiety in relation to the core gp120 structure (Fig. 5). The previously

defined neutralizing, nonneutralizing, and silent faces of gp120 (41, 83) are illustrated, as are the IgG1b12 (58) and 2G12 (83) epitopes. According to this model, the $gp41_{ECTO}$ moiety recognized by MAb 2F5 is located at 90° relative to the IgG1b12 epitope and 180° from the 2G12 epitope (Fig. 5B). This model is in broad agreement with the independently derived electron microscopy images of the complexes formed between SOS gp140 and combinations of these MAbs (Fig. 3E and F). This putative placement of $gp41_{ECTO}$ would cause it to largely occlude the nonneutralizing face of gp120, a result that is consistent with the MAb reactivity patterns observed for SOS gp140 both here and elsewhere (4).

Antigenic properties of unpurified SOS gp140 and $gp140_{UNC}$ proteins. (i) RIPAs

RIPA was used to determine whether the antigenicity of HIV-1_{JR-FL} SOS gp140 differed when the protein was expressed in stably transfected CHO cells from what was observed previously when the same protein was expressed in transiently transfected 293T cells (4). The SOS gp140 proteins in unpurified supernatants expressed from CHO cells were efficiently recognized by neutralizing agents to gp120 epitopes located in the C3/V4 region (MAb 2G12), the CD4 binding site (the CD4-IgG2 molecule), and the V3 loop (MAb 19b) (data not shown). In addition, the conserved CD4-induced neutralization epitope defined by MAb 17b was strongly induced on SOS gp140 by sCD4. SOS gp140 was also efficiently immunoprecipitated by the broadly neutralizing gp41 MAb 2F5. In contrast, SOS gp140 was largely unreactive with the nonneutralizing MAbs 23A and 2.2B to gp120 and gp41, respectively (data not shown). These findings are consistent with our previous observations (4) and indicate that CHO and 293T cell-derived HIV-1_{JR-FL} SOS gp140 proteins possess similar antigenic properties.

Relatively minor amounts of free gp120 were observed in the unpurified SOS gp140 CHO cell supernatants (data not shown), as reported previously for 293T-derived material (4). This free gp120 was preferentially recognized by MAb 23A, suggesting that its C5 epitope is largely obscured in SOS gp140 (data not shown). This is consistent with the electron microscopy-derived topology model described above (Fig. 5B) and with what is known about the gp120-gp41 interface (27, 41, 82). As with 293T-derived material (4), processing of SOS gp140 at the gp120-gp41 cleavage site was efficient in CHO cells, as determined by RIPAs performed under reducing and nonreducing conditions (data not shown). Similar levels of assembly and proteolytic processing were observed when unpurified SOS gp140 was analyzed by Western blotting rather than RIPA (data not shown). Thus, the folding, assembly, and processing of this protein appear to be largely independent of the cell line used for its production.

(ii) SPR assays

Surface plasmon resonance (SPR) was used to further characterize the antibody- and receptor-binding properties of unpurified, CHO cell-expressed SOS gp140 and $gp140_{UNC}$ proteins. A comparison of results obtained using SPR and RIPA with the same MAbs allows us to determine if the antigenicity of these proteins is method dependent. Whereas SPR is a kinetically limited procedure that is completed in one or more minutes, RIPA is an equilibrium method in which Env-MAb binding occurs over several hours. SPR analysis was also performed on purified

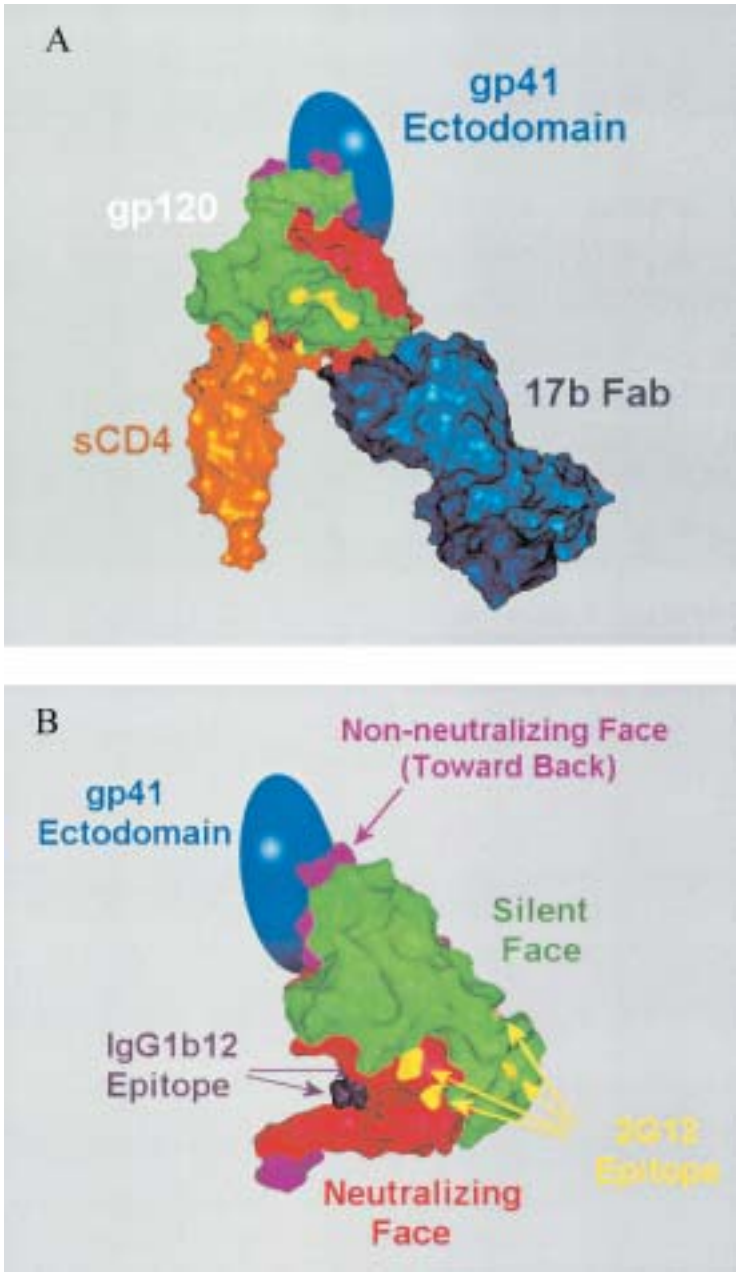

Fig. 5. Models indicating the approximate location of $gp41_{ECTO}$ in relation to gp120 as derived from electron microscopy data of SOS gp140. **A.** Presumptive location of $gp41_{ECTO}$ (represented by the blue oval) in relation to the X-ray crystal structure of the gp120 core (green, silent face; red, neutralizing face; lavender, nonneutralizing face [41, 83]) in complex with sCD4 (orange) and Fab 17b (dark blue) (PDB code 1GC1) (33). **B.** Surface rendering of the gp120 core with faces colored as above. Also indicated are the key residues of the IgG1b12 (58) (purple) and 2G12 (83) (yellow) epitopes. The image of the gp120 core in panel B is rotated 60° to the right about the vertical axis and 15° upward about the horizontal axis with respect to panel A.

and unpurified forms of the SOS gp140 and $gp140_{UNC}$ proteins, to assess whether protein antigenicity was significantly altered during purification. Purified $HIV\text{-}1_{JR\text{-}FL}$ gp120 was also studied. Although the purified SOS gp140 protein is a monomer, it does contain the gp120 subunit linked to the ectodomain of gp41. Since there is evidence that the presence of gp41 can affect the antigenic structure of gp120 (32, 53, 79), we thought it worth determining whether monomeric SOS gp140 behaved differently than monomeric gp120 in its interactions with neutralizing and non-neutralizing MAbs.

There was good concordance of results between RIPA- and SPR-based (Fig. 6) antigenicity analyses of unpurified SOS gp140 in CHO cell supernatants. For example, SOS gp140 bound the broadly neutralizing anti-gp41 MAb 2F5 (Fig. 6B) but not the nonneutralizing anti-gp41 MAb 2.2B (Fig. 6D). Similarly, binding of MAb 17b was strongly potentiated by sCD4 (Fig. 6F). Unpurified SOS gp140 bound the neutralizing anti-gp120 MAbs 2G12 and 19b but not the nonneutralizing anti-gp120 MAb 23A in both SPR and RIPA experiments (data not shown). Taken together, the RIPA and SPR data indicate that unpurified, CHO cell-derived SOS gp140 rapidly and avidly binds neutralizing anti-gp120 and anti-gp41 MAbs, whereas binding to the present set of nonneutralizing MAbs is not measurable by either technique.

SPR revealed some significant differences in the reactivities of SOS gp140 and $gp140_{UNC}$ proteins with anti-gp41 MAbs. Thus, SOS gp140 but not $gp140_{UNC}$ bound MAb 2F5 but not MAb 2.2B, whereas the converse was true for $gp140_{UNC}$. Notable, albeit less dramatic, differences were observed in the reactivity of SOS gp140 and $gp140_{UNC}$ with some anti-gp120 MAbs. Of the two proteins, SOS gp140 had the greater kinetics and magnitude of binding to the neutralizing MAbs IgG1b12 (Fig. 6G), 2G12 (Fig. 6H), and 17b in the presence of sCD4 (Fig. 6E and F). The binding of $gp140_{UNC}$ to 17b was clearly potentiated by sCD4, as has been reported elsewhere (90). Neither SOS gp140 nor $gp140_{UNC}$ bound the anti-gp120 MAb 23A (data not shown). This was expected for $gp140_{UNC}$, since the C5 amino-acid substitutions that eliminate the cleavage site directly affect the epitope for MAb 23A (43).

Qualitatively, the antigenicities of SOS gp140 and $gp140_{UNC}$ were little changed upon purification (Fig. 6, compare panels A, C, and E with panels B, D, and F). Hence the lectin affinity and gel filtration columns used for purification do not appear to significantly affect, or select for, a particular conformational state of these proteins. However, these studies do not allow for direct, quantitative comparisons of SPR data derived using purified and unpurified materials.

Compared with monomeric gp120, the purified $gp140_{UNC}$ protein reacted more strongly with MAb 2G12 but less strongly with MAb IgG1b12. Prior SPR studies have demonstrated that 2G12 avidly binds to oligomeric forms of Env (89), and it is possible that MAb 2G12 is capable of undergoing bivalent binding to oligomeric Envs. It will be informative to perform electron microscopy analyses of 2G12 in complex with $gp140_{UNC}$ or other oligomeric Envs in future studies, given the unusual nature of the 2G12-SOS gp140 complex (Fig. 3D).

Oligomeric properties of unpurified SOS gp140 and $gp140_{UNC}$ proteins

BN-PAGE was used to examine the oligomeric state of the SOS gp140 and $gp140_{UNC}$ proteins present in freshly prepared, CHO cell culture supernatants.

The SOS gp140 protein was largely monomeric by BN-PAGE, with only a minor proportion of higher-order proteins present (Fig. 7A). In some, but not all, 293T cell preparations, greater but highly variable amounts of dimers and higher-order oligomers were observed using BN-PAGE (data not shown, but see Fig. 7B). This probably accounts for our previous report that oligomers can be observed in unpurified SOS gp140 preparations using other techniques (4).

The unpurified $gp140_{UNC}$ protein typically migrated as well-resolved dimers, trimers, and tetramers, with trace amounts of monomer sometimes present (Fig. 7A). Qualitatively similar banding patterns were observed for purified (Fig. 2D) and unpurified (Fig. 7A) $gp140_{UNC}$ proteins. In each case, dimers of $gp140_{UNC}$ were the most abundant oligomeric species. HIV-1_{JR-FL} gp120 ran as a predominant 120-kDa monomeric band, although small amounts of gp120 dimers were observed in some unpurified supernatants. In general, the BN-PAGE analyses indicate that the oligomeric properties of the various Env proteins did not change appreciably upon purification (compare Fig. 7A and 2D).

The same CHO cell supernatants were also analyzed by analytical gel filtration, the column fractions being collected in 0.2-ml increments and analyzed for Env content by Western blotting. The retention times of unpurified gp120, SOS gp140, and $gp140_{UNC}$ proteins were determined to be 6.1, 5.9, and 5.2 min, respectively (data not shown). These values agree with those observed for the purified proteins (Fig. 2B) to within the precision of the method. The gel filtration studies thus corroborate the BN-PAGE data in that unpurified gp120 and SOS gp140 were mostly monomeric, while $gp140_{UNC}$ was mostly oligomeric (data not shown). However, unlike BN-PAGE, this analytical gel filtration procedure does not have sufficient resolving power to characterize the distribution of the oligomeric species present in the $gp140_{UNC}$ preparation.

SDS-PAGE followed by Western blot analyses of supernatants containing unpurified SOS gp140 and $gp140_{UNC}$ proteins yielded banding patterns similar to those shown in Fig. 1 for the purified proteins (data not shown). The gp120 preparation contained 10% dimer, which was observed only when SDS-PAGE analyses were carried out under nonreducing conditions. Thus, the gp120 dimer represents disulfide-linked and presumably misfolded material (46).

SOS gp140 glycoproteins with deletions of variable loops form more-stable oligomers

We previously described HIV-1_{JR-FL} SOS gp140 glycoproteins from which one or more of the gp120 variable loops were deleted to better expose underlying, conserved regions around the CD4- and coreceptor-binding sites. It was possible to remove the V1, V2, and V3 loop structures individually or in pairs without adversely affecting the formation of the intersubunit disulfide bond, proper proteolytic cleavage, or protein folding. However, the triple loop deletant was not efficiently cleaved (57). In order to explore the oligomeric properties of these modified SOS gp140 glycoproteins, the supernatants of 293T cells transiently cotransfected with these gp140 constructs and furin were analyzed by BN-PAGE. Unexpectedly, deletion of the variable loops, both alone and in combination, significantly enhanced the stability of the SOS gp140 oligomers. The V1V2 SOS gp140 preparation contained almost exclusively trimeric and tetrameric species,

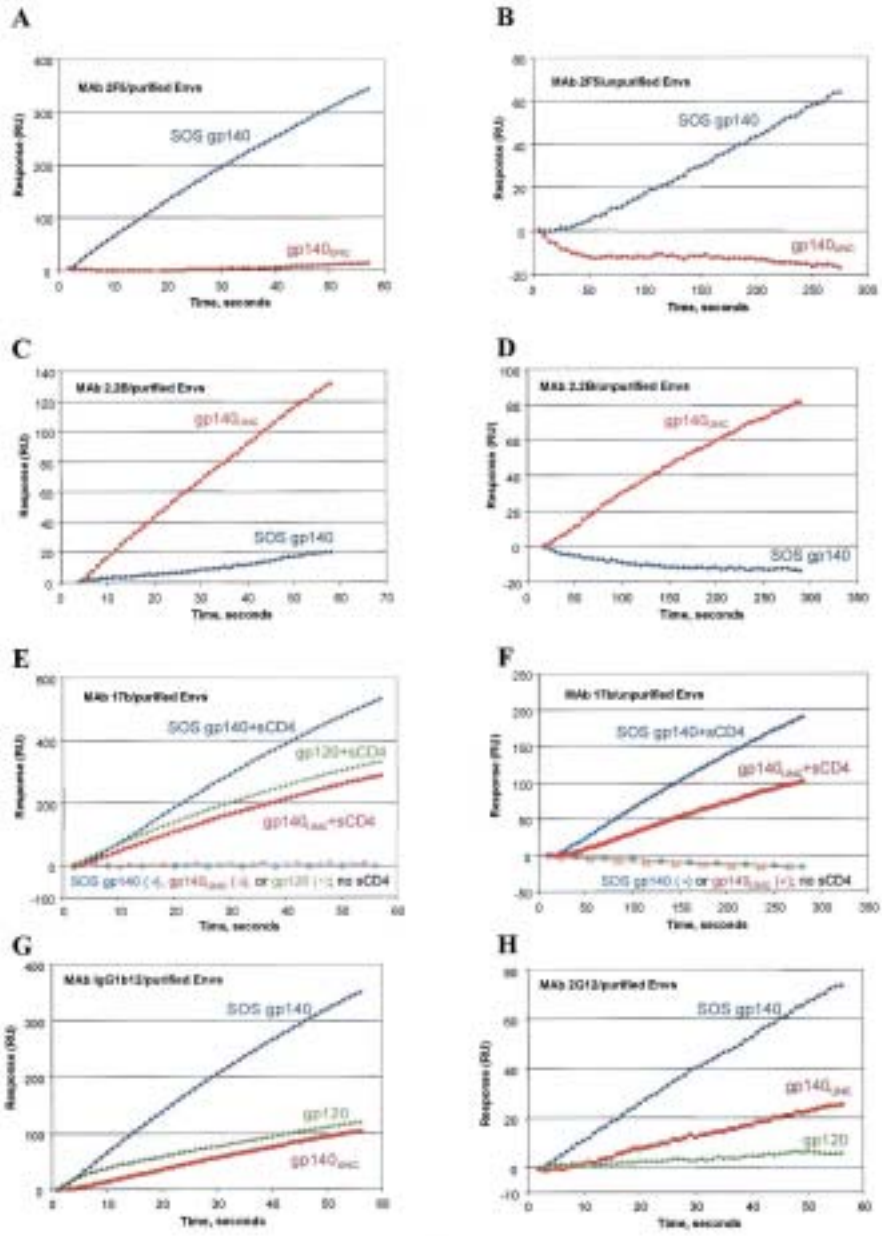

Fig. 6. SPR analysis of CHO cell-expressed HIV-$1_{JR\text{-}FL}$ SOS gp140, $gp140_{UNC}$, and gp120 proteins. Anti-gp120 and anti-gp41 MAbs were immobilized onto sensor chips and exposed to buffers containing the indicated gp120 or gp140 glycoproteins in either purified or unpurified form, as indicated. Where noted, Env proteins were mixed with an eightfold molar excess of sCD4 for 1 h prior to analysis. Culture supernatants from stably transfected CHO cells were used as the source of unpurified SOS gp140 and $gp140_{UNC}$ proteins. The concentrations of these proteins were measured by Western blotting and adjusted so that approximately equal amounts of each protein were loaded. Only the binding phases of the sensorgrams are shown; in general, the dissociation rates were too slow to provide meaningful information.

whereas V1 SOS gp140 formed a mixture of dimers, trimers, and tetramers similar to that seen with $gp140_{UNC}$ (data not shown). The V2 SOS gp140 protein was predominantly oligomeric, but it also contained significant quantities of monomer. Thus, in terms of oligomeric stability, the SOS proteins can be ranked as follows: first V1V2 SOS gp140, then V1 SOS gp140, then V2 SOS gp140, and then full-length SOS gp140. The reasons for this rank order are not yet clear but are under investigation.

Based on the above observations, we chose to generate a CHO cell line that stably expresses the V1V2 SOS gp140 protein. Supernatants from the optimized CHO cell line were first analyzed by SDS-PAGE under reducing and nonreducing conditions, followed by Western blot detection. The major Env band was seen at 120 kDa (V1V2 gp140 protein) in the nonreduced gel and at 100 kDa (V1V2 gp120 protein) in the reduced gel (data not shown). These results are consistent with our prior findings that deletion of the V1V2 loops decreases the apparent molecular mass of the protein by 20 kDa (57). Notably, the V1V2 SOS gp140 protein was largely free both of disulfide-linked aggregates and of the 100-kDa loop-deleted, free gp120 protein. Thus, proteolytic cleavage and SOS disulfide bond formation occur efficiently in the V1V2 SOS gp140 protein (data not shown).

CHO cell supernatants containing V1V2 SOS gp140, full-length SOS gp140, and $gp140_{UNC}$ were also analyzed by BN-PAGE and Western blotting (Fig. 7A). As was observed with the transiently transfected 293T cells, unpurified CHO cell-derived material was oligomeric. The CHO cell-derived V1V2 SOS gp140 migrated as a distinct single band with a molecular mass consistent with that of a trimer (360 kDa); the V1V2 SOS gp140 band lies between those of the $gp140_{UNC}$ dimer (280 kDa) and the $gp140_{UNC}$ trimer (420 kDa) (Fig. 7A). Hence the V1V2 SOS gp140 protein represents a proteolytically mature form of HIV-1 Env that oligomerizes into presumptive trimers via noncovalent interactions. Purification and additional biophysical studies of this protein are now in progress, and immunogenicity studies are planned.

The uncleaved SOS gp140 and gp140UNC proteins possess similar oligomeric properties

Overall, the above analyses reveal a clear difference in the oligomeric properties of the SOS gp140 and $gp140_{UNC}$ proteins. One structural difference between these proteins is their proteolytic cleavage status; another is the presence or absence of the intersubunit disulfide bond that defines SOS gp140 proteins. To address the question of whether it is gp120-gp41 cleavage or the introduced cysteine residues that destabilize the SOS gp140 oligomers, we made the SOS $gp140_{UNC}$ protein. Here, the cysteines capable of intersubunit disulfide bond formation are present, but the cleavage site between gp120 and $gp41_{ECTO}$ has also been modified to prevent cleavage. The SOS $gp140_{UNC}$, SOS gp140, and $gp140_{UNC}$ proteins were all expressed transiently in 293T cells and analyzed by BN-PAGE (Fig. 7B). In this and multiple repeat experiments, SOS $gp140_{UNC}$ and $gp140_{UNC}$ had similar migration patterns on the native gel, with the dimer band predominating and some monomers, trimers, and tetramers also present. In contrast, SOS gp140 was primarily monomeric, although small amounts of dimeric and trimeric species were also observed in this particular analysis (Fig. 7B).

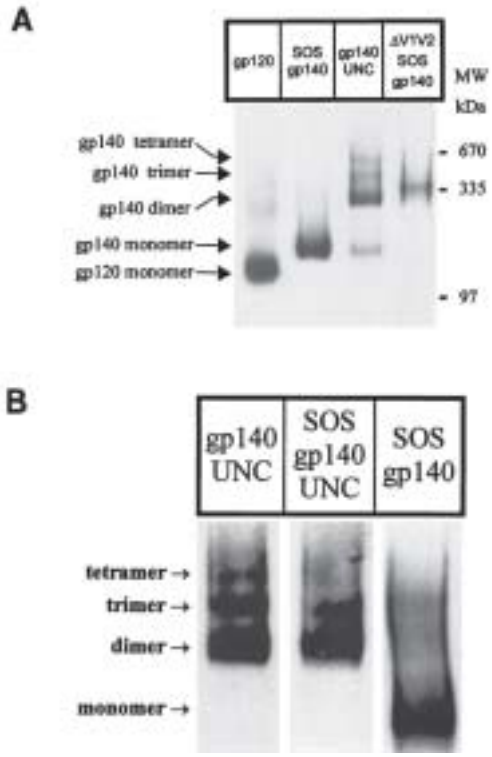

Fig. 7. BN-PAGE analyses of unfractionated cell culture supernatants. **A.** Comparison of HIV-1_{JR-FL} gp120, SOS gp140, $gp140_{UNC}$, and V1V2 SOS gp140 glycoproteins present in culture supernatants from stable CHO cell lines. **B.** Proteolytic cleavage destabilizes gp140 oligomers. 293T cells were transfected with furin and plasmids encoding SOS gp140, $gp140_{UNC}$, or SOS $gp140_{UNC}$. Cell culture supernatants were combined with MOPS buffer containing 0.1% Coomassie blue and resolved by BN-PAGE. Proteins were then transferred to PVDF membranes and visualized by Western blotting. Thyroglobulin and the BSA dimer were used as molecular mass (MW) markers (see Fig. 2C).

The above results suggest that the SOS $gp140_{UNC}$ protein behaves more like the $gp140_{UNC}$ protein than the SOS gp140 protein. This, in turn, implies that the cleavage of gp140 into gp120 and $gp41_{ECTO}$ has a substantial effect on how gp140 is oligomerized via interactions between the $gp41_{ECTO}$ moieties, whereas the presence of the cysteine substitutions in gp120 and gp41 has little effect on these interactions. We believe that this observation is central to understanding the relative instability of SOS gp140 oligomers, compared to those of the $gp140_{UNC}$ protein. We note, however, that we have not determined whether or not the intermolecular disulfide bond actually forms in SOS $gp140_{UNC}$; the simple method of DTT treatment to reduce this bond is inadequate, because the uncleaved peptide bond between the gp120 and $gp41_{ECTO}$ moieties still holds the two subunits together. Addressing this issue will require characterizing purified SOS $gp140_{UNC}$ by methods such as peptide mapping. Such studies are now in progress, to further explore the effect of gp140 cleavage on the structure of the gp120-$gp41_{ECTO}$ complex.

Discussion

We have previously described the antigenic properties of SOS gp140, an HIV-1 envelope glycoprotein variant in which an intermolecular disulfide bond has been introduced to covalently link the gp120 and $gp41_{ECTO}$ subunits (4, 57). In the original report, we demonstrated that the SOS gp140 protein, as contained in supernatants of transiently transfected 293T cells, was an antigenic mimic of virion-

associated Env (4). In that report, the methods employed were not sufficiently robust to conclusively determine the oligomeric state of unpurified 293T-derived SOS gp140 (4). Here we show with a smaller panel of MAbs that purified and unpurified CHO cell-derived SOS gp140 proteins also mimic native Env in terms of their patterns of antibody reactivity. However, unlike virus-associated Env, SOS gp140 is a monomeric protein.

Antigenicity and immunoelectron microscopy studies support a model for SOS gp140 in which the neutralizing face of gp120 is presented in a native conformation but the nonneutralizing face is occluded by $gp41_{ECTO}$ (Fig. 5). In one set of immunoelectron microscopy studies, SOS gp140 was examined in complex with combinations of anti-gp120 and anti-gp41 MAbs to defined epitopes (Fig. 3). The $gp41_{ECTO}$ subunit, as defined by the position of the anti-gp41 MAb 2F5, was located 180° from the MAb 2G12 epitope and 90° from the MAb IgG1b12 epitope, as is the nonneutralizing face. A second set of studies compared SOS gp140 and gp120 in complex with sCD4 and MAb 17b (Fig. 4). Here, a region of additional mass in the gp140 complex defined the presumptive $gp41_{ECTO}$; its location was similarly adjacent to the nonneutralizing face of gp120. This model of the geometry of the gp120-gp41 interaction is consistent with previous models based on mutagenesis techniques and the mapping of MAb epitopes (27, 41, 82). It also provides a basis for interpreting the patterns of MAb reactivity, as discussed below.

In the present report, the antigenicity of CHO-derived SOS gp140 was explored from a number of perspectives: (i) in comparison with $gp140_{UNC}$ and gp120, (ii) before and after purification, and (iii) in an equilibrium-based assay (RIPA) versus a kinetics-based assay (SPR). SOS gp140 proteins expressed in stably transfected CHO cells or transiently transfected 293T cells possessed qualitatively similar antigenic properties that were largely unaffected by purification. These analyses utilized a seven-member panel of MAbs and CD4-based proteins; it is possible that subtle antigenic differences could be discerned with additional MAbs or with peptides that target the amino- or carboxy-terminal heptad regions of gp41. We observed that most neutralizing anti-gp120 MAbs bound more strongly and more rapidly to SOS gp140 than to the gp120 or $gp140_{UNC}$ proteins, whereas the converse was true of nonneutralizing MAbs (Fig. 6). These results were largely independent of the analytical methodology used (RIPA or SPR) or the purification state of the glycoproteins and thus extend our earlier RIPA analyses of unpurified Env glycoproteins (4). We have addressed these issues on a largely qualitative basis in the present study; quantitative comparisons of MAb reactivities are now being explored.

It is not obvious why neutralizing MAbs recognize monomeric SOS gp140 better than monomeric gp120. One possibility relates to differences in the conformational freedom of the two glycoproteins. Monomeric gp120 has considerable conformational flexibility, such that "freezing" of the conformation by CD4 binding results in an unexpectedly large loss in entropy (45). Indeed, it has been suggested that reducing the conformational freedom of a gp120 immunogen may provide a means of generating broadly neutralizing antibodies, which generally recognize conformational epitopes (45). The presence of $gp41_{ECTO}$ may serve to minimize the conformational flexibility of the gp120 subunit of SOS gp140, stabilizing the protein in conformations recognized by neutralizing antibodies. However, the induc-

tion of 17b binding by sCD4 demonstrates that SOS gp140 is still capable of sampling multiple, relevant conformations. Studies are in progress to address these issues.

Variations in conformational flexibility may also underlie the antigenic differences observed between the SOS gp140 and $gp140_{UNC}$ proteins. Other possible explanations include differences in oligomerization and cleavage. Further studies using additional Env protein variants (e.g., SOS $gp140_{UNC}$), a broader range of anti-Env MAbs, and purified or size-fractionated proteins of a homogenous subunit composition will be required to explore these issues more thoroughly.

Standard biophysical techniques were used to demonstrate that the purified $HIV\text{-}1_{JR\text{-}FL}$ SOS gp140 glycoprotein is a monomer comprising one gp120 subunit that was disulfide linked to $gp41_{ECTO}$. Since it is generally accepted that the gp41 subunits are responsible for Env trimerization (8, 10, 38, 69, 78), we assume that the gp41-gp41 interactions within the cleaved SOS gp140 glycoprotein are weak, and that this instability precludes the purification of cleaved trimers. Others have reported that gp41-gp41 interactions are unstable in the context of gp140 (21, 85). Moreover, ultracentrifugation and nuclear magnetic resonance spectroscopy studies of the gp41 monomer-trimer equilibrium indicate that monomers are favored at concentrations of <3 μM (9, 80), which are comparable to the highest concentration of SOS gp140 attained in this report. The 1-mg/ml stock solution of purified SOS gp140 is approximately 7 μM, and the protein underwent further dilution during gel filtration, ultracentrifugation, and other biophysical analyses.

We also report the application of a rapid, simple, and high-resolution electrophoretic technique, BN-PAGE, for exploring the oligomeric state of HIV-1 envelope glycoproteins in unpurified as well as purified forms. In this technique, the proteins of interest are combined with the dye Coomassie blue, which binds to the exposed hydrophobic surfaces of proteins and usually enhances their solubility. In the presence of the dye, most proteins adopt a negative charge, migrate towards the anode in an electric field, and so can be sieved according to their Stokes radius in a polyacrylamide gradient gel. Whereas traditional native PAGE methods are typically performed under alkaline conditions (pH 9.5), BN-PAGE uses a physiological pH (pH 7.5), which is more compatible with protein stability. We demonstrate that a gp120/sCD4 complex and a variety of purified, oligomeric model proteins all remain associated during BN-PAGE analysis. When combined with Western blot detection, BN-PAGE can be used to determine the oligomeric state of HIV-1 envelope glycoproteins at all stages of purification. This high-resolution technique can resolve monomeric, dimeric, trimeric, and tetrameric forms of gp140.

As determined by BN-PAGE and other methods, the SOS gp140 protein was secreted in mostly monomeric form. In contrast, $gp140_{UNC}$ formed oligomers that are significantly more stable. Thus, we show that $HIV\text{-}1_{JR\text{-}FL}$ $gp140_{UNC}$ comprises a mixture of dimers, trimers, and tetramers, with dimers representing the major oligomeric form present under nondenaturing conditions. Although noncovalently associated oligomers constitute a significant percentage of the $gp140_{UNC}$ preparation, half or more of the material consists of disulfide-linked and presumably misfolded material (46). Others have made similar observations with uncleaved gp140 proteins from other HIV-1 strains and from simian immunodeficiency virus (11,

16-21, 28, 46, 54, 66, 67, 85-87). The question then arises as to why the SOS gp140 protein is a monomer but the uncleaved proteins are oligomeric. We believe that the cleavage of the gp120-gp41 peptide bond alters the overall conformation of the envelope glycoprotein complex, rendering it fusion competent but also destabilizing the association between the gp41 subunits. Support for this argument is provided by the evidence that the SOS $gp140_{UNC}$ protein resembles $gp140_{UNC}$ rather than SOS gp140; cleavage is clearly more important than the introduced cysteines in determining the oligomeric stability of gp140 proteins. We hypothesize that destabilization of gp41-gp41 interactions might be necessary for gp41-mediated fusion to occur efficiently upon activation of the Env complex by gp120-receptor interactions. Moreover, having cleavage and activation take place late in the synthetic process minimizes the risk of fusion events occurring prematurely, i.e., during intracellular transport of the envelope glycoprotein complex. Additional studies are in progress to explore the effect of cleavage on Env structure.

We can only speculate on the structure of $gp41_{ECTO}$ in SOS gp140. The strong reactivity of MAb 2F5 suggests that the C-terminal portion mimics the native, pre-fusion conformation, but there are few probes available for other portions of the native molecule. Clearly, $gp41_{ECTO}$ does not adopt a postfusion, coiled-coil conformation in the SOS gp140 monomer. It's not obvious how coiled-coil interactions are abrogated by a single cysteine substitution in an area outside the heptad repeat regions of gp41, but one possibility is that covalent attachment of gp120 at this "hinge" region of gp41 sterically prevents formation of intermediate or final intra- or intermolecular interactions that are required to achieve the coiled-coil state.

Taken together, the antigenic and biophysical data of SOS gp140, gp120, and $gp140_{UNC}$ suggest that SOS gp140 represents an improved yet clearly imperfect mimic of native Env. It is perhaps surprising that an SOS gp140 monomer mimics virus-associated Env in its reactivity with the present panel of MAbs. Immunochemical studies and the X-ray crystal structure of the gp120 core in complex with CD4 and MAb 17b have together defined the surface of gp120 in terms of neutralizing, nonneutralizing, and silent faces (33, 83). The data presented here and elsewhere (4) demonstrate the neutralizing face is readily accessible on SOS gp140, whereas the nonneutralizing face is not. There are still no immunologic ways to probe the exposure of the silent face of gp120 (41). A source of purified SOS gp140 glycoprotein, as described herein, will facilitate further studies of the antigenic structure of SOS gp140 in comparison with that of native Env.

Do $gp140_{UNC}$ proteins mimic the structure of the native, fusion-competent envelope glycoprotein complex on virions? We believe not, based on their exposure of nonneutralization epitopes in both gp120 and gp41 that are not accessible on the surface of native envelope glycoprotein complexes (4, 50, 61, 88). Similarly, the Env proteins of several other viruses undergo dramatic refolding upon cleavage as determined by electron microscopy and patterns of antibody reactivity (5, 15, 22, 26, 47, 64).

However, cleavage does not induce global conformational changes in all viral Envs. High-resolution crystal structures have been obtained for both cleaved and uncleaved forms of the influenza hemagglutinin protein, which is perhaps the best-characterized viral coat protein. Hemagglutinin cleavage induced mostly localized refolding and had little impact on the overall conformation of the molecule (12, 65).

Given that SOS gp140 is monomeric, what can be done to further stabilize the structure of fully cleaved, envelope glycoprotein complexes? The immunoelectron microscopy data of the 2G12/SOS gp140 complex suggest that appropriately directed antibodies could strengthen weak oligomeric interactions. The immunogenicity of such complexes may be worth testing, although a bivalent MAb might be expected to promote formation of Env dimers rather than trimers. We have already attempted to combine the SOS gp140 disulfide bond stabilization strategy with one in which the gp41 subunits were also stabilized by an intermolecular disulfide bond—this was unsuccessful, in that the mutated protein was poorly expressed and could not be cleaved into gp120 and gp41 subunits, even in the presence of cotransfected furin (R. W. Sanders et al., unpublished results). Similarly, adding GCN-4 domains onto the C terminus of gp41 hindered the proper cleavage of gp140 into gp120 and gp41 furin (Sanders et al., unpublished). Other approaches, based on site-directed mutagenesis of selected gp41 residues, are currently being evaluated.

Fortuitously, we have found that variable-loop-deleted forms of HIV-$1_{JR\text{-}FL}$ SOS gp140 form more-stable oligomers than their full-length counterparts. Thus, the SOS gp140 proteins lacking either the V1 or V2 variable loops contain a greater proportion of oligomers than the full-length protein, and the V1V2 double loop deletant is expressed primarily as noncovalently associated trimers. One hypothesis is that the extended and extensively glycosylated variable loops sterically impede the formation of stable gp41-gp41 interactions in the context of the full-length SOS gp140 protein. Indeed, using the crystal structure of the gp120/CD4/17b complex, Kwong et al. have developed a model of oligomeric gp120 that places V1V2 sequences at the trimer interface (34). The variable-loop-deleted SOS gp140 proteins may therefore represent proteolytically mature HIV-1 envelope glycoproteins that can perhaps eventually be produced and purified as oligomers. We previously demonstrated that unpurified forms of variable-loop-deleted SOS gp140 proteins possess favorable antigenic properties (57). These proteins are therefore worth further evaluation in structural and immunogenicity studies.

Acknowledgments

We thank Dennis Burton, Hermann Katinger, and James Robinson for the gifts of several MAbs. Additional MAbs were obtained through the AIDS Research and Reference Reagents Program. We thank Joseph Sodroski and Richard Wyatt for generously providing MAbs and recombinant HIV-1_{YU2} gp120 protein. This work was funded by NIH grants and contracts R01 AI39420, R01 AI42382, R01 AI45463, R21 AI44291, R21 AI49566, and U01 AI49764. J.P.M. is a Stavros S. Niarchos Scholar. The Department of Microbiology and Immunology at Weill Medical College gratefully acknowledges the support of the William Randolph Hearst Foundation.

References

1. **Allaway, G. P., K. L. Davis-Bruno, G. A. Beaudry, E. B. Garcia, E. L. Wong, A. M. Ryder, K. W. Hasel, M.-C. Gauduin, R. A. Koup, J. S. McDougal, and P. J. Maddon.** 1995. Expression and characterization of CD4-IgG2, a novel heterotetramer which neutralizes primary HIV-1 isolates. AIDS Res. Hum. Retrovir. **11:**533-539.
2. **Berman, P. W., T. J. Gregory, L. Riddle, G. R. Nakamura, M. A. Champe, J. P. Porter, F. M. Wurm, R. D. Hershberg, E. K. Cobb, and J. W. Eichberg.** 1990. Protection of chimpanzees from infection by HIV-1 after vaccination with recombinant glycoprotein gp120 but not gp160. Nature **345:**622-625.
3. **Berman, P. W., W. M. Nunes, and O. K. Haffar.** 1988. Expression of membrane-associated and secreted variants of gp160 of human immunodeficiency virus type 1 *in vitro* and in continuous cell lines. J. Virol. **62:**3135-3142.
4. **Binley, J. M., R. W. Sanders, B. Clas, N. Schuelke, A. Master, Y. Guo, F. Kajumo, D. J. Anselma, P. J. Maddon, W. C. Olson, and J. P. Moore.** 2000. A recombinant human immunodeficiency virus type 1 envelope glycoprotein complex stabilized by an intermolecular disulfide bond between the gp120 and gp41 subunits is an antigenic mimic of the trimeric virion-associated structure. J. Virol. **74:**627-643.
5. **Binley, J. M., R. W. Sanders, A. Master, C. S. Cayanan, C. L. Wiley, L. Schiffner, B. Travis, S. Kuhmann, D. R. Burton, S. L. Hu, W. C. Olson, and J. P. Moore.** 2002. Enhancing the proteolytic maturation of human immunodeficiency virus type 1 envelope glycoproteins. J. Virol. **76:**2606-2616.
6. **Burton, D. R., and D. C. Montefiori.** 1997. The antibody response in HIV-1 infection. AIDS **11**(Suppl. A)**:**S87-S98.
7. **Burton, D. R., J. Pyati, R. Koduri, S. J. Sharp, G. B. Thornton, P. W. H. I. Parren, L. S. Sawyer, R. M. Hendry, N. Dunlop, P. L. Nara, et al.** 1994. Efficient neutralization of primary isolates of HIV-1 by a recombinant human monoclonal antibody. Science **266:**1024-1027.
8. **Caffrey, M., M. Cai, J. Kaufman, S. J. Stahl, P. T. Wingfield, D. G. Covell, A. M. Gronenborn, and G. M. Clore.** 1998. Three-dimensional solution structure of the 44 kDa ectodomain of SIV gp41. EMBO J. **17:**4572-4584.
9. **Caffrey, M., J. Kaufman, S. Stahl, P. Wingfield, A. M. Gronenborn, and G. M. Clore.** 1999. Monomer-trimer equilibrium of the ectodomain of SIV gp41: insight into the mechanism of peptide inhibition of HIV infection. Protein Sci. **8:**1904-1907.
10. **Chan, D. C., D. Fass, J. M. Berger, and P. S. Kim.** 1997. Core structure of gp41 from the HIV envelope glycoprotein. Cell **89:**263-273.
11. **Chen, B., G. Zhou, M. Kim, Y. Chishti, R. E. Hussey, B. Ely, J. J. Skehel, E. L. Reinherz, S. C. Harrison, and D. C. Wiley.** 2000. Expression, purification, and characterization of gp160e, the soluble, trimeric ectodomain of the simian immunodeficiency virus envelope glycoprotein, gp160. J. Biol. Chem. **275:**34946-34953.
12. **Chen, J., K. H. Lee, D. A. Steinhauer, D. J. Stevens, J. J. Skehel, and D. C. Wiley.** 1998. Structure of the hemagglutinin precursor cleavage site, a determinant of influenza pathogenicity and the origin of the labile conformation. Cell **95:**409-417.
13. **Cherpelis, S., I. Shrivastava, A. Gettie, X. Jin, D. D. Ho, S. W. Barnett, and L. Stamatatos.** 2001. DNA vaccination with the human immunodeficiency virus type 1 SF162ÄV2 envelope elicits immune responses that offer partial protection from simian/human immunodeficiency virus infection to $CD8^+$ T-cell-depleted rhesus macaques. J. Virol. **75:**1547-1550.
14. **Doms, R. W., and J. P. Moore.** 2000. HIV-1 membrane fusion: targets of opportunity. J. Cell Biol. **151**:F9-F14.
15. **Dutch, R. E., R. N. Hagglund, M. A. Nagel, R. G. Paterson, and R. A. Lamb.** 2001. Paramyxovirus fusion (F) protein: a conformational change on cleavage activation. Virology **281:**138-150.
16. **Earl, P. L., C. C. Broder, R. W. Doms, and B. Moss.** 1997. Epitope map of human immunodeficiency virus type 1 gp41 derived from 47 monoclonal antibodies produced by immunization with oligomeric envelope protein. J. Virol. **71:**2674-2684.
17. **Earl, P. L., C. C. Broder, D. Long, S. A. Lee, J. Peterson, S. Chakrabarti, R. W. Doms, and B. Moss.** 1994. Native oligomeric human immunodeficiency virus type 1 envelope glycoprotein elicits diverse monoclonal antibody reactivities. J. Virol. **68:**3015-3026.

18. **Earl, P. L., R. W. Doms, and B. Moss.** 1990. Oligomeric structure of the human immunodeficiency virus type 1 envelope glycoprotein. Proc. Natl. Acad. Sci. USA **87:**648-652.
19. **Earl, P. L., W. Sugiura, D. C. Montefiori, C. C. Broder, S. A. Lee, C. Wild, J. Lifson, and B. Moss.** 2001. Immunogenicity and protective efficacy of oligomeric human immunodeficiency virus type 1 gp140. J. Virol. **75:**645-653.
20. **Edinger, A. L., M. Ahuja, T. Sung, K. C. Baxter, B. Haggarty, R. W. Doms, and J. A. Hoxie.** 2000. Characterization and epitope mapping of neutralizing monoclonal antibodies produced by immunization with oligomeric simian immunodeficiency virus envelope protein. J. Virol. **74:**7922-7935.
21. **Farzan, M., H. Choe, E. Desjardins, Y. Sun, J. Kuhn, J. Cao, D. Archambault, P. Kolchinsky, M. Koch, R. Wyatt, and J. Sodroski.** 1998. Stabilization of human immunodeficiency virus type 1 envelope glycoprotein trimers by disulfide bonds introduced into the gp41 glycoprotein ectodomain. J. Virol. **72:**7620-7625.
22. **Ferlenghi, I., B. Gowen, F. de Haas, E. J. Mancini, H. Garoff, M. Sjoberg, and S. D. Fuller.** 1998. The first step: activation of the Semliki Forest virus spike protein precursor causes a localized conformational change in the trimeric spike. J. Mol. Biol. **283:**71-81.
23. **Frank, J., M. Radermacher, P. Penczek, J. Zhu, Y. Li, M. Ladjadj, and A. Leith.** 1996. SPIDER and WEB: processing and visualization of images in 3D electron microscopy and related fields. J. Struct. Biol. **116:**190-199.
24. **Gerl, M., R. Jaenicke, J. M. Smith, and P. M. Harrison.** 1988. Self-assembly of apoferritin from horse spleen after reversible chemical modification with 2,3-dimethylmaleic anhydride. Biochemistry **27:**4089-4096.
25. **Guex, N., and M. C. Peitsch.** 1997. SWISS-MODEL and the Swiss-PdbViewer: an environment for comparative protein modeling. Electrophoresis **18:**2714-2723.
26. **Heinz, F. X., S. L. Allison, K. Stiasny, J. Schalich, H. Holzmann, C. W. Mandl, and C. Kunz.** 1995. Recombinant and virion-derived soluble and particulate immunogens for vaccination against tick-borne encephalitis. Vaccine **13:**1636-1642.
27. **Helseth, E., U. Olshevsky, C. Furman, and J. Sodroski.** 1991. Human immunodeficiency virus type 1 gp120 envelope glycoprotein regions important for association with the gp41 transmembrane glycoprotein. J. Virol. **65:**2119-2123.
28. **Hoffman, T. L., G. Canziani, L. Jia, J. Rucker, and R. W. Doms.** 2000. A biosensor assay for studying ligand-membrane receptor interactions: binding of antibodies and HIV-1 Env to chemokine receptors. Proc. Natl. Acad. Sci. USA **97:**11215-11220.
29. **Johnson, M. L., J. J. Correia, D. A. Yphantis, and H. R. Halvorson.** 1981. Analysis of data from the analytical ultracentrifuge by nonlinear least-squares techniques. Biophys. J. **36:**575-588.
30. **Jones, D. H., B. W. McBride, M. A. Roff, and G. H. Farrar.** 1995. Efficient purification and rigorous characterisation of a recombinant gp120 for HIV vaccine studies. Vaccine **13:**991-999.
30. **Jones, P. L., T. Korte, and R. Blumenthal.** 1998. Conformational changes in cell surface HIV-1 envelope glycoproteins are triggered by cooperation between cell surface CD4 and co-receptors. J. Biol. Chem. **273:**404-409.
32. **Klasse, P. J., J. A. McKeating, M. Schutten, M. S. Reitz, Jr., and M. Robert-Guroff.** 1993. An immune-selected point mutation in the transmembrane protein of human immunodeficiency virus type 1 (HXB2-Env:Ala 582(Thr)) decreases viral neutralization by monoclonal antibodies to the CD4-binding site. Virology **196:**332-337.
33. **Kwong, P. D., R. Wyatt, J. Robinson, R. W. Sweet, J. Sodroski, and W. A. Hendrickson.** 1998. Structure of an HIV gp120 envelope glycoprotein in complex with the CD4 receptor and a neutralizing human antibody. Nature **393:**648-659.
34. **Kwong, P. D., R. Wyatt, Q. J. Sattentau, J. Sodroski, and W. A. Hendrickson.** 2000. Oligomeric modeling and electrostatic analysis of the gp120 envelope glycoprotein of human immunodeficiency virus. J. Virol. **74:**1961-1972.
35. **Lambin, P., D. Rochu, N. Herance, and J. M. Fine.** 1982. High molecular-weight polymers in human albumin solutions. Quantitative determination by polyacrylamide gradient electrophoresis. Rev. Fr. Transfus. Immunohematol. **25:**487-498.
36. **Laue, T. M., B. D. Shah, T. M. Ridgeway, and S. L. Pelletier.** 1992. Computer-aided interpretation of analytical sedimentation data for proteins, p. 90-125. *In* S. E. Harding, A. J. Rowe, and J. C. Horton (ed.), Analytical ultracentrifugation in biochemistry and polymer science. Royal

Society of Chemistry, Cambridge, United Kingdom.
37. **Lewis, J. K., M. Bendahmane, T. J. Smith, R. N. Beachy, and G. Siuzdak.** 1998. Identification of viral mutants by mass spectrometry. Proc. Natl. Acad. Sci. USA **95:**8596-8601.
38. **Lu, M., S. C. Blacklow, and P. S. Kim.** 1995. A trimeric structural domain of the HIV-1 transmembrane glycoprotein. Nat. Struct. Biol. **2:**1075-1082.
39. **Melikyan, G. B., R. M. Markosyan, H. Hemmati, M. K. Delmedico, D. M. Lambert, and F. S. Cohen.** 2000. Evidence that the transition of HIV-1 gp41 into a six-helix bundle, not the bundle configuration, induces membrane fusion. J. Cell Biol. **151:**413-423.
40. **Moore, J. P., and D. D. Ho.** 1995. HIV-1 neutralization: the consequences of viral adaptation to growth on transformed T cells. AIDS **9**(Suppl. A)**:**S117-S136.
41. **Moore, J. P., and J. Sodroski.** 1996. Antibody cross-competition analysis of the human immunodeficiency virus type 1 gp120 exterior envelope glycoprotein. J. Virol. **70:**1863-1872.
42. **Moore, J. P., A. Trkola, B. Korber, L. J. Boots, J. A. Kessler, F. E. McCutchan, J. Mascola, D. D. Ho, J. Robinson, and A. J. Conley.** 1995. A human monoclonal antibody to a complex epitope in the V3 region of gp120 of human immunodeficiency virus type 1 has broad reactivity within and outside clade B. J. Virol. **69:**122-130.
43. **Moore, J. P., R. L. Willey, G. K. Lewis, J. Robinson, and J. Sodroski.** 1994. Immunological evidence for interactions between the first, second, and fifth conserved domains of the gp120 surface glycoprotein of human immunodeficiency virus type 1. J. Virol. **68:**6836-6847.
44. **Muster, T., F. Steindl, M. Purtscher, A. Trkola, A. Klima, G. Himmler, F. Ruker, and H. Katinger.** 1993. A conserved neutralizing epitope on gp41 of human immunodeficiency virus type 1. J. Virol. **67:**6642-6647.
45. **Myszka, D. G., R. W. Sweet, P. Hensley, M. Brigham-Burke, P. D. Kwong, W. A. Hendrickson, R. Wyatt, J. Sodroski, and M. L. Doyle.** 2000. Energetics of the HIV gp120-CD4 binding reaction. Proc. Natl. Acad. Sci. USA **97:**9026-9031.
46. **Owens, R. J., and R. W. Compans.** 1999. The human immunodeficiency virus type 1 envelope glycoprotein precursor acquires aberrant intermolecular disulfide bonds that may prevent normal proteolytic processing. Virology **179:**827-833.
47. **Paredes, A. M., H. Heidner, P. Thuman-Commike, B. V. Prasad, R. E. Johnston, and W. Chiu.** 1998. Structural localization of the E3 glycoprotein in attenuated Sindbis virus mutants. J. Virol. **72:**1534-1541.
48. **Parker, C. E., L. J. Deterding, C. Hager-Braun, J. M. Binley, N. Schülke, H. Katinger, J. P. Moore, and K. B. Tomer.** 2001. Fine definition of the epitope on the gp41 glycoprotein of human immunodeficiency virus type 1 for the neutralizing antibody, 2F5. J. Virol. **75:**10906-10911.
49. **Parren, P. W. H. I., and D. R. Burton.** 2001. The antiviral activity of antibodies *in vitro* and *in vivo*. Adv. Immunol. **77:**195-262.
50. **Parren, P. W. H. I., P. Fisicaro, A. F. Labrijn, J. M. Binley, W. P. Yang, H. J. Ditzel, C. F. Barbas, III, and D. R. Burton.** 1996. *In vitro* antigen challenge of human antibody libraries for vaccine evaluation: the human immunodeficiency virus type 1 envelope. J. Virol. **70:**9046-9050.
51. **Parren, P. W. H. I., J. P. Moore, D. R. Burton, and Q. J. Sattentau.** 1999. The neutralizing antibody response to HIV-1: viral evasion and escape from humoral immunity. AIDS **13**(Suppl. A)**:**S137-S162.
52. **Poignard, P., E. O. Saphire, P. W. H. I. Parren, and D. R. Burton.** 2001. gp120: biologic aspects of structural features. Annu. Rev. Immunol. **19:**253-274.
53. **Reitz, M. S. J., C. Wilson, C. Naugle, R. C. Gallo, and M. Robert-Guroff.** 1988. Generation of a neutralization-resistant variant of HIV-1 is due to selection for a point mutation in the envelope gene. Cell **54:**57-63.
54. **Richardson, T. M. J., B. L. Stryjewski, C. C. Broder, J. A. Hoxie, J. R. Mascola, P. L. Earl, and R. W. Doms.** 1996. Humoral response to oligomeric human immunodeficiency virus type 1 envelope protein. J. Virol. **70:**753-762.
55. **Roux, K. H.** 1989. Immunoelectron microscopy of idiotype-anti-idiotype complexes. Methods Enzymol. **178:**130-144.
56. **Roux, K. H.** 1996. Negative-stain immunoelectron-microscopic analysis of small macromolecules of immunologic significance. Methods **10:**247-256.
57. **Sanders, R. W., L. Schiffner, A. Master, F. Kajumo, Y. Guo, T. Dragic, J. P. Moore, and J. M. Binley.** 2000. Variable-loop-deleted variants of the human immunodeficiency virus type 1 enve-

lope glycoprotein can be stabilized by an intermolecular disulfide bond between the gp120 and gp41 subunits. J. Virol. **74:**5091-5100.

58. **Saphire, E. O., P. W. H. I. Parren, R. Pantophlet, M. B. Zwick, G. M. Morris, P. M. Rudd, R. A. Dwek, R. L. Stanfield, D. R. Burton, and I. A. Wilson.** 2001. Crystal structure of a neutralizing human IgG against HIV-1: a template for vaccine design. Science **293:**1155-1159.
29. **Sattentau, Q. J., and J. P. Moore.** 1991. Conformational changes induced in the human immunodeficiency virus envelope glycoprotein by soluble CD4 binding. J. Exp. Med. **174:**407-415.
60. **Sattentau, Q. J., S. Zolla-Pazner, and P. Poignard.** 1995. Epitope exposure on functional, oligomeric HIV-1 gp41 molecules. Virology **206:**713-717.
61. **Scandella, C. J., J. Kilpatrick, W. Lidster, C. Parker, J. P. Moore, G. K. Moore, K. A. Mann, P. Brown, S. Coates, and B. Chapman.** 1993. Nonaffinity purification of recombinant gp120 for use in AIDS vaccine development. AIDS Res. Hum. Retrovir. **9:**1233-1244.
62. **Schägger, H., W. A. Cramer, and G. von Jagow.** 1994. Analysis of molecular masses and oligomeric states of protein complexes by blue native electrophoresis and isolation of membrane protein complexes by two-dimensional native electrophoresis. Anal. Biochem. **217:**220-230.
63. **Schägger, H., and G. von Jagow.** 1991. Blue native electrophoresis for isolation of membrane protein complexes in enzymatically active form. Anal. Biochem. **199:**223-231.
64. **Schalich, J., S. L. Allison, K. Stiasny, C. W. Mandl, C. Kunz, and F. X. Heinz.** 1996. Recombinant subviral particles from tick-borne encephalitis virus are fusogenic and provide a model system for studying flavivirus envelope glycoprotein functions. J. Virol. **70:**4549-4557.
65. **Skehel, J. J., and D. C. Wiley.** 2000. Receptor binding and membrane fusion in virus entry: the influenza hemagglutinin. Annu. Rev. Biochem. **69:**531-569.
66. **Stamatatos, L., M. Lim, and C. Cheng-Mayer.** 2000. Generation and structural analysis of soluble oligomeric gp140 envelope proteins derived from neutralization-resistant and neutralization-susceptible primary HIV type 1 isolates. AIDS Res. Hum. Retrovir. **16:**981-994.
67. **Staropoli, I., C. Chanel, M. Girard, and R. Altmeyer.** 2000. Processing, stability, and receptor binding properties of oligomeric envelope glycoprotein from a primary HIV-1 isolate. J. Biol. Chem. **275:**35137-35145.
68. **Sullivan, N., Y. Sun, Q. Sattentau, M. Thali, D. Wu, G. Denisova, J. Gershoni, J. Robinson, J. Moore, and J. Sodroski.** 1998. CD4-induced conformational changes in the human immunodeficiency virus type 1 gp120 glycoprotein: consequences for virus entry and neutralization. J. Virol. **72:**4694-4703.
69. **Tan, K., J. Liu, J. Wang, S. Shen, and M. Lu.** 1997. Atomic structure of a thermostable subdomain of HIV-1 gp41. Proc. Natl. Acad. Sci. USA **94:**12303-12308.
70. **Thali, M., J. P. Moore, C. Furman, M. Charles, D. D. Ho, J. Robinson, and J. Sodroski.** 1993. Characterization of conserved human immunodeficiency virus type 1 gp120 neutralization epitopes exposed upon gp120-CD4 binding. J. Virol. **67:**3978-3988.
71. **Thomas, G., B. A. Thorne, L. Thomas, R. G. Allen, D. E. Hruby, R. Fuller, and J. Thorner.** 1988. Yeast KEX2 endopeptidase correctly cleaves a neuroendocrine prohormone in mammalian cells. Science **241:**226-230.
72. **Trkola, A., T. Dragic, J. Arthos, J. M. Binley, W. C. Olson, G. P. Allaway, C. Cheng-Mayer, J. Robinson, P. J. Maddon, and J. P. Moore.** 1996. CD4-dependent, antibody-sensitive interactions between HIV-1 and its co-receptor CCR-5. Nature **384:**184-187.
73. **Trkola, A., T. Ketas, V. N. KewalRamani, F. Endorf, J. M. Binley, H. Katinger, J. Robinson, D. R. Littman, and J. P. Moore.** 1998. Neutralization sensitivity of human immunodeficiency virus type 1 primary isolates to antibodies and CD4-based reagents is independent of coreceptor usage. J. Virol. **72:**1876-1885.
74. **Trkola, A., A. P. Pomales, H. Yuan, B. Korber, P. J. Maddon, G. P. Allaway, H. Katinger, C. F. Barbas, D. R. Burton, D. D. Ho, and J. P. Moore.** 1995. Cross-clade neutralization of primary isolates of human immunodeficiency virus type 1 by human monoclonal antibodies and tetrameric CD4-IgG2. J. Virol. **69:**6609-6617.
75. **Trkola, A., M. Purtscher, T. Muster, C. Ballaun, A. Buchacher, N. Sullivan, K. Srinivasan, J. Sodroski, J. P. Moore, and H. Katinger.** 1996. Human monoclonal antibody 2G12 defines a distinctive neutralization epitope on the gp120 glycoprotein of human immunodeficiency virus type 1. J. Virol. **70:**1100-1108.
76. **VanCott, T. C., J. R. Mascola, R. W. Kaminski, V. Kalyanaraman, P. L. Hallberg, P. R. Bur-**

nett, J. T. Ulrich, D. J. Rechtman, and D. L. Birx. 1997. Antibodies with specificity to native gp120 and neutralization activity against primary human immunodeficiency virus type 1 isolates elicited by immunization with oligomeric gp160. J. Virol. **71:**4319-4330.

77. **Venkatesh, S. G., and V. Deshpande.** 1999. A comparative review of the structure and biosynthesis of thyroglobulin. Comp. Biochem. Physiol. C. Pharmacol. Toxicol. Endocrinol. **122:**13-20.
78. **Weissenhorn, W., A. Dessen, S. C. Harrison, J. J. Skehel, and D. C. Wiley.** 1997. Atomic structure of the ectodomain from HIV-1 gp41. Nature **387:**426-430.
79. **Wilson, C., M. S. J. Reitz, K. Aldrich, P. J. Klasse, J. Blomberg, R. C. Gallo, and M. Robert-Guroff.** 1990. The site of an immune-selected point mutation in the transmembrane protein of human immunodeficiency virus type 1 does not constitute the neutralization epitope. J. Virol. **64:**3240-3248.
80. **Wingfield, P. T., S. J. Stahl, J. Kaufman, A. Zlotnick, C. C. Hyde, A. M. Gronenborn, and G. M. Clore.** 1997. The extracellular domain of immunodeficiency virus gp41 protein: expression in Escherichia coli, purification, and crystallization. Protein Sci. **6:**1653-1660.
81. **Wu, L., N. P. Gerard, R. Wyatt, H. Choe, C. Parolin, N. Ruffing, A. Borsetti, A. A. Cardoso, E. Desjardin, W. Newman, C. Gerard, and J. Sodroski.** 1996. CD4-induced interaction of primary HIV-1 gp120 glycoproteins with the chemokine receptor CCR-5. Nature **384:**179-183.
82. **Wyatt, R., E. Desjardin, U. Olshevsky, C. Nixon, J. Binley, V. Olshevsky, and J. Sodroski.** 1997. Analysis of the interaction of the human immunodeficiency virus type 1 gp120 envelope glycoprotein with the gp41 transmembrane glycoprotein. J. Virol. **71:**9722-9731.
83. **Wyatt, R., P. D. Kwong, E. Desjardins, R. W. Sweet, J. Robinson, W. A. Hendrickson, and J. G. Sodroski.** 1998. The antigenic structure of the HIV gp120 envelope glycoprotein. Nature **393:**705-711.
84. **Wyatt, R., and J. Sodroski.** 1998. The HIV-1 envelope glycoproteins: fusogens, antigens, and immunogens. Science **280:**1884-1888.
85. **Yang, X., M. Farzan, R. Wyatt, and J. Sodroski.** 2000. Characterization of stable, soluble trimers containing complete ectodomains of human immunodeficiency virus type 1 envelope glycoproteins. J. Virol. **74:**5716-5725.
86. **Yang, X., L. Florin, M. Farzan, P. Kolchinsky, P. D. Kwong, J. Sodroski, and R. Wyatt.** 2000. Modifications that stabilize human immunodeficiency virus envelope glycoprotein trimers in solution. J. Virol. **74:**4746-4754.
87. **Yang, X., R. Wyatt, and J. Sodroski.** 2001. Improved elicitation of neutralizing antibodies against primary human immunodeficiency viruses by soluble stabilized envelope glycoprotein trimers. J. Virol. **75:**1165-1171.
88. **York, J., K. E. Follis, M. Trahey, P. N. Nyambi, S. Zolla-Pazner, and J. H. Nunberg.** 2001. Antibody binding and neutralization of primary and T-cell line-adapted isolates of human immunodeficiency virus type 1. J. Virol. **75:**2741-2752.
89. **Zeder-Lutz, G., J. Hoebeke, and M. H. Van Regenmortel.** 2001. Differential recognition of epitopes present on monomeric and oligomeric forms of gp160 glycoprotein of human immunodeficiency virus type 1 by human monoclonal antibodies. Eur. J. Biochem. **268:**2856-2866.
90. **Zhang, C. W., Y. Chishti, R. E. Hussey, and E. L. Reinherz.** 2001. Expression, purification, and characterization of recombinant HIV gp140. The gp41 ectodomain of HIV or simian immunodeficiency virus is sufficient to maintain the retroviral envelope glycoprotein as a trimer. J. Biol. Chem. **276:**39577-39585.
91. **Zhang, W., G. Canziani, C. Plugariu, R. Wyatt, J. Sodroski, R. Sweet, P. Kwong, W. Hendrickson, and I. Chaiken.** 1999. Conformational changes of gp120 in epitopes near the CCR5 binding site are induced by CD4 and a CD4 miniprotein mimetic. Biochemistry **38:**9405-9416.
92. **Zhu, P., W. C. Olson, and K. H. Roux.** 2001. Structural flexibility and functional valency of CD4-IgG2 (PRO 542): potential for crosslinking HIV-1 envelope spikes. J. Virol. **75:**6682-6686.
93. **Zwick, M. B., A. F. Labrijn, M. Wang, C. Spenlehauer, E. O. Saphire, J. M. Binley, J. P. Moore, G. Stiegler, H. Katinger, D. R. Burton, and P. W. H. I. Parren.** 2001. Broadly neutralizing antibodies targeted to the membrane-proximal external region of human immunodeficiency virus type 1 glycoprotein gp41. J. Virol. **75:**10892-10905.

Chapter 5.4

Evolution of the HIV-1 envelope glycoproteins with a disulfide bond between gp120 and gp41

(Submitted for publication)

Rogier W. Sanders[1,2], Martijn M. Dankers[1], Els Busser[1], Michael Caffrey[3], John P. Moore[2], Ben Berkhout[1]

[1]Dept. of Human Retrovirology, Academic Medical Center, University of Amsterdam, 1105 AZ Amsterdam, The Netherlands
[2]Dept. of Microbiology and Immunology, Weill Medical College of Cornell University, 1300 York Ave., New York, NY 1002, USA
[3]Dept. of Biochemistry and Molecular Biology, University of Illinois at Chicago, Chicago, IL 60612, USA

We previously described the construction of an HIV-1 envelope glycoprotein complex (Env) that is stabilized by an engineered intermolecular disulfide bond (SOS) between gp120 and gp41. The modified Env protein antigenically mimics the functional wild-type Env complex. An HIV-1 molecular clone containing the SOS Env gene was only minimally replication competent, suggesting that the engineered disulfide bond substantially impaired Env function. However, virus evolution occurred in cell culture infections, and it eventually always led to elimination of the intermolecular disulfide bond. In the course of these evolution studies, we identified additional and unusual second-site reversions within gp41. These evolution paths highlight residues that play an important role in the interaction between gp120 and gp41.

Introduction

The trimeric HIV-1 envelope glycoprotein complex (Env) mediates viral entry into susceptible target cells. The surface subunit (SU; gp120) attaches to the receptor (CD4) and the coreceptor (CCR5 or CXCR4) on the cell surface, and subsequent conformational changes within the Env complex lead to membrane fusion mediated by the transmembrane subunit (TM; gp41) (10,13,14,51). After intracellular cleavage of the precursor gp160 protein, three gp120 subunits stay non-covalently associated with three gp41 subunits. However, these non-covalent interactions are weak and gp120 dissociates easily from gp41, a process that, if it occurs spontaneously and prematurely, inactivates the Env complex and leads to the exposure of non-neutralizing, immune-decoy epitopes on both gp120 and gp41 (29-31). HIV-1 vaccine strategies aimed at generating neutralizing antibodies have yielded various Env immunogens that have gp120 stably attached to gp41, usually by elimination of the natural cleavage site between gp120 and gp41. Uncleaved Env proteins, however, like the dissociated subunits, expose non-neutralizing epitopes (4,29-31,38).

We previously described the construction of a soluble Env variant that is stabilized by the introduction of an intermolecular disulfide bond between gp120 and the gp41 ectodomain (gp41e) (4,41). This SOS gp140 protein is cleaved and it is antigenically similar to native Env. Thus, neutralizing epitopes are exposed while several non-neutralizing epitopes, which are also not accessible on the functional Env complex, are occluded. The SOS gp140 protein is conformationally flexible in that CD4 can induce conformational changes that expose the coreceptor binding site. Moreover, SOS Env can be rendered fully functional by reduction of the intermolecular disulfide bond upon the engagement of CD4 and a coreceptor (1,3).

Stabilization of the native Env complex by disulfide bond linkage is likely to impose constraints on Env function because a certain degree of flexibility is probably essential for Env to undergo the conformational changes that eventually lead to fusion of the viral and cellular membranes. The gp120 – gp41 interface is considered to be structurally flexible, so constraining its motion might have adverse effects (37). For example, the conformational changes in gp120 that are induced by receptor and coreceptor binding might not be transduced to the gp41 fusion machinery because of the engineered disulfide bond between the two subunits. In addition, appropriately timed gp120 shedding may be necessary for receptor-mediated fusion, and this step is blocked by the SOS disulfide bond bridge. We have investigated whether HIV-1 would be able to accept the engineered disulfide bond by spontaneous adaptation and optimization during evolution in cell culture. This exercise could learn us more about the interaction between gp120 and gp41. Identifying compensatory mutations that would accommodate the SOS disulfide bond in a replicating virus might also be useful for the design of improved Env immunogens.

Materials and Methods

Plasmid Constructs

The plasmid pRS1, generated to subclone mutant *env* genes, was generated as follows. First, the SalI-BamHI fragment from a molecular clone of HIV-1_{LAI} (pLAI) (32) was cloned into pUC18 (Roche, Indianapolis, IN). A PstI-StuI fragment from the resulting plasmid was then cloned into a pBS-SK(+)-gp160 plasmid with the SalI-XhoI sequences of pLAI. Mutations were introduced in pRS1 using the Quickchange mutagenesis kit (Stratagene, La Jolla, CA) and verified by DNA sequencing. Mutant *env* genes in pRS1 were cloned into pLAI as SalI-BamHI fragments. The numbering of individual amino-acids is based on the HIV-1_{HXB2} gp160 sequence.

Cells and transfection

SupT1 T cells and C33A cervix carcinoma cells were maintained in RPMI 1640 medium and Dulbecco's modified eagle's medium (DMEM), respectively (Life Technologies Ltd., Paisley, UK), supplemented with 10% fetal calf serum (FCS), penicillin (100 U/ml) and streptomycin (100 µg/ml) as previously described (39). SupT1 and C33A cells were transfected with pLAI constructs by electroporation and $Ca_2(PO_4)_3$ precipitation, respectively, as described elsewhere (11).

Viruses and infection

Virus stocks were produced by transfecting C33A cells with the appropriate pLAI constructs. The virus containing supernatant was harvested 3 days post-transfection, filtered and stored at -80ºC. The virus concentration was quantified by capsid CA-p24 ELISA as described previously (18). The resulting values were used to normalize the amount of virus in subsequent infection experiments, which were performed as follows. T cells (3.75×10^5) were infected with 1.5 ng CA-p24 of HIV-1_{LAI} (produced in C33A cells) per well of a 24-well plate. Subsequent virus spread was monitored by CA-p24 ELISA for 14 days.

Virus evolution

For evolution experiments, 5×10^6 SupT1 cells were transfected with 40 µg pLAI by electroporation. The cultures were inspected regularly for the emergence of revertant viruses, using CA-p24 ELISA and/or the appearance of syncytia as indicators of virus replication. At regular intervals, cells and filtered supernatant were stored at -80ºC and virus was quantitated by CA-p24 ELISA. When a revertant virus was identified, DNA was extracted from infected cells (12), then proviral *env* sequences were PCR-amplified and sequenced. The complete *env* genes of the proviral DNA of cultures X, X3 and X4 were sequenced. Only the C5 region and gp41 were sequenced in subsequent evolution experiments.

Ultracentrifugation of virions

C33A cells were transfected with 40 µg pLAI per T75 flask. Medium was refreshed at day one post-transfection. The culture supernatant was harvested at 3 days post-transfection, centrifuged to remove cells and passed through a 0.45 µm filter to remove residual cells and debris. Cells were resuspended in 1.0 ml of lysis buffer (50mM Tris (pH 7.4), 10mM EDTA, 100mM NaCl, 1% SDS). Virus particles were pelleted from the supernatant by ultracentrifugation (100,000 x *g* for 45 min at 4°C) and resuspended in 0.5 ml lysis buffer. The virus-free supernatant, containing shed gp120, was concentrated using an Amicon centrifugal filter unit (Millipore, Bedford, MA), then SDS was added to a final concentration of 1%.

Quantitation of gp120 by ELISA

The gp120 contents of cell, virion and supernatant fractions were measured as described previously but with some modifications (26,42). ELISA plates were coated overnight with sheep antibody D7324 (10 µg/ml in 0.1 M $NaHCO_3$; Aalto Bioreagents, Rathfarnham, Dublin, Ireland), which is directed to the gp120 C5 region. After blocking by 2% milk in Tris-buffered saline (TBS) for 30 min, gp120 was captured by incubation for 2 h at room temperature. Recombinant HIV-1_{LAI} gp120 (Progenics Pharmaceuticals, Inc. Tarrytown, NY) was used as a reference standard. Unbound gp120 was washed away with TBS and purified HIV-1^+ serum Ig (HIVIg) was added for 1.5 h in 2% milk, 20% sheep serum (SS), 0.5% Tween. HIVIg binding was detected with alkaline phosphatase conjugated goat anti-human Fc (1:10000, Jackson Immunoresearch, West Grove, PA) in 2% milk, 20% SS, 0.5% Tween. Detection of alkaline phosphatase activity was performed using AMPAK (DAKO, Carpinteria, CA). The measured gp120 contents

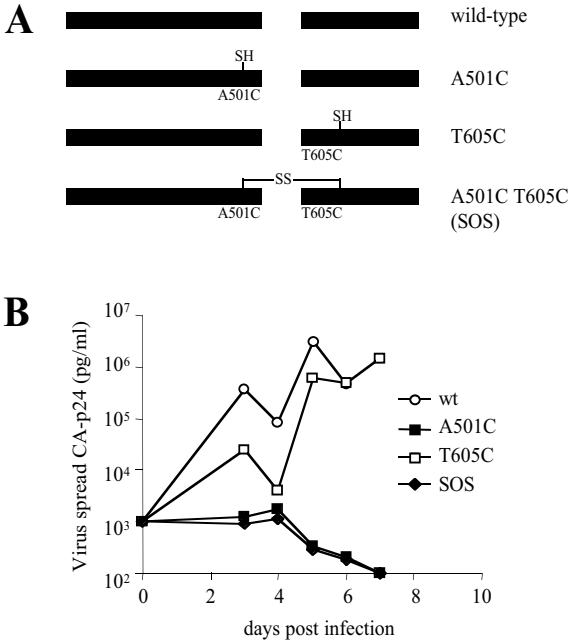

Fig. 1. HIV-1_{LAI} with an SOS-linked Env is replication-defective. **A.** Schematic representation of the A501C and T605C single and double (SOS) mutants used in this study. Free cysteines with a sulfhydryl group are indicated by SH and an intermolecular disulfide bond between gp120 and gp41 is indicated by SS. **B.** 375x10^3 MT-2 T cells were infected with 1.5 ng CA-p24 of C33A-produced virus and virus spread was monitored for 7 days by CA-p24 ELISA.

of cells, virus and supernatant were corrected for the CA-p24 content of the respective fractions. The resulting gp120/p24 ratios of the wild-type (wt) virus were arbitrarily set at 1.0 for each fraction and the corresponding ratios of the mutant and revertant viruses were calculated.

Results

Replication of HIV-1 mutants with cysteine substitutions in gp120 and gp41

We investigated the replication potential of HIV-1 containing cysteine substitutions that are able to form an intersubunit disulfide bond between gp120 and gp41. The A501C and T605C substitutions alone or in combination (SOS Env) were introduced into the molecular clone of the CXCR4-using strain HIV-1_{LAI} (Fig. 1A). Virus stocks were generated in non-susceptible C33A producer cells by transient transfection. The three mutant viruses and the wild-type (wt) parent all produced comparable amounts of CA-p24 antigen (results not shown). The virus stocks were then used to infect MT-2 T cells (Fig. 1B). The SOS virus was not able to initiate a spreading infection and the A501C single mutant was also replication-defective. In contrast and perhaps surprisingly, the T605C single mutant replicated efficiently, albeit with delayed kinetics compared to the wt control. Similar results were obtained using the SupT1 T cell line (results not shown). We conclude that the SOS Env protein does not support virus replication, consistent with previous studies using a cell-cell fusion assay or Env-pseudotyped viruses in a single-cycle infection protocol (1,3).

Evolution of HIV-1 with a disulfide bond between gp120 and gp41

To investigate the structural constraints imposed upon the SOS Env protein by the engineered disulfide bond and to identify viruses with potentially interesting second-site reversions, we passaged several virus cultures for a prolonged period (table 1, cultures A-C). One culture containing the A501C virus was also maintained for many weeks (table 1, culture D). Despite these efforts, we were unable to obtain any revertants of the two replication-impaired mutant viruses, underlining the deleterious effect of the intermolecular disulfide bond and the A501C single substitution on Env function. We therefore revised our experimental design by varying the cell type and increasing the amount of the transfected plasmid DNA. We also added low concentrations of β-mercaptoethanol (BME) to some of the cultures, reasoning that this reducing agent may reduce the SOS disulfide bond, thereby increasing the fusion capacity of SOS Env and virus evolution (1,3). We first determined the concentrations of BME that are toxic for MT-2 and SupT1 cells. At 0.3 mM, BME marginally impaired the growth of both cell types, so we did not exceed this concentration. The various cultures are listed in table 1. The evolution experiments were started by transfecting 5 x 10^6 cells with 10 or 40 μg of the SOS Env molecular clone. The cells were cultured in small (T25) flasks for 7 days and subsequently transferred to large (T75) flasks to increase the probability of detecting a rare evolution event.

The SOS Env virus acquires compensatory second-site reversions

After 7 weeks of culture, we detected virus spread, as measured by CA-p24 production, in one of the 15 cultures (culture X in table 1). This culture contained MT-2 cells grown with 0.3 mM BME. To investigate whether replication of the evolved virus was triggered by or even dependent on the reducing agent, we passaged the variant onto fresh MT-2 cells in the absence or presence of BME (Fig. 2). The evolved virus replicated poorly, but spread more efficiently without BME. This suggests that BME was not required for Env function and the toxicity of this compound may actually have hindered virus replication. Nevertheless, it remains possible that the initial evolution event itself was facilitated by BME, for instance by triggering entry of the original input SOS virus into cells.

Proviral DNA was isolated from the positive culture X after 7 weeks and the *env* gene was PCR-amplified. Sequencing of the viral quasispecies revealed that the original SOS cysteine substitutions were still present. Two additional reversions were found: L593Q in the gp41 loop 12 residues upstream of the introduced A605C SOS cysteine, and T719I in the gp41 intracytoplasmic tail (Fig. 3A).

Prolonged evolution leads to elimination of the SOS disulfide bond

The slowly replicating virus present in culture X (SOS-X) was used to initiate two new infections that were continued for another two months to monitor additional evolution events (cultures X3 and X4). Consistent with a further improvement of their fitness, the resulting viruses replicated faster than the original SOS-X virus, as monitored by the rate of appearance of syncytia and CA-p24 antigen production. The *env* genes were PCR-amplified from proviral DNA and sequenced (Fig. 3A). In both cultures, the SOS cysteine at position 605 had been replaced by a tyrosine, thus eliminating the intersubunit disulfide bond. Note that

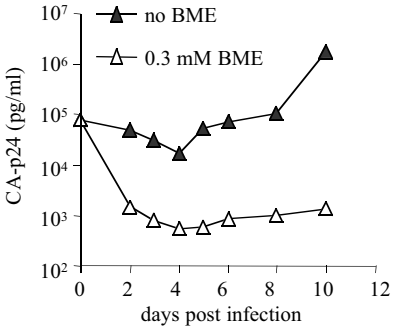

Fig. 2. Replication of the evolved SOS revertant virus in the absence and presence of reducing agent. 100 µl (78 ng CA-p24) of the cell-free culture supernatant of culture X (see the text) was passaged onto 5x10^6 fresh MT-2 T cells in the presence or absence of 0.3 mM BME and virus spread was measured for 10 days.

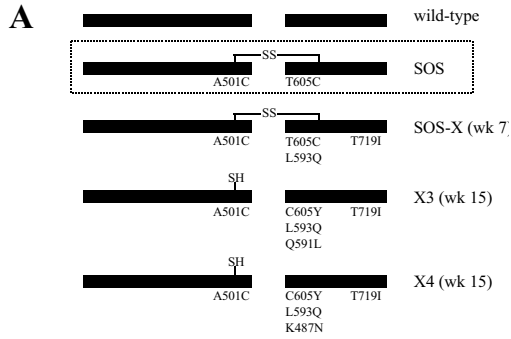

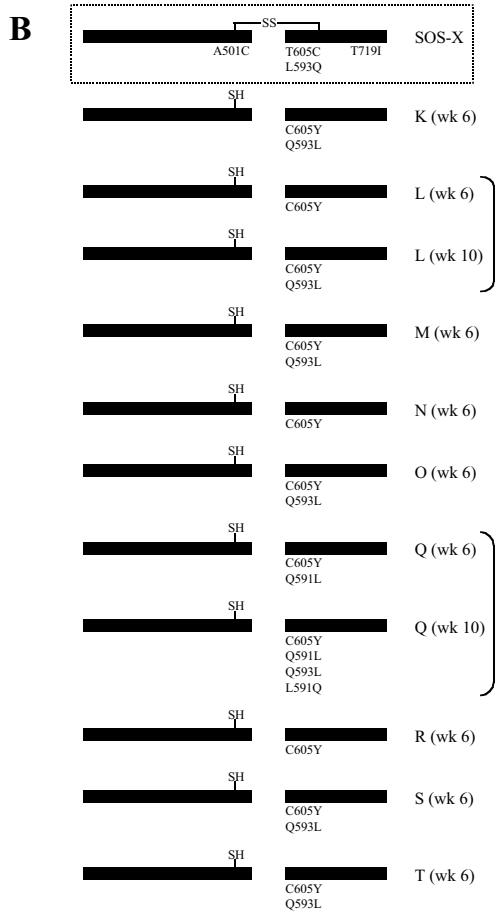

Fig. 3. Schematic of SOS virus evolution. **A.** The wt Env protein and the SOS mutant are shown. SOS Env formed the starting point for evolution of the revertant virus in culture X at week 7, and this culture was split in two and cultured up to week 15 (X3 and X4; see the text). **A.** Virus evolution starting with the SOS-X molecular clone (A501C T605C L593Q T719I). Nine independent cultures were followed over time.

the wt amino-acid at position 605 is a threonine, but reversion to the wt codon is unlikely because it requires two nucleotide changes; a change to tyrosine requires only a single G-to-A transition. An additional reversion event was observed in each culture: Q591L in culture X3 and K487N in culture X4 (Fig. 3A).

In an attempt to study the properties of a replication-competent, clonal virus that maintained the SOS disulfide bond, we cloned the *env* gene from the original escape virus in culture X and inserted it into the HIV-1_{LAI} molecular clone. The variant molecular clone contained the L593Q and T719I changes, but retained the SOS disulfide bond and is designated SOS-X (A501C T605C L593Q T719I). We used this molecular clone to initiate multiple new and independent evolution experiments, hoping that escape routes might be identified that would not result in elimination of the intersubunit disulfide bond. MT2 cells were transfected with 40 µg of pLAI-SOS-X and cultured for 6-10 weeks in the absence of BME. We eventually observed faster replicating viruses in most cultures, as indicated by the appearance of syncytia and the production of CA-p24. The proviral *env* genes were PCR-amplified and sequenced (Fig. 3B). Strikingly, the viruses in all 9 independent cultures eliminated the intersubunit disulfide bond via the C605Y first-site pseudo-reversion that we previously observed in the X3 and X4 cultures. In three cultures, no mutations other than this C605Y change occurred. Surprisingly, the L593Q substitution, which was selected in the initial SOS-X evolution, was eventually lost in 6 cultures by a *de novo* first-site reversion (Q593L). Two cultures exemplified that the Q593L reversion occurred after the loss of the cysteine at position 605 (cultures L and Q, compare sequences from weeks 6 and 10). The idea that the C605Y change has to precede Q593L reversion is supported by the fact that three cultures contain exclusively the C605Y reversion, but no cultures have Q593L as an individual substitution. In one culture, we detected a very similar amino-acid substitution nearby: Q591L (culture Q at week 6), which was already observed in culture X3. The Q culture evolved further in a surprising way: both the 593 and 591 residues eventually reverted to the wt residues (culture Q at week 10).

Oscillation and co-variation of the L593Q and Q591L substitutions in gp41

The various virus evolution pathways are depicted in figure 4. This scheme combines the results of the original cultures (X3 and X4) and the subsequent experiments (K through T), yielding 11 evolution events that started with SOS-X (A501C T605C L593Q T719I). The T719I substitution in the gp41 intracytoplasmic domain (in culture X) and the K487N substitution (in culture X4) were not tested further and are omitted from the scheme. It is possible that these reversions contributed to the gain of replication capacity by the SOS-X and X4 variants, respectively, but we chose to focus on residues in the gp41 ectodomain (residues 591 and 593). These residues are located near the SOS 605 cysteine in a region that is important for interaction with gp120 (4,7,9,22,37,40).

The selection of the L593Q substitution in the SOS to SOS-X evolution strongly suggests that it is advantageous for viral replication in the presence of the SOS disulfide bond. However, it appears to be disadvantageous and is eliminated once the disulfide bond is lost by the C605Y substitution. Alternatively, the negative effect of the L593Q substitution in the absence of the disulfide bond can

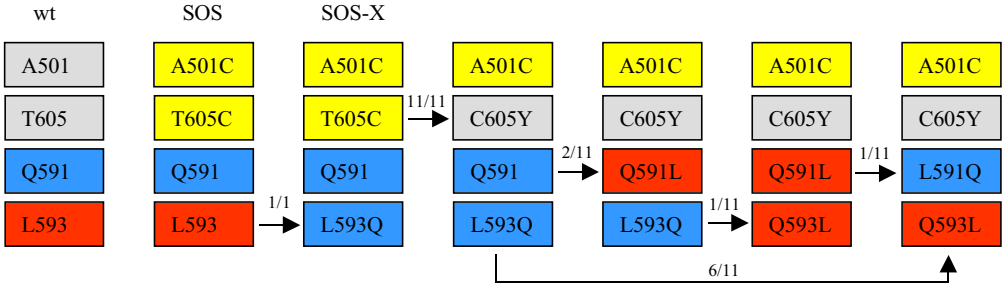

Fig. 4. SOS evolution pathways. The SOS-escape routes are summarized by focusing on four key amino-acid positions. The two SOS cysteines are marked in yellow, and loss of a cysteine changes the colour to grey. The oscillating 591 and 593 residues are also color-coded: red is L and, blue is Q. The observed frequencies of various reversions are indicated above the arrows. Both the original cultures (X3 and X4 in Fig. 3A) and the subsequent cultures (K through T in Fig. 3B) are included. The K487N reversion is left out of the scheme since it was only observed once (in X4) and the T719I reversion is not indicated since it was unchanged after its appearance in culture X.

be partially overcome by acquisition of the compensatory Q591L substitution, as exemplified by two virus cultures that follow this pathway (Fig. 3: X3 and Q, and Fig. 4). However, given sufficient evolution time in the absence of the SOS disulfide bond, both 591 and 593 residues revert back to the wt sequence (Fig. 3: culture Q).

To analyze the effects of the L593Q and Q591L changes, we constructed molecular clones containing these substitutions, either individually or in combination, in the context of SOS (A501C T605C) and the revertant virus (A501C C605Y). However, the poor replication capacity of these viruses did not allow any significant further testing (results not shown). We therefore studied the effect of the L593Q and Q591L substitutions in the context of the wt virus. MT-2 T cells were transfected with the appropriate molecular clones and virus spread was measured (Fig. 5). The L593Q mutant replicated with a delay of approximately 4 days compared to the wt virus. Replication of the Q591L mutant was significantly better, with a delay of only one day compared to the wt virus. Of note is that the double mutant L593Q Q591L had an intermediate phenotype, the delay being 3 days. Similar results were obtained in independent infection experiments (not

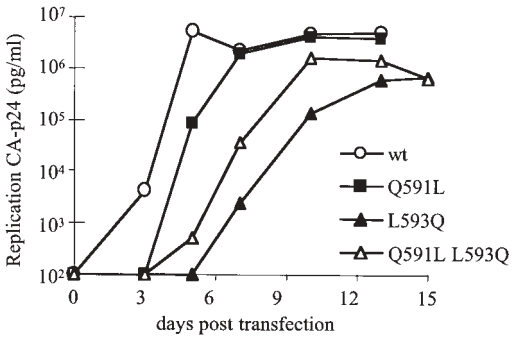

Fig. 5. Replication of the L593Q and Q591L mutant viruses. $5x10^6$ MT-2 cells were transfected with 5 µg of the indicated molecular clones and virus spread was monitored for 15 days by CA-p24 ELISA.

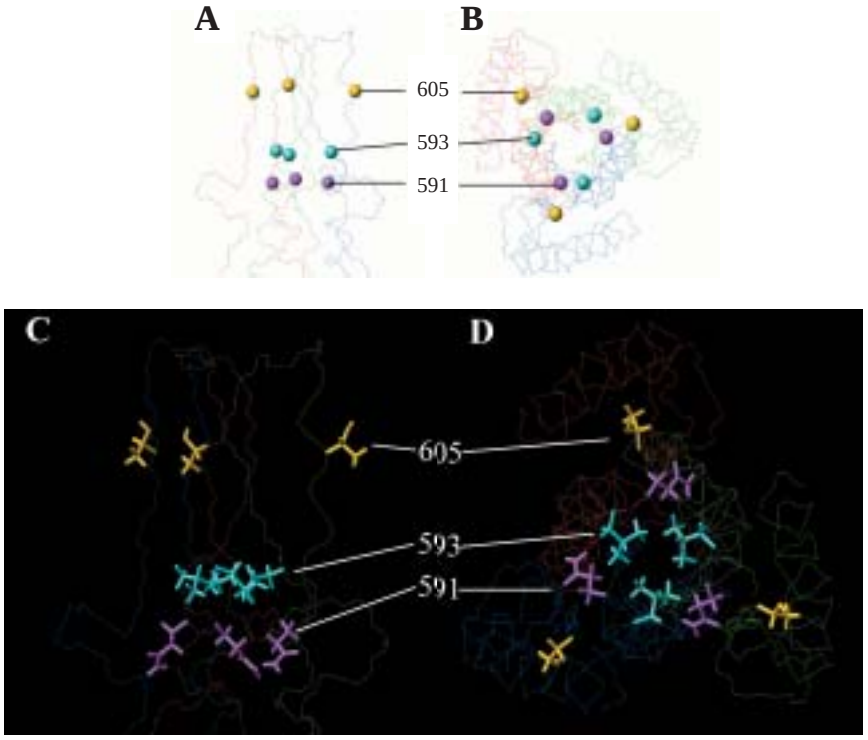

Fig. 6. Modeling of the SOS reversions in structure model of the HIV-1 gp41 ectodomain (5). The Cα atoms of the relevant residues are indicated as spheres in Fig. **A** and **B**, using the following color scheme: C605 is yellow, L593 is cyan, and Q591 is purple. The side chains in Fig. **C** and **D**, use the same color scheme. Panels A and C depict a side view of the gp41 loop region, panels B and D a top view from the perspective of the target membrane (and of gp120).

shown). Thus, whereas the Q591L substitution is slightly disadvantageous for the wt Env protein, it can partially compensate for the defect caused by the L593Q substitution.

Modeling of reversions in the gp41 structure model

To better understand the molecular mechanisms of the oscillating 591 and 593 substitutions, we analyzed the substitutions at positions 591, 593 and 605 in a structure model of the HIV-1 gp41 loop region (Fig. 6). The model is based on the SIV gp41 NMR structure and represents the post-fusion, six-helix bundle state of gp41 (5,6). It was used because the available crystal structures of the six-helix bundle do not include the loop region (8,45,49). Ideally, we would also like to model the substitutions in the pre-fusion structure of gp41 since they are likely to exert their effect on the Env complex at this stage. However, the structure of gp41 in the pre-fusion state is currently unknown. As reported previously, residue 605 (yellow in Fig. 6) is on the outside of the gp41 molecule and thus available for an interaction with gp120 (5). The side chain of residue 605 points outwards such that substitutions here would not be expected to disrupt the loop

structure. Indeed, the cysteine-to-tyrosine reversion that we observed can easily be accommodated at position 605.

Residues 591 and 593 are located at an equivalent position in the interior of the gp41 core, but the orientation of their side chains differs (Fig. 6). The side chain of residue 593 (cyan in Fig. 6) points towards the interior of the loop, thereby establishing an interaction with its counterparts in the other subunits at the trimer axis. This 593 Leu-Leu-Leu triplet stabilizes the loop structure by hydrophobic interactions. Similar hydrophobic Leu-Leu-Leu and Ile-Ile-Ile interactions stabilize the upstream coiled coil region (e.g. residues L545, I548, L555, I559, L566, I573, L576, L587). It is evident that L593 does not directly interact with residues 591 or 605. Leucine 593 can be replaced by glutamine without disrupting the backbone. This change might weaken the loop structure due to the introduction of hydrophilic side chains into the protein interior, but the glutamine side chains may rearrange to form hydrogen bonds to regain some of the lost energy, similar to Gln-Gln-Gln interactions that are present in the coiled coil domain (e.g. residues Q552, Q562).

The side chain of residue 591 (purple in Fig. 6) is located at the end of the N-terminal helix. It is partially occluded in the interior of gp41 and partially exposed on the surface. It does not directly interact with either residue 593 or 605. Replacing glutamine 591 with leucine is possible without perturbing the backbone (Fig. 6C and D). In conclusion, the Q591L and L593Q substitutions do not appear to have dramatic effects on the gp41 post-fusion conformation, which is consistent with the notion that these reversions may exert their effects on the gp41 – gp120 interaction in the pre-fusion form of the Env complex.

Discussion

The initial goal of our forced evolution studies was to generate SOS Env variants that could replicate despite having an intermolecular disulfide bond between gp120 and gp41. The presence of a disulfide bond between the SU and TM subunits of other viruses, including retroviruses, provides a rationale for this study (15-17,19,20,24,25,28,33-36,43,44,46-48,50). The evolutionary selection of a disulfide bond-stabilized, but functional HIV-1 Env complex would have been useful for mechanistic studies and the design of variant SOS Env immunogens. We did observe one SOS variant that replicated extremely poorly, but still retained the engineered cysteines (SOS-X, containing the L593Q reversion). This poorly replicating variant seemed a good candidate for subsequent evolution experiments. However, the cysteine at position 605 was always lost over time in multiple independent cultures. The L593Q reversion substitution may in fact destabilize the SOS disulfide bond (see below), thus biasing the subsequent evolution towards elimination of the disulfide bond. In conclusion, we were not able to obtain efficiently replicating viruses that retained the SOS disulfide bond. A rigid, covalent interaction between gp120 and gp41 is probably deleterious for HIV-1 replication. The dissociation of gp120 from gp41, or a significant shift in the geometry of the two subunits, may be essential for fusion to occur. This conclusion is supported by the observation that SOS Env will undergo fusion efficiently once a reducing agent is added to break the engineered disulfide bond subsequent to receptor engagement (1,3).

Table 1. SOS evolution cultures

culture	mutant	cell line	pLAI(µg)	BME (mM)	Reversion[a]
A	SOS	SupT1	10	-	-
B	SOS	SupT1	10	-	-
C	SOS	SupT1	10	-	-
D	A501C	SupT1	10	-	-
E	SOS	SupT1	10	-	-
F1	SOS	SupT1	10	0.1	-
F3	SOS	SupT1	10	0.3	-
I	SOS	SupT1	40	-	-
J1	SOS	SupT1	40	0.1	-
J3	SOS	SupT1	40	0.3	-
Q	SOS	MT-2	10	-	-
R	SOS	MT-2	10	0.1	-
T	SOS	MT-2	10	0.3	-
U	SOS	MT-2	40	-	-
V	SOS	MT-2	40	0.1	-
X	SOS	MT-2	40	0.3	+

[a] after 7 weeks (12 weeks for cultures A-D)

An intriguing question is why the loss of the SOS disulfide bond occurred in multiple independent cultures via a substitution of C605, but never of C501. This is a surprising finding given the fact that a virus with a single cysteine at position 605 is replication competent, whereas a virus with a single cysteine at position 501 is not (Fig. 1). It is possible that the evolutionary possibilities at position 501 are more restricted. For example, it may take more than one nucleotide change in codon 501 to acquire a functional amino-acid. The wt A501 is strongly conserved in natural isolates and it would require at least 2 nucleotide changes to remake the C501 codon into a triplet that is present in natural virus isolates. The underlying Rev responsive element may impose additional constraints on the evolution of this codon. In contrast, the C605Y reversion is generated by a relatively easy G-to-A transition (2), and tyrosine is tolerated at this position, as exemplified by the presence of a tyrosine in subtype O isolates (http://www.hiv.lanl.gov/content/hiv-db).

The evolutionary oscillation of the 591 and 593 residues (Q591 L593 or L591 Q593) has implications for understanding the molecular basis of the gp120-gp41 interaction. Molecular modeling indicated that these reversions do not have a drastic effect on the loop structure in the post-fusion, six-helix bundle configuration of gp41, although the initial L593Q substitution probably has a destabilizing effect. In the context of the SOS disulfide bond, destabilization of the loop region of gp41 could allow the disulfide bond-linked gp120 subunit to be more easily accommodated. However, inspection of the post-fusion gp41 structure does not readily explain why the Q591L secondary reversion compensates for the L593Q change in the absence of the SOS disulfide bond. We therefore favor an alternative explanation in which the initial L593Q change destabilizes the gp120–gp41 interaction. This would be consistent with previous mutagenesis studies (21,22,37). For example, the L593A substitution greatly weakens gp120-gp41 association (22). The L593Q reversion could either destabilize the SOS disulfide bond or prevent its formation. We were unable to detect such an effect in bio-

chemical assays using soluble SOS gp140 (results not shown), but the effect may be marginal, since the positive effect on SOS virus replication is also minor. Substitutions at position 591 (Q591A and Q591K) are much better tolerated with regard to Env function (22), which may explain why the Q591L reversion could act as an intermediate in two independent evolution cultures. In another study on the idiotypic mimicry of two monoclonal antibodies, the stretch of residues 591-594 was shown to be an interaction site for gp120 (21). Thus, previous mutagenesis studies, idiotypic mimicry and the forced evolution studies presented here all point to an important role for this gp41 domain in the interaction with gp120. The stability of the gp120–gp41 interaction is delicately balanced. Too weak an interaction is deleterious to virus replication because it results in premature gp120 shedding, loss of Env function and loss of virus replication. However, a too rigid, and certainly a covalent interaction is also incompatible with HIV-1 Env function, probably because this impedes conformational changes that are necessary for fusion to occur, which may even include the complete dissociation of gp120 from gp41 (23,27).

Acknowledgments

We thank Stephan Heynen for technical assistance. This work was sponsored by the Dutch AIDS Fund (Amsterdam) and by NIH grants AI 39420, AI 45463 and AI 54159.

References

1. **Abrahamyan, L. G., R. M. Markosyan, J. P. Moore, F. S. Cohen, and G. B. Melikyan**. 2003. Human immunodeficiency virus type 1 Env with an intersubunit disulfide bond engages coreceptors but requires bond reduction after engagement to induce fusion. J. Virol. **77**:5829-5836.
2. **Berkhout, B., A. T. Das, and N. Beerens.** 2001. HIV-1 RNA editing, hypermutation and error-prone reverse transcription. Science **292**:7.
3. **Binley, J. M., C. S. Cayanan, C. Wiley, N. Schulke, W. C. Olson, and D. R. Burton.** 2003. Redox-triggered infection by disulfide bond-shackled human immunodeficiency virus type 1 pseudovirions. J. Virol. **77**:5678-5684.
4. **Binley, J. M., R. W. Sanders, B. Clas, N. Schuelke, A. Master, Y. Guo, F. Kajumo, D. J. Anselma, P. J. Maddon, W. C. Olson, and J. P. Moore**. 2000. A recombinant HIV-1 envelope glycoprotein complex stabilized by an intermolecular disulfide bond between the gp120 and gp41 subunits is an antigenic mimic of the trimeric virion-associated structure. J. Virol. **74**:627-643.
5. **Caffrey, M.** 2001. Model for the structure of the HIV gp41 ectodomain: insight into the intermolecular interactions of the gp41 loop. Biochim. Biophys. Acta **1536**:116-122.
6. **Caffrey, M., M. Cai, J. Kaufman, S. J. Stahl, P. T. Wingfield, D. G. Covell, A. M. Gronenborn, and G. M. Clore.** 1998. Three-dimensional solution structure of the 44 kDa ectodomain of SIV gp41. EMBO J. **17**:4572-4584.
7. **Cao, J., L. Bergeron, E. Helseth, M. Thali, H. Repke, and J. Sodroski.** 1993. Effects of amino-acid changes in the extracellular domain of the human immunodeficiency virus type 1 gp41 envelope glycoprotein. J.Virol. **67**:2747-2755.
8. **Chan, D. C., D. Fass, J. M. Berger, and P. S. Kim**. 1997. Core structure of gp41 from the HIV envelope glycoprotein. Cell **89**:263-273.
9. **Chen, S. S**. 1994. Functional role of the zipper motif region of human immunodeficiency virus type 1 transmembrane protein gp41. J.Virol. **68**:2002-2010.

10. **Colman, P. M. and M. C. Lawrence**. 2003. The structural biology of type I viral membrane fusion. Nat.Rev.Mol. Cell Biol. **4**:309-319.
11. **Das, A. T., B. Klaver, and B. Berkhout**. 1999. A hairpin structure in the R region of the Human Immunodeficiency Virus type 1 RNA genome is instrumental in polyadenylation site selection. J. Virol. **73**:81-91.
12. **Das, A. T., B. Klaver, B. I. F. Klasens, J. L. B. van Wamel, and B. Berkhout.** 1997. A conserved hairpin motif in the R-U5 region of the human immunodeficiency virus type 1 RNA genome is essential for replication. J. Virol. **71**:2346-2356.
13. **Eckert, D. M. and P. S. Kim**. 2001. Mechanisms of viral membrane fusion and its inhibition. Annu. Rev. Biochem. **70**:777-810.
14. **Gallo, S. A., C. M. Finnegan, M. Viard, Y. Raviv, A. Dimitrov, S. S. Rawat, A. Puri, S. Durell, and R. Blumenthal**. 2003. The HIV Env-mediated fusion reaction. Biochim. Biophys. Acta **1614**:36-50.
15. **Gretch, D. R., R. C. Gehrz, and M. F. Stinski.** 1988. Characterization of a human cytomegalovirus glycoprotein complex (gcI). J. Gen. Virol. **69** (Pt 6):1205-1215.
16. **Gruber, C. and S. Levine**. 1983. Respiratory syncytial virus polypeptides. III. The envelope-associated proteins. J. Gen. Virol. **64** (Pt 4):825-832.
17. **Hardwick, J. M. and R. H. Bussell.** 1978. Glycoproteins of measles virus under reducing and nonreducing conditions. J. Virol. **25**:687-692.
18. **Jeeninga, R. E., M. Hoogenkamp, M. Armand-Ugon, M. de Baar, K. Verhoef, and B. Berkhout.** 2000. Functional differences between the LTR transcriptional promoters of HIV-1 subtypes A through G. J. Virol. **74**:3740-3751.
19. **Leamnson, R. N. and M. S. Halpern.** 1976. Subunit structure of the glycoprotein complex of avian tumor virus. J. Virol. **18**:956-968.
20. **Leamnson, R. N., M. H. Shander, and M. S. Halpern.** 1977. A structural protein complex in Moloney leukemia virus. Virology **76**:437-439.
21. **Lopalco, L., R. Longhi, F. Ciccomascolo, A. De Rossi, M. Pelagi, F. Andronico, J. P. Moore, T. Schulz, A. Beretta, and A. G. Siccardi.** 1993. Identification of human immunodeficiency virus type 1 glycoprotein gp120/gp41 interacting sites by the idiotypic mimicry of two monoclonal antibodies. AIDS Res. Hum. Retroviruses **9**:33-39.
22. **Maerz, A. L., H. E. Drummer, K. A. Wilson, and P. Poumbourios.** 2001. Functional analysis of the disulfide bond-bonded loop/chain reversal region of human immunodeficiency virus type 1 gp41 reveals a critical role in gp120-gp41 association. J. Virol. **75**:6635-6644.
23. M**cKeating, J. A., A. McKnight, and J. P. Moore.** 1991. Differential loss of envelope glycoprotein gp120 from virions of human immunodeficiency virus type 1 isolates: effects on infectivity and neutralization. J. Virol. **65**:852-860.
24. **Meredith, D. M., J. M. Stocks, G. R. Whittaker, I. W. Halliburton, B. W. Snowden, and R. A. Killington.** 1989. Identification of the gB homologues of equine herpesvirus types 1 and 4 as disulphide-linked heterodimers and their characterization using monoclonal antibodies. J. Gen. Virol. **70** (Pt 5):1161-1172.
25. **Montelaro, R. C., S. J. Sullivan, and D. P. Bolognesi.** 1978. An analysis of type-C retrovirus polypeptides and their associations in the virion. Virology **84**:19-31.
26. **Moore, J. P. and D. D. Ho**. 1993. Antibodies to discontinuous or conformationally sensitive epitopes on the gp120 glycoprotein of human immunodeficiency virus type 1 are highly prevalent in sera of infected humans. J. Virol. **67**:863-875.
27. **Moore, J. P., J. A. McKeating, R. A. Weiss, and Q. J. Sattentau**. 1990. Dissociation of gp120 from HIV-1 virions induced by soluble CD4. Science **250**:1139-1142.
28. **Opstelten, D. J., M. Wallin, and H. Garoff**. 1998. Moloney murine leukemia virus envelope protein subunits, gp70 and Pr15E, form a stable disulfide bond-linked complex. J. Virol. **72**:6537-6545.
29. **Parren, P. W., D. R. Burton, and Q. J. Sattentau.** 1997. HIV-1 antibody—debris or virion? Nat. Med. **3**:366-367.
30. **Parren, P. W., M. C. Gauduin, R. A. Koup, P. Poignard, P. Fisicaro, D. R. Burton, and Q. J. Sattentau.** 1997. Relevance of the antibody response against human immunodeficiency virus type 1 envelope to vaccine design. Immunol. Lett. **57**:105-112.
31. **Parren, P. W. H. I., J. P. Moore, D. R. Burton, and Q. J. Sattentau.** 1999. The neutralizing

antibody response to HIV-1: viral evasion and escape from humoral immunity. AIDS **13** (Suppl. A):S137-S162.

32. **Peden, K., M. Emerman, and L. Montagnier.** 1991. Changes in growth properties on passage in tissue culture of viruses derived from infectious molecular clones of HIV-1_{LAI}, HIV-1_{MAL}, and HIV-1_{ELI}. Virology **185**:661-672.
33. **Pinter, A. and E. Fleissner**. 1977. The presence of disulfide bond-linked gp70-p15(E) complexes in AKR murine leukemia virus. Virology **83**:417-422.
34. **Pinter, A. and E. Fleissner.** 1979. Structural studies of retroviruses: characterization of oligomeric complexes of murine and feline leukemia virus envelope and core components formed upon cross-linking. J. Virol. **30**:157-165.
35. **Pinter, A. and W. J. Honnen**. 1983. Comparison of structural domains of gp70s of ecotropic Akv and dualtropic MCF-247 MuLVs. Virology **129**:40-50.
36. **Pinter, A. and W. J. Honnen**. 1984. Characterization of structural and immunological properties of specific domains of Friend ecotropic and dual-tropic murine leukemia virus gp70s. J. Virol. **49**:452-458.
37. **Poumbourios, P., A. L. Maerz, and H. E. Drummer.** 2003. Functional evolution of the HIV-1 envelope glycoprotein gp120-association site of gp41. J. Biol. Chem. **278**: 42149-42160.
38. **Sakurai, H., R. A. Williamson, J. E. Crowe, J. A. Beeler, P. Poignard, R. B. Bastidas, R. M. Chanock, and D. R. Burton.** 1999. Human antibody responses to mature and immature forms of viral envelope in respiratory syncytial virus infection: significance for subunit vaccines. J. Virol. **73**:2956-2962.
39. **Sanders, R. W., E. C. de Jong, C. E. Baldwin, J. H. Schuitemaker, M. L. Kapsenberg, and B. Berkhout.** 2002. Differential transmission of human immunodeficiency virus type 1 by distinct subsets of effector dendritic cells. J. Virol. **76**:7812-7821.
40. **Sanders, R. W., B. Korber, M. Lu, B. Berkhout, and J. P. Moore**. 2002. Mutational analyses and natural variablility of the gp41 ectodomain, p. 43-68. *In* C. Kuiken, B. Foley, E. Freed, B. Hahn, P. Marx, F. McCutchan, J. Mellors, S. Wolinsky, and B. Korber (eds.), HIV Sequence compendium 2002. Los Alamos National Laboratory, Theoretical Biology and Biophysics Group, Los Alamos, New Mexico.
41. **Sanders, R. W., L. Schiffner, A. Master, F. Kajumo, Y. Guo, T. Dragic, J. P. Moore, and J. M. Binley**. 2000. Variable-loop-deleted variants of the human immunodeficiency virus type 1 envelope glycoprotein can be stabilized by an intermolecular disulfide bond between the gp120 and gp41 subunits. J. Virol. **74**:5091-5100.
42. **Sanders, R. W., M. Venturi, L. Schiffner, R. Kalyanaraman, H. Katinger, K. O. Lloyd, P. D. Kwong, and J. P. Moore.** 2002. The mannose-dependent epitope for neutralizing antibody 2G12 on human immunodeficiency virus type 1 glycoprotein gp120. J. Virol. **76**:7293-7305.
43. **Scheid, A. and P. W. Choppin**. 1977. Two disulfide bond-linked polypeptide chains constitute the active F protein of paramyxoviruses. Virology **80**:54-66.
44. **Storey, D. G., K. Dimock, and C. Y. Kang**. 1984. Structural characterization of virion proteins and genomic RNA of human parainfluenza virus 3. J. Virol. **52**:761-766.
45. **Tan, K., J. Liu, J. Wang, S. Shen, and M. Lu**. 1997. Atomic structure of a thermostable subdomain of HIV-1 gp41. Proc. Natl. Acad. Sci. USA **94**:12303-12308.
46. **van Drunen Littel-van den Hurk and L. A. Babiuk**. 1986. Synthesis and processing of bovine herpesvirus 1 glycoproteins. J. Virol. **59**:401-410.
47. **Waterfield, M., G. Scrace, and J. Skehel**. 1981. Disulphide bonds of haemagglutinin of Asian influenza virus. Nature **289**:422-424.
48. **Waxham, M. N. and J. S. Wolinsky**. 1983. Immunochemical identification of rubella virus hemagglutinin. Virology **126**:194-203.
49. **Weissenhorn, W., A. Dessen, S. C. Harrison, J. J. Skehel, and D. C. Wiley**. 1997. Atomic structure of the ectodomain from HIV-1 gp41. Nature **387**:426-430.
50. **Witte, O. N., A. Tsukamoto-Adey, and I. L. Weissman.** 19**77.** Cellular maturation of oncornavirus glycoproteins: topological arrangement of precursor and product forms in cellular membranes. Virology **76**:539-553.
51. **Wyatt, R. and J. Sodroski**. 1998. The HIV-1 envelope glycoproteins: fusogens, antigens, and immunogens. Science **280**:1884-1888.

Chapter 5.5

Enhancing the proteolytic maturation of the HIV-1 envelope glycoproteins

(*Journal of Virology,* May 2002, p. 2606-2616)

James M. Binley[1, 4], Rogier W. Sanders[1,2] , Aditi Master[1], Charmagne S. Cayanan[4], Cheryl L. Wiley[4,5], Linnea Schiffner[1], Bruce Travis[3], Shawn Kuhmann[1], Dennis R. Burton[4], Shiu-Lok Hu[3], William Olson[5], John P. Moore[1]

[1]*Dept. Microbiology and Immunology, Weill Medical College of Cornell University, 1300 York Ave., New York, NY 10021.*
[2]*Dept. of Human Retrovirology, Academic Medical Center, University of Amsterdam, 1105 AZ Amsterdam, The Netherlands.*
[3]*University of Washington, 3000 Western Ave., Seattle, WA 98121.*
[4]*The Scripps Research Institute, 10550 North Torrey Pines Rd., La Jolla CA 92037.*
[5]*Progenics Pharmaceuticals, 777 Old Saw Mill River Rd., Tarrytown, NY 10591.*

In virus-infected cells, the envelope glycoprotein (Env) precursor, gp160, of human immunodeficiency virus type 1 (HIV-1) is cleaved by cellular proteases into a fusion-competent gp120/gp41 heterodimer in which the two subunits are non-covalently associated. However, cleavage can be inefficient when recombinant Env is expressed at high levels, either as a full-length gp160 or as a soluble gp140 truncated immediately N-terminal to the transmembrane domain. We have explored several methods for obtaining fully cleaved Env for use as a vaccine antigen. We tested whether purified Env could be enzymatically digested with purified protease *in vitro.* Plasmin efficiently cleaved the Env precursor, but also cut at a second site in gp120, most probably the V3 loop. In contrast, a soluble form of furin was specific for the gp120/gp41 cleavage site, but cleaved inefficiently. Co-expression of Env with the full-length or soluble forms of furin enhanced Env cleavage but also reduced Env expression. When the Env cleavage site (REKR) was mutated to see if its use by cellular proteases could be enhanced, several mutants were more efficiently processed than the wild-type protein. The optimal cleavage-site sequences were RRRRRR, RRRRKR and RRRKKR. These mutations did not significantly alter the capacity of the Env protein to mediate fusion, so did not radically perturb the Env structure. Furthermore, unlike wild-type Env, expression of the cleavage-site mutants was not significantly reduced by furin co-expression. The co-expression of Env cleavage site mutants and furin is therefore a useful method for obtaining high-level expression of processed Env.

Introduction

The envelope glycoprotein complex (Env) mediates receptor binding and membrane fusion during human immunodeficiency virus type 1 (HIV-1) infection of

susceptible cells (66). It is synthesized as a polypeptide precursor (gp160) that oligomerizes to form a heavily glycosylated trimer (20, 24). At a late stage of synthesis, most probably in the trans-Golgi network (TGN), gp160 is cleaved by furin (17, 18, 55-58) or other, related subtilisin-like proteases (17, 18, 28, 38, 58, 90) into the surface (SU; gp120) and transmembrane subunits (TM; gp41) (34, 43, 55-58, 82). Cleavage occurs at a motif at the gp120-gp41 juncture that contains a basic amino-acid residue tetramer, R-X-R/K-R (where X is any amino-acid). The gp120 and gp41 proteins then remain non-covalently associated, forming the functional, native $gp120_3$-$gp41_3$ complex (20, 24, 66).

During fusion, the gp120 protein interacts with the receptor and co-receptor on target cells. This triggers conformational changes that lead to the insertion of a hydrophobic fusion peptide, located at the N-terminus of gp41, into the target cell membrane (66). Cleavage of gp160 is essential for fusion, since uncleaved gp160 is fusion-incompetent (9, 33, 39, 48). Generally, only cleaved Env is incorporated into virions (22), although uncleaved Env can be virion-associated (39, 48). By analogy with other enveloped viruses such as influenza A (5, 32, 36, 40-42, 60), Semliki forest virus (27,71) and Newcastle disease virus (76), gp160 cleavage may induce a shift from a low-energy state to a metastable Env configuration that is capable of fusion. The common requirement for cleavage of an Env precursor in many families of enveloped viruses is an indication of the general importance of this event in virus assembly (8, 27, 42, 70, 79, 83, 89, 91).

HIV-1 Env is the focus of vaccine design strategies intended to elicit virus-neutralizing antibodies. To neutralize HIV-1, an antibody must be able to bind to the native, trimeric virus-associated Env complex (11, 12, 63, 64). Most Env-based vaccine candidates tested to date have been either monomeric gp120 subunits or various forms of the uncleaved gp160 or gp140 (gp120 plus gp41 ectodomain) precursor proteins (4, 25, 26, 37, 47, 68, 80, 96-98). The use of uncleaved gp140 or gp160 proteins has been considered necessary because the labile, non-covalent gp120-gp41 association in cleaved Env leads to the dissociation of gp120 from gp41 (30, 49, 54, 73). However, gp120, uncleaved gp140 and gp160 proteins do not fully mimic the structure of the native trimeric Env complex. As a result, antibodies elicited to gp120 and uncleaved Env proteins can sometimes neutralize the homologous HIV-1 isolate, but generally do not cross-neutralize heterologous primary isolates (4, 25, 68, 98).

It is not yet clear what effect cleavage has on the overall structure of HIV-1 Env, especially from the perspective of antibody recognition. Cleavage of the influenza A hemagglutinin precursor (HA_0), causes only localized refolding with little impact on its overall structure (15). However, it is not clear how precise a model influenza A HA_0 is for HIV-1 gp160: The two viruses are distant relatives, and their fusion potential is triggered by quite different mechanisms, so it may not be appropriate to extrapolate what that has been learned from HA_0 to predict all aspects of gp160 structure and function. Indeed, uncleaved HIV-1 gp140 proteins are antigenically and, by implication structurally, different from cleaved proteins (6). Moreover, the Env proteins of several other enveloped viruses exhibit dramatic refolding of their envelope proteins upon cleavage (23, 27, 35, 62, 71, 74, 76, 79). Thus, the projecting domains of the trimeric spike precursor of Semliki Forest virus (SFV) coalesce to form a compact, mature spike (27, 71).

The structures of the mature forms of the tick-borne encephalitis virus (TBEV) E protein and the SV5 paramyxovirus F protein, as probed by antibodies, appears to be significantly different from the immature form (23, 35, 74, 79). Of note is that antibodies against the heptad repeat regions of the transmembrane domain of the SV5 F protein only recognized the uncleaved form (23). Overall, whether the above examples represent better paradigms than HA_0 for the structural impact of cleavage on HIV-1 Env is unknown, but clearly they justify further analysis of cleaved forms of HIV-1 Env.

Mimicking the native structure of Env may be a useful HIV-1 vaccine design strategy. The production of a native Env complex as a recombinant protein has, however, been hampered by the limited efficiency of Env cleavage (6, 55, 57, 58, 90, 95), and by the instability of the complex after cleavage has occurred (30, 49, 54, 73). The SU-TM association in cleaved forms of Env can be stabilized by the introduction of appropriately positioned cysteine residues that form an intermolecular disulfide bond between gp120 and gp41 (6). However, to achieve full cleavage of the gp140 precursor in Env-transfected cells, it was necessary to co-express furin (6). A disadvantage of this approach is that furin co-expression significantly reduced Env expression (6, 55, 57, 58, 95). Moreover, cleavage of some Env proteins was still not complete even with furin co-expression (17, 18, 55, 58, 95). Changes in the gp120 variable loops (72, 85), elsewhere in Env (19, 51, 84, 88, 94), and at residues proximal to the cleavage site (2, 29, 33, 84), can all affect Env cleavage efficiency, usually unpredictably. Overall, cleavage efficiency is a function of the folding, oligomerization and glycosylation of gp160, factors that influence the access of furin to its binding site at the gp120-gp41 juncture.

Here, we have investigated several ways to produce proteolytically cleaved HIV-1 Env proteins: The use of purified proteases to cleave purified Env; co-expression with Env of full-length and soluble forms of furin; and mutation of the cleavage site to enhance its processing by cellular proteases. We report that co-expression of Env cleavage site mutants with furin is a useful method for obtaining significant amounts of processed Env.

Materials and Methods

Plasmids and mutagenesis

The pPPI4 plasmid that expresses soluble gp140 lacking the transmembrane and intracytoplasmic domains of gp41 has been described elsewhere (6, 72, 86). Unless specified otherwise, the Env glycoproteins expressed in this study were derived from the HIV-$1_{JR\text{-}FL}$ molecular clone, a subtype B, R5 primary isolate. However, we also expressed gp140 proteins from the molecular clones HXB2, 89.6, 89.6_{KB9}, DH123 and Gun-1_{WT}, as previously described (6), and from a South African isolate, DU151, using a pT7blue-based source plasmid provided by Drs. Lynn Morris, Carolyn Williamson and Maria Papathanopoulous (National Institute of Virology, Johannesburg, South Africa). The gp140 proteins from SIVmac and SIVmne were expressed in a similar manner to HIV-$1_{JR\text{-}FL}$. Some of the above gp140 proteins were also made as mutants that contained cysteine substitutions designed to introduce an intermolecular disulfide bond between gp120 and gp41; the positioning of this disulfide bond corresponds to the one introduced

into JR-FL gp140, to make the protein designated as SOS gp140 ($gp140_{SOS}$), as described elsewhere (6). Wild-type gp140 proteins that lack the SOS mutations but retain the native SU/TM cleavage site are denoted $gp140_{WT}$. Other gp140 proteins were mutated to replace the wild-type SU/TM cleavage site REKR (see below) and are designated as follows: $gp140_{RRRKKR}$, $gp140_{RRRRKR}$, $gp140_{RRRRRR}$, $gp140_{KKRKKR}$ and $gp140_{RERRRKKR}$. All amino-acid substitutions were made using the Quikchange™ site-directed mutagenesis kit (Stratagene Inc) using appropriate primers. The plasmid pSV was used to express full-length JR-FL gp160 for infectivity and fusion assays (21). Mutants of this protein were constructed and named analogously to the pPPI4 gp140 mutants. Vesicular stomatitis virus (VSV) G protein was also expressed by the pSV plasmid (21). Furin was expressed from the plasmid pcDNA3.1-Furin as previously described (6). A stop codon was introduced within the furin gene in place of that for residue E-684, to make the plasmid pCDNA-furin∂TC. This mutation truncates furin close to the C-terminal end of its ectodomain, leading to the expression of a secreted, active form of furin (65). A pGEM furin source plasmid was obtained from Dr. Gary Thomas and Sean Molloy (Vollum Institute, Portland, OR) (52, 53).

Anti-HIV-1 and SIV antibodies and sera

Monoclonal antibody (MAb) B12 recognizes an epitope in the C2 domain of gp120 that is preferentially exposed on denatured forms of the molecule (1). This was provided by Dr. George Lewis (Institute of Human Virology, Baltimore, MD). MAb 2F5 recognizes a neutralizing epitope in the C-terminal region of the gp41 ectodomain (59), and was provided by Dr. Hermann Katinger (Polymun Scientific Inc., Vienna, Austria). Purified SIV immune globulin (SIVIG) was purified from the serum of SIVmac251-infected rhesus macaques as previously described (7). Purified human immune globulin from HIV-1-infected people (HIVIG) was obtained from Dr. John Mascola (Vaccine Research Center, NIH, Washington, DC).

Transfection, immunoprecipitation and Western blotting

Transfection and metabolic labeling of 293T cells and immunoprecipitations were performed as described previously (6, 72) using HIVIG or SIVIG to precipitate the labeled HIV-1 or SIV proteins, respectively. Ten micrograms of each plasmid were used for transfections in 10cm cell culture plates, unless otherwise stated. In other experiments, purified gp140 proteins were analyzed by denaturing SDS-PAGE and Western blotting, using either MAb 2F5 or MAb B12 as probes (6, 72).

Measurement of Env expression and cleavage efficiency

Densitometry measurements were performed using ImageQuant™ and NIH Image software. Env cleavage efficiency was calculated by the following formula (density of gp120 band)/(combined density of gp120+gp140 bands or gp120+gp160 bands), after subtracting the background density in each case. The values obtained were reproducible for each protein within a 6% deviation from the value presented in each case. Env protein expression levels were calculated by combining the densities of the gp120+gp140 or gp120+gp160 bands and sub-

tracting the background density. In each gel, expression is recorded as a ratio relative to the standard used for normalization in that particular experiment.

Vaccinia viruses

Viruses v-VSE5 (expressing full length SIVmne Env under control of the 7.5K promoter) and v-VS4 (expressing SIVmne gag-pol under the control of the 11K promoter) have been described previously (67). The vaccinia recombinant VV:hfur, expressing full length human furin, was obtained from Drs. Gary Thomas and Sean Molloy (52). For protein production, BSC40 cells were infected at a multiplicity of infection (MOI) of 5. Supernatant proteins metabolically labeled with [^{35}S]-cysteine and [^{35}S]-methionine were collected 2 days later. Samples were processed in a similar manner to the transfected cell supernatants above.

Purified Env proteins, enzymes and in vitro enzymatic digestion

Purified human furin was purchased from Affinity Bioreagents Inc., Golden, CO. This is a soluble form of furin with the transmembrane and cytoplasmic tail removed. The specific activity of 1 unit of furin is the amount required to release 1pmol of fluorogenic substrate peptide in 1 min. Purified human plasmin was purchased from Sigma Chemical Co. For determining optimal digestion conditions, a highly purified $gp140_{SOS}$ protein was used (prepared by Progenics Pharmaceuticals Inc.). This particular, early production batch of protein was approximately 50% cleaved. As a control, JR-FL gp120 produced and purified in the same manner was used (86). For plasmin digestions, 8µg (approximately 60pmol) of $gp140_{SOS}$ or gp120 was incubated at 37˚C with 200pmol (approximately 0.2U) of plasmin in 0.1M Tris-HCl pH 7.0 in a total volume of 80µl. For furin digestions, 8µg (approximately 60pmol) of $gp140_{SOS}$ was incubated at 37°C with 20U of furin in100mM HEPES, 1mM $CaCl_2$, pH 7.5 in a total volume of 80µl. The digests were then analyzed by SDS-PAGE and Western blot.

Viral infectivity and cell-cell fusion assays

Pseudotyped luciferase reporter viruses were produced by calcium phosphate transfection. Thus, 293T cells were co-transfected with 5µg of the Env-deficient NL4-3 HIV-1 virus construct pNL-luc and with 15µg of a pSV vector expressing either the full-length JR-FL Env glycoproteins or the positive control VSV-G protein (21). The pNL-luc virus carries the luciferase reporter gene. The pSV plasmids expressed either wild-type gp160 ($gp160_{WT}$) or a mutant with a cleavage site modified from REKR to RRRRRR, designated as JR-FL $gp160_{RRRRRR}$. The supernatants containing pseudotyped viruses from transfected cells were harvested after 48h and filtered through a 0.45µm filter. The viral stocks were then standardized for p24 protein content by ELISA (21), and infections were performed using HeLa-CD4-CCR5 cells. Infectivity was expressed as light units per nanogram of p24 protein in the viral inoculum (21).

Cell-cell fusion activity was measured using a fluorescent cytoplasmic dye transfer assay, as described elsewhere (50). Briefly, 293T cells on a 6cm dish were transfected with 10µg of the pSV7D vector expressing full-length JR-FL Env, then labeled with 1.5µM calcein AM (Molecular Probes, Inc., Eugene, OR)

in 2ml of phosphate buffered saline (PBS), according to the manufacturer's instructions. Cells were detached from the dish by incubating in PBS supplemented with 0.5mM EDTA and 0.5mM EGTA, then transferred into a centrifuge tube. Approximately $5x10^6$ CEM.NKR.CCR5 cells (87) were suspended in 2 ml of Opti-MEM (Gibco) containing 100μM 7-amino-4-chloro methylcoumarin (CMAC, Molecular Probes) and incubated for 30 min at 37°C. After extensive washing to remove the remaining free dye, the effector and target cells were mixed, transferred into poly-lysine coated, 8-well chambered slides and incubated for 2h at 37°C. The extent of fusion was determined by fluorescence video microscopy by normalizing the number of fusion products (stained with both cytoplasmic markers) against the number of target cells that were in contact with the effector cells.

Results

Enzymatic processing of purified, uncleaved $gp140_{SOS}$

In principle, one way to achieve Env cleavage is to treat purified Env proteins *in vitro* with proteases capable of recognizing the gp120-gp41 cleavage site. The highly active subtilisin-family protease plasmin was previously reported to cleave recombinant gp160 into gp120-gp41, whereas other trypsin-like proteases lacked this ability (61). Plasmin is also capable of processing influenza HA_0 at the cell surface (32). We therefore evaluated the effect of plasmin on a preparation of purified, soluble $gp140_{SOS}$ that was 50% cleaved. The partially cleaved $gp140_{SOS}$ preparation was incubated with an excess of plasmin for 2h or 16h at 37°C, and the proteins were analyzed by SDS-PAGE and Western blotting using the 2F5 anti-gp41 MAb (Fig.1). After 2h of plasmin treatment, there was a reduction in the intensity of the uncleaved gp140 band, but the longer reaction time (16h) was required for processing to be complete (Fig.1A). This is consistent with the previous report on gp160 cleavage by plasmin (61). However, when a Western blot of the 16h plasmin digest was probed with the gp120-specific MAb, B12, it was clear that plasmin also digests gp120 into fragments, one of which is of about 70kDa (Fig.1B). MAb B12 recognizes an epitope in the second conserved domain of gp120, N-terminal to the V3 loop (1). Thus, plasmin cleaves gp120 internally, most likely at the site in the V3 loop that is a substrate for other tryptic proteases and which typically yields 50kDa and 70kDa fragments (16, 49, 75). Although plasmin does process the gp120/gp41 cleavage site, the use of this enzyme to enhance Env cleavage is not, therefore, a practical technique.

We next investigated whether soluble furin would cleave gp140 efficiently but with greater specificity. During a 16h incubation, soluble furin significantly, albeit incompletely, cleaved $gp140_{SOS}$ into gp120 without causing additional gp120 degradation (Fig.1C, compare lanes 1 and 3). The efficiency of cleavage of gp140 by soluble furin was low, as shown by the following calculation: One unit (U) of soluble furin can process 1pmol of fluorogenic peptide substrate in 1 min (3). If gp140 were an equally efficient substrate, the 8μg of gp140, containing approximately 4μg (30pmol) of uncleaved gp140, would be digested by 20U of furin within 2min. However, only 50% of the gp140 was actually processed after 16h. If we assume the rate of processing was uniform over this period,

gp140 was cleaved at 0.7fmol/min; i.e. gp140 is ~1000-fold less efficiently cleaved by furin than are model peptides.

The pH of the furin digest may affect its efficiency. For example, the mildly acidic pH of the exocytic pathway alters the structure of the TEBV Env precursor to permit an increase in cleavage efficiency (79). Hence furin is able to cleave the TEBV Env precursor *in vitro* at pH 6.2, but not at pH 7.5 (79). Furthermore, NH_4Cl treatment of cells, which raises the pH of the secretory pathway, can interfere with HIV-1 Env processing (93). We therefore investigated whether a mildly acidic pH might allow more efficient cleavage of gp140 by soluble furin during a16h incubation. The optimal pH for Env cleavage was found to be 5.8 (Fig.1D), in contrast to a report that furin was most active (>80%) at a pH in the range 6.5 to 8 (18). However, even at pH 5.8, gp140 was only cleaved by about 60% (Fig.1D), so optimizing the reaction pH was insufficient to achieve complete cleavage. Overall, we conclude that because a large excess of furin is required to achieve only a modest increase in gp140 cleavage efficiency, this also is not a practical technique for routine use.

Recombinant Env proteins are incompletely processed by cellular proteases; effect of co-expressing furin and Env

We examined the extent of endogenous gp120/gp41 cleavage of seven HIV-1 and four SIV gp140 proteins by immunoprecipitation using HIVIG or SIVIG, as appropriate. Although the cleavage site (REKR) was conserved among all seven HIV-1 isolates, the $gp140_{SOS}$ cleavage efficiency (defined under Materials and Methods) varied from 38-58%, and in no case was cleavage complete (Fig.2A). Similar results were obtained with the corresponding seven HIV-1 $gp140_{WT}$ proteins that lack the SOS cysteine substitutions (data not shown). These proteins are secreted as a mixture of gp120 and uncleaved gp140 despite retaining the REKR cleavage site, because proteolysis is inefficient in the absence of co-transfected furin (6). The cleavage efficiency was generally slightly higher for each $gp140_{WT}$ protein than for the corresponding $gp140_{SOS}$ mutant (data not shown).

Incomplete cleavage was also observed with the SIVmac251 and SIVmne $gp140_{SOS}$ proteins and the SIVmne $gp140_{WT}$ protein, each of which has an RNKR cleavage site motif. In contrast, cleavage of the SIVmac251 $gp140_{WT}$ protein was almost complete (Fig.2A). Since the cleavage site motif in the latter protein is identical, indirect factors such as differences in folding must influence cleavage efficiency.

Co-expression of furin reduces the expression of Env proteins

We next examined the effects of co-expressing furin with JR-FL $gp140_{SOS}$ and $gp140_{WT}$ proteins, since this has previously been shown to increase cleavage efficiency (6, 55, 95). Varying amounts of the full-length, furin-expressing plasmid, pCDNA-furin, were co-transfected with a constant amount of Env-expressing plasmid (Fig.2B). The expression of sufficient furin resulted in almost complete (>90%) cleavage of both forms of gp140 protein, but it also caused a significant reduction in overall Env expression as measured by a decrease in the combined intensity of the gp140 and gp120 bands.

To verify the effect of Env and furin co-expression using a different form of

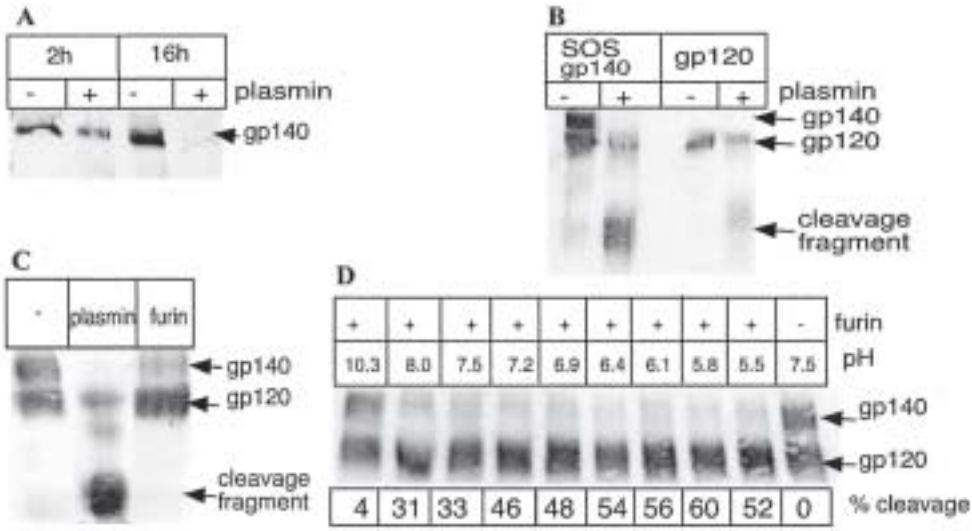

Fig. 1. In vitro enzymatic cleavage of Env with plasmin or soluble furin. Eight micrograms of partially (~50%) cleaved, purified JR-FL $gp140_{SOS}$ or gp120 were incubated with a protease for various times at 37°C. The Env proteins were then analyzed by reducing SDS-PAGE and Western blot. **A.** $gp140_{SOS}$ proteins from a 2h or 16h plasmin (20µg) digest. The Western blot was probed with the anti-gp41 MAb 2F5. **B.** $gp140_{SOS}$ or gp120 samples from a 16h plasmin (20µg) digest. The Western blot was probed with the anti-gp120 MAb B12. **C.**) $gp140_{SOS}$ was incubated at pH 7.5 with or without plasmin or soluble furin for 16h at 37°C. The Western blot was probed with MAb B12. **D.** JR-FL $gp140_{SOS}$ was incubated with or without furin for 16h at the pH indicated. The Western blot was probed with MAb B12. The percent cleavage achieved by soluble furin was calculated as described under Materials and Methods, and expressed with reference to the control in lane 10 (no furin, 0% cleavage).

Env protein and a different expression system, we expressed SIVmne E11S gp160 in BSC40 cells from a recombinant vaccinia virus, both alone and together with Gag and Pol. Co-expression of Env with Gag-Pol enabled us to examine the efficiency with which full-length, membrane-bound gp160, secreted as pseudovirions, was cleaved into gp120/gp41 complexes (Fig.2C). The expression of SIVmne gp160 was approximately 10-fold higher after vaccinia virus v-VSE5 infection than after transfection of the pPPI4-based plasmid encoding the identical gp160 (data not shown). In the absence of furin, gp160 cleavage was very low (Fig.2C, lanes 1 and 3). The extent of cleavage was increased only modestly by furin co-expression, but there was a substantial reduction in the overall expression of Env (Fig.2C, lanes 2 and 4). Indeed, when Gag-Pol and Env were co-expressed along with furin, the Env proteins were barely detectable (lane 2). Gag-Pol was also immunoprecipitated at diminished levels when furin was co-expressed (lane 2). This may be because the precipitation of Gag-Pol from pseudovirions occurs indirectly via antibody reactivity with surface Env, and Env expression is reduced by furin. Alternatively, this could be explained by non-specific competition for expression of proteins from the various plasmids. Some full-length gp160 was present in the supernatant even in the absence of co-expressed

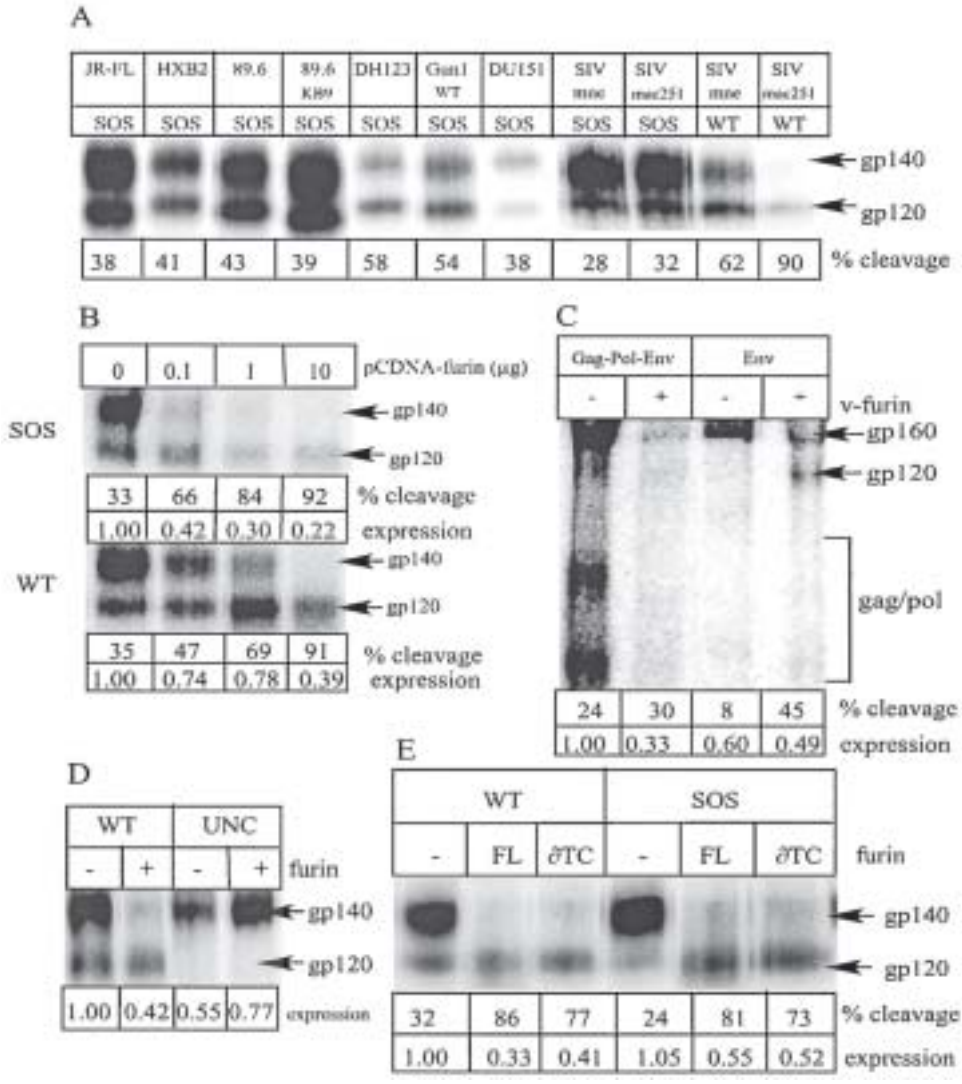

Fig. 2. Cleavage and expression of Env proteins with or without furin. Culture supernatants containing ^{35}S-labeled Env proteins were immunoprecipitated with either HIVIG or SIVIG as appropriate, then analyzed by reducing SDS-PAGE. The results shown are representative of three repeats. In each panel, the percent cleavage was calculated as per materials and methods. Additionally, the relative expression of the gp120+ gp140 or gp120+gp160 bands was calculated and expressed as a ratio relative to a standard (expression defined as 1.00) in each gel. **A.** Soluble gp140 proteins were expressed in 293T cells transfected with pPPI4-based plasmids. **B.** The JR-FL $gp140_{SOS}$ or $gp140_{WT}$ proteins were expressed as in panel A but in the presence of variable amounts of co-expressed, full-length furin. **C.** BSC40 cells were infected with vaccinia viruses v-VS4 (expressing SIVmne Gag-Pol) and/or v-SE5 (expressing SIVmne Env) at an MOI of 5, as indicated. Some of the cells were co-infected, also at an MOI of 5, with the vaccinia virus vv:hfur expressing full-length furin (lanes 2 and 4). **D.** JR-FL $gp140_{WT}$ and $gp140_{UNC}$ proteins were expressed in 293T cells transfected with pPPI4-based plasmids, with or without co-transfection of full-length furin. **E.** JR-FL $gp140_{WT}$ and $gp140_{SOS}$ proteins were expressed in 293T cells transfected with pPPI4-based plasmids, alone or with co-transfection of either full-length furin (FL) or truncated, soluble furin (∂TC), as indicated.

Gag-Pol (Fig.2C, lanes 3,4). This may be associated with cellular vesicles (31) or could have been released from dead cells.

Overall, it is clear that furin expression has qualitatively similar effects on both gp140 and gp160 proteins irrespective of the expression system. Moreover, the increase in Env expression in the vaccinia virus system is associated with a further reduction in the extent of Env cleavage.

Influence of the furin substrate sequence on Env expression in the presence of co-expressed furin

The co-expression of furin has previously been reported to reduce the expression of several furin substrates, perhaps due to the complexing and retention of the nascent proteins with furin in the TGN rather than to any overtly toxic effect of furin on the cells (52, 58, 81). To investigate this, we determined whether the reduction in Env expression caused by furin co-expression required that the Env protein exhibit a furin-recognition motif (Fig.2D). We observed that furin co-expression had little effect on expression of the JR-FL $gp140_{UNC}$ protein (Fig.2D, lanes 3, 4) in which the KRRVVQREKRAV furin-recognition sequence had been replaced by LRLRLRLRLRLR (6). Although, in this experiment, $gp140_{UNC}$ expression was slightly increased in the presence of furin, the increase was not usually observed in repeat assays (data not shown). The lack of effect of furin on $gp140_{UNC}$ expression contrasts markedly with its substantial inhibition of the expression of the $gp140_{WT}$ and $gp140_{SOS}$ proteins that have unmodified cleavage site sequences (Fig.2D, lanes 1, 2, Fig. 2B). These results are consistent with the hypothesis that furin-induced reduction in Env expression is attributable to the formation of Env-furin complexes that are retained within the cell.

A soluble form of furin allows efficient Env cleavage without dramatically reducing Env expression

In an attempt to overcome the apparent formation of furin-Env complexes in the TGN, we co-expressed Env with a soluble form of furin. The proteolytic activity of furin is contained entirely in its lumenal domain, and soluble forms of the enzyme retain enzymatic activity (52, 53, 65). When we expressed JR-FL $gp140_{WT}$ and $gp140_{SOS}$ in the presence of full-length furin, we saw the expected reduction in Env expression (Fig.2E, lanes 2 and 5). However, essentially the same result was observed when a soluble form of furin (furin∂TC) was used instead of the full-length, membrane-bound enzyme (Fig.2E, lanes 3 and 6). Thus, although the presence of the furin recognition sequence is important (Fig.2D), direct retention of Env in complex with furin in the TGN may not be the entire explanation for the reduction in Env expression upon furin co-expression (38, 52, 57, 93).

Altering the cleavage sequence can increase Env processing by cellular proteases

Our next approach towards increasing the efficiency of gp140 cleavage was to vary the furin recognition sequence. The rationale for this is partly derived from studies of other RNA viruses. For example, some influenza A virus variants have evolved proteolytic cleavage sites in the HA_0 precursor protein that contain basic residue insertions. This is associated with increased cleavage efficiency and a gain

in viral virulence. Thus, whereas avirulent clones contain only a single arginine residue within the HA_0 cleavage site, the corresponding sites of virulent clones contain multiple basic residues, leading to motifs such as RRRKKR (5, 32, 36, 40, 41, 60). Biochemical evidence using peptide-cleavage assays has confirmed that multi-arginine stretches are highly efficient targets for furin (13). The most efficiently recognized target sequences consist of hexa- or hepta-arginine repeats; for example, a peptide with the recognition sequence RRRRRR was cleaved approximately 50 times more efficiently than one with the RRRR motif (13).

In contrast to influenza A, HIV-1 and SIV strains contain only simple R-X-R/K-R furin-recognition sequences. We therefore introduced basic amino-acids into the cleavage site of the JR-FL $gp140_{SOS}$ and $gp140_{WT}$ proteins. The mutated gp140 proteins were processed more efficiently than those containing the normal REKR motif, although none of the mutants was completely cleaved by endogenous, cellular proteases (Fig.3A, Table 1).

Two of the most efficiently cleaved mutants contained the RRRRRR or RRRKKR motifs (Fig.3A; compare lanes 1, 3 and 5). When furin was co-expressed, these mutants were 100% cleaved, compared to only about 90% cleavage for wild-type Env (or less than 90% in other experiments; data not shown). An unexpected finding was that furin did not reduce the overall expression of the cleavage-site mutant gp140 proteins, whereas, as noted above, it significantly diminished the expression of the wild-type gp140 (Fig.3A; compare lanes 2, 4 and 6). This was confirmed when the RRRRRR gp140 mutant was co-expressed with variable amounts of pCDNA-furin (0.1µg, 1µg or 10µg) (Fig.3B). In this experiment, furin co-expression actually increased the overall amount of Env protein secreted, although an increase was not always seen with this or related mutants in other experiments.

The expression levels and cleavage efficiencies of a selection of gp140 mutants with basic insertions into the REKR cleavage site are summarized in Table 1. The closely related mutants RRRKKR, RRRRKR and RRRRRR all had similar properties, in that cleavage was enhanced in the absence of co-transfected furin, and was complete in the presence of furin, but without a significant decrease in the extent of Env expression. The mutants KKRKKR and RERRRKKR were also better cleaved than the wild-type protein, and their expression was unaffected by furin co-transfection. However, they were expressed at lower levels than the other mutants and less well than wild-type gp140 proteins containing the standard REKR motif. The effects of the basic residue insertions were similar whether the test protein was $gp140_{WT}$ or $gp140_{SOS}$, although some of the $gp140_{WT}$ proteins were expressed at slightly higher levels than the corresponding $gp140_{SOS}$ proteins (Table 1).

To address whether the insertion of basic amino-acids into the proteolytic cleavage site had a general effect on cleavage efficiency (i.e. was not restricted to the JR-FL clone), we mutated the cleavage site of $gp140_{SOS}$ of the subtype C primary isolate, DU151, from REKR to RRRRRR. In the absence of co-transfected furin, the unmodified DU151 $gp140_{SOS}$ protein was partially cleaved (Fig.3C, lane 1). When furin was co-expressed, Env expression was significantly reduced, in some experiments to the extent that the Env proteins were no longer visible on the gel (Fig.3C, lane 2; and data not shown). In contrast, the RRRRRR mutant

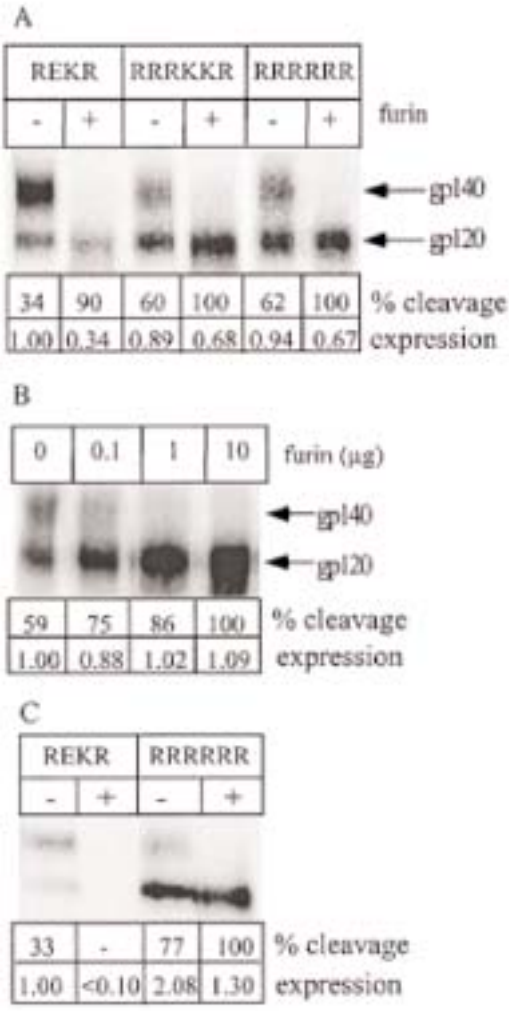

Fig. 3. Altering the cleavage sequence can increase Env processing by cellular proteases. **A.** JR-FL gp140 $_{SOS}$ with the wild type REKR cleavage site (lanes 1, 2) or the mutant RRRKKR (lanes 3, 4) or RRRRRR (lanes 5,6) cleavage site sequences was expressed in the absence (lanes 1, 3, 5) or presence (lanes 2, 4, 6) of co-transfected full-length furin. **B.** JR-FL gp140$_{SOS}$ RRRRRR was expressed with no (lane 1), 0.1µg (lane 2), 1µg (lane 3) or 10µg (lane 4) of co-transfected full-length furin. **C.** DU151 gp140$_{SOS}$ (lanes 1, 2) and its RRRRRR mutant (lanes 3, 4) was expressed in the absence (lanes 1,3) or presence of co-transfected full-length furin (lanes 2,4). All samples were labeled and immunoprecipitated as described in the legend to Fig. 2. The percent cleavage and relative expression of Env were calculated as in Fig. 2.

was more efficiently cleaved in the absence of furin, and was fully cleaved in the presence of furin. Furthermore, the overall expression of Env being greater than that of the wild-type gp140 (Fig.3C, compare lanes 2 and 4).

Effect of cleavage sites mutations on HIV-1 infectivity

We examined whether Env mutants containing basic cleavage site insertions were still functional for virus infection, using an Env-pseudotype assay (21). The JR-FL gp160$_{RRRRRR}$ mutant expressed by the pSV plasmid in 293T cells could successfully pseudotype pNL-luc, producing a virus capable of infecting HeLa-CD4-CCR5 cells. The infectivity of the JR-FL gp160$_{RRRRRR}$ Env pseudotype was about 3-4 fold lower than the JR-FL gp160$_{WT}$ pseudotype, but still in the range we find to be typical of pseudotyped virus stocks (Fig.4A). In an independent test of the functional activity of the mutant Env, we examined the ability of the JR-

FL $gp160_{RRRRRR}$ mutant to mediate cell-cell fusion, using a fluorescent cytoplasmic dye transfer assay (50). The modest, and statistically insignificant, increase in fusion with the RRRRRR mutant (Fig.4B) may be because it is expressed at 5 fold higher levels than the wild type gp160 by Western blot analysis of cell lysates. Overall, the REKR to RRRRRR substitution does not globally disrupt the Env conformation required for fusion and infection.

Discussion

The Env proteins of most enveloped viruses, including HIV-1, are synthesized as inactive precursors that are proteolytically processed to attain full functional activity. In the case of HIV-1, the gp160 precursor is cleaved into a fusion-active gp120/gp41 complex. The structures of a monomeric gp120 core fragment (45) and a post-fusion form of gp41 (14, 46, 92) have been determined. However, little is known about the structure of either uncleaved gp160 or the gp120/gp41 complex, although the latter is considered to be trimeric (14, 20, 46, 66, 92). The fusion-active complex is unstable, principally because the gp120-gp41 interaction is weak and gp120 is shed. We previously found that introducing a disulfide bond between gp120 and gp41 can prevent gp120-gp41 dissociation (6). However, the purified form of this protein ($gp140_{SOS}$) is monomeric, probably because of a further instability between the associated gp41 subunits (Chapter 5.3). To overcome this instability we are presently making both recombinant glycoproteins that mimic the native Env complex and also virus-like particles containing these Env forms. With or without additional modifications, Env glycoproteins of this type may be worth evaluating for their ability to elicit neutralizing antibodies.

Here we investigated methods to produce proteolytically processed proteins for future analytical and immunogenicity studies. The expression of gp140 or gp160 proteins at high levels usually leads to the production of a mixture of cleaved and uncleaved proteins, implying that processing of the cleavage site by host cell proteases is incomplete. Partial cleavage is a common phenomenon when Env is expressed in a variety of recombinant systems and cell lines (38, 55-58, 69, 78, 95). Differences in folding among natural and mutant Env proteins (19, 51, 84, 85, 88, 94) may affect the exposure of what is likely to be a loop structure containing the cleavage site (15). Another influence on Env cleavage is the direct or indirect masking of the furin recognition site by glycans (62). Overall, the accessibility of this site to the protease is a complex function of both Env folding and glycosylation (15, 58, 77).

We first evaluated the possibility of cleaving unprocessed, purified Env proteins by adding a purified protease *in vitro*. Although plasmin could efficiently process the gp120/gp41 cleavage site, as has been previously reported (61), it also cleaved gp120 at a second site, most probably within the V3 loop. This renders its use impractical. Purified furin can also cleave secreted Env (17, 18, 38, 56), albeit at low efficiency (17, 90). Our own findings were similar: Even when furin digestion of $gp140_{SOS}$ was performed at optimal pH with the enzyme in large excess, approximately 40% of the Env substrate remained uncleaved, suggesting that there may be a subpopulation of gp140 that is more resistant to cleavage. This may perhaps represent hyperglycosylated or misfolded proteins. Furin

Table 1. Summary of expression and cleavage efficiencies[a] of gp140 proteins with mutant cleavage sites

Cleavage	WT gp140		WT gp140 + furin		SOS gp140		SOS gp140 + furin	
	Cleavage (%)	Expression	Cleavage (%)	Expression	Cleavage (%)	Expression	Cleavage (%)	Expression
REKR	35	1.0	91	0.4	34	1.0	92	0.3
RRRKKR	66	0.9	100	0.7	60	0.9	100	0.8
RRRRKR	65	0.9	100	0.7	60	0.9	100	0.7
RRRRRR	71	1.0	100	0.9	62	0.9	100	0.9
KKRKKR	59	0.2	96	0.1	57	0.3	98	0.3
RERRRKKR	58	0.4	97	0.3	55	0.4	100	0.4

[a] The cleavage efficiency of various gp140 cleavage site mutants is given as a percentage derived from densitometric analysis. The percent cleavage value recorded represents the mean from at least 3 individual experiments in which the individual values did not deviate by more than 6% from the mean. Combined expression of gp140 and gp120 is also given as a ratio relative to the level of expression of the parental gp140+gp120 observed in transfections with $gp140_{WT}$ or $gp140_{SOS}$. Mean ratios from 3 repeats are given to the nearest decimal place and did not deviate more than 25% from this value. Data are shown for both $gp140_{WT}$ and $gp140_{SOS}$ proteins expressed both in the presence and absence of co-transfected furin.

is not an inherently inefficient enzyme - it is highly effective at cleaving synthetic peptides (13, 65) - but the conformation of its recognition site on gp160 limits its ability to cleave this particular substrate. That gp160 is an inherently poor substrate for furin is exemplified by a comparison of gp160 and anthrax toxin, the latter being cleaved by furin several orders of magnitude more efficiently than gp160 at pH 7.2 (53).

One way to augment gp160 cleavage is to co-express exogenous furin, but this can lead to a reduction in overall Env expression. The reduction of primary protein expression (including, but not limited to, HIV-1 Env) upon furin co-expression has been noted previously (6, 55, 57, 81, 90). One possible explanation is that furin may form stable complexes with Env proteins that it cleaves poorly, with these complexes being retained in the TGN or recycled to lysosomes, rather than secreted (38, 52, 57, 81, 93). This idea is supported by our observation that furin co-expression with Env mutants containing optimized cleavage sites caused very little reduction in Env expression. The co-expression of Env with either the full-length (membrane-bound) or the soluble form of furin reduced gp140 expression, so this reduction can occur without a direct association of the furin-Env complex with a membrane. Perhaps another, membrane-associated cellular protein is involved in the removal and degradation of complexes between uncleaved Env and furin. It has been shown that although truncated furin is shed into the culture medium, it can also still be isolated from membrane fractions like the full-length counterpart (52).

Although furin co-expression increases the cleavage of secreted gp140 proteins, it has been reported that this does not occur with full-length gp160 molecules expressed on the cell surface (38, 99, P. Poignard, personal communication). In contrast, we and others (90, 95), have found that gp160 cleavage can be at least partially augmented by furin, at least under some experimental conditions. Clearly, then, there are poorly understood variables that affect different

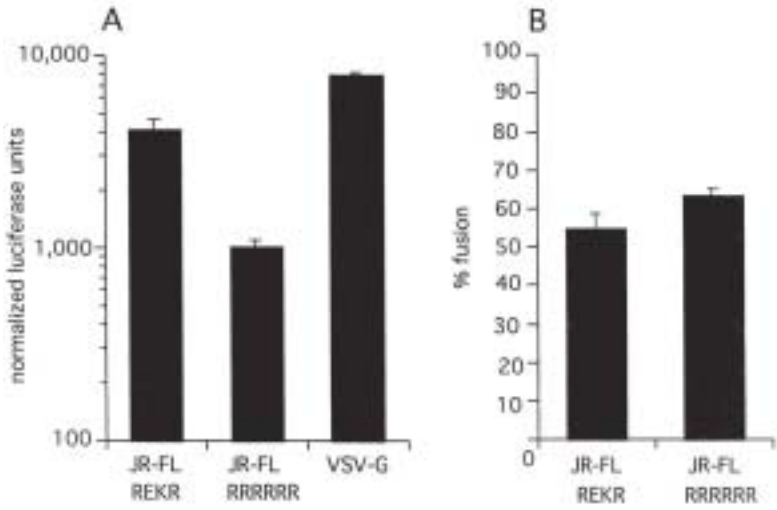

Fig. 4. Env cleavage site mutants are functional for infection and fusion. **A.** The infectivity for HeLa-CD4-CCR5 cells of pNL-luc viruses pseudotyped with wild-type JR-FL $gp160_{WT}$, the JR-FL $gp160_{RRRRRR}$ mutant or VSV-G was measured using a single round infection assay using a luciferase readout. Normalized luciferase values for negative control viruses lacking envelope (derived from pNL-luc transfection supernatants) were <1 unit. **B.** Cell-cell fusion mediated by the $gp160_{WT}$ or $gp160_{RRRRRR}$ proteins was analyzed in a dye transfer assay.

experimental systems differently, perhaps including the expression vectors, the particular Env gene and the cell line used.

Our most successful strategy for improving Env cleavage efficiency involved mutating the furin-recognition site. Studies of naturally occurring influenza A virus variants have revealed that insertion of basic amino-acids in and near the cleavage site of the HA_0 protein is associated with enhanced proteolysis (5), and frequently also with increased host cell range and virulence (5, 32, 36, 40, 41, 60). Moreover, improved cleavage of the influenza B glycoprotein was previously achieved by Brassard and Lamb, who substituted the conserved monobasic cleavage site with the multibasic cleavage sites found in virulent influenza A clones (10). We therefore considered it possible that altering the conserved, tetrameric cleavage recognition sequence of HIV-1 Env might increase cleavage efficiency. We found that several variant furin recognition sequences, based on those found in HA_0 proteins from pathogenic influenza A strains, allowed enhanced cleavage of HIV-1 Env in the absence of co-expressed furin. The best of these variant sequences were RRRKKR, RRRRKR and RRRRRR, which approximately doubled the extent of Env cleavage compared to that achieved when the standard REKR sequence was present. Furthermore, co-expression of furin did not reduce the expression of Env proteins containing these mutated sequences, but did allow the cleavage efficiency to now approach 100%. A consequence of the more efficient cleavage of these improved furin substrates may be the more rapid egress of Env from the secretory pathway, allowing a higher overall expression of fully processed Env. Furthermore, the REKR to RRRRRR

mutation had little impact on the infectivity of Env-complemented reporter viruses, or on Env-mediated membrane fusion. The cleavage site mutations do not, therefore, affect the overall folding of Env in any adverse manner, which is relevant to any consideration of the use of such Env mutants as vaccine antigens.
Although furin recognition of gp160 is rather inefficient, the strict conservation of the REKR sequence in HIV-1 (or of RNKR in SIV) suggests that this sequence confers a selective advantage to the virus. There are no examples of Env sequences with basic residue insertions adjacent to the consensus cleavage-site motif (44), so a higher rate of Env cleavage may be disadvantageous. For example, a too-rapid destruction of the infected cell by fusion caused by high levels of processed, cell-surface Env could reduce the yield of progeny virions from that cell. An immunological mechanism might be that uncleaved Env is actually beneficial to the virus by acting as a decoy that causes the induction of predominantly non-neutralizing antibodies (12, 63, 70).

Here we have demonstrated that we can produce HIV-1 Env mutants containing polybasic cleavage sites that are more efficient substrates for furin than the consensus, REKR, sequence. The use of these Env mutants should simplify the production of significant amounts of cleaved Env, which may be useful in HIV-1 vaccine design.

Acknowledgements

We are grateful to Sean Molloy and Gary Thomas for advice and for the vv:hfur virus. We thank Maceij Paluch and Daryl Schiller for technical assistance, Norbert Schülke for providing purified $gp140_{SOS}$, and Gregory Melikyan and Levon Abrahamyan for assistance and advice with the fusion experiments. We thank Pascal Poignard for useful discussions. This work was supported by NIH grants AI49566 (JMB) and AI45463 (JPM). JPM is an Elizabeth Glaser Scientist of the Pediatric AIDS Foundation, and a Stavros S. Niarchos Scholar. The Department of Microbiology and Immunology at the Weill Medical College gratefully acknowledges the support of the William Randolph Hearst Foundation.

References

1. **Abacioglu, Y. H., T. R. Fouts, J. D. Laman, E. Claassen, S. H. Pincus, J. P. Moore, C. A. Roby, R. Kamin-Lewis, and G. K. Lewis.** 1994. Epitope mapping and topology of baculovirus-expressed HIV-1 gp160 determined with a panel of murine monoclonal antibodies. AIDS Res. Hum. Retrovir. **10:**371-381.
2. **Adams, O., H. Schall, and A. Scheid.** 2000. Natural variation in the amino acid sequence around the HIV-1 glycoprotein gp160 cleavage site and its effect on cleavability, subunit association and membrane fusion. AIDS Res. Hum. Retrovir. **16:**1235-1245.
3. **Angliker, H., U. Neumann, S. S. Molloy, and G. Thomas.** 1995. Internally quenched fluorogenic substrate for furin. Anal. Biochem. **224**:409-412.
4. **Barnett, S. W., S. Lu, I. Srivastava, S. Cherpelis, A. Gettie, J. Blanchard, S. Wang, I. Mboudjeka, L. Leung, Y. Lian, A. Fong, C. Buckner, A. Ly, S. Hilt, J. Ulmer, C. T. Wild, J. R. Mascola, and L. Stamatatos.** 2001. The ability of an oligomeric human immunodeficiency virus type 1 (HIV-1) envelope antigen to elicit neutralizing antibodies against primary HIV-1 isolates is

improved following partial deletion of the second hypervariable region. J. Virol. **75:**5526-5540.
5. **Bender, C., H. Hall, J. Huang, A. Klimov, N. Cox, A. Hay, V. Gregory, K. Cameron, W. Lim, and K. Subbarao.** 1999. Characterization of the surface proteins of influenza A (H5N1) viruses isolated from humans in 1997-1998. Virology **254:**115-123.
6. **Binley, J. M., R. W. Sanders, B. Clas, N. Schuelke, A. Master, Y. Guo, F. Kajumo, D. J. Anselma, P. J. Maddon, W. C. Olson, and J. P. Moore.** 2000. A recombinant human immunodeficiency virus type 1 envelope glycoprotein complex stabilized by an intermolecular disulfide bond between the gp120 and gp41 subunits is an antigenic mimic of the trimeric virion-associated structure. J. Virol. **74:**627-643.
7. **Binley, J. M., B. Clas, A. Gettie, M. Vesanen, D. C. Montefiori, L. Sawyer, J. Booth, M. Lewis, P. A. Marx, S. Bonhoeffer, and J. P. Moore.** 2000. Passive infusion of immune serum into simian immunodeficiency virus-infected rhesus macaques undergoing a rapid disease course has minimal effect on plasma viremia. Virology **270:**237-249.
8. **Bolt, G., L. O. Pederson, and H. H. Birkeslund.** 2000. Cleavage of the respiratory syncytial virus fusion protein is required for its surface expression: role of furin. Virus Res. **68:**25-33.
9. **Bosch, V., and M. Pawlita.** 1990. Mutational analysis of the human immunodeficiency virus type 1 *env* gene product proteolytic cleavage site. J. Virol. **64:**2337-2344.
10. **Brassard, D. L., and R. A. Lamb.** 1997. Expression of influenza B virus hemagglutinin containing multibasic residue cleavage sites. Virology **236:**234-248.
11. **Burton, D. R.** 1997. A vaccine for HIV type 1: the antibody perspective. Proc. Natl. Acad. Sci. USA **94:**10018-10023.
12. **Burton, D. R., and P. H. W. I. Parren.** 2000. Vaccines and the induction of functional antibodies: time to look beyond the molecules of natural infection? Nat. Med. **6:**123-125.
13. **Cameron, A., J. Appel, R. A. Houghten, and I. Lindberg.** 2000. Polyarginines are potent furin inhibitors. J. Biol. Chem. **275:**36741-36749.
14. **Chan, D. C., D. Fass, J. M. Berger, and P. S. Kim.** 1997. Core structure of gp41 from the HIV envelope glycoprotein. Cell **89:**263-273.
15. **Chen, J., K. H. Lee, D. A. Steinhauer, D. J. Stevens, J. J. Skehel, and D. C. Wiley.** 1998. Structure of the hemagglutinin precursor cleavage site, a determinant of influenza pathogenicity and the origin of labile conformation. Cell **95:**409-417.
16. **Clements, G. J., M. J. Price-Jones, P. E. Stephens, C. Sutton, T. F. Schulz, P. R. Clapham, J. A. McKeating, M. O. McClure, S. Thomson, M. Marsh, J. Kay, R. A. Weiss, and J. P. Moore.** 1991. The V3 loops of the HIV-1 and HIV-2 surface glycoproteins contain proteolytic cleavage sites: a possible function in viral fusion? AIDS Res. Hum. Retrovir. **7:**3-16.
17. **Decroly, E., M. Vandenbranden, J. M. Ruysschaert, J. Cogniaux, G. S. Jacob, S. C. Howard, G. Marshall, A. Kompelli, A. Basak, F. Jean, C. Lazure, S. Benjannet, M. Chretien, R. Day, and N. G. Seidah.** 1994. The convertases furin and PC1 can both cleave the human immunodeficiency virus (HIV-1) envelope glycoprotein gp160 into gp120 (HIV-1 SU) and gp41 (HIV-I TM). J. Biol. Chem. **269:**12240-12247.
18. **Decroly, E., S. Wouters, C. Di Bello, C. Lazure, J.-M. Ruysschaert, and N. G. Seidah.** 1996. Identification of the paired basic convertases implicated in HIV gp160 processing based on in vitro assays and expression in $CD4^+$ cell lines. J. Biol. Chem. **271:**30442-30450.
19. **Dedera, D., R. L. Gu, and L. Ratner.** 1992. Conserved cysteine residues in the human immunodeficiency virus type 1 transmembrane envelope protein are essential for precursor envelope cleavage. J. Virol. **66:**1207-1209.
20. **Doms, R. W., R. A. Lamb, J. K. Rose, and A. Helenius.** 1993. Folding and assembly of viral membrane proteins. Virology **193:**545-562.
21. **Dragic, T., V. Litwin, G. P. Allaway, S. R. Martin, Y. Huang, K. A. Nagashima, C. Cayanan, P. J. Maddon, R. A. Koup, J. P. Moore, and W. A. Paxton.** 1996. HIV-1 entry into $CD4^+$ cells is mediated by the chemokine receptor CC-CKR-5. Nature **381:**667-673.
22. **Dubay, J. W., S. R. Dubay, H. J. Shin, and E. Hunter.** 1995. Analysis of the cleavage site of the human immunodeficiency virus type 1 glycoprotein: requirement of precursor cleavage for glycoprotein incorporation. J. Virol. **69:**4675-4682.
23. **Dutch, R. E., R. N. Hagglund, M. A. Nagel, R. G. Paterson, and R. A. Lamb.** 2001. Paramyxovirus fusion (F) protein: a conformational change on cleavage activation. Virology **281:**138-150.
24. **Earl, P. L., B. Moss, and R. W. Doms.** 1994. Folding, interaction with GRP78-BiP, assembly and

transport of the human immunodeficiency virus type 1 envelope protein. J. Virol. **65:**2047-2055.
25. **Earl, P. L., W. Sugiura, D. C. Montefiori, C. C. Broder, S. A. Lee, C. Wild, J. Lifson, and B. Moss.** 2001. Immunogenicity and protective efficacy of oligomeric human immunodeficiency virus type 1 gp140. J. Virol. **75:**645-653.
26. **Farzan, M., H. Choe, E. Desjardins, Y. Sun, J. Kuhn, J. Cao, D. Archambault, P. Kolchinsky, M. Koch, R. Wyatt, and J. Sodroski.** 1998. Stabilization of human immunodeficiency virus type 1 envelope glycoprotein trimers by disulfide bonds introduced into the gp41 glycoprotein ectodomain. J. Virol. **72:**7620-7625.
27. **Ferlenghi, I., B. Gowen, F. de Haas, E. J. Mancini, H. Garoff, M. Sjoberg, and S. J. Fuller.** 1998. The first step: activation of the Semliki Forest virus spike protein precursor causes a localized conformational change in the trimeric spike. J. Mol. Biol. **283:**71-81.
28. **Franzusoff, A., A. M. Volpe, D. Josse, S. Pichuantes, and J. R. Wolf.** 1995. Biochemical and genetic definition of the cellular protease required for HIV-1 gp160 processing. J. Biol. Chem. **270:**3154-3159.
29. **Freed, E. O., D. J. Myers, and R. Risser.** 1989. Mutational analysis of the cleavage sequence of the human immunodeficiency virus type 1 envelope glycoprotein precursor gp160. J. Virol. **63:**4670-4675.
30. **Gelderblom, H. R., H. Reupke, and G. Pauli.** 1985. Loss of envelope antigens of HTLV-III/LAV, a factor in AIDS pathogenesis? Lancet **ii:**1016-1017.
31. **Gluschankof, P., I. Mondor, H. R. Gelderblom, and Q. J. Sattentau.** 1997. Cell membrane vesicles are a major contaminant of gradient-enriched human immunodeficiency virus type-1 preparations. Virology **230:**125-133.
32. **Goto, H., and Y. Kawaoka.** 1998. A novel mechanism for the acquisition of virulence by a human influenza A virus. Proc. Natl. Acad. Sci. USA **95:**10224-10228.
33. **Guo, H. G., F. M. Veronese, E. Tschachler, R. Pal, V. S. Kalyanaraman, R. C. Gallo, and M. S. Reitz, Jr.** 1990. Characterization of an HIV-1 point mutant blocked in envelope glycoprotein cleavage. Virology **174:**217-224.
34. **Hallenberger, S., M. Moulard, M. Sordel, H.-D. Klenk, and W. Garten.** 1997. The role of eukaryotic subtilisin-like endoproteases for the activation of human immunodeficiency virus glycoproteins in natural host cells. J. Virol. **71:**1036-1045.
35. **Heinz, F. X., S. L. Allison, K. Stiasny, J. Schalich, H. Holzmann, C. W. Mandl, and C. Kunz.** 1995. Recombinant and virion-derived soluble and particulate immunogens for vaccination against tick-borne encephalitis. Vaccine **13:**1636-1642.
36. **Horimoto, T., E. Rivera, J. Pearson, D. Senne, S. Krauss, Y. Kawaoka, and R. G. Webster.** 1995. Origin and molecular changes associated with emergence of a highly pathogenic H5N2 influenza virus in Mexico. Virology **213:**223-230.
37. **Hu, S. L., J. Klaniecki, T. Dykers, P. Sridhar, and B. M. Travis.** 1991. Neutralizing antibodies against HIV-1 BRU and SF2 isolates generated in mice immunized with recombinant vaccinia virus expressing HIV-1 (BRU) envelope glycoproteins and boosted with homologous gp160. AIDS Res. Hum. Retrovir. **7:**615-620.
38. **Inocencio, N. M., J. F. Sucic, J. M. Moehring, M. J. Spence, and T. J. Moehring.** 1997. Endoprotease activities other than furin and PACE4 with a role in processing of HIV-I gp160 glycoproteins in CHO-K1 cells. J. Biol. Chem. **272:**1344-1348.
39. **Iwatani, Y., K. Kawano, T. Ueno, M. Tanaka, A. Ishimoto, M. Ito, and H. Sakai.** 2001. Analysis of dominant-negative effects of mutant env proteins of human immunodeficiency virus type 1. Virology **286:**45-53.
40. **Kawaoka, Y.** 1991. Structural features influencing hemagglutinin cleavability in a human influenza A virus. J. Virol. **65:**1195-1201.
41. **Kawaoka, Y., and R. G. Webster.** 1988. Sequence requirements for cleavage activation of influenza virus hemagglutinin expressed in mammalian cells. Proc. Natl. Acad. Sci. USA **85:**324-328.
42. **Klenk, H.-D., and W. Garten.** 1994. Activation of cleavage of viral spike proteins by host proteases, p. 241-280. *In* E. Wimmer (ed.), Cellular receptors for animal viruses. Cold Spring Harbor Laboratory Press, Cold Spring Harbor, N.Y.
43. **Kozarsky, K., M. Penman, L. Barsiripour, W. Haseltine, J. Sodroski, and M. Krieger.** 1989. Glycosylation and processing of the human immunodeficiency virus type 1 envelope protein. J.

Acquir. Immune Defic. Syndr. **2:**163-169.
44. **Kuiken, C., B. Foley, B. Hahn, P. Marx, F. McCutchan, J. Mellors, J. Mullins, S. Wolinsky, and B. Korber.** 2000. HIV sequence compendium. Theoretical Biology and Biophysics Group, Los Alamos National Laboratory, Los Alamos, N.Mex.
45. **Kwong, P. D., R. Wyatt, J. Robinson, R. W. Sweet, J. Sodroski, and W. A. Hendrickson.** 1998. Structure of an HIV gp120 envelope glycoprotein in complex with the CD4 receptor and a neutralizing human antibody. Nature **393:**648-659.
46. **Lu, M., S. Blackow, and P. Kim.** 1995. A trimeric structural domain of the HIV-1 transmembrane glycoprotein. Nat. Struct. Biol. **2:**1075-1085.
47. **Ly, A., and L. Stamatatos.** 2000. V2 loop glycosylation of the human immunodeficiency virus type 1 SF162 envelope facilitates interaction of this protein with CD4 and CCR5 receptors and protects the virus from neutralization by anti-V3 loop and anti-CD4 binding site antibodies. J. Virol. **74:**6769-6776.
48. **McCune, J. M., L. B. Rabin, M. B. Feinberg, M. Lieberman, J. C. Kosek, G. R. Reyes, and I. L. Weissman.** 1988. Endoproteolytic cleavage of gp160 is required for the activation of human immunodeficiency virus. Cell **53:**55-67.
49. **McKeating, J. A., A. McKnight, and J. P. Moore.** 1991. Differential loss of envelope glycoprotein gp120 from virions of human immunodeficiency virus type 1 isolates: effects on infectivity and neutralization. J. Virol. **65:**852-860.
50. **Melikyan, G. B., R. M. Markosyan, H. Hemmati, M. K. Delmedico, D. M. Lambert, and F. S. Cohen.** 2000. Evidence that the transition of HIV-1 gp41 into a six-helix bundle, not the bundle configuration, induces membrane fusion. J. Cell Biol. **151:**413-423.
51. **Merat, R., H. Raoul, T. Leste-Lasserre, P. Sonigo, and G. Pancino.** 1999. Variable constraints on the principal immunodominant domain of the transmembrane glycoprotein of human immunodeficiency virus type 1. J. Virol. **73:**5698-5706.
52. **Molloy, S., L. Thomas, J. K. VanSlyke, P. E. Stenberg, and G. Thomas.** 1994. Intracellular trafficking and activation of the furin proprotein convertase: localization to the TGN and recycling from the cell surface. EMBO J. **13:**18-33.
53. **Molloy, S. S., P. A. Bresnahan, S. H. Leppla, K. R. Klimpel, and G. Thomas.** 1992. Human furin is a calcium-dependent serine endoprotease that recognizes the sequence Arg-X-X-Arg and efficiently cleaves anthrax toxin protective antigen. J. Biol. Chem. **267:**16396-16402.
54. **Moore, J. P., J. A. McKeating, R. A. Weiss, and Q. J. Sattentau.** 1990. Dissociation of gp120 from HIV-1 virions induced by soluble CD4. Science **250:**1139-1142.
55. **Morikawa, Y., E. Barsov, and I. Jones.** 1993. Legitimate and illegitimate cleavage of human immunodeficiency virus glycoproteins by furin. J. Virol. **67:**3601-3604.
56. **Moulard, M., L. Chaloin, L. Canarelli, K. Mabrouk, H. Darbon, and L. Challoin.** 1998. Retroviral envelope processing: structural investigation of the cleavage site. Biochemistry **37:**4510-4517.
57. **Moulard, M., S. Hallenberger, W. Garten, and H. D. Klenk.** 1999. Processing and routage of HIV glycoproteins by furin to the cell surface. Virus Res. **60:**55-65.
58. **Moulard, M., and E. Decroly.** 2000. Maturation of HIV envelope glycoprotein precursors by cellular proteases. Biochem. Biophys. Acta **1469:**121-132.
59. **Muster, T., F. Steindl, M. Purtscher, A. Trkola, A. Klima, G. Himmler, F. Ruker, and H. Katinger.** 1993. A conserved neutralizing epitope on gp41 of human immunodeficiency virus type 1. J. Virol. **67:**6642-6647.
60. **Ohuchi, M., M. Orlich, R. Ohuchi, B. E. Simpson, W. Garten, H. D. Klenk, and R. Rott.** 1989. Mutations at the cleavage site of the hemagglutinin alter the pathogenicity of influenza virus A/chick/Penn/83 (H5/N2). Virology **168:**274-280.
61. **Okumura, Y., M. Yano, M. Murakami, S. Mori, T. Towatari, and H. Kido.** 1999. The extracellular processing of HIV-1 envelope glycoprotein gp160 by human plasmin. FEBS Lett. **442:**39-42.
62. **Paredes, A. M., H. Heidner, P. Thuman-Commike, B. V. Venkataram Prasad, R. E. Johnston, and W. Chiu.** 1998. Structural localization of the E3 glycoprotein in attenuated sindbis virus mutants. J. Virol. **72:**1534-1541.
63. **Parren, P. W. H. I., D. R. Burton, and Q. J. Sattentau.** 1997. HIV-1 antibody—debris or virion? Nat. Med. **3:**366-367.

64. **Parren, P. W. H. I., and D. R. Burton.** 2001. The antiviral activity of antibodies in vitro and in vivo. Adv. Immunol. **77:**195-262.
65. **Plaimauer, B., G. Mohr, W. Wernhart, M. Himmelspach, F. Dorner, and U. Schlokat.** 2001. 'Shed' furin: mapping of the cleavage determinants and identification of its C-terminus. Biochem. J. **354:**689-695.
66. **Poignard, P., E. Ollman Saphire, P. W. H. I. Parren, and D. R. Burton.** 2001. gp120: biologic aspects of structural features. Annu. Rev. Immunol. **19:**253-274.
67. **Polacino, P. S., V. Stallard, J. E. Klaniecki, S. Pennathur, D. C. Montefiori, A. J. Langlois, B. A. Richardson, W. R. Morton, R. E. Benveniste, and S. L. Hu.** 1999. Role of immune responses against the envelope and the core antigens of simian immunodeficiency virus SIVmne in protection against homologous cloned and uncloned virus challenge in macaques. J. Virol. **73:**8201-8215.
68. **Richardson, T. M., Jr., B. L. Stryjewski, C. C. Broder, J. A. Hoxie, J. R. Mascola, P. L. Earl, and R. W. Doms.** 1996. Humoral response to oligomeric human immunodeficiency virus type 1 envelope protein. J. Virol. **70:**753-762.
69. **Rodriguez, D., J. R. Rodriguez, and M. Esteban.** 1995. Enhanced proteolytic processing of the human immunodeficiency virus type 1 envelope protein in murine Ltk$^-$ cells. AIDS Res. Hum. Retrovir. **11:**81-85.
70. **Sakurai, H., R. A. Williamson, J. E. Crowe, J. A. Beeler, P. Poignard, R. B. Bastidas, R. M. Chanock, and D. R. Burton.** 1999. Human antibody responses to mature and immature forms of viral envelope in respiratory syncytial virus infection: significance for subunit vaccines. J. Virol. **73:**2956-2962.
71. **Salminen, A., J. M. Wahlberg, M. Lobigs, P. Liljestrom, and H. Garoff.** 1992. Membrane fusion process of Semliki Forest virus. II. Cleavage-dependent reorganization of the spike protein complex controls virus entry. J. Cell Biol. **116:**349-357.
72. **Sanders, R. W., L. Schiffner, A. Master, F. Kajumo, Y. Guo, T. Dragic, J. P. Moore, and J. M. Binley.** 2000. Variable-loop-deleted variants of the human immunodeficiency virus type 1 envelope glycoprotein can be stabilized by an intermolecular disulfide bond between the gp120 and gp41 subunits. J. Virol. **74:**5091-5100.
73. **Schalich, J., S. L. Allison, K. Stiasny, C. W. Mandl, C. Kunz, and F. X. Heinz.** 1996. Recombinant subviral particles from tick-borne encephalitis virus are fusogenic and provide a model system for studying flavivirus envelope glycoprotein functions. J. Virol. **70:**4549-4557.
74. **Schneider, J., O. Kaaden, T. D. Copeland, S. Oroszlan, and G. Hunsmann.** 1986. Shedding and interspecies type sero-reactivity of the envelope glycopolypeptide gp120 of the human immunodeficiency virus. J. Gen. Virol. **67:**2533-2538.
75. **Schulz, T. F., J. D. Reeves, J. G. Hoad, C. Tailor, P. Stephens, G. Clements, S. Ortlepp, K. A. Page, J. P. Moore, and R. A. Weiss.** 1993. Effect of mutations in the V3 loop of HIV-1 gp120 on infectivity and susceptibility to proteolytic cleavage. AIDS Res. Hum. Retrovir. **9:**159-166.
76. **Sergel, T. A., L. W. McGinnes, and T. G. Morrison.** 2001. Mutations in the fusion peptide and adjacent heptad repeat inhibit folding or activity of the Newcastle disease virus fusion protein. J. Virol. **75:**7934-7943.
77. **Singh, J., and T. Compton.** 2000. Characterization of a panel of insertion mutants in human cytomegalovirus glycoprotein B. J. Virol. **74:**1383-1392.
78. **Spies, C. P., and R. W. Compans.** 1994 Effects of cytoplasmic domain length on cell surface expression and syncytium-forming capacity of the simian immunodeficiency virus envelope glycoprotein. Virology **203:**8-19.
79. **Stadler, K., S. L. Allison, J. Schalich, and F. X. Heinz.** 1997. Proteolytic activation of tick-borne encephalitis virus by furin. J. Virol. **71:**8475-8481
80. **Stamatatos, L., M. Lim, and C. Cheng-Mayer.** 2000 Generation and structural analysis of soluble oligomeric gp140 envelope proteins derived from neutralization-resistant and neutralization-susceptible primary HIV type 1 isolates. AIDS Res. Hum. Retrovir. **16:**981-994.
81. **Staropoli, I., C. Chanel, M. Girard, and R. Altmeyer.** 2000. Processing, stability and receptor binding properties of oligomeric envelope glycoprotein from a primary HIV-1 isolate. J. Biol. Chem. **275:**35137-35145.
82. **Stein, B. S., and E. G. Engleman.** 1990. Intracellular processing of the gp160 HIV-1 envelope precursor. Endoproteolytic cleavage occurs in a *cis* or medial compartment of the Golgi complex.

J. Biol. Chem. **265:**2640-2649.
83. **Sugrue, R. J., C. Brown, G. Brown, J. Aitken, and H. W. M. Rixon.** 2001. Furin cleavage of the respiratory syncytial virus fusion protein is not a requirement for its transport to the surface of virus-infected cells. J. Gen. Virol **82:**1375-1386.
84. **Syu, W. J., W. R. Lee, B. Du, Q. C. Yu, M. Essex, and T. H. Lee.** 1991. Role of conserved gp41 cysteine residues in the processing of human immunodeficiency virus envelope precursor and viral infectivity. J. Virol. **65:**6349-6352.
85. **Travis, B. M., T. I. Dykers, D. Hewgill, J. Ledbetter, T. T. Tsu, S. L. Hu, and J. B. Lewis.** 1992. Functional roles of the V3 hypervariable region of HIV-1 gp160 in the processing of gp160 and in the formation of syncytia in $CD4^+$ cells. Virology **186:**313-317.
86. **Trkola, A., T. Dragic, J. Arthos, J. M. Binley, W. C. Olson, G. P. Allaway, C. Cheng Mayer, J. Robinson, P. J. Maddon, and J. P. Moore.** 1996. CD4-dependent, antibody-sensitive interactions between HIV-1 and its co-receptor CCR-5. Nature **384:**184-187.
87. **Trkola, A., J. Matthews, C. Gordon, T. Ketas, and J. P. Moore.** 1999. A cell line-based assay for primary human immunodeficiency virus type 1 isolates that use either the CCR5 or the CXCR4 coreceptor. J. Virol. **73:**8966-8974.
88. **Tschachler, E., H. Buchow, R. C. Gallo, and M. S. Reitz, Jr.** 1990. Functional contribution of cysteine residues to the human immunodeficiency virus type 1 envelope. J. Virol. **64:**2250-2259.
89. **Volchkov, V., H. Feldmann, V. A. Volchkova, and H.-D. Klenk.** 1998. Processing of the Ebola virus glycoprotein by the proprotein convertase furin. Proc. Natl. Acad. Sci. USA **95:**5762-5767.
90. **Vollenweider, F., S. Benjannet, E. Decroly, D. Savaria, C. Lazure, G. Thomas, M. Chretien, and N. G. Seidah.** 1996. Comparative cellular processing of the human immunodeficiency virus (HIV-1) envelope glycoprotein gp160 by the mammalian subtilisin/kexin-like convertases. Biochem. J. **314:**521-532.
91. **Weidmann, A., A. Maisner, W. Garten, M. Seufert, V. ter Meulen, and S. Schneider-Schaulies.** 2000. Proteolytic cleavage of the fusion protein but not membrane fusion is required for measles virus-induced immunosuppression in vitro. J. Virol. **74:**1985-1993.
92. **Weissenhorn, W., A. Dessen, S. C. Harrison, J. J. Skehel, and D. C. Wiley.** 1997. Atomic structure of the ectodomain from HIV-1 gp41. Nature **387:**426-430.
93. **Willey, R. L., J. S. Bonifacino, B. J. Potts, M. A. Martin, and R. D. Klausner.** 1988. Biosynthesis, cleavage, and degradation of the human immunodeficiency virus 1 envelope glycoprotein gp160. Proc. Natl. Acad. Sci. USA **85:**9580-9584.
94. **Willey, R. L., T. Klimkait, D. M. Frucht, J. S. Bonifacino, and M. A. Martin.** 1991. Mutations within the human immunodeficiency virus type 1 gp160 envelope glycoprotein alter its intracellular transport and processing. Virology **184:**313-321.
95. **Yamshchikov, G. V., G. D. Ritter, M. Vey, and R. W. Compans.** 1995. Assembly of SIV virus-like particles containing envelope proteins using a baculovirus expression system. Virology **214:**50-58.
96. **Yang, X., L. Florin, M. Farzan, P. Kolchinsky, P. Kwong, J. Sodroski, and R. Wyatt.** 2000. Modifications that stabilize human immunodeficiency virus envelope glycoprotein trimers in solution. J. Virol. **74:**4746-4754.
97. **Yang, X., M. Farzan, R. Wyatt, and J. Sodroski.** 2000. Characterization of stable, soluble trimers containing complete ectodomains of human immunodeficiency virus type 1 envelope glycoproteins. J. Virol. **74:**5716-5725.
98. **Yang, X., R. Wyatt, and J. Sodroski.** 2001. Improved elicitation of neutralizing antibodies against primary human immunodeficiency viruses by soluble stabilized envelope glycoprotein trimers. J. Virol. **75:**1165-1171.
99. **York, J., K. E. Follis, M. Trahey, P. N. Nyambi, S. Zolla-Pazner, and J. H. Nunberg.** 2001. Antibody binding and neutralization of primary and T-cell line-adapted isolates of human immunodeficiency virus type 1. J. Virol. **75:**2741-2752.

Chapter 5.6

Stabilization of the soluble, cleaved, trimeric form of the envelope glycoprotein complex of HIV-1

(*Journal of Virology,* September 2002, p. 8875-8889)

Rogier W. Sanders[1,2], Mika Vesanen[1], Norbert Schülke[3], Aditi Master[1], Linnea Schiffner[1], Roopa Kalyanaraman[1], Maciej Paluch[1], Ben Berkhout[2], Paul I. Maddon[3], William C. Olson[3], Min Lu[4], John P. Moore[1]

[1]Dept. of Microbiology and Immunology and [4]Dept. of Biochemistry, Weill Medical College of Cornell University, 1300 York Ave., New York, NY 10021.

[2]Dept. of Human Retrovirology, Academic Medical Center, University of Amsterdam, Meibergdreef 15, 1105 AZ Amsterdam, The Netherlands.

[3]Progenics Pharmaceuticals, 777 Old Saw Mill River Rd., Tarrytown, NY 10591.

The envelope glycoprotein (Env) complex of human immunodeficiency virus type 1 (HIV-1) has evolved a structure that is minimally immunogenic while retaining its natural function of receptor-mediated virus-cell fusion. The Env complex is trimeric; its six individual subunits (3 gp120's, 3 gp41's) are associated by relatively weak, non-covalent interactions. The induction of neutralizing antibodies after vaccination with individual Env subunits has proven very difficult, probably because they are inadequate mimics of the native complex. Our hypothesis is that a stable form of the Env complex, perhaps with additional modifications to rationally alter its antigenic structure, may be a better immunogen than the individual subunits. A soluble Env protein, SOS gp140, can be made that has gp120 stably linked to the gp41 ectodomain by an intermolecular disulfide bond. This protein is fully cleaved at the proteolysis site between gp120 and gp41. However, the gp41–gp41 interactions in SOS gp140 are too weak to maintain the protein in a trimeric configuration. Consequently, the purified SOS gp140 protein is a monomer (chapter 5.3). Here we describe modifications of the SOS gp140 protein that increase its trimer stability. A variant SOS gp140 protein, designated SOSIP gp140, contains an isoleucine-to-proline substitution at position 559 in the N-terminal heptad repeat region of gp41. This protein is fully cleaved, has favorable antigenic properties and is predominantly trimeric. SOSIP gp140 trimers are non-covalently associated and can be partially purified by gel-filtration chromatography. These gp140 trimers are dissociated into monomers by anionic detergent or heat, but are relatively resistant to non-ionic detergents, high salt concentrations or exposure to mildly acidic pH. The SOSIP gp140 protein should be a useful reagent for structural and immunogenicity studies.

Introduction

The envelope glycoprotein (Env) complex of human immunodeficiency virus type 1 (HIV-1) mediates viral entry into $CD4^+$ cells. The sequential binding of the surface subunit gp120 to the CD4 receptor and a co-receptor, usually CCR5 or CXCR4, induces conformational changes in the Env complex. These alterations in protein structure eventually enable the insertion of the hydrophobic fusion peptide of the transmembrane subunit, gp41, into the cell membrane. Subsequently, the viral and cell membranes fuse, allowing the release of the viral core into the cytoplasm and the initiation of a new cycle of infection (for reviews see (17,24,25,31,61,99)). The gp120 and gp41 proteins are synthesized as a gp160 precursor that is cleaved within the cell to yield the native, pre-fusion form of the envelope glycoprotein complex (39,55,63). This is generally considered to be a trimeric structure, containing three gp120 and three gp41 moieties, held together by non-covalent interactions (31,73,99). The native Env complex is unstable, because the non-covalent intersubunit interactions that hold gp120 onto gp41 are weak, as are the intermolecular interactions between the gp41 moieties (31,73,99). This instability is probably essential for the receptor-triggered conformational changes to occur, but it does cause a problem for attempts to express the native complex as a recombinant protein (5).

One reason to prepare recombinant forms of the native Env complex is for structural studies. At present, structural information on HIV-1 Env is limited to core fragments of gp120 in the CD4-associated configuration, and the six-helix bundle form of the gp41 core which represent its terminal, most stable configuration (10,16,45,46,51,54,89,94). Although the six-helix bundle is often referred to as the "fusogenic" form of gp41, this term can be misleading, because it is the formation and not the mere presence of the six-helix bundle that drives membrane fusion (25,35,56). Hence, antibodies to the six-helix bundle cannot interfere with fusion, and are non-neutralizing (42,59,65,71,90). We therefore use the term "post-fusion" form of gp41 when referring to the six-helix bundle, to reflect its persistence on infected cells as a major immunogen after the fusion process is complete, and on virions when conformational changes in Env leading to gp120 shedding have occurred prematurely or abortively (25). Most antibodies to gp41 in HIV-1-infected individuals recognize this post-fusion conformation (36,59,71,78,90,100).

A second reason to make the native Env complex is to study its immunogenicity and determine its suitability as a vaccine antigen. The few monoclonal antibodies (MAbs) that potently neutralize HIV-1 all recognize epitopes exposed on the native Env complex, and may well have been induced by such a complex (9,34,58,69-71,73,81). In contrast, non-neutralizing MAbs do not bind to the native complex, and probably represent immune responses to non-native forms of Env, such as uncleaved gp160 precursors, dissociated gp120 subunits or the six-helix bundle, post-fusion form of gp41 (9,59,69,70,73).

Eliciting neutralizing antibodies by vaccination with any form of Env is problematic, because of the mechanisms that the native Env complex has evolved to shield its most critical sites, and to limit its overall immunogenicity. Thus, conserved regions of gp120 involved in receptor binding are shielded by variable loops and by extensive glycosylation. The CD4 binding site is recessed, and the

co-receptor binding site is only formed or exposed for a short period after CD4 has already bound, thereby limiting the time and space available for antibody interference (57,58,66,97). Whether such defense mechanisms can be overcome by vaccine-induced antibodies remains uncertain (59,71). Our approach to the problem has been to try to make a stabilized native Env complex, which may then have to be further modified to improve its immunogenicity.

The lability of the non-covalent interaction between gp120 and the gp41 ectodomain ($gp41_{ECTO}$) is an obstacle to the production of stable, fully processed HIV-1 Env trimers. We have previously reported that the association between gp120 and $gp41_{ECTO}$ can be stabilized by the introduction of a correctly positioned intermolecular disulfide bond, to make the SOS gp140 protein (5,79). In the presence of co-transfected furin, the peptide bond linking gp120 to $gp41_{ECTO}$ is cleaved, allowing us to produce properly processed gp140 proteins (5,79). We initially reported that oligomeric proteins were present in supernatants from 293T cells transiently expressing SOS gp140 (5). However, these oligomers were not abundant, and they did not survive purification: purified SOS gp140 is a monomeric protein (83). We now describe a way to further stabilize the gp41-gp41 interactions in SOS gp140 proteins. We have introduced amino-acid substitutions into the N-terminal heptad-repeat region of gp41 that we hypothesize destabilize the post-fusion form of the protein and thereby render the transition to this configuration less likely. One such protein, SOS I559P gp140 (designated SOSIP), is properly folded, proteolytically cleaved, substantially trimeric and has appropriate receptor-binding and antigenic properties. The SOSIP gp140 trimer can be converted to the monomeric form by heat or anionic detergent, but is partially resistant to nonionic detergents.

Materials and methods

Env expression

Various forms of the JR-FL gp140 envelope glycoproteins were expressed in 293T cells from the pPPI4 vector, and furin was expressed from pcDNA3.1-Furin, as described previously (5,79). The uncleaved JR-FL gp140 protein ($gp140_{UNC}$) with amino-acid substitutions to prevent its proteolytic processing has also been described elsewhere (5). Specific mutations were made using the QuickChange mutagenesis kit (Stratagene, La Jolla, CA). Random mutations were generated with primers that could contain any nucleotide at the relevant positions. Numbering is based on the HXB2 Env sequence. Recombinant JR-FL gp120 has been described elsewhere (92).

Antibody binding assays

The procedures and MAbs used to perform radioimmunoprecipitation assays (RIPA) have all been described (1,5,60,80,93). MAbs were provided by James Robinson (17b, 2.2B), George Lewis (B12), Hermann Katinger (2F5, 2G12, 4D4, 4E10) and Dennis Burton (IgG1b12).

SDS-PAGE, BN-PAGE and Western blot analyses

Sodium dodecyl sulfate polyacrylamide gel electrophoresis (SDS-PAGE), Blue

Native (BN)-PAGE and Western blot analyses were performed as described previously (5,79,83). Culture supernatants from transiently transfected 293T cells were concentrated 10-fold before gel electrophoresis, using Ultrafree-15 concentrators (Millipore, Bedford, MA).

Gel-filtration analysis of envelope glycoproteins
Supernatants from 293T cells, transfected with pPPI4-gp140 plus pcDNA3.1-Furin, were concentrated 100-fold, then size-fractionated using an analytical Superdex 200 HR 10/30 column equilibrated with phosphate-buffered saline (PBS; Amersham-Pharmacia, Piscataway, NJ). Fractions (300 µl) were analyzed using SDS-PAGE and BN-PAGE; in both cases, Western blotting was used to detect Env glycoproteins. The column was calibrated using protein standards of known size (HMW-standard; Amersham-Pharmacia).

Trimer stability experiments
Eluates from gel filtration columns, containing SOSIP gp140 trimers, were incubated with various reagents or under different conditions, then analyzed using BN-PAGE and western blot procedures. The following detergents were obtained from the following suppliers: SDS, Sigma, St Louis, MO; t-octylphenoxypolyethoxyethanol (Triton X-100), Sigma; polyoxyethylene sorbitan monolaurate (Tween-20), Sigma; ethylphenyl-polyethylene glycol (NP-40), United States Biochemicals, Cleveland, OH; n-octyl β-D-glucopyranoside (oct-glucoside), Sigma; Empigen BB 30% solution, (Empigen) (Calbiochem, La Jolla, CA).

Peptide production
Plasmid pN36/C34$_{JR\text{-}FL}$, encoding the HIV-1$_{JR\text{-}FL}$ N36(L6)C34 model peptide, was derived from pN36/C34$_{HXB2}$ (51). Amino-acid substitutions were introduced into the N36 segment of pN36/34$_{JR\text{-}FL}$ using the method of Kunkel et al. (44), then verified by DNA sequencing. All recombinant peptides were expressed in *Escherichia coli* strain BL21(DE3)/pLysS (Novagen, Madison, WI). The bacteria were grown at 37°C in LB medium to an optical density of 0.8 at 600 nm, and induced with isopropylthio-β-D-galactoside for 3-4 h. Cells were lysed at 0°C with glacial acetic acid. The bacterial lysate was centrifuged (35,000 *g* for 30 min) to separate the soluble fraction from inclusion bodies. The soluble fraction, containing denatured peptide, was dialyzed into 5% acetic acid overnight at room temperature. Peptides were purified from the soluble fraction to homogeneity by reverse-phase high-performance liquid chromatography (Waters, Milford, MA) using a Vydac C-18 preparative column (Vydac, Hesperia, CA) and a water-acetonitrile gradient in the presence of 0.1% trifluoroacetic acid, then lyophilized. The molecular weight of each peptide was confirmed by using matrix-assisted laser desorption ionization-time-of-flight mass spectrometry (PerSeptive Biosystems, Framingham, MA). The concentration of each peptide was determined at 280 nm after solubilization in 6 M guanidinium chloride (32).

Circular dichroism (CD) spectroscopy
HPLC-purified peptides were solubilized in 6 M guanidinium chloride and 10 mM Tris-HCl (pH 7.0), and refolded by dilution into PBS at neutral pH. The sin-

gle-point substituted variant peptides were named according to the position of the substitution. CD experiments were performed using an Aviv 62A DS circular dichroism spectrometer. The wavelength dependence of molar ellipticity, [θ], was monitored at 4°C, using a 10 μM peptide solution in 100 mM NaCl, 50 mM sodium phosphate, pH 7.0 (PBS). Helix content was calculated by the method of Chen et al. (22). Thermal stability was determined by monitoring the change in the CD signal at 222nm ($[\theta]_{222}$) as a function of temperature. Thermal melts were performed in 2°C increments with an equilibration time of 2 min at the desired temperature and an integration time of 30s. All melts were reversible. Superimposable folding and unfolding curves were observed, and >90% of the signal was regained upon cooling. The melting temperatures, or midpoints of the cooperative thermal unfolding transitions (T_m), were determined from the maximum of the first derivative, with respect to the reciprocal of the temperature, of the $[\theta]_{222}$ values (12). The error in estimation of T_m is ± 0.5°C.

Sedimentation equilibrium analysis

A Beckman XL-A (Beckman Coulter, Fullerton, CA) analytical ultracentrifuge equipped with an An-60 Ti rotor (Beckman Coulter) was used. Peptide solutions were dialyzed overnight against PBS (pH 7.0), loaded at initial concentrations of 10, 30, and 100 μM, and analyzed at rotor speeds at 20,000 and 23,000 rpm at 20°C. Data sets were fitted simultaneously to a single-species model of ln(absorbance) versus (radial distances)^2 using the program NONLIN (43). Protein partial specific volume and solvent density were calculated as described by Laue et al. (48).

Results

Stabilization of the SOS gp140 trimer by mutagenesis

Although the purified, cleaved SOS gp140 protein is a monomer, we have observed oligomeric forms of this protein in freshly prepared supernatants from transiently transfected 293T cells (5,83). An example of SOS gp140 oligomers, together with the experiment-to-experiment variation in their abundance, is provided by a BN-PAGE analysis of several different 293T cell transfections. In some preparations, a significant fraction of SOS gp140 proteins is oligomeric; in others, a negligible proportion (Fig. 1A).

The above observations suggest that the oligomeric form of SOS gp140, although clearly unstable, might not be too far from stability. We therefore adopted a mutagenesis strategy to try to increase the stability of the cleaved, oligomeric SOS gp140 protein. We focused on altering the $gp41_{ECTO}$ sequence, because of the clear preponderance of evidence that interactions between $gp41_{ECTO}$ subunits are responsible for the oligomerization of gp140 (29,85,99). However, no structural or other data are available on the likely points of contact between the gp41 moieties in the native, pre-fusion form of the envelope glycoprotein trimer. We therefore adopted a more theoretical approach, based on the premise that destabilization of the post-fusion state of gp41 might stabilize its pre-fusion configuration, by shifting the conformational equilibrium in favor of the pre-fusion state (40,41,49-51). A plethora of structural and genetic data on the post-fusion, six-

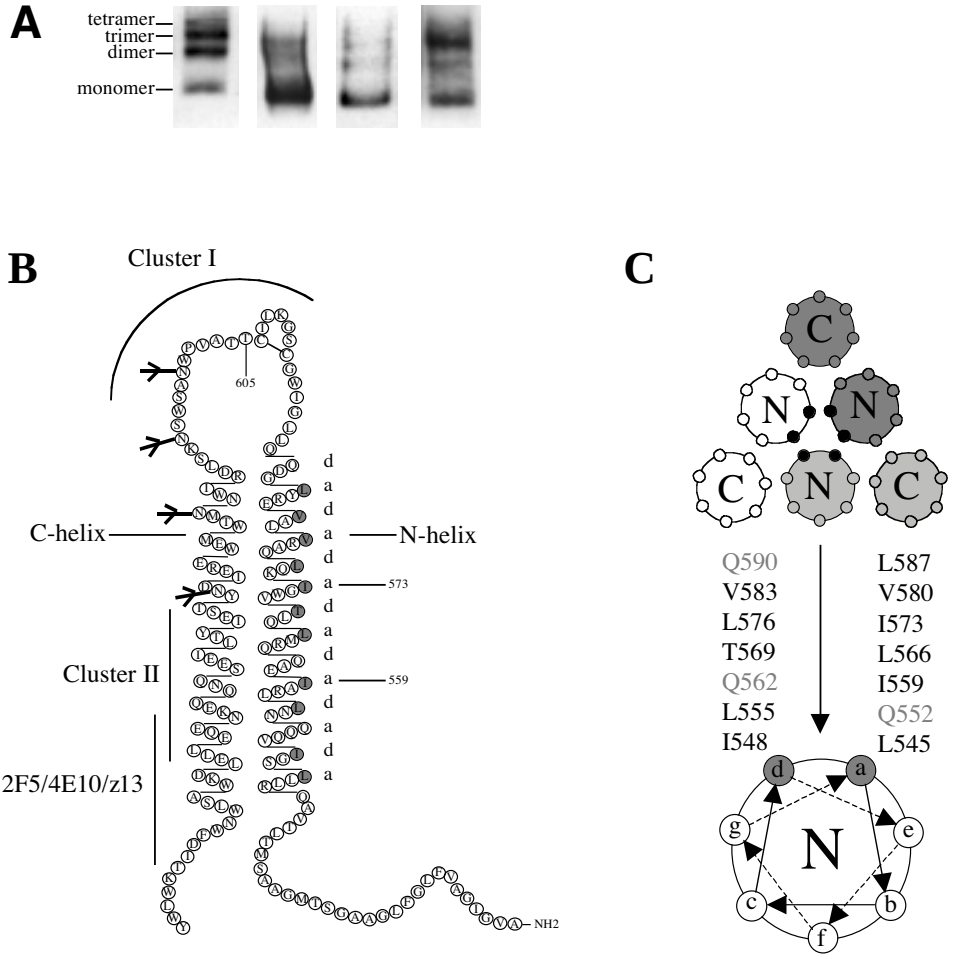

Fig. 1. Instability of SOS gp140 and a mutagenesis strategy for gp41$_{ECTO}$. A. BN-PAGE analysis of transiently expressed SOS gp140 proteins from different 293T cell supernatants. **B**. The residues at the ***a*** and ***d*** positions in the N-terminal heptad repeat of gp41$_{ECTO}$, depicted in gray in the secondary structure, were substituted in this study. Major MAb epitopes are indicated (26,68,100,106). **C**. A schematic representation of a cross-section of the six-helix bundle, post-fusion form of gp41$_{ECTO}$, and an helical wheel representation of one N-terminal helix, are depicted. The residues at the ***a*** and ***d*** positions of the N-terminal heptad repeat (black) form the trimer interface.

helix bundle structure of gp41 was available to guide our mutagenesis strategy (3,10,13,16,20,21,39,49,51,54,74,89,94-96).

The trimeric stability of gp41 in the six-helix bundle form of the protein is determined by the residues at the *a* and *d* positions of the N-terminal heptad-repeat region (40,41,52) (Fig. 1B,C). Most of these amino-acids are absolutely conserved. Hydrophobic Val, Leu and Ile residues form the apolar interface between the three N-terminal helices; these residues are critical determinants of the folding and thermal stability of the six-helix bundle (84). We assumed that

making non-conservative substitutions at these conserved, hydrophobic residues would destabilize the six-helix bundle and so, by reducing the probability of its formation, cause the $gp41_{ECTO}$ subunits to remain in their desired, pre-fusion configuration. The hydrophilic glutamine residues at positions 552, 562 and 590 were initially left unaltered, since buried polar interactions involving these residues confer structural specificity for formation of the N-terminal coiled-coil trimer at the expense of its thermal stability (41) (Fig. 1B,C). Substitutions at residue Thr-569 were also evaluated.

Because we could not predict what amino-acids would be tolerated in the pre-fusion configuration of $gp41_{ECTO}$, we performed random mutagenesis. Hence various amino-acids with different biochemical properties were introduced in place of the targeted Val, Ile and Leu residues. An emphasis of our mutagenesis approach was to alter the Ile-559 and Ile-573 residues, because core isoleucines are known to confer the greatest stability to trimeric coiled coils (also known as isoleucine zippers) (38). In most simian immunodeficiency virus (SIV) strains, Val and Thr residues are found, respectively, at these positions, where they may serve to destabilize the post-fusion, coiled-coil structure (40,49,50). Of note is that the SIV $gp140_{UNC}$ protein has a greater tendency to be trimeric than the corresponding HIV-1 protein (15,19).

We have described elsewhere the use of blue native (BN)-PAGE to monitor the oligomeric state of HIV-1 gp140 proteins (83). This technique served as a screening assay to identify more stable SOS gp140 variants - i.e., ones that remained trimeric under conditions in which the unmodified SOS gp140 protein ran mainly as a monomer. The variant SOS gp140 proteins were expressed in transiently transfected 293T cells, in the presence of co-transfected furin to facilitate gp120-gp41 cleavage. The effects of various, single-residue substitutions on the expression and trimer stability of these SOS gp140 proteins are summarized in Table 1A. An example of how BN-PAGE was used to derive this information is shown in Fig. 2A.

Many of the randomly generated SOS gp140 mutants were not expressed, or were expressed poorly, particularly those with substitutions at residues 555, 576 and 587. This is probably because amino-acid changes at these positions have adverse effects on protein folding. However, other conserved residues (e.g., 548, 573, 580 and 583) were more tolerant of substitution, in that the altered SOS gp140 proteins were still expressed efficiently. The effect on SOS gp140 expression of substitutions at other positions, notably at residues 545, 559, 566 and 569, was dependent on the identity of the amino-acid introduced. Thus, at position 545, a Leu-to-Phe change (L545F) reduced SOS gp140 expression, whereas the introduction of Asn (L545N), Pro (L545P) or Gly (L545G) at this position had little effect. Similarly, Ile-to-Phe or Ile-to-Asn substitutions at position 559 (I559F, I559N) severely diminished gp140 expression (Fig. 2A, lanes 3,6). In contrast, the introduction of Val (I559V), Gly (I559G) or Arg (I559R) residues at position 559 had a lesser effect on SOS gp140 expression, and a Pro (I559P) substitution had no adverse effect at all (Fig. 2A, lanes 4,7,8). Other examples of how the introduced residue can have a variable effect on SOS gp140 expression include changes at residues 566 and 569 (Table 1A).

We used BN-PAGE to determine whether there were differences in oligomer stability among the subset of altered SOS gp140 proteins that were efficiently

expressed. Under native conditions, the wild-type SOS gp140 protein migrates predominantly as a monomer, with some dimeric and trimeric species also present (Fig. 2A, lane 2). The proportion of the SOS gp140 protein that is oligomeric varies from experiment to experiment, but the gel shown in Fig. 2A is typical of what is most commonly observed. In contrast, the $gp140_{UNC}$ protein migrates as oligomeric forms, with the dimer predominating (Fig. 2A, lane 1).

Most of the amino-acid substitutions consistent with the efficient expression of SOS gp140 had little effect on the extent of its oligomerization (Table 1A). However, several substitutions at position 559 clearly altered the oligomerization state of SOS gp140 (Fig. 2A). Thus, when Ile-559 was replaced by a non-conservative Gly (I559G), Arg (I559R) or Pro (I559P) residue, the most abundant protein form was consistently the trimer (Fig. 2A, lanes 4,5,8). In contrast, the conservative Ile-to-Val substitution at position 559 had no effect, in that the I559V and wild-type SOS gp140 proteins were indistinguishable (Fig. 2A, lanes 2,7). Some substitutions at positions 566 and 569 (e.g., L566V, T569P) marginally increased the proportion of SOS gp140 proteins that were trimeric (Table 1A). Note that the percentage of trimers varied per transfection, but the amount of trimer in the SOS gp140 I559P preparations shown in Fig. 2A (and Fig. 3, see below) was typical. Sometimes, higher amounts of trimer, up to 90% were observed.

There appeared to be a correlation between the expression of some SOS gp140 mutants and the extent to which they were oligomeric. Thus, substitutions at positions 559, 566 and 569 affected both the expression and the oligomerization of SOS gp140 (Table 1A, Fig. 2A). These residues may be particularly important for the correct folding of the trimeric, pre-fusion form of gp140 glycoproteins.

The above experiments show that the introduction of the helix-destabilizing residues Gly or Pro at position 559 increased the tendency of the SOS gp140 protein to form trimers. Hence this region of gp140 may not be helical in the pre-fusion configuration of the protein. In the influenza HA_2 protein, a loop-to-helix transition induced by exposure to low pH is essential for the formation of the fusion-intermediate, extended coiled-coil conformation (8). Various proline substitutions in this particular region of HA_2 permit the production of proteolytically cleaved trimers, but these mutants are fusion-impaired because they cannot undergo the critical loop-to-helix transition (37,75). We therefore investigated whether proline substitutions at other residues near position 559 of HIV-1 gp41 could have the same, trimer-stabilizing effect as the I559P substitution. However, although most of these mutants could be efficiently expressed, none of them stabilized the trimeric form of SOS gp140 in the same way that the I559P substitution did (Table 1B).

We also tested various combinations of amino-acid substitutions. Generally, in all the double or triple mutants that were evaluated, the presence of one or other of the I559P or I559G changes was essential to obtain the trimer-stabilized phenotype. A few other substitutions (e.g., L566V and T569P) had a marginally stabilizing effect on the SOS gp140 trimers (Table 1).

The I559G and I559P substitutions shown above to confer increased stability on the SOS gp140 protein, were also made in the context of a $HIV\text{-}1_{LAI}$ virus containing a membrane-bound Env glycoprotein, to see whether they were compatible with Env function. Both substitutions completely abrogated Env function and

Table 1. Summary of characteristics of SOS gp140 variants

Residue	Mutation in SOS gp140	Expression[a]	Trimer stability[b]	Cleavage[c]	Residue	Mutation in SOS gp140	Expression[a]	Trimer stability[b]	Cleavage[c]
L545	F	±	±		I573	L	++	±	
	N	++	±			F	++	±	
	P	++	±			Y	++	±	
	G	++	±			Q	++	±	
I548	V	++	±			N	++	±	
	L	++	±			T	++	±	
	H	++	±			P	++	±	
	N	++	±			G	++	±	
	S	++	±			K	++	±	
	G	++	±		L576	V	±	±	
	R	++	±			F	±	±	
L555	V	-	ND			Y	±	±	
	W	-	ND			Q	±	±	
	Y	-	ND			N	±	±	
	S	-	ND			G	±	±	
	P	-	ND			K	±	±	
I559	V	+	±		V580	L	++	±	
	F	±	++			H	++	±	
	N	-	ND			T	++	±	
	P	++	++	++		P	++	±	
	G	+	++	++		G	++	±	
	R	+	++		V583	L	++	±	
L566	V	+	+	++		Q	++	±	
	I	±	±			N	++	±	
	N	+	+			S	++	±	
	T	+	+			P	++	±	
	P	+	±			R	++	±	
	K	±	±			K	++	±	
T569	S	+	±		L587	A	±	±	
	P	+	+	++		P	±	±	
	K	+	+			R	±	±	
	E	-	ND			D	±	±	
						E	±	±	

[a] Relative scale: -, no expression; ±, minimal expression; +, expression level lower than that of wild-type SOS gp140; ++, expression level equivalent to that of wild-type SOS gp140; +++, expression level greater than that of wild-type SOS gp140. All proteins were expressed in the presence of cotransfected furin, which decreases gp140 expression (5, 6, 79). The data were derived from at least three independent transfections.

[b] As assessed by BN-PAGE. The trimer stability of SOS gp140 was set at ± (some trimers were present in some transfections). The maximum amount of trimers (++) was found only in gp140 variants containing substitutions at residue Ile-559 and ranged from 40 to >90% of total Env expression in independent transfections. The data were derived from at least three independent transfections. ND, not determined (no expression).

[c] Data were derived from Fig. 2C. Symbols are as defined in footnote a.

virus replication (chapter 5.7). This is consistent with previous reports of the deleterious effects of most substitutions in this region of gp41 (13,20,21,74, 95,96).

Stabilized SOS trimers form non-covalently and are cleaved

Based on the above results, we focused on the SOS I559P and I559G gp140 proteins for further analysis. These proteins are designated the SOSIP and SOSIG gp140 proteins, respectively. Although the SOSIP gp140 protein was consistently expressed at higher levels than SOSIG gp140, the presence of a glycine residue at position 559 might confer flexibility to the latter protein. We considered that any such flexibility might prove useful if and when the I559G substitution were combined with other modifications. We also further studied the SOS L566V and T569P gp140 proteins, to see whether similar results were obtained with trimers that had been stabilized, even to only a limited extent, by substitutions at positions other than residue 559.

To investigate whether the oligomeric species present in the preparations of the SOSIP, SOSIG, SOS L566V and SOS T569P gp140 proteins were covalently or non-covalently associated, we analyzed them using denaturing, but non-reducing SDS-PAGE (Fig. 2B). The $gp140_{UNC}$ protein was included for comparison (Fig. 2B, lane 1). As expected, SOS gp140 migrated predominantly as a 140 kDa species (Fig. 2B, lane 2). However, some higher molecular weight, SDS-resistant species were also present in both the SOS gp140 and the $gp140_{UNC}$ preparations. The higher molecular weight species were only a minor component of the SOS gp140 preparation, but they were the predominant form of the $gp140_{UNC}$ protein (Fig. 2B, lane 1). We believe that the higher molecular weight forms of these proteins are predominantly covalently associated dimers and, in some cases, tetramers that could be dimers of dimers (see below).

The SOS gp140 variants were all indistinguishable from the wild-type SOS gp140 protein, in that the predominant species after SDS treatment were always 140 kDa monomers (Fig. 2B, lanes 3-7). Thus, the trimeric forms of the SOSIP and SOSIG gp140 proteins are not created by the aberrant formation of intermolecular disulfide bonds; instead, the protein is associated by non-covalent interactions.

Our goal is to make stable, oligomeric gp140 proteins that are properly processed at the cleavage site between the gp120 and gp41 subunits. We therefore analyzed whether the SOSIP, SOSIG, SOS L566V and SOS T569P gp140 variants were processed appropriately. The proteins were boiled in the presence of SDS and dithiothreitol (DTT), to achieve both denaturation and reduction, before SDS-PAGE analysis (Fig. 2C). Under these conditions, each of the various SOS gp140 proteins was converted to gp120 and $gp41_{ECTO}$ forms (Fig. 2C, and data not shown). Thus, each of the gp140 proteins was substantially (>90%) cleaved, in that the 140 kDa bands did not survive DTT treatment (Fig. 2C, lanes 2-7). In contrast, the $gp140_{UNC}$ protein was unaffected by DTT and still migrated as a 140 kDa band, because it possesses a peptide bond between the gp120 and gp41 subunits (Fig. 2C, lane 1). Thus, the increased trimer stability of the SOSIP, SOSIG, SOS L566V and SOS T569P gp140 proteins is not caused by, or associated with, any cleavage defect.

Most of the SOS gp140 preparations analyzed by SDS-PAGE contained a small percentage of SDS-resistant oligomers, and these forms of gp140 were relatively abundant in the $gp140_{UNC}$ preparation (Fig. 2B). Since these higher molecular weight forms of gp140 were not observed when DTT was also present to reduce disulfide bonds (Fig. 2C), they presumably represent protein forms that

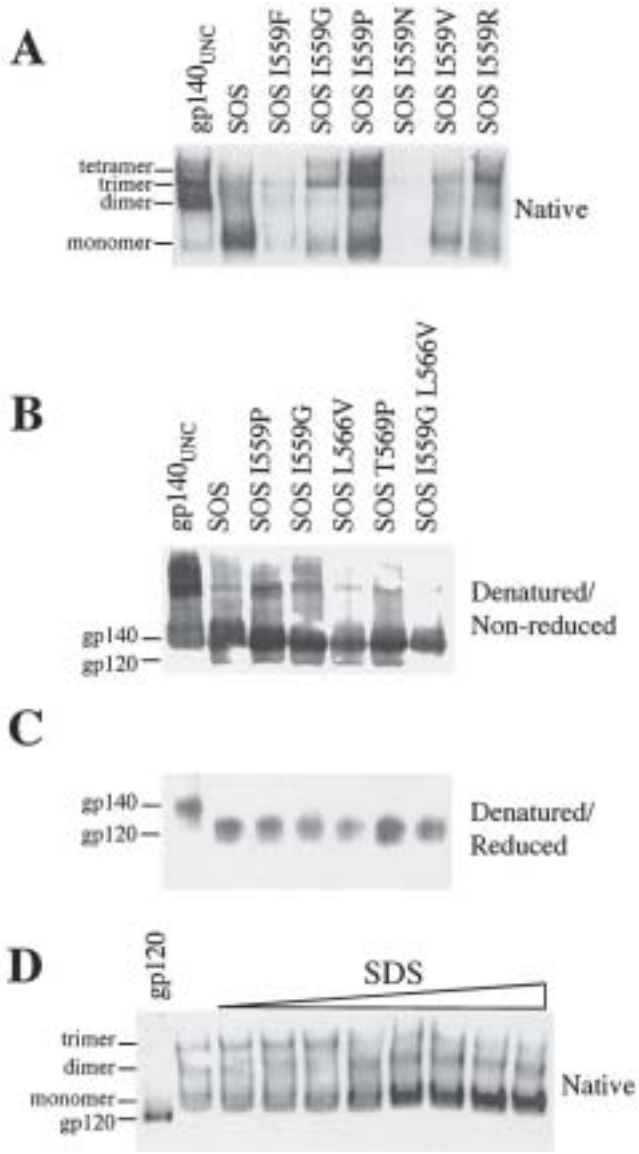

Fig. 2. PAGE analysis of SOS gp140 proteins. **A**. BN-PAGE of SOS gp140 proteins containing changes at position 559. The $gp140_{UNC}$ protein was included for comparison. **B**, **C**. SDS-PAGE of SOS gp140 variants under non-reducing (**B**) or reducing (**C**) conditions. **D**. The SOSIG gp140 protein was treated with SDS for 1h at 25°C. The SDS concentrations used were 0%, 0.005%, 0.01%, 0.015%, 0.02%, 0.025%, 0.03%, 0.035% and 0.04%, increasing from left to right. BN-PAGE analysis was then performed. Monomeric gp120 (20 ng) served as a molecular weight standard.

are linked via aberrant, intermolecular disulfide bonds (83). To see whether the higher molecular weight proteins were dimers or trimers, we treated the SOSIG gp140 protein with increasing amounts of SDS, then performed a BN-PAGE analysis (Fig. 2D). In the absence of SDS, trimers, dimers and monomers were

present at roughly equal proportions in this preparation of the SOSIG gp140 protein (Fig. 2D, lane 2). As the SDS concentration increased, however, the trimer band completely disappeared, whereas the dimer band survived exposure to SDS concentrations even as high as 1% (Fig. 2D; Fig. 2B, lane 4). The stronger intensity of the dimer band on the western blot is probably attributable to an increased reactivity of the detecting MAb once the gp140 protein has been denatured with SDS. The more pronounced increase in the intensity of the monomer band suggests that trimers dissociate to three monomers, rather than to a dimer and a monomer (see below). Overall, we conclude that the SOSIG gp140 trimers are formed by non-covalent, SDS-sensitive bonds, but that the dimers are associated via aberrant, intersubunit disulfide bonds. Similar results were obtained with the SOSIP gp140 protein (data not shown, but see Fig. 4 below). The wild-type SOS gp140 protein could not, of course, be tested in this way as its trimeric form was too unstable.

Fractionation of oligomeric gp140 species by gel filtration

The BN-PAGE analyses showed that amino-acid substitutions, in particular at the 559 position, can stabilize SOS gp140 trimers. To corroborate this by an independent technique, unpurified gp140 proteins secreted from Env-transfected 293T cells were studied by analytical gel-filtration chromatography using a Superdex 200 column. Proteins with known molecular weight provided reference standards. These were catalase (232 kDa), ferritin (440 kDa) and thyroglobulin (669 kDa). However, it should be noted that fully glycosylated gp120 and gp140 molecules are non-globular in shape, so gel filtration cannot precisely determine their absolute molecular weights (14,15,83).

The eluate fractions were collected, then analyzed by SDS-PAGE and Western blotting to identify the migration positions of various Env protein forms (Fig. 3). Because the input Env proteins were unpurified, unrelated proteins are also present in the eluate, so the fractions in which Env proteins eluted could not be determined by non-specific methods. The SOS gp140 protein was predominantly found in fractions 13, 14 and 15, corresponding to an apparent molecular weight similar to that of catalase (232 kDa) (Fig. 3A, top panel). Thus, the average apparent molecular weight of the eluted SOS gp140 monomer was ~240 kDa, which is consistent with the value of ~220 kDa that we reported previously, also using gel filtration (83). The small amount of gp120 present in this preparation of SOS gp140 had a slightly lower apparent molecular weight of ~220 kDa (Fig.3A). In most preparations of SOS gp140, a small quantity of covalently linked oligomers, probably dimers, was also seen, centered around fractions 9 and 10 (data not shown). These results confirm our report that SOS gp140 is usually, predominantly a monomeric protein (83) (Fig. 1A).

In contrast, the SOSIP gp140 proteins eluted over a broad range in fractions 1-16, indicating that both oligomeric and monomeric species are present (Fig. 3A, bottom panel). A small amount of covalently linked oligomers was also observed (see also Fig. 2B, lane 3), just as similar oligomers were usually present in SOS gp140 preparations (Fig. 2B, lane 2). To resolve the different oligomeric species, the same SOSIP gp140 gel-filtration fractions were then analyzed by BN-PAGE. This showed that trimeric, dimeric and monomeric proteins had been clearly

resolved on the Superdex 200 column; the trimers were predominantly in fractions 4-9, the dimers in fractions 7-11 and the monomers in fractions 11-15 (Fig. 3B). Similar results were obtained with an SOS gp140 triple mutant containing the I559P, L566V and T569P mutations (data not shown).

The apparent molecular weight of the SOSIP gp140 monomer corresponds to what was observed with wild-type SOS gp140 (~240 kDa, see above). The retention of dimers, centered around fraction 9, corresponds to an average apparent molecular weight of ~410 kDa, whereas the trimer (peak fraction 6) has an average apparent molecular weight of ~520 kDa. It is notable that the trimers do not elute in a position consistent with their expected size of three times the size of a gp140 monomer. Thus they elute at a position corresponding to a molecular weight of ~520kDa, as opposed to the "expected" ~660-720 kDa (i.e., 3 x ~220-240 kDa). The same is true, to a lesser extent, of the dimers, which elute at ~410 kDa, compared to the "expected" ~440-480 kDa (i.e., 2 x ~220-240 kDa). The explanation for this is probably that the trimers, and perhaps also the dimers, are folded into a conformation which is more compact than that of gp140 monomers. Electron microscopy studies may be able to confirm this suggestion. Alternatively, the nature and extent of glycosylation of the different oligomeric forms of gp140 may vary, because glycosylation sites on the trimer could be less accessible to modifying enzymes than the same sites on the monomer. Overall, given the limitations of gel filtration for estimating the molecular weights of non-globular proteins (14,15,83), we will need to use other techniques (e.g., mass spectrometry) to establish the absolute molecular weights of the various, purified oligomeric species of SOS gp140 proteins.

Clearly, SOSIP gp140 preparations are not pure trimers prior to fractionation by gel-filtration (Figs. 2A and 3); monomers, dimers and tetramers are also present. We estimate that typically 40% of an SOSIP gp140 preparation elutes in the trimer fraction. We assume that the dimers and tetramers are aberrant forms of Env that are generated by much the same, albeit unknown, processes that also cause them to be present in $gp140_{UNC}$ preparations (Fig. 2) (28-30,33,83,101, 102). The small amount of monomers present in SOSIP gp140 preparations probably arise because the effect of the trimer-stabilizing I559P substitution is imperfect. We are presently determining how to purify SOSIP gp140 trimers away from other non-Env proteins that elute at similar positions from gel-filtration columns.

Stability of SOSIP gp140 trimers

The Superdex 200 column fractions corresponding to the trimer peak of the SOS I559P gp140 protein (fractions 6 and 7) were pooled for analysis of their stability (Fig. 4). The trimers were stable to incubation for 1h at 25°C and 37°C (Fig. 4A, lanes 1 and 2), but some monomers became visible after 1h at 45°C (lane 3) and almost all of the protein was in monomeric form after heating for 1h at 55°C or 65°C (lanes 4 and 5). Three freeze-thaw cycles at -80°C did not convert the trimer into a monomer (lane 7). We next incubated the fractionated trimers with various detergents for 1h at 25°C (Fig. 4B). The trimers dissociated into monomers upon incubation with 0.1% SDS, an anionic detergent (lane 2), but they were at least partially resistant to the same concentration of the nonionic or

zwitterionic detergents Triton X-100, Tween-20, NP-40, Octyl-glucoside and Empigen (lanes 3-7). We have also observed that SOSIP gp140 trimers did not dissociate into monomers in the presence of NaCl concentrations of up to 1.0 M, or after exposure to mild acid (pH 4.0) (data not shown). The effects of various adjuvants and of long-term storage at various temperatures on the trimeric state of purified SOSIP gp140 trimers are currently under investigation.

Dimers were present at only very low levels in heat- or detergent-treated SOSIP gp140 trimers. This suggests that the assembly units of the trimers are three equivalent monomers, rather than a monomer and a dimer.

Antigenic structure analysis of the stabilized SOS gp140 proteins

Since our goal is to make cleaved, stable gp140 trimers that mimic as closely as possible the antigenic structure of virion-associated Env, we studied the reactivity of the unpurified, SOSIP gp140 protein with a panel of MAbs and CD4-based reagents. The SOS gp140 and $gp140_{UNC}$ proteins were also studied, for comparison (Fig. 5). Both the wild-type SOS gp140 and the SOSIP gp140 proteins were immunoprecipitated by the CD4-IgG2 molecule, indicating that the CD4-binding site (CD4BS) was intact on the gp120 subunits of both proteins (lane 2). The neutralizing MAb IgG1b12 to a CD4BS-associated epitope also bound to both proteins efficiently, as did the neutralizing MAb 2G12 to a mannose-dependent gp120 epitope (80,93) (lanes 1 and 3). Furthermore, sCD4 induction of the 17b epitope was highly efficient in both the SOS and SOSIP gp140 proteins (lanes 4 and 5). This epitope overlaps the CD4-inducible, co-receptor binding site on gp120 (77,91,97,98). Thus, the I559P substitution in $gp41_{ECTO}$ does not affect the ability of the gp120 subunits of an SOS gp140 protein to bind the CD4 receptor, and to then undergo receptor-mediated conformational changes within the gp120 subunits. The SOSIP gp140 protein appears indistinguishable from the wild-type SOS gp140 protein in this regard.

There are three predominant epitope clusters in $gp41_{ECTO}$. One cluster is rec-

Table 2. Effect of proline substitutions at residues near position 559

Residue	Expression[a]	Trimer stability[b]	Cleavage[c]
L555[d]	-	ND	
L556	++	±	
R557	++	±	
A558	++	±	
I559[d]	++	++	++
E560	+++	±	
A561	+++	±	
Q562	+++	±	
Q563	+++	±	
R564	+++	±	
M565	++	±	
L566[d]	±	±	

[a] See Table 1, footnote a.
[b] See Table 1, footnote b.
[c] See Table 1, footnote c.
[d] Also shown in Table 1.

ognized by the neutralizing MAbs 2F5, 4E10 and z13, and is located close to the C-terminus of $gp41_{ECTO}$ (68,88,106) (Fig. 1B). This region of $gp41_{ECTO}$ is well exposed on the SOS and SOSIP gp140 proteins, as indicated by their efficient binding of 2F5 (Fig. 5, lane 6) and 4E10 (data not shown). The cluster I and cluster II $gp41_{ECTO}$ epitopes are highly immunogenic. However, antibodies to these regions of gp41 are non-neutralizing because their epitopes are occluded in the native, pre-fusion form of the envelope glycoprotein complex, either by interactions between $gp41_{ECTO}$ moieties or because of the presence of the gp120 subunits (5,42,59,65,71,82,90). MAbs to cluster I (2.2B) and cluster II (4D4) epitopes interact with the $gp140_{UNC}$ protein efficiently but do not bind to the SOS or SOSIP gp140 proteins (lanes 7 and 8). Similar results were obtained with other MAbs to these epitope clusters (data not shown). This pattern of results is consistent with our previous reports on the antigenic structure of SOS gp140 (5,79,83). It is possible that the introduction of the cysteine substitution at residue 605 in the SOS gp140 proteins directly perturbs the nearby epitopes for some or all of the cluster I MAbs. However, this cannot be the case for the cluster II MAb epitopes, since these are located in the C-terminal helical region, approximately 40 residues from the Cys-605 substitution (Fig. 1B).

The SOS gp140 variants I559G, L566V and T569P were also tested for reactivity with the above MAbs and CD4-based reagents. Each of them behaved similarly to the SOS and SOSIP gp140 proteins (data not shown). Further studies on the receptor- and MAb-binding properties of purified SOSIP gp140 trimers will be described elsewhere, as a comparison with other forms of gp140 proteins (MSV, RWS and JPM, unpublished results). These experiments, together with other planned structural analyses, should determine whether the $gp41_{ECTO}$ moieties of SOSIP gp140 proteins adopt a native configuration, or whether the helix-destabilizing effect of the I559P substitution creates a non-native $gp41_{ECTO}$ conformation that is not recognized by some anti-gp41 MAbs.

Destabilization of the six-helix bundle form of gp41

Our mutagenesis results indicate that the SOS gp140 trimers can be stabilized by the I559G, I559P and, to some extent, L566V and T569P substitutions in the N-terminal heptad-repeat region of the $gp41_{ECTO}$ subunit. Given that hydrophobic interactions are a dominant factor in the stabilization of the gp41 core (40,51), it would appear that these amino-acid substitutions destabilize the six-helix bundle structure. To directly test this hypothesis, we determined the effects of each of the four amino-acid substitutions on the overall structure and stability of the JR-FL $gp41_{ECTO}$ core. We therefore constructed a recombinant peptide model of this soluble gp41 core. This model peptide, designated N36(L6)C34, consists of the N36 and C34 peptides connected via a short peptide linker that replaces the disulfide-bonded loop region of $gp41_{ECTO}$ (Fig. 6A) (51). The N36 peptide consists of residues 546-581, the C34 peptide of residues 628-661 of the JR-FL gp41 protein sequence. Each of the above four amino-acid changes was introduced into the N36(L6)C34 peptide. Sedimentation equilibrium analysis showed that the molecular weights of N36(L6)C34 variants, except for the I559P mutant, were all within 10% of those calculated for an ideal trimer, with no systematic deviation of the residuals (data not shown).

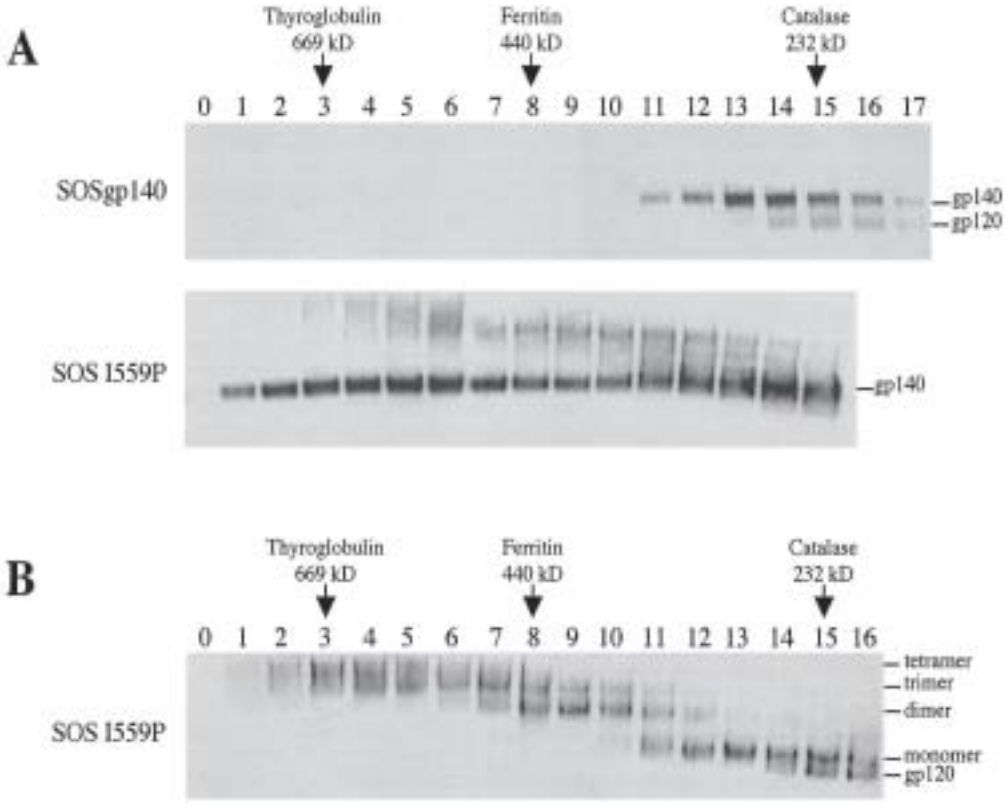

Fig. 3. Gel-filtration analysis of SOSIP gp140. **A**. The SOS and SOSIP (SOS I559P) gp140 proteins were fractionated on a Superdex 200 column. The individual fractions were analyzed by SDS-PAGE and Western blotting. **B**. The same SOSIP gp140 fractions from **A** were analyzed by BN-PAGE and western blotting. The elution positions (peak fractions) of standard proteins are indicated.

Circular dichroism (CD) measurements indicated that the N36(L6)C34 wild-type, and the I559G, L566V and T569P variant peptides were each >95% a-helical at 4°C, whereas the I559P variant peptide was apparently only ~75% a-helical (Table 2). Under these conditions, the midpoints of thermal denaturation (T_m's) of the I559G, I559P, L566V, and T569P peptides are 46, 34, 72 and 44°C, respectively, as compared to a T_m of 78°C for the wild-type peptide (Table 2). The pre- and post-transitional slopes and the steepness of the main transition are very similar for the N36(L6)C34, I559G, and L566V peptides (Fig. 6B). In contrast, the I559P and T569P peptides display broad thermal unfolding transitions (Fig. 6B). Sedimentation equilibrium experiments indicate that the N36(L6)C34 peptide and its I559G, L566V and T569P variants each sediment as discrete trimers over a ten-fold range of peptide concentration (10 to 100 µM) (Table 2; Fig. 6C). The I559P peptide is also trimeric in solution at concentrations below 15 µM, but it exhibits a systematic deviation from the trimer molecular weight between 10 to 100 µM, indicating that I559P is prone to aggregation. Taken together, these results indicate that the Ile-559 to Gly and Thr-569 to Pro substitutions each lead

to an appreciable destabilization of the six-helix bundle structure, but do not affect its overall fold. In contrast, the Ile-559 to Pro substitution essentially disrupts the six-helix bundle formation. Moreover, the Leu-566 to Val change is associated with a small, unfavorable, residual destabilization of the six-helix bundle.

Overall, these experiments confirm that the I559P, I559G, L566V and T569P substitutions do, in fact, destabilize the six-helix bundle, post-fusion conformation of $gp41_{ECTO}$. Indeed, the I559P change appears sufficient to completely prevent the formation of the post-fusion state, by destabilizing the N-terminal helix. The results obtained using model peptides are therefore consistent with what was observed when the corresponding amino-acid substitutions were introduced into the SOS gp140 protein. Moreover, both sets of results support the underlying hypothesis that destabilizing, or otherwise preventing the formation of the six-helix bundle form of $gp41_{ECTO}$ helps maintain the gp140 protein in its native, trimeric, pre-fusion configuration.

Discussion

We describe here the generation and characterization of soluble, cleaved HIV-1 envelope glycoprotein trimers. In these gp140 proteins, the gp120-gp41 interactions are stabilized by an intermolecular disulfide bond, and the gp41-gp41 interactions are stabilized by specific amino-acid substitutions in the N-terminal heptad repeat of $gp41_{ECTO}$, most notably at position 559. The need for this study arose when we observed that the SOS gp140 protein was unstable, in that it dissociated into gp140 monomers and could not be purified in trimeric form (83). The fragility of the SOS gp140 trimer is created by the proteolytic cleavage event that eliminates the peptide bond between gp120 and $gp41_{ECTO}$ as the gp140 precursor is processed to maturity. Thus, $gp140_{UNC}$ proteins form stable oligomers, whether or not the disulfide bond that characterizes the SOS gp140 proteins is also present (2,83,87,101,102,105). Since we want to make cleaved, stable Env trimers for structural and immunogenicity studies, we needed to find a way to overcome the instability of the gp41-gp41 ectodomain interactions in the pre-fusion form of the gp140 protein.

Our efforts were guided by the hypothesis that destabilization of the post-fusion state of gp41 might lead to stabilization of the native, trimeric SOS gp140 complex. The native HIV-1 Env complex is metastable and undergoes a transition to the post-fusion, six-helix bundle structure after activation by receptor-binding, probably losing gp120 in the process (17,24,25,31,61,99). The gp120 moiety of the SOS gp140 protein can bind CD4 and undergo conformational changes within gp120 that expose the co-receptor binding site. We do not know whether any additional conformational changes are initiated in the $gp41_{ECTO}$ moiety of the SOS gp140 protein upon CD4 and/or co-receptor binding. If they are, these changes cannot be completed. However, whether or not the SOS gp140 protein has bound to CD4, the gp41–gp41 interactions that are responsible for its trimerization are unstable; the protein readily becomes a monomer (83).

Our hypothesis for stabilizing the trimeric form of SOS gp140 was based on an increasing understanding of the delicate balance between the metastable, pre-

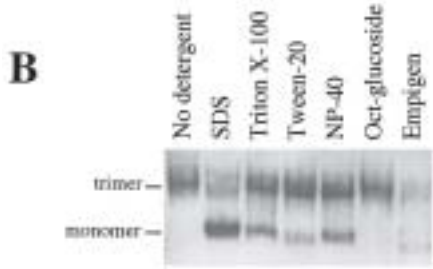

Fig. 4. Stability of SOSIP gp140 trimers. Fractions 6 and 7 from a gel-filtration profile similar to that shown in Fig. 3 were pooled as a source of SOSIP gp140 trimers. The trimers were (**A**) incubated for 1h at the temperatures indicated or (**B**) exposed to a 0.1% concentration of various detergents for 1h at 25°C. The proteins were then analyzed using BN-PAGE and Western blotting.

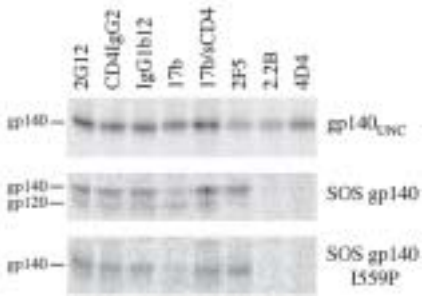

Fig. 5. Antigenic structure analysis of gp140 proteins. RIPAs were performed using the $gp140_{UNC}$, SOS gp140 and SOSIP gp140 proteins and various neutralizing and non-neutralizing MAbs, as previously described (5).

fusion state of gp140 and its stable, post-fusion, six-helix bundle configuration. The balance involves not only the trimeric interactions between $gp41_{ECTO}$ moieties, but also the association between gp120 and $gp41_{ECTO}$. Several lines of evidence support our experimental approach. Thus, the SIV_{mac} gp140 protein seems to be a more stably trimeric protein than HIV-1 gp140 (15,19). In contrast, the post-fusion state of SIV_{mac} Env is less stable than that of HIV-1 Env (50); it may or may not be relevant that the SIV_{mac} Env glycoprotein contains a valine and not an isoleucine residue at position 559. Furthermore, a SIV_{mac} envelope glycoprotein with an unusually strong gp120-gp41 association has a destabilized, post-fusion, six-helix bundle conformation compared to the parental virus from which it evolved (47,50). Also consistent with our hypothesis are studies with a variant $HIV\text{-}1_{LAI}$ virus engineered to contain the SOS substitutions, and so to have gp120 covalently linked to gp41. This virus is minimally infectious, but evolves in culture to a more infectious form via reversions at a region of $gp41_{ECTO}$ that corresponds to the trimer interface of the post-fusion form (chapter 5.7). These changes in $gp41_{ECTO}$ may influence the interactions both between gp120 and gp41 and between the gp41 moieties.

We believe that the substitutions we have introduced at position 559 to make

the SOSIP or SOSIG gp140 proteins, block one or more of the conformational transitions in $gp41_{ECTO}$ (39). A model of how the substitutions might act is presented in Fig. 7. We argue that preventing these transitions stabilizes the SOS gp140 protein as a trimer. However, we do not yet know which among the several conformational transitions that $gp41_{ECTO}$ undergoes during fusion is impaired by the changes at residue 559. Two possibilities are that the transition from the elusive native state to the pre-hairpin intermediate could be affected, or the subsequent transition from the pre-hairpin intermediate to the six-helix bundle structure might be prevented (Fig. 7). The observation that the N36(L6)C34 I559P peptide is only ~75% helical argues in favor of the first possibility – interference with the formation of the N-terminal helix – although additional studies will be required to confirm this. Peptide-based studies on the gp41 N-terminal helix have shown that the first part of this helix, including the region around residue 559, is more flexible than the last part (18). There is evidence that the pre-hairpin intermediate may exist as an equilibrium between a monomeric state and a trimeric coiled-coil and that disrupting the homotrimeric coiled-coil is an efficient way to block fusion (4,11,72). We think that preventing the formation of the inherently instable prehairprin intermediate state, stabilizes the Env complex in its native conformation.

Stabilizing the pre-fusion, trimeric structure of a fusogenic viral glycoprotein, by destabilizing or disrupting its N-terminal helix via a proline substitution, is not without precedent. In the influenza HA_2 glycoprotein, a stretch of 22 amino-acids is not helical in the pre-fusion form. However, upon exposure to low pH to trigger fusion, this region of HA_2 undergoes a loop-to-helix transition to form the fusion-active configuration of the protein (8). Proline substitutions here in HA_2 allow the expression of properly processed, but fusion-incompetent proteins (37,75). Similarly, a proline substitution at position 559 in HIV-1 gp41 is known to abolish the fusogenicity of an otherwise infectious virus (20,21).

The SOSIP, SOSIG, SOS L566V and SOS T569P gp140 proteins do not suffer from any proteolytic cleavage defects. This is in contrast with the cleavage defects that are caused by amino-acid substitutions at the same positions in the context of wild-type gp160 proteins (13,20,21,74). An explanation for the apparent discrepancy may be provided by our earlier observations that the presence of the SOS inter-subunit disulfide bond can rescue some cleavage defects in gp140 proteins (79). Moreover, the various SOS gp140 proteins are expressed in the presence of co-transfected furin, so the increased concentration of this enzyme may compensate for any partial reduction in cleavage efficiency. We have described elsewhere the use of basic substitutions within the gp140 cleavage site to increase the efficiency with which SOS gp140 proteins are processed by endogenous and exogenous furin proteases (6). The utility of these cleavage site changes in the context of the SOSIP gp140 protein is now being evaluated.

Several unpurified and purified $gp140_{UNC}$ proteins from both HIV-1 and SIV_{mac} have been described previously (2,15,19,28,86,87,105). There is general agreement that SIV_{mac} $gp140_{UNC}$ proteins are predominantly trimeric (15,19). In contrast, the oligomeric state of HIV-1 $gp140_{UNC}$ proteins varies from study to study. After a purification procedure that included an earlier size exclusion chromatography step, HIV-1 ADA $gp140_{UNC}$ proteins were eluted homogeneously from size exclusion columns with a molecular weight that indicates they are

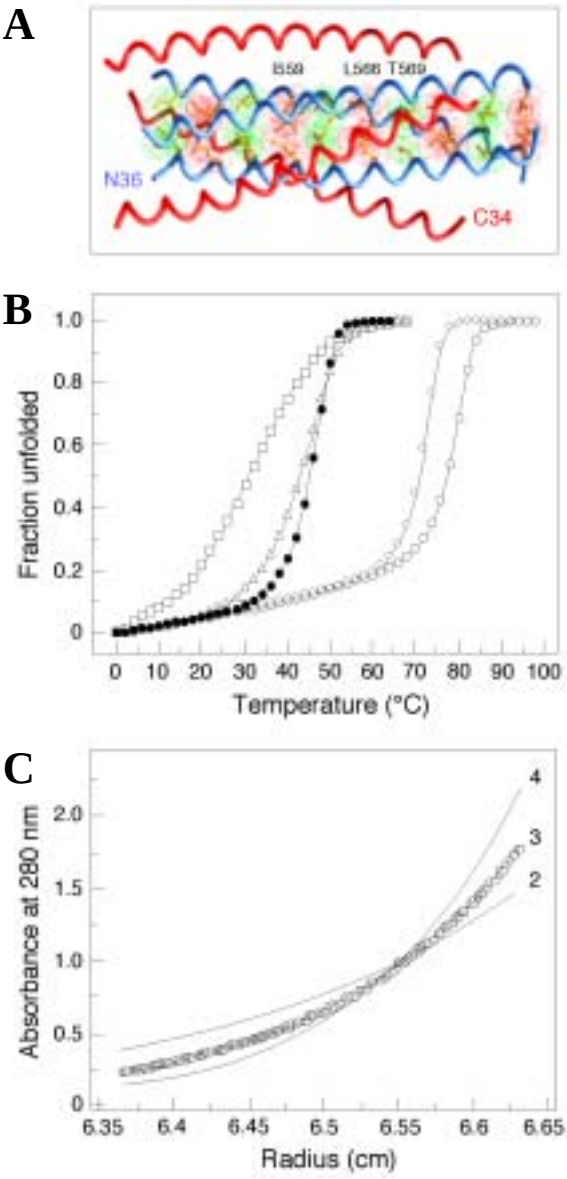

Fig. 6. HIV-1 $gp41_{ECTO}$ core structure and mutant peptides. **A**. The N36/C34 crystal structure is shown with one N36 and one C34 helix labeled at the amino terminus. Three C34 helices (red) pack against the N36 trimeric coiled coil (blue). The van der Waal surfaces of residues at the ***a*** (red) and ***d*** (green) positions are superimposed on the helix backbone of the N36 coiled coil. Amino-acids substituted in this study are indicated above the ***a*** and ***d*** layers. The Fig. was prepared using the program GRASP (64). **B**. Thermal melting transition curves of the N36(L6)C34 (open circles), I559G (closed circles), I559P (open squares), L566V (open rhombs) and T569P peptides (open triangles) were determined by CD spectroscopy at 222 nm, and at a peptide concentration of 10 μM in PBS (pH 7.0). The increase in the fraction of unfolded molecules is shown as a function of temperature. All melts were reversible. Superimposable folding and unfolding curves were observed, and >90% of the signal was regained upon cooling. **C**. Equilibrium sedimentation analysis of the T569P peptide. Representative data for this peptide were collected at 20°C and 20,000 rpm in PBS (pH 7.0), at a peptide concentration of ~30 μM. The data fit best to a trimer model (curve 3). Curves for a dimer (curve 2) and a tetramer (curve 4) are depicted for comparison. Analyses of residual differences from curve 3 do not reveal a systematic error.

trimers (105). The production of an oligomeric US4 $gp140_{UNC}$ protein that might be trimeric has also been reported (86). The presence of both dimers and tetramers in uncleaved versions of both membrane-bound gp160 and soluble gp140 molecules has been observed in several previous studies (27-30,33,101-103). Our own experience, using the BN-PAGE assay, is that a mixture of dimers, trimers and tetramers is present in unpurified and purified HIV-1_{JR-FL} $gp140_{UNC}$ preparations, with dimers being the most abundant species (83). Moreover, the dimeric and tetrameric forms of HIV-1 $gp140_{UNC}$ and gp160 proteins are probably oligomerized by aberrant intermolecular disulfide bonds (Fig. 2) (67,83). It is

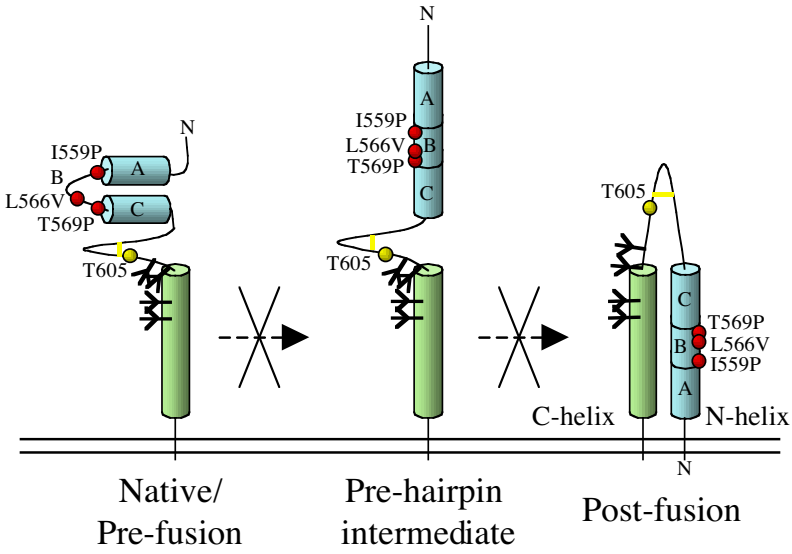

Fig. 7. Model of gp41$_{ECTO}$ and its transitions during fusion. Left panel: the hypothetical, native pre-fusion configuration of gp41 (39). Middle panel: The pre-hairpin intermediate form. Right panel: The post-fusion state. In the pre-fusion configuration the N-terminal helix is not present, and the region around position 559-569 is not helical. The I559P and related substitutions are proposed to disrupt either the formation of the N-terminal helix in the pre-hairpin intermediate, or the formation of the six-helix bundle. By doing so, the modified SOS gp140 proteins are maintained in the pre-fusion configuration. The position of the T605C substitution that creates the SOS gp140 protein is also specified, as is the adjacent intermolecular disulfide bond (yellow bar) and the position of *N*-linked glycans. Only the two helices from one gp41 molecule are shown, for clarity.

unlikely that oligomeric gp140 proteins of this type will fully mimic the native conformation of Env. Indeed, we have found that unpurified gp140$_{UNC}$ proteins have a different antigenic structure than unpurified SOS gp140 monomers and SOSIP gp140 trimers. Thus, non-neutralizing antibody epitopes in both the gp120 and gp41$_{ECTO}$ moieties are exposed to a much greater extent in gp140$_{UNC}$ proteins than in the SOS gp140 proteins (Fig. 5) (5,79,83). We are now comparing purified, cleaved and uncleaved trimers, as well as purified, uncleaved dimers and tetramers, to assess their antigenic structures, their migration on BN-PAGE gels after various treatments, and their receptor-binding properties. These and other planned structural studies studies should help determine whether SOSIP gp140 proteins truly have properties that mimic those of the native Env trimer, or whether the I559P or related substitutions have converted the gp41$_{ECTO}$ moieties into a non-native, irrelevant conformation.

The trimer-stabilizing substitutions we have described here should simplify the production of cleaved Env trimers, which may be useful in vaccine design and for structural studies. Whether cleaved, stabilized trimeric Env proteins such as SOSIP gp140 will turn out to be better or worse immunogens than other forms of Env (e.g., gp140$_{UNC}$ proteins) can only be determined empirically. It may be necessary to further modify the structure of SOSIP gp140 to increase its immuno-

Table 3. Biophysical characterization of JR-FL gp41 core mutants[a]

Mutant	θ_{222} (degrees/cm²/dmol)	T_m (°C)	M_{obs}/M_{calc}
N36(L6)C34	32,500	78	3.1
I559G	32,300	46	2.9
I559P	25,600	34	—[b]
L566V	32,100	72	3.1
T569P	29,400	44	3.0

[a] All CD scans and melts were performed with 10 μM peptide solutions in PBS (pH 7.0). T_m was estimated from the thermal dependence of θ_{222}. Sedimentation equilibrium results are reported as a ratio of the experimentally determined molecular weight to the calculated molecular weight for a monomer (M_{obs}/M_{calc}).
[b] —, Aggregated, as determined by sedimentation equilibrium analysis.

genicity, for example, by removing the variable loops to increase the exposure of underlying conserved epitopes, or by reducing the extent to which the protein is glycosylated (2,7,23,53,62,76,104). Proteins with such changes are now also being constructed for future structural and immunogenicity studies.

Acknowledgements

We are grateful to James Robinson, George Lewis, Hermann Katinger and Dennis Burton for the gifts of MAbs used in these studies**.** Paul Maddon's advice and support is greatly appreciated. We thank Steven Harrison providing SIV $gp140_{UNC}$ trimers for calibration of gel-filtration columns. This work was supported by NIH grants AI39420, AI42382, AI45463 and AI49764. JPM is a Stavros S. Niarchos Scholar. The Department of Microbiology and Immunology at the Weill Medical College gratefully acknowledges the support of the William Randolph Hearst Foundation.

References

1. **Allaway, G. P., K. L. Davis-Bruno, G. A. Beaudry, E. B. Garcia, E. L. Wong, A. M. Ryder, K. W. Hasel, M. C. Gauduin, R. A. Koup, J. S. McDougal, and P. J. Maddon**. 1995. Expression and characterization of CD4-IgG2, a novel heterotetramer that neutralizes primary HIV type 1 isolates. AIDS Res. Hum. Retrovir. **11**:533-539.
2. **Barnett, S. W., S. Lu, I. Srivastava, S. Cherpelis, A. Gettie, J. Blanchard, S. Wang, I. Mboudjeka, L. Leung, Y. Lian, A. Fong, C. Buckner, A. Ly, S. Hilt, J. Ulmer, C. T. Wild, J. R. Mascola, and L. Stamatatos**. 2001. The ability of an oligomeric human immunodeficiency virus type 1 (HIV- 1) envelope antigen to elicit neutralizing antibodies against primary HIV-1 isolates is improved following partial deletion of the second hypervariable region. J. Virol. **75**:5526-5540.
3. **Bernstein, H. B., S. P. Tucker, S. R. Kar, S. A. McPherson, D. T. McPherson, J. W. Dubay, J. Lebowitz, R. W. Compans, and E. Hunter**. 1995. Oligomerization of the hydrophobic heptad repeat of gp41. J. Virol. **69**:2745-2750.
4. **Bewley, C. A., J. M. Louis, R. Ghirlando, and G. M. Clore**. 2002. Design of a novel peptide inhibitor of HIV fusion that disrupts the internal trimeric coiled-coil of gp41. J. Biol. Chem. **277**:14238-14245.
5. **Binley, J. M., R. W. Sanders, B. Clas, N. Schuelke, A. Master, Y. Guo, F. Kajumo, D. J. Anselma, P. J. Maddon, W. C. Olson, and J. P. Moore**. 2000. A recombinant HIV-1 envelope glyco-

protein complex stabilized by an intermolecular disulfide bond between the gp120 and gp41 subunits is an antigenic mimic of the trimeric virion-associated structure. J. Virol. **74**:627-643.

6. **Binley, J. M., R. W. Sanders, A. Master, C. S. Cayanan, C. L. Wiley, L. Schiffner, B. Travis, S. Kuhmann, D. R. Burton, S.-L. Hu, W. C. Olson, and J. P. Moore**. 2002. Enhancing the proteolytic maturation of human immunodeficiency virus type 1 envelope glycoproteins. J. Virol. **76**:2606-2616.
7. **Bolmstedt, A., J. Hinkula, E. Rowcliffe, M. Biller, B. Wahren, and S. Olofsson**. 2001. Enhanced immunogenicity of a human immunodeficiency virus type 1 env DNA vaccine by manipulating N-glycosylation signals. Effects of elimination of the V3 N306 glycan. Vaccine **20**:397-405.
8. **Bullough, P. A., F. M. Hughson, J. J. Skehel, and D. C. Wiley**. 1994. Structure of influenza haemagglutinin at the pH of membrane fusion. Nature **371**:37-43.
9. **Burton, D. R. and P. W. Parren**. 2000. Vaccines and the induction of functional antibodies: time to look beyond the molecules of natural infection? Nat. Med. **6**:123-125.
10. **Caffrey, M., M. Cai, J. Kaufman, S. J. Stahl, P. T. Wingfield, D. G. Covell, A. M. Gronenborn, and G. M. Clore**. 1998. Three-dimensional solution structure of the 44 kDa ectodomain of SIV gp41. EMBO J. **17**:4572-4584.
11. **Caffrey, M., J. Kaufman, S. Stahl, P. Wingfield, A. M. Gronenborn, and G. M. Clore**. 1999. Monomer-trimer equilibrium of the ectodomain of SIV gp41: insight into the mechanism of peptide inhibition of HIV infection. Protein Sci. **8**:1904-1907.
12. **Cantor, C. and P. Schimmel**. 1980. Biophysical chemistry, part III. W. H. Freeman and company, New York, N.Y.
13. **Cao, J., L. Bergeron, E. Helseth, M. Thali, H. Repke, and J. Sodroski**. 1993. Effects of amino-acid changes in the extracellular domain of the human immunodeficiency virus type 1 gp41 envelope glycoprotein. J. Virol. **67**:2747-2755.
14. **Center, R. J., P. L. Earl, J. Lebowitz, P. Schuck, and B. Moss**. 2000. The human immunodeficiency virus type 1 gp120 V2 domain mediates gp41- independent intersubunit contacts. J. Virol. **74**:4448-4455.
15. **Center, R. J., P. Schuck, R. D. Leapman, L. O. Arthur, P. L. Earl, B. Moss, and J. Lebowitz**. 2001. Oligomeric structure of virion-associated and soluble forms of the simian immunodeficiency virus envelope protein in the prefusion activated conformation. Proc. Natl. Acad. Sci. USA **98**:14877-14882.
16. **Chan, D. C., D. Fass, J. M. Berger, and P. S. Kim**. 1997. Core structure of gp41 from the HIV envelope glycoprotein. Cell **89**:263-273.
17. **Chan, D. C. and P. S. Kim**. 1998. HIV entry and its inhibition. Cell **93**:681-684.
18. **Chang, D. K., V. D. Trivedi, S. F. Cheng, and S. Francis**. 2001. The leucine zipper motif of the envelope glycoprotein ectodomain of human immunodeficiency virus type 1 contains conformationally flexible regions as revealed by NMR and circular dichroism studies in different media. J. Pept. Res. **57**:234-239.
19. **Chen, B., G. Zhou, M. Kim, Y. Chishti, R. E. Hussey, B. Ely, J. J. Skehel, E. L. Reinherz, S. C. Harrison, and D. C. Wiley**. 2000. Expression, purification, and characterization of gp160e, the soluble, trimeric ectodomain of the simian immunodeficiency virus envelope glycoprotein, gp160. J. Biol. Chem. **275**:34946-34953.
20. **Chen, S. S.** 1994. Functional role of the zipper motif region of human immunodeficiency virus type 1 transmembrane protein gp41. J. Virol. **68**:2002-2010.
21. **Chen, S. S., S. F. Lee, H. J. Hao, and C. K. Chuang**. 1998. Mutations in the leucine zipper-like heptad repeat sequence of human immunodeficiency virus type 1 gp41 dominantly interfere with wild-type virus infectivity. J. Virol. **72**:4765-4774.
22. **Chen, Y. H., J. T. Yang, and K. H. Chau**. 1974. Determination of the helix and beta form of proteins in aqueous solution by circular dichroism. Biochemistry **13**:3350-3359.
23. **Cherpelis, S., I. Shrivastava, A. Gettie, X. Jin, D. D. Ho, S. W. Barnett, and L. Stamatatos**. 2001. DNA vaccination with the human immunodeficiency virus type 1 SF162DeltaV2 envelope elicits immune responses that offer partial protection from simian/human immunodeficiency virus infection to CD8(+) T-cell-depleted rhesus macaques. J. Virol. **75**:1547-1550.
24. **Doms, R. W.** 2000. Beyond receptor expression: the influence of receptor conformation, density, and affinity in HIV-1 infection. Virology **276**:229-237.

25. **Doms, R. W. and J. P. Moore**. 2000. HIV-1 membrane fusion: targets of opportunity. J. Cell Biol. **151**:F9-14.
26. **Earl, P. L., C. C. Broder, R. W. Doms, and B. Moss**. 1997. Epitope map of human immunodeficiency virus type 1 gp41 derived from 47 monoclonal antibodies produced by immunization with oligomeric envelope protein. J. Virol. **71**:2674-2684.
27. **Earl, P. L., C. C. Broder, D. Long, S. A. Lee, J. Peterson, S. Chakrabarti, R. W. Doms, and B. Moss**. 1994. Native oligomeric human immunodeficiency virus type 1 envelope glycoprotein elicits diverse monoclonal antibody reactivities. J. Virol. **68**:3015-3026.
28. **Earl, P. L., R. W. Doms, and B. Moss**. 1990. Oligomeric structure of the human immunodeficiency virus type 1 envelope glycoprotein. Proc. Natl. Acad. Sci. USA **87**:648-652.
29. **Earl, P. L. and B. Moss**. 1993. Mutational analysis of the assembly domain of the HIV-1 envelope glycoprotein. AIDS Res. Hum. Retrovir. **9**:589-594.
30. **Earl, P. L., B. Moss, and R. W. Doms**. 1991. Folding, interaction with GRP78-BiP, assembly, and transport of the human immunodeficiency virus type 1 envelope protein. J. Virol. **65**:2047-2055.
31. **Eckert, D. M. and P. S. Kim**. 2001. Mechanisms of viral membrane fusion and its inhibition. Annu. Rev. Biochem. **70**:777-810.
32. **Edelhoch, H.** 1967. Spectroscopic determination of tryptophan and tyrosine in proteins. Biochemistry **6**:1948-1954.
33. **Farzan, M., H. Choe, E. Desjardins, Y. Sun, J. Kuhn, J. Cao, D. Archambault, P. Kolchinsky, M. Koch, R. Wyatt, and J. Sodroski**. 1998. Stabilization of human immunodeficiency virus type 1 envelope glycoprotein trimers by disulfide bonds introduced into the gp41 glycoprotein ectodomain. J. Virol. **72**:7620-7625.
34. **Fouts, T. R., A. Trkola, M. S. Fung, and J. P. Moore**. 1998. Interactions of polyclonal and monoclonal anti-glycoprotein 120 antibodies with oligomeric glycoprotein 120-glycoprotein 41 complexes of a primary HIV type 1 isolate: relationship to neutralization. AIDS Res. Hum. Retrovir. **14**:591-597.
35. **Gallo, S. A., A. Puri, and R. Blumenthal**. 2001. HIV-1 gp41 six-helix bundle formation occurs rapidly after the engagement of gp120 by CXCR4 in the HIV-1 Env-mediated fusion process. Biochemistry **40**:12231-12236.
36. **Gorny, M. K. and S. Zolla-Pazner**. 2000. Recognition by human monoclonal antibodies of free and complexed peptides representing the prefusogenic and fusogenic forms of human immunodeficiency virus type 1 gp41. J. Virol. **74**:6186-6192.
37. **Gruenke, J. A., R. T. Armstrong, W. W. Newcomb, J. C. Brown, and J. M. White**. 2002. New insights into the spring-loaded conformational change of influenza virus hemagglutinin. J. Virol. **76**:4456-4466.
38. **Harbury, P. B., P. S. Kim, and T. Alber**. 1994. Crystal structure of an isoleucine-zipper trimer. Nature **371**:80-83.
39. **Hunter, E.** 1997. gp41, a multifunctional protein involved in HIV entry and pathogenesis, p. III-55-III-73. *In* B. Korber, B. Hahn, B. Foley, J. W. Mellors, T. Leitner, G. Myers, F. McCutchan, and C. L. Kuiken (eds.), Human Retroviruses and AIDS 1997. Theoretical Biology and Biophysics Group, Los Alamos National Laboratory, Los Alamos, NM.
40. **Jelesarov, I. and M. Lu**. 2001. Thermodynamics of trimer-of-hairpins formation by the SIV gp41 envelope protein. J. Mol. Biol. **307**:637-656.
41. **Ji, H., C. Bracken, and M. Lu**. 2000. Buried polar interactions and conformational stability in the simian immunodeficiency virus (SIV) gp41 core. Biochemistry **39**:676-685.
42. **Jiang, S., K. Lin, and M. Lu**. 1998. A conformation-specific monoclonal antibody reacting with fusion-active gp41 from the human immunodeficiency virus type 1 envelope glycoprotein. J. Virol. **72**:10213-10217.
43. **Johnson, M. L., J. J. Correia, D. A. Yphantis, and H. R. Halvorson**. 1981. Analysis of data from the analytical ultracentrifuge by nonlinear least- squares techniques. Biophys. J. **36**:575-588.
44. **Kunkel, T. A., J. D. Roberts, and R. A. Zakour**. 1987. Rapid and efficient site-specific mutagenesis without phenotypic selection, p. 367-382. *In* R. Wu and L. Grossman (eds.), Methods in Enzymology. Academic Press, San Diego.
45. **Kwong, P. D., R. Wyatt, S. Majeed, J. Robinson, R. W. Sweet, J. Sodroski, and W. A. Hendrickson**. 2000. Structures of HIV-1 gp120 envelope glycoproteins from laboratory- adapted and

primary isolates. Structure Fold. Des. **8**:1329-1339.
46. **Kwong, P. D., R. Wyatt, J. Robinson, R. W. Sweet, J. Sodroski, and W. A. Hendrickson**. 1998. Structure of an HIV gp120 envelope glycoprotein in a complex with the CD4 receptor and a neutralizing human antibody. Nature **393**:648-659.
47. **LaBranche, C. C., M. M. Sauter, B. S. Haggarty, P. J. Vance, J. Romano, T. K. Hart, P. J. Bugelski, M. Marsh, and J. A. Hoxie**. 1995. A single amino-acid change in the cytoplasmic domain of the simian immunodeficiency virus transmembrane molecule increases envelope glycoprotein expression on infected cells. J. Virol. **69**:5217-5227.
48. **Laue, T. M., B. D. Shah, T. M. Ridgeway, and S. L. Pelletier**. 1992. Computer-aided interpretation of analytical sedimentation data for proteins, p. 90-125. *In* S. E. Harding, A. J. Rowe, and J. C. Horton (eds.), Analytical ultracentrifugation in biochemistry and polymer science. Royal Society of Chemistry, Cambridge, England.
49. **Liu, J., W. Shu, M. B. Fagan, J. H. Nunberg, and M. Lu**. 2001. Structural and functional analysis of the HIV gp41 core containing an Ile573 to Thr substitution: implications for membrane fusion. Biochemistry **40**:2797-2807.
50. **Liu, J., S. Wang, J. A. Hoxie, C. C. LaBranche, and M. Lu**. 2002. Mutations that destabilize the gp41core are determinants for stabilizing the Simian Immunodeficiency Virus-CPmac envelope glycoprotein complex. J. Biol. Chem. **277**:12891-12900.
51. **Lu, M., H. Ji, and S. Shen**. 1999. Subdomain folding and biological activity of the core structure from human immunodeficiency virus type 1 gp41: implications for viral membrane fusion. J. Virol. **73**:4433-4438.
52. **Lu, M., M. O. Stoller, S. Wang, J. Liu, M. B. Fagan, and J. H. Nunberg**. 2001. Structural and functional analysis of interhelical interactions in the human immunodeficiency virus type 1 gp41 envelope glycoprotein by alanine-scanning mutagenesis. J. Virol. **75**:11146-11156.
53. **Lu, S., R. Wyatt, J. F. Richmond, F. Mustafa, S. Wang, J. Weng, D. C. Montefiori, J. Sodroski, and H. L. Robinson**. 1998. Immunogenicity of DNA vaccines expressing human immunodeficiency virus type 1 envelope glycoprotein with and without deletions in the V1/2 and V3 regions. AIDS Res. Hum. Retrovir. **14**:151-155.
54. **Malashkevich, V. N., D. C. Chan, C. T. Chutkowski, and P. S. Kim**. 1998. Crystal structure of the simian immunodeficiency virus (SIV) gp41 core: conserved helical interactions underlie the broad inhibitory activity of gp41 peptides. Proc. Natl. Acad. Sci. USA **95**:9134-9139.
55. **McCune, J. M., L. B. Rabin, M. B. Feinberg, M. Lieberman, J. C. Kosek, G. R. Reyes, and I. L. Weissman**. 1988. Endoproteolytic cleavage of gp160 is required for the activation of human immunodeficiency virus. Cell **53**:55-67.
56. **Melikyan, G. B., R. M. Markosyan, H. Hemmati, M. K. Delmedico, D. M. Lambert, and F. S. Cohen**. 2000. Evidence that the transition of HIV-1 gp41 into a six-helix bundle, not the bundle configuration, induces membrane fusion. J. Cell Biol. **151**:413-423.
57. **Moore, J. P. and J. Binley**. 1998. HIV. Envelope's letters boxed into shape. Nature **393**:630-631.
58. **Moore, J. P. and D. D. Ho**. 1995. HIV-1 neutralization: the consequences of viral adaptation to growth on transformed T cells. AIDS **9 (Suppl. A)**:S117-S136.
59. **Moore, J. P., P. W. H. I. Parren, and D. R. Burton**. 2001. Genetic subtypes, humoral immunity, and human immunodeficiency virus type 1 vaccine development. J. Virol. **75**:5721-5729.
60. **Moore, J. P. and J. Sodroski**. 1996. Antibody cross-competition analysis of the human immunodeficiency virus type 1 gp120 exterior envelope glycoprotein. J. Virol. **70**:1863-1872.
61. **Moore, J. P. and M. Stevenson**. 2000. New targets for inhibitors of HIV-1 replication. Nat. Rev. Mol. Cell Biol. **1**:40-49.
62. **Mori, K., Y. Yasutomi, S. Ohgimoto, T. Nakasone, S. Takamura, T. Shioda, and Y. Nagai**. 2001. Quintuple deglycosylation mutant of simian immunodeficiency virus SIVmac239 in rhesus macaques: robust primary replication, tightly contained chronic infection, and elicitation of potent immunity against the parental wild-type strain. J. Virol. **75**:4023-4028.
63. **Moulard, M. and E. Decroly**. 2000. Maturation of HIV envelope glycoprotein precursors by cellular endoproteases. Biochim. Biophys. Acta **1469**:121-132.
64. **Nicholls, A., K. A. Sharp, and B. Honig**. 1991. Protein folding and association: insights from the interfacial and thermodynamic properties of hydrocarbons. Proteins **11**:281-296.
65. **Nyambi, P. N., M. K. Gorny, L. Bastiani, G. G. van der, C. Williams, and S. Zolla-Pazner**. 1998. Mapping of epitopes exposed on intact human immunodeficiency virus type 1 (HIV-1) viri-

ons: a new strategy for studying the immunologic relatedness of HIV-1. J. Virol. **72**:9384-9391.
66. **Olofsson, S. and J. E. Hansen**. 1998. Host cell glycosylation of viral glycoproteins—a battlefield for host defence and viral resistance. Scand. J. Infect. Dis. **30**:435-440.
67. **Owens, R. J. and R. W. Compans**. 1990. The human immunodeficiency virus type 1 envelope glycoprotein precursor acquires aberrant intermolecular disulfide bonds that may prevent normal proteolytic processing. Virology **179**:827-833.
68. **Parker, C. E., L. J. Deterding, C. Hager-Braun, J. M. Binley, N. Schulke, H. Katinger, J. P. Moore, and K. B. Tomer**. 2001. Fine Definition of the Epitope on the gp41 Glycoprotein of Human Immunodeficiency Virus Type 1 for the Neutralizing Monoclonal Antibody 2F5. J. Virol. **75**:10906-10911.
69. **Parren, P. W., D. R. Burton, and Q. J. Sattentau**. 1997. HIV-1 antibody—debris or virion? Nat. Med. **3**:366-367.
70. **Parren, P. W., I. Mondor, D. Naniche, H. J. Ditzel, P. J. Klasse, D. R. Burton, and Q. J. Sattentau**. 1998. Neutralization of human immunodeficiency virus type 1 by antibody to gp120 is determined primarily by occupancy of sites on the virion irrespective of epitope specificity. J. Virol. **72**:3512-3519.
71. **Parren, P. W. H. I., J. P. Moore, D. R. Burton, and Q. J. Sattentau**. 1999. The neutralizing antibody response to HIV-1: viral evasion and escape from humoral immunity. AIDS **13 (Suppl. A)**:S137-S162.
72. **Peisajovich, S. G. and Y. Shai**. 2001. SIV gp41 binds to membranes both in the monomeric and trimeric states: consequences for the neuropathology and inhibition of HIV infection. J. Mol. Biol. **311**:249-254.
73. **Poignard, P., E. O. Saphire, P. W. Parren, and D. R. Burton**. 2001. gp120: Biologic aspects of structural features. Annu. Rev. Immunol. **19**:253-274.
74. **Poumbourios, P., K. A. Wilson, R. J. Center, W. El Ahmar, and B. E. Kemp**. 1997. Human immunodeficiency virus type 1 envelope glycoprotein oligomerization requires the gp41 amphipathic alpha-helical/leucine zipper-like sequence. J. Virol. **71**:2041-2049.
75. **Qiao, H., S. L. Pelletier, L. Hoffman, J. Hacker, R. T. Armstrong, and J. M. White**. 1998. Specific single or double proline substitutions in the "spring-loaded" coiled-coil region of the influenza hemagglutinin impair or abolish membrane fusion activity. J. Cell Biol. **141**:1335-1347.
76. **Reitter, J. N., R. E. Means, and R. C. Desrosiers**. 1998. A role for carbohydrates in immune evasion in AIDS. Nat. Med. **4**:679-684.
77. **Rizzuto, C. D., R. Wyatt, N. Hernandez-Ramos, Y. Sun, P. D. Kwong, W. A. Hendrickson, and J. Sodroski**. 1998. A conserved HIV gp120 glycoprotein structure involved in chemokine receptor binding. Science **280**:1949-1953.
78. **Robinson, W. E., Jr., T. Kawamura, M. K. Gorny, D. lake, J. Y. Xu, Y. Matsumoto, T. Sugano, Y. Masuho, W. M. Mitchell, E. Hersh, and S. Zolla-Pazner**. 1990. Human monoclonal antibodies to the human immunodeficiency virus type 1 (HIV-1) transmembrane glycoprotein gp41 enhance HIV-1 infection *in vitro*. Proc. Natl. Acad. Sci. USA **87**:3185-3189.
79. **Sanders, R. W., L. Schiffner, A. Master, F. Kajumo, Y. Guo, T. Dragic, J. P. Moore, and J. M. Binley**. 2000. Variable-loop-deleted variants of the human immunodeficiency virus type 1 envelope glycoprotein can be stabilized by an intermolecular disulfide bond between the gp120 and gp41 subunits. J. Virol. **74**:5091-5100.
80. **Sanders, R. W., M. Venturi, L. Schiffner, R. Kalyanaraman, H. Katinger, P. D. Kwong, and J. P. Moore**. 2002. The mannose-dependent epitope for the neutralizing antibody 2G12 on the gp120 glycoprotein of human immunodeficiency virus type-1. J. Virol. **in press**.
81. **Sattentau, Q. J. and J. P. Moore**. 1995. Human immunodeficiency virus type 1 neutralization is determined by epitope exposure on the gp120 oligomer. J. Exp. Med. **182**:185-196.
82. **Sattentau, Q. J., S. Zolla-Pazner, and P. Poignard**. 1995. Epitope exposure on functional, oligomeric HIV-1 gp41 molecules. Virology **206**:713-717.
83. **Schuelke, N., M. S. Vesanen, R. W. Sanders, P. Zhu, D. J. Anselma, A. R. Villa, P. W. H. I. Parren, J. M. Binley, K. H. Roux, P. J. Maddon, J. P. Moore, and W. C. Olson**. 2002. Structural and antigenic properties of a proteolytically mature, disulfide-stabilized human immunodeficiency virus type 1 gp140 envelope glycoprotein. J. Virol. **in press**.
84. **Shu, W., H. Ji, and M. Lu**. 1999. Trimerization specificity in HIV-1 gp41: analysis with a GCN4 leucine zipper model. Biochemistry **38**:5378-5385.

85. **Shugars, D. C., C. T. Wild, T. K. Greenwell, and T. J. Matthews**. 1996. Biophysical characterization of recombinant proteins expressing the leucine zipper-like domain of the human immunodeficiency virus type 1 transmembrane protein gp41. J. Virol. **70**:2982-2991.
86. **Srivastava, I. K., L. Stamatatos, H. Legg, E. Kan, S. Coates, L. Leung, A. Fong, M. Wininger, A. R. Tipton, J. Donnelly, J. B. Ulmer, and S. W. Barnett**. 2002. Purification and characterization of oligomeric glycoprotein from a primary R5 subtype B human immunodeficiency virus for vaccine applications. J. Virol. **76**:2835-2847.
87. **Stamatatos, L., M. Lim, and C. Cheng-Mayer**. 2000. Generation and structural analysis of soluble oligomeric gp140 envelope proteins derived from neutralization-resistant and neutralization- susceptible primary HIV type 1 isolates. AIDS Res. Hum. Retrovir. **16**:981-994.
88. **Stiegler, G., R. Kunert, M. Purtscher, S. Wolbank, R. Voglauer, F. Steindl, and H. Katinger**. 2001. A potent cross-clade neutralizing human monoclonal antibody against a novel epitope on gp41 of human immunodeficiency virus type 1. AIDS Res. Hum. Retrovir. **17**:1757-1765.
89. **Tan, K., J. Liu, J. Wang, S. Shen, and M. Lu**. 1997. Atomic structure of a thermostable subdomain of HIV-1 gp41. Proc. Natl. Acad. Sci. USA **94**:12303-12308.
90. **Taniguchi, Y., S. Zolla-Pazner, Y. Xu, X. Zhang, S. Takeda, and T. Hattori**. 2000. Human monoclonal antibody 98-6 reacts with the fusogenic form of gp41. Virology **273**:333-340.
91. **Thali, M., J. P. Moore, C. Furman, M. Charles, D. D. Ho, J. Robinson, and J. Sodroski**. 1993. Characterization of conserved human immunodeficiency virus type 1 gp120 neutralization epitopes exposed upon gp120-CD4 binding. J. Virol. **67**:3978-3988.
92. **Trkola, A., T. Dragic, J. Arthos, J. M. Binley, W. C. Olson, G. P. Allaway, C. Cheng-Mayer, J. Robinson, P. J. Maddon, and J. P. Moore**. 1996. CD4-dependent, antibody-sensitive interactions between HIV-1 and its co-receptor CCR-5. Nature **384**:184-187.
93. **Trkola, A., M. Purtscher, T. Muster, C. Ballaun, A. Buchacher, N. Sullivan, K. Srinivasan, J. Sodroski, J. P. Moore, and H. Katinger**. 1996. Human monoclonal antibody 2G12 defines a distinctive neutralization epitope on the gp120 glycoprotein of human immunodeficiency virus type 1. J. Virol. **70**:1100-1108.
94. **Weissenhorn, W., A. Dessen, S. C. Harrison, J. J. Skehel, and D. C. Wiley**. 1997. Atomic structure of the ectodomain from HIV-1 gp41. Nature **387**:426-430.
95. **Weng, Y. and C. D. Weiss**. 1998. Mutational analysis of residues in the coiled-coil domain of human immunodeficiency virus type 1 transmembrane protein gp41. J. Virol. **72**:9676-9682.
96. **Weng, Y., Z. Yang, and C. D. Weiss**. 2000. Structure-function studies of the self-assembly domain of the human immunodeficiency virus type 1 transmembrane protein gp41. J. Virol. **74**:5368-5372.
97. **Wyatt, R., P. D. Kwong, E. Desjardins, R. W. Sweet, J. Robinson, W. A. Hendrickson, and J. G. Sodroski**. 1998. The antigenic structure of the HIV gp120 envelope glycoprotein. Nature **393**:705-711.
98. **Wyatt, R., J. Moore, M. Accola, E. Desjardin, J. Robinson, and J. Sodroski**. 1995. Involvement of the V1/V2 variable loop structure in the exposure of human immunodeficiency virus type 1 gp120 epitopes induced by receptor binding. J. Virol. **69**:5723-5733.
99. **Wyatt, R. and J. Sodroski**. 1998. The HIV-1 envelope glycoproteins: fusogens, antigens, and immunogens. Science **280**:1884-1888.
100. **Xu, J. Y., M. K. Gorny, T. Palker, S. Karwowska, and S. Zolla-Pazner**. 1991. Epitope mapping of two immunodominant domains of gp41, the transmembrane protein of human immunodeficiency virus type 1, using ten human monoclonal antibodies. J. Virol. **65**:4832-4838.
101. **Yang, X., M. Farzan, R. Wyatt, and J. Sodroski**. 2000. Characterization of stable, soluble trimers containing complete ectodomains of human immunodeficiency virus type 1 envelope glycoproteins. J. Virol. **74**:5716-5725.
102. **Yang, X., L. Florin, M. Farzan, P. Kolchinsky, P. D. Kwong, J. Sodroski, and R. Wyatt**. 2000. Modifications that stabilize human immunodeficiency virus envelope glycoprotein trimers in solution. J. Virol. **74**:4746-4754.
103. **Yang, X., J. Lee, E. M. Mahony, P. D. Kwong, R. Wyatt, and J. Sodroski**. 2002. Highly stable trimers formed by human immunodeficiency virus type 1 envelope glycoproteins fused with the trimeric motif of T4 bacteriophage fibritin. J. Virol. **76**:4634-4642.
104. **Yang, X., R. Wyatt, and J. Sodroski**. 2001. Improved elicitation of neutralizing antibodies against primary human immunodeficiency viruses by soluble stabilized envelope glycoprotein

trimers. J. Virol. **75**:1165-1171.

105. **Zhang, C. W., Y. Chishti, R. E. Hussey, and E. L. Reinherz**. 2001. Expression, purification, and characterization of recombinant HIV gp140. The gp41 ectodomain of HIV or simian immunodeficiency virus is sufficient to maintain the retroviral envelope glycoprotein as a trimer. J. Biol. Chem. **276**:39577-39585.
106. **Zwick, M. B., A. F. Labrijn, M. Wang, C. Spenlehauer, E. O. Saphire, J. M. Binley, J. P. Moore, G. Stiegler, H. Katinger, D. R. Burton, and P. W. Parren**. 2001. Broadly neutralizing antibodies targeted to the membrane-proximal external region of human immunodeficiency virus type 1 glycoprotein gp41. J. Virol. **75**:10892-10905.

Chapter 5.7

Evolutionary repair of HIV-1 gp41 with a kink in the N-terminal helix leads to restoration of the six-helix bundle structure

(Submitted for publication)

Rogier W. Sanders[1], Els Busser[1], John P. Moore[2], Min Lu[3], Ben Berkhout[1]

[1] Department of Human Retrovirology, Academic Medical Center, University of Amsterdam, the Netherlands

[2] Department of Microbiology and Immunology and [3] Department of Biochemistry, Weill Medical College, Cornell University, NewYork, NY 10021, USA

The HIV-1 envelope glycoprotein complex (Env) can be stabilized by the introduction of a disulfide bond between the gp120 and gp41 subunits. The resulting protein is monomeric, but trimerization can be improved by the introduction of a single helix-breaking residue at the conserved Ile559 site in the N-terminal heptad repeat region of gp41. To provide more insight into how such a substitution in gp41 affects Env structure and function, we evaluated the effect on the wild-type Env in the context of replicating virus. The Ile559Gly and Ile559Pro mutations adversely affect Env biosynthesis and Env incorporation into virions. Biophysical studies show that the Ile559Pro mutation essentially disrupts the folding of a recombinant gp41 ectodomain core into a six-helix bundle structure. Viruses containing the Ile559Gly and Ile559Pro substitutions replicate poorly, but an evolution route is described that restores replication competence. In the escape virus, which contains a Pro559Leu first-site pseudo-reversion, the local helical structure and, as a consequence, Env biosynthesis and function are restored.

Introduction

The HIV-1 envelope glycoproteins (Env) mediate viral attachment and entry into susceptible target cells. A gp160 precursor protein is processed intracellularly to yield the native form of the envelope complex, consisting of three gp120 and three gp41 molecules associated through non-covalent interactions. Upon binding of the cell-surface receptor (CD4) and a co-receptor (CCR5 or CXCR4) to the surface subunit gp120, a series of conformational changes within the Env complex enable the insertion of the hydrophobic fusion peptide of the transmembrane subunit gp41 into the target membrane (31,45). Structural rearrangements within gp41 eventually trigger the association of the N-terminal helix (the first heptad repeat; HR1) with a C-terminal helix (the second heptad repeat; HR2) into a six-helix bundle, thereby juxtaposing the viral and cellular membranes for fusion (12,15,18). These late structural changes are targeted by the entry inhibitor T-20 (2,15).

The gp120 and gp41 glycoproteins are embedded in the viral membrane, and form the major targets for virus-neutralizing antibodies (29,31). Hence these proteins are the focus for the development of subunit vaccines based on the induction of humoral immunity. However, monomeric gp120 has not been able to elicit adequate neutralizing antibody responses (29,42). Although more sophisticated, modified Env immunogens have been designed, the design of such proteins is greatly hampered by an incomplete understanding of the intracellular folding, processing and oligomerization steps, and the structure of the assembled Env complex. Thus, modified forms of Env can sometimes be misfolded, uncleaved, monomeric/dimeric instead of trimeric or otherwise structurally different from the native Env conformation. A better understanding of these modified Env constructs may help in the design of further modifications and, eventually, in the development of improved Env immunogens.

We have previously shown that gp120 and gp41 can be stably linked by an appropriately positioned disulfide (5,37,41). Antibody probing indicated that the resulting soluble SOS gp140 protein is correctly folded, but subsequent studies indicated that it does not form a stable trimer (41). The membrane-bound form of the disulfide-stabilized protein (SOS Env) is capable of receptor-activated fusion when a reducing agent is added at the appropriate time to break the engineered bond (1,4). We subsequently demonstrated that the replacement of the absolutely conserved Ile at position 559 in the gp41 ectodomain (gp41e) by Gly (I559G) or Pro (I559P), can further stabilize the soluble SOS gp140 protein in substantially trimeric form (39). The resulting protein is termed SOSIP gp140 and may serve as a scaffold for further modifications to expose neutralizing epitopes. The immunogenicity of trimeric SOSIP gp140 is currently under investigation. The critical importance of gp41e residue 559 in trimer stabilization warrants further investigation of this position. To provide more insight into how substitutions at position 559 confer stability upon Env trimers, their effect on Env function was evaluated. We report here that viruses with the I559G and I559P substitutions replicate poorly, but that viral evolution is able to repair the replication capacity. The pathway involves restoring the potential of the HR1 region to form an a-helix that is capable of interacting with the HR2 region to form the six-helix bundle structure.

Materials and Methods

Plasmid constructs

The plasmid pRS1, generated to subclone mutant *env* genes, was generated as follows. First, the *Sal*I-*Bam*HI fragment from a molecular clone of HIV-1_{LAI} (pLAI)(30) was cloned into pUC18 (Roche, Indianapolis, IN). Second, a *Pst*I-*Stu*I fragment from the resulting plasmid was cloned into a pBS-SK(+)-gp160 plasmid with the *Sal*I-*Xho*I sequences of pLAI. Mutations were introduced in pRS1 using the Quickchange mutagenesis kit (Stratagene, La Jolla, CA) and verified by DNA sequencing. Mutant env genes in pRS1 were cloned into pLAI as *Sal*I-*Bam*HI fragments. Plasmid pN36/$C34_{JR-FL}$, encoding the HIV-1_{JR-FL} N36 (L6)C34 model peptide, was described previously (39). Amino-acid substitutions were introduced into the N36 segment of pN36/34_{JR-FL} by the method of Kunkel

et al. (23) and verified by DNA sequencing. Numbering of individual amino-acids is based on the HXB2 gp160 sequence.

Cells and transfection

SupT1 T cells and C33A cervix carcinoma cells were maintained in RPMI 1640 and DMEM, respectively (Life Technologies Ltd., Paisley, UK), supplemented with 10% fetal calf serum (FCS), penicillin (100 U/ml) and streptomycin (100 µg/ml) as previously described (35). SupT1 and C33A cells were transfected with pLAI constructs by electroporation and $Ca_2(PO_4)_3$ precipitation, respectively, as described previously (13).

Viruses and infection

Virus stocks were produced by transfecting C33A cells with the appropriate pLAI constructs. The virus containing supernatant was harvested 3 days post-transfection, filtered and stored at -80°C. The virus concentration was quantitated by capsid (CA)-p24 ELISA as described previously (20). These values were used to normalize the amount of virus in subsequent infection experiments, which were performed as follows. $200x10^3$ T cells were infected with C33A-produced HIV-1_{LAI} (20 ng CA-p24 per well on a 24-well plate), and virus spread was monitored for 14 days by CA-p24 ELISA.

Virus infectivity

LuSIV cells, stably transfected with an LTR-luciferase construct (34), were infected with 200 ng CA-p24/$300x10^3$ cells/ml/well on a 48-well plate. Cells were maintained in the presence of 200 nM saquinavir to prevent subsequent rounds of replication. Luciferase activity was measured after 48 h.

Virus evolution

For evolution experiments, SupT1 cells were transfected with 40 g pLAI by electroporation. The cultures were monitored regularly for the emergence of revertant viruses, using CA-p24 ELISA and/or the appearance of syncytia as indicators of virus replication. At regular intervals, cells and filtered supernatant were stored at -80°C and virus was quantitated by CA-p24 ELISA. When a revertant virus was identified, DNA was extracted from infected cells (14). Proviral gp41e sequences were PCR-amplified with primers A (5'-GTTTTAATTGTGGAGGGGAAT-3') and B (5'-ATTCCAATAATTCTTGTTCATTC-3'), then sequenced.

Ultracentrifugation of virions

C33A cells were transfected with 40 µg pLAI per T75 flask. Medium was refreshed at day one post-transfection. The culture supernatant was harvested at 3 days post-transfection, centrifuged and passed through a 0.45 µm filter to remove residual cells and debris. Cells were resuspended in 1.0 ml of lysis buffer (50mM Tris (pH 7.4), 10mM EDTA, 100mM NaCl, 1% SDS). Virus particles were pelleted from the supernatant by ultracentrifugation (100,000 x *g* for 45 min at 4°C) and resuspended in 0.5 ml lysis buffer. The virus free supernatant, containing shed gp120, was concentrated using Amicon centrifugal filter units (Millipore, Bedford, MA), then SDS was added to a final concentration of 1%.

Quantitation of gp120 by ELISA

Gp120 in cell, virion and supernatant fractions was measured as described previously with some modifications (28,38). ELISA plates were coated overnight with sheep antibody D7324 (10 µg/ml in 0.1 M $NaHCO_3$; Aalto Bioreagents, Rathfarnham, Dublin, Ireland), which is directed to the gp120 C5 region. After blocking by 2% milk in Tris-buffered saline (TBS) for 30 min, gp120 was captured by incubation for 2 h at room temperature. Recombinant HIV-1_{LAI} gp120 (Progenics Pharmaceuticals, Inc. Tarrytown, NY) was used as a reference standard. Unbound gp120 was washed away with TBS and purified HIV-1^+ serum Ig (HIVIg) was added for 1.5 h in 2% milk, 20% sheep serum (SS), 0.5% Tween. HIVIg binding was detected with alkaline phosphatase conjugated goat anti-human Fc (1:10000, Jackson Immunoresearch, West Grove, PA) in 2% milk, 20% SS, 0.5% Tween. Detection of alkaline phosphatase activity was performed using AMPAK reagents (DAKO, Carpinteria, CA). The measured gp120 contents of cells, virus and supernatant were corrected for the CA-p24 content of the respective fractions. The resulting gp120/p24 ratio's of the wt virus were arbitrarily set at 1.0 for each fraction and the relative gp120/gp24 ratio's of mutant and revertant viruses were established.

Peptide production

All recombinant peptides were expressed in *Escherichia coli* strain BL21(DE3)/pLysS (Novagen, Madison, WI). The bacteria were grown at 37°C in LB medium to an optical density of 0.8 at 600 nm, and induced with isopropylthio-b-D-galactoside for 3-4 h. Cells were lysed at 0°C with glacial acetic acid. The bacterial lysate was centrifuged (35,000 x *g* for 30 min) to separate the soluble fraction from inclusion bodies. The soluble fraction, containing denatured peptide, was dialyzed into 5% acetic acid overnight at room temperature. Peptides were purified from the soluble fraction to homogeneity by reverse-phase high-performance liquid chromatography (Waters, Milford, MA) using a Vydac C-18 preparative column (Vydac, Hesperia, CA) and a water-acetonitrile gradient in the presence of 0.1% trifluoroacetic acid and then lyophilized. The molecular weight of each peptide was confirmed by matrix-assisted laser desorption ionization-time-of-flight mass spectrometry (PerSeptive Biosystems, Framingham, MA). The concentration of each peptide was determined at 280 nm after solubilization in 6 M guanidinium chloride (16).

Circular dichroism (CD) spectroscopy

HPLC-purified peptides were solubilized in 6 M guanidinium chloride and 10 mM Tris-HCl (pH 7.0), and refolded by dilution into 100 mM NaCl, 50 mM Na_3PO_4, pH 7.0 (PBS). The single-point substituted variant peptides were named according to the position of the substitution. CD experiments were performed on an Aviv 62A DS circular dichroism spectrometer. The wavelength dependence of molar ellipticity, [θ], was monitored at 4°C, using a 10 µM peptide solution in PBS. Helix content was calculated by the method of Chen et al. (11). Thermal stability was determined by monitoring the change in the CD signal at 222nm ($[\theta]_{222}$) as a function of temperature. Thermal melting experiments were performed in 2°C increments with an equilibration time of 2 min at the desired tem-

perature and an integration time of 30 s. All melts were reversible. Superimposable folding and unfolding curves were observed, and >90% of the signal was regained upon cooling. The melting temperatures, or midpoints of the cooperative thermal unfolding transitions (T_m), were determined from the maximum of the first derivative, with respect to the reciprocal of the temperature, of the $[\theta]_{222}$ values (6). The error in estimation of T_m is ± 0.5 °C.

Sedimentation equilibrium analysis

A Beckman XL-A (Beckman Coulter, Fullerton, CA) analytical ultracentrifuge equipped with an An-60 Ti rotor (Beckman Coulter) was used. Peptide solutions were dialyzed overnight against PBS (pH 7.0), loaded at initial concentrations of 10, 30 and 100 µM, and analyzed at rotor speeds at 20,000 and 23,000 rpm at 20°C. Data sets were fitted simultaneously to a single-species model of ln(absorbance) versus (radial distances)^2 using the program NONLIN (21). Protein partial specific volume and solvent density were calculated as described by Laue et al. (24).

Results

The HIV-1 I559G and I559P mutants are replication defective

Helix-breaking residues introduced at position 559 in gp41 can stabilize prefusion Env trimers (39). Located centrally in the core of the six-helix bundle (Fig. 1), these substitutions are thought to disfavour conformational changes that lead

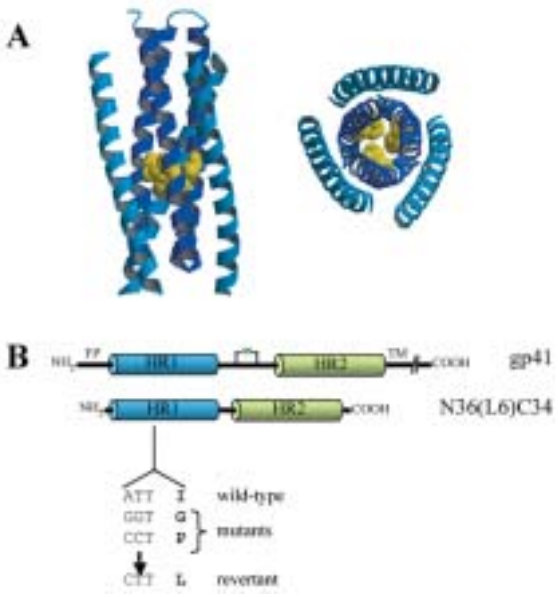

Fig. 1. **A**. The location of Ile-559 in the gp41 core domain. Residue Ile-559 (yellow spheres) is shown in the crystal structure of the gp41e core in the six-helix bundle conformation (pdb accession code 1AIK (8)). Ile-559 is located in the middle of the N-terminal helix and in the center of the trimeric coiled-coil, participating in hydrophobic interactions that contribute to the stability of the six-helix bundle. The Fig. was drawn using MOLSCRIPT (22) and RASTER3D (27). **B**. Linear representation of gp41 and the N36(L6)C34 peptide used for biophysical experiments (FP, fusion-peptide; HR1, first heptad-repeat region or N-terminal helix; HR2, second heptad-repeat region or C-terminal helix; TM, trans-membrane domain). The location of residue 559 in HR1 is indicated with the codons for the wt, mutant and revertant residues. The revertant codon was dominantly present in the population sequence of the viral quasispecies at day 24 and subsequent time-points.

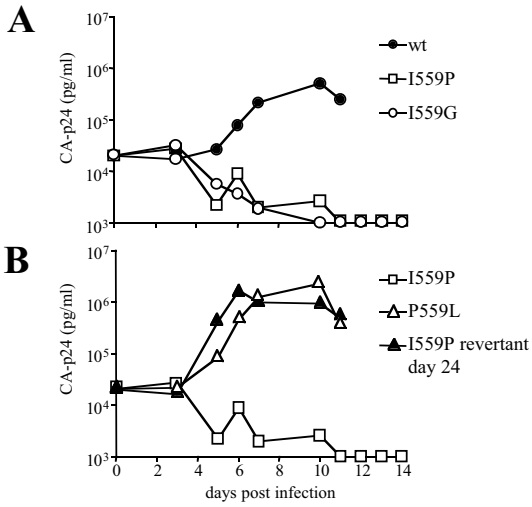

Fig. 2. Replication of the I559G/I559P mutant and the P559L revertant viruses. **A**. 3 x 10^5 SupT1 cells were infected with the wt and mutant viruses (20 ng CA-p24) and virus spread was monitored by CA-p24 ELISA for 14 days. **B**. Infection of SupT1 cells with the evolved I559P virus harvested at day 24 (quasi-species directly isolated from the evolution culture), the parental I559P mutant virus and the P559L virus (20 ng CA-p24).

to fusion, thereby stabilizing the inherently metastable pre-fusion state of the Env complex (39). To study the effects of the I559P and I559G substitutions on replication of the wild-type (wt) virus, they were introduced into a molecular clone of HIV-1_{LAI}. Virus stocks were generated, and mutant and wt viruses were analysed for their ability to replicate in the SupT1 T cell line. These studies indicate that replication of both mutant viruses is completely abolished (Fig. 2A). This result is consistent with the strong conservation of Ile at position 559 among natural virus isolates (36).

The HIV-1 I559P mutant evolves through first-site pseudoreversion

To obtain a better understanding of why the I559P and I559G mutant viruses were not able to replicate, we performed forced evolution experiments (3,26,44). Multiple independent cultures of SupT1 cells were transfected with the molecular clone of I559G or I559P. The mutant codons creating the I559G or I559P changes were designed such that first-site reversion to the wt sequence was possible only by means of at least two nucleotide changes, which is an unlikely event (Fig. 1B). The transfected cells were maintained in culture for a prolonged period. After 24 days of culturing, we identified a replicating virus in a single I559P culture. The infectivity of this virus variant was then directly compared with the original I559P mutant, demonstrating that the variant had a significantly increased replication capacity (Fig. 2B). The replication of the variant virus did not further improve in more extended cultures (results not shown). No virus evolution was ever detected in other I559P and I559G cultures.

Total cellular DNA was extracted from cells infected with the evolved virus. The gp41-coding region of the proviral *env* gene was PCR-amplified and sequencing of the viral quasispecies at day 24 revealed the occurrence of a first-site pseudo-reversion P559L via a single C-to-T transition (Fig. 1B). We did not detect other mutations in gp41e. Although leucine is biochemically similar to

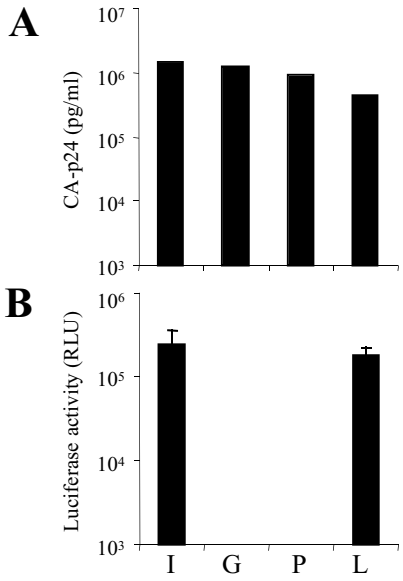

Fig. 3. The P559L reversion restores viral entry. **A**. Virus stocks were produced by transient transfection of C33A cells and the amount of virus was quantitated by CA-p24 ELISA. **B**. 3 x 10^5 LuSIV cells were infected with 100 ng CA-p24 in the presence of 200 nM Saquinavir. Viral entry was quantified by measuring the luciferase activity 48 h after infection.

isoleucine, it is never found at this position in natural virus isolates (36). To exclude the possibility that additional mutations in the viral genome caused or contributed to the revertant phenotype, we constructed a molecular clone containing only the P559L change. Virus stocks were generated and the replication capacity was evaluated in infection experiments. The P559L virus replicated efficiently, confirming that the first-site pseudo-reversion was sufficient to account for the variant phenotype (Fig. 2B). Similar results were obtained in other T cell lines (results not shown). We could not readily observe differences in replication between the wt and P559L viruses in competition experiments (results not shown).

The severe replication defect of the gp41 mutants probably arises at the level of virus-cell fusion and entry. To assess this, we used a single cycle infection assay in which the target cell contains an LTR-luciferase reporter construct that is activated by newly synthesized Tat protein encoded by the incoming virus. First, we made stocks of the wt, mutant and revertant viruses by transfection of C33A producer cells. There was no significant difference in the production of the three viruses in these cells: this was expected because virus assembly and budding is essentially Env-independent (Fig. 3A). We next tested equal amounts of the three viruses in an infection assay, measuring luciferase activity after 2 days (Fig. 3B). Consistent with the replication results, we measured no entry for the I559G and I559P mutant viruses, whereas entry of the revertant virus was restored to levels comparable to that of the wt virus.

Env production and virion incorporation

To investigate whether Env biosynthesis, incorporation into the virion and/or gp120 shedding were affected by the I559G and I559P substitutions, we quantified the gp120 content of virus-producing cells, pelleted virions and the super-

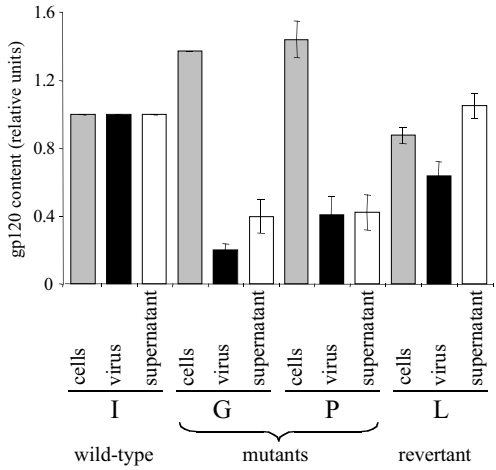

Fig. 4. The P559L reversion restores Env incorporation into virions. The gp120 content of cells, virus and supernatant fractions of virus-producing cells were measured. gp120 and CA-p24 contents were measured by ELISA. The gp120 amounts were standardized for CA-p24 input and the gp120 content of the mutants is presented relative to that of wt gp120. The respective residues at position 559 are indicated at the bottom of the figure. The experiment was performed in triplicate and the standard errors of deviation are indicated by error bars. Similar results were obtained in three independent experiments.

natant from the virion pellet that contained dissociated gp120. To do this, C33A cells were transfected with a molecular clone of either the wt virus or one of the I559G, I559P or P559L mutants. The cell fraction was separated by centrifugation and the virions were collected by ultracentrifugation. The amount of CA-p24 in the various fractions was quantified for the wt virus and the three mutants, then used to normalize the gp120 content of each fraction. Each of the four viruses produced a similar amount of CA-p24 in each fraction (results not shown). The I559G and I559P mutants accumulated gp120 intracellularly, while low amounts of gp120 were shed into the medium and incorporated onto virions (20% and 41% incorporation compared to wt; Fig. 4), indicating that these mutants have biosynthesis problems. The P559L reversion is able to restore Env incorporation onto virions to 63% compared to wt, while the gp120 content of the supernatant is comparable to wt (105%), indicating that relatively more gp120 is shed from the virus and/or cell surface.

Together, the above results indicate that the replication defects of the I559P and I559G mutants can be attributed to problems with Env biosynthesis and Env incorporation onto virions. The P559L reversion partially overcomes these problems, but causes an increase in gp120 shedding. Nevertheless, although gp120 was virtually absent from virions of the I559G mutant, a considerable amount of Env (41% of wt) was present on the I559P mutant virions. Thus, other defects may contribute to the overall reduction in the fusion capacity of the latter mutant.

The P559L reversion restores the α-helical content of gp41e

We next investigated the effects of the P559L reversion on the structure and stability of the gp41 ectodomain core formed by the recombinant polypeptide N36(L6)C34 (Fig. 1B). The P559L substitution was introduced into N36(L6)C34 and its biophysical properties were compared to those of the wt peptide and the I559P mutant. Circular dichroism was used to measure the extent of the α-helical structure. The wt peptide is >95% α-helical at 4ºC as indicated by the typical wavelength dependency pattern shown in figure 5A. In contrast, the I559P mutant is only ~75% α-helical (Fig. 5A, table 1 and ref (39)). The revertant P559L pep-

Table 1. Summary of circular dichroism and sedimentation equilibrium data for the HIV-1 gp41 core mutants

N36(L6)C34 peptide	$-[\theta]_{222}$[a] (deg cm^2 dmol^{-1})	T_m[a] (°C)	Molecular mass (kDa)
wt[b]	32,500	78	27.6
P559L	32,700	76	26.8
I559G[b]	32,300	46	25.9
I559P[b]	25,600	34	NA[c]

[a] All scans and melts were performed at 10 µM protein concentration.
[b] Data derived from ref (39)
[c] NA, aggregated.

tide is >95% α-helical and its wavelength dependency is similar to that of the wt peptide, indicating that the Pro-to-Leu reversion restores the wt α-helical structure. Under these conditions, the mid-point of thermal denaturation (T_m) of the wt peptide is 78ºC, the T_m for the I559P and P559L peptides are 34ºC and 76ºC, respectively (table 1, Fig. 5B and ref (39)). The pre- and post-transitional slopes and the steepness of the main transition are very similar for the wt and P559L peptides (Fig. 5B). In contrast, the I559P peptide displays broad thermal unfolding transitions (39). Sedimentation equilibrium experiments indicate that the P559L peptide forms discrete trimers over a ten-fold range of peptide concentration (10 to 100 µM) (table 1, Fig. 5C). In conclusion, these data indicate that the I559P substitution disrupts α-helical structure and thus reduces six-helix bundle stability. Both these effects probably contribute to the fusion-defective phenotype of the I559P mutant virions. The P559L reversion, however, restores both α-helical structure and six-helix bundle stability.

Discussion

We have studied viral replication and evolution of viruses that have substitutions at position 559 in the gp41e core. These substitutions stabilize the oligomeric state of disulfide-linked gp120-gp41 complexes (39). In the context of soluble gp140 with a disulfide (SOS) bond between gp120 and gp41e, the I559P substitution increases trimerization, but does not seem to have any adverse consequences. The I559G substitution reduced expression of SOS gp140, but it too increased gp140 trimer stability. The mechanism of trimer stabilization by the substitutions at position 559 is incompletely understood, but we think that the introduction of helix-breaking residues blocks a transition of a non-helical segment to an α-helical structure (39). This conformational change could be necessary for the formation of the pre-hairpin intermediate, in which the N-terminal fusion peptides are directed towards the target membrane. A similar conformational change is required for membrane fusion mediated by the influenza hemagglutinin, and the introduction of prolines in an analogous non-helical segment blocks the transition to the fusion-active state (33). Thus, the inherently instable native conformation of the Env complex can be stabilized by blocking a conformational change that is normally necessary for function.

The I559G and I559P viruses are both replication defective. The defect in the I559G mutant is probably explained by the absence of Env from virions, but it is

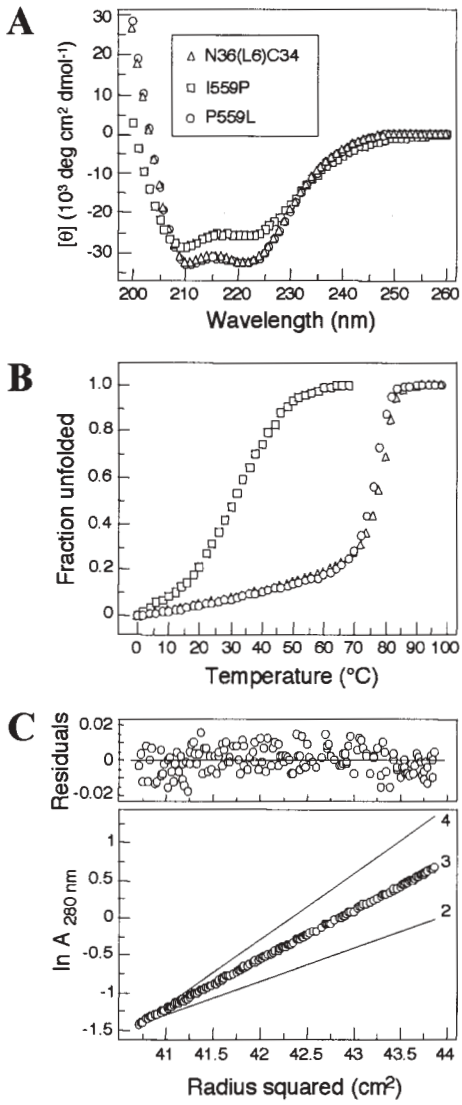

Fig. 5. The P559L peptide folds as a stable α-helical trimer. **A**. Circular dichroism (CD) spectrum of wt N36(L6)C34, I559P and P559L peptides at 4°C. **B**. Thermal melts of wt N36(L6)C34 (open triangles) and P559L (open circles) peptides monitored by CD at 222 nm at 10 μM protein concentration in PBS (pH 7.0). **C**. Representative sedimentation equilibrium data (20 krpm) of the P559L peptide collected at 20°C in PBS (pH 7.0) at ~30 μM protein concentration. The natural logarithm of the absorbance at 280 nm is plotted against the square of the radial position. The random distributions of the residuals indicate that the data fit well to an ideal single-species model. The slope of the plotted data indicates the P559L peptide is a trimeric species. The calculated data for dimeric and tetrameric models are indicated by solid and dashed lines, respectively. Note that the data on the I559P peptide are reproduced from ref (39) for clarity.

unlikely that the defect in the I559P mutant is solely attributable to the observed 59% reduction of Env incorporation or retention in virions. In general, the effect of these substitutions in the context of infectious virus seems to be more severe and complicated than when they are present in soluble SOS gp140. This is consistent with previous reports on the adverse impact of the I559P change on protein expression, cleavage and gp120 association (9,10). In the context of SOS gp140, the I559P mutation does not affect expression and cleavage, which may not be entirely unexpected since we reported elsewhere that the SOS disulfide bond can rescue the folding and cleavage of otherwise misfolded Env variants (37).

The Env biosynthesis defect imposed upon infectious viruses by the I559G and I559P substitutions implies that the integrity of the gp41 N-terminal helix is

important not only for the post-fusion structure, as shown by our biophysical experiments, but also for the formation of a different gp41 configuration that is required for Env biosynthesis in the first place. One explanation is that the N-terminal helix in gp41 is important for the structure of a folding intermediate of the nascent Env protein, or of the uncleaved gp160 precursor. There is evidence that gp41e in the uncleaved precursor protein shares some characteristics with the post-fusion gp41e structure. For instance, cluster I and II non-neutralizing epitopes are exposed both on uncleaved protein and on the six-helix bundle, but not on the native pre-fusion complex (5,17,19,40,43). Thus, the I559P substitution causes Env to fold in a structure that is not easily cleaved (9,10). The P559L reversion restores this defect, but results in a weakened gp120 - gp41 interaction. Hence this residue may play an important role in the interaction of gp41 with gp120. Consistent with this supposition, we and others have found that other residues in this gp41 domain are also involved in the gp120-gp41 interaction (chapter 4.3)(5,7,9,25,32,36). Why, however, is a leucine residue never found at position 559 in natural isolates? The increased gp120 shedding associated with the P559L variant apparently has little or no impact on virus replication *in vitro*, but there may be less obvious disadvantages *in vivo*.

Although we did not test the P559L substitution in our previous studies on stabilizing disulfide-linked soluble gp140 trimers through substitutions at position 559, we did test the similar I559V substitution (39). In contrast to the helix-breaking I559G and I559P substitutions, the I559V substitution had no trimer stabilizing effect, so it is unlikely that the I559L substitution will have such an effect. Apparently, stabilizing the native trimer is not advantageous for virus replication, since a metastable, spring-loaded Env complex is required to trigger receptor-mediated fusion. Overall, a better understanding of Env conformation and, in particular, of how sequence changes affect Env folding, structure and function, may help in the design of future modifications intended to improve Env immunogenicity.

Acknowledgements

We thank Norbert Schülke and Bill Olson for the gift of recombinant gp120, James Binley for the gift of HIVIg, Janice Clements for the donation of LuSIV cells, and Stephan Heynen for technical assistance. This work was sponsored by the Dutch AIDS Fund (Amsterdam) and by NIH grants AI 39420, AI 45463 and AI 54159.

References

1. **Abrahamyan, L. G., R. M. Markosyan, J. P. Moore, F. S. Cohen, and G. B. Melikyan**. 2003. Human immunodeficiency virus type 1 Env with an intersubunit disulfide bond engages coreceptors but requires bond reduction after engagement to induce fusion. J. Virol. **77**:5829-5836.
2. **Baldwin, C. E., R. W. Sanders, and B. Berkhout**. 2003. Inhibiting HIV-1 Entry with Fusion Inhibitors. Curr. Med. Chem. **10**:1633-1642.
3. **Berkhout, B., K. Verhoef, J. L. B. van Wamel, and B. Back**. 1999. Genetic instability of live-attenuated HIV-1 vaccine strains. J. Virol. **73**:1138-1145.
4. **Binley, J. M., C. S. Cayanan, C. Wiley, N. Schulke, W. C. Olson, and D. R. Burton**. 2003. Redox-triggered infection by disulfide-shackled human immunodeficiency virus type 1 pseudovirions. J. Virol. **77**:5678-5684.
5. **Binley, J. M., R. W. Sanders, B. Clas, N. Schuelke, A. Master, Y. Guo, F. Kajumo, D. J. Anselma, P. J. Maddon, W. C. Olson, and J. P. Moore**. 2000. A recombinant HIV-1 envelope glycoprotein complex stabilized by an intermolecular disulfide bond between the gp120 and gp41 subunits is an antigenic mimic of the trimeric virion-associated structure. J. Virol. **74**:627-643.
6. **Cantor, C. and P. Schimmel**. 1980. Biophysical chemistry, part III. W. H. Freeman and company, New York, N.Y.
7. **Cao, J., L. Bergeron, E. Helseth, M. Thali, H. Repke, and J. Sodroski**. 1993. Effects of amino-acid changes in the extracellular domain of the human immunodeficiency virus type 1 gp41 envelope glycoprotein. J. Virol. **67**:2747-2755.
8. **Chan, D. C., D. Fass, J. M. Berger, and P. S. Kim**. 1997. Core structure of gp41 from the HIV envelope glycoprotein. Cell **89**:263-273.
9. **Chen, S. S.** 1994. Functional role of the zipper motif region of human immunodeficiency virus type 1 transmembrane protein gp41. J. Virol. **68**:2002-2010.
10. **Chen, S. S., C. N. Lee, W. R. Lee, K. McIntosh, and T. H. Lee**. 1993. Mutational analysis of the leucine zipper-like motif of the human immunodeficiency virus type 1 envelope transmembrane glycoprotein. J. Virol. **67**:3615-3619.
11. **Chen, Y. H., J. T. Yang, and K. H. Chau**. 1974. Determination of the helix and beta form of proteins in aqueous solution by circular dichroism. Biochemistry **13**:3350-3359.
12. **Colman, P. M. and M. C. Lawrence**. 2003. The structural biology of type I viral membrane fusion. Nat. Rev. Mol. Cell Biol. **4**:309-319.
13. **Das, A. T., B. Klaver, and B. Berkhout**. 1999. A hairpin structure in the R region of the Human Immunodeficiency Virus type 1 RNA genome is instrumental in polyadenylation site selection. J. Virol. **73**:81-91.
14. **Das, A. T., B. Klaver, B. I. F. Klasens, J. L. B. van Wamel, and B. Berkhout**. 1997. A conserved hairpin motif in the R-U5 region of the human immunodeficiency virus type 1 RNA genome is essential for replication. J. Virol. **71**:2346-2356.
15. **Eckert, D. M. and P. S. Kim**. 2001. Mechanisms of viral membrane fusion and its inhibition. Annu. Rev. Biochem. **70**:777-810.
16. **Edelhoch, H.** 1967. Spectroscopic determination of tryptophan and tyrosine in proteins. Biochemistry **6**:1948-1954.
17. **Finnegan, C. M., W. Berg, G. K. Lewis, and A. L. DeVico**. 2002. Antigenic properties of the human immunodeficiency virus transmembrane glycoprotein during cell-cell fusion. J. Virol. **76**:12123-12134.
18. **Gallo, S. A., C. M. Finnegan, M. Viard, Y. Raviv, A. Dimitrov, S. S. Rawat, A. Puri, S. Durell, and R. Blumenthal**. 2003. The HIV Env-mediated fusion reaction. Biochim. Biophys. Acta **1614**:36-50.
19. **Gorny, M. K. and S. Zolla-Pazner**. 2000. Recognition by human monoclonal antibodies of free and complexed peptides representing the prefusogenic and fusogenic forms of human immunodeficiency virus type 1 gp41. J. Virol. **74**:6186-6192.
20. **Jeeninga, R. E., M. Hoogenkamp, M. Armand-Ugon, M. de Baar, K. Verhoef, and B. Berkhout**. 2000. Functional differences between the LTR transcriptional promoters of HIV-1 subtypes A through G. J. Virol. **74**:3740-3751.
21. **Johnson, M. L., J. J. Correia, D. A. Yphantis, and H. R. Halvorson**. 1981. Analysis of data from the analytical ultracentrifuge by nonlinear least- squares techniques. Biophys. J. **36**:575-588.

22. **Kraulis, P. J.** 1991. MOLSCRIPT: A program to produce both detailed and schematic plots of protein structures. J. Appl. Crystallogr. **24**:946-950.
23. **Kunkel, T. A., J. D. Roberts, and R. A. Zakour**. 1987. Rapid and efficient site-specific mutagenesis without phenotypic selection, p. 367-382. *In* R. Wu and L. Grossman (eds.), Methods in Enzymology. Academic Press, San Diego.
24. **Laue, T. M., B. D. Shah, T. M. Ridgeway, and S. L. Pelletier**. 1992. Computer-aided interpretation of analytical sedimentation data for proteins, p. 90-125. *In* S. E. Harding, A. J. Rowe, and J. C. Horton (eds.), Analytical ultracentrifugation in biochemistry and polymer science. Royal Society of Chemistry, Cambridge, England.
25. **Maerz, A. L., H. E. Drummer, K. A. Wilson, and P. Poumbourios**. 2001. Functional analysis of the disulfide-bonded loop/chain reversal region of human immunodeficiency virus type 1 gp41 reveals a critical role in gp120-gp41 association. J. Virol. **75**:6635-6644.
26. **Marzio, G., K. Verhoef, M. Vink, and B. Berkhout**. 2001. *In vitro* evolution of a highly replicating, doxycycline-dependent HIV for applications in vaccine studies. Proc. Natl. Acad. Sci. USA **98**:6342-6347.
27. **Merritt, E. A. and D. J. Bacon**. 1997. Raster3D: Photorealistic molecular graphics. Methods Enzymol. **277**:505-525.
28. **Moore, J. P. and D. D. Ho**. 1993. Antibodies to discontinuous or conformationally sensitive epitopes on the gp120 glycoprotein of human immunodeficiency virus type 1 are highly prevalent in sera of infected humans. J. Virol. **67**:863-875.
29. **Parren, P. W. H. I., J. P. Moore, D. R. Burton, and Q. J. Sattentau**. 1999. The neutralizing antibody response to HIV-1: viral evasion and escape from humoral immunity. AIDS **13 (Suppl. A)**:S137-S162.
30. **Peden, K., M. Emerman, and L. Montagnier**. 1991. Changes in growth properties on passage in tissue culture of viruses derived from infectious molecular clones of HIV-1_{LAI}, HIV-1_{MAL}, and HIV-1_{ELI}. Virology **185**:661-672.
31. **Poignard, P., E. O. Saphire, P. W. Parren, and D. R. Burton**. 2001. gp120: Biologic aspects of structural features. Annu. Rev. Immunol. **19**:253-274.
32. **Poumbourios, P., A. L. Maerz, and H. E. Drummer**. 2003. Functional evolution of the HIV-1 envelope glycoprotein gp120-association site of gp41. J. Biol. Chem. **278**: 42149-42160.
33. **Qiao, H., S. L. Pelletier, L. Hoffman, J. Hacker, R. T. Armstrong, and J. M. White**. 1998. Specific single or double proline substitutions in the "spring-loaded" coiled-coil region of the influenza hemagglutinin impair or abolish membrane fusion activity. J. Cell Biol. **141**:1335-1347.
34. **Roos, J. W., M. F. Maughan, Z. Liao, J. E. Hildreth, and J. E. Clements**. 2000. LuSIV cells: a reporter cell line for the detection and quantitation of a single cycle of HIV and SIV replication. Virology **273**:307-315.
35. **Sanders, R. W., E. C. de Jong, C. E. Baldwin, J. H. Schuitemaker, M. L. Kapsenberg, and B. Berkhout**. 2002. Differential transmission of human immunodeficiency virus type 1 by distinct subsets of effector dendritic cells. J. Virol. **76**:7812-7821.
36. **Sanders, R. W., B. Korber, M. Lu, B. Berkhout, and J. P. Moore**. 2002. Mutational analyses and natural variablility of the gp41 ectodomain, p. 43-68. *In* C. Kuiken, B. Foley, E. Freed, B. Hahn, P. Marx, F. McCutchan, J. Mellors, S. Wolinsky, and B. Korber (eds.), HIV Sequence compendium 2002. Los Alamos National Laboratory, Theoretical Biology and Biophysics Group, Los Alamos, New Mexico.
37. **Sanders, R. W., L. Schiffner, A. Master, F. Kajumo, Y. Guo, T. Dragic, J. P. Moore, and J. M. Binley**. 2000. Variable-loop-deleted variants of the human immunodeficiency virus type 1 envelope glycoprotein can be stabilized by an intermolecular disulfide bond between the gp120 and gp41 subunits. J. Virol. **74**:5091-5100.
38. **Sanders, R. W., M. Venturi, L. Schiffner, R. Kalyanaraman, H. Katinger, K. O. Lloyd, P. D. Kwong, and J. P. Moore**. 2002. The mannose-dependent epitope for neutralizing antibody 2G12 on human immunodeficiency virus type 1 glycoprotein gp120. J. Virol. **76**:7293-7305.
39. **Sanders, R. W., M. Vesanen, N. Schuelke, A. Master, L. Schiffner, R. Kalyanaraman, M. Paluch, B. Berkhout, P. J. Maddon, W. C. Olson, M. Lu, and J. P. Moore**. 2002. Stabilization of the soluble, cleaved, trimeric form of the envelope glycoprotein complex of human immunodeficiency virus type 1. J. Virol. **76**:8875-8889.
40. **Sattentau, Q. J., S. Zolla-Pazner, and P. Poignard**. 1995. Epitope exposure on functional,

oligomeric HIV-1 gp41 molecules. Virology **206**:713-717.

41. **Schulke, N., M. S. Vesanen, R. W. Sanders, P. Zhu, M. Lu, D. J. Anselma, A. R. Villa, P. W. Parren, J. M. Binley, K. H. Roux, P. J. Maddon, J. P. Moore, and W. C. Olson**. 2002. Oligomeric and conformational properties of a proteolytically mature, disulfide-stabilized human immunodeficiency virus type 1 gp140 envelope glycoprotein. J. Virol. **76**:7760-7776.
42. **Schultz, A. M. and J. A. Bradac**. 2001. The HIV vaccine pipeline, from preclinical to phase III. AIDS **15 Suppl 5**:S147-S158.
43. **Taniguchi, Y., S. Zolla-Pazner, Y. Xu, X. Zhang, S. Takeda, and T. Hattori**. 2000. Human monoclonal antibody 98-6 reacts with the fusogenic form of gp41. Virology **273**:333-340.
44. **Verhoef, K., R. W. Sanders, V. Fontaine, S. Kitajima, and B. Berkhout**. 1999. Evolution of the HIV-1 LTR promoter by conversion of an NF-κB enhancer element into a GABP binding site. J. Virol. **73**:1331-1340.
45. **Wyatt, R. and J. Sodroski**. 1998. The HIV-1 envelope glycoproteins: fusogens, antigens, and immunogens. Science **280**:1884-1888.

Chapter 6

Concluding remarks

The work presented in this thesis encompasses several aspects of HIV-1 biology, with a particular focus on the envelope glycoprotein complex (Env). Although some studies may seem unrelated, only a complete integration of Env science from different disciplines may tackle the HIV vaccine problem. Almost all aspects of Env research have consequences for Env vaccine design. Not only Env immunology, but also Env biochemistry and biophysics to study protein structure, folding and function have important implications for Env vaccine design. This is particularly true because unmodified Env has no prospect as an HIV vaccine and Env thus has to be modified, perhaps extensively. Modifications of Env may affect its folding, structure, glycosylation and function, but also the type of antibody responses it elicits in vaccinated individuals. Thus, a differently folded Env immunogen may alter the elicitation of neutralizing antibodies, non-neutralizing antibodies and enhancing antibodies. A better understanding on the biochemical and functional properties of Env in combination with an understanding of the antibody response against Env should eventually lead to the design of Env immunogens that can elicit protective antibody responses.

To get a better understanding of Env-mediated transmission by dendritic cells (DC) and to identify which molecules besides Env are involved in this process, we studied HIV-1 transmission by different subsets of mature DC that differentially express surface molecules involved in HIV-1 transmission and infection (chapter 2 (25)). The experiments revealed that the ICAM-1 – LFA-1 interaction, which plays an important role in the immunological contact between DC and T cells, also plays a key role in the transfer of HIV virus particles from DC to the T cell. The relevance of this study became apparent in a recent article published in *Science* by McDonald et al. (18), in which the authors describe the visualization of DC-mediated HIV transmission by time-lapse microscopy. They elegantly show that an 'infectious synapse' is formed between DC and T cell, analogous to the immunological synapse between the two cell types, which facilitates transfer of the virion due to clustering of relevant receptors and adhesion molecules. Among the molecules on the T cell surface that cluster at the infectious synapse are CD4, CXCR4, CCR5 and LFA-1, the latter of which we proposed to facilitate HIV transmission by an interaction with its counterpart ICAM-1 on the donor DC (see chapter 2.1, Fig. 6).

One aspect that is relevant to several chapters in this thesis is the interaction between gp120 and gp41. This interaction is important for vaccine design for several reasons. The interactive regions form the non-neutralizing decoy epitopes that are exposed in the dissociated subunits and immature gp160. Stabilization of the intersubunit interactions is important to create a stable mimic of the function-

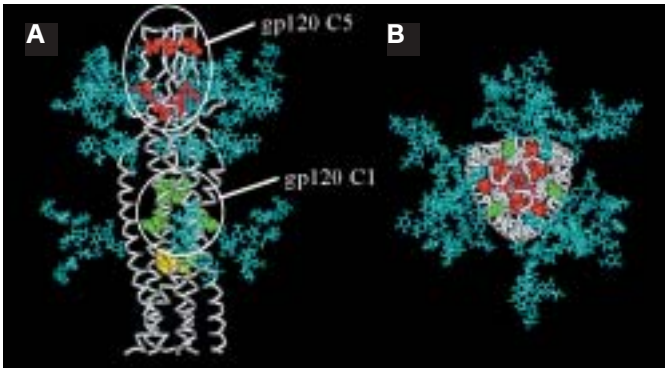

Fig. 1. Residues in gp41 that are described in this thesis are highlighted in the post-fusion structure model of gp41 (8). Panel **A** represents a side view of trimeric gp41 oriented such that the 2F5 epitope and the membrane would be at the bottom. Panel **B** gives a top view of the loop region. The glycans (cyan) were modeled by dr. Mark Wormald (Oxford Glycobiology Institute, Oxford, UK). Residues 591, 593 and 605 (chapters 5.1 and 5.4) that are involved in the interaction with the gp120 C5 region are coloured in red. Residues 567 and 573 (chapter 4.3) that are involved the interaction in the gp120 C1 region are marked green, and residue 559 (chapters 5.6 and 5.7) is in yellow. The contact site of residue 559 is not known. Note that the structure model represents the post-fusion conformation of gp41, not the gp120 bound conformation, which is currently unknown.

al trimer that does not expose these decoy epitopes. During the work presented in this thesis, we acquired more knowledge on the interaction between gp120 and gp41. It was previously known that the C1 and C5 regions in gp120 and the loop and HR1 regions in gp41 were involved in the intersubunit interactions (see appendix and (26)). We show here that the C5 region has its contact site in the gp41 loop region. More precisely, position 501 in gp120 has to be in close proximity to position 605 in gp41 in order to form the SOS intermolecular disulfide bond (chapters 5.1 and 5.2). We also showed that gp41 residues 591 and 593 can influence the interaction between 501 and 605 (chapter 5.4). Furthermore, it became apparent that residue 559 affects the interaction with gp120, although we can not point to a specific interaction domain in gp120 (chapter 5.7). The results presented in chapter 4.3 show that reversion in the C1 region or in the leader peptide in combination with reversion in HR1 in gp41, specifically at residues 567 and 573, contribute to the restoration of folding and viral replication of a virus that lacks a disulfide bond in the C1 region. This strongly suggests that the C1 region contacts HR1 and that this interaction is important at some stage during folding. The above mentioned results are summarized in the structure model of the gp41 ectodomain (Fig. 1), in which the suggested contact regions for the C1 and C5 regions are indicated. The gp41 loop region contacts C5, HR1 contacts C1, the fusion peptide (not shown) may contact gp120 or may be buried in the hydrophobic core of the complex.

Glycosylation of Env is important for many reasons. First, glycans are very important for proper folding in the ER (chapter 4). Second, they have a functional role in binding DC-SIGN and other lectins to facilitate DC-mediated transmission (chapter 2.1). Third, they are important for immune evasion (chapters 1 and 3.1). Strikingly, they are also the target of the broadly neutralizing antibody

2G12. It is relevant to vaccine design to dissect which glycans are important for which function, since one important modification strategy will be the removal of specific glycans in order to unshield potential neutralizing epitopes and to increase the elicitation of neutralizing antibodies. Thus, it seems reasonable to leave intact the glycans that are directly and indirectly involved in 2G12 binding, to give the immune system an opportunity to elicit 2G12-like antibodies. The results from our analysis of the 2G12 epitope (chapter 3)(28) were recently confirmed in a *Science* article by Calarese et al. (9), which describes the crystal structure of a dimeric Fab fragment of 2G12. Docking of the dimeric antigen binding site of the 2G12 Fab onto gp120 revealed that the carbohydrates attached to asparagines 332 and 392 are key to 2G12 binding with some direct or indirect contribution of other glycans. These conclusions largely confirm our findings. Interestingly, Hong and co-workers recently showed that the epitope of 2G12 does not overlap with the binding site of DC-SIGN (12).

An understanding of Env folding is of importance for vaccine design. In particular, knowledge of oxidative folding of Env in the ER and the role of disulfide bonds in this process (chapter 4) is of importance when changing the disulfide bonded architecture as in our SOS modified Env variants (chapter 5). We found that Env is relatively flexible in changing this architecture. First of all, we could remove certain disulfide bonds without effects on oxidative folding. Two disulfide bonds were even dispensable for Env function. Furthermore, some disulfide bonds (54/74 (chapter 4.3) and 385/418 (chapter 4.2)) could be replaced by other means through virus evolution. The addition of an appropriately positioned non-native disulfide bond between gp120 and gp41 also did not have a negative effect on oxidative folding, although incorrectly placed cysteines actually did have adverse effects (chapter 5.1). In contrast, SOS Env is fully functional upon reduction of the disulfide bond (1,3). Thus, Env displays a remarkable flexibility in its disulfide bonded architecture, and this can be used in the design of novel immunogens.

Our ongoing work on the design of novel Env immunogens is presented in chapter 5 (4,5,27,29,30). Although we and others have deployed sophisticated vaccine strategies, combinations of various strategies used by different groups are probably required to significantly improve the elicitation of neutralizing antibody responses. In the SOSIP gp140 protein, we have combined several modifications. First, we ensure complete cleavage, either by the co-expression of furin during the production of soluble SOSIP gp140 or by introduction of an improved cleavage site in the context of SOSIP gp160 DNA immunizations (chapter 5.5). Second, the gp120-gp41 is stabilized by the SOS disulfide bond (chapter 5.1). Third, the trimer interactions are stabilized by the I559P substitution in gp41 (chapter 5.6). At this moment we do not know whether the elicitation of neutralizing antibodies by SOSIP immunogens is improved compared to conventional Env subunit vaccines, but we anticipate that additional modification will be necessary. There are several options to combine our work with that of other groups to improve SOSIPs immunogenicity (see chapter 1). For example, we could stabilize the gp120 subunits in the CD4-bound state or the pre-CD4-binding state (32). We could also increase the affinity for the neutralizing antibody b12 (22). Furthermore, we could uncover the receptor binding sites by deletion of variable

loops (chapter 5.2) and/or elimination of selected glycans that shield the receptor binding sites, but that do not contribute to the neutralizing 2G12 epitope (chapter 3.1)(2,6,7,10,13-15,17,19,21,24,27,31).

Thus, SOS gp140 and SOSIP gp140 are interesting reagents not only for immunogenicity studies, but also for structural, antigenic and functional studies. These reagents have already been of value for studies by us and others, for example for the characterization of neutralizing antibodies to gp120 and gp41, the delineation of the location of gp41 relative to gp120 in the three-dimensional structure, and the characterization of fusion intermediate conformations (1,3,11,16,20,23,30,33). In collaboration with Ian Wilson, Robyn Stanfield and Dennis Burton at the Scripps Research Institute, we have initiated attempts to crystallize SOSIP trimers in complex with CD4 and various combinations of neutralizing antibodies to gp120 and gp41. So far, these attempts were unsuccessful, but we hope that in the future, an increase in structural information on various Env variants and neutralizing antibodies can assist in the design of improved SOSIP variants.

References

1. **Abrahamyan, L. G., R. M. Markosyan, J. P. Moore, F. S. Cohen, and G. B. Melikyan**. 2003. Human immunodeficiency virus type 1 Env with an intersubunit disulfide bond engages coreceptors but requires bond reduction after engagement to induce fusion. J. Virol. **77**:5829-5836.
2. **Barnett, S. W., S. Lu, I. Srivastava, S. Cherpelis, A. Gettie, J. Blanchard, S. Wang, I. Mboudjeka, L. Leung, Y. Lian, A. Fong, C. Buckner, A. Ly, S. Hilt, J. Ulmer, C. T. Wild, J. R. Mascola, and L. Stamatatos**. 2001. The ability of an oligomeric human immunodeficiency virus type 1 (HIV- 1) envelope antigen to elicit neutralizing antibodies against primary HIV-1 isolates is improved following partial deletion of the second hypervariable region. J. Virol. **75**:5526-5540.
3. **Binley, J. M., C. S. Cayanan, C. Wiley, N. Schulke, W. C. Olson, and D. R. Burton**. 2003. Redox-triggered infection by disulfide bond-shackled human immunodeficiency virus type 1 pseudovirions. J. Virol. **77**:5678-5684.
4. **Binley, J. M., R. W. Sanders, B. Clas, N. Schuelke, A. Master, Y. Guo, F. Kajumo, D. J. Anselma, P. J. Maddon, W. C. Olson, and J. P. Moore**. 2000. A recombinant HIV-1 envelope glycoprotein complex stabilized by an intermolecular disulfide bond between the gp120 and gp41 subunits is an antigenic mimic of the trimeric virion-associated structure. J. Virol. **74**:627-643.
5. **Binley, J. M., R. W. Sanders, A. Master, C. S. Cayanan, C. L. Wiley, L. Schiffner, B. Travis, S. Kuhmann, D. R. Burton, S.-L. Hu, W. C. Olson, and J. P. Moore**. 2002. Enhancing the proteolytic maturation of human immunodeficiency virus type 1 envelope glycoproteins. J. Virol. **76**:2606-2616.
6. **Binley, J. M., R. Wyatt, E. Desjardins, P. D. Kwong, W. Hendrickson, J. P. Moore, and J. Sodroski**. 1998. Analysis of the interaction of antibodies with a conserved enzymatically deglycosylated core of the HIV type 1 envelope glycoprotein 120. AIDS Res. Hum. Retroviruses **14**:191-198.
7. **Bolmstedt, A., J. Hinkula, E. Rowcliffe, M. Biller, B. Wahren, and S. Olofsson**. 2001. Enhanced immunogenicity of a human immunodeficiency virus type 1 env DNA vaccine by manipulating N-glycosylation signals. Effects of elimination of the V3 N306 glycan. Vaccine **20**:397-405.
8. **Caffrey, M.** 2001. Model for the structure of the HIV gp41 ectodomain: insight into the intermolecular interactions of the gp41 loop. Biochim. Biophys. Acta **1536**:116-122.
9. **Calarese, D. A., C. N. Scanlan, M. B. Zwick, S. Deechongkit, Y. Mimura, R. Kunert, P. Zhu, M. R. Wormald, R. L. Stanfield, K. H. Roux, J. W. Kelly, P. M. Rudd, R. A. Dwek, H. Katinger,**

D. R. Burton, and I. A. Wilson. 2003. Antibody domain exchange is an immunological solution to carbohydrate cluster recognition. Science **300**:2065-2071.

10. **Cao, J., N. Sullivan, E. Desjardin, C. Parolin, J. Robinson, R. Wyatt, and J. Sodroski**. 1997. Replication and neutralization of human immunodeficiency virus type 1 lacking the V1 and V2 variable loops of the gp120 envelope glycoprotein. J. Virol. **71**:9808-9812.
11. **Herrera, C., C. Spenlehauer, M. S. Fung, D. R. Burton, S. Beddows, and J. P. Moore**. 2003. Nonneutralizing antibodies to the CD4-binding site on the gp120 subunit of human immunodeficiency virus type 1 do not interfere with the activity of a neutralizing antibody against the same site. J. Virol. **77**:1084-1091.
12. **Hong, P. W., K. B. Flummerfelt, A. de Parseval, K. Gurney, J. H. Elder, and B. Lee**. 2002. Human immunodeficiency virus envelope (gp120) binding to DC-SIGN and primary dendritic cells is carbohydrate dependent but does not involve 2G12 or cyanovirin binding sites: implications for structural analyses of gp120-DC-SIGN binding. J. Virol. **76**:12855-12865.
13. **Jeffs, S. A., C. Shotton, P. Balfe, and J. A. McKeating**. 2002. Truncated gp120 envelope glycoprotein of human immunodeficiency virus 1 elicits a broadly reactive neutralizing immune response. J. Gen. Virol. **83**:2723-2732.
14. **Johnson, W. E., J. Morgan, J. Reitter, B. A. Puffer, S. Czajak, R. W. Doms, and R. C. Desrosiers**. 2002. A replication-competent, neutralization-sensitive variant of simian immunodeficiency virus lacking 100 amino-acids of envelope. J. Virol. **76**:2075-2086.
15. **Koch, M., M. Pancera, P. D. Kwong, P. Kolchinsky, C. Grundner, L. Wang, W. A. Hendrickson, J. Sodroski, and R. Wyatt**. 2003. Structure-based, targeted deglycosylation of HIV-1 gp120 and effects on neutralization sensitivity and antibody recognition. Virology **313**:387-400.
16. **Labrijn, A. F., P. Poignard, A. Raja, M. B. Zwick, K. Delgado, M. Franti, J. Binley, V. Vivona C. Grundner, C. C. Huang, M. Venturi, C. J. Petropoulos, T. Wrin, D. S. Dimitrov, J. Robinson, P. D. Kwong, R. T. Wyatt, J. Sodroski, and D. R. Burton**. 2003. Access of Antibody Molecules to the Conserved Coreceptor Binding Site on Glycoprotein gp120 Is Sterically Restricted on Primary Human Immunodeficiency Virus Type 1. J. Virol. **77**:10557-10565.
17. **Lu, S., R. Wyatt, J. F. Richmond, F. Mustafa, S. Wang, J. Weng, D. C. Montefiori, J. Sodroski, and H. L. Robinson**. 1998. Immunogenicity of DNA vaccines expressing human immunodeficiency virus type 1 envelope glycoprotein with and without deletions in the V1/2 and V3 regions. AIDS Res. Hum. Retroviruses **14**:151-155.
18. **McDonald, D., L. Wu, S. M. Bohks, V. N. KewalRamani, D. Unutmaz, and T. J. Hope**. 2003. Recruitment of HIV and its receptors to dendritic cell-T cell junctions. Science **300**:1295-1297.
19. **McKeating, J. A., C. Shotton, S. Jeffs, C. Palmer, A. Hammond, J. Lewis, K. Oliver, J. May, and P. Balfe**. 1996. Immunogenicity of full length and truncated forms of the human immunodeficiency virus type I envelope glycoprotein. Immunol. Lett. **51**:101-105.
20. **Moulard, M., S. K. Phogat, Y. Shu, A. F. Labrijn, X. Xiao, J. M. Binley, M. Y. Zhang, I. A. Sidorov, C. C. Broder, J. Robinson, P. W. Parren, D. R. Burton, and D. S. Dimitrov**. 2002. Broadly cross-reactive HIV-1-neutralizing human monoclonal Fab selected for binding to gp120-CD4-CCR5 complexes. Proc. Natl. Acad. Sci. USA **99**:6913-6918.
21. **Olofsson, S. and J. E. Hansen**. 1998. Host cell glycosylation of viral glycoproteins—a battlefield for host defence and viral resistance. Scand. J. Infect. Dis. **30**:435-440.
22. **Pantophlet, R., S. E. Ollmann, P. Poignard, P. W. Parren, I. A. Wilson, and D. R. Burton**. 2003. Fine mapping of the interaction of neutralizing and nonneutralizing monoclonal antibodies with the CD4 binding site of human immunodeficiency virus type 1 gp120. J. Virol. **77**:642-658.
23. **Parker, C. E., L. J. Deterding, C. Hager-Braun, J. M. Binley, N. Schulke, H. Katinger, J. P. Moore, and K. B. Tomer**. 2001. Fine Definition of the Epitope on the gp41 Glycoprotein of Human Immunodeficiency Virus Type 1 for the Neutralizing Monoclonal Antibody 2F5. J. Virol. **75**:10906-10911.
24. **Reitter, J. N., R. E. Means, and R. C. Desrosiers**. 1998. A role for carbohydrates in immune eva sion in AIDS. Nat. Med. **4**:679-684.
25. **Sanders, R. W., E. C. de Jong, C. E. Baldwin, J. H. Schuitemaker, M. L. Kapsenberg, and B. Berkhout**. 2002. Differential transmission of human immunodeficiency virus type 1 by distinct subsets of effector dendritic cells. J. Virol. **76**:7812-7821.
26. **Sanders, R. W., B. Korber, M. Lu, B. Berkhout, and J. P. Moore**. 2002. Mutational analyses and natural variablility of the gp41 ectodomain, p. 43-68. *In* C. Kuiken, B. Foley, E. Freed, B. Hahn,

P. Marx, F. McCutchan, J. Mellors, S. Wolinsky, and B. Korber (eds.), HIV Sequence compendium 2002. Los Alamos National Laboratory, Theoretical Biology and Biophysics Group, Los Alamos, New Mexico.

27. **Sanders, R. W., L. Schiffner, A. Master, F. Kajumo, Y. Guo, T. Dragic, J. P. Moore, and J. M. Binley**. 2000. Variable-loop-deleted variants of the human immunodeficiency virus type 1 envelope glycoprotein can be stabilized by an intermolecular disulfide bond between the gp120 and gp41 subunits. J.Virol. **74**:5091-5100.
28. **Sanders, R. W., M. Venturi, L. Schiffner, R. Kalyanaraman, H. Katinger, K. O. Lloyd, P. D. Kwong, and J. P. Moore**. 2002. The mannose-dependent epitope for neutralizing antibody 2G12 on human immunodeficiency virus type 1 glycoprotein gp120. J.Virol. **76**:7293-7305.
29. **Sanders, R. W., M. Vesanen, N. Schuelke, A. Master, L. Schiffner, R. Kalyanaraman, M. Paluch, B. Berkhout, P. J. Maddon, W. C. Olson, M. Lu, and J. P. Moore**. 2002. Stabilization of the soluble, cleaved, trimeric form of the envelope glycoprotein complex of human immunodeficiency virus type 1. J.Virol. **76**:8875-8889.
30. **Schulke, N., M. S. Vesanen, R. W. Sanders, P. Zhu, M. Lu, D. J. Anselma, A. R. Villa, P. W. Parren, J. M. Binley, K. H. Roux, P. J. Maddon, J. P. Moore, and W. C. Olson**. 2002. Oligomeric and conformational properties of a proteolytically mature, disulfide bond-stabilized human immunodeficiency virus type 1 gp140 envelope glycoprotein. J.Virol. **76**:7760-7776.
31. **Stamatatos, L., M. Wiskerchen, and C. Cheng-Mayer**. 1998. Effect of major deletions in the V1 and V2 loops of a macrophage-tropic HIV type 1 isolate on viral envelope structure, cell entry, and replication. AIDS Res. Hum. Retroviruses **14**:1129-1139.
32. **Xiang, S. H., P. D. Kwong, R. Gupta, C. D. Rizzuto, D. J. Casper, R. Wyatt, L. Wang, W. A. Hendrickson, M. L. Doyle, and J. Sodroski**. 2002. Mutagenic stabilization and/or disruption of a CD4-bound state reveals distinct conformations of the human immunodeficiency virus type 1 gp120 envelope glycoprotein. J. Virol.**76**:9888-9899.
33. **Zwick, M. B., A. F. Labrijn, M. Wang, C. Spenlehauer, E. O. Saphire, J. M. Binley, J. P. Moore, G. Stiegler, H. Katinger, D. R. Burton, and P. W. Parren**. 2001. Broadly neutralizing antibodies targeted to the membrane-proximal external region of human immunodeficiency virus type 1 glycoprotein gp41. J.Virol. **75**:10892-10905.

Appendix

Mutational analyses and natural variability of the gp41 ectodomain

(pp. 1-23-47 in *HIVMolecular Immunology Database 2OO2*.
Edited by: Korber B, Brander C, Haynes BF, Koup R, Kuiken C, Moore IP, Walker BD, and Watkins DI. Published by: Theoretical Biology and Biophysics, Los Alamos National Laboratory, Los Alamos, NM)

Rogier W. Sanders[1], Bette Korber[2], Min Lu[3], Ben Berkhout[1], John P. Moore[4]

[1]Department of Human Retrovirology, Academic Medical Center, University of Amsterdam, 1105 AZ Amsterdam, The Netherlands; r.w.sanders@amc.uva.nl
[2]Theoretical Biology and Biophysics, MS K710, Los Alamos National Laboratory, Los Alamos, New Mexico 87545
[3]Department of Biochemistry and [4]Department of Microbiology and Immunology, Weill Medical College, Cornell University, New York, New York 10021

The HIV-1 envelope glycoproteins mediate viral attachment and release of the viral core in susceptible target cells. A single gp160 precursor protein is processed intracellularly to yield the native form of the envelope complex, consisting of three gp120 and three gp41 molecules associated through non-covalent interactions. Upon receptor and co-receptor binding to the surface subunit gp120, conformational changes within the envelope glycoprotein complex enable the insertion of the hydrophobic fusion peptide of the transmembrane subunit gp41 into the target membrane. Subsequent rearrangements within gp41 allow fusion of viral and cellular membranes. These late structural alterations are targeted by the entry inhibitor T-20 (for reviews see 13, 20, 21, 24, 46, 75).

A considerable body of mutagenesis data on structure-function relationships within the HIV-1 gp41 ectodomain (gp41e) has been published over the years. The value of this data-set has been increased considerably by the determination of the structure of the gp41e core, allowing some of the mutational effects to be interpreted and at least partially understood (9, 12, 38, 41, 68, 71). The native, pre-fusion structure of gp41e in the trimeric gp120-gp41 complex on the virion surface prior to receptor engagement is not known, however, and the various transitional structures of gp41 during the virus-cell fusion process are still ill-defined. Consequently, the structural and functional consequences of many amino acid substitutions in gp41e remain unclear.

Here, we have summarized the results of published mutagenesis studies on gp41e (see the accompanying table). The HXB2 reference strain has been used as a basis for numbering individual amino acid residues (Figure 1). This information should facilitate the research of those who study the HIV-1 envelope glycopro-

teins as fusogens or vaccine antigens. In general, we have tabulated only data for single mutants, but several publications contain information on the effects of multiple amino acid substitutions (25, 43, 44, 49, 56, 57, 62). The table does not include information on every naturally occurring gp41e sequence variant, as the variation is extensive. However, a summary of natural variability in clades B and C is presented in Figure 2. Also, the last two columns in the table present the entropy scores for gp41e positions that have a defined impact on Env function, for both the B clade and the C clade. Not surprisingly, positions identified through mutational analysis as those where substitutions can abrogate key functions, also tend to be highly conserved among the natural variants. The clearest example is provided by positions where substitutions essentially eliminate cell-cell fusion (*i.e.*, where fusion efficiencies in syncytium assays or reporter gene assays have been reduced to less than 3% of the wild-type value). Sites at which substitutions can abrogate cell-cell fusion tended to be more invariant among 123 B clade sequences (26/44, 59%), compared to those sites where amino acid changes did not dramatically reduce fusion (11/39, 28%, Fisher's exact test $p = 0.004$). Some unusual gp41e variants found in neutralization-resistant isolates are also included in the table, as are variants that arise in response to selection pressure, both *in vitro* and *in vivo*, from the entry inhibitor T-20, which targets gp41e.

The precision with which the available data could be analyzed was sometimes limited because different viral clones, isolates and assays were used to obtain the experimental data. We have therefore chosen to summarize quantitative parameters using the grading system —, +, ++ and +++, as indicated in the footnotes. In some cases these grades had to be deduced from the primary reports, so readers are encouraged to consult the original papers for quantitative details; we regret any errors of interpretation we may have made during this estimation process. Not surprisingly, perhaps, different studies sometimes yielded conflicting results. We have recorded the conflicting data sets but shall leave it to the readers to judge which are the more plausible.

The natural variability of residues in clade B and C isolates was analyzed and mapped on the structure of gp41 (see Figure 2 and Figure 3). A focus of variable residues in clade B sequences is located in the upper part of the C-terminal helix centered around the highly variable leucine-glutamate-glutamine (LEQ) triplet, indicating that this region is under selective pressure. However, it is also possible that certain changes in residues in this region have little impact on Env function, particularly if there is some flexibility in Env structure(s) around this region. This relatively variable region also contains four glycosylation sites, which could be involved in immune evasion (30). Indeed, mutations that affect glycosylation in this region can modulate neutralization sensitivity (65). Of note is that no CTL or antibody epitopes have been mapped to this region despite the intense positive selection. One interpretation of this observation is that the selection pressure is exerted indirectly on distant antibody epitopes elsewhere in gp41e or even in gp120 (32). Another is that some neutralizing antibodies remain as yet undiscovered in this region of gp41e. In clade C viruses the variability is somewhat shifted towards the 2F5 epitope, compared to clade B. Furthermore, certain residues are significantly more variable in clade C viruses compared to clade B, and vice

versa, suggesting that subtly different selection pressures may operate on viruses from the two clades.

Acknowledgments

We thank Brian Foley and Charles Calef for their help with graphical presentation of Figures and Tables. Financial support was obtained from the Dutch AIDS Fund, Amsterdam.

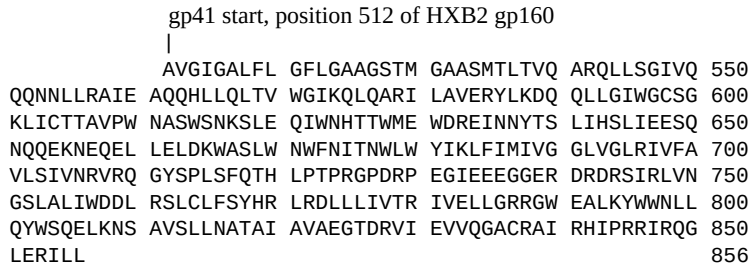

Fig. 1. The HXB2 reference strain and the numbering of positions in the gp41 sequence. Only information on the ectodomain (residues 512-684) is incorporated in subsequent analyses.

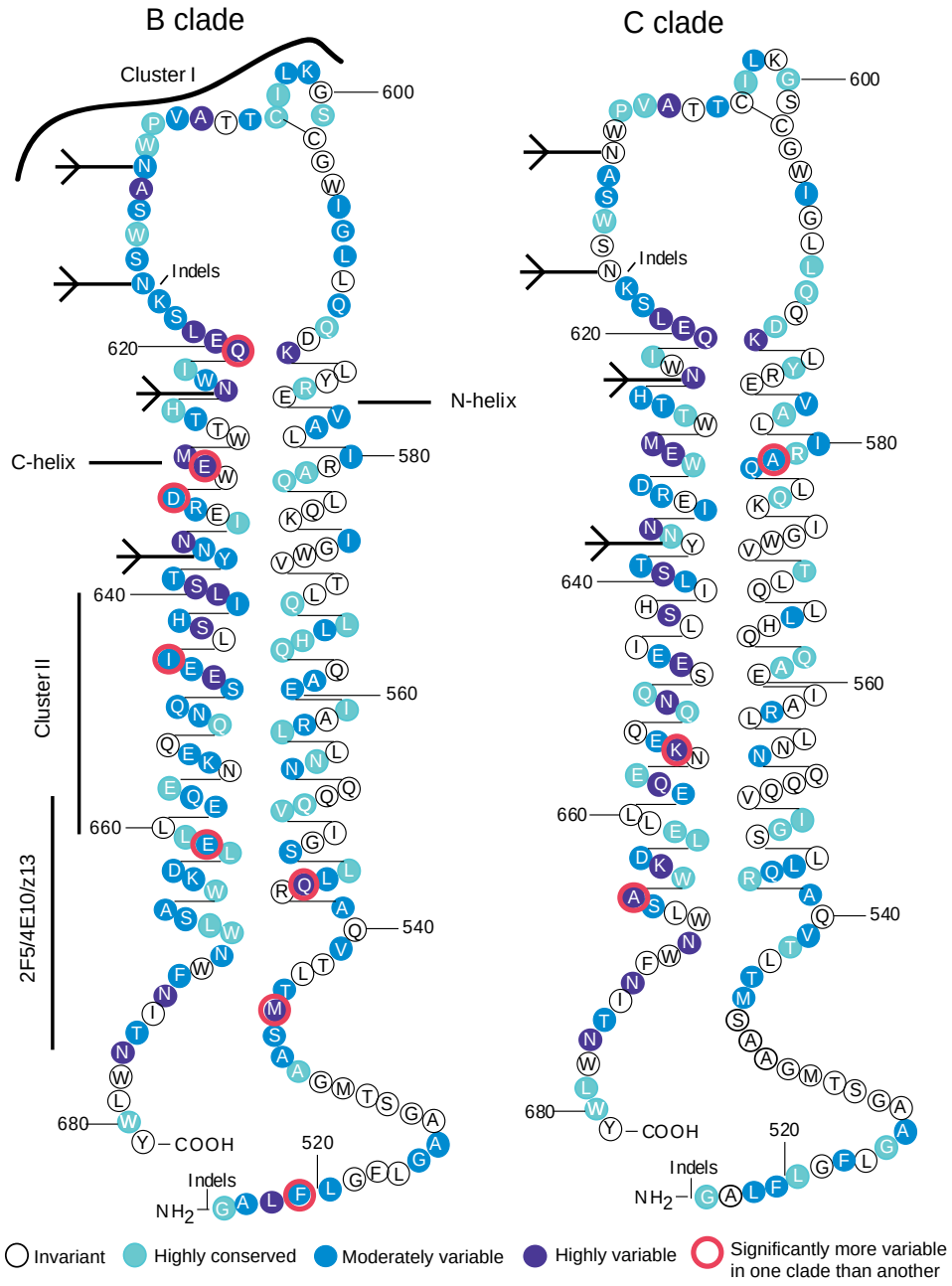

Fig. 2. Variability of gp41e. The relative entropies of residues were mapped onto a 2D representation of the HXB2 gp41e (adapted from 29, 61). The variability of residues in clade **B** isolates (left panel) and clade **C** isolates (right panel) is indicated according to their entropy values. The entropy is a simple measure of variation in each position based on a sequence alignment (33). Not surprisingly, entropy values for each amino acid were highly correlated with the ratio of the nonsynonymous/synonymous substitution rates, a measure which is indicative of selective pressure, calculated using PAML (76) (Spearman's rank correlation

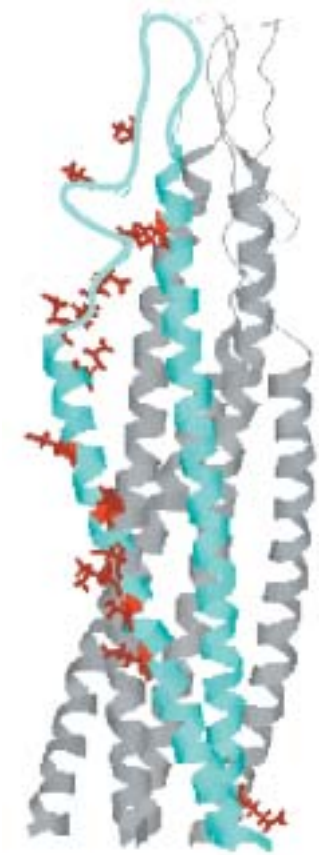

Fig. 3. The residues with the highest 10% of entropy scores in clade B are indicated in red on the 3D structure model of Caffrey (pdb accession number 1IF3, (8)). These residues are only indicated in one monomer. The other two monomers are shown in grey for orientation purposes.

tests gave z = 7.3, p = 2 x 10^{-13} for the B clade, and z = 7.5, p = 5 x 10^{-14} for the C clade). We used the entropy scores as our measure of variability here because they lent themselves to testing for differences in variability between the B clade and C clade (33). The color coding for the sites is as follows: white, invariant (entropy score of zero); light blue, very conserved (entropy score below the median, corresponding to only one observed substitution); medium blue, variable (entropy score above the median: 2 or more observed substitutions); dark blue, highly variable (highest 10% of entropy scores: > 0.8 for clade B and > 0.75 for clade C). Residues that are significantly more variable in clade B than in clade C or vice versa (p value <= 0.03 after a Bonferroni correction for multiple tests, using a Monte Carlo scheme and randomizing the B and C clade data 10,000 times) are indicated by red circles. 123 clade B sequences and 48 clade C sequences were used for the analyses. The four glycans and the major antibody epitopes (non-neutralizing clusters I and II and the neutralizing 2F5/4E10/z13 cluster) are also indicated, as are regions labelled "indel" where insertions and deletions are frequently observed in natural variants.

Residue[1]	Comments	Substitution	Isolate[2]	Reference	Expression (cell lysate)[3]	Expression (cell surface)[4]	gp160 processing[5]	gp120 association[6]	CD4-binding[7]	CD4-induced shedding[8]	Cell-cell fusion[9]	Virion incorporation[10]	Virus entry[11]	Viral Replication[12]	Oligomerization (gp160/gp140)[13]	Trimerization (SOS gp140)[14]	Thermal stability (gp41 core)[15]	B-clade entropy	C-clade entropy
WT					++	++	++	++	++	‡		‡	‡	++	‡‡	+	++		
A512		V[16]	NL4-3	Freed90	++	++	++	++	++		+							0.136	0
		E	NL4-3	Freed90	++		++	++	++		+								
V513		E	NL4-3	Freed90	++		++	++	++		–							0.326	0.44
		A	NL4-3	Buchschacher95							‡‡								
		G	NL4-3								‡‡								
		R	NL4-3		++		++				–							0.628	0.594
G514		V	NL4-3	Delahunty96	++		++	++			++							0.047	0.101
G516		V	NL4-3	Delahunty96	+++		++	++	++		++							0.115	0
A517		[17]	HXB2	Kowalski91	++	++	++	++	++					++					
		[18]	HXB2	Kowalski91										–					
M518		V[19]	ELI1	Kozak97					+++					++				0.985	0.658
F519		L[16]	NL4-3	Freed90	++		++	++	++		+							0.19	0.473
		V	NL4-3	Delahunty96	+++		++	++			‡‡			++					
L520		R	NL4-3	Freed90	++		++	++	++		–							0.13	0.101
G521		V	NL4-3	Delahunty96	+	++	++	++			–			–				0	0
F522		V	NL4-3	Delahunty96	+++		++	++			+							0	0.302
		G	BH8	Pritsker99	++		++				+								
G524		V	NL4-3	Delahunty96	+++	++	++	++			+			+				0.083	0.101
A525		T[20]	LAI	Bahbouhi01	++		++						‡‡	++				0.115	0.202
A526		E	NL4-3	Freed90	++		+	+	++		–							0	0
G527		V	NL4-3	Delahunty96	+++		++	–			–							0	0
S528		T	HXB2	Cao93		+	+	–		+	–		+					0	0
M530		S	HXB2	Cao93		++	–	–		+	–							0	0
G531		V	NL4-3	Delahunty96	+++		++	++	++		‡‡							0	0
L537		R	NL4-3	Freed90	++		+	+	++		–							0	0
V539		E	NL4-3	Freed90	++		++	++	++		+							0.083	0.334
Q540		L	NL4-3	Freed90	++		+	+	++		–							0	0

Residue[1]	Comments	Substitution	Isolate[3]	Reference	Expression (cell lysate)[3]	Expression (cell surface)[4]	gp160 processing[5]	gp120 association[6]	CD4-binding[7]	CD4-induced shedding[8]	Cell-cell fusion[9]	Virion incorporation[10]	Virus entry[11]	Viral Replication[12]	Oligomerization (gp160/gp140)[13]	Trimerization (SOS gp140)[14]	Thermal stability (gp41 core)[15]	B-clade entropy	C-clade entropy
R542	e in heptad-repeat	G	NL4-3	Freed90	++		++	++	++		+							0	0.101
Q543	f in heptad-repeat	H	PI	Wei02, Kilby02										++				0.811	0.202
		R												++					
P543		L^{28}	MN	Park00										++					
L544	g in heptad-repeat	S^{22}	PI	Fikkert02										++				0.094	0.234
L545	a in heptad-repeat	F^{21}	JR-FL	Sanders02		–										+		0.047	0
		N^{21}	JR-FL			++										+			
		P^{21}	JR-FL			++										+			
		G^{21}	JR-FL			++										+			
G547	c in heptad-repeat	S^{22}	NL4-3	Rimsky98										++				0	0.101
		D^{22}	NL4-3											++					
		D^{22}	PI	Baldwin03										++					
		V^{22}	PI	Poveda02										++					
		D^{22}	PI	Wei02										++					
I548	d in heptad-repeat	A	HXB2	Cao93	++	++	+	+++		++	+		++					0	0.101
		T^{22}	NL4-3	Rimsky98										++					
		K^{22}	PI	Baldwin03										++					
		V^{22}	PI	Wei02, Kilby02										++					
		V^{21}	JR-FL	Sanders02		++										+			
		L^{21}	JR-FL			++										+			
		H^{21}	JR-FL			++										+			
		N^{21}	JR-FL			++										+			
		S^{21}	JR-FL			++										+			
		G^{21}	JR-FL			++										+			
		R^{21}	JR-FL			++										+			

Residue[1]	Comments	Substitution	Isolate[2]	Reference	Expression (cell lysate)[3]	Expression (cell surface)[4]	gp160 processing[5]	gp120 association[6]	CD4-binding[7]	CD4-induced shedding[8]	Cell-cell fusion[9]	Virion incorporation[10]	Virus entry[11]	Viral Replication[12]	Oligomerization (gp160/gp140)[13]	Trimerization (SOS gp140)[14]	Thermal stability (gp41 core)[15]	B-clade entropy	C-clade entropy
V549	e in heptad-repeat	M[22]	NL4-3	Rimsky98										++				0.047	0
		M[22]	PI	Wei02										++					
		A[22]	PI											++					
		A[22]	PI	Baldwin03										++					
		W[22]	PI											++					
		G[22]	PI											++					
		A	HXB2	Lu01		++	++	++			++						++		
Q551	g in heptad-repeat	A	HXB2	Lu01, Follis02		++	++	++			++		++				++	0	0
Q552	a in heptad-repeat	L	HXB2	Cao93	++		–	–			–							0	0
N554	c in heptad-repeat	K[22]	PI	Fikkert02										++				0.047	0
L555	d in heptad-repeat	G	HXB2	Cao93	++		–	–			–							0	0
		A	BH8	Poumbourios97	++		–		++		–				++				
		V[21]	JR-FL	Sanders02		–													
		W[21]	JR-FL			–													
		Y[21]	JR-FL			–													
		S[21]	JR-FL			–													
		P[21]	JR-FL			–													
L556	e in heptad-repeat	P	HXB2	Chen94	++		+	–					–					0.047	0
		R	HXB2	Weng98	–						–		–						
		E	HXB2		–						–		–						
		A	HXB2		+	–							–						
		D	HXB2	Weng00	++		++					++	–						
		G	HXB2		++		++					++	–						
		K	HXB2		–								–						
		N	HXB2		++		++					++	–						
		A	HXB2	Lu01, Follis02		++	+	++			–		+				++		
		P[21]	JR-FL	Sanders02		++										+			

Residue[1]	Comments	Substitution	Isolate[2]	Reference	Expression (cell lysate)[3]	Expression (cell surface)[4]	gp160 processing[5]	gp120 association[6]	CD4-binding[7]	CD4-induced shedding[8]	Cell-cell fusion[9]	Virion incorporation[10]	Virus entry[11]	Viral Replication[12]	Oligomerization (gp160/gp140)[13]	Trimerization (SOS gp140)[14]	Thermal stability (gp41 core)[15]	B-clade entropy	C-clade entropy
R557	f in heptad-repeat	P^{21}	JR-FL	Sanders02		++										+		0.237	0.334
		M	PI	Wei02										±					
A558	g in heptad-repeat	R	HXB2	Weng98	–								–					0	0
		E	HXB2		+								–						
		C	HXB2	Weng00	++		++					++	–						
		G	HXB2		++		++					++	–						
		T	HXB2		++		++					++	+						
		P^{21}	JR-FL	Sanders02		++										+			
I559	a in heptad-repeat	P	HXB2	Chen93, Chen94	++	++	–	–	++		–		–		++			0.047	0
		A	BH8	Poumbourios97	++		–	–	++		–				++				
		V^{21}	JR-FL	Sanders02		+										+			
		P^{21}	JR-FL			–										+++			
		N^{21}	JR-FL			–										+++			
		P^{21}	JR-FL			++	++									+++	–		
		G^{21}	JR-FL			+	++									+++	+		
		R^{21}	JR-FL			+										+++			
		P	LAI/ JR-FL	Sanders03b										–			–		
		G	LAI/ JR-FL											–			+		
		L	LAI/ JR-FL											++			++		
E560	b in heptad-repeat	P^{21}	JR-FL	Sanders02		+++										+		0.217	0
		G^{19}	ELI1	Kozak97							+								
A561	c in heptad-repeat	P^{21}	JR-FL	Sanders02		+++										+		0.094	0.101
S561		A^{28}	MN	Park00										++					

Residue[1]	Comments	Substitution	Isolate[2]	Reference	Expression (cell lysate)[3]	Expression (cell surface)[4]	gp160 processing[5]	gp120 association[6]	CD4-binding[7]	CD4-induced shedding[8]	Cell-cell fusion[9]	Virion incorporation[10]	Virus entry[11]	Viral Replication[12]	Oligomerization (gp160/gp140)[13]	Trimerization (SOS gp140)[14]	Thermal stability (gp41 core)[15]	B-clade entropy	C-clade entropy
Q562	d in heptad-repeat	L	HXB2	Cao93	++		+	–			–							0	0.101
		A	BH8	Poumbourios97	++		++	+	‡						++				
		P^{21}	JR-FL	Sanders02		+++										+			
Q563	e in heptad-repeat	A	HXB2	Weng00	++		++					++	++					0.047	0
		E	HXB2		++		++					++	–						
		M	HXB2		++		++					++	–						
		G	HXB2		++		++					++	++						
		R	HXB2		++		++					++	+						
		A	HXB2	Lu01, Follis02		++	++	++			++		++				++		
		P^{21}	JR-FL	Sanders02		+++										+			
R564	f in heptad-repeat	P^{21}	JR-FL	Sanders02		+++												0.047	0
H564		N^{28}	MN	Park00										++					
		C^{26}	HXB2	Rabenstein95											++				
L565	g in heptad-repeat	P	HXB2	Chen94	++	++	+	++	‡		–							0.402	0.584
		A	HXB2	Lu01, Follis02		++	++	++			–		–						
		P^{21}	JR-FL	Sanders02		++										+			
L566	a in heptad-repeat	G	HXB2	Cao93		++	+	+		–			+						
		P	HXB2	Chen93, Chen94	++	++	+	+	++		–		–		++			0.047	0
		A	BH8	Poumbourios97	++		–		++		–				++				
		V^{23}	BH8	Earl93		++	++		++						++				
		V^{21}	JR-FL	Sanders02		+	++									++	++		
		I^{21}	JR-FL			–										+	+		
		N^{21}	JR-FL			+										++	++		
		T^{21}	JR-FL			+										++	++		
		P^{21}	JR-FL			+	++									+	+		
		K^{21}	JR-FL			–										+	+		

Residue[1]	Comments	Substitution	Isolate[2]	Reference	Expression (cell lysate)[3]	Expression (cell surface)[4]	gp160 processing[5]	gp120 association[6]	CD4-binding[7]	CD4-induced shedding[8]	Cell-cell fusion[9]	Virion incorporation[10]	Virus entry[11]	Viral Replication[12]	Oligomerization (gp160/gp140)[13]	Trimerization (SOS gp140)[14]	Thermal stability (gp41 core)[15]	B-clade entropy	C-clade entropy
Q567	b in heptad-repeat	R	LAI	Sanders03a						±				±			±	0.177	0
L568	c in heptad-repeat	A	HXB2	Cao93	++	++	+	++	++	±	–	++	+					0	0
		P	HXB2	Chen94	++	++	+	+	++		–								
		A	HXB2	Ji00													+		
T569	d in heptad-repeat	A	BH8	Poumbourios97	++		–		++		–				±			0	0.101
		C	HXB2	Farzan98			–												
		S^{21}	JR-FL	Sanders02		+		+								+			
		P^{21}	JR-FL			+	++									++	+		
		K^{21}	JR-FL			+										++			
		E^{21}	JR-FL			–													
V570	e in heptad-repeat	R	HXB2	Weng98	++	++			++		–	++	–					0	0
		E^{35}	HXB2		++	++			++			++							
		A	HXB2	Weng00	++		++					++	–						
		D	HXB2		++		++					++	–						
		E	HXB2		++		++					++	–						
		G	HXB2		++		++					++	–						
		I	HXB2		++		++					++	±						
		A	HXB2	Lu01, Follis02		++	++	++			–		–				+		
W571	f in heptad-repeat	R	HXB2	Cao93	++	++	+	++	++	–	–		–					0	0
		R	HXB2	Ji00													++		
		C^{26}	HXB2	Rabenstein95											++				
G572	g in heptad-repeat	G	HXB2	Weng98	++	–			++		–	–	–					0	0
		A	HXB2	Lu01		++	++	++			–								

Residue[1]	Comments	Substitution	Isolate[2]	Reference	Expression (cell lysate)[3]	Expression (cell surface)[4]	gp160 processing[5]	gp120 association[6]	CD4-binding[7]	CD4-induced shedding[8]	Cell-cell fusion[9]	Virion incorporation[10]	Virus entry[11]	Viral Replication[12]	Oligomerization (gp160/gp140)[13]	Trimerization (SOS gp140)[14]	Thermal stability (gp41 core)[15]	B-clade entropy	C-clade entropy
I573	a in heptad-repeat	L	HXB2	Dubay92	++		++	++			++	++		‡	++			0.083	0
		V	HXB2		++	++	++	++			++	++		‡	++				
		A	HXB2		++		++	++			+	++		+	++				
		G	HXB2		++	++	++	++			–	++		–	++				
		E	HXB2		++	++	++	++			–	++		–	++				
		D	HXB2		++		++	++			–	++		–	++				
		S	HXB2		++		++	++			–	++		–	++				
		P^{24}	HXB2	Bernstein95											–				
		A^{24}	HXB2												+				
		D^{24}	HXB2												–				
		A^{25}	HXB3	Shugars96											‡				
		S^{25}	HXB3												–				
		P	HXB2	Chen93, Chen94	++	‡	+	+	++		–		–		‡				
		P^{26}	HXB2, LAI	Wild94	++		‡	+			–								
		A^{26}	HXB2, LAI		++	++	++	++			+			+			–		
		S^{26}	HXB2, LAI		++	++	++	++			–			–			–		
		P^{26}	HXB2	Rabenstein95											–				
		D^{26}	HXB2												–				
		S^{26}	HXB2												–				
		S	168P	Liu01		++	++	++			++	++	‡				–		
		T	168P														+		
		V	LAI	Sanders03a										‡			‡		
		A	BH8	Poumbourios97	++		++	++	++		–				++				
		V	HXB2	Markosyan02													‡		
		A	HXB2														+		
		S	HXB2														+		

Residue[1]	I573 cont.	Comments	Substitution	Isolate[2]	Reference	Expression (cell lysate)[3]	Expression (cell surface)[4]	gp160 processing[5]	gp120 association[6]	CD4-binding[7]	CD4-induced shedding[8]	Cell-cell fusion[9]	Virion incorporation[10]	Virus entry[11]	Viral Replication[12]	Oligomerization (gp160/gp140)[13]	Trimerization (SOS gp140)[14]	Thermal stability (gp41 core)[15]	B-clade entropy	C-clade entropy
			P	HXB2														-		
			L^{21}	JR-FL	Sanders02		++										+			
			F^{21}	JR-FL			++										+			
			Y^{21}	JR-FL			++										+			
			Q^{21}	JR-FL			++										+			
			N^{21}	JR-FL			++										+			
			T^{21}	JR-FL			++										+			
			P^{21}	JR-FL			++										+			
			G^{21}	JR-FL			++										+			
			K^{21}	JR-FL			++										+			
K574		b in heptad-repeat	R	BH8	McInerney98	++		+	+	++	++	+							0	0
L576		d in heptad-repeat	P	HXB2	Chen94	++		+	+	++		−							0	0
			A	BH8	Poumbourios97	++		−		++		−				++				
			C^{27}	HXB2	Farzan98	++	+	−								+++				
			V^{21}	JR-FL	Sanders02		−										+			
			F^{21}	JR-FL			−										+			
			Y^{21}	JR-FL			−										+			
			Q^{21}	JR-FL			−										+			
			N^{21}	JR-FL			−										+			
			G^{21}	JR-FL			−										+			
			K^{21}	JR-FL			−										+			

Residue[1]	Comments	Substitution	Isolate[2]	Reference	Expression (cell lysate)[3]	Expression (cell surface)[4]	gp160 processing[5]	gp120 association[6]	CD4-binding[7]	CD4-induced shedding[8]	Cell-cell fusion[9]	Virion incorporation[10]	Virus entry[11]	Viral Replication[12]	Oligomerization (gp160/gp140)[13]	Trimerization (SOS gp140)[14]	Thermal stability (gp41 core)[15]	B-clade entropy	C-clade entropy
Q577	e in heptad-repeat	R	HXB2	Weng98	++	++	++		++			++	–					0.047	0.173
		E	HXB2		++	++			++		+	+	+						
		A	HXB2	Weng00	++		++					++	+						
		D	HXB2		++		++					++	++						
		E	HXB2		++		++					++	+						
		G	HXB2		++		++					++	++						
		M	HXB2		++		++					++	+						
		C[27]	HXB2	Farzan98	++	+	–								+++				
		A	HXB2	Lu01		++	++	++			++								
A578	f in heptad-repeat	G[27]	HXB2	Farzan98	++	+	–								+++			0.047	0.483
R579	g in heptad-repeat	G	HXB2	Weng00	++		+					++	–					0	0.101
		A	HXB2	Lu01		++	+	++			–						++		
I580	a in heptad-repeat	P	HXB2	Chen94	++	++	+	–	++		–							0.432	0.173
		A	BH8	Poumbourios97	++		++	++	++		–				++				
		L[21]	JR-FL	Sanders02		++										+			
		H[21]	JR-FL			++										+			
		T[21]	JR-FL			++										+			
		P[21]	JR-FL			++										+			
		G[21]	JR-FL			++										+			
L581	b in heptad-repeat	Q[28]	MN	Park00										++				0	0
A582	c in heptad-repeat	T[28]	PI	Reitz88										++				0.094	0.101
		C[26]	HXB2	Rabenstein95											++				

Residue[1]	Comments	Substitution	Isolate[2]	Reference	Expression (cell lysate)[3]	Expression (cell surface)[4]	gp160 processing[5]	gp120 association[6]	CD4-binding[7]	CD4-induced shedding[8]	Cell-cell fusion[9]	Virion incorporation[10]	Virus entry[11]	Viral Replication[12]	Oligomerization (gp160/gp140)[13]	Trimerization (SOS gp140)[14]	Thermal stability (gp41 core)[15]	B-clade entropy	C-clade entropy
V583	d in heptad-repeat	A	BH8	Poumbourios97	++		+	++	++		–				++			0.244	0.503
		C	HXB2	Farzan98			–												
		L^{21}	JR-FL	Sanders02		++										+			
		Q^{21}	JR-FL			++										+			
		N^{21}	JR-FL			++										+			
		S^{21}	JR-FL			++										+			
		P^{21}	JR-FL			++										+			
		R^{21}	JR-FL			++										+			
		K^{21}	JR-FL			++										+			
E584	e in heptad-repeat	A	HXB2	Cao93		++	–	–	++	+	–		–					0	0
		Q	BH8	Maerz01	++	++	++	+	++		+								
		D	BH8		++		++				+								
		N	BH8		++		++				–								
Y586	f in heptad repeat	R	HXB2	Weng98	++	+			++			+	–					0	0.101
		E	HXB2		++	+			++			+	–						
		C^{29}	HXB2	Farzan98			–												
L587	a in heptad-repeat	P	HXB2	Chen93, Chen94	++	++	++	–	++		–		–		++			0	0
		A	BH8	Poumbourios97	++		++	++	++		–				++				
		C^{29}	HXB2	Farzan98			–												
		A^{21}	JR-FL	Sanders02		–										+			
		P^{21}	JR-FL			–										+			
		R^{21}	JR-FL			–										+			
		D^{21}	JR-FL			–										+			
		E^{21}	JR-FL			–										+			
K588		R	BH8	McInerney98	++		++	++	++	++	++							1.112	0.775
D589		L	HXB2	Cao93	++	++	+++	+	++	+	–		+					0	0.101
		C^{30}	JR-FL	Binley00		++													
		K	BH8	Maerz01	++	++	++	+			–								

Residue[1]	Comments	Substitution	Isolate[2]	Reference	Expression (cell lysate)[3]	Expression (cell surface)[4]	gp160 processing[5]	gp120 association[6]	CD4-binding[7]	CD4-induced shedding[8]	Cell-cell fusion[9]	Virion incorporation[10]	Virus entry[11]	Viral Replication[12]	Oligomerization (gp160/gp140)[13]	Trimerization (SOS gp140)[14]	Thermal stability (gp41 core)[15]	B-clade entropy	C-clade entropy
Q591		A	BH8	Maerz01	++	++	++	±			++							0.083	0.101
		K	BH8		++		++				++								
		L	LAI	Sanders03c										+				0	0.101
L592		V	BH8	Maerz01	++		++				++								
		A	BH8		++		++				++								
L593		V	BH8	Maerz01	++		++				+		–					0.143	0
		A	BH8		++	++	++	–			+		–						
		Q	LAI	Sanders03c										+/–					
I595		F^{31}	PI	Moore93										++				0.162	0.555
W596		M	HXB2	Cao93, Cao94	++	++	++	+	++		–		++	++	++			0	0
		Y	LAI, NL4-3	Rovinski99		++	++					++							
		A	LAI, NL4-3				–					+							
		C^{30}	JR-FL	Binley00		++													
		F	BH8	Maerz01	++	++	++	+			++		++						
		H	BH8		++		++				+								
		L	BH8		++	++	++	+			+								
G597		P	BH8	Maerz01	++	++	++	–			–							0	0
		A	BH8		++	++	++	–			–								
		S	BH8		++	++	++	–			–								
C598		S	HXB2	Dedera92a	++		–				–							0	0
		S^{23}	BH8	Earl93		++	++		++						++				
		G	HXB2	Syu91	++		–							–					
		A	LAI	Van Anken03										–					
G600		A	LAI, NL4-3	Rovinski99		++	++					++						0	0.101

Residue[1]	Comments	Substitution	Isolate[2]	Reference	Expression (cell lysate)[3]	Expression (cell surface)[4]	gp160 processing[5]	gp120 association[6]	CD4-binding[7]	CD4-induced shedding[8]	Cell-cell fusion[9]	Virion incorporation[10]	Virus entry[11]	Viral Replication[12]	Oligomerization (gp160/gp140)[13]	Trimerization (SOS gp140)[14]	Thermal stability (gp41 core)[15]	B-clade entropy	C-clade entropy
K601		R	BH8	McInemey98	++		++	+	++	++	–							0.218	0
		R	LAI, NL4-3	Rovinski99			++					++							
		E	LAI, NL4-3			++	++					++							
		E	BH8	Mera99	++		+				++								
		E	BH8	Maerz01	++	++	++	+			++								
		H	BH8		++	++	++	+			++								
		Q	BH8		++	++	++	+			++								
		A	BH8		++	++	++				++								
C604		S	HXB2	Dedera92a	++		–				–							0.047	0
		S^{23}	BH8	Earl93		++	++		++						++				
		G	HXB2	Syu91	++		–							–					
		A	LAI	Van Anken03										–					
T605		C^{30}	JR-FL, HXB2, DH123, 89.6, GUN1-wt	Binley00		++	++	+++	++						+			0.177	0.173
		C	LAI	Sanders03c										++					
		Y	LAI											++					
V608		S	HXB2	Cao93			–	–			–							0.094	0.101
		C^{30}	JR-FL	Binley00		++													
P609		C^{30}	JR-FL	Binley00		++												0.047	0.101
W610		C^{30}	JR-FL	Binley00		++												0.047	0
		F	BH8	Maerz01	++	++	++	–			–								
		H	BH8		++	++	++	–			–								

Residue[1]	Comments	Substitution	Isolate[2]	Reference	Expression (cell lysate)[3]	Expression (cell surface)[4]	gp160 processing[5]	gp120 association[6]	CD4-binding[7]	CD4-induced shedding[8]	Cell-cell fusion[9]	Virion incorporation[10]	Virus entry[11]	Viral Replication[12]	Oligomerization (gp160/gp140)[13]	Trimerization (SOS gp140)[14]	Thermal stability (gp41 core)[15]	B-clade entropy	C-clade entropy
N611	Glycosylation site	Q	HXB2	Dedera92b	++		++	‡			+			++	++			0.141	0
		H	HXB2	Lee92	++		++					‡		+					
		S	NL4-3	Dash94	++	++	++				‡								
		Q	SHIV-KB9	Johnson01	++		++							++					
S613	Glycosylation site N611	A	HXB2	Lee92	++		++							+				0.94	0.274
N616	Glycosylation site	Q	HXB2	Dedera92b							+			++				0.237	0
		Q^{23}	BH8	Earl93		++	++		++						++				
		H	HXB2	Lee92	++		++					++		++					
		S	NL4-3	Dash94	++	++	++				‡								
		Q	BH10	Perrin98	++		++				+								
		Q	SHIV-KB9	Johnson01	++		++							++					
K617		R	BH8	McInerney98	++		++	++	++	++	++							0.348	0.658
S618	Glycosylation site N616	A	HXB2	Lee92	++		++	–						–				0.495	0.483
N624	d in heptad-repeat Glycosylation site (N625 in most isolates)	H	HXB2	Lee92	++		++					++		+				1.153	1.305
		Q	BH10	Perrin98	++		++				‡								
		Q	SHIV-KB9	Johnson01	++		++							++					
N625	e in heptad-repeat Glycosylation site	Q^{23}	BH8	Earl93		++	++		++						++			0.047	0.274
T626	f in heptad-repeat Glycosylation site N624	M	HXB2	Cao93	++	–	–	–		–	–		–					0.244	0.444
		M^{28}	SHIV-HXBc2P	Si01										++					

Residue[1]	Comments	Substitution	Isolate[2]	Reference	Expression (cell lysate)[3]	Expression (cell surface)[4]	gp160 processing[5]	gp120 association[6]	CD4-binding[7]	CD4-induced shedding[8]	Cell-cell fusion[9]	Virion incorporation[10]	Virus entry[11]	Viral Replication[12]	Oligomerization (gp160/gp140)[13]	Trimerization (SOS gp140)[14]	Thermal stability (gp41 core)[15]	B-clade entropy	C-clade entropy
W628	a in heptad-repeat	M	HXB2	Cao93			–	–		–	–							0	0
		A	HXB2	Weng00	++		–					++	–						
		F	HXB2		++		–					++	–						
		A	HXB2	Wang02		++	–	++			–						+		
W631	d in heptad-repeat	A	HXB2	Wang02		++	–	++			–						–	0	0.101
D632	e in heptad-repeat	N[32]	BH10	Perrin98	++		++				–							0.591	0.287
R633	f in heptad-repeat	G	PI	Wei02										++				0.55	0.451
I635	a in heptad-repeat	A	HXB2	Wang02		++		++			–						+	0.047	0.173
N637	c in heptad-repeat	K[22]	PI	Baldwin03										++				0.141	0.101
	Glycosylation site	Q	HXB2	Dedera92b							++			++					
		Q[23]	BH8	Earl93		++	++		++						++				
		H	HXB2	Lee92	++		++					++		–					
		S	NL4-3	Dash94	++	–	–				–								
		Q	BH10	Perrin98	++		++				++								
		Q	SHIV-KB9	Johnson01	++		++							++					
Y638	d in heptad-repeat	A	HXB2	Wang02		++	++	++					++				++	0.13	0
T639	e in heptad-repeat	V	HXB2	Lee92	++		++							+				0.083	0.202
	Glycosylation site N637	A	HXB2	Cao93	++	–	–			–	–								
I642	a in heptad-repeat	A	HXB2	Wang02		++	–	++			–						++	0.094	0
		A	HXB2	Markosyan02													++		
		S	HXB2														++		
H643	b in heptad-repeat	Y[20]	LAI	Bahbouhi01	++		++					++		++				0.115	0
		Y	LAI	Sanders03a										++					
L645	d in heptad-repeat	A	H64333	Wang02		++	++	++					++				++	0	0

Residue[1]	Comments	Substitution	Isolate[2]	Reference	Expression (cell lysate)[3]	Expression (cell surface)[4]	gp160 processing[5]	gp120 association[6]	CD4-binding[7]	CD4-induced shedding[8]	Cell-cell fusion[9]	Virion incorporation[10]	Virus entry[11]	Viral Replication[12]	Oligomerization (gp160/gp140)[13]	Trimerization (SOS gp140)[14]	Thermal stability (gp41 core)[15]	B-clade entropy	C-clade entropy
E647	f in heptad-repeat	L	HXB2	Cao93		++	+++	+			++		++					0.188	0.173
S649	a in heptad-repeat	A	HXB2	Wang02		++	++	++					++				++	0.401	0
Q652	d in heptad-repeat	L	HXB2	Cao93		++	++	+			++		++					0.047	0.101
		L	HXB2	Shu00													++		
		A	HXB2	Wang02		++	++	++					++				++		
K655	g in heptad-repeat	R^{33}	BH8	Poumbourios95	++		++	++			++							0.213	1.093
N656	a in heptad-repeat	L	HXB2	Cao93	++	++	+	++	++		–		+					0	0
L663	2F5 epitope	F	HXB2	Cao93		++	+++	++			++		++					0.047	0.101
K665	2F5 epitope	R^{33}	BH8	Poumbourios95	++		++	++			++							0.451	0.922
W666	2F5 epitope	P	HXB2	Cao93		++	++	++			++		++					0.047	0.101
		A	HXB2, NL4-3	Salzwedel99	++		++	++			++								
S668	2F5 epitope	N^{28}	HXB2	Back93										++				0.497	0.573
L669		P	HXB2	Cao93		+++	++	+		+++	++		++					0.047	0
W670		A	HXB2, NL4-3	Salzwedel99	++		++	++			++							0.047	0
N671	4E10/z13 epitope	P	HXB2	Cao93		++	++	++			++		++					0.713	0.945
W672	4E10/z13 epitope	S	HXB2	Cao93	++	++	++	+		+++	++		++					0	0
		S	HXB2, NL4-3	Salzwedel99	++		++	++			++								
		P	HXB2, NL4-3		++		++	++			++	–	+						
		F	HXB2, NL4-3		++		++	++			++	+	+						
F673	4E10/z13 epitope	P	HXB2	Cao93	++	++	++	+			++		++					0.94	0
		S^{34}	HXB2	Stern95							++			++					

Residue[1]	Comments	Substitution	Isolate[2]	Reference	Expression (cell lysate)[3]	Expression (cell surface)[4]	gp160 processing[5]	gp120 association[6]	CD4-binding[7]	CD4-induced shedding[8]	Cell-cell fusion[9]	Virion incorporation[10]	Virus entry[11]	Viral Replication[12]	Oligomerization (gp160/gp140)[13]	Trimerization (SOS gp140)[14]	Thermal stability (gp41 core)[15]	B-clade entropy	C-clade entropy
N674	4E10/z13 epitope	H	HXB2	Lee92	++		++					++		++				1.038	1.375
		S	NL4-3	Dash94	++	++	++				++								
		D[28]	SHIV-HXBc2P	Si01										++					
I675	4E10/z13 epitope	S	HXB2	Cao93		++	++	+			++		++					0	0
		M[28]	HXB2	Back93										++					
N677		R	HXB2	Cao93		++	++	+			++		++					1.237	0.769
W678		A	HXB2	Cao93		++	++	+			++		++					0	0
		A	HXB2, NL4-3	Salzwedel99	++		++	++			++								
W680		A	HXB2, NL4-3	Salzwedel99	++		++	++			++							0.047	0.101
Y681		P	HXB2	Cao93			++	++			++		++					0	0
K683		R	BH8	McInerney98	++		++	++	++	++	++							0.375	0.325

Table footnotes:

[1]Residue numbering is based on HXB2 gp160, although the amino-acids studied may be different in the isolate used. The one-letter code for amino acids is used

[2]PI: primary isolate

[3]As assessed by western blot or immunoprecipitation. –, minimal or no expression; +, reduced expression; ++, expression similar to WT; +++, increased expression

[4]As assessed by surface biotinylation, iodination or FACS. When soluble gp140 constructs were used, the relative secretion levels (western blot or immunoprecipitation) are given. –, minimal or no expression; +, reduced expression; ++, expression similar to WT; +++, increased expression

[5]As assessed by western blot or immunoprecipitation in combination with densitometric measurements. –, minimal or no processing; +, reduced processing; ++, processing similar to WT; +++, increased processing

[6]As assessed by western blot or immunoprecipitation in combination with densitometric measurements. –, minimal or no association; +, reduced association; ++, association similar to WT; +++, increased association

[7]As assessed by immunoprecipitation with CD4-based reagents. ++, similar to WT; +++, increased CD4 binding

[8]As assessed by immunoprecipitation. –, no shedding; +, reduced shedding; ++, shedding similar to WT; +++, increased shedding. Note that CD4-induced shedding and to a lesser extent gp120 association (*i.e.*, the reverse of shedding), when measured in laboratory isolates, might be diminished in primary isolates that can retain gp120 more efficiently.

[9]As assessed by syncytium formation or reporter gene assays. –, fusion lower than 3% of WT; +, fusion between 3 and 30% of WT; ++, fusion greater than 30% of WT

[10]As assessed by western blot or immunoprecipitation. –, minimal or no incorporation; +, reduced incorporation; ++, incorporation similar to WT

[11]As assessed by various assays (replication complementation, use of reporter genes, p24 production). –, entry lower than 3% of WT; +, entry between 3 and 30% of WT; ++, entry

greater that 30% of WT

[12]–, no apparent replication; +, replication with a delay of more than 2 days compared to WT; ++ replication similar to WT

[13]As assessed by sucrose gradient fractionation, immunoprecipitation, velocity sedimentation or FPLC, unless indicated otherwise. –, oligomerization below 25% of WT; +, oligomerization between 25% and 50% of WT; ++, oligomerization similar to WT. No distinction between dimerization, trimerization or tetramerization is made.

[14]As assessed by Blue Native-PAGE. +, trimerization similar to WT SOS gp140 (occasional trimerization); ++, slightly more trimerization than in WT; +++, significantly more trimerization than in WT.

[15]As analyzed using the N34(L6)C28 or N36(L6)C34 peptide model, unless indicated otherwise. –, melting temperature (T_m) below 40°C; +, T_m between 40°C and 60°C; ++, T_m between 60°C and 80°C; +++, T_m over 80°C

[16]Analyzed in a double mutant, A512V + F519L

[17]Four amino-acid insertion GIPA

[18]Six amino-acid insertion IHRWIA

[19]Involved in cell line adaptation

[20]Identified in an isolate which is resistant to the furin inhibitor (α1-PDX)

[21]Analyzed in soluble SOS gp140 constructs and so also contain the A501C and T605C substitutions

[22]Involved in T-20 resistance

[23]Analyzed in soluble gp140

[24]Analyzed in an N-peptide/Protein A fusion protein

[25]Analyzed in an N-peptide/maltose binding protein (MBP) fusion protein

[26]Thermal stability (74) or oligomerization (53) of N-peptides analyzed in the absence of C-peptides

[27]Analyzed in a triple mutant L576C + Q577C + A578G

[28]Involved in neutralization resistance

[29]Analyzed in a double mutant Y586C + L587C

[30]Analyzed in combination with gp120 cysteine substitutions in the context of soluble gp140

[31]Involved in resistance to soluble CD4

[32]Generates a new glycosylation site

[33]Analyzed in a double mutant K655R + K665R

[34]Analyzed in a double mutant A582T + F673S

[35]Data on this mutant were corrected in reference 73

References

1. **Van Anken, E., R. W. Sanders, B. Berkhout, and I. Braakman.** 2003. unpublished results.
2. **Back, N. K., L. Smit, M. Schutten, P. L. Nara, M. Tersmette, and J. Goudsmit.** 1993. Mutations in human immunodeficiency virus type 1 gp41 affect sensitivity to neutralization by gp120 antibodies. *J. Virol.* **67**:6897-6902.
3. **Bahbouhi, B., N. G. Seidah, and E. Bahraoui.** 2001. Replication of HIV-1 viruses in the presence of the Portland alpha1- antitrypsin variant (alpha1-PDX) inhibitor. *Biochem. J.* **360**:127-134.
4. **Baldwin, C. E., R. W. Sanders, S. Jurriaans, J. M. Lange, and B. Berkhout.** 2002. Two step evolution of HIV-1 gp41 during therapy with the T20 entry inhibitor. Submitted.
5. **Bernstein, H. B., S. P. Tucker, S. R. Kar, S. A. McPherson, D. T. McPherson, J. W. Dubay, J. Lebowitz, R. W. Compans, and E. Hunter.** 1995. Oligomerization of the hydrophobic heptad repeat of gp41. *J. Virol.* **69**:2745-2750.
6. **Binley, J. M., R. W. Sanders, B. Clas, N. Schuelke, A. Master, Y. Guo, F. Kajumo, D. J. Anselma, P. J. Maddon, W. C. Olson, and J. P. Moore.** 2000. A recombinant HIV-1 envelope glycoprotein complex stabilized by an intermolecular disulfide bond between the gp120 and gp41 subunits is an antigenic mimic of the trimeric virion-associated structure. *J. Virol.* **74**:627-643.
7. **Buchschacher, G. L., Jr., E. O. Freed, and A. T. Panganiban.** 1995. Effects of second-site mutations on dominant interference by a human immunodeficiency virus type 1 envelope glycoprotein mutant. *J. Virol.* **69**:1344-1348.
8. **Caffrey, M.** 2001. Model for the structure of the HIV gp41 ectodomain: insight into the intermolecular interactions of the gp41 loop. *Biochim. Biophys. Acta.* **1536**:116-122.
9. **Caffrey, M., M. Cai, J. Kaufman, S. J. Stahl, P. T. Wingfield, D. G. Covell, A. M. Gronenborn, and G. M. Clore.** 1998. Three-dimensional solution structure of the 44 kDa ectodomain of SIV gp41. *EMBO J.* **17**:4572-4584.
10. **Cao, J., L. Bergeron, E. Helseth, M. Thali, H. Repke, and J. Sodroski.** 1993. Effects of amino acid changes in the extracellular domain of the human immunodeficiency virus type 1 gp41 envelope glycoprotein. *J. Virol.* **67**:2747-2755.
11. **Cao, J., B. Vasir, and J. G. Sodroski.** 1994. Changes in the cytopathic effects of human immunodeficiency virus type 1 associated with a single amino acid alteration in the ectodomain of the gp41 transmembrane glycoprotein. *J. Virol.* **68**:4662-4668.
12. **Chan, D. C., D. Fass, J. M. Berger, and P. S. Kim.** 1997. Core structure of gp41 from the HIV envelope glycoprotein. *Cell* **89**:263-273.
13. **Chan, D. C. and P. S. Kim.** 1998. HIV entry and its inhibition. *Cell* **93**:681-684.
14. **Chen, S. S.** 1994. Functional role of the zipper motif region of human immunodeficiency virus type 1 transmembrane protein gp41. *J. Virol.* **68**:2002-2010.
15. **Chen, S. S., C. N. Lee, W. R. Lee, K. McIntosh, and T. H. Lee.** 1993. Mutational analysis of the leucine zipper-like motif of the human immunodeficiency virus type 1 envelope transmembrane glycoprotein. *J. Virol.* **67**:3615-3619.
16. **Dash, B., A. McIntosh, W. Barrett, and R. Daniels.** 1994. Deletion of a single N-linked glycosylation site from the transmembrane envelope protein of human immunodeficiency virus type 1 stops cleavage and transport of gp160 preventing env-mediated fusion. *J. Gen. Virol.* **75** (Pt 6):1389-1397.
17. **Dedera, D., R. L. Gu, and L. Ratner.** 1992a. Conserved cysteine residues in the human immunodeficiency virus type 1 transmembrane envelope protein are essential for precursor envelope cleavage. *J. Virol.* **66**:1207-1209.
18. **Dedera, D. A., R. L. Gu, and L. Ratner.** 1992b. Role of asparagine-linked glycosylation in human immunodeficiency virus type 1 transmembrane envelope function. *Virol.* **187**:377-382.
19. **Delahunty, M. D., I. Rhee, E. O. Freed, and J. S. Bonifacino.** 1996. Mutational analysis of the fusion peptide of the human immunodeficiency virus type 1: identification of critical glycine residues. *Virol.* **218**:94-102.
20. **Doms, R. W.** 2000. Beyond receptor expression: the influence of receptor conformation, density, and affinity in HIV-1 infection. *Virol.* **276**:229-237.
21. **Doms, R. W. and J. P. Moore.** 2000. HIV-1 membrane fusion: targets of opportunity. *J. Cell Biol.* **151**:F9-14.
22. **Dubay, J. W., S. J. Roberts, B. Brody, and E. Hunter.** 1992. Mutations in the leucine zipper of

the human immunodeficiency virus type 1 transmembrane glycoprotein affect fusion and infectivity. *J. Virol.* **66**:4748-4756.
23. **Earl, P. L. and B. Moss.** 1993. Mutational analysis of the assembly domain of the HIV-1 envelope glycoprotein. *AIDS Res. Hum. Retroviruses* **9**:589-594.
24. **Eckert, D. M. and P. S. Kim.** 2001. Mechanisms of viral membrane fusion and its inhibition. *Annu. Rev. Biochem*. **70**:777-810.
25. **Farzan, M., H. Choe, E. Desjardins, Y. Sun, J. Kuhn, J. Cao, D. Archambault, P. Kolchinsky, M. Koch, R. Wyatt, and J. Sodroski.** 1998. Stabilization of human immunodeficiency virus type 1 envelope glycoprotein trimers by disulfide bonds introduced into the gp41 glycoprotein ectodomain. *J. Virol.* **72**:7620-7625.
26. **Fikkert, V., P. Cherepanov, K. van Laethum, A. Hantson, B. van Remoortel, C. Pannecouque, E. de Clercq, Z. Debyser, A. Vandamme, and M. Witvrouw.** 2002. Env chimeric virus technology for evaluating human immunodeficiency virus susceptility to entry inhibitors. *Antimicrob. Agents Chemother*. **46**:3954-3962
27. **Follis, K. E., S. J. Larson, M. Lu, and J. H. Nunberg.** 2002. Genetic evidence that interhelical packing interactions in the gp41 core are critical for transition of the human immunodeficiency virus type 1 envelope glycoprotein to the fusion-active state. *J. Virol*. **76**:7356-7362.
28. **Freed, E. O., D. J. Myers, and R. Risser.** 1990. Characterization of the fusion domain of the human immunodeficiency virus type 1 envelope glycoprotein gp41. *Proc. Natl. Acad. Sci. USA* **87**:4650-4654.
29. **Gallaher, W. R., J. M. Ball, R. F. Garry, A. M. Martin-Amedec, and R. C. Montelaro.** 1989. A general model for the transmembrane proteins of HIV and other retroviruses. *AIDS Res. Hum. Retroviruses* **5**:431-440.
30. **Johnson, W. E., J. M. Sauvron, and R. C. Desrosiers.** 2001. Conserved, N-linked carbohydrates of human immunodeficiency virus type 1 gp41 are largely dispensable for viral replication. *J. Virol*. **75**:11426-11436.
31. **Kilby, J. M., J. P. Lalezari, J. J. Eron, M. Carlson, C. Cohen, R. C. Arduino, J. C. Goodgame, J. E. Gallant, P. Volberding, R. L. Murphy, F. Valentine, M. S. Saag, E. L. Nelson, P. R. Sista, and A. Dusek.** 2002. The Safety, Plasma Pharmacokinetics, and Antiviral Activity of Subcutaneous Enfuvirtide (T-20), a Peptide Inhibitor of gp41-Mediated Virus Fusion, in HIV-Infected Adults. *AIDS Res. Hum. Retroviruses* **18**:685-693.
32. **Klasse, P. J., J. A. McKeating, M. Schutten, M. S. Reitz Jr., and M. Robert-Guroff.** 1993. An immune-selected point mutation in the transmembrane protein of human immunodeficiency virus type 1 (HXB2-Env:Ala 582(>Thr)) decreases viral neutralization by monoclonal antibodies to the CD4-binding site. *Virol.* **196**:332-337.
33. **Korber BT, K Kunstman, BK Patterson, M Furtado, M McEvilly, R Levy, and SM Wolinsky.** 1994. Genetic differences between blood- and brain-derived viral sequences from human immunodeficiency virus type 1-infected patients: evidence of conserved elements in the V3 region of the envelope protein of brain-derived sequences. *J. Virol.* **68**(11):7467-81
34. **Kowalski, M., L. Bergeron, T. Dorfman, W. Haseltine, and J. Sodroski.** 1991. Attenuation of human immunodeficiency virus type 1 cytopathic effect by a mutation affecting the transmembrane envelope glycoprotein. *J. Virol.* **65**:281-291.
35. **Kozak, S. L., E. J. Platt, N. Madani, F. E. Ferro, K. Peden, and D. Kabat.** 1997. CD4, CXCR-4, and CCR-5 dependencies for infections by primary patient and laboratory-adapted isolates of human immunodeficiency virus type 1. *J. Virol.* **71**:873-882.
36. **Lee, W. R., X. F. Yu, W. J. Syu, M. Essex, and T. H. Lee.** 1992. Mutational analysis of conserved N-linked glycosylation sites of human immunodeficiency virus type 1 gp41. *J. Virol.* **66**:1799-1803.
37. **Liu, J., W. Shu, M. B. Fagan, J. H. Nunberg, and M. Lu.** 2001. Structural and functional analysis of the HIV gp41 core containing an Ile573 to Thr substitution: implications for membrane fusion. *Biochem.* **40**:2797-2807.
38. **Lu, M., H. Ji, and S. Shen.** 1999. Subdomain folding and biological activity of the core structure from human immunodeficiency virus type 1 gp41: implications for viral membrane fusion. *J. Virol.* **73**:4433-4438.
39. **Lu, M., M. O. Stoller, S. Wang, J. Liu, M. B. Fagan, and J. H. Nunberg.** 2001. Structural and functional analysis of interhelical interactions in the human immunodeficiency virus type 1 gp41

envelope glycoprotein by alanine-scanning mutagenesis. *J. Virol.* **75**:11146-11156.
40. **Maerz, A. L., H. E. Drummer, K. A. Wilson, and P. Poumbourios.** 2001. Functional analysis of the disulfide-bonded loop/chain reversal region of human immunodeficiency virus type 1 gp41 reveals a critical role in gp120-gp41 association. *J. Virol.* **75**:6635-6644.
41. **Malashkevich, V. N., D. C. Chan, C. T. Chutkowski, and P. S. Kim.** 1998. Crystal structure of the simian immunodeficiency virus (SIV) gp41 core: conserved helical interactions underlie the broad inhibitory activity of gp41 peptides. *Proc. Natl. Acad. Sci. USA* **95**:9134-9139.
42. **Markosyan, R. B., X. Ma, M. Lu, F. Cohen, and G. Melikyan.** 2002. The mechanism of HIV-1 Env-mediated cell-cell fusion by recombinant cores of gp41 ectodomain. *Virol.* **302**:174-184.
43. **McInerney, T. L., W. El Ahmar, B. E. Kemp, and P. Poumbourios.** 1998. Mutation-directed chemical cross-linking of human immunodeficiency virus type 1 gp41 oligomers. *J. Virol.* **72**:1523-1533.
44. **Merat, R., H. Raoul, T. Leste-Lasserre, P. Sonigo, and G. Pancino.** 1999. Variable constraints on the principal immunodominant domain of the transmembrane glycoprotein of human immunodeficiency virus type 1. *J. Virol.* **73**:5698-5706.
45. **Moore, J. P., L. C. Burkly, R. I. Connor, Y. Cao, R. Tizard, D. D. Ho, and R. A. Fisher.** 1993. Adaptation of two primary human immunodeficiency virus type 1 isolates to growth in transformed T cell lines correlates with alterations in the responses of their envelope glycoproteins to soluble CD4. *AIDS Res. Hum. Retroviruses* **9**:529-539.
46. **Moore, J. P. and M. Stevenson.** 2000. New targets for inhibitors of HIV-1 replication. *Nat. Rev. Mol. Cell Biol.* **1**:40-49.
47. **Park, E. J., M. K. Gorny, S. Zolla-Pazner, and G. V. Quinnan, Jr.** 2000. A global neutralization resistance phenotype of human immunodeficiency virus type 1 is determined by distinct mechanisms mediating enhanced infectivity and conformational change of the envelope complex. *J. Virol.* **74**:4183-4191.
48. **Perrin, C., E. Fenouillet, and I. M. Jones.** 1998. Role of gp41 glycosylation sites in the biological activity of human immunodeficiency virus type 1 envelope glycoprotein. *Virol.* **242**:338-345.
49. Poumbourios, P., W. El Ahmar, D. A. McPhee, and B. E. Kemp. 1995. Determinants of human immunodeficiency virus type 1 envelope glycoprotein oligomeric structure. *J. Virol.* **69**:1209-1218.
50. **Poumbourios, P., K. A. Wilson, R. J. Center, W. El Ahmar, and B. E. Kemp.** 1997. Human immunodeficiency virus type 1 envelope glycoprotein oligomerization requires the gp41 amphipathic alpha-helical/leucine zipper-like sequence. *J. Virol.* **71**:2041-2049.
51. **Poveda, E., B. Rodes, C. Toro, L. Martinez-Carbonero, J. Gonzalez-Lahoz, and V. Soriano.** 2002. Evolution of the gp41 env region in HIV-infected patients receiving T-20, a fusion inhibitor. *AIDS* **16**:1959-1980.
52. **Pritsker, M., J. Rucker, T. L. Hoffman, R. W. Doms, and Y. Shai.** 1999. Effect of nonpolar substitutions of the conserved Phe11 in the fusion peptide of HIV-1 gp41 on its function, structure, and organization in membranes. *Biochem.* **38**:11359-11371.
53. **Rabenstein, M. and Y. K. Shin.** 1995. A peptide from the heptad repeat of human immunodeficiency virus gp41 shows both membrane binding and coiled-coil formation. *Biochem.* **34**:13390-13397.
54. **Reitz, M. S., Jr., C. Wilson, C. Naugle, R. C. Gallo, and M. Robert-Guroff.** 1988. Generation of a neutralization-resistant variant of HIV-1 is due to selection for a point mutation in the envelope gene. *Cell* **54**:57-63.
55. **Rimsky, L. T., D. C. Shugars, and T. J. Matthews.** 1998. Determinants of human immunodeficiency virus type 1 resistance to gp41- derived inhibitory peptides. *J. Virol.* **72**:986-993.
56. **Rovinski, B., G. A. Dekaban, S. X. Cao, F. L. Yao, R. Persson, T. J. Matthews, and M. H. Klein.** 1999. Engineering of noninfectious HIV-1-like particles containing mutant gp41 glycoproteins as vaccine candidates that allow vaccinees to be distinguished from HIV-1 infectees. *Virol.* **257**:438-448.
57. **Salzwedel, K., J. T. West, and E. Hunter.** 1999. A conserved tryptophan-rich motif in the membrane-proximal region of the human immunodeficiency virus type 1 gp41 ectodomain is important for Env-mediated fusion and virus infectivity. *J. Virol.* **73**:2469-2480.
58. **Sanders, R. W., E. Van Anken, M. Lu, I. Braakman, and B. Berkhout.** 2003a. unpublished results.

59. **Sanders, R. W., E. Busser, J. P. Moore, M. Lu, and B. Berkhout.** 2003b. unpublished results.
60. **Sanders, R. W., M. Dankers, J. P. Moore, and B. Berkhout.** 2003c. unpublished results.
61. **Sanders, R. W., M. Vesanen, N. Schuelke, A. Master, L. Schiffner, R. Kalyanaraman, M. Paluch, B. Berkhout, P. J. Maddon, W. C. Olson, M. Lu, and J. P. Moore.** 2002c. Stabilization of the soluble, cleaved, trimeric form of the envelope glycoprotein complex of human immunodeficiency virus type 1. *J. Virol.* **76**:8875-8889.
62. **Schaal, H., M. Klein, P. Gehrmann, O. Adams, and A. Scheid.** 1995. Requirement of N-terminal amino acid residues of gp41 for human immunodeficiency virus type 1-mediated cell fusion. *J. Virol.* **69**:3308-3314.
63. **Shu, W., J. Liu, H. Ji, L. Radigen, S. Jiang, and M. Lu.** 2000. Helical interactions in the HIV-1 gp41 core reveal structural basis for the inhibitory activity of gp41 peptides. *Biochem.* **39**:1634-1642.
64. **Shugars, D. C., C. T. Wild, T. K. Greenwell, and T. J. Matthews.** 1996. Biophysical characterization of recombinant proteins expressing the leucine zipper-like domain of the human immunodeficiency virus type 1 transmembrane protein gp41. *J. Virol.* **70**:2982-2991.
65. **Si, Z., M. Cayabyab, and J. Sodroski.** 2001. Envelope glycoprotein determinants of neutralization resistance in a simian-human immunodeficiency virus (SHIV-HXBc2P 3. 2) derived by passage in monkeys. *J. Virol.* **75**:4208-4218
66. **Stern, T. L., M. S. Reitz, Jr., and M. Robert-Guroff.** 1995. Spontaneous reversion of human immunodeficiency virus type 1 neutralization-resistant variant HXB2thr582: in vitro selection against cytopathicity highlights gp120-gp41 interactive regions. *J. Virol.* **69**:1860-1867.
67. **Syu, W. J., W. R. Lee, B. Du, Q. C. Yu, M. Essex, and T. H. Lee.** 1991. Role of conserved gp41 cysteine residues in the processing of human immunodeficiency virus envelope precursor and viral infectivity. *J. Virol.* **65**:6349-6352.
68. **Tan, K., J. Liu, J. Wang, S. Shen, and M. Lu.** 1997. Atomic structure of a thermostable subdomain of HIV-1 gp41. *Proc. Natl. Acad. Sci. USA* **94**:12303-12308.
69. **Wang, S., J. York, W. Shu, M. O. Stoller, J. H. Nunberg, and M. Lu.** 2002. Interhelical interactions in the gp41 core: implications for activation of HIV-1 membrane fusion. *Biochem.* **41**:7283-7292.
70. **Wei, X., J. M. Decker, H. Liu, Z. Zhang, R. B. Arani, J. M. Kilby, M. S. Saag, X. Wu, G. M. Shaw, and J. C. Kappes.** 2002. Emergence of resistant human immunodeficiency virus type 1 in patients receiving fusion inhibitor (T-20) monotherapy. *Antimicrob. Agents Chemother*. **46**:1896-1905.
71. **Weissenhorn, W., A. Dessen, S. C. Harrison, J. J. Skehel, and D. C. Wiley.** 1997. Atomic structure of the ectodomain from HIV-1 gp41. *Nature* **387**:426-430.
72. **Weng, Y. and C. D. Weiss.** 1998. Mutational analysis of residues in the coiled-coil domain of human immunodeficiency virus type 1 transmembrane protein gp41. *J. Virol.* **72**:9676-9682.
73. **Weng, Y., Z. Yang, and C. D. Weiss.** 2000. Structure-function studies of the self-assembly domain of the human immunodeficiency virus type 1 transmembrane protein gp41. *J. Virol.* **74**:5368-5372.
74. **Wild, C., J. W. Dubay, T. Greenwell, T. Baird, Jr., T. G. Oas, C. McDanal, E. Hunter, and T. Matthews.** 1994. Propensity for a leucine zipper-like domain of human immunodeficiency virus type 1 gp41 to form oligomers correlates with a role in virus- induced fusion rather than assembly of the glycoprotein complex. *Proc. Natl. Acad. Sci. USA* **91**:12676-12680.
75. **Wyatt, R. and J. Sodroski.** 1998. The HIV-1 envelope glycoproteins: fusogens, antigens, and immunogens. *Science* **280**:1884-1888.
76. **Yang Z, Nielsen R, Goldman N, Pedersen AM.** 2000. Codon-substitution models for heterogeneous selection pressure at amino acid sites. *Genetics* **155**(1):431-49.

Summary

The HIV-1 envelope glycoproteins (Env) mediate viral entry into cells that express the appropriate receptors: the CD4 receptor and either CCR5 or CXCR4 as a coreceptor. Env is arranged on the virus particle in trimeric spikes, comprising three gp120 (SU) and three gp41 (TM) molecules, and is anchored within the viral membrane through the gp41 transmembrane domain. Since the Env complex resides in the lipid membrane that constitutes the outside of the virus particle, it is the major target for virus-neutralizing antibodies. Currently, our knowledge on Env folding, structure and function and the implications for immunogenicity is insufficient. Fundamental research in combination with rational vaccine design may contribute to a better understanding of Env and the immune responses raised against it. Hopefully, this will eventually lead to the design of Env immunogens that are capable of inducing potent neutralizing antibodies to prevent transmission or to clear infection. Chapter 2, 3 and 4 describe our fundamental research on various properties of Env. The current knowledge is used in chapter 5 to modify Env for vaccine purposes.

Dendritic cells (DC) support HIV-1 transmission by capture of the virus particle in the mucosa and subsequent transport to the draining lymph node, where HIV-1 is presented to $CD4^+$ T helper (Th) cells. Virus transmission involves an interaction of the DC-specific surface molecule DC-SIGN or other lectins with gp120 and subsequent internalization of the virus, which remains infectious. The mechanism of viral transmission from DC to T cells is currently unknown. Sentinel immature DC (iDC) develop into Th1-promoting effector DC1 or Th2-promoting DC2, depending on the activation signals. We studied the ability of these effector DC subsets to support HIV-1 transmission *in vitro*. Compared with iDC, virus transmission is greatly upregulated for the DC1 subset, whereas DC2 cells are inactive. Increased transmission by DC1 did not correlate with increased surface expression of the HIV-1 receptors CD4, CXCR4 or CCR5. Furthermore, the expression of DC-SIGN, which binds mannose residues on gp120 and facilitates HIV-1 transmission, was not upregulated. In contrast, we found that the increased transmission by DC1 correlates with increased expression of ICAM-1, and blocking studies confirm that ICAM-1 expression on DC1 is important for HIV transmission. The ICAM-1 – LFA-1 interaction is known to be important for immunological cross-talk between DC and T cells, and our results indicate that this cell – cell contact is exploited by HIV-1 for efficient transmission.

We have analyzed the unique epitope for the broadly neutralizing human monoclonal antibody 2G12 on gp120. Sequence analysis, thereby focusing on the conservation of relevant residues across multiple HIV-1 isolates, refined the epitope

that was previously defined by substitutional mutagenesis. In a biochemical study, we digested recombinant gp120 with various glycosidase enzymes with known specificity, and showed that the 2G12 epitope is lost when gp120 is treated with mannosidases. Computational analyses were used to position the epitope in the context of the virion-associated Env complex, to determine the variability of the surrounding surface, and to calculate the surface accessibility of possible glycan- and polypeptide-epitope components. Together, these analyses suggest that the 2G12 epitope is centered around the high mannose/hybrid glycans of residues 295, 332 and 392, with peripheral glycans from 386 and 448 on either flank. The epitope is mannose-dependent and composed primarily of carbohydrate, with probably no direct involvement of the gp120 polypeptide surface. It resides on a face orthogonal to the CD4 binding face, on a surface proximal to, but distinct from, that implicated in coreceptor binding. Its conservation amidst an otherwise highly variable gp120 surface suggests a functional role for the 2G12 binding site, perhaps related to the mannose-dependent attachment of HIV-1 to DC-SIGN or related lectins that facilitate DC-mediated virus transmission.

The strict conservation of the ten disulfide bonds in Env suggests that they are important for the oxidative folding in the endoplasmic reticulum (ER) or for Env function in viral entry. To investigate the role of individual disulfide bonds, we systematically replaced cysteines by alanines. We found that five disulfide bonds are essential for both folding and viral entry. Surprisingly, two disulfide bonds could be mutagenized without abrogating folding or function. The remaining three disulfide bonds are elementary for viral fitness despite their dispensability for folding. Thus, approval from the quality control to leave the ER is based on 'foldedness', which in turn does not necessarily warrant protein functionality. We describe evolved Env variants lacking the disulfide bond in the N-terminal C1 domain of the gp120 subunit. Compensatory changes were found both locally near the leader cleavage site and distally in the gp41 ectodomain. The results suggest that these two Env domains interact during folding.

Protein folding is studied at several levels. First, the formation of secondary structure elements such as α-helices and β-sheets can be investigated. Second, the acquisition of tertiary structure and disulfide bonds during oxidative folding in the endoplasmic reticulum (ER) *in vivo* can be studied. Third, one can analyze the results of a completed folding process as a protein is secreted or expressed at the cell surface, the ultimate test being the analysis of function. The correlates of these different levels of protein folding are mostly unclear. We generated a gp120 variant through virus evolution that is functional despite the lack of the disulfide bond at the base of the V4 domain that is otherwise required for virus replication and gp120 activity. Biochemical and computational analyses indicate that virus replication is restored through the improvement of local hydrogen bonding and stabilization of a local β-sheet fold. This study provides proof that a critically important disulfide bond can be functionally replaced by an alternative protein structure motif. It also provides evidence for the proposal that local protein stability is an important factor in escape from ER quality control during protein biosynthesis. Furthermore, our data indicate that β-sheet preference is a determinant in directing protein stability and protein folding *in vivo* and that β-sheet rules deduced from experiments with small model proteins also hold for the intricate

chaperone-assisted folding of a complicated glycoprotein such as gp120.

In the second part of this thesis, we describe Env modifications that may improve immunogenicity. The few antibodies that potently neutralize HIV-1 recognize a limited number of Env epitopes exposed on the functional Env complex on infectious virions. These native Env complexes comprise three gp120 subunits noncovalently and weakly associated with three gp41 moieties. The individual subunits induce neutralizing antibodies rather inefficiently but raise mainly non-neutralizing antibodies. Consequently, recombinant Env does not elicit strong antiviral antibody responses, particularly against primary isolates. To develop recombinant proteins that are better antigenic mimics of the native Env complex, we have introduced a disulfide bond between the C-terminal region in gp120 and the immunodominant segment in the gp41 ectodomain. The resulting gp140 protein, termed SOS gp140, is processed efficiently and produces a properly folded Env complex. The association of gp120 with gp41 is now stabilized by the supplementary intermolecular disulfide bond. Importantly, the SOS gp140 protein has antigenic properties that resemble those of the virion-associated complex.

We describe the generation and characterization of gp140 variants that have deletions in the first, second and/or third variable loops. We observed that deletion of the third variable (V3) loop interferes with the proteolytic processing of gp140, leading to the production of proteins in which gp120 remains linked to the gp41 ectodomain by a peptide bond. However, V3 loop-deleted SOS gp140 proteins were proteolytically processed efficiently. Thus, the introduction of the intermolecular disulfide bond reverses the cleavage defect created by deletion of the V3 loop. An Env variant that combines the V1, V2 and V3 loops deletions could not be stabilized by the intermolecular disulfide. Antigenic characterization of the variant SOS gp140 proteins revealed that deletion of the variable loops uncovers cryptic, conserved neutralization epitopes overlapping with the coreceptor binding site on gp120.

SOS gp140, proteolytically uncleaved gp140 ($gp140_{UNC}$) and gp120 were expressed in stably transfected Chinese hamster ovary (CHO) cells and analyzed for antigenic and structural properties before and after purification. Compared with $gp140_{UNC}$, SOS gp140 reacted more strongly in surface plasmon resonance and radioimmunoprecipitation assays with the neutralizing monoclonal antibodies 2G12 (anti-gp120), 2F5 (anti-gp41) and 17b (directed to a CD4-induced epitope that overlaps the CCR5 binding site). In contrast, $gp140_{UNC}$ displayed greater reactivity with non-neutralizing anti-gp120 and anti-gp41 antibodies. Immuno-electron microscopy studies suggested a model for SOS gp140 wherein the gp41 ectodomain ($gp41_{ECTO}$) occludes the non-neutralizing face of gp120, consistent with the antigenic properties of this protein. We also report the application of Blue Native polyacrylamide gel electrophoresis (BN-PAGE), a high-resolution molecular sizing method, to the study of viral envelope proteins. BN-PAGE and other biophysical studies demonstrated that SOS gp140 is monomeric, whereas $gp140_{UNC}$ comprised a mixture of non-covalently associated and disulfide-linked dimers, trimers and tetramers. The oligomeric and antigenic properties of SOS gp140 and $gp140_{UNC}$ were largely unaffected by purification. An uncleaved gp140 protein containing the SOS cysteine mutations (SOS $gp140_{UNC}$) was also oligomeric. Surprisingly, variable-loop-deleted SOS gp140 proteins

were expressed as cleaved, non-covalently associated oligomers that were significantly more stable than the full-length SOS gp140.

We have investigated whether HIV-1 would be able to accept the engineered SOS disulfide bond by spontaneous adaptation and optimization through evolution in cell culture infection. This approach may provide information on the interaction between gp120 and gp41. Identifying compensatory mutations that would accommodate the SOS disulfide bond in a replicating virus might also be useful for the design of improved Env immunogens. An HIV-1 molecular clone containing the SOS Env gene was only minimally replication competent, indicating that the engineered disulfide bond substantially impaired Env function. Virus escape mutants could be selected, but virus evolution eventually always led to elimination of the intermolecular disulfide bond. During these evolution experiments, we identified additional and unusual second-site reversions at position 591 and 593 within gp41. These changes highlight residues that may play an important role in the interaction between gp120 and gp41.

In virus-infected cells, the Env precursor gp160 is cleaved by cellular proteases into a fusion-competent gp120/gp41 heterodimer in which the two subunits are non-covalently associated. However, cleavage can be inefficient when recombinant Env is expressed at high levels, either as a full-length gp160 or as a soluble gp140 truncated immediately N-terminal to the transmembrane domain. We have explored several methods for obtaining fully cleaved Env for use as a vaccine antigen. We tested whether purified Env could be enzymatically digested with purified protease *in vitro.* Plasmin efficiently cleaved the Env precursor, but also cut at a second site in gp120, most probably the V3 loop. In contrast, a soluble form of furin was specific for the gp120/gp41 cleavage site, but cleaved inefficiently. Co-expression of Env with the full-length or soluble forms of furin enhanced Env cleavage but also reduced Env expression. When the Env cleavage site (REKR) was mutated to see if its use by cellular proteases could be enhanced, several mutants were identified that are indeed processed more efficiently than the wild-type protein. The optimal cleavage-site sequences are RRRRRR, RRRRKR and RRRKKR. These mutations do not significantly alter the capacity of the Env protein to mediate fusion and do not radically perturb the Env structure. Furthermore, unlike wild-type Env, expression of the cleavage-site mutants is not significantly reduced by furin co-expression. The co-expression of Env cleavage site mutants and furin is therefore a useful method for the high-level expression of processed Env.

Although SOS gp140 is an antigenic mimic of the functional Env complex, the gp41–gp41 interactions are too weak to maintain the protein in a trimeric configuration. Consequently, the purified SOS gp140 protein is a monomer. We describe modifications of the SOS gp140 protein that increase its trimer stability. A variant SOS gp140 protein, designated SOSIP gp140, contains an isoleucine-to-proline substitution at position 559 in the N-terminal heptad repeat region of gp41. This protein is fully cleaved, has favorable antigenic properties and is predominantly trimeric. SOSIP gp140 trimers are non-covalently associated and can be purified by gel-filtration chromatography. These gp140 trimers are dissociated into monomers by anionic detergent or heat, but are relatively resistant to non-ionic detergents, high salt concentrations or exposure to mildly acidic pH.

To provide more insight into how helix-breaking substitutions at position 559 affect Env structure and function, we evaluated their effects on wild-type Env in the context of replicating virus. Viruses containing an isoleucine-to-proline or isoleucine-to-glycine substitution at this position replicate poorly, but an evolution route is described that restores replication competence. Both substitutions adversely affect Env expression, Env incorporation into virions and the interaction between gp120 and gp41. Biophysical studies show that the isoleucine-to-proline mutation essentially disrupts the folding of a recombinant gp41 ectodomain core model into a six-helix bundle structure. In the escape virus, which contains a proline-to-leucine first-site pseudo-reversion, most of these properties are restored.

Thus, we managed to overcome several problems in Env vaccine research, while increasing our knowledge of Env. First, complete precursor cleavage can be ensured, either by co-transfection of furin when producing recombinant proteins, or by optimization of the cleavage site. Second, the weak intermolecular interactions between gp120 and gp41 can be stabilized by the introduction of a disulfide bond. Third, the trimer interactions can be stabilized by the introduction of helix-breaking residues in gp41. Fourth, variable loops can be deleted to uncover the receptor binding sites. The resulting proteins may be useful reagents for structural and immunogenicity studies, although it seems likely that further modification is necessary to address other aspects of Env-related immune evasion by HIV.

Samenvatting

Introductie

Het humaan immunodeficiëntie virus (HIV) is de veroorzaker van AIDS. Het envelop eiwitcomplex van HIV, dat zich aan de buitenkant (de "envelop") van het virus bevindt, is verantwoordelijk voor het binnendringen van het virus in een menselijke gastheercel. Cellen van het menselijk immuunsysteem die geïnfecteerd kunnen worden door HIV, brengen de CD4 receptor en een van de coreceptoren CCR5 en CXCR4 tot expressie op hun oppervlak. De envelop eiwitten hebben deze receptoren nodig om de fusie van de virale membraan met de celmembraan te bewerkstelligen, met als gevolg entree van het virale erfelijk materiaal. Het functionele envelop eiwitcomplex op een virusdeeltje bestaat uit zes glycoproteïnen (suikereiwitten), te weten drie oppervlakte (gp120) moleculen, en drie transmembraan (gp41) moleculen. De transmembraan domeinen in de gp41 moleculen verankeren het complex in de virale membraan. Omdat de envelop eiwitten gp120 en gp41 zich aan de buitenkant van het virusdeeltje bevinden, zijn zij het belangrijkste doel voor antilichamen die kunnen verhinderen dat het virus de cel binnenkomt, de zogenaamde virus-neutraliserende antilichamen. Daarom zijn de envelop eiwitten zeer belangrijk voor vaccinonderzoek. De huidige kennis over de vouwing, structuur en functie van het envelop eiwitcomplex en de implicaties voor de immuunrespons, waaronder antilichamen, die het eiwitcomplex opwekt, is niet genoeg om een werkzaam vaccin te ontwerpen. In de hoofdstukken 2, 3 en 4 beschrijven we ons fundamentele onderzoek naar een aantal aspecten van het envelop eiwitcomplex en de huidige kennis hebben we gebruikt om nieuwe envelop eiwitvarianten te ontwerpen die gebruikt kunnen worden in vaccins.

Een opvallend kenmerk van HIV is het enorme vermogen zich aan te passen aan een veranderende omgeving. Dit komt onder andere omdat het virale reverse transciptase enzym, dat verantwoordelijk is voor omzetting van het virale genetisch materiaal van RNA in DNA, veel fouten maakt. Gemiddeld bevat ieder nieuw virusdeeltje één fout in het erfelijk materiaal. Als deze "fout" een evolutionair voordeel oplevert onder nieuwe omstandigheden, bijvoorbeeld de aanwezigheid van een medicijn, worden virussen met deze fout geselecteerd. Hierdoor kan HIV snel resistent worden tegen medicijnen. Ook kan HIV zo gemakkelijk ontsnappen aan het immuunsysteem, bijvoorbeeld aan neutraliserende antilichamen. In het laboratorium gebruiken we de veranderlijkheid van HIV om dingen te leren over het virus. We laten een virus met een bepaald defect zich een aantal weken of maanden vermenigvuldigen en bekijken dan hoe het virus het door ons geïntroduceerde probleem oplost. De compensatoire veranderingen geven vaak veel inzicht in bepaalde aspecten van de virale levenscyclus. In de hoofdstukken

4.2, 4.3, 5.4 en 5.7 hebben we gebruikt gemaakt van deze techniek, die we "gedwongen virusevolutie" noemen omdat we het virus dwingen een oplossing te vinden voor een door ons geïntroduceerd probleem.

De envelop eiwitten worden als een voorloper gp160 eiwit gemaakt, en gp160 is zoals alle eiwitten opgebouwd uit aminozuren, die in een keten aan elkaar gezet worden. Aminozuurketens vouwen ingewikkelde eiwitstructuren. Tijdens de synthese van een aminozuurketen wordt deze naar het endoplasmatisch reticulum (ER) verplaatst, de eiwitfabriek van de cel. In eerste instantie vouwen aminozuurketens hier in secundaire structuren, waarvan α-helices en β-sheets de belangrijkste voorbeelden zijn. Ook worden in het ER cysteïnebruggen gevormd. Een cysteïnebrug is een stevige verbinding tussen twee cysteïne aminozuren en kan gevormd worden tussen twee cysteïnes in dezelfde aminozuurketen of in een andere aminozuurketen, en deze brug vergemakkelijkt het ontstaan van de tertiaire structuur van het eiwit. Uiteindelijk vormen drie voorloper envelop eiwitten (gp160) de quaternaire structuur: het trimeer complex. Ook worden in het ER suikerketens aan de eiwitketen gekoppeld. De envelop eiwitten bestaan voor bijna de helft uit suiker, vandaar de benaming glycoproteïnen (suikereiwitten).

Nadat het goed gevouwen voorloper gp160 eiwit toestemming krijgt om het ER te verlaten, komt het terecht in het Golgi complex. Hier wordt gp160 geknipt in de afzonderlijke onderdelen gp120 en gp41, die labiel aan elkaar blijven zitten. In het Golgi complex worden ook de suikers gemodificeerd. Daarna wordt het functionele envelop eiwitcomplex, dat nu dus bestaat uit trimeren van drie gp120 en drie gp41 moleculen, naar het celmembraan getransporteerd waar het samen met andere virale eiwitten en het genetisch materiaal nieuwe virus deeltjes vormt die de cel verlaten en een nieuwe cel kunnen gaan infecteren.

Van de twintig natuurlijk voorkomende aminozuren zijn er drie van belang voor dit proefschrift. De eerder genoemde cysteïne kan dus met een andere cysteïne een sterke binding vormen, een cysteïnebrug. Het normale envelop eiwitcomplex heeft tien cysteïnebruggen en de rol van deze cysteïnebruggen wordt beschreven in hoofdstukken 4.1, 4.2 en 4.3. In hoofdstuk 5.1 beschrijven we een variant met een extra, elfde cysteïnebrug, namelijk tussen gp120 en gp41, zodat deze stabiel aan elkaar verankerd worden. Van belang is ook het proline aminozuur, omdat dit secundaire structuren destabiliseert. In hoofdstuk 5.6 hebben we hier gebruik van gemaakt. We hebben een extra proline ingebouwd in een α-helix, waardoor deze helix niet meer gevormd kan worden. Asparagine is het derde aminozuur dat van speciaal belang is, omdat de suikerketens aan asparagines worden vastgemaakt. Deze suikerketens zijn van belang voor eiwitvouwing (hoofdstuk 4), voor binding aan receptoren (hoofdstuk 2) en als afscherming tegen antilichamen (hoofdstukken 1 en 3).

Verschillende facetten van het envelop eiwitcomplex dragen bij aan de eigenschap dat het nauwelijks neutraliserende antilichamen opwekt, zowel in een natuurlijke infectie als in gevaccineerde personen. Ten eerste worden de domeinen die aan de receptor en aan de coreceptor binden - mogelijke doelwitten voor neutraliserende antilichamen - beschermd door variabele domeinen en suikerketens. Variabele domeinen kunnen via evolutie gemakkelijk veranderd worden zodat de neutraliserende antilichamen niet meer kunnen binden. Suikers worden door het immuunsysteem niet herkend als lichaamsvreemd en wekken daardoor

nauwelijks specifieke antilichamen op. Een uitzondering is het 2G12 antilichaam (hoofdstuk 3). Daarnaast leiden de envelop eiwitten het immuunsysteem om de tuin met behulp van domeinen die niet-neutraliserende antilichamen opwekken. gp120 en gp41 vallen gemakkelijk van elkaar en gp160 wordt niet altijd geknipt. Beiden eigenschappen leiden tot de expositie van domeinen die op het functionele eiwitcomplex niet toegankelijk zijn. Deze domeinen zijn erg goed in het opwekken van antilichamen, maar deze kunnen het virus niet neutraliseren. Een aantal van deze eigenschappen die het envelop eiwitcomplex beschermen tegen het immuunsysteem hebben we proberen te doorbreken (hoofdstuk 5).

Het envelop eiwit en HIV transmissie (hoofdstuk 2)
Seksuele transmissie van HIV wordt mogelijk gemaakt door dendritische cellen die virusdeeltjes binden in de mucosa en vervolgens naar de lymfeknopen vervoeren waar deze virusdeeltjes T cellen kunnen infecteren. Dendritische cellen binden HIV via een molecuul op hun oppervlak, DC-SIGN, dat bind aan gp120, waarna het infectieuze virus wordt opgenomen in de dendritische cel. Tijdens de tocht van mucosa naar lymfeknopen differentiëren de dendritische cellen. Afhankelijk van de activeringsignalen die deze cellen krijgen zijn er twee typen gedifferentieerde dendritische cellen te onderscheiden. We hebben bestudeerd of deze gedifferentieerde dendritische cellen verschillen in hun vermogen HIV transmissie te bewerkstelligen. Het blijkt dat dendritische cellen van type 1 heel erg effectief zijn in HIV transmissie, terwijl type 2 cellen inactief zijn. Er is geen correlatie tussen de verhoogde transmissiecapaciteit van type 1 cellen en de expressie van de HIV receptoren CD4, CXCR4, CCR5 of DC-SIGN. We hebben wel een correlatie kunnen aantonen met een verhoogde oppervlakte expressie van ICAM-1, een adhesiemolecuul dat normaal gesproken verantwoordelijk is voor de binding van dendritische cellen aan T cellen, en HIV misbruikt volgens ons deze binding voor efficiënte transmissie. Het blokkeren van deze interactie verhindert transmissie van HIV door dendritische cellen.

Envelop eiwitbinding aan het 2G12 antilichaam (hoofdstuk 3)
We hebben het bindingsdomein op gp120 bestudeerd van het 2G12 antilichaam, een van de weinige antilichamen die HIV wel neutraliseren. Uit onze analyses komt naar voren dat het 2G12 bindingsdomein is opgebouwd uit de suikerketens die aan de asparagines 295, 332 en 392 vastzitten, met een kleine en/of indirecte bijdrage van de suikerketens aan de asparagines 386 en 448. 2G12 binding aan gp120 is afhankelijk van de aanwezigheid van mannose, één van de bouwstenen waaruit suikerketens opgebouwd kunnen zijn. Waarschijnlijk bestaat het bindingsdomein geheel uit suiker en is er geen eiwitbijdrage. De locatie van het 2G12 bindingsdomein is orthogonaal ten opzichte van het CD4 bindingsdomein, en dichtbij het coreceptor bindingsdomein. Dit verklaart het mechanisme van 2G12 neutralisatie: 2G12 blokkeert binding van gp120 aan de coreceptor, een binding die noodzakelijk is voor het virus om een cel binnen te komen. Het feit dat veel virusstammen het 2G12 bindingsdomein bezitten, suggereert dat het domein een functie heeft in de levenscyclus van het virus. Wellicht zijn de suikerketens die het 2G12 bindingsdomein vormen van belang voor binding van gp120 aan dendritische cellen en dus voor HIV transmissie.

Envelop eiwitvouwing en cysteïnebruggen (hoofdstuk 4)
De conservering van de tien cysteïnebruggen in gp160 in alle HIV stammen suggereert dat deze belangrijk zijn voor vouwing van het eiwit in het ER of voor functie van de envelop eiwitten in virus replicatie. Om de rol van individuele cysteïnebruggen te bestuderen, hebben we deze systematisch verwijderd en vouwing en functie van deze gemuteerde eiwitten bekeken (hoofdstuk 4.1). We vonden dat vijf cysteïnebruggen onmisbaar zijn voor een goede vouwing. Opvallend was dat twee cysteïnebruggen niet belangrijk bleken te zijn voor vouwing of functie. De overige drie cysteïnebruggen zijn niet belangrijk voor vouwing in het ER, maar wel voor functie en virusreplicatie. Dus, toestemming om het ER te verlaten vereist een bepaalde mate van vouwing, maar dit resulteert niet per se in een functioneel eiwit.

Met behulp van "gedwongen virusevolutie" experimenten hebben we een functionele gp120 variant geïdentificeerd die een cysteïnebrug mist welk normaal gesproken essentieel is voor envelop eiwitvouwing, namelijk de cysteïnebrug aan de basis van het vierde variabele domein (hoofdstuk 4.2). Onze studies tonen aan dat de vouwing van deze variant hersteld wordt door stabilisering van een plaatselijke β-sheet. Dit bewijst dat een essentiële cysteïnebrug vervangen kan worden door een alternatieve eiwitstructuur. Het geeft ook aan dat eiwitstabiliteit een belangrijke factor is voor toestemming om het ER te verlaten tijdens eiwitbiosynthese. Daarnaast suggereren onze proeven dat de voorkeur van aminozuren om een β-sheet te vormen een belangrijke factor is voor eiwitstabiliteit en voor het aansturen van eiwitvouwing in het ER. Tevens blijkt dat de simpele β-sheet voorkeuren van aminozuren, zoals die vastgesteld zijn voor kleine modeleiwitten, ook gelden voor vouwing in het ER van een gecompliceerd eiwit zoals gp120. In "gedwongen virusevolutie" met een mutant virus dat de eerste cysteïnebrug in gp120 mist zijn naast lokale veranderingen in gp120, ook aanpassingen in gp41 gevonden (hoofdstuk 4.3). Dit resultaat geeft aan dat er tijdens gp160 vouwing een belangrijke interactie is tussen de gp120 en gp41 delen.

Envelop eiwitaanpassingen voor vaccinontwerp (hoofdstuk 5)
In het tweede deel van dit proefschrift (hoofdstuk 5) beschrijven we modificaties van de envelop eiwitten die nuttig kunnen zijn voor vaccins. Er zijn maar weinig antilichamen die HIV kunnen neutraliseren. Deze herkennen een paar eiwitdomeinen die toegankelijk zijn op het functionele envelop eiwitcomplex zoals dat aanwezig is op infectieuze virusdeeltjes. Dit complex bestaat uit drie gp120 moleculen die labiel verbonden zijn met drie gp41 moleculen. De labiliteit van deze interactie is problematisch, omdat de individuele moleculen vrijwel geen neutraliserende antilichamen opwekken, maar wel veel antilichamen die niet in staat zijn HIV te neutraliseren (niet-neutraliserende antilichamen). Een gevolg hiervan is dat gp120 vaccins geen sterke antivirale antilichaamrespons opwekken. Om een envelop eiwit te maken dat meer lijkt op het functionele complex zoals dat aanwezig is op virusdeeltjes, hebben we een extra cysteïnebrug ingebouwd tussen gp120 en gp41 (hoofdstuk 5.1). In het resulterende SOS eiwit zijn gp120 en gp41 stabiel aan elkaar verbonden.

In hoofdstuk 5.2 beschrijven we varianten van het SOS eiwit waarvan een deel van de variabele domeinen verwijderd zijn, om zo de receptor bindingsdomeinen

meer zichtbaar te maken voor het immuunsysteem. Uit onze studies blijkt dat het mogelijk is om het eerste en tweede variabele domein van gp120 te verwijderen. Het is ook mogelijk om het derde variabele domein te verwijderen. Dit resulteert inderdaad in een betere toegang tot de receptor bindingsdomeinen. Het is echter onmogelijk om de drie variabele domeinen tegelijk te verwijderen. In dat geval wordt de extra SOS cysteïnebrug niet gevormd en worden gp120 en gp41 dus niet stabiel aan elkaar verankerd.

In hoofdstuk 5.3 bekeken we de eigenschappen van gezuiverd SOS eiwit in meer detail en vergeleken het met gp120 en ongeknipt envelop eiwit, d.w.z. eiwit waarbij de knip tussen gp120 en gp41 niet heeft plaatsgevonden. Het SOS eiwit blijkt sterker te binden aan een aantal neutraliserende antilichamen, waaronder het eerder beschreven 2G12 antilichaam. We konden ook aantonen dat gp41 bindt aan de zijde van gp120 waar de niet-neutraliserende antilichamen binden. Deze kunnen dus niet aan het SOS eiwit binden, omdat de aanwezigheid van gp41 dat verhindert. Met diverse technieken hebben we de quaternaire structuur van het SOS eiwit bekeken. Terwijl ongeknipt envelop eiwit een mix van dimeren (twee gp120 moleculen en twee gp41 moleculen), trimeren en tetrameren vormt, vormt SOS alleen monomeren (één gp120 molecuul plus één gp41 molecuul). Beide eiwitvormen wijken dus af van het envelop eiwitcomplex op virusdeeltjes dat trimeren vormt. Verrassend genoeg worden wel stabiele trimeren gevormd door SOS eiwitten waarvan het eerste en tweede variabele domein verwijderd zijn.

We hebben gekeken of HIV de SOS cysteïnebrug zou kunnen accepteren en wellicht optimaliseren door “gedwongen virusevolutie” (hoofdstuk 5.4). Compensatoire mutaties die er voor zouden zorgen dat HIV de SOS cysteïnebrug kan accepteren in een levend virus, zouden waardevol kunnen zijn voor vaccinontwerp. We verkregen een virus dat minimaal infectieus was, terwijl de SOS cysteïnes nog steeds aanwezig waren. Dit leek een goede kandidaat voor vervolg evolutieproeven. Echter, in deze vervolg evolutieproeven verloor het virus altijd de SOS cysteïnebrug. Blijkbaar is de aanwezigheid van de SOS cysteïnebrug niet verenigbaar met efficiënte virusreplicatie. Wel vonden we tijdens deze studies interessante compensatoire mutaties die ons inzicht verschaffen in de interactie tussen gp120 en gp41.

De knip van gp160 in de individuele onderdelen gp120 en gp41 is niet altijd efficiënt (hoofdstuk 5.5). Dit kan een probleem zijn als men een volledig geknipt envelop eiwit als vaccin wil maken. Om dit probleem op te lossen hebben we getracht het envelop eiwit te knippen met plasmine, een protease enzym dat het juiste knipmotief in gp160 herkent. Dit resulteerde inderdaad in een efficiënte knip, maar er werd nog een tweede keer geknipt, waarschijnlijk in het derde variabele domein. De knip kan ook verbeterd worden met furine, een ander protease enzym, maar furine vermindert de hoeveelheid geproduceerd envelop eiwit. Daarna hebben we gekeken of we het knipmotief (bestaande uit de aminozuren arginine-glutamaat-lysine-arginine) in gp160 konden vervangen door knipmotieven die efficiënter gebruikt worden. Verschillende varianten bleken efficiënter geknipt te worden. De beste zijn arginine-arginine-arginine-arginine-arginine-arginine, arginine-arginine-arginine-arginine-lysine-arginine, en arginine-arginine-arginine-lysine-lysine-arginine. Deze mutaties hebben geen negatieve invloed op de eiwitstructuur en virusreplicatie. Een bijkomend voordeel is dat de

productie van deze varianten niet verminderd wordt door furine.

Het SOS eiwit lijkt op het functionele envelop eiwit zoals dat op virusdeeltjes voorkomt, maar de trimeer interacties bleken te zwak om de trimeer bij elkaar te houden, met als gevolg dat gezuiverd SOS eiwit een monomeer is met één gp120 en één gp41 molecuul. In hoofdstuk 5.6 beschrijven we aanpassingen van het SOS eiwit die de trimeer interactie stabiliseren. Het resulterende eiwit, het SOSIP eiwit, waarin een isoleucine op een specifieke positie in gp41 is vervangen door proline, lijkt op het SOS eiwit met dit verschil dat het stabiele trimeren vormt. Deze trimeren kunnen gezuiverd worden en zijn resistent tegen sommige detergentia, hoge zout concentraties, matige hitte en zuren.

Om te begrijpen hoe de vervanging van een isoleucine door een proline in gp41 SOS trimeren kan verstevigen, hebben we het effect van deze mutatie bekeken op het envelop eiwit in de context van replicerend virus (hoofdstuk 5.7). De mutatie bleek de envelop eiwitproductie, de incorporatie in virusdeeltjes en de gp120 - gp41 interactie negatief te beïnvloeden, met als resultaat dat een virus met deze mutatie niet functioneert. Biofysische proeven gaven aan dat het mutant gp41 niet goed kan vouwen in een α-helix structuur. Echter na “gedwongen virusevolutie” konden we een virus identificeren dat weer repliceert door herstel van de α-helix structuur. De proline die wij in het virus hadden aangebracht was verwijderd door een verandering naar een leucine.

We hebben dus verschillende problemen in envelop eiwitvaccin onderzoek kunnen oplossen, terwijl onze kennis over het eiwit is toegenomen. Ten eerste kunnen we de gp160 knip verbeteren, door het toevoegen van furine en/of door de introductie van een beter knipmotief. Ten tweede hebben we de zwakke interactie tussen gp120 en gp41 weten te verstevigen door de introductie van de extra SOS cysteïnebrug. Ten derde hebben we de trimeer interacties in het SOS eiwitcomplex kunnen stabiliseren door de specifieke introductie van een proline in gp41. Ten vierde kunnen we SOS eiwitvarianten produceren waarvan meerdere variabele domeinen verwijderd zijn om zo de receptor bindingsdomeinen toegankelijk te maken voor antilichamen. De resulterende eiwitten zijn interessante reagentia voor vaccinonderzoek, alhoewel er hoogstwaarschijnlijk nog meer aanpassingen nodig zijn om een effectief vaccin te ontwikkelen.

Dankwoord

Dit proefschrift had niet tot stand kunnen komen zonder de volgende mensen die ik daarom hartelijk dank:

Allereerst natuurlijk mijn promotores. Ben, voor een fantastische begeleiding. Jouw enthousiaste manier van wetenschapsbeoefening en je een enorme flexibiliteit m.b.t. plannen om weer eens wat proeven op een ander continent te gaan doen, zijn essentieel geweest voor de succesvolle afgelopen jaren. John, many thanks for giving me the opportunity to work in your lab on a great project, first at Aaron Diamond and later at Cornell, for the valuable lessons in scientific writing, and for supervising an important part of my PhD. Many thanks for coming over to Amsterdam on the occasion of the defense of this thesis. De hooggeleerde dame Braakman en de hooggeleerde heren Goudsmit, Kapsenberg, Osterhaus, Miedema en Rottier voor zittingname in de promotiecommissie.

Koen, voor je immer enthousiaste begeleiding van mijn eerste schreden op een wetenschappelijk pad. Martijn en Els, bedankt voor een hele prettige samenwerking en heel erg mooie resultaten. Ondanks mijn soms ietwat lange afwezigheid – het bespreken van experimenten over de e-mail is natuurlijk niet ideaal – hebben jullie fantastisch werk geleverd, getuige jullie bijdrage aan een aantal hoofdstukken. Rienk, Atze, Truus, Bep en Jeroen voor immer nuttige labadviezen. Henk, samen student, samen AIO, samen klaar. Chris voor een prettige samenwerking. Bill&Georgios, voor de suggestie een stage te gaan doen bij John, en ook voor een prettige samenwerking. Angela, voor de gelegenheid om af en toe Nederlands te praten in New York en natuurlijk voor een mooi stukje werk. Ik hoop dat je ooit nog iets in de wetenschap gaat doen na je co-schappen. Iedereen binnen de vakgroep humane retrovirologie voor veel gezelligheid, waardevol advies, en leuke discussies.

James, for supervising my internship at Aaron Diamond and for many discussions (sometimes scientific) in Liquids and other bars the New York East Village and later in San Diego. Brian and Francis at Aaron Diamond, Linnea, Aditi, Roopa and Maciej at Cornell for a great time in New York and for great work. Mika, for good discussions, helpful advise and a fantastic weekend in the Catskill mountains. Norbert, Bill and Paul for motivating discussions. Robyn, Ian, Dennis and other people in the Burton and Wilson labs at Scripps for trying to teach me X-ray crystallography. Hopefully we can resume lessons at some point in the future.

Esther, Joost, Martien, voor een geweldige samenwerking en wijze lessen immunologie. Eelco, Ineke, Danny, Alexandre eveneens voor een geweldige samenwerking en veel leerzame discussies over het vouwen van enveloppen. Min Lu, Peter Kwong, Michael Caffrey, Mark Wormald and Bette Korber for fruitful collaborations and helpful discussions.

Mijn paranimfen, Erik en Arno, voor jullie inzet tijdens de voorbereidingen voor de promotiedag. Mijn ouders en Martijn voor een niet aflatende steun ondanks dat jullie meestal niet wisten waar ik nou echt mee bezig was. Maartje, voor alle steun en voor de tijden dat je alleen thuis zat als ik weer eens in New York was. Je hebt me later behoorlijk teruggepakt….

Publications

Verhoef K, **Sanders RW**, Fontaine V, Kitajima S, Berkhout B. 1999. Evolution of the human immunodeficiency virus type 1 Long Terminal Repeat promoter: conversion of a NF-kB enhancer element into a GABP binding site.
Journal of Virology **73**: 1331-1340

Binley JM, **Sanders RW**, Clas B, Schülke N, Master A, Guo Y, Kajumo F, Anselma DH, Maddon PJ, Olson WC, Moore JP. 2000. A recombinant human immunodeficiency virus type 1 envelope glycoprotein complex stabilized by an intermolecular disulfide bond between the gp120 and gp41 subunits is an antigenic mimic of the trimeric virion-associtated structure.
Journal of Virology **74**: 627-643

Sanders RW, Schiffner L, Master A, Kajumo F, Guo Y, Dragic T, Moore JP, Binley JM. 2000. Variable loop-deleted variants of the human immunodeficiency virus type 1 envelope glycoprotein can be stabilized by the introduction of an intermolecular disulfide bridge between gp120 and the gp41 subunits.
Journal of Virology **74**: 5091-5100

Jeeninga RE, Keulen W, Boucher C, **Sanders RW**, Berkhout B. Evolution of AZT-resistance in HIV-1: The 41-70 intermediate that is not observed in vivo has a replication defect.
Virology **283**: 294-305

Binley JM, **Sanders RW,** Master A, Cayanan CS, Wiley CL, Schiffner L, Travis B, Kuhmann S, Burton DR, Hu S-L, Olson W, Moore JP. 2002. Enhancing the proteolytic maturation of human immunodeficiency virus type 1 envelope glycoproteins.
Journal of Virology **76**: 2606-2616

Sanders RW, Venturi M, Schiffner L, Kalyanaraman R, Katinger H, Lloyd KO, Kwong PD, Moore JP. 2002. The mannose-dependent epitope for neutralizing antibody 2G12 on human immunodeficiency virus type 1 glycoprotein gp120.
Journal of Virology **76**: 7293-7305

Schülke N, Vesanen MS, **Sanders RW,** Lu M, Anselma DJ, Villa AR, Nagashima KA, Rosenfield SI, Binley JM, Maddon PJ, Moore JP, Olson WC. 2002. Biophysical and antigenic properties of a proteolytically mature, disulfide stabilized human immunodeficiency virus type 1 gp140 envelope glycoprotein.

Journal of Virology **76**: 7760-7776

Sanders RW, De Jong EC, Baldwin CE, Schuitemaker J, Kapsenberg ML, Berkhout B. 2002. Differential transmission of human immunodeficiency virus type 1 by distinct subsets of effector dendritic cells.

Journal of Virology **76**: 7812-7821

Sanders RW, Vesanen M, Schülke N, Master A, Schiffner L, Kalyanaraman R, Paluch M, Berkhout B, Olson WC, Lu M, Moore JP. 2002. Stabilization of the soluble, trimeric form of the envelope glycoprotein complex of human immunodeficiency virus type 1.

Journal of Virology **76**: 8875-8889

Sanders RW, Korber B, Lu M, Berkhout B, and Moore JP 2002. Mutational analyses and natural variability of the gp41 ectodomain.

pp. 43-68 in *HIV Sequence Compendium 2002*. Edited by: Kuiken C, Foley B, Freed E, Hahn B, Korber B, Marx PA, McCutchan F, Mellors, JW, and Wolinksy S. Published by: Theoretical Biology and Biophysics, Los Alamos National Laboratory, Los Alamos, NM

Baldwin CE, **Sanders RW**, Berkhout B. 2003. Inhibiting HIV-1 entry with fusion inhibitors.

Current Medicinal Chemistry **10**: 1633-1642

Baldwin CE, **Sanders RW,** Jurriaans S, Lange JM, Berkhout B. 2003. Emergence of drug-resistant and drug-dependent HIV-1 variants during therapy with the T20 fusion inhibitor.

(submitted for publication)

Sanders RW, Busser E, Moore JP, Lu M, Berkhout B. Evolution of HIV-1 gp41 with a kink in the N-terminal helix results in restoration of the six-helix bundle structure.

(submitted for publication)

Sanders RW, Dankers MD, Busser E, Caffrey M, Moore JP, Berkhout B. Evolution of the HIV-1 envelope glycoproteins with a disulfide bond between gp120 and gp41.

(manuscript in preparation)

Van Anken E, **Sanders RW,** Liscaljet M, De Kok M, Tilleman S, Holopainen K, Dankers M, Dierdorp M, Busser E, Berkhout B, Braakman I. Folding and functionality of HIV-1 envelope glycoprotein disulfide bond mutants: discrepancies between ER quality control verdicts and viral fitness requirements.

(manuscript in preparation)

Sanders RW, Hsu SD, Van Anken E, Liscaljet M, Tilleman S, Busser E, Dankers M, Braakman I, Bonvin AMJJ, Berkhout B. A stable b-sheet fold can substitute for a disulfide bond in HIV-1 gp120.

(manuscript in preparation)